British Journal of Pharmacology

May 1995

Volume 115 Number 2 pages 217–380

British Journal of Pharmacology (1995) 115, 217–219

OBITUARY

Franz Hobbiger MD PhD DSc MRCP (1920-1994)

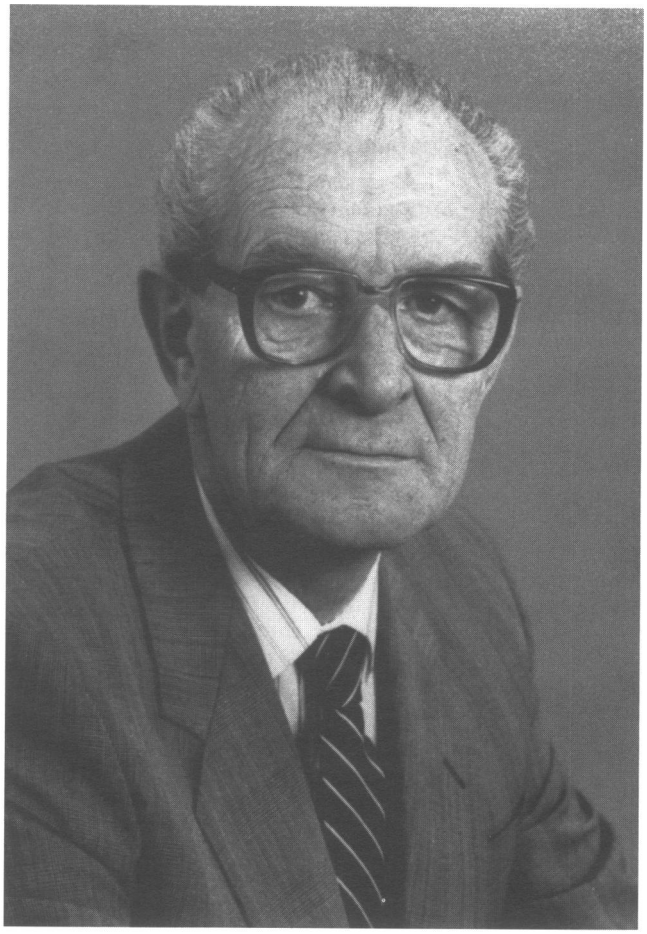

Franz Hobbiger

Franz Hobbiger, who died on June 4, 1994, was a familiar and respected member of the British Pharmacological Society, and for 6 years was an editor of this journal. A regular attender at meetings his participation, voiced in a strong Austrian accent, livened up many discussions. Arriving in Britain in 1948, his entire working life in this country was spent at the Middlesex Hospital Medical School.

Born in 1920 in the small village of Kleedorf, Austria, near the Czech border, he began his medical studies in Vienna in 1938 immediately after the anschluss. He qualified MD in 1946 but his studies were interrupted by intermittent military service on the eastern front. During the last weeks of the war a wound to a leg and misuse of a tourniquet, necessitated an above knee amputation. His original intention to specialize in surgery was changed to pharmacology. He qualified with distinctions in all parts of the MD and was clearly well-equipped intellectually to pursue a scientific career. Disenchanted by prospects in the divided Vienna of the immediate post-war years he came to the Middlesex as a WHO fellow in 1948 and worked initially with A.S.V. Burgen, who left the following year. Franz was appointed demonstrator in 1949 then promoted through the lecturer grades to reader (1959), professor (1964) and head of department (1968 succeeding C.A. Keele) before retiring in 1988. He was away from London for a few months only, on a fellowship at the Montreal Neurological Institute in 1957-58.

Franz Hobbiger arrived at the Middlesex at an opportune time for research. A.S.V. Burgen (with Dickens and Zatman) had defined the mechanism of action of botulinum toxin in a classic paper now sadly ignored, despite increasing therapeutic use of the toxin, and the work was done without a single radioactive isotope! Armstrong and Keele soon began to clarify the area of substances producing pain and itch. Tait and Simpson were discovering aldosterone, and Doniach and Roitt the fertile field of autoimmune diseases. In physiology, Eric Neil was elucidating the chemoreceptor mechanism and importance of reduced oxygen tension, work forming a basis for the practical advances in the management of respiratory failure introduced by Campbell and Westlake in the early 1960s. The young Austrian quickly found this environment to his liking, enjoying not only the laboratories and school, but the common room, clubs and pubs.

Franz Hobbiger's principal research field was the cholinesterases, work which had begun in Vienna and several publications, all in German, predate his arrival in England. At the Middlesex he was able to expand it and make fundamental discoveries. He worked in a laboratory on the ground floor of the old medical school, later demolished to build the Thorn Building. The laboratory appeared like something out of an Ealing comedy film. Smoked drums and kymographs abounded, with linked-up organ baths and rubber tubing which spurted leaks when some incompetent clamped off the wrong conduit with a Spencer Wells. Pride of place was the Warburg, an oblong tank filled with water, and containing racks of glass manometers which moved backwards and forwards. This instrument, almost ridiculous in appearance, was central to the manometric techniques essential for early enzymology enabling the biochemical pharmacology to relate to effects on isolated organs and whole animals. Franz was a superb technical experimenter using these temperamental techniques with great skill and affection. He concentrated early on studies of the mechanism by which organophosphorus compounds (potential war gases or more optimistically, insecticides) inhibited cholinesterases, and observed in 1951 (with A.S.V. Burgen) that inhibited enzyme could reactivate spontaneously. Received wisdom at that time defined the organophosphorus inhibitors as irreversible in type, chemically changing the active site by co-valent bonding: end of story. Franz Hobbiger was one of a small group of scientific heretics who challenged orthodoxy and demonstrated that practical reactivation could be achieved, with all the therapeutic implications that could ensue.

It is difficult to be certain of the exact sequence of events in this very active field through the 1950s and early sixties. Bo Holmstedt, a careful historian, made this point close to the events in 1959 and held the same view in 1985 when the dust had settled. Dates of publication are an uncertain guide through a field heavy with security and military implications. The groups with whom Franz Hobbiger interrelated included Davies and co-workers at Porton Down (where he consulted for many years), Aldridge and others at Carshalton, and I.B. Wilson and co-workers in the U.S.A. In 1951 both Hobbiger and Wilson independently reported spontaneous reactivation of the inhibited enzyme. Wilson noted also that choline and hydroxylamine speed up the process while Hobbiger showed that the rate of reactivation was related to the dialkyl structure of the inhibitor. Over the next four years much work was published on reactivation by nucleophilic compounds by the different research groups. Dr Norman Aldridge kindly drew my attention to Hobbiger's 1955 paper on 'ageing' of the inhibited enzyme. In this he examined the effects of nicotine hydroxamic acid methiodide (NHA) on human plasma cholinesterase inhibited by organophosphates containing either diethyl or disopropylphosphato groups. The

longer the time of contact between inhibitor and enzyme, the more difficult it was to reactivate with NHA. Two types of phosphorylated enzyme, I and II were postulated; type I could be reactivated whereas type II could not. (Dr Aldridge points out that it is now known that ageing is a reaction occurring in phosphorylated cholinesterases in the absence of inhibitor and the rate depends on the particular enzyme derivative). With DFP contact must not exceed 1 h whereas with some diethyl compounds reactivation could be achieved after longer periods. Also in 1955 Davies and Green at Porton and Wilson and Ginsburg in the USA reported on the reactivating properties of P-2-AM the oxime later available as pralidoxime, the currently available antidote for organophosphorus poisoning. Each group appears to have obtained their compound independently, Davies acknowledging the chemical help of G.L. Sainsbury and C. Stratford and Wilson acknowledging K. Pfister and Merck and Co. Inc. Hobbiger the following year extended his studies on ageing to true cholinesterase (human and bovine) and their reactivation from enzyme I by the potent pralidoxime supplied by Davies. Subsequently in 1966 (with Vojvodic) he extended the work to the even more potent obidoxime. In 1963 he reviewed the whole subject of reactivation in *Heffter's Handbuch Der Experimentellen Pharmacologie* edited by his friend George Koelle, a review which 30 years on is still an outstanding work of reference. Of the 25 contributors he was the only one who needed to follow his main chapter with an eleven page Addendum and 63 new references to cover the period between writing and publication, testifying both to his thoroughness and completeness, and to the scientific activity of the field. It is sad that this review is the only published example of his work referred to in the current edition of Goodman & Gilman (the 8th). Earlier volumes gave him more recognition.

Through the late 1960s and 70s the earlier single author publications gave way to joint work with his PhD students, all closely and individually supervised. Gradually, teaching and administrative work (departmental and university) took precedence over the laboratory bench, to his regret. Always cautious, anxious to confirm and pedantic to a degree in the writing of this adopted language, he was never one to publish precipitately. Additionally his love of skilful techniques made him disparaging of some of the newer isotope methods of biochemical pharmacology. He denigrated the 'PhD factories' and this led at times to conflicts with colleagues. Those who knew him well admired and respected his dedication to the very highest scientific traditions, but realised and regretted that these were increasingly compromised in many units by the changing scene of the 1980s when the future of departments depended on the number of publications.

In the early 1960s the laboratory moved to the new medical school overlooking the elegant Georgian terraces of Charlotte Street which had housed Wellcome's Physiological Research Laboratories sixty years earlier. New state of the art equipment appeared. The Warburgs now gyrated and winked Dalek-like and were capped by an appropriate rocket shape. Recorders by Devices and strain gauges now replaced the kymographs. To his responsibilities as departmental head, were added those of secretary (1965–6) followed by chairmanship (1966–9) of The Board of Studies in pharmacology at the University. In 1979 he became chairman of the Higher Degrees Committee at the medical school and in 1981 Post-graduate sub dean (Science). From 1970–88 he was a member of the veterinary products committee of the Medicines Commission. Inevitably administrative and teaching commitments through the 1970s took precedence over his research. He always regarded teaching very highly and interrelated it with research both at undergraduate and post-graduate level. Generations of medical students at the Middlesex owe to him the scientific basis of their therapeutics. Again the Middlesex in the early 1950s was blessed with distinguished teachers, notably Samson Wright with his socratic dialogues, requiring blackboard, chalk, good discussion and not a slide in sight, and Eldred Walls who could build up the most complex anatomical relationships with a few coloured chalks. Franz continued and extended this tradition.

Primo Levi disparaged the value of the scientific demonstration. Alas he never experienced Franz Hobbiger's ability to reproduce epoch-making discoveries in pharmacology: the Weber brothers' inhibition of cardiac rate by stimulation of the peripheral vagus and the same effects from i.v. acetylcholine; the hypertensive effects of adrenaline, discovered by Oliver and Schaffer; the reversal of this effect by ergotamine in the classic serendipitous observation of H.H. Dale (only to be adequately explained after Ahlquist, 1948) and many others. Only with hindsight does one realise the importance of these demonstrations for one's education; someone once said something about youth being wasted on the young! The animal demonstrations were extended to man in the pharmacology practical class before the discipline of 'clinical pharmacology' existed. Student groups explored the effects of histamine on gastric acid, glyceryltrinitrate on the cardiovascular system, and drugs on the eye. Franz collated the findings, skilfully introducing statistics and using any anomalies to teach on variability. For him there was no distinction between the animal laboratory and the human work, there was only pharmacology; clinical pharmacology was an unnecessary subdivision.

In late 1969 the Middlesex hosted the BPS meeting. A satellite meeting of clinical pharmacologists was convened and met at University College Hospital, to discuss initiating a clinical section within the BPS, which subsequently occurred. Franz undoubtedly disapproved of the separate section in principle, and felt slighted by the manner in which it was done. He saw no need for a separate department at the Middlesex and that this was practically unique among UK medical schools in no way worried him. With the fiscal contractions of the 1980s he realised he had saved the public purse much money, a sentiment which doubtless appealed to his somewhat mischievous sense of humour. Despite his political objection to clinical pharmacology, he was never obstructive to human work; indeed he encouraged it, often collaborating with anaesthetists, helping neurologists with the management of myasthenia gravis and ophthalmologists with glaucoma patients. For several years he provided a service for the diagnosis or exclusion of phaeochromocytoma until reliable chemical methods became available. Recognition by his clinical colleagues with his appointment as honorary pharmacologist to the North East District (1976) and his MRCP (1984) gave him particular pleasure, as did the establishment of the Hobbiger Prize for clinical pharmacology by the medical school.

A devout Catholic, attending mass at Sunningdale most Sundays despite the physical limitation of his amputation, he rarely discussed religion. Politics both general and university, he loved and these were frequent topics over half-pints of bitter at 5.30pm on many evenings in The King & Queen. He had a melancholic sense of humour, frequently predicting the apocalypse of the 1980s though not believed by more optimistic colleagues. When it arrived one sensed his mischievous glee. He loved to relate unfortunate bad luck–like being hit by pigeon droppings in Trafalgar Square, or butting a police officer up the backside with his protruding prosthesis when on the back of Jim Tait's motorbike negotiating Hyde Park Corner. While his English was impeccable and many of his students only learned to write clear unambiguous English while working on their theses, his spoken English remained strongly accented. He could have improved this but I suspect chose not to. He related with relish the story of how Heller (during some controversial discussion), remarked to Zaimis 'Vee Breeteesh must steek togezzer'.

Always clearly an Austrian expatriate he became a naturalized British subject in 1956. He had approached Samson Wright for sponsorship–but the generous Sammy

could not help; he had become an Israeli citizen. Hobbiger married Eluned Underhay, a biochemist at the Middlesex Hospital Medical School, in 1956, and they had a son and daughter, both doctors. In 1987 he suffered a stroke while attending the Xth International Congress of Pharmacology in Sydney. With characteristic courage he largely recovered from this, only to develop Crohns disease. In 1993 an extensive resection was very successful and he appeared his old self again. His terminal illness lasted only days and resulted from extensive vascular disease of the gut. Franz was a man with strongly-held views, at times clashing with colleagues on controversial issues. Described by his old secretary, Miss Bainbridge (now 97) as a 'Christian gentleman' he was a dedicated researcher and teacher, generous always with his time and knowledge. He is greatly missed by his many colleagues and students who owe him so much.

Anthony W. Peck
Dept of Clinical Pharmacology,
University College London Medical School

British Journal of Pharmacology (1995) 115, 220-221

SPECIAL REPORT

Reduction of vasoconstriction mediated by neuropeptide Y Y_2 receptors in arterioles of the guinea-pig small intestine

[1]T.O. Neild & C.J. Lewis

Department of Human Physiology, Flinders University, GPO Box 2100, Adelaide 5001, Australia

Brief applications of a high-K^+ solution were used to evoke transient constrictions of arterioles from the guinea-pig small intestine. Analogues of neuropeptide Y (NPY) selective for Y_2-receptors reduced the constrictions, whereas NPY or a Y_1-selective analogue potentiated the constrictions. We conclude that arteriolar smooth muscle has both Y_1 and Y_2 receptors, and suggest that Y_2 receptors inhibit vasoconstriction by modulating the opening of voltage-sensitive Ca^{2+} channels. This may be related to the role of NPY that is present in some vasodilator nerves.

Keywords: Neuropeptide Y; Y_1 receptor, Y_2 receptor; potentiation; vasoconstrictor nerves; vasodiltor nerves; vascular smooth muscle; arterioles; Ca^{2+} channels

Introduction Neuropeptide Y (NPY) is found in the sympathetic nerves around most arteries and it acts on the arterial muscle to cause vasoconstriction and potentiate the responses to other vasoconstrictor substances (Wahlestedt *et al.*, 1990). This action is mediated by the Y_1 subtype of NPY receptor (Xia *et al.*, 1992). Another receptor, the Y_2 receptor, has been found on nerve terminals where it reduces neurotransmitter release (Potter, 1987), probably by a reduction of Ca^{2+} influx through voltage-sensitive Ca^{2+} channels (Foucart *et al.*, 1993). There is also some evidence that Y_2 receptors are present on arterial smooth muscle, because Y_2-selective agonists cause vasoconstriction in some arteries (Tessel *et al.*, 1993). Here we describe experiments in which Y_2-selective agonists *reduced* vasoconstrictor responses to K^+ acting on vascular smooth muscle. This is a novel observation, but may be useful in explaining the role of the NPY that has been detected in many vasodilator nerves.

Methods Guinea-pigs of either sex and weighing 200-300 g were killed by a heavy blow to the head followed by exsanguination. A piece of ileum was removed, slit open, and the mucosa peeled off. A sheet of connective tissue containing the submucous arterioles and nerve plexus was then separated from the circular muscle and pinned out in a small chamber with a transparent base. The preparation was viewed with an inverted compound microscope equipped with a television camera, and arteriole diameter was monitored by computer analysis of the television images. This method measures average diameter over a chosen region of arteriole less than 100 μm long.

The preparation was superfused continuously with warmed oxygenated physiological saline, composition (mmol l^{-1}): Na^+ 146, K^+ 5, Ca^{2+} 2.5, Mg^{2+} 2, Cl^- 134, HCO_3^- 1, glucose 11, and was equilibrated with 95%O_2/5%CO_2. High potassium solution was made by replacing 95 mmol l^{-1} of NaCl with KCl, to give a final K^+ concentration of 100 mM. It was applied to the arteriole by pressure ejection from a micropipette using pulses 100-400 ms in duration, or in the superfusing solution to determine the maximum constriction for the arteriole (Neild & Kotecha, 1989).

Drugs used were neuropeptide Y (porcine sequence, synthesized in the Department of Biochemistry, Monash University); PYY-(13-36), [Leu^{31},Pro^{34}]NPY (Auspep, Melbourne, Australia); ω-conotoxin GVIA (Sapphire Bioscience, Alexandria, NSW, Australia). *N*-acety[Leu^{28},Leu^{31}]NPY-(24-36) was a gift from Dr E.K. Potter, Prince of Wales Medical Research Institute, Sydney, Australia.

The potentiating effect of NPY was calculated using an index P (Xia *et al.*, 1992) defined as:

$$P = \left(\frac{n}{max - n}\right) / \left(\frac{c}{max - c}\right)$$

where c is the amplitude of the control constriction, n is the amplitude of the constriction to the same stimulus in the presence of NPY or a selective agonist for Y_1 or Y_2 receptors, and max is the maximum constriction of which the arteriole is capable. P gives an index of the potentiating effect; $P = 1$ for no effect, $P > 1$ for potentiation and $P < 1$ for depression. Differences between P values were analysed by ANOVA followed by Bonferroni test. Student's *t* test was used to determine whether individual values differed from 1. A probability value < 0.05 was considered significant.

Results Brief applications of high-K^+ solution at 5 min intervals gave small repeatable constrictions of the arteriole. The amplitude of the constriction was unaffected by 30 nM ω-conotoxin GVIA, showing that the K^+ was acting on the arteriolar smooth muscle and not by releasing substances from the perivascular nerves.

The constriction was slightly potentiated by a 2 min exposure to 50 nM NPY in the superfusing solution. The potentiation was significantly greater when 50 nM [Leu^{31}, Pro^{34}]NPY, a Y_1-selective agonist (Aakerlund *et al.*, 1990) was used. The Y_2-selective agonists, PYY-(13-36) (Wahlestedt & Hakanson, 1986) or *N*-acetyl[Leu^{28},Leu^{31}]NPY-(24-36) (Potter *et al.*, 1994) in the same concentration (50 nM) significantly decreased the response. Representative traces are shown in Figure 1, and quantitation of the potentiation is summarised in Table 1.

Discussion These experiments show that arterioles of the guinea-pig intestinal submucosa express NPY Y_2 receptors in addition to the Y_1 receptors described previously (Xia *et al.*, 1992). These Y_2 receptors mediate a reduction of the constriction caused by high K^+, a constriction that is due entirely to depolarization of the smooth muscle and subsequent entry of Ca^{2+} through depolarization-activated channels. We have previously shown that responses to noradrenaline, which rely mainly on Ca^{2+} release from the internal stores, are not affected by one of the Y_2-selective agonists used here, PYY-(13-36) (Xia *et al.*, 1992). We therefore suggest that there are Y_2 receptors on the smooth muscle which modulate the opening of voltage-sensitive Ca^{2+} channels, as they do in nerve terminals (Foucart *et al.*, 1993).

[1] Author for correspondence.

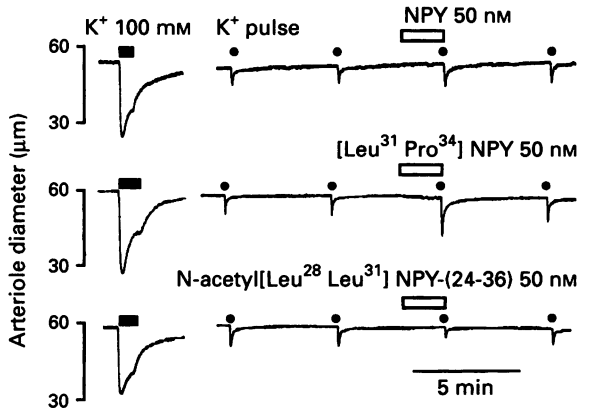

Figure 1 Traces of arteriole diameter from 3 different arterioles, showing the effects of 50 nM neuropeptide Y (NPY) and agonists selective for Y_1 and Y_2 receptors on constrictions caused by brief applications of high K^+ solution. Each trace begins with a maximum constriction caused by superfusion with 100 mM K^+ solution (solid bar). Subsequent small brief constrictions were evoked by application of 100 mM K^+ by pressure ejection from a micropipette every 5 min (●). NPY receptor agonists were applied in the superfusing solution for 2 min (open bar) prior to one application of K^+.

It appears that the action of NPY on these arterioles was a mixture of two opposing effects; a Y_1-mediated potentiating effect tending to make all vasoconstrictor responses larger, and a Ca^{2+} channel modulating effect mediated by Y_2 receptors which will reduce only those vasoconstrictor responses that rely on Ca^{2+} influx. The potentiating effect of 50 nM NPY was therefore significantly less than the potentiation caused by a Y_1 agonist. The effect of other concentrations of NPY cannot be predicted at present, as the concentration-dependence of the Y_1- and Y_2-mediated actions of NPY in these arterioles, and therefore the relative balance of constrictor and inhibitory effects, is not known.

Table 1 Values of P (mean ± s.e.mean) calculated from the effects of 50 nM neuropeptide Y (NPY) and selective agonists for Y_1 and Y_2 receptors on the constriction caused by brief applications of high K^+

	NPY (50 nM)	*[Leu³¹,Pro³⁴] NPY (50 nM)*	*N-acetyl [Leu²⁸,Leu³¹] NPY-(24-36) (50 nM)*	*PYY-(13-36) (50 nM)*
P	1.17 ± 0.077 (*n* = 13)	2.28 ± 0.368 (*n* = 6)	0.49 ± 0.095 (*n* = 6)	0.44 ± 0.044 (*n* = 6)

A value > 1 indicates potentiation of the response, < 1 indicates depression. All values were significantly different from 1. All values are significantly different from each other except for those from the two Y_2-selective agonists *N*-acetyl[Leu²⁸,Leu³¹]NPY-(24-36) and PYY-(13-36).

We have shown that mechanisms exist by which NPY can both potentiate and inhibit vasoconstriction, and this may explain its distribution in various types of perivascular nerves. It is found in many sympathetic vasoconstrictor nerves, which is quite compatible with its role as a potentiator of vasoconstriction, but it is also found in some vasoactive intestinal polypeptide (VIP)-containing nerves that are probably vasodilator (Morris *et al.*, 1985). It is now evident that its action on Y_2 receptors can reduce depolarization-induced vasoconstriction, so its presence in vasodilator nerves seems quite logical if the vessels supplied by these nerves have a significant population of Y_2 receptors. We suggest that in some vessels, NPY may have a physiological role as a vasodilator acting selectively against depolarization-induced vasoconstriction.

References

AAKERLUND, L., GETHER, U., FUHLENDORFF, J., SCHWARTZ, T.W. & THASTRUP, O. (1990). Y1 receptors for neuropeptide Y are coupled to mobilization of intracellular calcium and inhibition of adenylate cyclase. *FEBS Lett.*, **260**, 73–78.

FOUCART, S., BLEAKMAN, D., BINDOKAS, V.P. & MILLER, R.J. (1993). Neuropeptide Y and pancreatic polypeptide reduce calcium currents in acutely dissociated neurons from adult rat superior cervical ganglia. *J. Pharmacol. Exp. Ther.*, **265**, 903–909.

MORRIS, J.L., GIBBINS, I.L., FURNESS, J.B., COSTA, M. & MURPHY, R. (1985). Co-localization of neuropeptide Y, vasoactive intestinal polypeptide and dynorphin in non-noradrenergic axons of the guinea-pig uterine artery. *Neurosci. Lett.*, **62**, 31–37.

NEILD, T.O. & KOTECHA, N. (1989). A study of the phasic response of arterioles of the guinea-pig small intestine to prolonged exposure to norepinephrine. *Microvasc. Res.*, **38**, 186–199.

POTTER, E.K. (1987). Presynaptic inhibition of cardiac vagal postganglionic nerves by neuropeptide Y. *Neurosci. Lett.*, **83**, 101–107.

POTTER, E.K., BARDEN, J., MCCLOSKEY, M., SELBIE, L., TSENG, A., HERZOG, H. & SHINE, J. (1994). A novel neuropeptide Y analog N-acetyl[Leu²⁸,Leu³¹]NPY(24–36) with functional specificity for the presynaptic (Y2) receptor. *Eur. J. Pharmacol.*, **267**, 253–262.

TESSEL, R.E., MILLER, D.W., MISSE, G.A., DONG, X. & DOUGHTY, M.B. (1993). Characterization of vascular postsynaptic NPY receptor function and regulation and differential sensitivity of Y1 and Y2 receptor function to changes in extracellular calcium availability and prior in vitro peptide exposure. *Neuropeptides*, **25**, 289–298.

WAHLESTEDT, C. & HAKANSON, R. (1986). Effects of neuropeptide Y (NPY) at the sympathetic neuroeffector junction. Can pre- and postjunctional receptors be distinguished? *Med. Biol.*, **64**, 85–88.

WAHLESTEDT, C., GRUNDEMAR, L., HAKANSON, R., HEILEG, M., SHEN, G.H., ZUKOWSKA-GROJEK, Z. & REIS, D.J. (1990). Neuropeptide Y receptor subtypes, Y1 and Y2. *Ann. N.Y. Acad. Sci.*, **611**, 7–26.

XIA, J., NEILD, T.O. & KOTECHA, N. (1992). Effects of neuropeptide Y and agonists selective for neuropeptide Y sub-types on arterioles of the guinea-pig small intestine and the rat brain. *Br. J. Pharmacol.*, **107**, 771–776.

(Received February 13, 1995
Accepted February 28, 1995)

British Journal of Pharmacology (1995) 115, 222-224

SPECIAL REPORT

Involvement of protein kinase C in the delayed cytoprotection following sublethal ischaemia in rabbit myocardium

G.F. Baxter, [1]F.M. Goma & [2]D.M. Yellon

The Hatter Institute for Cardiovascular Studies, Division of Cardiology, University College London Hospital and Medical School, Grafton Way, London WC1E 6DB

Rabbit hearts were preconditioned with four 5 min coronary artery occlusions 24 h before 30 min coronary occlusion with 120 min reperfusion. Preconditioning significantly reduced the percentage of myocardium infarcting within the risk zone from 49.1 ± 4.3% to 31.8 ± 3.5% ($P<0.05$). When the protein kinase C (PKC) inhibitor, chelerythrine, was administered just before preconditioning, the delayed protection against infarction 24 h later was abolished. We conclude that the delayed cytoprotective response associated with ischaemic preconditioning of myocardium is likely to involve the early activation of one or more PKC subtypes.

Keywords: Ischaemic preconditioning; second window of protection; myocardial protection; ischaemia; infarction; protein kinase C (PKC); chelerythrine

Introduction Recently, a delayed phase of resistance to ischaemia in myocardium has been described that develops many hours after preconditioning with transient ischaemia. This 'second window of protection' (Yellon & Baxter, 1995) is associated with infarct size reduction in the rabbit (Marber *et al.*, 1993; Baxter *et al.*, 1994) and the dog (Kuzuya *et al.*, 1993), and with anti-arrhythmic effects in the dog (Vegh *et al.*, 1994). Alterations in the transcriptional regulation of protective proteins, as part of the adaptive response to sublethal ischaemic stress, may be involved in this late protection (Hoshida *et al.*, 1993; Marber *et al.*, 1993). Adenosine A_1 receptor activation during ischaemic preconditioning may be an important trigger for the delayed protection in the rabbit (Baxter *et al.*, 1994) but the intracellular signalling cascade is unknown. Since the A_1 receptor is known to link to protein kinase C (PKC) and since PKC can regulate gene transcription (Hug & Sarre, 1993), we tested the hypothesis that PKC activation during preconditioning is involved in the development of the delayed protection.

Methods The two-stage experimental protocol has been described in detail (Baxter *et al.*, 1994). Under anaesthesia ('Hypnorm' and diazepam), male New Zealand White rabbits (2.0-3.0 kg) underwent a midline sternotomy. Preconditioning was effected by four 5 min occlusions of an anterolateral branch of the circumflex coronary artery, each separated by 10 min reperfusion. Sham-operated animals served as controls. During these procedures, animals received either chelerythrine chloride 5 mg kg^{-1} (Calbiochem, Nottingham, UK) or vehicle (water with 7% v/v ethanol, total volume 6 ml), administered by slow i.v. injection over 5 min, beginning 8-10 min before the first coronary occlusion or sham preconditioning period. Four experimental groups were prepared: preconditioned + vehicle ($n=7$); preconditioned + chelerythrine ($n=6$); sham + vehicle ($n=8$); sham + chelerythrine ($n=5$). Twenty four hours later the animals were re-anaesthetized with pentobarbitone sodium and the coronary artery was occluded for 30 min with 120 min reperfusion. The myocardial risk volume (R) was determined *ex vivo* by infusion of zinc cadmium sulphide microspheres (Duke Scientific, Palo Alto, CA, U.S.A.) and the infarcted zone (I) was determined with triphenyltetrazolium chloride staining (Sigma, Poole, UK). The ratio I/R was calculated. Data were analysed with ANOVA followed by Fisher's least significant difference test and $P<0.05$ was considered as significant.

Results The principal endpoint of protection in this study was I/R (Figure 1a). I/R was reduced from 49.1 ± 4.3% in sham + vehicle to 31.8 ± 3.5% in preconditioned + vehicle ($P<0.05$), a reduction in infarct size constituting the second window of protection. Chelerythrine during the sham operation had no significant effect on infarct size 24 h later (I/R 56.9 ± 3.6% v 49.1 ± 4.3% in sham + vehicle). However, chelerythrine during preconditioning abolished the protection 24 h later (preconditioned + chelerythrine 55.4 ± 8.4% v preconditioned + vehicle 31.8 ± 3.5%; $P<0.05$). Since the rabbit is a species deficient in preformed collateral vessels, the baseline predictors of infarct size in this model are R and systemic haemodynamic status during the infarction procedure. R was similar in all the experimental groups at around 0.8-1.0 cm^3 (Figure 1b). Arterial pressure and heart rate did not differ among the experimental groups at any time point (Table 1).

Discussion This study extends our earlier observation of adenosine A_1 receptor involvement in the delayed protection (Baxter *et al.*, 1994) and suggests that a PKC signalling pathway may link adenosine receptor activation during preconditioning to the observed cytoprotection many hours later. These data provide the first evidence that PKC activation is a pivotal step in the development of the delayed protection after ischaemic preconditioning *in vivo*. Chelerythrine has been reported to be a very potent inhibitor of PKC (IC_{50} approximately 0.7 μM), showing marked selectivity for this kinase rather than other protein kinases (Herbert *et al.*, 1990). Little is known about other actions of chelerythrine. For example, inhibition of hepatic alanine aminotransferase and Na-K ATPase have been reported to occur in the micromolar range. Thus, we cannot exclude the possibility that non-kinase related activity of the compound may have been involved in our observation.

Many oncogenes and transcription factors are known to be activated by various PKC subtypes (Hug & Sarre, 1993). We have hypothesized that alterations in the regulation of heat stress proteins and/or anti-oxidant enzyme genes in the preconditioned myocardium may play a role in the mediation

[1] On leave from the Department of Physiology, University of Zambia Medical School, Lusaka
[2] Author for correspondence.

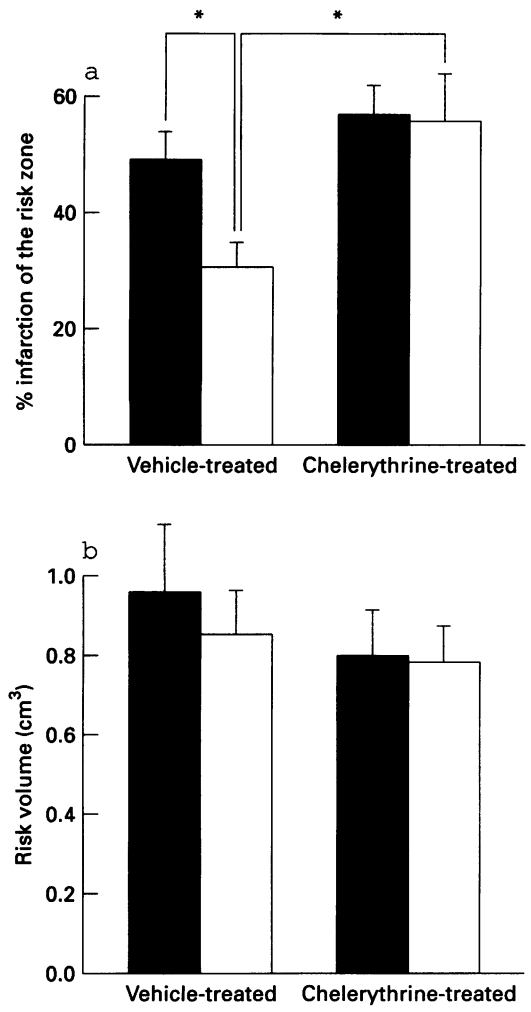

of this protection (Yellon & Baxter, 1995) while Vegh *et al.* (1994) have suggested that upregulation of the inducible nitric oxide synthase and/or cyclo-oxygenase may be involved. The nuclear translocation of activated PKC subtypes could be an important step in the transcription or modulation of these putative cytoprotective proteins. Evidence to support a direct link between adenosine receptor activation and subsequent enhancement of endogenous anti-oxidant activity has come recently from cell culture studies by Maggirwar *et al.* (1994). In addition, Yamashita *et al.* (1994) showed that hypoxic preconditioning of rat isolated cardiomyocytes resulted in enhanced tolerance to a more prolonged hypoxic period 24 h later. This delayed protection was associated with elevation of Mn-SOD activity in response to hypoxic preconditioning and was abolished by incubation with staurosporine, a relatively non-selective protein kinase inhibitor.

In summary our results provide a further demonstration of an infarct limiting effect 24 h after ischaemic preconditioning in rabbit myocardium and show that this delayed protection can be abolished by PKC inhibition with chelerythrine during the preconditioning stimulus. Thus, it seems that the second window of protection against infarction in the rabbit is likely to involve the early activation of chelerythrine-sensitive PKC subtype(s).

F.M.G. was funded by a British Council bursary. We thank the Hatter Foundation, the Wellcome Trust and Glaxo for their support.

Figure 1 (a) Percentage infarction of the risk zone (I/R) in rabbit hearts subjected to 30 min left coronary occlusion and 120 min reperfusion. Twenty fours hours previously, rabbits were treated with either chelerythrine or vehicle and were preconditioned (open columns) or were sham-operated (solid columns). In vehicle-treated rabbits, there was a marked reduction in infarct size in the group preconditioned 24 h earlier. When chelerythrine was given at the same time as preconditioning, the subsequent protection against infarction was abolished. (b) Volume of myocardium at risk during coronary occlusion was similar in all the experimental groups. The values given are mean ± s.e.mean for 5–8 animals. $*P<0.05$ (ANOVA).

Table 1 Summary of systemic haemodynamic parameters during the infarction protocol

	Baseline	*29 min ischaemia*	*60 min reperfusion*	*120 min reperfusion*
Sham + vehicle, $n=8$				
HR (min^{-1})	261 ± 12	239 ± 13	228 ± 11	241 ± 12
MAP (mmHg)	69 ± 3	55 ± 1	57 ± 3	57 ± 2
Preconditioned + vehicle, $n=7$				
HR (min^{-1})	236 + 9	234 + 16	230 ± 16	225 ± 17
MAP (mmHg)	60 + 3	46 ± 4	50 ± 4	48 ± 4
Sham + chelerythrine, $n=5$				
HR (min^{-1})	256 ± 19	250 ± 18	240 ± 21	215 ± 20
MAP (mmHg)	66 ± 5	54 ± 6	49 ± 6	56 ± 3
Preconditioned + chelerythrine, $n=6$				
HR (min^{-1})	248 ± 21	248 ± 20	252 ± 21	253 ± 22
MAP (mmHg)	68 ± 2	59 ± 2	55 ± 3	60 ± 4

Heart rate (HR) and mean arterial pressure (MAP) were recorded continuously from a cannula placed in the right carotid artery. Data are expressed as mean ± s.e.mean.

References

BAXTER, G.F., MARBER, M.S., PATEL, V.C. & YELLON, D.M. (1994). Adenosine receptor involvement in a delayed phase of protection 24 hours following ischemic preconditioning. *Circulation*, **90**, 2993–3000.

HERBERT, J.M., AUGEREAU, J.M. & MAFFRAND, J.P. (1990). Chelerythrine is a potent and specific inhibitor of protein kinase C. *Biochem. Biophys. Res. Commun.*, **172**, 993–999.

HOSHIDA, S., KUZUYA, T., FUJI, H., YAMASHITA, N., OE, H., HORI, M., SUZUKI, K., TANIGUCHI, N. & TADA, M. (1993). Sublethal ischemia alters myocardial antioxidant activity in canine heart. *Am. J. Physiol.*, **264**, H33–H39.

HUG, H. & SARRE, T.F. (1993). Protein kinase C isoenzymes: divergence in signal transduction. *Biochem. J.*, **291**, 329–343.

KUZUYA, T., HOSHIDA, S., YAMASHITA, N., FUJI, H., OE, H., HORI, M., KAMADA, T. & TADA, M. (1993). Delayed effects of sublethal ischemia on the acquisition of tolerance to ischemia. *Circ. Res.*, **72,** 1293–1299.

MAGGIRWAR, S.B., DHANRAJ, D.N., SOMANI, S.M. & RAMKUMAR, V. (1994). Adenosine acts as an endogenous activator of the cellular antioxidant defence system. *Biochem. Biophys. Res. Commun.*, **201,** 508–515.

MARBER, M.S., LATCHMAN, D.S., WALKER, J.M. & YELLON, D.M. (1993). Cardiac stress proten elevation 24 hours following brief ischemia or heat stress is associated with resistance to myocardial infarction. *Circulation*, **88,** 1264–1272.

VEGH, A., PAPP, J.G. & PARRATT, J.R. (1994). Prevention by dexamethasone of the marked antiarrhythmic effects of preconditioning induced 20 h after rapid cardiac pacing. *Br. J. Pharmacol.*, **113,** 1081–1082.

YAMASHITA, N., NISHIDA, M., HOSHIDA, S., KUZUYA, T., HORI, M., TANIGUCHI, N., KAMADA, T. & TADA, M. (1994). Induction of manganese superoxide dismutase in rat cardiac myocytes increases tolerance to hypoxia 24 hours after preconditioning. *J. Clin. Invest.*, **94,** 2193–2199.

YELLON, D.M. & BAXTER, G.F. (1995). A 'second window of protection' or delayed preconditioning phenomenon: future horizons for myocardial protection? *J. Mol. Cell. Cardiol.*, **27,** (in press).

(Received February 7, 1995
Accepted March 1, 1995)

British Journal of Pharmacology (1995) 115, 225-226

SPECIAL REPORT

Effect of a new non-steroidal anti-inflammatory drug, nitroflurbiprofen, on the expression of inducible nitric oxide synthase in rat neutrophils

S. Mariotto, *L. Cuzzolin, *A. Adami, †P. Del Soldato, [1]H. Suzuki & *G. Benoni

Istituto di Chimica Biologica and *Farmacologia, Università di Verona, Verona and †Pharmaceutical Discovery Service, Milano, Italy

The effects of a non-steroidal anti-inflammatory drug, flurbiprofen, and its nitro-derivative, nitroflurbiprofen, on inducible nitric oxide synthase in rat neutrophils were examined. Nitroflurbiprofen was shown to inhibit nitric oxide synthase induction caused by lipopolysaccharide administration, while flurbiprofen had no effect on nitric oxide synthase induction. This inhibitory action may be ascribed to nitric oxide released from nitroflurbiprofen.

Keywords: Nitroflurbiprofen; nitric oxide; nitric oxide synthase; neutrophil

Introduction Inflammation is a pathological event to which nitric oxide (NO), released by NO synthase (NOS) induced in activated macrophages, neutrophils and hepatocytes at the injured site, seems to contribute. Some steroid hormones such as dexamethasone were reported to be inhibitory agents of the expression of the inducible form of NOS (Boughton-Smith *et al.*, 1993): this seems to account in part for the anti-inflammatory effects of dexamethasone.

Non-steroidal anti-inflammatory drugs are widely used in the treatment of inflammatory conditions, but gastrointestinal lesions have often limited their clinical utilization (Carson & Strom, 1992). Flurbiprofen (FP) is a well-established anti-inflammatory agent having a potent pharmacological action mostly due to its ability to inhibit cyclo-oxygenase activity, causing a concomitant deficiency of cellular prostacyclin content and tissue damage. Nitroflurbiprofen (NFP) is a new anti-inflammatory drug obtained by the incorporation of a nitroxybutyl moiety through an ester linkage to the carboxylic group of FP; previous experiments have shown its anti-inflammatory efficacy and good gastrointestinal tolerability (Wallace *et al.*, 1994).

In the present work, we investigated the possible effects of the two non-steroidal anti-inflammatory drugs on NOS induction in the neutrophils of lipopolysaccharide (LPS)-treated rats.

Methods *Animal treatment* Female Sprague-Dawley rats (Charles River, Italy), weighing 220-240 g, were treated with FP or NFP (10 mg kg^{-1} body weight) suspended in carboxymethylcellulose 0.5% and administered orally in a volume of 1 ml 100 g^{-1} body weight; control rats received an equal volume of the vehicle. In rats co-treated with LPS (5 mg kg^{-1} body weight), it was given via the tail vein 1 h after the drug administration. Four hours later, the rats were killed by injection of sodium pentobarbitone (60 mg kg^{-1} body weight) i.p.

Neutrophil preparation Neutrophils were separated by Ficoll-Paque density gradient centrifugation as described previously (Mariotto *et al.*, 1995).

Quantitation of nitrite/nitrate in the plasma Nitrite/nitrate concentrations in the plasma were measured according to a modification of a method described previously (Bartholomew, 1984): nitrate reductase prepared from *E. coli* ATCC 25922 (Difco) was used to convert nitrate to nitrite. Nitrite was quantitated colorimetrically after reaction with the Griess reagent (Green *et al.*, 1982).

Assay of NOS activity in the neutrophils NOS activity was estimated by measurement of the conversion of L-[^{3}H]-arginine to L-[^{3}H]-citrulline as described by Bredt & Snyder (1990) with a slight modification.

Chemicals L-[2,3,4,5-^{3}H]-arginine monohydrochloride (specific activity: 60 Ci $mmol^{-1}$; 1 Ci = 27 GBq) was from Amersham Life Science. (6**R**)-5,6,7,8-tetrahydro-l-biopterin was from Dr B Schircks Laboratories (Jona, Switzerland). Nitroflurbiprofen was synthesized and kindly supplied by Pharmaceutical Discovery Service (Milano, Italy).

Statistical analysis Statistical analysis of the data was performed by one-way analysis of variance followed by Student's *t* test. $P < 0.05$ or less was considered as indicative of a significant difference.

Results and Discussion NOS activity in the neutrophils of control rats was undetectable under our assay conditions. Neither FP nor NFP had any effects on the induction of NOS activity in the neutrophils. On the other hand, NFP treatment caused a 3 fold increase in nitrite/nitrate plasma concentrations compared to the basal value: this indicates an exogenous NO release from NFP and confirms recent data on the elevation of plasma nitrite levels *in vivo* following NFP administration (Wallace *et al.*, 1994). After LPS-treatment, NOS activity became detectable, with a 8 fold increase in nitrite/nitrate plasma levels. When FP was co-administered, NOS activity did not change significantly, while the plasma nitrite/nitrate level halved compared to LPS-treated rats. Since FP alone did not change the basal plasma nitrite/nitrate concentration and had no effects on the induction of neutrophil NOS, the decreased nitrite/nitrate levels observed in rats co-treated with LPS and FP could be partially due to the cyclo-oxygenases inhibition with production of free radicals reacting with NO and/or to an inhibition of NOS present in other tissues (Table 1).

[1] Author for correspondence.

Table 1 Plasma NO_2^-/NO_3^- levels and neutrophil NOS activity

Group	*Plasma NO_2^-/NO_3^- (μM)*	*NOS activity (pmol/10^6 cells)*
Controls	32.80 ± 18.03	0
Flurbiprofen	36.08 ± 15.67	0
Nitroflurbiprofen	83.20 ± 26.25(*)	0
LPS	230.00 ± 88.36(**)	10.25 ± 6.28
LPS + flurbiprofen	121.20 ± 41.25(•)	11.94 ± 6.28
LPS + nitroflurbiprofen	252.80 ± 74.59	6.13 ± 4.97

The values are expressed as mean ± s.d. of 5–7 experiments for each treatment. Student's *t* test: nitroflurbiprofen vs controls, $*P<0.01$; LPS vs controls, $**P<0.001$; LPS + flurbiprofen vs LPS, $•P<0.05$.

NFP and LPS co-administration caused a marked decrease (40%) in neutrophil NOS activity, while no change in nitrite/nitrate plasma levels was observed; these data raise the question of the inhibitory effect of NFP on iNOS activity.

Since NFP is hydrolyzed *in vivo* to FP and NO as reported recently (Wallace *et al.*, 1994) and as indicated also in this work, and FP alone does not exert any inhibitory action on neutrophil NOS induction, it seems reasonable to postulate that the inhibitory action of NFP should be ascribed to NO released from NFP. Our recent report on a possible inhibition of neutrophil NOS induction by exogenous NO derived from sodium nitroprusside (Mariotto *et al.*, 1995) seems to be consistent with the present data. Furthermore, similar results were reported recently on an inhibitory action of NFP on iNOS in J774 cells (Cirino *et al.*, 1994). Recent work has pointed out a possible feedback inhibition of the induction of iNOS expression by endogenously produced NO (Park *et al.*, 1994); our data do not exclude this possibility.

Another aspect should be considered concerning the inhibition of neutrophil NOS by NFP. Recently Assreuy *et al.* (1993) demonstrated a direct inhibition of iNOS by NO; on the other hand, Cirino *et al.* (1994) reported that NFP did not inhibit J774 iNOS activity. This does not exclude a possible direct inhibition of neutrophil NOS activity by NFP during the course of experiments.

The present data indicate the possibility that exogenous NO derived from NFP, as endogenous NO (Park *et al.*, 1994), exerts an inhibitory action on iNOS expression, probably at the transcriptional level. The nature of exogenous NO remains to be elucidated.

According to the above description, plasma nitrite/nitrate levels in rats receiving both NFP and LPS should result from the balance between the following two distinct phenomena: (1) increase in plasma nitrite/nitrate concentration after oxidation of NO released from NFP and (2) decrease in nitrite/nitrate concentrations caused by inhibition of NOS induction due to NO released from NFP.

In conclusion, a novel non-steroidal anti-inflammatory drug, NFP, seems to act as an inhibitory agent on the induction of NOS expression in neutrophils, while its analogue, FP, does not.

References

ASSREUY, J., CUNHA, F.Q., LIEW, F.Y. & MONCADA, S. (1993). Feedback inhibition of nitric oxide synthase activity by nitric oxide. *Br. J. Pharmacol.*, **108,** 833–837.

BARTHOLOMEW, B. (1984). A rapid method for the assay of nitrate in urine using the nitrate reductase enzyme of E. coli. *Food Chem. Toxicol.*, **22,** 541–543.

BOUGHTON-SMITH, N.K., EVANS, S.N., LASZLO, F., WHITTLE, B.J.R. & MONCADA, S. (1993). The induction of nitric oxide synthase and intestinal vascular permeability by endotoxin in the rat. *Br. J. Pharmacol.*, **110,** 1189–1195.

BREDT, D.S. & SNYDER, S.H. (1990). Isolation of nitric oxide synthase, a calmodulin-requiring enzyme. *Proc. Natl. Acad. Sci. U.S.A.*, **87,** 682–685.

CARSON, J.L. & STROM, B.L. (1992). The gastrointestinal toxicity of the non-steroidal anti-inflammatory drugs. In *Side effects of Anti-inflammatory Drugs*, ed. Rainsford, K.D. & Velo, G.P. pp. 1–8. Lancaster and Boston: MTP Press.

CIRINO, G., TIGLEY, A.W., D'ACQUISTO, F., WALLACE, J.L. & BAYDOUN, A.R. (1994). Inhibition of inducible nitric oxide synthase expression in J774 cells by the novel nonsteroidal anti-inflammatory compound, flurbiprofen-nitroxybutylester. *Br. J. Pharmacol.* (proceedings) (in press).

GREEN, L.C., WAGNER, D.A., GLOGOWSKI, J., SKIPPER, P.L., WISHNOK, J.S. & TANNENBAUM, S.R. (1982). Analysis of nitrate, nitrite and ^{15}N nitrate in biological fluids. *Anal. Biochem.*, **126,** 131–138.

MARIOTTO, S., CUZZOLIN, L., ADAMI, A., DEL SOLDATO, P., SUZUKI, H. & BENONI, G. (1995). Sodium nitroprusside inhibits the expression of the inducible oxide synthase in rat neutrophil. *Br. J. Pharmacol.*, (in press).

PARK, S.K., LIN, H.L., & MURPHY, S. (1994). Nitric oxide limits transcriptional induction of nitric oxide synthase in CNS glial cells. *Biochem. Biophys. Res. Commun.*, **201,** 762–768.

WALLACE, J.L., REUTER, B., CICALA, C., MCKNIGHT, W., GRISHAM, M.B. & CIRINO, G. (1994). Novel NSAID derivatives with markedly reduced ulcerogenic properties in the rat. *Gastroenterol.*, **107,** 173–179.

(Received January 25, 1995
Accepted March 1, 1995)

British Journal of Pharmacology (1995) 115, 227-236

Acute pro-inflammatory actions of endothelin-1 in the guinea-pig lung: involvement of ET_A and ET_B receptors

[1]János G. Filep, *Alain Fournier & Éva Földes-Filep

Research Center, Maisonneuve-Rosemont Hospital, Department of Medicine, University of Montréal, Montréal, P.Q., Canada H1T 2M4 and *Institut National de la Recherche Scientifique-Santé, Pointe-Claire, P.Q., Canada H9R 1G6

1 Although recent observations suggest that endothelin-1 (ET-1) may play a role in the pathogenesis of asthma, to date little is known about the effects of ET-1 on parameters other than bronchoconstriction. The objectives of the present experiments were to study whether intravenously administered ET-1 could exert pro-inflammatory actions in the guinea-pig lung and to assess the involvement of endothelin ET_A and ET_B receptors in these events by using the ET_A receptor-selective antagonist, FR 139317, the novel ET_A/ET_B receptor antagonist, bosentan and the ET_B receptor-selective agonist, IRL 1620.

2 Bolus i.v. injection of ET-1 (0.1–1 nmol kg^{-1}) to anaesthetized guinea-pigs evoked dose-dependent increases in mean arterial blood pressure which lasted for 6–12 min. This was accompanied by a dose-dependent haemoconcentration (8–15% plasma volume losses) and increases (up to 546%) in albumin extravasation in the trachea, upper and lower bronchi, but not in the pulmonary parenchyma. Qualitatively similar changes were observed following i.v. injection of the ET_B receptor agonist, IRL 1620 (0.3 and 1 nmol kg^{-1}), although IRL 1620 appeared to be about 3 times less potent than ET-1. The ET_A receptor-selective antagonist, FR 139317 (2.5 mg kg^{-1}) inhibited the ET-1 (1 nmol kg^{-1})-induced pressor response, haemoconcentration and albumin extravasation by 75, 77 and 60–70%, respectively, whereas it did not attenuate IRL 1620 (1 nmol kg^{-1})-induced changes. The ET_A/ET_B receptor antagonist, bosentan (10 mg kg^{-1}) almost completely inhibited the pressor, haemoconcentration and permeability effects of both ET-1 and IRL 1620.

3 ET-1, but not IRL 1620 (0.1–1 nmol kg^{-1}), produced a dose-dependent neutropenia with relative lymphocytosis and monocytosis, but did not induce influx of neutrophil granulocytes into pulmonary tissues or the bronchoalveolar space. ET-1 (1 nmol kg^{-1})-induced neutropenia was prevented by pretreatment of the animals with FR 139317 (2.5 mg kg^{-1}), bosentan (10 mg kg^{-1}) or adrenaline (90 nmol kg^{-1}), indicating that ET-1 caused intravascular sequestration of neutrophil granulocytes.

4 ET-1 or IRL 1620 (10^{-10}–10^{-6} M) alone did not activate alveolar macrophages *in vitro*, whereas at a concentration of 10^{-8} M, ET-1, but not IRL 1620, markedly potentiated superoxide production in response to f-Met-Leu-Phe (10^{-9}–10^{-7} M) and platelet-activating factor (PAF, 10^{-9}–10^{-7} M), but not to phorbol 12-myristate 13-acetate (10^{-9} M). ET-1 did not affect f-Met-Leu-Phe- or PAF-induced increases in intracellular free calcium concentration. This potentiating effect of ET-1 was abolished by FR 139317 (1.5×10^{-7} M).

5 We conclude that, in addition to evoking airway contractions, ET-1 exerts pro-inflammatory actions via activation of the ET_A and to a lesser extent the ET_B receptors, and therefore, might contribute to the airway inflammation present in asthma. These findings also suggest the therapeutic potential of ET_A/ET_B receptor and perhaps ET_A receptor-selective antagonists in this disease.

Keywords: Endothelin-1; ET_A and ET_B receptors; FR 139317; bosentan; IRL 1620; vascular permeability; neutropenia; neutrophil sequestration; superoxide; alveolar macrophages; inflammation; asthma

Introduction

Recent observations suggest that an increased intrapulmonary production of endothelin-1 (ET-1) may specifically occur in asthma. The bronchial epithelium of asthmatic patients has been found to express preproendothelin-1 mRNA (Vittori *et al.*, 1992), to contain endothelin immunoreactivity (Springall *et al.*, 1991) and to release high amounts of ET-1 (Mattoli *et al.*, 1990; Vittori *et al.*, 1992). Furthermore, elevated concentrations of ET-1 in the bronchoalveolar lavage fluid from patients with symptomatic asthma have also been detected (Nomura *et al.*, 1989; Mattoli *et al.*, 1991). The high potency of ET-1 in inducing contraction of airway smooth muscle both *in vivo* and *in vitro* (for recent reviews see Filep, 1993; Hay *et al.*, 1993a) led to the assumption that it plays a pathophysiological role in asthma. To date, the existence of at least two distinct subtypes of endothelin receptors has been demonstrated in mammalian cells (Arai *et al.*, 1990; Sakurai *et al.*, 1990): one is highly selective for ET-1 (ET_A), and the other is equally sensitive to isopeptides of the endothelin family (ET_B). ET-1 appears to elicit airway contractions via ET_A receptors in the sheep (Abraham *et al.*, 1993), whereas both ET_A and ET_B receptors mediate ET-1-induced contractions in guinea-pig airways (Cardell *et al.*, 1993; Hay *et al.*, 1993b) and rat trachea (Henry, 1993).

Although airway smooth muscle contraction is the most obvious symptom and an important component of asthma, several clinical observations have provided evidence that inflammation is the basis of the disease (cf. Holgate *et al.*, 1992). These pathologies involve increased microvascular permeability and oedema formation (McFadden, 1992) and influx and activation of inflammatory cells (Holgate *et al.*, 1992; Lee & Lane, 1992) even at a clinically early stage of the disease (Laitinen *et al.*, 1993). To date, however, little information is available on the pro-inflammatory actions of ET-1. Previous studies have reported that ET-1 activates a subpopulation of human alveolar macrophages (Haller *et al.*, 1991), stimulates oxygen radical formation in the distal rat lung (Nagase *et al.*, 1990) and can enhance albumin extravasation in certain vascular beds in the rat (Filep *et al.*, 1991;

[1] Author for correspondence.

1992). The present experiments were designed to study whether or not ET-1 could affect (1) pulmonary microvascular albumin extravasation, (2) influx of inflammatory cells into pulmonary tissues and airspace and (3) activation of alveolar macrophages in the guinea-pig. In addition, the involvement of ET_A and ET_B receptors was assessed in these events by use of a highly selective, competitive ET_A receptor antagonist, FR 139317 (Aramori *et al.*, 1993; Sogabe *et al.*, 1993), a non-peptide ET_A/ET_B receptor antagonist, bosentan (Clozel *et al.*, 1994) and the ET_B receptor-selective agonist, IRL 1620 (Takai *et al.*, 1992).

Methods

In vivo *experiments*

Male Dunkin-Hartley guinea-pigs weighing 360–420 g (Charles River Canada Inc., St. Constant, Qué., Canada) were anaesthetized with pentobarbitone sodium (37.5 mg kg^{-1}, i.p.), the trachea was cannulated and catheters were inserted into the left jugular vein and carotid artery. Mean arterial blood pressure (MABP) was monitored continuously by an electromanometer (Digi-Med, Louisville, KY, U.S.A.) using a COBE CDX III pressure transducer. After control measurements, ET-1 (0.1, 0.3 or 1 nmol kg^{-1}) or IRL 1620 (0.3 or 1 nmol kg^{-1}) was injected i.v. in a volume of 50 $\mu l\ kg^{-1}$ body weight. Ten min before and after ET-1 or IRL 1620 administration, blood (approximately 400 μl) was obtained through the arterial catheter to determine the haematocrit and total and differential blood cell counts. A group of animals were either pretreated with FR 139317 (2.5 mg kg^{-1}) or bosentan (10 mg kg^{-1}) for 10 min before injection of ET-1 (1 nmol kg^{-1}) or IRL 1620 (1 nmol kg^{-1}). Another group of animals received adrenaline (90 nmol kg^{-1}, i.v.) together with ET-1 (1 nmol kg^{-1}). The animals were killed 10 or 20 min after injection of ET-1, and either bronchoalveolar lavage was performed for analysis of bronchoalveolar resident cells or the lungs were immediately removed for the determination of tissue myeloperoxidase activity. In separate experiments, the effects of ET-1 and IRL 1620 on pulmonary albumin extravasation were studied by using Evans blue dye as a marker of vascular permeability (see below). In an additional group of guinea-pigs, the pulmonary permeability effects of platelet-activating factor (PAF, 0.9 nmol kg^{-1}) were compared in the absence and presence of FR 139317 (2.5 mg kg^{-1}) or bosentan (10 mg kg^{-1}). All procedures were in accordance with the Guidelines of the Canadian Council of Animal Care and were approved by the local Animal Care Committee.

Measurement of albumin extravasation

Albumin extravasation was estimated by measuring tissue accumulation of Evans blue dye, which binds to plasma albumin (Rawson, 1943) as described previously (Filep *et al.*, 1991). In brief, Evans blue dye (20 mg kg^{-1}, 25 mg ml^{-1} in 0.9% NaCl) was injected i.v. together with ET-1, IRL 1620 or their vehicle (0.9% NaCl). Ten min later, the thorax was cut open and the lungs were perfused with 40 ml 0.9% NaCl through a catheter inserted into the pulmonary vein. Then the trachea, upper bronchi (airways extending from the bifurcation of the trachea to its entry to parenchyma), lower bronchi (defined as major airways surrounded by parenchyma that can be easily dissected without magnification) and peripheral parenchyma strips were prepared. Tissue Evans blue dye content was measured spectrophotometrically at 650 nm following extraction with formamide (4 ml per g wet tissue weight at 24°C for 24 h) and was expressed as μg dye per g dry tissue weight to avoid underestimation of changes due to oedema formation. Previous studies have shown highly significant correlation between the tissue content of Evans blue dye and radiolabelled human serum albumin in guinea-pig airways (Rogers *et al.*, 1989).

Myeloperoxidase assay

Myeloperoxidase activity, a marker of neutrophil granulocyte infiltration (Krawisz *et al.*, 1984; Mullane *et al.*, 1985), was measured in lung tissues according to the method of Krawisz *et al.* (1984). In brief, tissue samples were homogenized and sonicated in phosphate buffer (50 mM, pH 6.0) containing 0.5% hexadecyltrimethyl ammonium bromide, frozen at −70°C and thawed three times, then centrifuged at 40,000 *g* for 15 min. Myeloperoxidase activity in supernatants was measured by changes in optical density (at 460 nm) resulting from decomposition of H_2O_2 in the presence of O-dianisidine. Myeloperoxidase from human leukocytes (EC 1.11.1.7) was used as a standard.

Absolute and differential cell counts

Total red blood cell, white blood cell and platelet counts were obtained from the arterial blood. Absolute cell counts were performed with a Coulter JT3 Automated Haematology Analyzer (Hialech, FL, U.S.A.). White blood cell differential counts were performed on samples stained with Wright's stain. One hundred cells were counted at × 1000 magnification with a microscope and classified as segmented neutrophils, lymphocytes, monocytes, eosinophils and basophils.

Bronchoalveolar lavage

Three times 15 ml of phosphate-buffered saline (in mM: NaCl 140, KCl 2.7, Na_2HPO_4 0.8 and KH_2PO_4 1.5) at 37°C, pH 7.4 were gently instilled into the lungs, withdrawn, collected and centrifuged with 400 *g* at 4°C for 10 min. The pellet was resuspended in 2 ml phosphate-buffered saline and examined for cell content.

In vitro *experiments*

Alveolar macrophages were prepared from untreated guinea-pigs as described previously (Földes-Filep *et al.*, 1992). In brief, the cells obtained by bronchoalveolar lavage were layered onto 50% continuous Percoll (Pharmacia, Uppsala, Sweden). After centrifugation at 400 *g* for 30 min, alveolar macrophages were collected from the top of the Percoll gradient, washed and resuspended in ice-cold Hanks' balanced salt solution (HBSS) without Ca^{2+} and Mg^{2+}. Cell viability was higher than 95% as determined by trypan blue exclusion and macrophage purity was always greater than 98% (estimated following Wright staining). The contaminating cells were lymphocytes and neutrophil granulocytes.

Measurement of superoxide production

Superoxide production was measured as superoxide dismutase-inhibitable reduction of ferricytochrome c (Földes-Filep *et al.*, 1992). Alveolar macrophages (10^6 cells ml^{-1}) were incubated with FR 139317 (1.5×10^{-7} M) or its vehicle for 10 min at 37°C in HBSS supplemented with 1.1 mM $CaCl_2$ and 0.6 mM $MgSO_4$, then ET-1 (10^{-10}–10^{-6} M) was added for 5 min. The cells were challenged with f-Met-Leu-Phe (10^{-9}–10^{-7} M), platelet-activating factor (PAF, 10^{-9}–10^{-7} M) or phorbol 12-myristate 13-acetate (PMA, 10^{-9} M) for 30 min in the presence of ferricytochrome c (240 $\mu g\ ml^{-1}$), with or without superoxide dismutase (100 $\mu g\ ml^{-1}$). FR 139317 was in contact with the cells for the entire experiment. The amount of superoxide generated was calculated using the extinction coefficient of $21.1 \times 10^3\ M^{-1}\ cm^{-1}$ at 550 nm for the reduced cytochrome c. At the concentration of 100 $\mu g\ ml^{-1}$, superoxide dismutase attenuated superoxide generation by more than 98% in this system.

Measurement of intracellular free calcium concentration

Intracellular free calcium was measured by loading alveolar macrophages with the fluorescent dye fure 2/AM, 1 μM for 20 min at 37°C. After washing, the cells were incubated for 15 min at 37°C to allow complete hydrolysis of the entrapped ester. Loaded cells (3×10^6 ml^{-1}) were resuspended in HBSS-HEPES buffer (in mM: NaCl 137, KCl 5.36, Na_2HPO_4 0.33, KH_2PO_4 0.44, $CaCl_2$ 1.6, $MgSO_4$ 1.2, HEPES 10 and glucose 5.5) and were incubated with various concentrations of ET-1 (10^{-9}–10^{-6} M) and challenged with f-Met-Leu-Phe (10^{-7} M) or PAF (10^{-7} M). Fluorescence was measured with an LKB fluorescence spectrophotometer (Turku, Finland) with an excitation wavelength of 340 nm and an emission wavelength of 500 nm. Intracellular free calcium concentrations were calculated according to the method of Tsien *et al.* (1982).

Drugs and chemicals

ET-1 and IRL 1620 (Suc-[Glu^9, Ala^{11,15}]endothelin-1(18-21) were synthesized in our laboratories using solid phase methodology. The purity of the preparations was greater than 97% as measured by high performance liquid chromatography. FR 139317 ((**R**)2-[(**R**)-2-[(5)-2-[[1-(hexahydro-1*H*-azepinyl)]carbonyl]amino-4-methylpentanoyl]amino-3-[3-(1-methyl-1*H*-indoyl)]propionyl] amino-3-(2-pyridyl) propionic acid, Fujisawa Pharmaceutical Co., Osaka, Japan) was dissolved in 0.9% NaCl. Bosentan (Ro 47-0203, 4-*tert*-butyl-*N*-[6-(2-hydroxy-ethoxy)-5-(2-methoxy-phenoxy)-2,2′ bipyrimidin- 4-yl]-benzene-sulphonamide sodium salt, Hoffmann-LaRoche, Basel, Switzerland) was dissolved in distilled water containing 300 mM glucose. PAF (1-O-hexadecyl-2-O-acetyl-sn-glycero-3-phosphorylcholine) was purchased from Calbiochem, La Jolla, CA, U.S.A. All other chemicals were purchased from Sigma Chemical Co., St. Louis, MO, U.S.A.

Data analysis

Results are expressed as means ± s.e.mean. Changes in plasma volume were calculated according to the formula Δplasma volume (%) = $(100/100\text{-}Hct_i) \times ((Hct_i\text{-}Hct_f)/Hct_f) \times 100$, where Hct_i and Hct_f are the haematocrit values obtained 10 min before (initial or control) and 10 min after (final Hct) injection of ET-1, respectively.

Statistical analysis of the data was performed by one way analysis of variance using ranks (Kruskal-Wallis test) followed by Dunn's multiple contrast hypothesis test (Dunn, 1964) to compare various treatments to the same control, and by Wilcoxon's signed rank test and Mann-Whitney's U test for paired and unpaired observations, respectively. A $P<0.05$ level was considered significant for all tests.

Results

Effects of FR 139317 and bosentan on vascular responses to ET-1

As expected, bolus i.v. injection of ET-1 (0.1–1 nmol kg^{-1}) evoked dose-dependent increases in MABP (Table 1). MABP reached a maximum within 50–110 s, then returned to baseline values in the next 6–12 min. The pressor response was not preceded by transient hypotension. The pressor action of ET-1 was accompanied by dose-dependent increases in haematocrit (Table 1). Following injection of ET-1, 0.1, 0.3 and 1 nmol kg^{-1}, the haematocrit increased by 5, 8 and 10%, respectively, corresponding to 8, 12 and 15% plasma volume losses, respectively. Neither FR 139317 (2.5 mg kg^{-1}) nor bosentan (10 mg kg^{-1}) by itself produced significant changes in MABP and haematocrit. FR 139317 (2.5 mg kg^{-1}) attenuated both the vasopressor and haemoconcentration actions of ET-1 (1 nmol kg^{-1}) by about 75% (Table 1). Increasing the dose of FR 139317 to 10 mg kg^{-1} did not cause further inhibition of the pressor effect of ET-1. Both the peak pressor and haemoconcentration effects of ET-1 (1 nmol kg^{-1}) were inhibited on average by 93 and 95%, respectively, following bosentan (10 mg kg^{-1}) (Table 1). The maximum inhibition of the pressor and haemoconcentration effects of ET-1 that can be achieved with bosentan was significantly greater ($P<0.05$) than that observed following FR 139317 treatment.

Injection of ET-1 (0.3 or 1 nmol kg^{-1}) increased up to 373, 546 and 264% tissue Evans blue dye content in the trachea, upper and lower bronchi, respectively, but not pulmonary parenchyma, in a dose-dependent manner (Figure 1). FR 139317 (2.5 mg kg^{-1}) reduced the extravasation of Evans blue dye elicited by ET-1 (1 nmol kg^{-1}) by 70, 61 and 69% in the trachea, upper and lower bronchi, respectively (Figure 1). Furthermore, ET-1 (1 nmol kg^{-1})-induced albumin extravasation in these tissues was reduced on average by 95, 93 and 85%, respectively, in the presence of bosentan (10 mg kg^{-1}) (Figure 1). Neither FR 139317 nor bosentan by itself affected

Table 1 Effects of FR 139317 and bosentan on endothelin-1 (ET-1) and IRL 1620-induced changes in mean arterial blood pressure (MABP), haematocrit and plasma volume in anaesthetized guinea-pigs

				Haematocrit (vol. %)				
	n	*Basal MABP* (mmHg)	*Maximum increase in MABP* (mmHg)	*10 min before injection*	*10 min after of ET-1*	P[a]	*Δplasma volume* (%)	P[b]
Vehicle	7	74 ± 2	–	38.8 ± 0.9	39.0 ± 0.4	–	−0.7 ± 2.1	–
ET-1, 0.1 nmol kg^{-1}	6	71 ± 5	3 ± 0.5	38.2 ± 0.7	40.3 ± 0.5	0.05	−8.3 ± 1.5	0.05
ET-1, 0.3 nmol kg^{-1}	3	70 ± 3	13 ± 2*	38.4 ± 0.9	41.5 ± 1.0	0.05	−12.0 ± 1.6	0.05
ET-1, 1 nmol kg^{-1}	7	72 ± 2	29 ± 5**	38.5 ± 0.9	42.4 ± 0.6	0.05	−14.9 ± 1.7	0.01
FR 139317	4	69 ± 2	1 ± 1	38.8 ± 0.9	39.6 ± 0.5	NS	−2.6 ± 2.2	NS
FR 139317 plus ET-1, 1 nmol kg^{-1}	5	69 ± 1	7 ± 1**	39.3 ± 0.9	40.1 ± 1.0	0.05	−3.5 ± 0.5**	0.05
Bosentan	3	73 ± 2	1 ± 1	38.4 ± 0.6	38.6 ± 0.6	NS	−0.7 ± 0.9	NS
Bosentan plus ET-1, 1 nmol kg^{-1}	3	73 ± 3	2 ± 3**	38.5 ± 0.6	38.8 ± 0.4	NS	−1.4 ± 0.9**	NS
IRL 1620, 0.3 nmol kg^{-1}	4	72 ± 7	6 ± 2	38.4 ± 0.7	39.0 ± 0.4	NS	−2.1 ± 0.9	NS
IRL 1620, 1 nmol kg^{-1}	4	74 ± 8	10 ± 2	38.7 ± 0.4	40.9 ± 0.4	0.05	−8.7 ± 1.5	0.05
FR 139317 plus IRL 1620, 1 nmol kg^{-1}	3	70 ± 8	9 ± 3	37.6 ± 0.4	39.9 ± 0.4	0.05	−9.0 ± 2.4	0.05
Bosentan plus IRL 1620, 1 nmol kg^{-1}	3	69 ± 3	1 ± 1	38.0 ± 1.2	38.4 ± 0.8	NS	−1.5 ± 1.6	NS

Values are means ± s.e.mean. FR 139317 (2.5 mg kg^{-1}) or bosentan (10 mg kg^{-1}) was injected i.v. 10 min before administration of ET-1 or IRL 1620.

**$P<0.01$, compared to ET-1 (1 nmol kg^{-1}) by Mann-Whitney's U test.

[a]Compared to haematocrit values before injection of ET-1 by Wilcoxon's signed rank test; [b]compared to vehicle by Dunn's multiple contrast hypothesis test.

NS, not significant.

significantly accumulation of Evans blue dye in the vascular beds studied (Figure 1).

The magnitude of ET-1 (1 nmol kg^{-1})-induced albumin extravasation in the trachea, upper and lower bronchi was similar to that evoked by PAF (0.9 nmol kg^{-1}) (Figure 2). There were no significant differences in the permeability effects of PAF in the absence and presence of FR 139317 (2.5 mg kg^{-1}) or bosentan (10 mg kg^{-1}) (Figure 2).

Effects of FR 139317 and bosentan on vascular responses to IRL 1620

Bolus i.v. injection of the ET_B receptor-selective agonist, IRL 1620 (0.3 or 1 nmol kg^{-1}) produced dose-dependent pressor responses (Table 1) that were not preceded by a transient depressor action. The duration of the pressor effect of IRL 1620 was shorter (4–8 min) than that of equimolar doses of ET-1. On a molar basis, IRL 1620 was about 3 times less potent than ET-1. Following injection of IRL 1620, 0.3 and 1 nmol kg^{-1} the haematocrit increased by 2 and 6%, respectively, corresponding to 2 and 9% decreases in plasma volume, respectively (Table 1). FR 139317 (2.5 mg kg^{-1}) did not affect IRL 1620 (1 nmol kg^{-1})-induced changes in MABP and plasma volume, whereas bosentan (10 mg kg^{-1}) inhibited both the pressor and haemoconcentration effects of IRL 1620 by 93 and 95%, respectively (Table 1).

Like ET-1, injection of IRL 1620 (0.3 or 1 nmol kg^{-1}) also evoked dose-dependent increases (up to 392%) in albumin extravasation in the trachea, upper and lower bronchi, but not pulmonary parenchyma (Figure 3). IRL 1620 (1 nmol kg^{-1})-induced changes in tissue Evans blue dye content were not affected significantly by FR 139317 (2.5 mg kg^{-1}) pretreatment, whereas they were almost completely prevented by bosentan (10 mg kg^{-1}) (Figure 3).

ET-1-induced neutropenia

In arterial blood, ET-1 (0.1–1 nmol kg^{-1}) caused a significant dose-dependent neutropenia without significant changes in red blood cell and platelet counts within 10 min (Table 2). White blood cell count decreased from $5.5 \pm 0.4 \times 10^3$ cells μl^{-1} to $2.5 \pm 0.4 \times 10^3$ cells μl^{-1} and $2.9 \pm 0.4 \times 10^3$ cells μl^{-1} 10 and 20 min after injection of ET-1 (1 nmol kg^{-1}), respectively. The leukopenia was characterized by a sharp decrease in the percentage of neutrophil granulocytes with a concomitant increase in the percentage of lymphocytes and monocytes (Table 2). Guinea-pigs receiving an injection of either vehicle or IRL 1620 (0.3 or 1 nmol kg^{-1}) did not experience a decrease in circulating leukocytes (Table 2).

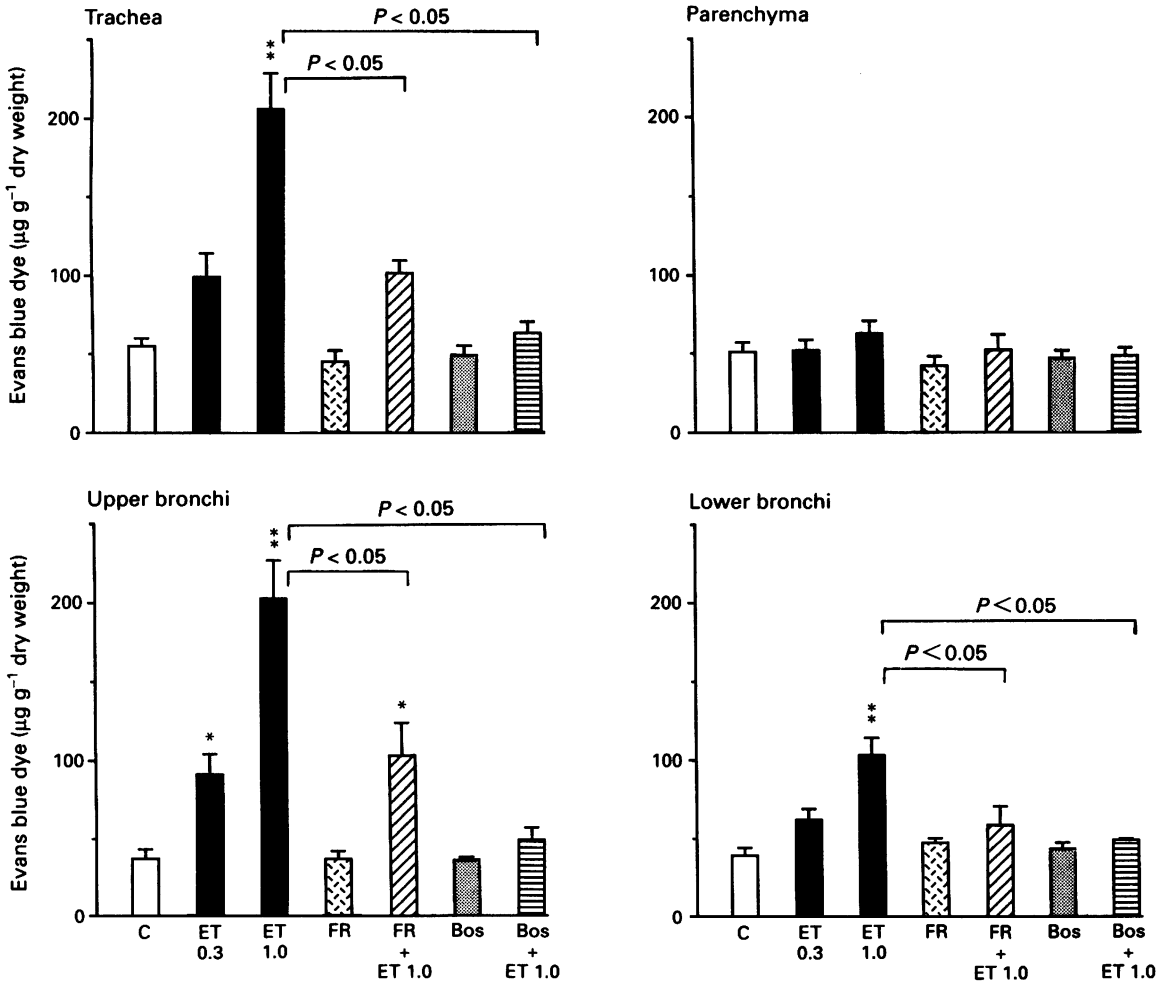

Figure 1 Effects of the ET_A receptor-selective antagonist, FR 139317 and the ET_A/ET_B receptor antagonist, bosentan on endothelin-1 (ET-1)-induced albumin extravasation in guinea-pig airways. The animals were pretreated with FR 139317 (FR, 2.5 mg kg^{-1}), bosentan (Bos, 10 mg kg^{-1}) or 0.9% NaCl (control, C) for 10 min before i.v. bolus injection of ET-1 (ET, 0.3 or 1 nmol kg^{-1}) plus Evans blue dye (20 mg kg^{-1}). The guinea-pigs were killed 10 min after injection of ET-1 and the lungs were perfused with 0.9% NaCl via the pulmonary artery. The permeability measurements were made 15 min after injection of ET-1. Values are means with s.e.mean. $n = 7$ for control, $n = 6$ for ET-1 (1 nmol kg^{-1}), $n = 5$ for ET-1 (0.3 nmol kg^{-1}) and FR 139317 plus ET-1 (1 nmol kg^{-1}) and $n = 4$ for FR 139317, bosentan and bosentan plus ET-1 (1 nmol kg^{-1}). $^*P<0.05$; $^{**}P<0.01$ (compared to control by Dunn's multiple contrast hypothesis test).

Effects of FR 139317, bosentan and adrenaline on ET-1-induced neutropenia

The mechanisms of ET-1-induced neutropenia were investigated by administering FR 139317 (2.5 mg kg^{-1}), bosentan (10 mg kg^{-1}) or adrenaline (90 nmol kg^{-1}) before injection of ET-1 (1 nmol kg^{-1}). Pretreatment of the animals with either FR 139317 or bosentan almost completely prevented ET-1-induced neutropenia (Table 2). White blood cell counts were $5.4 \pm 0.3 \times 10^3$, $5.0 \pm 0.4 \times 10^3$ and $5.8 \pm 0.3 \times 10^3$ cells μl^{-1} 20 min before and 10 and 20 min after injection of ET-1 in animals pretreated with FR 139317, respectively ($n = 5$, $P > 0.3$, Kruskal-Wallis test). No significant changes could be detected in white blood cell counts in response to ET-1 in animals pretreated with bosentan (white blood cell counts were $5.6 \pm 0.8 \times 10^3$, $5.7 \pm 0.6 \times 10^3$ and $5.3 \pm 0.7 \times 10^3$ cells μl^{-1} 20 min before and 10 and 20 min after injection of ET-1, respectively, $n = 3$, $P > 0.6$, Kruskal-Wallis test). Similarly, adrenaline administered at the same time as ET-1 abrogated ET-1-induced neutropenia at 10 min (Table 2) and actually resulted in a slight neutrophilia at 20 min (white blood cell counts were $5.2 \pm 0.3 \times 10^3$ and $6.0 \pm 0.2 \times 10^3$ cells μl^{-1} 10 min before and 20 min after injection of ET-1, respectively, $n = 5$, $P < 0.05$). FR 139317 or bosentan alone did not cause significant changes in blood cell counts 20 min after its administration.

Effect of ET-1 on pulmonary neutrophil infiltration

In order to investigate whether ET-1 could induce influx of neutrophils from the circulation into the bronchoalveolar space and pulmonary tissues, bronchoalveolar lavage was performed and tissue myeloperoxidase activity was measured in separate animals receiving ET-1 (1 nmol kg^{-1}) or its vehicle. Bronchoalveolar lavage yielded $10 \pm 2 \times 10^6$ cells ($n = 7$) in control animals, and $9 \pm 2 \times 10^6$ cells ($n = 6$, $P > 0.9$) and $9 \pm 4 \times 10^6$ cells ($n = 5$, $P > 0.8$) 10 and 20 min after injection of ET-1 (1 nmol kg^{-1}), respectively. Of these cells 95–97%, 1–3%, 1–2% and 1–2% were alveolar macrophages, neutrophil granulocytes, lymphocytes and eosinophils, respectively, and no significant differences could be detected among the groups. Myeloperoxidase activity in the pulmonary parenchyma was 108 ± 28, 130 ± 17 and 128 ± 25 u g^{-1} dry tissue weight in control animals and 10 and 20 min after i.v. injection of ET-1 (1 nmol kg^{-1}), respectively ($n = 4$, $P > 0.8$, Kruskal-Wallis test).

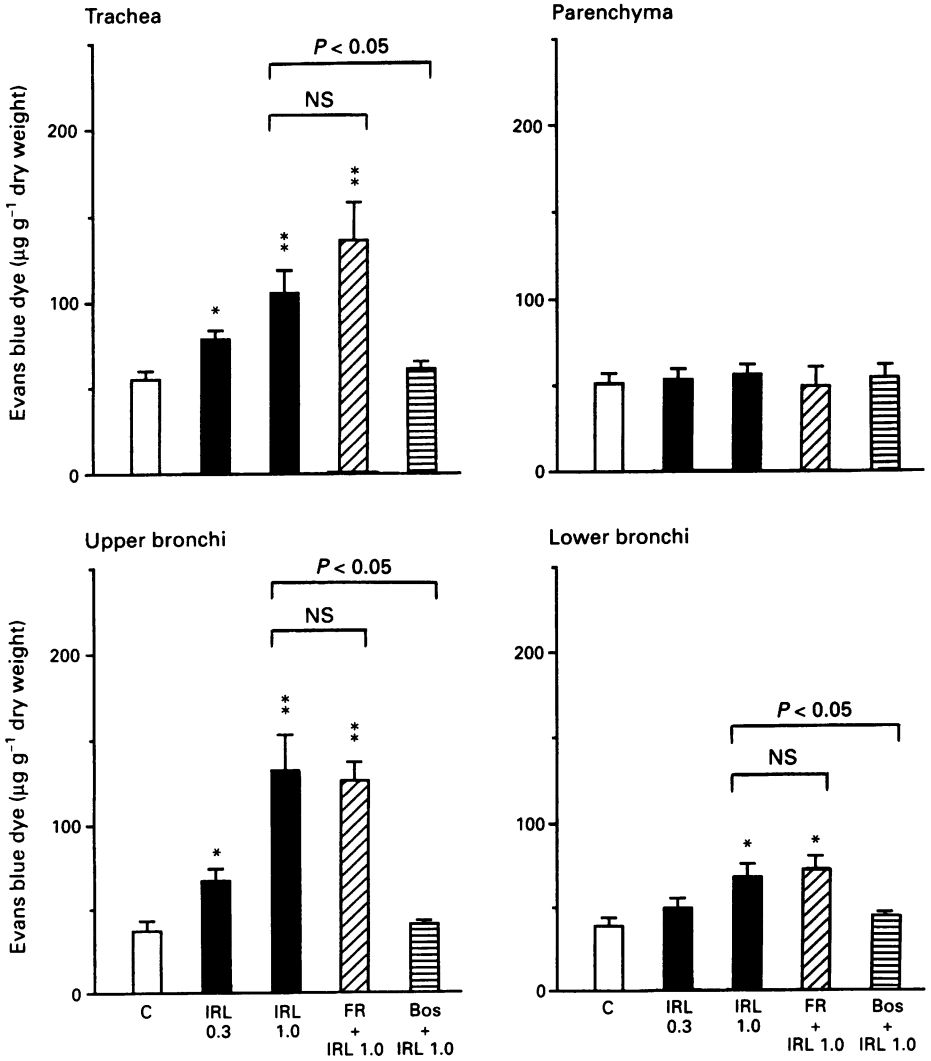

Figure 2 Effects of the FR 139317 and bosentan on IRL 1620-induced albumin extravasation in guinea-pig airways. The animals were pretreated with FR 139317 (FR, 2.5 mg kg^{-1}), bosentan (Bos, 10 mg kg^{-1}) or 0.9% NaCl (control, C) for 10 min before i.v. bolus injection of IRL 1620 (IRL, 0.3 or 1 nmol kg^{-1}) plus Evans blue dye (20 mg kg^{-1}). The guinea-pigs were killed 10 min after injection of IRL 1620 and the lungs were perfused with 0.9% NaCl via the pulmonary artery. The permeability measurements were made 15 min after injection of IRL 1620. Values are means with s.e.mean shown by vertical lines. $n = 7$ for control, $n = 6$ for IRL 1620 (1 nmol kg^{-1}), $n = 4$ for the other groups. $^*P < 0.05$; $^{**}P < 0.01$ (compared to control by Dunn's multiple contrast hypothesis test).

Effects of ET-1 on superoxide production by alveolar macrophages

ET-1 or IRL 1620 (10^{-10}–10^{-6} M) alone neither induced superoxide production by alveolar macrophages nor affected lactate dehydrogenase release (lactate dehydrogenase release was similar in macrophages incubated with saline, IRL 1620, 10^{-6} M or ET-1, 10^{-6} M, and never exceeded 2% of the total cellular lactate dehydrogenase content). For instance, unstimulated macrophages reduced 11 ± 1 nmol ferricytochrome c per 5×10^5 cells 30 min^{-1} ($n = 8$) versus 13 ± 2 nmol ferricytochrome c reduction per 5×10^5 cells 30 min^{-1} in the presence of 10^{-6} M ET-1 ($n = 6$, $P > 0.1$). However, ET-1 (10^{-8} M), but not IRL 1620, significantly enhanced superoxide production evoked by f-Met-Leu-Phe or PAF when alveolar macrophages were preincubated with ET-1 for

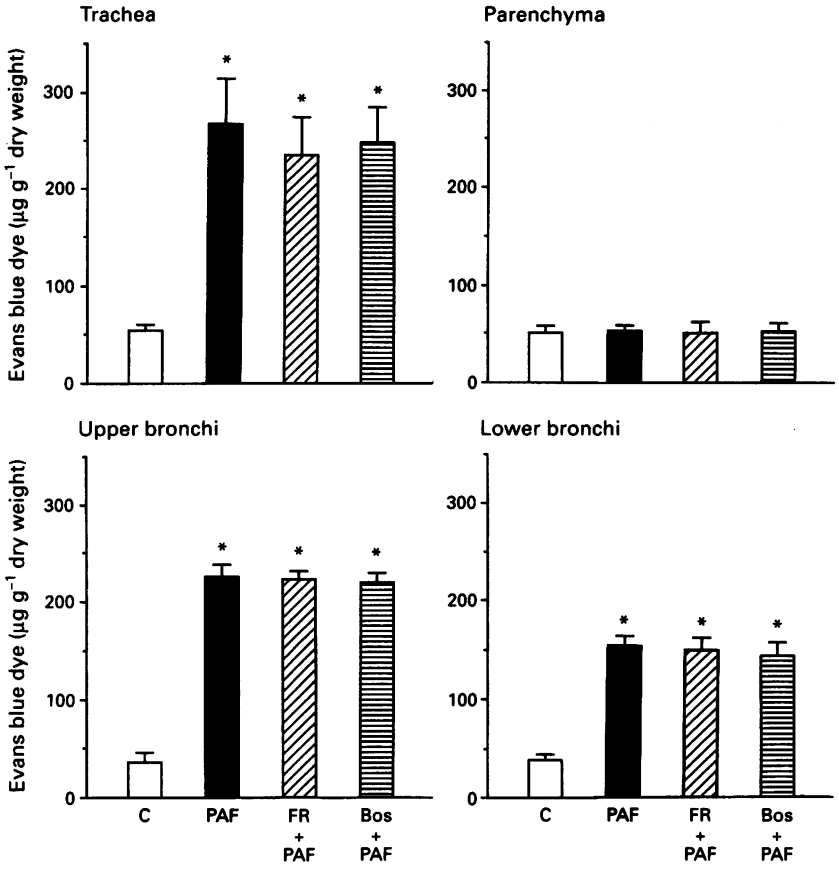

Figure 3 Lack of effect of the FR 139317 and bosentan on PAF-induced albumin extravasation in guinea-pig airways. The animals were pretreated with FR 139317 (FR, 2.5 mg kg^{-1}), bosentan (Bos, 10 mg kg^{-1}) or 0.9% NaCl (control, C) for 10 min before i.v. bolus injection of PAF (0.9 nmol kg^{-1}) plus Evans blue dye (20 mg kg^{-1}). The guinea-pigs were killed 10 min after injection of PAF and the lungs were perfused with 0.9% NaCl via the pulmonary artery. The permeability measurements were made 15 min after injection of PAF. Values are means with s.e.mean shown by vertical lines. $n = 6$ for control, $n = 4$ for all other treatments. $^*P < 0.05$ (compared to control by Dunn's multiple contrast hypothesis test).

Table 2 Endothelin-1 (ET-1)-induced changes in red blood cell count (RBC), platelet count, white blood cell count (WBC) and white blood cell differential counts in guinea-pig arterial blood, and prevention by FR 139317, bosentan and adrenaline

	n	*RBC* ($\times 10^6 \mu l^{-1}$)	*Platelets* ($\times 10^3 \mu l^{-1}$)	*WBC* ($\times 10^3 \mu l^{-1}$)	*Lymphocytes* (%)	*Neutrophils* (%)	*Monocytes* (%)	*Eosinophils* (%)	*Basophils* (%)
Vehicle	7	4.9 ± 0.2	345 ± 18	5.8 ± 0.4	60.3 ± 3.5	32.1 ± 4.0	6.9 ± 0.3	0.6 ± 0.3	0.4 ± 0.3
ET-1, 0.1 nmol kg^{-1}	4	4.9 ± 0.1	353 ± 33	4.8 ± 0.3	65.0 ± 1.6	22.8 ± 1.4	9.8 ± 0.8	1.5 ± 0.3	1.0 ± 0.4
ET-1, 0.3 nmol kg^{-1}	4	5.1 ± 0.2	378 ± 11	3.4 ± 0.3*	71.3 ± 1.4*	16.0 ± 1.3*	11.8 ± 0.9*	0.8 ± 0.5	0.5 ± 0.3
ET-1, 1 nmol kg^{-1}	7	5.2 ± 0.2	382 ± 37	2.5 ± 0.4**	75.4 ± 2.2*	13.1 ± 1.8*	10.7 ± 0.7*	0.4 ± 0.2	0.4 ± 0.2
IRL 1620, 0.3 nmol kg^{-1}	4	4.8 ± 0.1	329 ± 30	5.5 ± 0.5	63.0 ± 2.2	28.6 ± 1.8	7.9 ± 0.9	0.8 ± 0.1	0.4 ± 0.3
IRL 1620, 1 nmol kg^{-1}	4	4.9 ± 0.1	378 ± 14	5.2 ± 0.4	58.5 ± 2.9	32.8 ± 3.0	8.6 ± 1.1	0.3 ± 0.1	0.2 ± 0.2
FR 139317	4	5.0 ± 0.1	310 ± 40	5.2 ± 0.2	61.5 ± 2.1	30.5 ± 1.8	6.5 ± 0.6	1.0 ± 0.4	0.5 ± 0.3
FR 139317 plus ET-1, 1 nmol kg^{-1}	5	5.2 ± 0.2	376 ± 26	5.0 ± 0.4**	59.6 ± 3.0**	31.4 ± 2.3**	8.4 ± 1.0	0.4 ± 0.2	0.2 ± 0.2
Bosentan	3	4.8 ± 0.2	315 ± 52	5.5 ± 0.2	59.6 ± 1.1	32.5 ± 1.5	7.1 ± 0.7	0.6 ± 0.3	0.2 ± 0.1
Bosentan plus ET-1, 1 nmol kg^{-1}	3	4.8 ± 0.3	317 ± 19	5.7 ± 0.6**	62.3 ± 2.1**	29.8 ± 1.8**	7.1 ± 0.5	0.6 ± 0.3	0.2 ± 0.1
Adrenaline	5	4.9 ± 0.2	301 ± 31	5.6 ± 0.4	60.6 ± 3.6	32.4 ± 3.4	6.2 ± 0.4	0.8 ± 0.4	0.2 ± 0.2
Adrenaline plus ET-1, 1 nmol kg^{-1}	5	5.0 ± 0.1	313 ± 15	5.7 ± 0.2**	57.8 ± 3.8**	34.8 ± 3.4**	6.0 ± 0.3#	1.0 ± 0.3	0.4 ± 0.2

Values are means ± s.e.mean. The animals were pretreated with FR 139317 (2.5 mg kg^{-1} i.v.) or bosentan (10 mg kg^{-1} i.v.) for 10 min before administration of ET-1. Adrenaline (90 nmol kg^{-1}) was injected together with ET-1.
$^*P < 0.05$; $^{**}P < 0.01$ (compared to vehicle), $^\#P < 0.05$; $^{\#\#}P < 0.01$ (compared to 1 nmol kg^{-1} ET-1 by Dunn's multiple contrast hypothesis test).

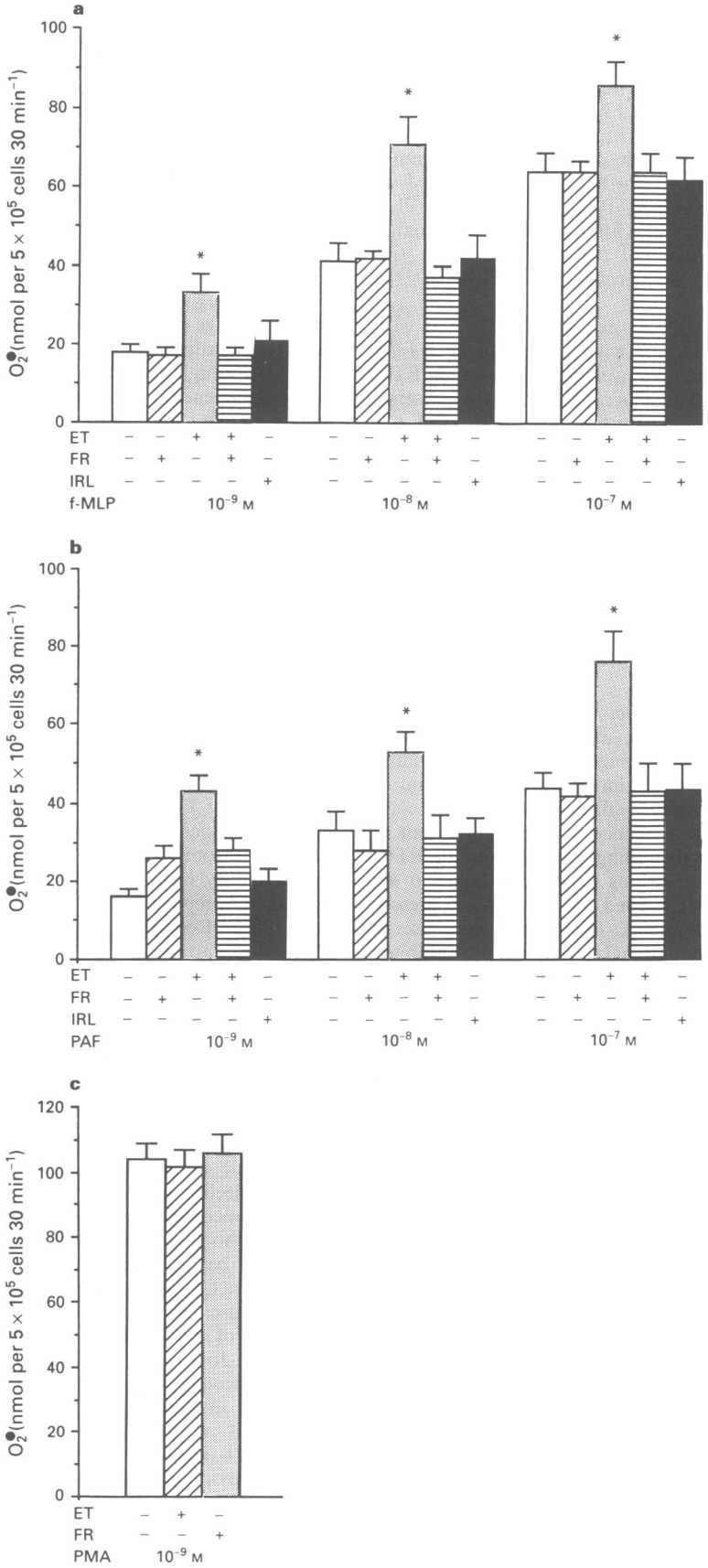

Figure 4 Potentiation by ET-1 of f-Met-Leu-Phe and PAF-induced superoxide production by guinea-pig alveolar macrophages. Macrophages (10^6 cells ml^{-1}) were preincubated with FR 139317 (FR, 1.5×10^{-7} M) or 0.9% NaCl for 10 min at 37°C, then endothelin-1 (ET, 10^{-8} M), IRL 1620 (10^{-8} M) or their vehicle (0.9% NaCl) was added for 5 min. The cells were then challenged with (**a**) f-Met-Leu-Phe, (**b**) PAF or (**c**) phorbol 12-myristate 13-acetate (PMA, 10^{-9} M) for 30 min in the presence of ferricytochrome c with or without superoxide dismutase. Superoxide production is reported as net release (i.e. the amount released by challenged cells minus the amount released by identically handled but untreated and unchallenged cells). Basal superoxide release was 11 ± 1 nmol O_2^- per 5×10^5 cells 30 min^{-1} ($n = 8$) in the absence of any agonists. Values are means with s.e.mean for four to eight separate experiments. $^*P < 0.05$ compared to control by Dunn's multiple contrast hypothesis test.

10 min at 37°C (Figure 4a,b). Preliminary experiments showed that the maximal enhancement of superoxide production can be observed under these conditions. The potentiating effect of ET-1 was completely inhibited by pre-incubation of the cells with FR 139317 (1.5×10^{-7} M) for 1 min before addition of ET-1 (Figure 4a,b). FR 139317 alone neither stimulated superoxide production (12 ± 1 nmol O_2^- per 5×10^5 cells 30 min^{-1}, $n = 8$, $P > 0.1$ compared to unstimulated cells) nor modified PAF or f-Met-Leu-Phe-induced superoxide production (Figure 4a,b). Superoxide production elicited by PMA, 10^{-9} M did not differ significantly in the absence and presence of ET-1, 10^{-8} M (Figure 4c).

Basal $[Ca^{2+}]_i$ values of alveolar macrophages loaded with fura-2 ranged from 63 to 112 nM with a mean of 83 ± 4 nM ($n = 11$). No significant changes were detected when ET-1 (10^{-10}–10^{-6} M) was applied to macrophages in the presence of 1 mM extracellular calcium. Furthermore, ET-1 did not potentiate f-Met-Leu-Phe or PAF-induced increases in $[Ca^{2+}]_i$. For instance, $[Ca^{2+}]_i$ rose from 79 ± 6 nM to 144 ± 14 nM and to 146 ± 14 nM ($n = 5$) in response to f-Met-Leu-Phe (10^{-7} M) in the absence and presence of ET-1 (10^{-8} M), respectively, and $[Ca^{2+}]_i$ rose from 86 ± 6 nM to 118 ± 11 nM and 122 ± 8 nM ($n = 6$) in response to PAF (10^{-7} M) in the absence and presence of ET-1 (10^{-8} M), respectively.

Discussion

This study indicates that, by inducing intravascular sequestration of neutrophil granulocytes, modulating activation of alveolar macrophages and enhancing microvascular albumin extravasation, ET-1 is a pro-inflammatory mediator and/or modulator of the pulmonary inflammatory response in guinea-pigs and also provide evidence for the involvement of ET_A and ET_B receptors in mediating these actions of ET-1.

Confirming previous observations (Macquin-Mavier *et al.*, 1989), the present study also showed the monophasic pressor action of ET-1 in the guinea-pig. The pressor response to ET-1 was substantially, though never completely, inhibited by FR 139317, a highly selective ET_A receptor antagonist, whereas almost complete inhibition was observed with the ET_A/ET_B receptor antagonist, bosentan. FR 139317 has been reported to be 7000 times more potent in inhibiting the binding of ET-1 to ET_A than ET_B receptors *in vitro* (Aramori *et al.*, 1993; Sogabe *et al.*, 1993). At the dose used, FR 139317 appeared to be a selective ET_A receptor antagonist *in vivo*, as it did not inhibit the responses to the ET_B receptor-selective agonist, IRL 1620 in the guinea-pig. Bosentan has been shown to antagonize the specific binding of ET-1 on ET_A (human umbilical vein vascular smooth muscle cells) as well as on ET_B receptors (microsomal membranes from human placenta) with similar K_i values (Clozel *et al.*, 1994). These observations indicate that similarly to the rat (Ihara *et al.*, 1992; Filep *et al.*, 1992), both ET_A and ET_B receptors are involved in the generation of a pressor effect in the guinea-pig. The findings that the ET_B receptor-selective agonist, IRL 1620 also evoked increases in MABP lend further support to this notion.

Bolus injection of ET-1 resulted in a dose-dependent haemoconcentration that was almost completely inhibited by bosentan and significantly, though not totally, attenuated by FR 139317. ET-1 also enhanced albumin extravasation in the trachea, upper and lower bronchi, but not in the pulmonary parenchyma in a dose-dependent fashion. The effects of 1 nmol kg^{-1} ET-1 were comparable to those elicited by 0.9 nmol kg^{-1} PAF. The present results clearly show that the permeability enhancing effect of ET-1 is mediated through both ET_A and ET_B receptors as (a) ET_A receptor blockade caused only 60–70% inhibition of the ET-1-induced albumin extravasation in the large airways, (b) ET_A/ET_B receptor blockade with bosentan resulted in significantly greater degree of inhibition of ET-1-induced albumin extravasation than FR 139317 and (c) selective activation of ET_B receptors with IRL 1620 also led to enhanced albumin accumulation in the trachea, upper and lower bronchi. The lack of effect of bosentan or FR 139317 on PAF-induced albumin extravasation would exclude a non-specific protective effect of these compounds on endothelial cells. In the present experiments, parallel changes were observed in albumin extravasation and MABP. However, the increase in blood pressure, *per se*, could not be the basis for the observed albumin extravasation. Indeed, the mediator-stimulated increase in albumin extravasation is thought to be attributable primarily to induction of interendothelial gap formation exclusively in the venules (Grega *et al.*, 1986). This leads to opening of the variable large-pore system, the dominant macromolecular transport pathway operant in inflammation (Grega *et al.*, 1986). Although activation of this transport pathway appears to be independent of haemodynamic changes, elevation of microvascular hydrostatic pressure can promote protein infiltration if large pores are open (Grega *et al.*, 1986). Although we did not measure pulmonary microvessel hydrostatic pressure, one may assume that ET-1 could increase microvascular hydrostatic pressure, as it is a considerably more potent constrictor of venous than arterial vessels (Yang *et al.*, 1989; Warner, 1990). However, this alone would not lead to enhanced albumin extravasation. The increased permeability to water but not to protein over pulmonary venous pressure from 20 to 105 Torr in dog isolated perfused lungs (Ehrhart & Hofman, 1992) indicates that permeability to water and protein can change independently, and is counter to the theory that elevated vascular pressure 'stretches' vascular pores. Given that ET_B receptors predominate on vascular endothelial cells (Hosoda *et al.*, 1991), ET-1 and IRL 1620 may induce gap formation directly via activation of ET_B receptors or through release of secondary mediators such as platelet-activating factor (Filep *et al.*, 1991) or thromboxane A_2 (Filep *et al.*, 1994) or both. Release of secondary mediators may be mediated via ET_A receptors as has been reported for the rat coronary circulation (Filep *et al.*, 1994). Regardless of the mechanisms underlying gap formation, attenuation of ET-1-induced pulmonary vasoconstriction by FR 139317 or bosentan would lead to a reduction of capillary hydrostatic pressure, which, in turn, could result in a decrease in albumin extravasation.

The present study showed that bolus i.v. injections of ET-1, but not IRL 1620, into guinea-pigs induces leukopenia in a dose-dependent manner. Since leukopenia occurred at the time when significant decreases in plasma volume were also detected, it is likely that the actual decreases in white blood cell count might have been underestimated. The marked decline in the percentage of neutrophil granulocytes with a concomitant increase in the percentage of monocytes and lymphocytes indicates that ET-1-induced leukopenia can primarily be attributed to a decrease in the number of circulating neutrophil granulocytes. The ability of adrenaline, which causes neutrophilia by demargination of the substantial pool of marginated intravascular neutrophils (Athens *et al.*, 1961; Joyce *et al.*, 1976), to prevent ET-1-induced neutropenia would suggest that the underlying mechanism is increased intravascular sequestration rather than egress of neutrophil granulocytes from the circulation into tissues. The findings that ET-1 had no significant effect on pulmonary myeloperoxidase activity, a sensitive marker of neutrophil infiltration (Krawisz *et al.*, 1984; Mullane *et al.*, 1985), and on the number and composition of bronchoalveolar lavage cells lend further support to this notion. These latter findings are consistent with previous observations that exposure of guinea-pig lungs to aerosolized ET-1 also fails to affect the number and composition of lavage fluid cells (Boichot *et al.*, 1991). Furthermore, histological studies have shown that ET-1 does not cause inflammatory cell influx into the alveolar or vascular walls or into the bronchial epithelium within 30 min of its administration (Macquin-Mavier *et al.*, 1989). Since neutropenia was observed 10 min after injection of ET-1, it

seems unlikely that ET-1 inhibited entry of neutrophil granulocytes into the circulation. The prevention of ET-1-induced neutropenia by adrenaline would also argue against a direct cytotoxic effect of ET-1 on neutrophil granulocytes. Previous studies have demonstrated that the lung and spleen are the two most important sites of sequestration of neutrophil granulocytes (cf. Hogg, 1987). Neutrophil margination is most probably the result of reversible binding of neutrophil granulocytes to the endothelium (Gamble *et al.*, 1985). As the neutropenia elicited by ET-1 cannot be mimicked by IRL 1620 but can be prevented by the ET_A receptor-selective antagonist, FR 139317, and endothelial cells do not possess ET_A receptors (Hosoda *et al.*, 1991), it seems likely that ET-1 elicits a pro-adhesive effect primarily on neutrophil granulocytes. It should be noted that migration of neutrophil granulocytes into tissues is not a prerequisite for their contribution to the development or propagation of tissue damage, as it has been reported for the cat coronary reperfusion injury model, where most of the neutrophils were adherent to the microvasculature, particularly the capillaries and venules despite massive tissue necrosis (Lefer *et al.*, 1993).

Our results demonstrate that ET-1 alone neither increases free calcium concentration nor augments superoxide production in guinea-pig alveolar macrophages. These findings are at variance with similar measurements made in human alveolar macrophages (Haller *et al.*, 1991). The reason(s) for these differences is (are) unclear, but possibly species differences in the distribution and/or coupling of ET receptors may occur. Indeed, Haller *et al.* (1991) have reported that ~50% of human isolated single macrophages did not respond to ET-1 at all. Therefore, it is possible that guinea-pigs, unlike human subjects, lack a subpopulation of macrophages that responds to ET-1.

While ET-1 or IRL 1620 by itself failed to activate guinea-pig alveolar macrophages, ET-1, but not IRL 1620, markedly potentiated superoxide production in macrophages challenged with f-Met-Leu-Phe or PAF without affecting f-Met-Leu-Phe or PAF-induced changes in intracellular free calcium concentration. This potentiating effect of ET-1 was completely reversed by FR 139317, indicating that this action of ET-1 is mediated through ET_A receptors. Accordingly, ET-1 failed to affect PAF-induced aggregation of guinea-pig platelets (Filep *et al.*, unpublished data) that do not possess functional ET receptors. On the other hand, ET-1 did not enhance superoxide production elicited by PMA, a direct activator of protein kinase C. These findings suggest that ET-1 might have modulated the signal transduction pathway for superoxide production at a level between f-Met-Leu-Phe or PAF receptors and protein kinase C. A likely explanation is that ET-1 induces production of diacylglycerol via activation of phospholipase D, which, in turn, would lead to activation of protein kinase C. Protein kinase C then proceeds to phosphorylate elements of the response mechanism and may also enhance the actions of PAF as well as other stimuli (see O'Flaherty *et al.*, 1989). These bidirectional influences of protein kinase C may be critical to cellular priming. Although we did not measure phospholipase D activity in alveolar macrophages, ET-1 has been reported to activate phospholipase D in cultured vascular smooth muscle cells (Konishi *et al.*, 1991), which possess predominantly ET_A receptors (Hosoda *et al.*, 1991). It is worth mentioning that similar potentiation by ET-1 of f-Met-Leu-Phe-induced superoxide formation has been reported for human neutrophil granulocytes (Ishida *et al.*, 1990).

In conclusion, the present data indicate that ET-1 may exert pro-inflammatory actions in the guinea-pig lung. Albumin extravasation and subsequent local oedema formation elicited by ET-1 would induce or predispose to tissue damage, and would contribute to airway narrowing (McFadden, 1992). ET-1 can also initiate intravascular sequestration of neutrophil granulocytes, the first step required for neutrophil influx into tissues, albeit it did not evoke neutrophil infiltration. However, sequestration and subsequent activation of neutrophil granulocytes could lead to propagation of tissue damage. Although locally produced ET-1 may be released from the lung into the circulation (Shirakami *et al.*, 1991) and intravascular and aerosol administration of ET-1 elicit similar increases in airway tone in the guinea-pig isolated lung (Pons *et al.*, 1991), intravenous administration of ET-1 does not necessarily mimic the local actions of the peptide. Therefore, additional experiments using aerosolized ET-1 are required to confirm these effects of ET-1. The present study also showed that ET-1 could prime alveolar macrophages for enhanced superoxide production in response to other inflammatory mediators, which may contribute to the inflammatory reaction. These findings suggest that ET-1 may be an important modulator of the inflammatory response. The observations that these pro-inflammatory actions of ET-1 can effectively be attenuated by bosentan and, in part, by FR 139317, suggest a therapeutic potential for ET_A/ET_B receptor and perhaps ET_A receptor-selective antagonists in the treatment of airway inflammation associated with asthma or other respiratory disorders.

We thank Dr Martine Clozel (Hoffmann-La Roche Ltd., Basel, Switzerland) and Fujisawa Pharmaceutical Co., Ltd., Osaka, Japan for generously supplying us with bosentan and FR 139317, respectively. This study was supported by the Medical Research Council of Canada and the Maisonneuve-Rosemont Hospital. A.F. and J.G.F. are Scholars of the Fonds de la Recherche en Santé du Québec.

References

ABRAHAM, W.H., AHMED, A., CORTES, A., SPINELLA, M.J., MALIK, A.B. & ANDERSEN, T.T. (1993). A specific endothelin-1 antagonist blocks inhaled endothelin-1-induced bronchoconstriction in sheep. *J. Appl. Physiol.*, **74**, 2537–2542.

ARAI, H., HORI, S., ARAMORI, I., OHKUBO, H. & NAKANISHI, S. (1990). Cloning and expression of a cDNA encoding an endothelin receptor. *Nature*, **348**, 730–732.

ARAMORI, I., NIREI, H., SHOUBO, M., SOGABE, K., NAKAMURA, K., KOJO, H., NOTSU, Y., ONO, T. & NAKANISHI, S. (1993). Subtype selectivity of a novel endothelin antagonist, FR 139317, for the two endothelin receptors in transfected Chinese hamster ovary cells. *Mol. Pharmacol.*, **43**, 127–131.

ATHENS, J.W., HAAB, O.P., RAAB, S.O., MAUER, M.A., ASCHENBRUCKER, H., CARTWRIGHT, G.E. & WINTROBE, M.M. (1961). Leukokinetic studies. IV. The total blood, circulating, and marginal granulocyte pools and the granulocyte turnover rate in normal subjects. *J. Clin. Invest.*, **40**, 989–997.

BOICHOT, E., CARRE, C., LAGENTE, V., PONS, F., MENCIA-HUERTA, J.M. & BRAQUET, P. (1991). Endothelin-1 and bronchial hyperresponsiveness in the guinea pig. *J. Cardiovasc. Pharmacol.*, **17** (Suppl. 7), S329–S331.

CARDELL, L.O., UDDMAN, R. & EDVINSON, L. (1993). A novel ET_A-receptor antagonist, FR 139317, inhibits endothelin-induced contractions of guinea-pig pulmonary arteries, but not trachea. *Br. J. Pharmacol.*, **108**, 448–452.

CLOZEL, M., BREU, V., GRAY, G.A., KALINA, B., LÖFFLER, B.M., BURRI, K., CASSAL, J.M., HIRTH, G., MÜLLER, M., NEIDHART, W. & RAMUZ, H. (1994). Pharmacological characterization of bosentan, a new potent orally active non-peptide endothelin receptor antagonist. *J. Pharmacol. Exp. Ther.*, **270**, 228–235.

DUNN, O.J. (1964). Multiple comparisons using rank sums. *Technometrics*, **6**, 241–252.

EHRHART, I.C. & HOFMAN, W.F. (1992). Pressure-dependent increase in lung vascular permeability to water but not protein. *J. Appl. Physiol.*, **72**, 211–218.

FILEP, J.G. (1993). Endothelin peptides: biological actions and pathophysiological significance in the lung. *Life Sci.*, **52**, 119–133.

FILEP, J.G., FÖLDES-FILEP, E., ROUSSEAU, A., FOURNIER, A., SIROIS, P. & YANO, M. (1992). Endothelin-1 enhances vascular permeability in the rat heart through the ET_A receptor. *Eur. J. Pharmacol.*, **219**, 343–344.

FILEP, J.G., FOURNIER, A. & FÖLDES, FILEP, E. (1994). Endothelin-1-induced myocardial ischaemia and oedema in the rat: involvement of the ET_A receptor, platelet-activating factor and thromboxane A_2. *Br. J. Pharmacol.*, **112**, 963–971.

FILEP, J.G., SIROIS, M.G., ROUSSEAU, A., FOURNIER, A. & SIROIS, P. (1991). Effects of endothelin-1 on vascular permeability in the conscious rat: interactions with platelet-activating factor. *Br. J. Pharmacol.*, **104**, 797–804.

FÖLDES-FILEP, E., FILEP, J.G. & SIROIS, P. (1992). C-reactive protein inhibits intracellular calcium mobilization and superoxide production of guinea pig alveolar macrophages. *J. Leukoc. Biol.*, **51**, 13–18.

GAMBLE, J.R., HARLAN, J.H., KLEBANOFF, S.J. & VADAS, M.A. (1985). Stimulation of the adherence of neutrophils to umbilical vein endothelium by human recombinant tumor necrosis factor. *Proc. Natl. Acad. Sci. U.S.A.*, **82**, 8687–8671.

GREGA, J.G., ADAMSKI, S.W. & DOBBINS, D.E. (1986). Physiological and pharmacological evidence for the regulation of permeability. *Fed. Proc.*, **45**, 96–100.

HALLER, H., SCHABERG, T., LINDSCHAU, C., LODE, H. & DISTLER, A. (1991). Endothelin increases $[Ca^{2+}]_i$, protein phosphorylation, and O_2^- production in human alveolar macrophages. *Am. J. Physiol.*, **261**, L478–L484.

HAY, D.W.P., HENRY, P.J. & GOLDIE, R.G. (1993a). Endothelin and the respiratory system. *Trends Pharmacol. Sci.*, **14**, 29–32.

HAY, D.W.P., LUTTMANN, M.A., HUBBARD, W.C. & UNDEM, B.J. (1993b). Endothelin receptor subtypes in human and guinea-pig pulmonary tissues. *Br. J. Pharmacol.*, **110**, 1175–1183.

HENRY, P.J. (1993). Endothelin-1 (ET-1)-induced contraction in rat isolated trachea: involvement of ET_A and ET_B receptors and multiple signal transduction systems. *Br. J. Pharmacol.*, **110**, 435–441.

HOGG, J.C. (1987). Neutrophil kinetics and lung injury. *Physiol. Rev.*, **67**, 1249–1295.

HOLGATE, S.T., WILSON, J.R. & HOWARTH, P.H. (1992). New insights into airway inflammation by endobronchial biopsy. *Am. Rev. Respir. Dis.*, **145**, S2–S6.

HOSODA, K., NAKAO, K., ARAI, H., SUGA, S., OGAWA, Y., MUKOYAMA, M., SHIRAKAMI, G., SAITO, Y., NAKANISHI, S. & IMURA, H. (1991). Cloning and expression of human endothelin-1 receptor cDNA. *FEBS Lett.*, **287**, 23–26.

IHARA, M., NOGUCHI, K., SAEKI, T., FUKURODA, T., TSUCHIDA, S., KIMURA, S., FUKAMI, T., ISHIKAWA, K., NISHIKIBE, M. & YANO, M. (1992). Biological profiles of highly potent novel endothelin antagonists selective for the ET_A receptor. *Life Sci.*, **50**, 247–255.

ISHIDA, K., TAKESHIGE, K. & MINAKAMI, S. (1990). Endothelin-1 enhances superoxide generation of human neutrophils stimulated by the chemotactic peptide, N-formyl-methionyl-leucyl-phenylalanine. *Biochem. Biophys. Res. Commun.*, **173**, 496–500.

JOYCE, R.A., BOGGS, D.R., HASIBA, U. & SRODES, C.H. (1976). Marginal neutrophil pool size in normal subjects and neutropenic patients as measured by epinephrine infusion. *J. Lab. Clin. Med.*, **88**, 614–620.

KONISHI, F., KONDO, T. & INAGAMI, T. (1991). Phospholipase D in cultured rat vascular smooth muscle cells and its activation by phorbol esters. *Biochem. Biophys. Res. Commun.*, **179**, 1070–1076.

KRAWISZ, J.E., SHARON, P. & STENSON, W.F. (1984). Quantitative assay for acute intestinal inflammation based on myeloperoxidase activity. Assessment of inflammation in rat and hamster models. *Gastroenterology*, **87**, 1344–1350.

LAITINEN, L.A., LAITINEN, A. & HAAHTELA, T. (1993). Airway mucosal inflammation even in patient with newly diagnosed asthma. *Am. Rev. Respir. Dis.*, **147**, 697–704.

LEE, T.H. & LANE, S.J. (1992). The role of macrophages in the mechanisms of airway inflammation in asthma. *Am. Rev. Respir. Dis.*, **145**, S27–S30.

LEFER, A.M., ALBERTINE, K.H., WEYRICH, A.S. & MA, X.L. (1993). Polymorphonuclear (PMN) leukocytes accumulate intravascularly but do not migrate to the myocardium following ischemia/reperfusion in the cat (Abstract). *FASEB J.*, **7**, A344.

MACQUIN-MAVIER, I., LEVAME, M., ISTIN, N. & HARF, A. (1989). Mechanisms of endothelin-mediated bronchoconstriction in the guinea pig. *J. Pharmacol. Exp. Ther.*, **250**, 740–745.

MATTOLI, S., MEZZETTI, M., RIVA, G., ALLEGRA, L. & FASOLI, A. (1990). Specific binding of endothelin on human bronchial smooth muscle cells in culture and secretion of endothelin-like material from bronchial epithelial cells. *Am. J. Respir. Cell. Mol. Biol.*, **3**, 145–151.

MATTOLI, S., SOLOPERTE, M., MARINI, M. & FASOLI, A. (1991). Levels of endothelin in the bronchoalveolar lavage fluid of patients with symptomatic asthma and reversible airflow obstruction. *J. Allergy Clin. Immunol.*, **88**, 376–384.

MCFADDEN. E.R.Jr. (1992). Microvasculature and airway responses. *Am. Rev. Respir. Dis.*, **145**, S42–S43.

MULLANE, K.M., KRAEMER, R. & SMITH, B. (1985). Myeloperoxidase activity as a quantitative assessment of neutrophil infiltration into ischemic myocardium. *J. Pharmacol. Methods*, **14**, 157–167.

NAGASE, T., FUKUCHI, Y., JO, C., TERAMOTO, S., UEJIMA, Y., SHIMIZU, T. & ORIMO, H. (1990). Endothelin-1 stimulates arachidonate 15-lipoxygenase activity and oxygen radical formation in the rat distal lung. *Biochem. Biophys. Res. Commun.*, **168**, 485–489.

NOMURA, A., UCHIDA, Y., KANEYAMA, M., SAOTOME, M., OHI, K. & HASEGAWA, S. (1989). Endothelin and bronchial asthma. *Lancet*, **ii**, 747–748.

O'FLAHERTY, J.T., JACOBSON, D.P. & REDMAN, J.F. (1989). Bidirectional effects of protein kinase C activators. Studies with human neutrophils and platelet-activating factor. *J. Biol. Chem.*, **264**, 6836–6843.

PONS, F., TOUVAY, C., LAGENTE, V., MENCIA-HUERTA, J.M. & BRAQUET, P. (1991). Comparison of the effects of intra-arterial and aerosol administration of endothelin-1 (ET-1) in the guinea-pig isolated lung. *Br. J. Pharmacol.*, **102**, 791–796.

RAWSON, R.A. (1943). The binding of T-1824 and structurally related diazo dyes by the plasma protein. *Am. J. Physiol.*, **138**, 708–717.

ROGERS, D.F., BOSCHETTO, P. & BARNES, P.J. (1989). Plasma exudation. Correlation between Evans blue dye and radiolabeled albumin in guinea pig airways in vivo. *J. Pharmacol. Methods*, **21**, 309–315.

SAKURAI, T., YANAGISAWA, M., TAKUWA, Y., MIYAZAKI, H., KIMURA, S., GOTO, K. & MASAKI, T. (1990). Cloning of a cDNA encoding a non-isopeptide selective subtype of the endothelin receptor. *Nature*, **348**, 732–735.

SHIRAKAMI, G., NAKAO, K., SAITO, Y., MAGARIBUCHI, T., JOUGASAKA, M., MUKOYAMA, Y., ARAI, H., HOSODA, K., SUGA, S.I., OGAWA, Y., YAMADA, T., MORI, K. & IMURA, H. (1991). Acute pulmonary alveolar hypoxia increases lung and plasma levels of endothelin-1 levels in conscious rats. *Life Sci.*, **48**, 969–976.

SOGABE, K., NIREI, H., SHOUBO, M., NOMOTO, A., AO, S., NOTSU, Y. & ONO, T. (1993). Pharmacological profile of FR 139317, a novel, potent endothelin ET_A receptor antagonist. *J. Pharmacol. Exp. Ther.*, **264**, 1040–1046.

SPRINGALL, D.R., HOWARTH, P.H., COUNIHAN, H., DJUKANOVIC, R., HOLGATE, S. & POLAK, J.M. (1991). Endothelin immunoreactivity of airway epithelium in asthmatic patients. *Lancet*, **337**, 697–701.

TAKEI, M., UMEMURA, I., YAMASAKI, K., WATANABE, T., FUJITANI, Y., ODA, K., URADE, Y., INUI, T., YAMAMURA, T. & OKADA, T. (1992). A potent and specific agonist, Suc-[Glu^9, $Ala^{11,15}$]endothelin-1(18-21), IRL 1620, for the ET_B receptor. *Biochem. Biophys. Res. Commun.*, **184**, 953–959.

TSIEN, R.Y., POZZAN, T. & RINK, T.J. (1982). Calcium homeostasis in intact lymphocytes: cytoplasmic free calcium monitored with a new, intracellularly trapped fluorescent indicator. *J. Cell. Biol.*, **94**, 325–334.

VITTORI, E., MARINI, M., FASOLI, A., DE FRANCHIS, R. & MATTOLI, S. (1992). Increased expression of endothelin in bronchial epithelial cells of asthmatic patients and effects of corticosteroids. *Am. Rev. Respir. Dis.*, **146**, 1320–1325.

WARNER, T.D. (1990). Simultaneous perfusion of rat isolated superior mesenteric arterial and venous beds: comparison of their vasoconstrictor and vasodilator responses to agonists. *Br. J. Pharmacol.*, **99**, 427–433.

YANG, Z.H., BÜHLER, F.R., DIEDERICH, D. & LÜSCHER, T.F. (1989). Different effects of endothelin-1 on cAMP-, and cGMP-mediated vascular relaxation in human arteries and veins: comparison with norepinephrine. *J. Cardiovasc. Pharmacol.*, **13** (Suppl. 5), S129–S131.

(Received October 25, 1994
Revised January 11, 1995
Accepted January 30, 1995)

British Journal of Pharmacology (1995) 115, 237-246

Evidence that tachykinin NK_1 and NK_2 receptors mediate non-adrenergic non-cholinergic excitation and contraction in the circular muscle of guinea-pig duodenum

*Vladimir Zagorodnyuk, Paolo Santicioli, [1]Carlo Alberto Maggi & Antonio Giachetti

Pharmacology Department, A. Menarini Pharmaceuticals, Florence, Italy and *Department of Neuro-muscular Physiology, Bogomoletz Institute of Physiology, Kiev, Ukraine

1 In the presence of atropine (1 μM), guanethidine (3 μM), indomethacin (3 μM), apamin (0.1 μM) and L-nitroarginine (L-NOARG, 30 μM), electrical field simulation (EFS) produced a nonadrenergic, non-cholinergic (NANC) excitatory junctional potential (e.j.p.), action potentials and contraction of the circular muscle of the guinea-pig proximal duodenum, recorded by the single sucrose gap technique.

2 The selective tachykinin (TK) NK_1 receptor antagonist, GR 82,334 (30 nM–3 μM) produced a concentration-dependent inhibition of the EFS-evoked NANC e.j.p. and contraction. Similarly, the selective NK_2 receptor antagonists, MEN 10,627 (30 nM–3 μM) and GR 94,800 (100 nM–10 μM), both produced a concentration-dependent inhibition of the EFS-evoked NANC e.j.p. and contraction. GR 82,334 inhibited the electrical and mechanical NANC responses to EFS in an almost parallel manner, while MEN 10,627 and GR 94,800 were more effective in inhibiting the mechanical than the electrical response to EFS.

3 Activation of the NK_1 or NK_2 receptor by the selective agonists, [Sar^9]substance P (SP) sulphone and [βAla^8]neurokinin A (NKA) (4-10), respectively (0.3 μM each), produced depolarization, action potentials and contractions. GR 82,334 selectively inhibited the responses to [Sar^9]SP sulphone, without affecting the responses to [βAla^8]NKA (4-10). MEN 10,627 and GR 94,800 inhibited or abolished the responses to [βAla^8]NKA (4-10), without affecting the responses to [Sar^9]SP sulphone.

4 Nifedipine (1 μM) abolished the action potentials and contraction produced either by EFS or by the TK receptor agonists [Sar^9]SP sulphone or [βAla^8]NKA (4-10).

5 In the presence of nifedipine, the NANC e.j.p. produced by EFS was biphasic: in the majority of strips tested (21 out of 29) an early fast phase of depolarization was followed by a second slow component. The combined administration of GR 82,334 and GR 94,800 (3 μM each) reduced both components, the slow phase being inhibited to a greater extent than the fast phase.

6 The P_2 purinoreceptor antagonist, suramin (100 μM) reduced the fast phase of the e.j.p. produced by EFS in the presence of nifedipine, without affecting the slow phase. The combined administration of suramin, GR 82,334 and GR 94,800 produced a nearly complete blockade of the e.j.p. produced by EFS in the presence of nifedipine.

7 When tested in the absence of apamin and L-NOARG, EFS induced a NANC inhibitory junction potential (i.j.p.) followed by an e.j.p., and the selective P_{2Y} receptor agonist, adenosine-5'-O-(2-thiodiphosphate) (ADPβS, 10 μM), produced membrane hyperpolarization. After addition of apamin and L-NOARG, the i.j.p. was blocked, and EFS produced a pure NANC e.j.p.; ADPβS produced depolarization, action potentials and contraction.

8 Suramin (100 μM) blocked the depolarization, action potentials and contractions produced by ADPβS in the presence of apamin and L-NOARG, without affecting the responses produced by the NK_1 receptor agonist, [Sar^9]SP sulphone.

9 We conclude that NK_1 and NK_2 receptors cooperate in producing NANC excitation and contraction of the circular muscle in the guinea-pig proximal duodenum. Activation of either TK receptor produces membrane depolarization and both receptors contribute to generate action potentials which are essential for producing muscle contraction, via nifedipine-sensitive calcium channels. It appears that endogenous ATP chiefly acts as an inhibitory transmitter but, after blockade of NANC inhibitory mechanism(s), ATP may act as a fast signalling excitatory transmitter.

Keywords: Guinea-pig duodenum; NANC; excitatory junction potentials; tachykinins; tachykinin receptors; ATP

Introduction

Anatomical, neurochemical and pharmacological evidence indicates a major role for peptides of the tachykinin (TK) family as mediators of NANC excitatory neurotransmission to the smooth muscle of the mammalian intestine (Bartho & Holzer, 1985, for review). Two TKs, substance P (SP) and neurokinin A (NKA), via the expression of the preprotachykinin I gene, are produced by some neuronal elements in the myenteric plexus (Deacon *et al.*, 1987; Sternini *et al.*, 1989) which have the adequate anatomical projections to act as effector motoneurones to the circular muscle of the intestine (Brookes *et al.*, 1991). The status of TKs as enteric excitatory transmitters is further documented by the notion that SP- and NKA-like immunoreactive material(s) are released in the gut following neuronal depolarization (Holzer, 1984; Theodorsson *et al.*, 1991; Broad *et al.*, 1992) and by the powerful, receptor-mediated, contractile activity exerted by exogenous TKs in various regions of the mammalian

[1] Author for correspondence.

intestine. Three types of TK receptors have been isolated and cloned, which are termed NK_1, NK_2 and NK_3, respectively (Maggi *et al.*, 1993, for review): in the circular muscle of the guinea-pig small and large intestine, both NK_1 and NK_2 receptors mediate the direct smooth muscle contraction to TKs, while NK_3 receptors, apparently located on neuronal elements, indirectly affect motility by stimulating the release of other mediators (Maggi *et al.*, 1990; 1994a).

From the above, it appears that TKergic excitatory neurotransmission to the circular muscle of the intestine could involve two mediators (SP and NKA) and two receptors (NK_1 and NK_2). In previous electrophysiological experiments, non-cholinergic excitatory junction potentials (e.j.ps) have been recorded in the longitudinal (Bauer & Kuriyama, 1982) and circular muscle (Niel *et al.*, 1983; Bywater & Taylor, 1986; Crist *et al.*, 1991) of the guinea-pig ileum. In some of these studies, a biphasic noncholinergic e.j.p. has been described, and a differential degree of inhibition of the two phases of e.j.p. was observed with SP antagonists such as [D-Arg[1],D-Pro[2],D-Trp[7,9],Leu[11]]SP (RPWWL-SP, Niel *et al.*, 1983; Bywater & Taylor, 1991) and spantide (Crist *et al.*, 1991). The residual phase of e.j.p. appears to be mediated by an unknown transmitter (Bywater & Taylor, 1986; Crist *et al.*, 1991). Because of their low potency and selectivity, and presence of nonspecific effects (e.g. local anaesthetic action), ligands like RPWWL-SP or spantide, have a limited value for assessing the transmitter role of TKs; furthermore, these ligands are essentially poor instruments to discern a differential contribution of NK_1 and NK_2 receptors in TKergic co-transmission (Buck & Shatzer, 1988; Maggi *et al.*, 1993, for review).

Thanks to the recent availability of antagonists that selectively block the NK_1 (SP-preferring) or NK_2 (NKA-preferring) receptors (Maggi *et al.*, 1993) it has become possible to obtain information about the relative contribution of various TKs and different TK receptors in excitatory NANC responses (Bartho *et al.*, 1992; Zagorodnyuk *et al.*, 1993; Holzer *et al.*, 1993; Holzer & Maggi, 1994; Maggi *et al.*, 1994b). Both NK_1 and NK_2 receptors appear to play a relevant role in NANC contraction evoked by electrical nerve stimulation or intraluminal balloon distension in the circular muscle of the guinea-pig ileum (Bartho *et al.*, 1992; Maggi *et al.*, 1994b), while mainly NK_1 receptors mediate the NANC e.j.p. in the circular muscle of the guinea-pig proximal colon (Zagorodnyuk *et al.*, 1993).

The aim of this study was to assess the relative contribution of NK_1 and NK_2 receptors to NANC excitatory neurotransmission in the circular muscle of the guinea-pig duodenum, by studying the effect of potent and selective receptor antagonists, GR 82,334 (Hagan *et al.*, 1991) for NK_1 receptors, GR 94,800 (McElroy *et al.*, 1992) and MEN 10,627 (Patacchini *et al.*, 1994; Maggi *et al.*, 1994c) for NK_2 receptors. From these studies we found evidence that only part of the NANC e.j.p. produced by EFS in the circular muscle of guinea-pig duodenum can be accounted for by the release of endogenous TKs. In the smooth muscle of guinea-pig stomach and caecum, it has been suggested that apamin unmasks a fast purinergic NANC e.j.p. (Shuba & Vladimirova, 1980). To address the possible role of adenosine-triphosphate (ATP) in the NANC e.j.p. in guinea-pig duodenum, we investigated the effect of the general P_2 purinoceptor antagonist, suramin (Dunn & Blakeley, 1988; Hoyle *et al.*, 1990) and of the selective P_{2Y} receptor agonist, adenosine-5'-O-(2-thiodiphosphate) (ADPβS) (Bertrand *et al.*, 1991).

Methods

A modified single sucrose-gap (Artemenko *et al.*, 1982; Hoyle, 1987) was used to investigate simultaneously changes in membrane potential and contractile activity of the smooth muscle to EFS, as described in detail previously (Zagorodnyuk *et al.*, 1993; 1994). Circular muscle strips of proximal duodenum (1–3 cm from the pyloric sphincter), approximately 0.5–0.8 mm wide and 10 mm long were superfused, at a rate of 1 ml min^{-1}, with oxygenated Krebs solution (35 ± 0.5°C) of the following composition (mM): NaCl 119, $NaHCO_3$ 25, KH_2PO_4 1.2, $MgSO_4$ 1.5, KCl 4.7, $CaCl_2$ 2.5 and glucose 11.

Junction potentials were evoked by submaximal electrical field stimulation (EFS): train of stimuli (30–40 V, 0.15–0.2 ms pulse width) were delivered at a frequency of 32 Hz for 1 s every 3–4 min. In preliminary experiments, we found that the electrical and mechanical responses produced with these parameters of EFS are reproducible for the experimental period (1–2 h) of this study. The Krebs solution routinely contained atropine (1 μM) and guanethidine (3 μM) to block the effect of excitatory cholinergic nerves and adrenergic inhibitory nerves, respectively. Indomethacin (3 μM) was used to exclude the possible involvement of prostanoids. Unless otherwise stated, N^{ω}-nitro-L-arginine (L-NOARG, 30 μM) and apamin (0.1 μM) were used to block NANC inhibitory junction potentials (i.j.ps) evoked by EFS (He & Goyal, 1993; Zagorodnyuk *et al.*, 1993).

In a first series of experiments, performed in the presence of atropine (1 μM), guanethidine (3 μM), indomethacin (3 μM), apamin (0.1 μM) and L-NOARG (30 μM), NANC e.j.ps were produced by train EFS at 3–4 min intervals and the effect of tachykinin receptor antagonists (GR 82,334, MEN 10,627 and GR 94,800) on the electrical and mechanical responses produced by EFS was determined. The effect of antagonists was evaluated as % inhibition of the area of electrical and mechanical responses produced by EFS.

In parallel experiments, the selective NK_1 or NK_2 receptor agonists, [Sar[9]]SP sulphone or [βAla[8]]NKA(4-10), respectively (cf. Zagorodnyuk *et al.*, 1993; 1994), were applied to the circular smooth muscle in the absence or presence of tachykinin receptor antagonists. In preliminary experiments, we found that a concentration of 0.3 μM (applied in superfusion for 20 s) of each agonist determined a reproducible electrical and contractile responses when elicited at 15 min intervals.

In a second series of experiments, performed in the presence of atropine (1 μM), guanethidine (3 μM), indomethacin (3 μM), apamin (0.1 μM) and L-NOARG (30 μM), the role of nifedipine-sensitive calcium channels was determined by studying the effect of 1 μM nifedipine (superfused for at least 30 min) on the NANC responses produced by EFS and on the electrical and mechanical responses to tachykinin receptor agonists, [Sar[9]]SP sulphone and [βAla[8]]NKA(4-10). From these experiments, it was found that a biphasic NANC e.j.p. is produced by EFS in the presence of nifedipine: the effect of GR 82,334 and GR 94,800, alone or in combination, on the nifedipine-resistant NANC e.j.p. was also investigated. Since a fraction of this NANC e.j.p. was still present after the combined administration of the TK receptor antagonists, the hypothesis was advanced that ATP may also act as excitatory transmitter in these experimental conditions. To check this point we investigated the effect of the P_2 purinoceptor antagonist, suramin (100 μM, applied in superfusion for 20–30 min) on the NANC e.j.p.

In a final series of experiments we studied the effect of the selective P_{2Y} receptor agonist adenosine-5'-O-(2-thiodiphosphate) (ADPβS) (10 μM) on the electrical and mechanical activity of the guinea-pig duodenum: ADPβS was applied in superfusion for 30 s at 15 min intervals and its effects were investigated in the absence and presence of apamin and L-NOARG.

Statistical analysis

All data in the text are mean ± s.e.mean. Statistical analysis was performed by means of Student's *t* test for paired or

unpaired data, or by means of analysis of variance followed by Dunnett's test, if applicable. A P level <0.05 was considered as statistically significant.

Drugs

Drugs used were: atropine HCl (Serva), guanethidine sulphate (ICF), GR 82,334 or [D-Pro^9,(spiro-γ-lactam) Leu^{10}, Trp^{11}] physalaemin(1-11) (Neosystem), N$^{\omega}$-nitro-L-arginine (L-NOARG), apamin, indomethacin, ADPβS and nifedipine (Sigma). MEN 10,627 or cyclo(Met-Asp-Trp-Phe-Dap-Leu) cyclo(2β-5β) and GR 94,800 or PhCO-Ala-Ala-D.Trp-Phe-D.Pro-Pro-NleNH$_2$ were synthesized at the Chemistry Department of Menarini Pharmaceuticals. Suramin was a kind gift of Prof. M. Costa, Dept. of Human Physiology, Flinders University SA, Bedford Park, Australia.

Results

General

In the presence of atropine (1 μM), guanethidine (3 μM), indomethacin (3 μM), apamin (0.1 μM) and L-NOARG (30 μM), EFS (30 V, 0.15–0.2 ms pulse width, 32 Hz for 1 s) evoked a NANC e.j.p. (mean amplitude of depolarization 10.5 ± 0.7 mV, $n = 42$, latency 426 ± 33 ms, $n = 24$) with superimposed action potentials (mean amplitude 23.8 ± 1.1 mV, $n = 42$) and contraction (5.8 ± 0.4 mN, $n = 42$) (Figures 1, 2 and 3). The mean duration of the NANC e.j.p. was 23.8 ± 3.5 s ($n = 32$). The parameters used to produce a NANC e.j.p. are about two times larger than the threshold EFS stimulation required to produce an e.j.p. followed by action potentials and contraction. Under the

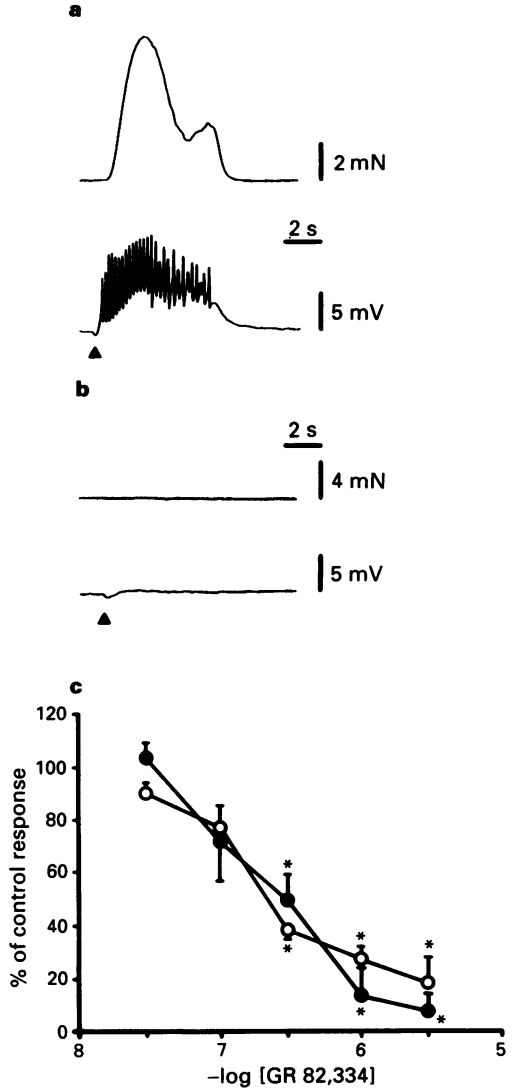

Figure 1 Effect of the tachykinin NK$_1$ receptor antagonist GR 82,334 on the NANC e.j.p. and contraction produced by EFS in the circular muscle of the guinea-pig duodenum. (a and b) Control responses to EFS (32 Hz for 1 s, a), applied at arrowhead and effect of GR 82,334 (3 μM, b) on the responses to EFS in the same preparation. In both panels, upper tracing is muscle tension, lower tracing show changes in membrane potential. (c) Concentration-dependent inhibition of the response to EFS by GR 82,334. The effect of GR 82,334 on the area of depolarization of the NANC e.j.p. (○) and of the area of NANC contraction (●) produced by EFS is expressed as % of the control responses obtained in the absence of the antagonist. Each value is the mean ± s.e.mean of 3–5 experiments. *Significantly different from control, $P<0.05$.

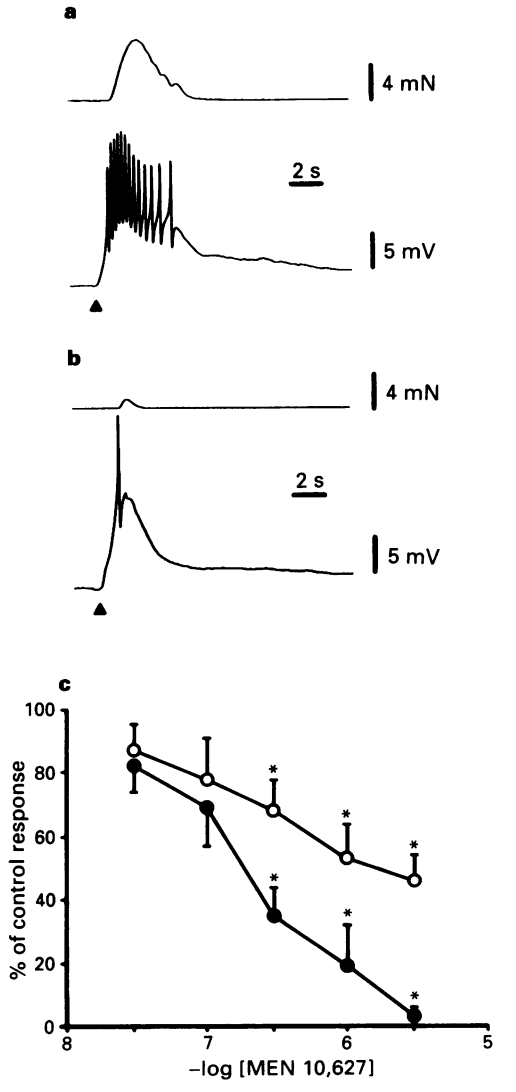

Figure 2 Effect of tachykinin NK$_2$ receptor antagonist MEN 10,627 on the NANC e.j.p. and contraction produced by EFS in the circular muscle of the guinea-pig duodenum. (a and b) Control response to EFS (32 Hz for 1 s, a), applied at arrowhead and effect of MEN 10,627 (3 μM, b) on the responses to EFS in the same preparation. In both panels, upper tracing is muscle tension, lower tracing shows changes in membrane potential. (c) Concentration-dependent inhibition of the response to EFS by MEN 10,627. The effect of MEN 10,627 on the area of depolarization of the NANC e.j.p. (○) and of the area of NANC contraction (●) produced by EFS is expressed as % of the control responses obtained in the absence of the antagonist. Each value is the mean ± s.e.mean of 5–7 experiments. *Significantly different from control, $P<0.05$.

present experimental conditions, the development of contractile responses to EFS (e.g. Figures 1a, 2a and 3a) or exogenous agonists (e.g. Figures 4a, 5a, 8b and 9a) was strictly associated with the presence of action potentials.

Effects of NK_1 and NK_2 receptor antagonists on the NANC e.j.p. and contractions produced by EFS

The NK_1 receptor antagonist, GR 82,334 (30 nM–3 μM), concentration-dependently inhibited the NANC e.j.p. and contractions, EC_{50} values (95% c.l. in parentheses) being 0.23 μM (0.09–0.5 μM) and 0.30 μM (0.19–0.46 μM), respectively. The maximal inhibition of depolarization and contraction produced by GR 82,334 averaged 82 ± 10% ($n = 5$) and 93 ± 7% ($n = 5$), respectively, and the two concentration-response curves were almost superimposable (Figure 1).

The NK_2 receptor antagonist, MEN 10,627 (30 nM–3 μM) concentration-dependently inhibited the NANC e.j.p. and contraction, EC_{50} values (95% c.l. in parentheses) being 0.15 μM (0.11–0.21 μM) and 0.18 μM (0.11–0.29 μM), respectively. As shown in Figure 2, the maximal inhibitory effect of MEN 10,627 on contractility (97 ± 3% inhibition at 3 μM, $n = 7$) was larger than its inhibitory effect on depolarization (54 ± 8% inhibition, $n = 7$). The NK_2 receptor antagonist, GR 94,800 (100 nM–10 μM) concentration-dependently reduced the NANC e.j.p. and contraction, EC_{50} values (95% c.l. in parentheses) being 0.45 μM (0.32–0.63 μM) and 0.20 μM (0.05–0.75 μM), respectively. Also GR 94,800 was more effective in inhibiting contractility (79 ± 8% inhibition, $n = 4$) than depolarization (46 ± 8% inhibition, $n = 4$) (Figure 3). Neither GR 82,334 (up to 3 μM) nor MEN 10,627 (up to 3 μM) or GR 94,800 (up to 10 μM) had any agonist effect on the electrical or contractile activity.

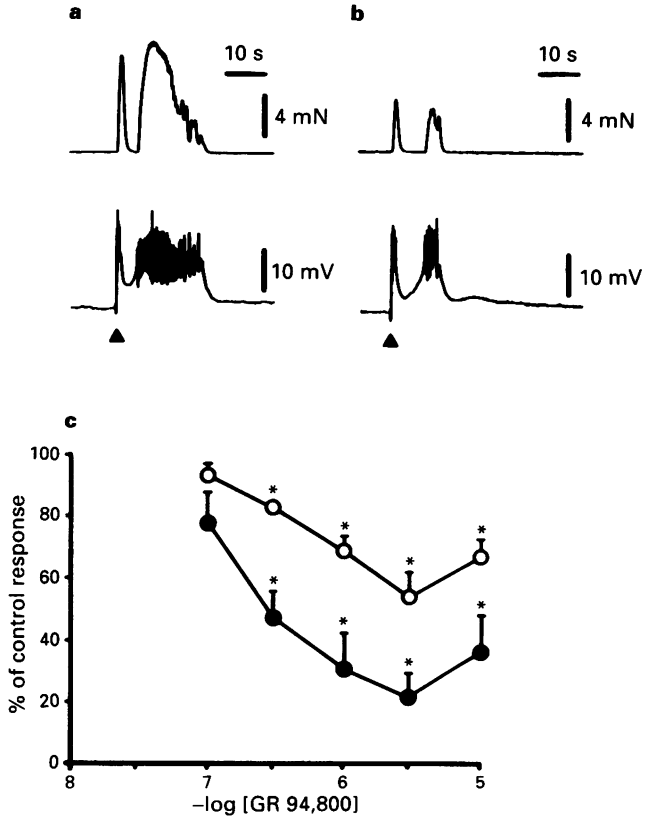

Figure 3 Effect of the tachykinin NK_2 receptor antagonist GR 94,800 on the NANC e.j.p. and contraction produced by EFS in the circular muscle of the guinea-pig duodenum. (a and b) Control response to EFS (32 Hz for 1 s, a), applied at arrowhead and effect of GR 94,800 (3 μM, b) on the responses to EFS in the same preparation. In both panels, upper tracing is muscle tension, lower tracing shows changes in membrane potential. (c) Concentration-dependent inhibition of the response to EFS by GR 94,800. The effect of GR 94,800 on the area of depolarization of the NANC e.j.p. (○) and of the area of NANC contraction (●) produced by EFS is expressed as % of the control responses obtained in the absence of the antagonist. Each value is the mean ± s.e.mean of 4–5 experiments. *Significantly different from control, $P < 0.05$.

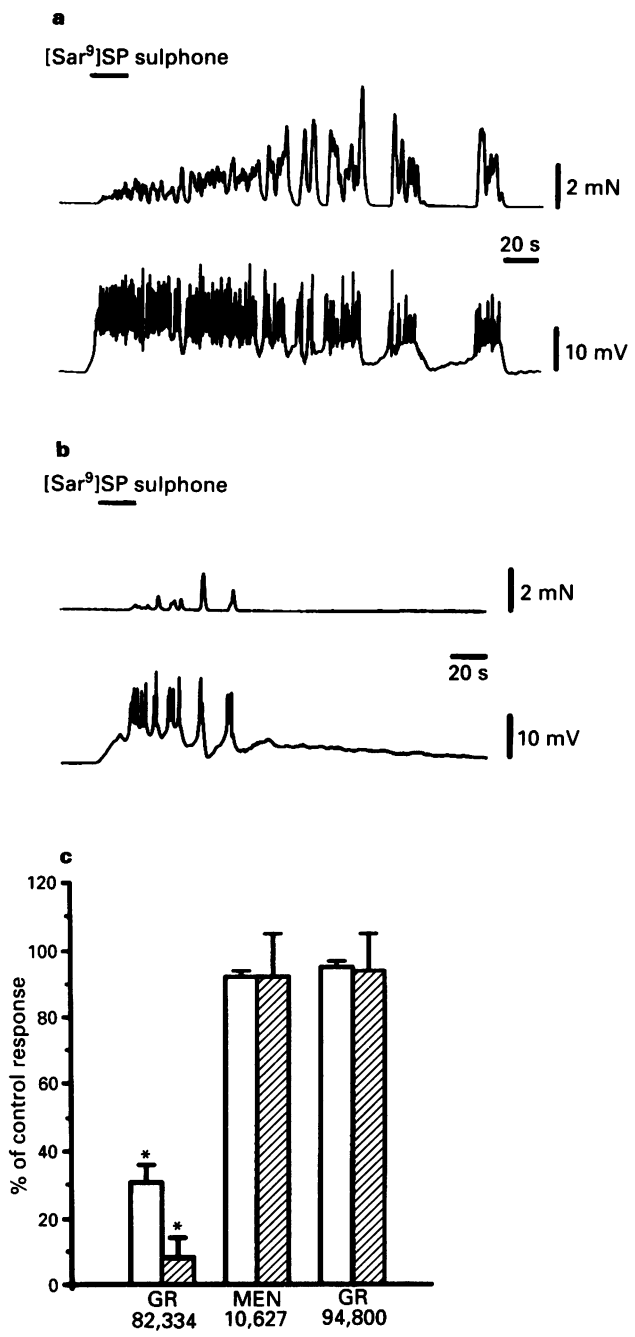

Figure 4 Effect of the tachykinin NK_1 receptor antagonist, GR 82,334 and of the NK_2 receptor antagonists, MEN 10,627 and GR 94,800 on the response induced by the selective tachykinin NK_1 receptor agonist [Sar⁹]SP sulphone. (a) Control response to [Sar⁹]SP sulphone (period of application of the agonist is indicated by the horizontal bar); (b) response to [Sar⁹]SP sulphone in the presence of GR 82, 334 (3 μM); in both panels, upper tracing is muscle tension, lower tracing shows changes in membrane potential. (c) Effect of GR 82,334 (3 μM), MEN 10,627 (3 μM) and GR 94,800 (3 μM) on the area of depolarization (open columns) and area of contraction (hatched columns) induced by [Sar⁹]SP sulphone (0.3 μM for 20 s). The responses to the agonist obtained in the presence of the antagonist are expressed as % of the control response. Each value is the mean ± s.e.mean of 4–5 experiments. *Significantly different from control, $P < 0.05$.

Effect of tachykinin receptor antagonists on the electrical and mechanical responses to selective NK_1 and NK_2 receptor agonists

In the presence of atropine (1 μM), guanethidine (3 μM), indomethacin (3 μM), apamin (0.1 μM) and L-NOARG (30 μM), application of the NK_1 receptor selective agonist, [Sar^9]SP sulphone or of the NK_2 receptor selective agonist, [βAla^8]NKA (4-10) (0.3 μM for 20 s in each case, $n = 8-11$) produced membrane depolarization followed by slow waves with superimposed action potentials and contraction (Figures 4 and 5).

The amplitude of depolarization evoked by the agonists averaged 13.8 ± 0.8 mV ($n = 10$) and 12.1 ± 0.9 mV ($n = 9$) for [Sar^9]SP sulphone and [βAla^8]NKA (4-10), respectively; the amplitude of action potentials averaged 27.5 ± 1.4 and 26 ± 1.9 mV, respectively ($n = 11$ and 8, respectively); the amplitude of evoked contraction averaged 6.2 ± 0.95 and 6.5 ± 0.64 mN, respectively ($n = 11$ and 8, respectively).

GR 82,334 (3 μM) inhibited the [Sar^9]SP sulphone-induced depolarization and contraction by 69 ± 5 and 92 ± 6%, ($n = 4$), respectively, while it did not affect the response to [βAla^8]NKA (4-10) (Figures 4 and 5). MEN 10,627 (1 μM) almost completely abolished the [βAla^8]NKA (4-10)-induced depolarization and contraction (93 ± 4 and 99.8 ± 0.2% inhibition, $n = 3$, respectively). The responses induced by [Sar^9]SP sulphone were not significantly changed by MEN 10,627 (3 μM) (Figures 4 and 5). GR 94,800 (3 μM) completely blocked the [βAla^8]NKA (4-10)-induced depolarization and contraction while the responses evoked by [Sar^9]SP sulphone were not significantly affected (Figures 4 and 5).

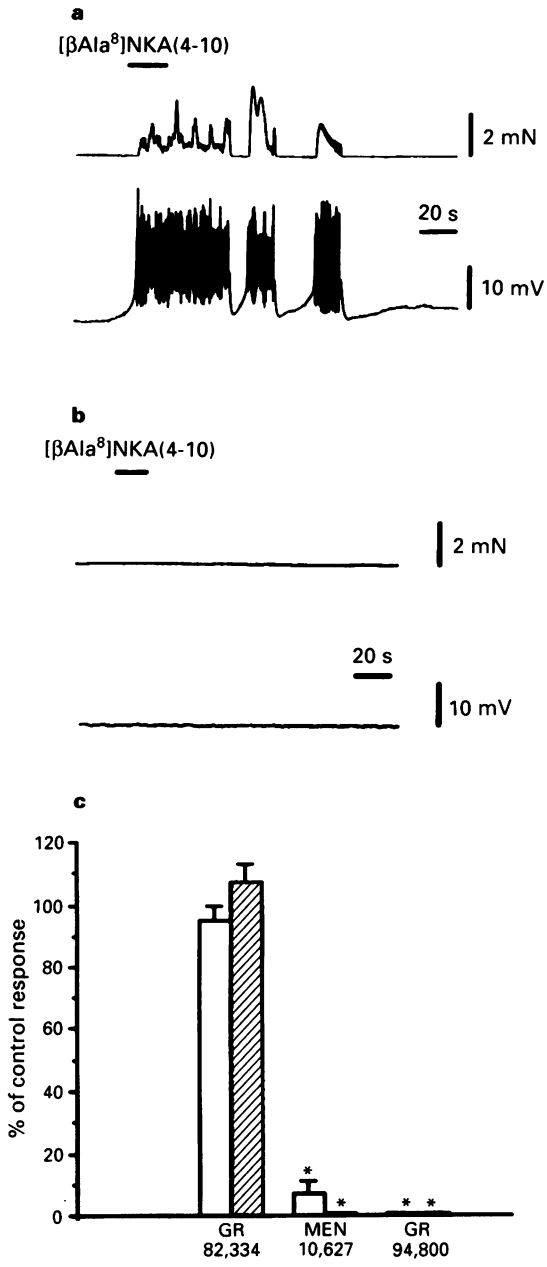

Figure 5 Effect of the tachykinin NK_1 receptor antagonist, GR 82,334 and of the NK_2 receptor antagonist, MEN 10,627 and GR 94,800 on the response induced by the selective tachykinin NK_2 receptor agonist [βAla^8]NKA(4-10). (a) Control response to [βAla^8]NKA(4-10) (period of application of the agonist is indicated by the horizontal bar); (b) response to [βAla^8]NKA(4-10) in the presence of GR 94,800 (3 μM); in both panels, upper tracing is muscle tension, lower tracing shows changes in membrane potential. (c) Effect of GR 82,334 (3 μM), MEN 10,627 (1 μM) and GR 94,800 (3 μM) on the area of depolarization (open columns) and area of contraction (hatched columns) induced by [βAla^8]NKA(4-10) (0.3 μM for 20 s). The responses to the agonist obtained in the presence of the antagonist are expressed as % of the control response. Each value is the mean ± s.e.mean of 3–4 experiments. *Significantly different from control, $P < 0.05$.

Effect of nifedipine on the NANC e.j.p. and responses produced by [Sar^9]SP sulphone or [βAla^8]NKA (4-10)

Nifedipine (1 μM for 30 min) blocked the action potentials superimposed on the EFS-evoked NANC e.j.p. and totally abolished contraction (Figure 6). Nifedipine also reduced the EFS-evoked NANC e.j.p.: the maximal amplitude of depolarization was 15.2 ± 3 mV and 4.7 ± 0.6 mV (70% inhibition, $n = 9$) in the absence and presence of nifedipine, respectively. In most cases (21 out of 29 strips) the NANC e.j.p. evoked by EFS (32 Hz for 1 s, 40 V, 0.2 ms) in the presence of nifedipine was biphasic, a first fast phase of e.j.p. being followed by a second slow component (Figure 6). In 8 out of 29 preparations, the e.j.p. was slow and monophasic. The total duration of the e.j.p. (measured as the duration from the onset of e.j.p. to the 90% of recovery from maximum) averaged 84 ± 9 s ($n = 13$).

Nifedipine totally abolished the action potentials and contraction evoked by [Sar^9]SP sulphone or [βAla^8]NKA(4-10) (0.3 μM and $n = 3$ for each agonist). The depolarization produced by [Sar^9]SP sulphone was inhibited by 72 ± 5% ($n = 3$) while that induced by [βAla^8]NKA(4-10) was reduced at a lesser extent (38 ± 6% inhibition, $n = 3$).

Effect of tachykinin receptor antagonists on the NANC e.j.p. in the presence of nifedipine

In the presence of nifedipine, GR 82,334 (3 μM) reduced the area of the EFS-evoked e.j.p. by 65 ± 7% ($n = 5$); GR 82,334 decreased to a similar extent the peak amplitude of the fast and slow phases of e.j.p. (63 ± 7 and 61 ± 4% inhibition, respectively, $n = 4$ and 5) (Figure 6).

GR 94,800 (3 μM) inhibited the area of the EFS-evoked e.j.p. by 48 ± 5% ($n = 3$) (Figure 6); GR 94,800 decreased to a similar extent the amplitude of the fast and slow phases of the e.j.p. (43 ± 5 and 50 ± 4% inhibition, respectively, $n = 3$).

The combined administration of GR 82,334 (3 μM) and GR 94,800 (3 μM) produced a further inhibition of the area of the EFS-evoked e.j.p. in the presence of nifedipine: only 15 ± 2% ($n = 9$) of the control response remained after 20 min of combined application of the NK_1 and NK_2 receptor antagonists (Figure 6). The combined administration of GR 82,334 and GR 94,800 decreased the peak amplitude of first and second phase of the e.j.p. by 45 ± 12 and 82 ± 4% ($n = 6$ and 7), i.e. the second slow phase of the e.j.p. was preferentially inhibited as compared to the first one.

Effect of suramin on the NANC e.j.p. in the presence of nifedipine

From the above experiments, it appears that a consistent part of the biphasic NANC e.j.p. evoked by EFS in the presence of nifedipine, and especially its fast component, is resistant to the combined blockade of NK_1 and NK_2 receptors by GR 82,334 and GR 94,800. We speculated that adenosine-triphosphate (ATP) maybe involved in this residual response. A NANC e.j.p. was evoked by train EFS (32 Hz for 1 s, 40 V, 0.2 ms pulse width, $n = 10$; Figure 7) and, in some strips ($n = 5$), also by single pulse EFS (30 V, 0.2 ms pulse width). Either suramin (100 μM for 25–30 min) was administered first and the effect of GR 82,334 plus GR 94,800 (3 μM each for 15 min) was investigated on the suramin-resistant response ($n = 6$) *or* GR 82,334 plus GR 94,800 were administered first and the effect of suramin was investigated on the response resistant to the TK receptor antagonists ($n = 4$).

The combined administration of GR 82,334 (3 μM) and GR 94,800 (3 μM) decreased the peak amplitude of the fast phase of e.j.p. in response to train EFS (37 ± 13% inhibition, $n = 4$) and remarkably reduced the area of the second slow phase (73 ± 8% inhibition, $n = 4$; Figure 7). The application of suramin (100 μM) in the presence of GR 82,334 and GR 94,800 produced a further marked inhibition of the peak amplitude of first fast phase of e.j.p. (87 ± 3% inhibition, $n = 4$) while leaving unaffected the residual area of the slow phase of e.j.p. (6 ± 8% increase, $n = 4$, Figure 7).

When applied first, suramin (100 μM) inhibited the peak amplitude of the first fast phase of the e.j.p. in response to train EFS in 4 out of 6 strips by 91 ± 2% ($n = 4$) without affecting the area of the slow phase of the e.j.p. (2 ± 15% increase, $n = 4$) (Figure 7). The combined administration of GR 82,334 and GR 94,800 (3 μM each for 15 min) in the presence of suramin (100 μM) did not affect significantly the peak amplitude of the first residual phase of e.j.p. (3 ± 9% increase, $n = 4$) but remarkably reduced the area of second slow phase of the e.j.p. (83 ± 4% inhibition, $n = 4$). It is also worth noting that suramin significantly increased (2.2 times) the latency of e.j.p.-evoked by train EFS: the latency averaged 268 ± 57 and 590 ± 83 ms ($n = 7$, $P < 0.05$) before and after suramin (100 μM), respectively.

In 2 strips, in which the e.j.p. was also biphasic in response to train EFS, suramin (100 μM) slightly increased (9%) or decreased (16%) the peak amplitude of the first phase and increased the area (35 and 22%) of the second slow phase of the e.j.p. In both cases, the e.j.p. had a large latency (590 and 400 ms, not modified by suramin) and was markedly reduced by the combined administration of GR 82,334 and GR 94,800 (82 and 91% inhibition, respectively) in the presence of suramin.

In the presence of nifedipine, single pulse EFS (30 V, 0.15 ms) evoked a fast NANC e.j.p. with an amplitude of

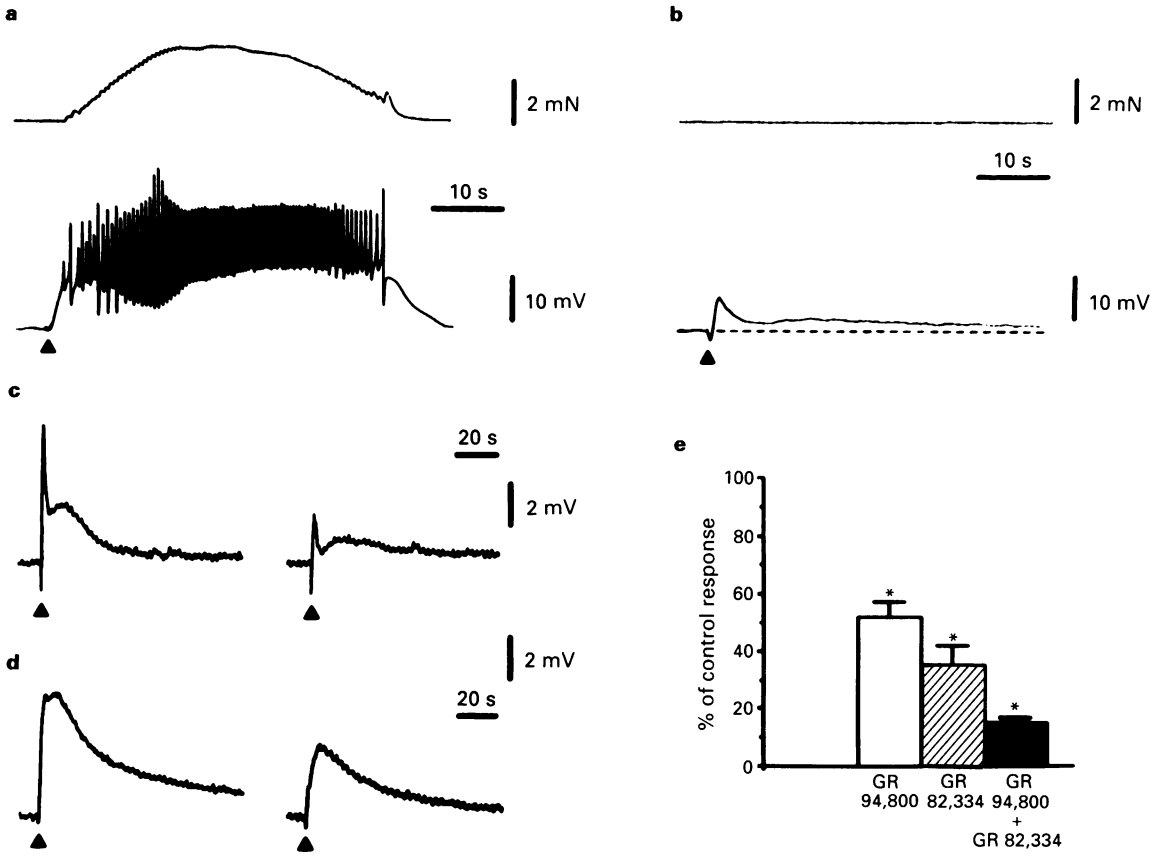

Figure 6 Effect of nifedipine on the NANC e.j.p. produced by EFS (32 Hz for 1 s, applied at arrowheads) and effect of the tachykinin NK_1 receptor antagonist, GR 82,334 and NK_2 receptor antagonist, GR 94,800 on the e.j.p. produced by EFS in the presence of nifedipine. (a and b) Electrical and mechanical responses to train EFS (32 Hz for 1 s, applied to arrowhead) in the absence (a) and presence (b) of nifedipine (1 μM); in both panels, upper tracing is muscle tension, lower tracing shows changes in membrane potential. (c) Effect of GR 82,334 (3 μM) on the nifedipine-resistant e.j.p. to train EFS (32 Hz for 1 s, applied at arrowhead); the control response to EFS is shown on the left, that obtained in the presence of GR 82,334 on the right. (d) Effect of GR 94,800 (3 μM) on the nifedipine-resistant e.j.p. to train EFS (32 Hz for 1 s, applied at arrowhead); the control response to EFS is shown on the left, that obtained in the presence of GR 94,800 on the right. (e) Effect of GR 94,800 (3 μM, open columns), GR 82,334 (3 μM, hatched columns), and combined administration of the two antagonists (solid columns) on the area of the nifedipine-resistant e.j.p. to train EFS. The area of e.j.p. obtained in the presence of antagonists is expressed as % of the control response. Each value is the mean ± s.e.mean of 3–9 experiments. *Significantly different from control response, $P < 0.05$.

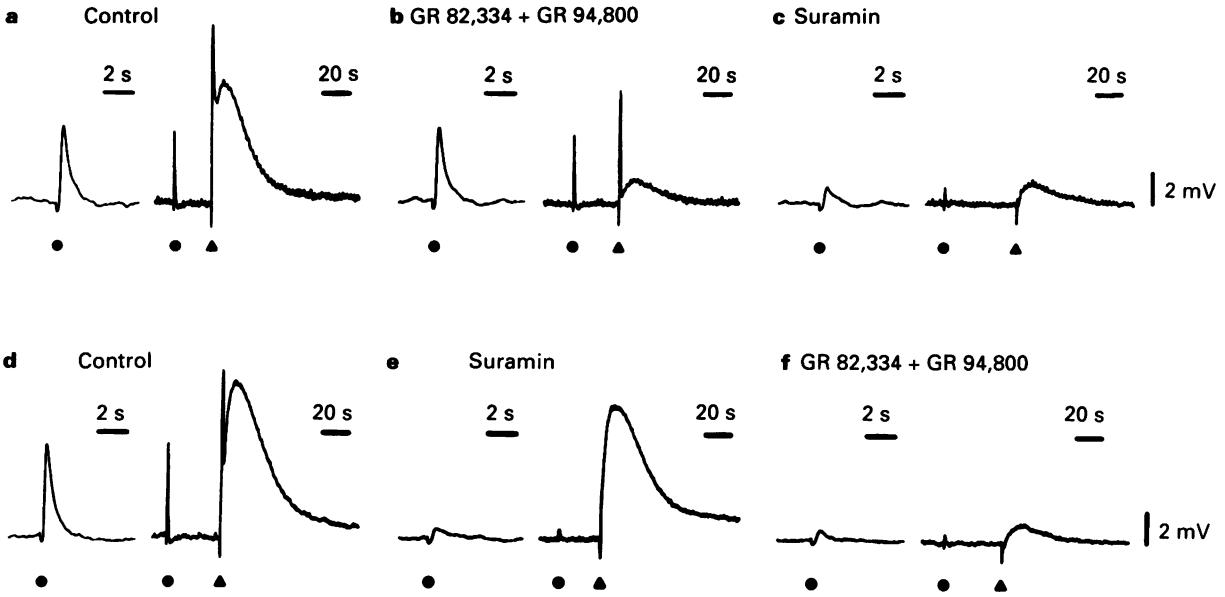

Figure 7 Effect of suramin (100 μM) and of the combined administration of tachykinin receptor antagonist GR 82,334 and GR 94,800 (3 μM each) on the e.j.p. produced by EFS in the presence of nifedipine. In each panel, dots indicate the application of single pulse EFS (30 V, 0.15 ms) and arrowheads indicate the application of train EFS (32 Hz for 1 s, 40 V, 0.25 ms). In the left part of each panel the e.j.p. produced by single pulse EFS is also shown on a magnified time scale. (a) Control responses to EFS; (b) the effect of combined administration of GR 82,334 and GR 94,800; (c) the effect of suramin in the presence of GR 82,334 and GR 94,800. (d) Control responses to EFS; (e) the effect of suramin; (f) the effect of GR 82,334 and GR 94,800 in the presence of suramin.

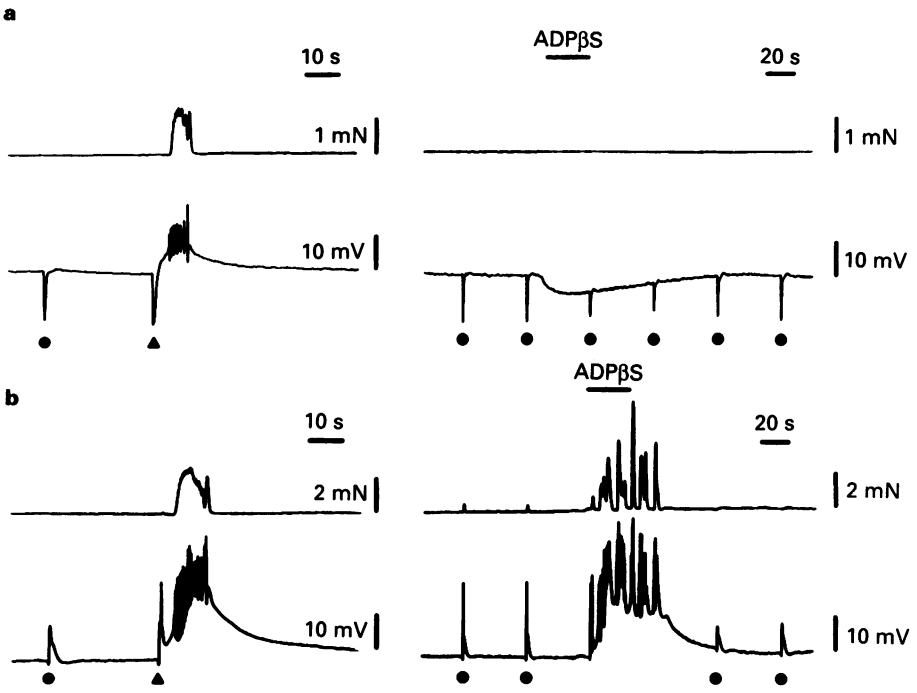

Figure 8 Effect of apamin and N^{ω}-nitro-L-arginine (L-NOARG) on the electrical and mechanical responses to EFS, junction potential and on the electrical and mechanical responses induced by ADPβS (10 μM for 30 s) in the circular muscle of the guinea-pig duodenum. Single pulse (30 V, 0.15 ms) and train EFS (32 Hz for 1 s, 40 V, 0.25 ms) were applied at dots and arrowheads, respectively. In right panels, the period of application of ADPβS is shown by horizontal bars. In each panel upper tracing shows mechanical activity and lower tracing shows changes in membrane potential. (a) Control responses to EFS and ADPβS; (b) responses obtained after 30 min combined administration of apamin (0.3 μM) and L-NOARG (30 μM). Note that, in the absence of apamin and L-NOARG (a, Krebs solution containing atropine, guanethidine and indomethacin) single pulse EFS produced a pure NANC inhibitory junction potential (i.j.p.) and train EFS produced a NANC i.j.p. followed by a NANC e.j.p. and contraction. After addition of apamin and L-NOARG, both single pulse and train EFS evoked a pure NANC e.j.p.; the e.j.p. and contraction were enhanced by administration of apamin and L-NOARG. In the absence of apamin and L-NOARG (a, Krebs solution containing atropine, guanethidine and indomethacin) the P_{2Y} receptor agonist ADPβS produced hyperpolarization of the membrane; this response was converted to depolarization with action potentials and contraction in the presence of apamin and L-NOARG (b).

4.4 ± 1.1 mV; the latency and duration of this e.j.p. were 195 ± 4 ms and 2.1 ± 0.3 s, respectively ($n = 8$). In the same strips, the amplitude of the fast component of the biphasic e.j.p. in response to train EFS averaged 6.5 ± 1.2 mV ($n = 8$). All the strips which showed a fast e.j.p. in response to single pulse EFS ($n = 8$) also showed a biphasic response to train EFS. The combined administration of GR 82,334 and GR 94,800 (3 μM each for 15 min) did not affect significantly (2 ± 4% increase, $n = 3$) the amplitude of the e.j.p. evoked by single pulse EFS. The application of suramin (100 μM for 30 min) in the presence of GR 82,334 and GR 94,800 inhibited the e.j.p. by 84 ± 6% ($n = 3$) (Figure 7). When applied first, suramin inhibited the amplitude of the e.j.p. evoked by single pulse EFS by 90 ± 3% ($n = 5$) while the combined administration of GR 82,334 and GR 94,800 did not affect the residual e.j.p. in the presence of suramin (Figure 7, $n = 5$).

Effect of suramin on the responses induced by ADP βS and [Sar⁹]SP sulphone in the absence of nifedipine

From the above, it would appear that, under certain circumstances, endogenous ATP may act via suramin-sensitive receptors as an excitatory transmitter. We then studied the effect of the selective P_{2Y} receptor agonist, ADPβS before and after blockade of NANC inhibitory transmission.

In the presence of atropine (1 μM), guanethidine (3 μM) and indomethacin (3 μM) single pulse or train (32 Hz for 1 s) EFS evoked an inhibitory junction potential (i.j.p., 16.1 ± 1.2 and 17.8 ± 1.3 mV, $n = 5$, respectively) followed by a NANC e.j.p., action potentials and contraction. The application of ADPβS (10 μM for 30 s) produced a hyperpolarization (7.8 ± 1.3 mV, $n = 5$) of the circular muscle of the guinea-pig duodenum (Figure 8). The combined administration of apamin (0.3 μM) and L-NOARG (30 μM) blocked the EFS-evoked i.j.p. and disclosed a pure NANC e.j.p. in response to train EFS in all cases tested. In 3 out of 5 strips a fast e.j.p. was also evoked by single pulse of EFS (Figure 8).

In the presence of apamin and L-NOARG, the application of ADPβS (10 μM for 30 s) induced a depolarization (7.3 ± 1.1 mV, $n = 9$), appearance of slow waves with action potentials (27.4 ± 2.2 mV, $n = 9$) and contraction (3.7 ± 0.5 mN, $n = 9$) of smooth muscle (Figures 8 and 9). The responses induced by [Sap⁹]SP sulphone (0.3 μM for 10 s) were comparable to those produced by ADPβS: depolarization (7.5 ± 1.3 mV, $n = 3$), action potentials (24.7 ± 4.3 mV, $n = 3$), contraction (2.8 ± 0.8 mN, $n = 3$, Figure 8).

After incubation with suramin (100 μM for 20–30 min), the depolarization and contraction induced by ADPβS were markedly reduced (72 ± 6 and 98 ± 8% inhibition, respectively, $n = 4$) while the responses to [Sar⁹]SP sulphone were not significantly affected (Figure 9).

Discussion

Tachykinin NK_1 and NK_2 receptors mediate NANC excitatory neurotransmission in the circular muscle of guinea-pig duodenum

The natural TKs synthesized by myenteric neurones, SP and NKA, act as full agonists at NK_1 and NK_2 receptors although with different potencies (Maggi *et al.*, 1993); they also act as full agonists at NK_3 receptors, producing neuronal excitation and release of other mediators, including acetylcholine, TKs and NO (e.g. Maggi *et al.*, 1990; 1994e). Therefore natural TKs are not suitable tools for establishing the relative role of NK_1 and NK_2 receptors in neuromuscular transmission; this can be precisely assessed by using receptor-selective agonists and antagonists. The interpretation of the findings presented in this study is based on the assumption that, at the concentrations used, GR 82,334 selectively blocked NK_1 receptors while MEN 10,627 and GR 94,800 selectively blocked NK_2 receptors. The assumption is based on the known pharmacological properties of these ligands (Hagan *et al.*, 1991; McElroy *et al.*, 1992; Patacchini *et al.*, 1994; Maggi *et al.*, 1994c) and has been further checked here by studying their action toward the responses produced by the receptor selective agonists, [Sar⁹]SP sulphone for NK_1 receptors and [βAla⁸]NKA(4-10) for NK_2 receptors (Maggi *et al.*, 1993 for review).

The present results demonstrate that NK_1 and NK_2 receptors are both involved in mediating a NANC e.j.p. and contraction in the circular muscle of the guinea-pig duodenum. This conclusion is supported by the following: (i) GR 82,334 *or* GR 94,800 and MEN 10,627 produced a

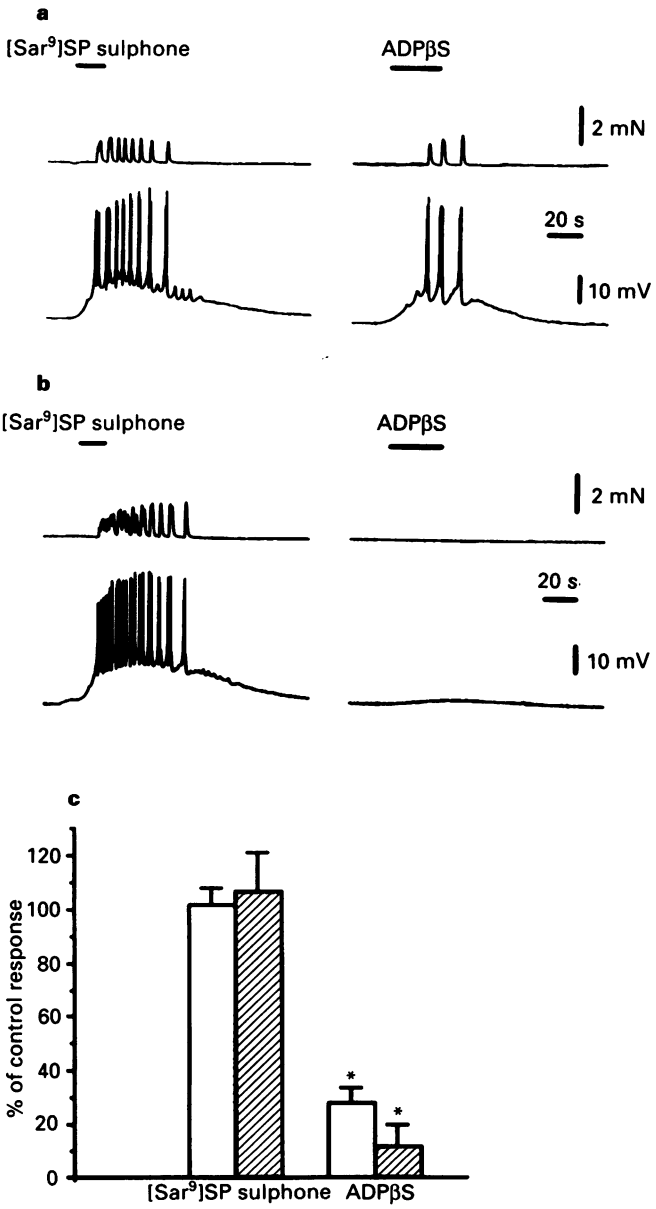

Figure 9 Effect of suramin (100 μM for 20 min) on the responses induced by ADPβS (10 μM for 30 s) and [Sar⁹]SP sulphone (0.3 μM for 10 s) in the circular muscle of the guinea-pig duodenum. (a) Control responses to ADPβS and [Sar⁹]SP sulphone; (b) responses obtained in the presence of suramin. Horizontal bars indicate the period of application of the agonist. In both panels, upper tracing shows muscle tension and lower tracing shows changes in membrane potential. (c) Effect of suramin (100 μM) on the area of depolarization (open columns) and area of contraction (hatched columns) induced by [Sar⁹]SP sulphone and ADPβS. Each value is the mean ± s.e.mean of 3–4 experiments. *Significantly different from control, $P < 0.05$.

concentration-dependent inhibition of the NANC e.j.p. and contraction evoked by EFS; (ii) GR 82,334 and GR 94,800 exerted an additive inhibitory effect on the area of the NANC e.j.p. evoked by EFS in the presence of nifedipine; (iii) GR 82,334, inhibited depolarization and contraction produced by [Sar^9]SP sulphone, without affecting that produced by [βAla^8]NKA(4-10); (iv) MEN 10,627 and GR 94,800 blocked depolarization and contraction produced by [βAla^8]NKA(4-10) but not that produced by [Sar^9]SP sulphone.

Nifedipine abolished the action potentials and totally suppressed the contraction produced by selective NK_1 and NK_2 receptor agonists in the circular muscle of the guinea-pig duodenum, similar to its effect in the guinea-pig ileum (Maggi *et al.*, 1994a). Therefore, L-type calcium channels appear essential for NANC excitation-contraction coupling throughout the guinea-pig small intestine. The experiments using receptor selective agonists demonstrate that, for a certain degree of receptor stimulation, activation of NK_1 *or* NK_2 receptor alone, via depolarization and triggering of action potentials, is sufficient to produce contraction of the guinea-pig duodenum. This does not necessarily reflect the situation occurring when endogenous TKs are released to produce the NANC e.j.p. Indeed, the inhibitory effect of GR 82,334 toward depolarization and contractility in response to EFS is almost parallel while, for both NK_2 receptor antagonists tested, contractility was preferentially inhibited. Moreover, blockade of either NK_1 or NK_2 receptor alone produced a very large inhibition of NANC contraction. We speculate that, at the relative amounts released from intramural nerves during EFS, the action exerted by the endogenous ligand(s) for NK_1 receptor (i.e. SP) could be relatively more efficient than that of the endogenous ligand(s) for NK_2 receptors (i.e. NKA) in producing depolarization. However, the activation of NK_2 receptor may contribute an amplifying mechanism, reinforcing the depolarization produced by NK_1 receptors and facilitating the attainment of threshold for action potentials and contraction. This may provide an explanation for the ability of NK_2 receptor antagonists to produce a large suppression of EFS-evoked NANC contraction while leaving a large proportion of e.j.p. unaffected (e.g. Figure 2a and 2b).

The inhibitory effect produced by NK_1 or NK_2 receptor antagonists was quite variable from one strip to another, yet examples have been found (Figure 1a and b) in which blockade of NK_1 receptor only was sufficient to produce an almost full blockade of both electrical and mechanical responses to EFS. This variability may involve differences in relative amounts of endogenous ligands for NK_1 and NK_2 receptors released from intramural nerves and/or differences in the expression of NK_1 and NK_2 receptors on smooth muscle. A further element of variability arises from the contribution of a third excitatory transmitter (see below) to the fast NANC e.j.p. evoked in the presence of L-NOARG and apamin, since this component showed quite a large variation in strips from different animals.

The relative contribution of the two TK receptors in the overall e.j.p. produced by endogenous TKs is more clearly appreciated in the presence of nifedipine which eliminated the action potentials: in the presence of nifedipine, the NK_1 and NK_2 receptor antagonists were about equieffective (65 and 48% inhibition of the area of e.j.p. by GR 82,334 and GR 94,800, respectively) in reducing the e.j.p. and their combined administration produced an additive inhibitory effect on the area of evoked depolarization (Figure 6e). Nifedipine apparently reduced in a preferential manner the relative contribution of NK_1 receptors to the NANC e.j.p., in agreement with the larger inhibitory effect of nifedipine toward the depolarization induced by the NK_1 vs. NK_2 receptor agonist.

Overall, the present findings support the view that both NK_1 and NK_2 receptors are junctionally activated during NANC e.j.p. in guinea-pig duodenum, yet the clear additivity was evident only after blockade of calcium channels. The observed differential profile of antagonism produced by GR 82,334 and MEN 10,627 *or* GR 94,800 on the electrical and mechanical components of NANC excitatory transmission may be explained by a co-operation of the signal generated by NK_1 and NK_2 receptors in attaining threshold for firing action potentials. Further studies are needed to verify this hypothesis. In any case, the pattern observed in the circular muscle of the guinea-pig duodenum differs markedly from that found in the proximal colon, where the response initiated by activation of NK_1 and NK_2 receptors shows a remarkable specialization leading to NANC excitatory responses with distinct and separate time courses and onset/offset kinetics of contraction (Zagorodnyuk *et al.*, 1993; 1994; Maggi *et al.*, 1994d).

Biphasic NANC e.j.p. in the presence of nifedipine and role of ATP as excitatory transmitter

In most strips tested in the presence of apamin, L-NOARG and nifedipine, train EFS produced a biphasic e.j.p. which involves several mediators; in some strips a fast NANC e.j.p. was also produced by single pulse EFS. These findings are strongly reminiscent of the results obtained in the circular muscle of the guinea-pig ileum, in which a biphasic e.j.p. to nerve stimulation was likewise observed (Niel *et al.*, 1983; Bywater & Taylor, 1986; Crist *et al.*, 1991). Our findings indicate that, in addition to TKs, another excitatory transmitter, possibly ATP (see below), mediates the fast NANC e.j.p. in the guinea-pig duodenum, while the slow e.j.p. is mediated almost exclusively by TKs. Various studies have implicated ATP as a mediator of the NANC i.j.p in the circular muscle of the guinea-pig intestine (e.g. Crist *et al.*, 1991; Zagorodnyuk & Maggi, 1994). In the guinea-pig duodenum, the i.j.p. evoked by EFS was totally eliminated by apamin and L-NOARG: although we did not investigate the effect of these two drugs separately, it appears conceivable that, in analogy with circular muscle of the ileum (cf. He & Goyal, 1993), apamin alone may be sufficient to block the inhibitory action of ATP. The ability of apamin to convert the hyperpolarizing effect of ATP into a depolarization was reported previously in guinea-pig intestine (Shuba & Vladimirova, 1980). The application of apamin and L-NOARG totally eliminated the NANC i.j.p. and, in parallel, converted the hyperpolarization induced by ADPβS into a depolarization. We speculate that after blockade of apamin-sensitive K channels, a depolarizing effect of endogenous ATP was unmasked, involving changes of permeability for some ions. For instance, receptor-gated, calcium permeable, nonselective cation channels are activated by ATP in vascular smooth muscle (Benham & Tsien, 1987).

The evidence for an involvement of ATP in the fast NANC e.j.p. can be summarized as follows: (i) suramin selectively reduced the fast phase of NANC e.j.p.; (ii) when tested in presence of apamin and L-NOARG, ADPβS produced depolarization and contraction; (iii) suramin selectively suppressed the electrical and mechanical responses to ADPβS without affecting that to [Sar^9]SP sulphone. Previously, we suggested that, in addition to acetylcholine and TKs, a third excitatory mediator could be involved in the ascending excitatory reflex to the circular muscle of the guinea-pig ileum, especially in the presence of apamin and L-NOARG (Maggi *et al.*, 1994b). The present findings raise the possibility that, under certain circumstances, ATP may act as excitatory mediator participating in some form of atropine-resistant neuromuscular transmission. On the other hand, the need to block NANC inhibitory mechanisms to demonstrate an ATP-mediated NANC e.j.p. casts some doubt on the physiological relevance of this mechanism.

Interestingly, the fast e.j.p. evoked by single pulse EFS in the presence of apamin and L-NOARG was inhibited by suramin while it was unaffected by the combined administration of GR 82,334 and GR 94,800; on the other hand, a

partial inhibitory effect of the TK receptor antagonists was evident on the fast e.j.p. evoked by train EFS. Therefore the fast e.j.p. to single pulse EFS may represent a pure ATP-mediated event, possibly reflecting the need of more intense stimulation for release of TKs.

In conclusion, both NK_1 and NK_2 receptors mediate NANC e.j.p. and contraction in the circular muscle of the guinea-pig duodenum, and a co-operation of the signal(s) generated by the two receptors appears important to activate the effector mechanism (L-type calcium channels) which mediates excitation-contraction coupling at this level. In the presence of apamin, L-NOARG and nifedipine, the e.j.p. evoked by a train of EFS is biphasic: the fast component involves tachykinins and another excitatory transmitter, putatively ATP; the second slow phase of e.j.p. is TK-mediated and involves both NK_1 and NK_2 receptors.

References

ARTEMENKO, D.P., BURY, V.A., VLADIMIROVA, I.A. & SHUBA, M.F. (1982). Modification of the single sucrose-gap method. *Physiol. Zhur.*, **28**, 374–380.

BARTHO, L. & HOLZER, P. (1985). Search for a physiological role of substance P in gastrointestinal motility. *Neuroscience*, **16**, 1–32.

BARTHO, L., SANTICIOLI, P., PATACCHINI, R. & MAGGI, C.A. (1992). Tachykininergic transmission to the circular muscle of the guinea-pig ileum: evidence for the involvement of NK_2 receptors. *Br. J. Pharmacol.*, **105**, 805–810.

BAUER, V. & KURIYAMA, H. (1982). The nature of noncholinergic nonadrenergic transmission in longitudinal and circular muscle of the guinea-pig ileum. *J. Physiol.*, **332**, 375–391.

BENHAM, C.D. & TSIEN, R.W. (1987). ATP receptor-operated channels permeable to Ca^{2+} in arterial smooth muscle. *Nature*, **328**, 275–277.

BERTRAND, G., CHAPAL, J., PUECH, R. & LOUBATIERES-MARIANI, M.M. (1991). Adenosine-5'-O(2-thiodiphosphate) is a potent agonist at P_2 purinoceptors mediating insulin secretion from perfused rat pancreas. *Br. J. Pharmacol.*, **102**, 627–630.

BOARD, R.M., McDONALD, T.J., BRODIN, E. & COOK, M.A. (1992). Adenosine A_1 receptors mediate inhibition of tachykinin release from perifused enteric nerve endings. *Am. J. Physiol.*, **262**, G525–531.

BROOKES, S.J.H., STEELE, P.A. & COSTA, M. (1991). Identification and immunohistochemistry of cholinergic and noncholinergic circular muscle motor neurons in the guinea-pig small intestine. *Neuroscience*, **42**, 863–878.

BUCK, S.H. & SHATZER, S.A. (1988). Agonist and antagonist binding to tachykinin peptide NK_2 receptors. *Life Sciences*, **42**, 2701–2708.

BYWATER, R.A. & TAYLOR, G.S. (1986). Noncholinergic excitatory and inhibitory junction potentials in the circular smooth muscle of the guinea-pig ileum. *J. Physiol.*, **374**, 153–164.

CRIST, J.R., HE, X.D. & GOYAL, R.K. (1991). The nature of noncholinergic membrane potential responses to transmural stimulation in guinea-pig ileum. *Gastroenterology*, **100**, 1006–1015.

DEACON, C.F., AGOSTON, D.V., NAU, R. & CONLON, J.M. (1987). Conversion of neuropeptide K to neurokinin A and vesicular colocalization of neurokinin A and substance P in neurons of the guinea-pig small intestine. *J. Neurochem.*, **48**, 141–146.

DUNN, P.M. & BLAKELEY, A.G.H. (1988). Suramin: a reversible P_2 purinoceptor antagonist in the mouse vas deferens. *Br. J. Pharmacol.*, **90**, 383–391.

HAGAN, R.M., IRELAND, S.J., BAILEY, F., McBRIDE, C., JORDAN, C.A. & WARD, P. (1991). A spirolactam conformationally-constrained analogue of physalaemin which is a peptidase resistant, selective NK_1 receptor agonist. *Br. J. Pharmacol.*, **102**, 168P.

HE, X.D. & GOYAL, R.K. (1993). Nitric oxide involvement in the peptide VIP-associated inhibitory junction potential in the guinea-pig ileum. *J. Physiol.*, **461**, 485–499.

HOLZER, P. (1984). Characterization of the stimulus-induced release of immunoreactive SP from the myenteric plexus of the guinea-pig small intestine. *Brain Res.*, **297**, 127–136.

HOLZER, P. & MAGGI, C.A. (1994). Synergistic role of muscarinic acetylcholine and tachykinin NK_2 receptors in intestinal peristalsis. *Naunyn Schmied. Arch. Pharmacol.*, **349**, 194–201.

HOLZER, P., SCHLUET, W. & MAGGI, C.A. (1993). Ascending enteric reflex contraction: roles of acetylcholine and tachykinins in relation to distension and propagation of excitation. *J. Pharmacol. Exp. Ther.*, **264**, 391–396.

HOYLE, C.H.V. (1987). A modified single sucrose gap -junction potentials and electrotonic potentials in gastrointestinal smooth muscle. *J. Pharmacol. Methods*, **18**, 219–226.

HOYLE, C.H.V., KNIGHT, G.E. & BURNSTOCK, G. (1990). Suramin antagonizes responses to P_2 purinoceptor agonists and purinergic nerve stimulation in the guinea-pig urinary bladder and taenia coli. *Br. J. Pharmacol.*, **99**, 617–621.

MAGGI, C.A., ASTOLFI, M., GIULIANI, S., GOSO, C., MANZINI, S., MEINI, S., PATACCHINI, R., PAVONE, V., PEDONE, C., QUARTARA, L., RENZETTI, A.R. & GIACHETTI, A. (1994c). MEN 10,627, a novel polycyclic peptide antagonist of tachykinin NK_2 receptors. *J. Pharmacol. Exp. Ther.*, **271**, 1489–1500.

MAGGI, C.A., PATACCHINI, R., BARTHO, L., HOLZER, P. & SANTICIOLI, P. (1994b). Tachykinin NK_1 and NK_2 receptor antagonists and atropine-resistant ascending excitatory reflex to the circular muscle of the guinea-pig ileum. *Br. J. Pharmacol.*, **112**, 161–168.

MAGGI, C.A., PATACCHINI, R., GIACHETTI, A. & MELI, A. (1990). Tachykinin receptors in the circular muscle of the guinea-pig ileum. *Br. J. Pharmacol.*, **101**, 996–1000.

MAGGI, C.A., PATACCHINI, R., MEINI, S., QUARTARA, L., SISTO, A., POTIER, E., GIULIANI, A. & GIACHETTI, A. (1994a). Comparison of tachykinin NK_1 and NK_2 receptors of the guinea-pig ileum and proximal colon. *Br. J. Pharmacol.*, **112**, 150–160.

MAGGI, C.A., PATACCHINI, R., ROVERO, P. & GIACHETTI, A. (1993). Tachykinin receptors and tachykinin receptor antagonists. *J. Autonom. Pharmacol.*, **13**, 23–93.

MAGGI, C.A., ZAGORODNYUK, V. & GIULIANI, S. (1994d). Specialization of tachykinin NK_1 and NK_2 receptors in producing fast and slow atropine-resistant neurotransmission to the circular muscle of the guinea-pig colon. *Neuroscience*, **63**, 1137–1152.

MAGGI, C.A., ZAGORODNYUK, V. & GIULIANI, S. (1994e). Tachykinin NK_3 receptor mediates NANC hyperpolarization and relaxation via NO release in the circular muscle of guinea-pig colon. *Regul. Pept.*, **53**, 259–274.

McELROY, A.B., CLEGG, S.P., DEAL, M.J., EWAN, G.B., HAGAN, R.M., IRELAND, S.J., JORDAN, C.C., PORTER, B., ROSS, B.C., WARD, P. & WHITTINGTON, A.R. (1992). Highly potent and selective heptapeptide antagonists of the neurokinin NK_2 receptor. *J. Med. Chem.*, **35**, 2582–2591.

NIEL, J.P., BYWATER, R.A. & TAYLOR, G.S. (1983). Effect of substance P on noncholinergic fast and slow post-stimulus depolarization in the guinea-pig ileum. *J. Autonom. Nerv. System*, **9**, 573–584.

PATACCHINI, R., QUARTARA, L., ASTOLFI, M., PAVONE, V., PEDONE, C., LOMBARDI, A., GIACHETTI, A. & MAGGI, C.A. (1994). MEN 10,627, a potent polycyclic peptide antagonist at tachykinin NK_2 receptors. *Br. J. Pharmacol.*, **111**, 316P.

SHUBA, M.F. & VLADIMIROVA, I.A. (1980). Effect of apamin on the electrical responses of smooth muscle to ATP and to NANC nerve stimulation. *Neuroscience*, **5**, 853–859.

STERNINI, C., ANDERSON, K., FRANTZ, G., KRAUSE, J.E. & BRECHA, N. (1989). Expression of substance P/neurokinin A encoding preprotachykinin messenger ribonucleic acids in the rat enteric nervous system. *Gastroenterology*, **97**, 348–356.

THEODORSSON, E., MEDFORS, B., HELLSTROM, P., SODER, O., ALY, A., MUSAT, A., PANJA, A.B. & JOHANSSON, C. (1991). Aspects on the role of tachykinins and VIP in control of secretion, motility and blood flow in the gut. *Adv. Exp. Med. Biol.*, **298**, 233–240.

ZAGORODNYUK, V. & MAGGI, C.A. (1994). Electrophysiological evidence for different release mechanism of ATP and NO as inhibitory NANC transmitters in guinea-pig colon. *Br. J. Pharmacol.*, **112**, 1077–1082.

ZAGORODNYUK, V., SANTICIOLI, P. & MAGGI, C.A. (1994). Tachykinin NK_1 but not NK_2 receptors mediate noncholinergic excitatory junction potential in the circular muscle of guinea-pig colon. *Br. J. Pharmacol.*, **110**, 795–803.

ZAGORODNYUK, V., SANTICIOLI, P. & MAGGI, C.A. (1994). Different calcium influx pathways mediate tachykinin contraction in circular muscle of guinea-pig colon. *Eur. J. Pharmacol.*, **255**, 9–15.

(Received September 5, 1994
Revised January 31, 1995
Accepted February 2, 1995)

British Journal of Pharmacology (1995) 115, 247-254

P_2-purinoceptor-mediated inhibition of noradrenaline release in rat atria

[1]Ivar von Kügelgen, Daniel Stoffel & Klaus Starke

Pharmakologisches Institut, Universität Freiburg, Hermann-Herder-Strasse 5, D79104 Freiburg i. Br., Germany

1 We looked for P_2-purinoceptors modulating noradrenaline release in rat heart atria. Segments of the atria were preincubated with [^{3}H]-noradrenaline and then superfused with medium containing desipramine (1 μM) and yohimbine (1 μM) and stimulated electrically, by 30 pulses/1 Hz unless stated otherwise.

2 The adenosine A_1-receptor agonist, N^6-cyclopentyl-adenosine (CPA; EC_{50} 9.7 nM) and the nucleotides, ATP (EC_{50} 6.6 μM) and adenosine-5'-O-(3-thiotriphosphate) (ATPγS; EC_{50} 4.8 μM), decreased the evoked overflow of tritium. The adenosine A_{2a}-agonist, 2-*p*-(2-carbonylethyl)-phenethylamino-5'-N-ethylcarboxamido-adenosine (CGS-21680; 0.03–0.3 μM) and the P_{2X}-purinoceptor agonist β,γ-methylene-L-ATP (30 μM) caused no change.

3 The concentration-response curve of CPA was shifted to the right by the adenosine A_1-receptor antagonist, 8-cyclopentyl-1,3-dipropyl-xanthine (DPCPX; 3 nM; apparent pK_B value 9.7) but hardly affected by the P_2-purinoceptor antagonist, cibacron blue 3GA (30 μM). In contrast, the concentration-response curves of ATP and ATPγS were shifted to the right by DPCPX (3 nM; apparent pK_B values 9.3 and 9.4, respectively) as well as by cibacron blue 3GA (30 μM; apparent pK_B values 5.0 and 5.1, respectively). Combined administration of DPCPX and cibacron blue 3GA caused a much greater shift of the concentration-response curve of ATP than either antagonist alone. The concentration-response curve of ATP was not changed by indomethacin, atropine or the 5'-nucleotidase blocker α,β-methylene-ADP.

4 Cibacron blue 3GA (30 μM) increased the evoked overflow of tritium by about 70%. The increase was smaller when the slices were stimulated by 9 pulses/100 Hz instead of 30 pulses/1 Hz.

5 The results indicate that the postganglionic sympathetic axons in rat atria possess P_2-purinoceptors in addition to the known adenosine A_1-receptor. Both mediate inhibition of noradrenaline release. Some adenine nucleotides such as ATP and ATPγS act at both receptors. The presynaptic P_2-purinoceptor seems to be activated by an endogenous ligand, presumably ATP, under the condition of these experiments. This is the first evidence for presynaptic P_2-purinoceptors at cardiac postganglionic sympathetic axons.

Keywords: Rat heart atrium; P_1-purinoceptor; P_2-purinoceptor; presynaptic purinoceptors; noradrenaline release; adenine nucleotides; ATP; adenosine-5'-O-(3-thiotriphosphate) (ATPγS); cibacron blue 3GA; suramin

Introduction

Among other locations, P_2-purinoceptors occur presynaptically at terminal noradrenergic axons. Activation of presynaptic P_2-purinoceptors of various types has been reported to *increase* the release of noradrenaline in rabbit ear artery (Miyahara & Suzuki, 1987), guinea-pig ileum (Sperlagh & Vizi, 1991), and chick cultured sympathetic neurones (Allgaier *et al.*, 1994). In mouse and rat vas deferens, rat iris and rat brain cortex, activation of presynaptic P_{2Y}-like purinoceptors *decreases* the release of noradrenaline (von Kügelgen *et al.*, 1989; 1993; 1994b,c; Fuder & Muth, 1993; Kurz *et al.*, 1993). Chick cultured sympathetic neurones possess release-inhibiting P_2-purinoceptors, not classified further, in addition to the release-enhancing receptors (Allgaier *et al.*, 1994). Some peripheral release-inhibiting P_2-purinoceptors seem to function as autoreceptors, i.e. to be activated by endogenous ATP released as postganglionic sympathetic co-transmitter of noradrenaline (Fujioka & Cheung, 1987; Fuder & Muth, 1993; Kurz *et al.*, 1993; von Kügelgen *et al.*, 1993; 1994a,b; Gonçalves & Queiroz, 1994; Grimm *et al.*, 1994).

Adenine nucleotides such as ATP exert P_2-purinoceptor-mediated effects on the heart; the force of contraction, for example, is increased (for review see Ralevic & Burnstock, 1991). We have now looked for presynaptic P_2-purinoceptors at the sympathetic axons innervating rat atria. Adenine nucleosides (Wakade & Wakade, 1978; Khan & Malik, 1980; Richardt *et al.*, 1987) and nucleotides (Khan & Malik, 1980) reduce the release of noradrenaline in the rat heart. The nucleosides act through adenosine A_1-receptors (Richardt *et al.*, 1987). The possibility of an involvement of P_2-purinoceptors in the effect of adenine nucleotides (Khan & Malik, 1980) was not (and at that time could not be) examined. Some results have been published in abstract form (Stoffel *et al.*, 1994).

Methods

Male Wistar rats weighing 240–300 g (Savo, Kisslegg, Germany) were killed by cervical dislocation and exsanguination. The atria were cut into about 14 segments of 4–6 mg (from two rats). Six atrial segments were preincubated at 37°C for 30 min in each of two vials containing 4 ml medium with (−)-[^{3}H]-noradrenaline (0.1 μM). The segments were then washed three times with [^{3}H]-noradrenaline-free medium. One segment was transferred to each of twelve superfusion chambers where it was held by a polypropylene mesh between platinum plate electrodes 4 mm apart. The tissue was superfused with [^{3}H]-noradrenaline-free medium for 144 min at 1 ml min^{-1} and 37°C. A Stimulator I (Hugo Sachs Elektronik, March-Hugstetten, Germany) operating in the constant current mode was used for electrical field stimulation. Five periods of stimulation were applied (rectangular

[1] Author for correspondence.

pulses of 1 ms width and 60 mA current strength). The first, delivered after 30 min of superfusion and consisting of 30 pulses/1 Hz, was not used for determination of tritium overflow. The following stimulation periods (S_1–S_4) began after 66, 87, 108 and 129 min of superfusion and consisted of 30 pulses/1 Hz unless stated otherwise. The collection of successive 3-min superfusate samples began 6 min before S_1. After superfusion, each tissue segment was solubilized, and tritium was measured in superfusate samples and solubilized tissues by liquid scintillation counting.

The superfusion medium contained (mM): NaCl 118, KCl 4.8, $CaCl_2$ 2.5, $MgSO_4$ 1.2, $NaHCO_3$ 25, KH_2PO_4 0.9, glucose 11, ascorbic acid 0.3 and disodium EDTA 0.03. The medium used for preincubation contained $CaCl_2$ 0.2 mM instead of 2.5 mM (see Limberger *et al.*, 1992). Media were saturated with 5% CO_2 in O_2. The pH was adjusted to 7.4 with NaOH 1 M. The superfusion but not the preincubation medium contained in addition, desipramine (1 μM) and, in most experiments, yohimbine (1 μM) in order to block uptake$_1$ and presynaptic α_2-adrenoceptors, respectively. Other drugs were present either throughout superfusion, or from 6 min before S_2 for the remainder of the experiment, or, at increasing concentrations, from 6 min before to 15 min after the onset of S_2, S_3 and S_4. The delay from addition of drug to medium to arrival at tissue was about 60 s.

The outflow of tritium was expressed as fractional rate (min^{-1}) (Kurz *et al.*, 1993). The electrically evoked overflow was calculated as the difference 'total overflow during the 9 min after onset of stimulation' minus 'estimated basal outflow'; the basal outflow was assumed to decline linearly from the 3-min interval before, to the interval 9–12 min after, onset of stimulation. The difference (total minus basal; Bq) was expressed as a percentage of the tritium content (Bq) of the tissue at the onset of stimulation. Effects of drugs that were added after S_1 on basal tritium efflux were evaluated as ratios of the fractional rate immediately before S_2, S_3 and S_4 and the fractional rate immediately before S_1 (b_n/b_1). Effects of drugs that were added after S_1 on electrically evoked overflow were evaluated as ratios of the overflow elicited by S_2, S_3 and S_4 and the overflow elicited by S_1 (S_n/S_1). S_n/S_1 ratios obtained in individual experiments in which a test compound A was added after S_1 were calculated as a percentage of the respective mean ratio in the appropriate control group (solvent instead of A). When the interaction of A, added after S_1, and a drug B, added throughout superfusion, was studied, the 'appropriate control' was a group in which B alone was used.

Where relevant, the sigmoid-shaped function No. 25 of Waud (1976) was fitted to averaged agonist concentration-inhibition data. The function yielded the maximal inhibition and the EC_{50} (concentration that caused 50% of the maximal inhibition). For concentration-inhibition data from experiments carried out in the presence of the antagonists DPCPX or cibacron blue 3GA, the maximal inhibition was fixed to that obtained in the absence of antagonist (cf. Kurz *et al.*, 1993). pK_B ($-\log K_B$) values of DPCPX and cibacron blue 3GA were calculated from the increase in EC_{50} values. Since only one antagonist concentration was used and a competitive character of the antagonism was not verified, the values are *apparent* pK_B values (cf. von Kügelgen *et al.*, 1994c).

Drugs used were: suramin hexasodium (Bayer, Wuppertal, Germany), (−)-[ring-2,5,6-^{3}H]-noradrenaline, specific activity 1.48–2.65 TBq $mmol^{-1}$ (Du Pont, Dreieich, Germany), atropine sulphate (Merck, Darmstadt, Germany), 2-*p*-(2-carbonylethyl)-phenethylamino-5′-N-ethylcarboxamido-adenosine HCl (CGS-21680), N^6-cyclopentyl-adenosine (CPA), 8-cyclopentyl-1,3-dipropylxanthine (DPCPX), β,γ-methylene-L-adenosine-5′-triphosphate tetrasodium (β,γ-methylene-L-ATP), (−)-propranolol HCl (Research Biochemicals, Biotrend, Köln, Germany), yohimbine HCl (Roth, Karlsruhe, Germany), adenosine-5′-O-(3-thiotriphosphate) tetralithium (ATPγS), ATP disodium, cibacron blue 3GA (C-9534 in Sigma catalogue 1994; isomer of reactive blue 2 in which the sulphonic acid residue at the terminal benzene ring is in the *o*-position; see footnote on p. 130 of von Kügelgen *et al.*, 1994b), desipramine HCl, indomethacin, α,β-methylene-adenosine-5′-diphosphate (α,β-methylene-ADP), tetrodotoxin (Sigma, Deisenhofen, Germany). Solutions of drugs were prepared with either distilled water, or (indomethacin) the KH_2PO_4- and $NaHCO_3$-containing stock solution of the medium, or (CGS-21680, DPCPX) dimethyl sulphoxide (final concentration about 0.1 mM), or (CPA) ethanol (final concentration about 1 mM), or (tetrodotoxin) sodium acetate buffer (0.1 M, pH 4.8). The solvents did not change basal tritium efflux or the evoked overflow. Dimethyl sulphoxide (0.1 mM) was added in all experiments throughout superfusion to make them directly comparable.

Means ± s.e.mean are given throughout. Differences between means were tested for significance by the Mann-Whitney test. $P<0.05$ or lower was taken as the criterion of statistical significance. For multiple comparisons with the same control, P levels were adjusted according to Bonferroni. n is the number of tissue pieces.

Results

Stimulation by 30 pulses/1 Hz markedly increased the outflow of tritium from atrial segments preincubated with [^{3}H]-noradrenaline (Figure 1a). When the superfusion medium contained yohimbine (1 μM) in addition to desipramine (1 μM), as in the majority of experiments, the fractional rate of efflux immediately before S_1 (b_1) averaged 0.00161 ± 0.00003 min^{-1}, corresponding to 21.6 ± 0.6 Bq min^{-1}, and the overflow at S_1 (Table 1) 1.025 ± 0.037% of the tritium content of the tissue, corresponding to 150.7 ± 8.4 Bq (n = 132). Experimentally induced changes will be mentioned below.

When solvent was administered after S_1 (6 min before S_2), the b_2/b_1, b_3/b_1, and b_4/b_1 ratios were 0.97 ± 0.01, 0.97 ± 0.01 and 0.94 ± 0.02, and S_2/S_1, S_3/S_1, and S_4/S_1 ratios 1.01 ± 0.01, 0.99 ± 0.01 and 0.98 ± 0.01, respectively (n = 12; Figure 1a). Average b_n/b_1 ratios also were slightly below unity, and S_n/S_1 ratios close to unity, when the additional compounds listed in Table 1 were present in the medium throughout superfusion and solvent was added after S_1 (not shown).

Evoked tritium overflow: adenine nucleosides and nucleotides

In an initial series of experiments, drugs were added after S_1 and then kept at a constant concentration. Tetrodotoxin (0.3 μM) abolished the evoked overflow of tritium (Figure 2a). The adenosine A_1-receptor agonist CPA (0.3 μM; Williams *et al.*, 1986) as well as the nucleotides ATP (30 and 300 μM) and ATPγS (30 μM), a metabolically more stable analogue (Welford *et al.*, 1986), caused marked inhibition which was approximately constant from S_2, after 6 min of exposure, to S_4, after 48 min of exposure (Figure 2). No change was observed with the adenosine A_{2a}-agonist, CGS-21680 (0.03 and 0.3 μM; Jarvis *et al.*, 1989; Figure 2a) and the metabolically stable P_{2X}-selective ATP analogue β,γ-methylene-L-ATP (30 μM; Hourani *et al.*, 1986; Figure 2c).

When added after S_1 at increasing concentrations, CPA, ATP and ATPγS reduced the evoked overflow of tritium in a concentration-dependent manner (ATP in Figure 1b; concentration-inhibition curves in Figures 3 to 5, open symbols). The EC_{50} values (maximal inhibitions) were 9.7 nM (89%) for CPA, 6.6 μM (95%) for ATP, and 4.8 μM (88%) for ATPγS.

Evoked tritium overflow: interactions

Drugs tested for their interaction with CPA, ATP and ATPγS were added throughout superfusion (in addition to desipramine and yohimbine). When thus applied, the

adenosine A_1-receptor antagonist, DPCPX (3 nM; Bruns *et al.*, 1987; Lohse *et al.*, 1987) slightly increased the overflow evoked by S_1 (Table 1). It shifted the concentration-inhibition curves of CPA, ATP and ATPγS to the right by similar degrees (Figure 3; solid symbols). The shifts correspond to apparent pK_B values of DPCPX against CPA, ATP and ATPγS of 9.7, 9.3 and 9.4, respectively.

The P_2-purinoceptor antagonist, cibacron blue 3GA (30 μM; Kerr & Krantis, 1979; Fuder & Muth, 1993; see footnote in von Kügelgen *et al.*, 1994b) increased the

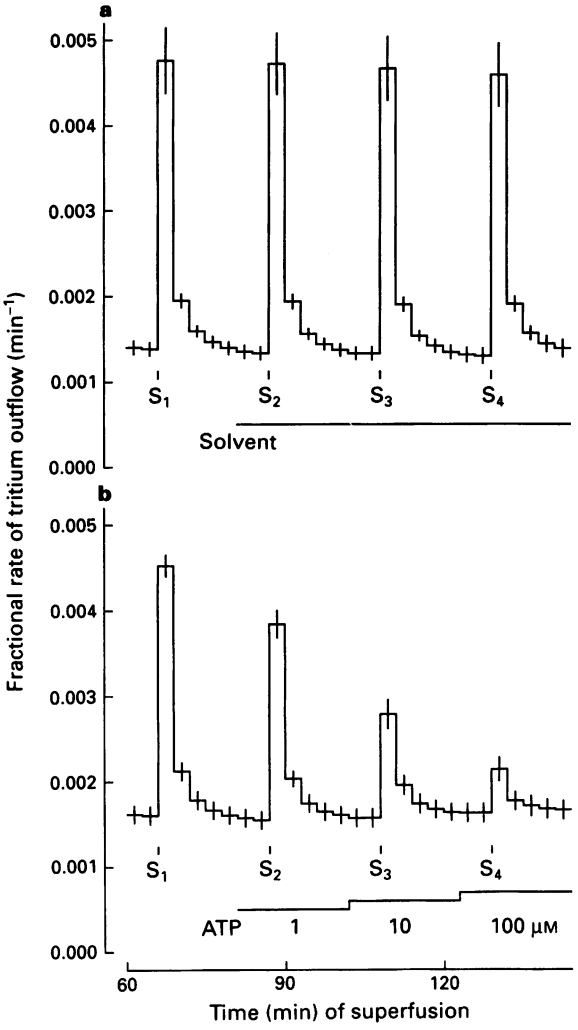

Figure 1 Time course of tritium outflow from segments of rat atria and effect of ATP. After preincubation with [^{3}H]-noradrenaline, tissue segments were superfused with medium containing desipramine (1 μM) and yohimbine (1 μM). They were stimulated four times by 30 pulses/1 Hz (S_1–S_4). Solvent (a; $n = 12$) or ATP (b; $n = 10$) was added as indicated.

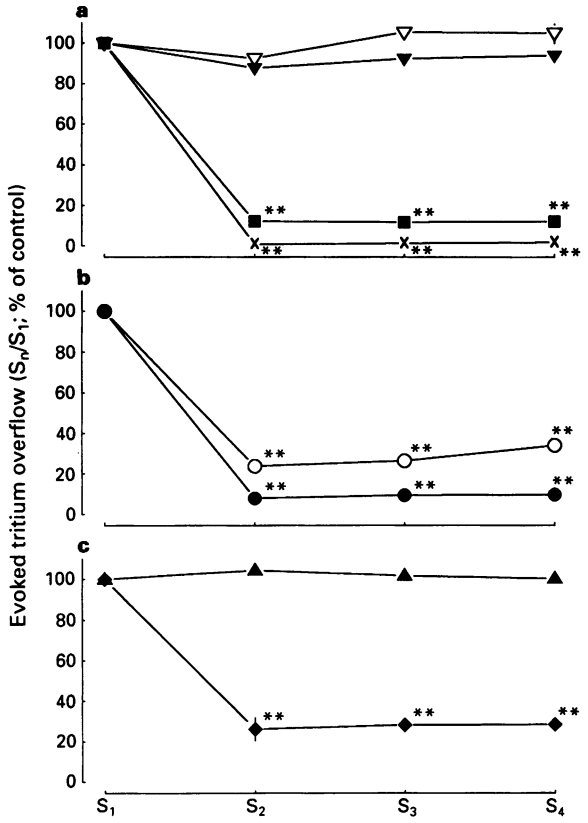

Figure 2 Effects of purinoceptor agonists and tetrodotoxin on electrically evoked overflow of tritium. After preincubation with [^{3}H]-noradrenaline, atrial segments were superfused with medium containing desipramine (1 μM) and yohimbine (1 μM). They were stimulated four times by 30 pulses/1 Hz (S_1–S_4). 2-*p*-(2-Carbonyethyl)-phenethylamino-5′-N-ethylcarboxamido-adenosine (CGS-21680; ▽ 0.03 and ▼ 0.3 μM; a), N^6-cyclopentyl-adenosine (CPA; ■ 0.3 μM; a), tetrodotoxin (×, 0.3 μM; a), ATP (○ 30 and ● 300 μM; b), β,γ-methylene-L-ATP (▲ 30 μM; c) or adenosine-5′-O-(3-thiotriphosphate) (ATPγS; ◆ 30 μM; c) was added 6 min before S_2 for the remainder of the experiment. Ordinates, evoked tritium overflow: S_n/S_1 ratios obtained in individual tissue segments were calculated as percentage of the corresponding average control S_n/S_1 ratio. Means ± s.e.mean from 4–11 tissue segments. Significant differences from corresponding control: $^{**}P < 0.01$.

Table 1 Electrically evoked tritium overflow (S_1)

Drugs present throughout superfusion	*Overflow evoked by S_1* (% of tissue tritium)	n
–	1.025 ± 0.037	132
DPCPX 3 nM	1.272 ± 0.046**	48
Cibacron blue 3GA 30 μM	1.914 ± 0.057**	43
Cibacron blue 3GA 30 μM[a]	1.465 ± 0.151*	24
DPCPX 3 nM + cibacron blue 3GA 30 μM	2.142 ± 0.135**	16
α,β-Methylene-ADP 100 μM	1.228 ± 0.125	11
Indomethacin 10 μM	1.263 ± 0.082*	24
Indomethacin 10 μM + cibacron blue 3GA 30 μM	1.795 ± 0.090**	24
Atropine 1 μM	1.631 ± 0.097**	20
Indomethacin 10 μM + atropine 1 μM + propranolol 1 μM + DPCPX 3 nM	1.359 ± 0.071**	12

After preincubation with [^{3}H]-noradrenaline, atrial segments were superfused with medium containing the drugs indicated (in addition to desipramine, 1 μM, and yohimbine, 1 μM, which were also present throughout superfusion). S_1 was applied after 66 min of superfusion and consisted of 30 pulses/1 Hz. DPCPX, 8-cyclopentyl-1,3-dipropylxanthine. Means ± s.e.mean from *n* tissue segments.
[a]Current strength 30 instead of 60 mA.
Significant differences from experiments, shown in first line, in which only desipramine and yohimbine were present: $^*P < 0.05$ and $^{**}P < 0.01$.

overflow at S_1 by 87% (Table 1). It caused little if any change in the concentration-response curve of CPA but shifted the curves of ATP and ATPγS clearly to the right (Figure 4; solid symbols). Apparent pK_B values of cibacron blue 3GA against ATP and ATPγS were 5.0 and 5.1, respectively.

An increase in transmitter release may *per se* attenuates the modulation of release through presynaptic receptors, irrespective of the cause of the increase (see p. 926 of Starke *et al.*, 1989). Therefore, in some experiments with cibacron blue 3GA (30 μM) the current strength was lowered from 60 to 30 mA in order to bring the reference overflow, at S_1, in the presence of cibacron blue 3GA, closer to values obtained in the absence of the antagonist (Table 1). Cibacron blue 3GA 30 μM shifted the concentration-inhibition curve of ATP to the right despite the S_1 adjustment (compare Figure 4b and 4d), indicating that the shift was in fact due to blockade of P_2-purinoceptors rather than to the increase in transmitter release *per se* (see von Kügelgen *et al.*, 1992). [We did not determine a concentration-inhibition curve of ATP at 30 mA in the absence of cibacron blue 3GA; from all that is known on presynaptic receptors it would lie to the left of the curve determined at 60 mA (p. 102 of Starke, 1987), so the shift by cibacron blue 3GA would be even more pronounced than shown in Figure 4d.]

Combined administration of cibacron blue 3GA (30 μM) and DPCPX (3 nM) enhanced the overflow evoked by S_1 by 109% (Table 1) and shifted the concentration-response curve of ATP beyond the shifts caused by DPCPX alone (Figure 3b) and cibacron blue 3GA alone (Figure 4b). The shift beyond that produced by DPCPX alone (Figure 3b) corresponds to an apparent pK_B of cibacron blue 3GA against ATP of 4.7, close to the 5.0 obtained in the absence of DPCPX (Figure 4b).

Further interaction experiments were carried out in search for possible mediators of the inhibitory effect of ATP. α,β-Methylene-ADP (100 μM) was used to block 5'-nucleotidase (Fredholm *et al.*, 1982; Fleetwood & Gordon, 1987; Borst & Schrader, 1991), the enzyme that catalyses the dephosphorylation of AMP to adenosine. α,β-Methylene-ADP did not change S_1 (Table 1) and did not affect the concentration-response curve of ATP (Figure 5a). Indomethacin (10 μM) and atropine (1 μM) were used at concentrations known to block the synthesis of prostaglandins in the heart (Starke *et al.*, 1977; Khan & Malik, 1980) and presynaptic muscarinic receptors (Fozard & Muscholl, 1972), respectively. Both increased the overflow at S_1 (Table 1), possibly by removing a presynaptic inhibition by prostaglandins and acetylcholine (see Fuder & Muscholl, 1995). Neither indomethacin (Figure

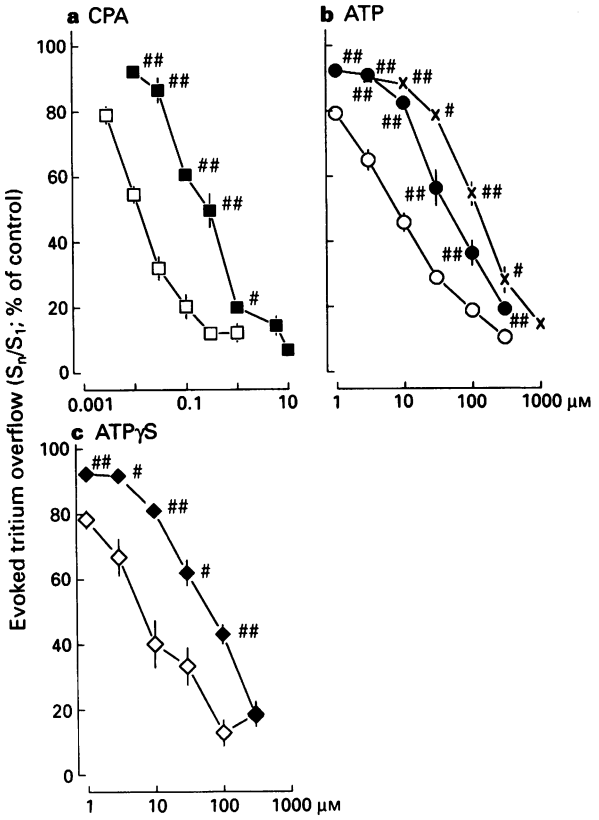

Figure 3 Interaction of purinoceptor agonists with 8-cyclopentyl-1,3-dipropylxanthine (DPCPX) or cibacron blue 3GA combined with DPCPX. After preincubation with [^{3}H]-noradrenaline, atrial segments were superfused with medium containing desipramine (1 μM) and yohimbine (1 μM). They were stimulated four times by 30 pulses/1 Hz (S_1–S_4). N^6-cyclopentyl-adenosine (CPA, a), ATP (b) or adenosine-5'-O-(3-thiotriphosphate) (ATPγS, c) was added at increasing concentrations from 6 min before to 15 min after onset of S_2, S_3 and S_4. Open symbols, experiments in which CPA, ATP or ATPγS was given alone; solid symbols, experiments in which medium contained DPCPX (3 nM) throughout superfusion; (×) experiments in which medium contained both DPCPX (3 nM) and cibacron blue 3GA (30 μM) throughout superfusion (b). Ordinates, evoked tritium overflow: S_n/S_1 ratios obtained in individual tissue segments were calculated as percentage of the corresponding average control S_n/S_1 ratio. Means ± s.e.mean from 4–10 tissue segments. Significant differences from experiments in which CPA, ATP or ATPγS was given alone: $^{\#}P<0.05$ and $^{\#\#}P<0.01$.

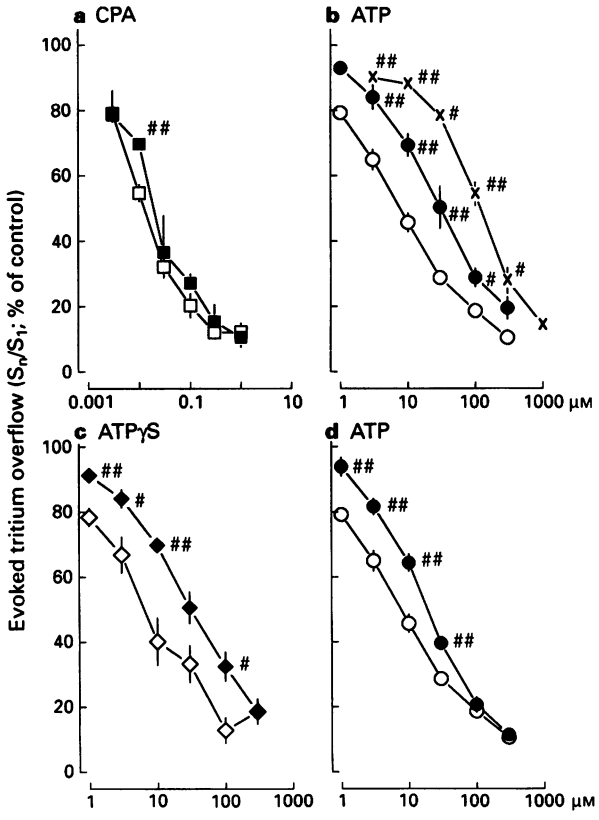

Figure 4 Interaction of purinoceptor agonists with cibacron blue 3GA or 8-cyclopentyl-1,3-dipropylxanthine (DPCPX) combined with cibacron blue 3GA. Open symbols, experiments in which N^6-cyclopentyl-adenosine (CPA, a), ATP (b and d) or adenosine-5'-O-(3-thiotriphosphate) (ATPγS, c) was given alone (identical with Figure 3); solid symbols, experiments in which medium contained cibacron blue 3GA (30 μM) throughout superfusion; (×) experiments in which medium contained both cibacron blue 3GA (30 μM) and DPCPX (3 nM) throughout superfusion (b; identical with (×) in Figure 3b). In some experiments in which cibacron blue 3GA was tested against ATP the current strength for electrical stimulation was reduced from 60 to 30 mA (solid symbols in d). Means ± s.e.mean from 4–11 tissue segments. Other details as in Figure 3.

5b) nor atropine (Figure 5c) changed the concentration-response curve of ATP. Cibacron blue 3GA (30 μM) shifted the concentration-response curve of ATP to the right also in the presence of indomethacin (10 μM; Figure 5b). The combination of indomethacin and cibacron blue 3GA increased the overflow of tritium at S_1 as did each compound alone (Table 1).

Evoked tritium overflow: purinoceptor antagonists

Effects of purinoceptor antagonists on the evoked overflow of tritium were already observed when they were present throughout superfusion (S_1; Table 1). However, drug effects are better assessed in this kind of experiment when the drugs are given after S_1 so that S_1 is the reference for each tissue segment (von Kügelgen *et al.*, 1994b). Cibacron blue 3GA 30 μM, when thus administered in desipramine- and yohimbine-containing medium, increased the overflow of tritium evoked by 30 pulses/1 Hz by 67% (Table 2), similar to the 87% increase of S_1 when cibacron blue 3GA was applied throughout superfusion (Table 1). The P_2-purinoceptor antagonist, suramin (300 μM; Dunn & Blakeley, 1988) increased the evoked overflow by 9% only (Table 2). DPCPX (3 nM) caused no change (Table 2), and this questions the relevance of the slight increases in S_1 observed when DPCPX was present throughout superfusion.

Cibacron blue 3GA 30 μM increased the overflow of tritium evoked by 30 pulses/1 Hz to a similar extent, namely by 72.6 ± 7.4%, when the medium contained indomethacin (10 μM), atropine (1 μM), propranolol (1 μM) and DPCPX (3 nM) in addition to desipramine and yohimbine throughout superfusion ($n = 6$; protocol of Table 2; S_1 in Table 1).

Cibacron blue 3GA also increased the tritium overflow evoked by 30 pulses/1 Hz, and DPCPX also failed to cause a significant change, when yohimbine was omitted from the medium (Table 2). In these experiments the overflow at S_1 was 0.316 ± 0.019% of the tritium content of the tissue ($n = 24$), about one third of that observed in presence of desipramine and yohimbine (Table 1). Accordingly, yohimbine (1 μM) increased the overflow evoked by 30 pulses/1 Hz about threefold when added after S_1 to previously yohimbine-free medium (Table 2).

Finally, trains consisting of 9 pulses/100 Hz were used for stimulation (Table 2). The overflow of tritium elicited by S_1 was 0.217 ± 0.014% of tissue tritium ($n = 24$). DPCPX and yohimbine did not affect the evoked overflow. Cibacron blue 3GA caused an increase by 38%, significantly ($P < 0.01$) less than in slices stimulated by trains of 30 pulses/1 Hz (Table 2).

Basal tritium efflux

None of the drugs, whether present throughout superfusion (in addition to desipramine) or added after S_1, changed significantly the basal efflux of tritium, with two exceptions: ATP (100 μM) caused a slight increase (see Figure 1b), and DPCPX (3 nM), when present throughout superfusion, caused a small decrease (not shown).

Discussion

The electrically evoked overflow of tritium in experiments of this kind reflects action potential-induced, neural release of [^{3}H]-noradrenaline (cf. for rat heart Fuder *et al.*, 1982). The

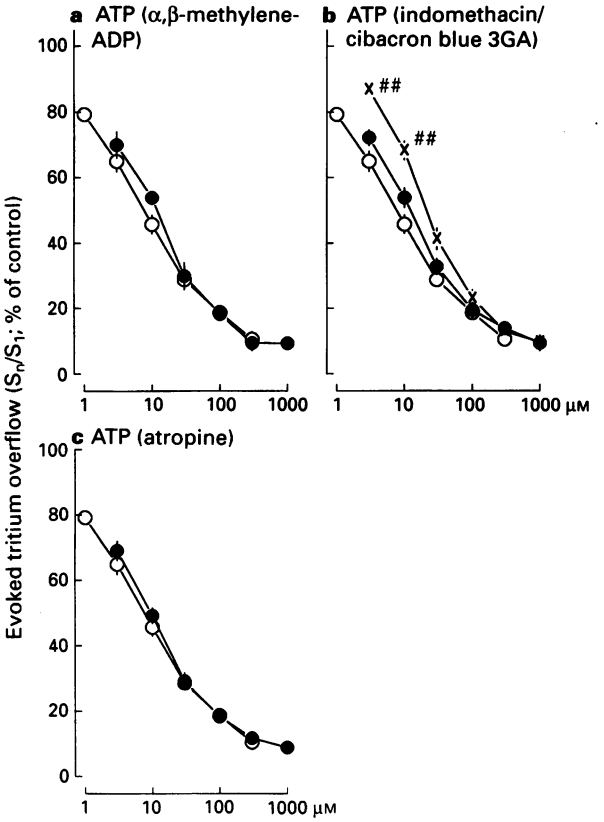

Figure 5 Interaction of ATP with α,β-methylene-ADP, indomethacin or indomethacin combined with cibacron blue 3GA, and atropine. Open symbols, experiments in which ATP was given alone (identical with Figure 3); solid symbols, experiments in which medium contained α,β-methylene-ADP (100 μM; a), indomethacin (10 μM; b) or atropine (1 μM; c) throughout superfusion; (×) experiments in which medium contained both indomethacin (10 μM) and cibacron blue 3GA (30 μM) throughout superfusion (b). Means ± s.e.mean from 4–11 tissue segments. Other details as in Figure 3.

Table 2 Effects of purinoceptor antagonists and yohimbine on electrically evoked tritium overflow

Drugs added 6 min before S_2	*Evoked tritium overflow* (S_2 to S_4/S_1; % of control) 30 p/1 Hz Yohimbine (1 μM) present	30 p/1 Hz No yohimbine	9 p/100 Hz No yohimbine
–	100.0 ± 0.9 (6)	100.0 ± 2.9 (6)	100.0 ± 5.0 (6)
DPCPX 3 nM	103.9 ± 3.8 (5)	107.8 ± 3.9 (6)	108.5 ± 6.0 (6)
Cibacron blue 3GA 30 μM	166.9 ± 5.1 (5)*	191.2 ± 11.5 (6)**	138.0 ± 9.5 (6)*
Suramin 300 μM	108.6 ± 1.7 (6)**	–	–
Yohimbine 1 μM	–	326.1 ± 23.1 (6)**	110.7 ± 4.5 (5)

After preincubation with [^{3}H]-noradrenaline, atrial segments were superfused with medium containing desipramine (1 μM) and, where indicated in heading, yohimbine (1 μM). They were stimulated electrically four times (S_1–S_4) at pulse numbers and frequencies indicated. 8-Cyclopentyl-1,3-dipropylxanthine (DPCPX), cibacron blue 3GA, suramin or yohimbine was added 6 min before S_2 for the remainder of the experiment. Ratios 'average overflow at S_2 to S_4 over overflow at S_1' obtained in individual tissue segments were calculated as a percentage of the corresponding average control ratio. Means ± s.e.mean from (n) tissue segments.
Significant differences from corresponding control (first line): *$P < 0.05$ and **$P < 0.01$.

medium contained desipramine (1 μM) and in most experiments yohimbine (1 μM), thus ensuring that changes in evoked tritium overflow caused by purinoceptor ligands were not due to an interference with uptake$_1$ or α_2-adrenoceptors.

Presynaptic adenosine A_1-receptors

Our experiments confirm the operation of release-inhibiting P_1-purinoceptors of the A_1-subtype at the sympathetic terminal axons in rat heart (see Introduction). In accord with this assumption, only the A_1-receptor agonist, CPA, but not the A_{2a}-receptor agonist, CGS-21680 affected the release of noradrenaline. Moreover, the adenosine A_1-receptor antagonist, DPCPX shifted the concentration-response curve of CPA to the right with an apparent pK_B value (9.7) close to values found at presynaptic A_1-receptors in other rat tissues (9.3–9.8; Sebastião *et al.*, 1990; Fuder *et al.*, 1992; Kurz *et al.*, 1993; von Kügelgen *et al.*, 1994c). The release-inhibiting P_1-purinoceptors at the sympathetic axons of guinea-pig papillary muscles also belong to the A_1-subtype (Schütz *et al.*, 1991).

The presynaptic A_1-receptors also mediated part of the inhibition caused by adenine nucleotides. DPCPX shifted the concentration-response curves of ATP and ATPγS to the right with apparent pK_B values (9.3 and 9.4) similar to the pK_B against CPA (9.7). Blockade of 5'-nucleotidase by α,β-methylene-ADP did not change the inhibition produced by ATP, indicating that breakdown to adenosine was not necessary for the effect. The result supports previous conclusions that some adenine nucleotides activate adenosine (A_1)-receptors directly (noradrenergic axons: von Kügelgen *et al.*, 1992; 1994b,c; Fuder & Muth, 1993; Kurz *et al.*, 1993; non-noradrenergic axons: Moody *et al.*, 1984; Wiklund *et al.*, 1985; Rubino *et al.*, 1992; non-neural cells: Collis & Pettinger, 1982; Bailey *et al.*, 1992). The common presynaptic receptor for adenine nucleosides and nucleotides at the sympathetic fibres of rat tail artery and rabbit vas deferens has been proposed to be a new 'hybrid' P_3-purinoceptor (Shinozuka *et al.*, 1988; Todorov *et al.*, 1994). In rat atria, the identical pK_B values of DPCPX against CPA, ATP and ATPγS (9.3–9.7; see above) indicate that the presynaptic receptor is the classical adenosine A_1-receptor (compare von Kügelgen *et al.*, 1992; 1994c; Kurz *et al.*, 1993).

Presynaptic P_2-purinoceptors

Presynaptic A_1-receptors were not the only site of inhibition by ATP and ATPγS: there was an additional, P_2-purinoceptor, site. The P_2 antagonist, cibacron blue 3GA, hardly changed the effect of CPA, but clearly shifted the concentration-inhibition curves of ATP and ATPγS to the right, with apparent pK_B values (5.0 and 5.1) close to those found at the presynaptic P_2-purinoceptors in rat iris (4.7; Fuder & Muth, 1993) and brain cortex (5.0; von Kügelgen *et al.*, 1994c). Cibacron blue 3GA produced a similar shift (apparent pK_B 4.7) when tested in combination with DPCPX (beyond the shift caused by DPCPX alone), as predicted from theory when there are two different receptors for an agonist. Atropine failed to change the effect of ATP, thus excluding a cholinergic link. Indomethacin also did not alter the effect of ATP (confirming Khan & Malik, 1980), and cibacron blue 3GA shifted the concentration-inhibition curve of ATP even in the presence of indomethacin, although the shift was somewhat reduced; at least the major part of the inhibition by ATP, therefore, was independent of cyclo-oxygenase products. In all likelihood, the P_2-purinoceptors are located at the sympathetic terminal axons themselves. Co-existence of presynaptic A_1- and P_2-purinoceptors has also been found in mouse and rat vas deferens, rat iris and rat brain cortex (von Kügelgen *et al.*, 1989; 1994b,c; Fuder & Muth, 1993; Kurz *et al.*, 1993).

The P_2-purinoceptors at the noradrenergic axons of mouse and rat vas deferens, rat iris and rat brain cortex are P_{2Y}-like (von Kügelgen *et al.*, 1989; 1993; 1994b,c; Fuder & Muth, 1993; Kurz *et al.*, 1993). The lack of any effect of the highly selective P_{2x}-purinoceptor agonist β,γ-methylene-L-ATP and the similarity of the pK_B values of cibacron blue 3GA in rat atria, iris and brain cortex (see above) suggest the same for rat atria.

Endogenous input

The P_2-purinoceptors at the postganglionic sympathetic axons innervating mouse, rat and rabbit vas deferens, rat iris, rat tail artery and guinea-pig saphenous artery seem to be autoreceptors, i.e. to be activated by an endogenous ligand, presumably ATP, released as cotransmitter of noradrenaline (see Introduction). The present results suggest the same for rat atria: cibacron blue 3GA and, although to a much smaller extent, suramin, but not (or not consistently) DPCPX, increased the release of [^{3}H]-noradrenaline. The increase by cibacron blue 3GA was observed in the combined presence of desipramine, yohimbine, atropine, DPCPX, indomethacin and propranolol, thus excluding the uptake$_1$ carrier, α_2-adrenoceptors, muscarinic receptors, adenosine A_1-receptors, cyclo-oxygenase and β-adrenoceptors as potential sites of, or links in, the action of cibacron blue 3GA. Also in accord with an autoreceptor role is the dependence of the increase on the stimulation conditions: it was larger for relatively long (30 pulses/1 Hz) than for very short pulse trains (9 pulses/100 Hz); similar conditions of operation have been established for the P_2-autoreceptors in mouse and rat vas deferens (von Kügelgen *et al.*, 1993; 1994b) as well as for other presynaptic autoreceptors (Starke *et al.*, 1989; α_2-autoreceptors in rat atria: Limberger *et al.*, 1992).

However, alternative sources of the endogenous agonist have to be taken into consideration. Adenine nucleotides are released from postganglionic parasympathetic in addition to sympathetic axon terminals (see Burnstock, 1990; von Kügelgen & Starke, 1991; Hoyle, 1992; Zimmermann, 1994) as well as from non-neural cells such as, in the heart, cardiomyocytes and endocardial cells (Paddle & Burnstock, 1974; Fredholm *et al.*, 1982; Borst & Schrader, 1991). Antagonism against ATP coming from these cells may have contributed to the increase of [^{3}H]-noradrenaline release caused by cibacron blue 3GA and suramin. Hypoxia greatly increases the release of ATP from cardiac non-neural cells (Paddle & Burnstock, 1974; Borst & Schrader, 1991). Whether responding to cotransmitter ATP, ATP from parasympathetic axons, or ATP of non-neural origin, the P_2-purinoceptors at cardiac sympathetic axon terminals will mediate inhibition of noradrenaline release and therefore, like the presynaptic A_1-receptors (see Richardt *et al.*, 1987), may protect the heart from sympathetic overdrive. Activation of excitatory soma-dendritic P_2-purinoceptors at the cholinergic neurones of the heart (Fieber & Adams, 1991) would act in the same direction.

The study was supported by the Deutsche Forschungsgemeinschaft (SFB 325). We thank Prof. H.J. Ruoff (Bayer, Fachbereich Klinische Forschung, Wuppertal, Germany) and Merck (Darmstadt, Germany) for drugs.

References

ALLGAIER, C., PULLMANN, F., SCHOBERT, A., VON KÜGELGEN, I. & HERTTING, G. (1994). P_2 purinoceptors modulating noradrenaline release from sympathetic neurons in culture. *Eur. J. Pharmacol.*, **252**, R7–R8.

BAILEY, S.J., HICKMAN, D. & HOURANI, S.M.O. (1992). Characterization of P_1-purinoceptors mediating contraction of the rat colon muscularis mucosae. *Br. J. Pharmacol.*, **105**, 400–404.

BORST, M.M. & SCHRADER, J. (1991). Adenine nucleotide release from isolated perfused guinea pig hearts and extracellular formation of adenosine. *Circ. Res.*, **68**, 797–806.

BRUNS, R.F., FERGUS, J.H., BADGER, E.W., BRISTOL, J.A., SANTAY, L.A., HARTMAN, J.D., HAYS, S.J. & HUANG, C.C. (1987). Binding of the A_1-selective adenosine antagonist 8-cyclopentyl-1,3-dipropylxanthine to rat brain membranes. *Naunyn-Schmied. Arch. Pharmacol.*, **335**, 59–63.

BURNSTOCK, G. (1990). Co-transmission. *Arch. Int. Pharmacodyn.*, **304**, 7–33.

COLLIS, M.G. & PETTINGER, S.J. (1982). Can ATP stimulate P_1-receptors in guinea-pig atrium without conversion to adenosine? *Eur. J. Pharmacol.*, **81**, 521–529.

DUNN, P.M. & BLAKELEY, A.G.H. (1988). Suramin: a reversible P_2-purinoceptor antagonist in the mouse vas deferens. *Br. J. Pharmacol.*, **93**, 243–245.

FIEBER, L.A. & ADAMS, D.J. (1991). Adenosine triphosphate-evoked currents in cultured neurones dissociated from rat parasympathetic cardiac ganglia. *J. Physiol.*, **434**, 239–256.

FLEETWOOD, G. & GORDON, J.L. (1987). Purinoceptors in the rat heart. *Br. J. Pharmacol.*, **90**, 219–227.

FOZARD, J.R. & MUSCHOLL, E. (1972). Effects of several muscarinic agonists on cardiac performance and the release of noradrenaline from sympathetic nerves of the perfused rabbit heart. *Br. J. Pharmacol.*, **45**, 616–629.

FREDHOLM, B.B., HEDQVIST, P., LINDSTRÖM, K. & WENNMALM, M. (1982). Release of nucleosides and nucleotides from the rabbit heart by sympathetic nerve stimulation. *Acta Physiol. Scand.*, **116**, 285–295.

FUDER, H., BRINK, A., MEINCKE, M. & TAUBER, U. (1992). Purinoceptor-mediated modulation by endogenous and exogenous agonists of stimulation-evoked [^{3}H]noradrenaline release on rat iris. *Naunyn-Schmied. Arch. Pharmacol.*, **345**, 417–423.

FUDER, H. & MUSCHOLL, E. (1995). Heteroreceptor-mediated modulation of noradrenaline and acetylcholine release from peripheral nerves. *Rev. Physiol. Biochem. Pharmacol.*, **126**, 265–412.

FUDER, H. & MUTH, U. (1993). ATP and endogenous agonists inhibit evoked [^{3}H]-noradrenaline release in rat iris via A_1- and P_{2Y}-like purinoceptors. *Naunyn-Schmied. Arch. Pharmacol.*, **348**, 352–357.

FUDER, H., SIEBENBORN, R. & MUSCHOLL, E. (1982). Nicotine receptors do not modulate the ^{3}H-noradrenaline release from the isolated rat heart evoked by sympathetic nerve stimulation. *Naunyn-Schmied. Arch. Pharmacol.*, **318**, 301–307.

FUJIOKA, M. & CHEUNG, D.W. (1987). Autoregulation of neuromuscular transmission in the guinea-pig saphenous artery. *Eur. J. Pharmacol.*, **139**, 147–153.

GONÇALVES, J. & QUEIROZ, M.G. (1994). Endogenous purines modulate noradrenaline release in the rat tail artery via A_{2A} and P_2 purinoceptors. *Drug Devel. Res.*, **31**, 274.

GRIMM, U., FUDER, H., MOSER, U., BÄUMERT, H.G., MUTSCHLER, E. & LAMBRECHT, G. (1994). Characterization of the prejunctional muscarinic receptors mediating inhibition of evoked release of endogenous noradrenaline in rabbit isolated vas deferens. *Naunyn-Schmied. Arch. Pharmacol.*, **349**, 1–10.

HOURANI, S.M.O., LOIZOU, G.D. & CUSACK, N.J. (1986). Pharmacological effects of L-AMP-PCP on ATP receptors in smooth muscle. *Eur. J. Pharmacol.*, **131**, 99–103.

HOYLE, C.H.V. (1992). Transmission: purines. In *Autonomic Neuroeffector Mechanisms*. ed. Burnstock, G. & Hoyle, C.H.V. pp. 367–407. Chur: Harwood.

JARVIS, M.F., SCHULZ, R., HUTCHISON, A.J., DO, U.H., SILLS, M.A. & WILLIAMS, M. (1989). [^{3}H]CGS 21680, a selective A_2 adenosine receptor agonist directly labels A_2 receptors in rat brain. *J. Pharmacol. Exp. Ther.*, **251**, 888–893.

KERR, D.I.B. & KRANTIS, A. (1979). A new class of ATP antagonist. *Proc. Aust. Physiol. Pharmacol. Soc.*, **10**, 156P.

KHAN, M.T. & MALIK, K.U. (1980). Inhibitory effect of adenosine and adenine nucleotides on potassium-evoked efflux of [^{3}H]-noradrenaline from the rat isolated heart: lack of relationship to prostaglandins. *Br. J. Pharmacol.*, **68**, 551–561.

KURZ, K., VON KÜGELGEN, I. & STARKE, K. (1993). Prejunctional modulation of noradrenaline release in mouse and rat vas deferens: contribution of P_1- and P_2-purinoceptors. *Br. J. Pharmacol.*, **110**, 1465–1472.

LIMBERGER, N., TRENDELENBURG, A.U. & STARKE, K. (1992). Pharmacological characterization of presynaptic α_2-autoreceptors in rat submaxillary gland and heart atrium. *Br. J. Pharmacol.*, **107**, 246–255.

LOHSE, M.J., KLOTZ, K.N., LINDENBORN-FOTINOS, J., REDDINGTON, M., SCHWABE, U. & OLSSON, R.A. (1987). 8-Cyclopentyl-1,3-dipropylxanthine (DPCPX) – a selective high affinity antagonist radioligand for A_1 adenosine receptors. *Naunyn-Schmied. Arch. Pharmacol.*, **336**, 204–210.

MIYAHARA, H. & SUZUKI, H. (1987). Pre- and post-junctional effects of adenosine triphosphate on noradrenergic transmission in the rabbit ear artery. *J. Physiol.*, **389**, 423–440.

MOODY, C.J., MEGHJI, P. & BURNSTOCK, G. (1984). Stimulation of P_1-purinoceptors by ATP depends partly on its conversion to AMP and adenosine and partly on direct action. *Eur. J. Pharmacol.*, **97**, 47–54.

PADDLE, B.M. & BURNSTOCK, G. (1974). Release of ATP from perfused heart during coronary vasodilatation. *Blood Vessels*, **11**, 110–119.

RALEVIC, V. & BURNSTOCK, G. (1991). Roles of P_2-purinoceptors in the cardiovascular system. *Circulation*, **84**, 1–14.

RICHARDT, G., WAAS, W., KRANZHÖFER, R., MAYER, E. & SCHÖMIG, A. (1987). Adenosine inhibits exocytotic release of endogenous noradrenaline in rat heart: a protective mechanism in early myocardial ischemia. *Circ. Res.*, **61**, 117–123.

RUBINO, A., AMERINI, S., LEDDA, F. & MANTELLI, L. (1992). ATP modulates the efferent function of capsaicin-sensitive neurones in guinea-pig isolated atria. *Br. J. Pharmacol.*, **105**, 516–520.

SCHÜTZ, W., STRÖHER, M., FREISSMUTH, M., VALENTA, B. & SINGER, E.A. (1991). Adenosine receptors mediate a pertussis toxin-insensitive prejunctional inhibition of noradrenaline release on a papillary muscle model. *Naunyn-Schmied. Arch. Pharmacol.*, **343**, 311–316.

SEBASTIÃO, A.M., STONE, T.W. & RIBEIRO, J.A. (1990). The inhibitory adenosine receptor at the neuromuscular junction and hippocampus of the rat: antagonism by 1,3,8-substituted xanthines. *Br. J. Pharmacol.*, **101**, 453–459.

SHINOZUKA, K., BJUR, R.A. & WESTFALL, D.P. (1988). Characterization of prejunctional purinoceptors on adrenergic nerves of the rat caudal artery. *Naunyn-Schmied. Arch. Pharmacol.*, **338**, 221–227.

SPERLAGH, B. & VIZI, E.S. (1991). Effect of presynaptic P_2 receptor stimulation on transmitter release. *J. Neurochem.*, **56**, 1466–1470.

STARKE, K. (1987). Presynaptic α-autoreceptors. *Rev. Physiol. Biochem. Pharmacol.*, **107**, 73–146.

STARKE, K., GÖTHERT, M. & KILBINGER, H. (1989). Modulation of neurotransmitter release by presynaptic autoreceptors. *Physiol. Rev.*, **69**, 864–989.

STARKE, K., PESKAR, B.A., SCHUMACHER, K.A. & TAUBE, H.D. (1977). Bradykinin and postganglionic sympathetic transmission. *Naunyn-Schmied. Arch. Pharmacol.*, **299**, 23–32.

STOFFEL, D., VON KÜGELGEN, I. & STARKE, K. (1994). Presynaptic P_2-purinoceptors inhibiting the release of [^{3}H]-noradrenaline in rat heart atrium. *Naunyn-Schmied. Arch. Pharmacol.*, **350**, R19.

TODOROV, L.D., BJUR, R.A. & WESTFALL, D.P. (1994). Inhibitory and facilitatory effects of purines on transmitter release from sympathetic nerves. *J. Pharmacol. Exp. Ther.*, **268**, 985–989.

VON KÜGELGEN, I., KURZ, K., BÜLTMANN, R., DRIESSEN, B. & STARKE, K. (1994a). Presynaptic modulation of the release of the co-transmitters noradrenaline and ATP. *Fundam. Clin. Pharmacol.*, **8**, 207–213.

VON KÜGELGEN, I., KURZ, K. & STARKE, K. (1993). Axon terminal P_2-purinoceptors in feedback control of sympathetic transmitter release. *Neuroscience*, **56**, 263–267.

VON KÜGELGEN, I., KURZ, K. & STARKE, K. (1994b). P_2-purinoceptor-mediated autoinhibition of sympathetic transmitter release in mouse and rat vas deferens. *Naunyn-Schmied. Arch. Pharmacol.*, **349**, 125–134.

VON KÜGELGEN, I., SCHÖFFEL, E. & STARKE, K. (1989). Inhibition by nucleotides acting at presynaptic P_2-receptors of sympathetic neuro-effector transmission in the mouse isolated vas deferens. *Naunyn-Schmied. Arch. Pharmacol.*, **340**, 522–532.

VON KÜGELGEN, I., SPÄTH, L. & STARKE, K. (1992). Stable adenine nucleotides inhibit [^{3}H]-noradrenaline release in rabbit brain cortex slices by direct action at presynaptic adenosine A_1-receptors. *Naunyn-Schmied. Arch. Pharmacol.*, **346**, 187–196.

VON KÜGELGEN, I., SPÄTH, L. & STARKE, K. (1994c). Evidence for P_2-purinoceptor-mediated inhibition of noradrenaline release in rat brain cortex. *Br. J. Pharmacol.*, **113**, 815–822.

VON KÜGELGEN, I. & STARKE, K. (1991). Noradrenaline-ATP co-transmission in the sympathetic nervous system. *Trends Pharmacol. Sci.*, **12**, 319–324.

WAKADE, A.R. & WAKADE, T.D. (1978). Inhibition of noradrenaline release by adenosine. *J. Physiol.*, **282**, 35–49.

WAUD, D.R. (1976). Analysis of dose-response relationships. In *Advances in General and Cellular Pharmacology*. ed. Narahashi, T. & Bianchi, C.P. pp. 145–178. New York: Plenum.

WELFORD, L.A., CUSACK, N.J. & HOURNAI, S.M.O. (1986). ATP analogues and the guinea-pig taenia coli: a comparison of the structure-activity relationships of ectonucleotidases with those of the P_2-purinoceptor. *Eur. J. Pharmacol.*, **129**, 217–224.

WIKLUNG, N.P., GUSTAFSSON, L.E. & LUNDIN, J. (1985). Pre- and postjunctional modulation of cholinergic neuroeffector transmission by adenine nucleotides. Experiments with agonist and antagonist. *Acta Physiol. Scand.*, **125**, 681–691.

WILLIAMS, M., BRAUNWALDER, A. & ERICKSON, T.J. (1986). Evaluation of the binding of the A-1 selective adenosine radioligand, cyclopentyladenosine (CPA), to rat brain tissue. *Naunyn-Schmied. Arch. Pharmacol.*, **332**, 179–183.

ZIMMERMANN, H. (1994). Signalling via ATP in the nervous system. *Trends Neurosci.*, **17**, 420–426.

(Received December 1, 1994
Revised January 21, 1995
Accepted February 2, 1995)

British Journal of Pharmacology (1995) 115, 255-260

Potentiation of the hyporeactivity induced by *in vivo* endothelial injury in the rat carotid artery by chronic treatment with fish oil

[1]Ghislaine A. Joly, Valerie B. Schini, Helen Hughes & Paul M. Vanhoutte

Center for Experimental Therapeutics, Baylor College of Medicine, Houston TX 77030, U.S.A.

1 The present study investigates whether or not chronic feeding of rats with a diet enriched in fish oil affects the reactivity of balloon-injured carotid arteries. The left carotid arteries were injured *in vivo* by the repeated passage of a balloon catheter. Both the right (control artery) and the left carotid arteries were excised 24 h after the injury, and suspended in organ chambers for the measurement of changes in isometric tension in the presence of indomethacin.

2 Phenylephrine evoked similar concentration-contraction curves in the right (control) carotid arteries without endothelium from control and fish oil-fed rats. Balloon injury decreased the contractility of carotid arteries to phenylephrine in both types of rats and the pEC_{50} for phenylephrine was significantly decreased in balloon-injured arteries from control rats compared to those obtained in arteries from fish oil-fed rats (pEC_{50} 7.59 ± 0.1 and 7.28 ± 0.06, respectively) while maximal contractions were similar (1.93 ± 0.15 g and 1.79 ± 0.12 g, respectively).

3 The treatment of control right carotid arteries without endothelium with either N^G-nitro-L-arginine (an inhibitor of nitric oxide synthase) or superoxide dismutase (which protects nitric oxide from degradation) did not affect significantly the contractions to phenylephrine in either group. In these preparations, methylene blue (an inhibitor of soluble guanylate cyclase) decreased slightly but significantly maximal contractions to phenylephrine in both groups. The treatment of balloon-injured carotid arteries with N^G-nitro-L-arginine or methylene blue partly restored contractions to phenylephrine in arteries from both types of rat. Superoxide dismutase further depressed the contractility to the α_1-adrenoceptor agonist in balloon-injured arteries from control diet-fed rats but had no effect in balloon-injured preparations from fish oil-fed rats.

4 3-Morpholino-sydnonimine (SIN-1, a donor of nitric oxide) evoked similar concentration-dependent relaxations in control and balloon-injured carotid arteries from both types of rat.

5 Balloon injury caused an increase in the tissue content of cyclic GMP in carotid arteries from control diet-fed rats. This production of cyclic GMP was abolished by N^G-nitro-L-arginine. Superoxide dismutase potentiated significantly the production of cyclic GMP caused by balloon injury in control but not in fish oil-fed rats.

6 These observations confirm that *in vivo* balloon injury causes the production of nitric oxide in the injured blood vessel wall. This production of nitric oxide from L-arginine accounts for the decreased contractility to phenylephrine and the accumulation of cyclic GMP in balloon-injured arteries. They further indicate that chronic feeding of rats with fish oil potentiates the L-arginine-nitric oxide pathway in the injured vessel leading to an enhanced hyporeactivity to phenylephrine.

Keywords: Endothelial injury; fish oil; nitric oxide; vascular injury

Introduction

Inflammatory mediators such as interleukin-1β activate vascular smooth muscle cells to produce nitric oxide following the induction of nitric oxide synthase (Wood *et al.*, 1990; Radomski *et al.*, 1990; Kilbourn & Belloni, 1990; Fleming *et al.*, 1990; Knowles *et al.*, 1990; Beasley *et al.*, 1991; Schini *et al.*, 1991). This response of vascular smooth muscle to inflammatory mediators is likely to account for the endothelium-independent and nitric oxide-mediated hyporeactivity of the carotid artery, which is elicited by the *in vivo* removal of the endothelial cells and injury to the smooth muscle by the repeated passage of a balloon catheter (Joly *et al.*, 1992). The injury-induced production of nitric oxide may compensate for the lack of endothelium-derived nitric oxide and contribute to the regulation of vascular functions at the sites of injury. Nitric oxide inhibits vascular tone and growth (Furchgott & Vanhoutte, 1989; Ignarro, 1989; Scott-Burden *et al.*, 1992), and also prevents the activation of platelets (Busse *et al.*, 1987; Radomski *et al.*, 1991).

[1] Author for correspondence at: M.D. Anderson Cancer Center, Department of Genitourinary Oncology Box 13, 1515 Holcombe Boulvard, Houston, Texas 77030 U.S.A.

Diet enriched in fish oil containing high levels of ω-3 unsaturated fatty acids such as eicosapentaenoic and docosahexaenoic acid, have beneficial effects in experimental models of vascular injury (see Vanhoutte & Dhouste-Blazy, 1991; Harker *et al.*, 1993). The fish oil-diets reduce the abnormal proliferation of vascular smooth cells in vein-grafts (Landymore *et al.*, 1985; Cahill *et al.*, 1988; Smith *et al.*, 1989), and balloon-injured blood vessels (Weiner *et al.*, 1986) in animals fed with a high cholesterol diet. The deposition of platelets and constriction of the carotid artery caused by balloon injury are reduced by the chronic supplementation of pigs' diet with fish oil (Lam *et al.*, 1992). In addition, fish oil feeding decreases the contractility of isolated aortae of the rat (Lockette *et al.*, 1982) and enhances the endothelium-dependent relaxations in porcine coronary arteries (Shimokawa *et al.*, 1987; Shimokawa & Vanhoutte, 1989).

The present study investigates whether or not chronic feeding with fish oil potentiates the production of nitric oxide induced by balloon injury. An enhanced endogenous production of nitric oxide is likely to prevent vasospasm and control the activation of platelets at sites of injury. This hypothesis is supported by the observation that the exposure of cultured

vascular smooth muscle cells to eicosapentaenoic acid potentiates the production of nitric oxide evoked by interleukin-1β (Schini *et al.*, 1993).

Methods

Male Wistar rats (275–300 g) were fed a semi-synthetic diet containing 20% (by weight) of either 'Max EPA' fish oils (fish oil group) or hydrogenated coconut oil containing 3% safflower oil (control group). The dry component of the feed consisted of (by weight): casein (17.76%), AIN 76 Min Mix (1.76%), AIN Vit Mix (0.66%), cellulose BW oil (20%) (prepared by Food-Tek, Inc.). The rats were placed on this diet for four weeks. Twenty four hours before vascular reactivity experiments, the rats were anaesthetized by an intraperitoneal injection of ketamine (100 mg kg^{-1}) and chlorpromazine (3 mg kg^{-1}), and the endothelium was injured unilaterally, *in vivo*, by inserting a Fogarty embolectomy catheter (2F) into the external left carotid artery. The contralateral right carotid artery without endothelium was used as control (Joly *et al.*, 1992). In addition, 24 h after balloon injury and prior to the vascular reactivity study, the left femoral artery was cannulated and connected to a pressure transducer P23XL (Gould) for the measurement of arterial pressure and the withdrawal of blood (2 ml) for the measurement of serum fatty acids, under anaesthesia (sodium pentobarbitone, 60 mg kg^{-1}, i.p.).

Vascular reactivity

The left and right carotid arteries were excised and stored in modified Krebs-Ringer bicarbonate solution containing, in mM: NaCl 118.3, KCl 4.7, $MgSO_4$ 1.2, KH_2PO_4 1.2, $CaCl_2$ 2.5, $NaHCO_3$ 25.0, CaEDTA 0.016, and glucose 11.1 (control solution). The arteries were cleaned of connective tissue and fat, cut into rings and suspended in conventional organ chambers containing 20 ml of control solution (37°C, pH 7.4) and aerated with 95% O_2 and 5% CO_2. In the right carotid arteries the endothelium was removed mechanically by inserting a small metal wire into the lumen and rolling the tissue back and forth several times on a paper towel wetted with control solution. The rings of carotid arteries were stretched progressively to 1 g (optimal length for maximal contraction as determined in preliminary experiments with phenylephrine, 1 μM). Changes in isometric tension were recorded by means of an isometric force transducer (model UC2, Gould, Cleveland, OH, U.S.A.). The absence of the endothelium was verified by the lack of relaxations to acetylcholine (1 μM) in arteries contracted with phenylephrine (1 μM). The arteries were rinsed three times with warm control solution, and after a resting period (30 min) they were incubated for 30 min either with solvent, N^G-nitro-L-arginine (L-NNA) (100 μM; an inhibitor of nitric oxide synthesis; Mulsch & Busse, 1990), superoxide dismutase (SOD) (100 iu ml^{-1}; a scavenger of superoxide anions; Rubany & Vanhoutte, 1986; McCord & Fridovich, 1970), or methylene blue (10 μM; an inhibitor of soluble guanylate cyclase; Martin *et al.*, 1985; Bullock *et al.*, 1986). Next, a concentration-contraction curve to phenylephrine (1 nM–10 μM), or a concentration-relaxation curve to SIN-1 (1 nM–10 μM; in rings contracted with phenylephrine, 10 μM) was obtained. All experiments were performed in the presence of indomethacin (10 μM) to prevent the synthesis of vasoactive prostanoids.

Tissue content of guanosine 3':5'-cyclic monophosphate (cyclic GMP)

Rings were incubated in warm (37°C) control solution (5 ml) containing indomethacin (10 μM) and 3-isobutyl-1-methylxanthine (IBMX; 100 μM; a nonselective inhibitor of phosphodiesterases) for 30 min, to inhibit the production of prostanoids and the degradation of cyclic nucleotides by phosphodiesterases, respectively. During this period, the rings were incubated with L-NNA (100 μM), SOD (100 iu ml^{-1}) or solvent. They were frozen quickly with an aluminium clamp cooled in liquid nitrogen. Subsequently, the rings were homogenized in 1 ml of 6% trichloroacetic acid, sonicated for 5 s, and centrifuged for 15 min (13,600 *g*). Supernatants were extracted with 4 vol water-satured ethylether before being lyophilized. Each sample was resuspended in 0.3 ml of sodium acetate buffer (0.05 M, pH 6.2), and the content of cyclic GMP was determined with a cyclic GMP Kit (Biochemical Technologies Inc., Stoughton, MA, U.S.A.), with an acetylation step induced to increase sensitivity. After lyophilization the pellets were incubated with NaOH (0.3 ml of 0.1 N) at 37°C for 24 h and the protein concentration of each sample was determined using the BCA Protein Assay Reagent (Pierce Chemical Co., Rockford, Ill, U.S.A.).

Serum fatty acid analysis

Blood samples were allowed to clot at room temperature for 2 h and were centrifuged at 2500 r.p.m. for 10 min. Aliquots of 150 μl were taken for fatty acid analysis and stored at −70°C. Plasma samples were extracted by the method of Bligh & Dyer (1959) and transesterified with sodium methoxide (0.5 M). The resulting fatty acid methyl esters were analyzed by gas chromatography flame ionization detection. A DB-23 capillary column (15 m × 0.25 mm, J & W Scientific) was heated from 100°C to 230°C at 4° min^{-1}. A modified 5710A gas chromatography was used for the analysis and a CR501 chromatopac (Bio-Rad) integrator for the quantitation of peak areas.

Drugs

Phenylephrine hydrochloride, acetylcholine chloride, indomethacin, 3-isobutyl-1-methylxanthine, methylene blue, and superoxide dismutase were purchased from Sigma Chemical Co., St. Louis, Mo, U.S.A. N^G-nitro-L-arginine was obtained from Boehringer Mannheim, Indianapolis, Inc., and 3-morpholino-sydnonimine (SIN-1) was a gift from laboratories Hoechst, Paris. Fish oil 'Max EPA' was a gift from Pierre Fabre Santé, Castres France. Indomethacin was prepared in an equimolar concentration of sodium carbonate (10 μM). All other drugs were prepared in distilled water.

Statistical analysis

Results are expressed as means ± s.e.mean. The number of rats studied is represented by *n*. The statistical evaluation of the data was performed by Student's *t* test for paired or unpaired observations. When data from more than two groups were compared, an analysis of variance (ANOVA) was used, and individual means were compared with Scheffe's *F* test. Values were considered to be statistically significant when *P* was less than 0.05. E_{max} (g) was the maximum contractile effect and pEC_{50} was the negative logarithm of the effective molar concentration of phenylephrine causing 50% of the maximal contraction.

Results

Body weights, arterial blood pressure and serum fatty acids

The body weight was significantly lower ($P < 0.05$) in rats fed with 20% fish oil compared to control (473 ± 13 g and 512 ± 8 g, respectively; $n = 9$).

The mean arterial blood pressure was significantly higher ($P < 0.05$) in the control group (127 ± 3 mmHg) than in the fish oil group (115 ± 2 mmHg; $n = 8$). In fish oil-fed rats, the proportion of the ω-3 polyunsaturated fatty acids, eicosapen-

taenoic acid (EPA 20:5) and docosahexaenoic acid (DHA 22:6) was significantly increased. The levels of stearic acid (18:0), oleic acid (18:1) and linoleic acid (18:2) were significantly lower in the serum of fish oil-fed rats compared to the control group. The plasma content of arachidonic acid (20:4) was similar in both groups (Table 1).

Effect of balloon injury: vascular reactivity

Phenylephrine (1 nM–10 μM) evoked concentration-dependent contractions in control carotid arteries without endothelium as well as in balloon-injured arteries, from both control and fish oil-fed rats (Figure 1). The contractions evoked by phenylephrine were similar in control arteries without endothelium in both group of rats (E_{max}: 2.43 ± 0.17 g and 2.28 ± 0.11 g, respectively) (Figure 1 and Table 2). In balloon-injured carotid arteries from both control and fish oil-fed rats, the contractions evoked by phenylephrine were depressed significantly compared to those obtained in control arteries ($P<0.05$). The reduction in contractions to phenylephrine induced by balloon injury was significantly more pronounced in rings from fish oil-fed than from control rats (Figure 1). The maximal contractions were similar (E_{max}: 1.79 ± 0.12 g and 1.93 ± 0.15 g respectively) but pEC_{50} were significantly decreased in arteries from fish oil-fed rats compared to those obtained in arteries from control diet-fed rats (Table 2).

The addition of N^G-nitro-L-arginine (L-NNA, 100 μM) or superoxide dismutase (SOD, 100 iu ml^{-1}) to control carotid rings without endothelium did not significantly affect the basal tension or the concentration-contraction curves to phenylephrine in rings from both control and fish oil-fed rats (Figure 2a and b, respectively, and Table 2). Methylene blue (MB, 10 μM) had no effect on basal tension, but significantly decreased the maximal contractions to phenylephrine without affecting pEC_{50} in both groups of rats (E_{max}: 2.43 ± 0.17 g and 1.9 ± 0.14 g; 2.28 ± 0.11 and 2 ± 0.14 g, without and with MB, respectively, $P<0.05$). L-NNA, SOD or MB had no effects on the basal tension of balloon-injured carotid arteries from both control and fish oil-fed rats. In balloon-injured carotid arteries from control rats, L-NNA shifted the concentration-response curves to phenylephrine significantly to the left and increased the maximal responses (E_{max}: 1.93 ± 0.15 g and 2.47 ± 0.12 g without and with L-NNA, respectively, ($P<0.05$), Figure 3a and Table 2) while SOD further significantly depressed contractions to this α_1-agonist (Table 2) without affecting maximal contractions in both types of rats (Figure 3a).

In balloon-injured carotid arteries of fish oil-fed rats, L-NNA shifted the concentration-contraction curves to phenylephrine significantly to the left and augmented the maximal contractions (E_{max}: 1.79 ± 0.12 g and 2.5 ± 0.17 g without and with L-NNA, respectively, ($P<0.05$) Figure 3b and Table 2). SOD had no effect on the contractions to phenylephrine (Figure 3b). MB, (10 μM) significantly enhanced the contractions evoked by phenylephrine (0.1 and 0.3 μM) in balloon-injured carotid arteries from control diet-fed rats and also those evoked by phenylephrine (0.3 and 1 μM) in balloon-injured carotid arteries from fish oil-fed rats (Figure 3). However, MB did not affect significantly the pEC_{50} values in both groups of rats (Table 2). The concentration-dependent relaxations to SIN-1 were not significantly different in control (without endothelium) and balloon-injured arteries from either control or fish oil-fed rats (Figure 4).

Production of cyclic GMP

The basal production of cyclic GMP was low in control carotid arteries without endothelium from both groups of

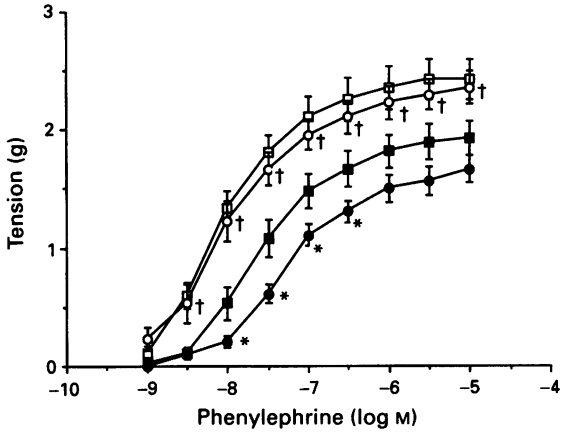

Figure 1 Concentration-contraction curves to phenylephrine in control right carotid (without endothelium) from control (□) and fish oil-fed rats (○); and in balloon-injured carotid arteries (24 h after endothelial injury) from control (■) and fish oil-fed rats (●). The experiments were performed in the presence of indomethacin (10 μM). Results are presented as mean ± s.e.mean of six different experiments and are shown as absolute values. *Statistically significant differences between control and fish-oil diet, in balloon-injured arteries and †between control without endothelium and balloon-injured arteries from both groups ($P<0.05$).

Table 1 Serum fatty acids

Fatty acids	*Control rats*	*Fil oil-fed rats*
16.0	28.83 ± 0.66	24.29 ± 0.31*
18.0	13.47 ± 0.59	11.39 ± 0.21*
18.1	15.36 ± 0.74	8.06 ± 0.12*
18.2	21.24 ± 0.58	7.38 ± 0.27*
20.4	16.93 ± 0.70	15.73 ± 0.48
20.5	trace	21.52 ± 0.51*
22.6	1.19 ± 0.07	9.07 ± 0.12*

Results expressed as % serum fatty acid composition. Data shown as means ± s.e.mean ($n = 11$). *Statistically significant differences between the two groups ($P<0.05$).

Table 2 Effects of N^G-nitro-L-arginine (L-NNA) 100 μM, superoxide dismutase (SOD) 100 iu ml^{-1} and methylene blue (MB) 10 μM on the concentration-contraction curves evoked by phenylephrine in control arteries without endothelium and in balloon-injured arteries from control diet-fed rats and fish oil-fed rats

	pEC_{50}			
	Control diet		*Fish oil diet*	
	Control	*Balloon*	*Control*	*Balloon*
Untreated	8.08 ± 0.05	7.59 ± 0.1	8.03 ± 0.1	7.28 ± 0.06†
L-NNA	8.15 ± 0.05	7.9 ± 0.09*	8.25 ± 0.12	7.73 ± 0.07*
SOD	7.96 ± 0.09	7.25 ± 0.09*	8.17 ± 0.08	7.36 ± 0.1
MB	7.83 ± 0.1	7.74 ± 0.13	7.89 ± 0.08	7.44 ± 0.12

pEC_{50}: negative logarithm of the effective molar concentration of phenylephrine causing 50% of the maximal contaction. *Statistically significant differences between the treated (L-NNA), (SOD), or (MB) and untreated arteries and †between the arteries from control and fish oil-diet rats ($P<0.05$).

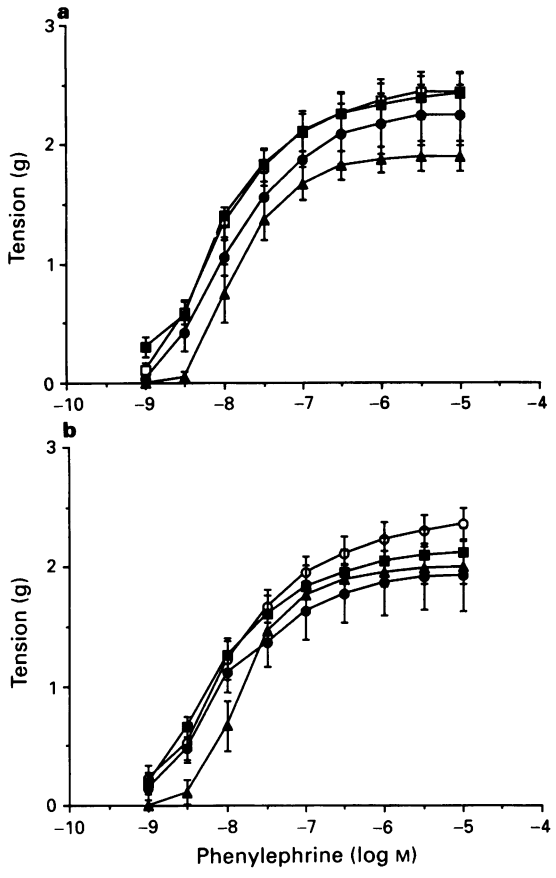

Figure 2 Lack of effect of N^G-nitro-L-arginine (■), superoxide dismutase (●), and methylene blue (▲) on the concentration-contraction curves to phenylephrine in right carotid arteries (without endothelium) from control (□) (a) and fish oil-fed (○) (b) rats. The experiments were performed in the presence of indomethacin (10 μM). Results are presented as mean ± s.e.mean of four to six different experiments, and are shown as absolute values.

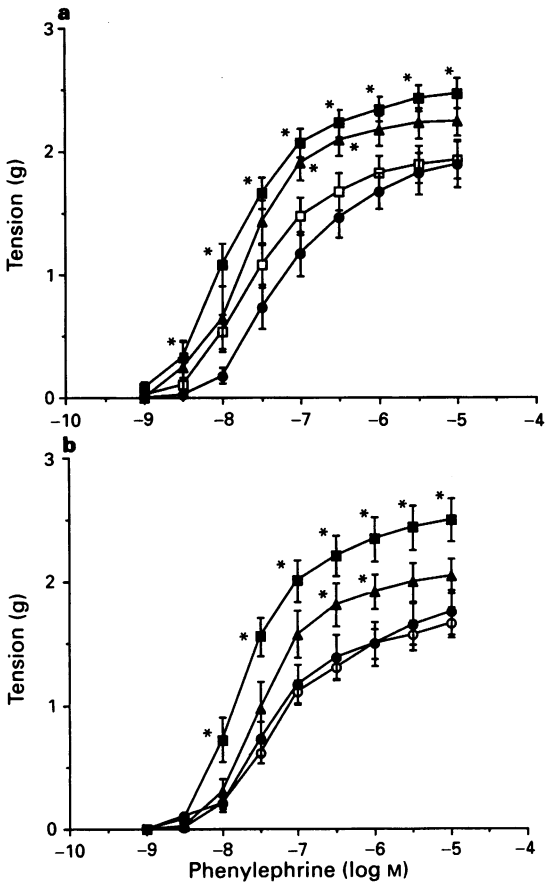

Figure 3 Effects of N^G-nitro-L-arginine (L-NNA, ■), superoxide dismutase (●), and methylene blue (MB, ▲) on concentration-contraction curves to phenylephrine in balloon-injured carotid arteries (24 h prior to sampling) from control (□) (a) and fish oil-fed (○) (b) rats. The experiments were performed in the presence of indomethacin (10 μM). Results are presented as means ± s.e.mean of six different experiments, and shown as absolute values. *Statistically significant differences between control and treated (L-NNA or MB) balloon-injured carotid arteries ($P<0.05$).

rats (Figure 5). Incubation of these arteries in the presence of either L-NNA or SOD did not significantly affect the content of cyclic GMP (Figure 5). In balloon-injured carotid arteries from control diet-fed rats, the basal content of cyclic GMP was significantly higher than in the control arteries without endothelium. Incubation of balloon injured arteries with L-NNA reduced while SOD increased significantly the basal production of cyclic GMP (Figure 5). In balloon-injured carotid arteries from fish oil-fed rats the basal production of cyclic GMP was significantly higher than that in the control arteries without endothelium in the presence but not in the absence of SOD (Figure 5). Incubation of balloon-injured arteries from fish oil-fed rats with L-NNA did not significantly affect the basal content of cyclic GMP (Figure 5).

Discussion

This study demonstrated that fish oil feeding increased the hyporesponsiveness to phenylephrine observed 24 h after injury of the endothelium in the rat carotid artery.

The analysis of plasma fatty acids demonstrated that the rats fed the fish oil diet had absorbed the ω-3 fatty acid, since eicosapentaenoic acid (EPA) and docosahexaenoic acid (DHA) were both elevated, in accordance with previous studies (Yin *et al.*, 1991). Fish oil rich in EPA have been claimed to prevent hypertension in the SHR (Yin *et al.*, 1991) and that induced by dexamethasone (Yin *et al.*, 1992). The

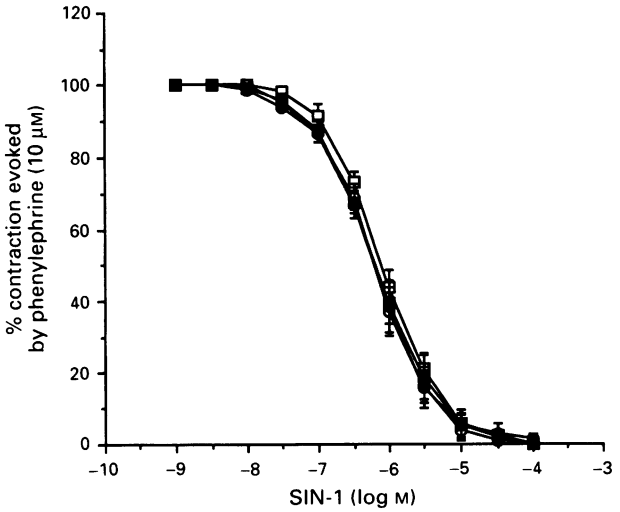

Figure 4 Concentration-relaxation curves to 3-morpholino-sydnonimine (SIN-1) in control arteries (without endothelium) from control (□) and fish oil-fed rats (○); and in balloon-injured carotid arteries from control (■) and fish oil rats (●). The experiments were performed in the presence of indomethacin (10 μM). Results are presented as means ± s.e.mean of six different experiments, and are expressed as the percentage of the contraction evoked by phenylephrine (10 μM).

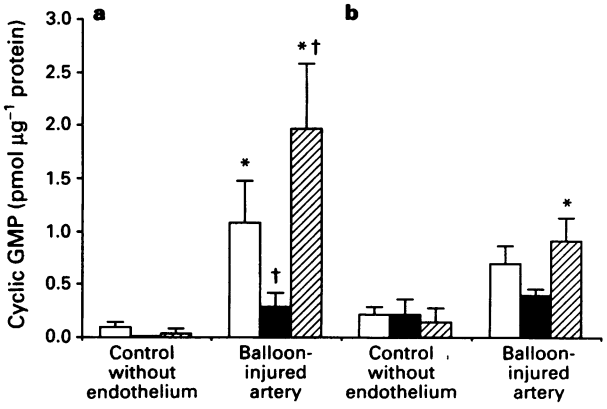

Figure 5 Effects of N^G-nitro-L-arginine (L-NNA, solid columns) and superoxide dismutase (hatched columns) on the basal production of cyclic GMP (open columns) in right carotid arteries (without endothelium) and in balloon-injured carotid arteries from control (a) and fish oil-fed rats (b). The experiments were performed in the presence of indomethacin (10 µM) and 3-isobutyl-1-methylxanthine (100 µM). Results are presented as means ± s.e.mean of four to five different experiments and are shown as absolute values. *Statistically significant differences between balloon-injured and control carotid arteries of two groups and †between control and treated (L-NNA) balloon-injured carotid arteries ($P<0.05$).

hypotensive effect of fish oil was associated with an increase in endothelium-dependent relaxations to acetylcholine in the aorta and a decreased endothelium-independent contraction to noradrenaline in mesenteric resistance arteries (Yin *et al.*, 1992). An increase of constitutive nitric oxide synthase (NOS) induced NO synthesis in endothelial cells probably explains these alterations in vascular reactivity in relation to the blood pressure lowering effects of fish oil and may underlie the slight but significant decrease in blood pressure observed in the present study in rats treated with fish oil.

Vascular smooth muscle cells from the rat carotid artery can generate nitric oxide from L-arginine and this is activated following vascular injury *in vivo* (Joly *et al.*, 1992). The present findings confirm that *in vivo* the injury caused by the repeated passage of a balloon catheter in the carotid artery from normal diet-fed rats causes the induction of NOS activity in the injured blood vessel wall (Joly *et al.*, 1992). This response to injury explains both the hyporeactivity to contractile agonists and the increased formation of cyclic GMP in the injured arteries. Chronic feeding of rats with a diet enriched in EPA enhances the hyporesponsiveness to phenylephrine caused by balloon injury without affecting the maximal responses to the α_1-adrenoceptor agonist. This loss of contractility, observed 24 h after *in vivo* endothelial injury, was inhibited by an inhibitor of NOS, L-NNA, and also partly by an inhibitor of soluble guanylate cyclase, MB. Furthermore, exposure of cultured vascular smooth muscle cells to EPA potentiates the production of nitric oxide evoked by cytokines (Schini *et al.*, 1993). Altogether, these observations suggest that chronic feeding of rats with fish oil enhances the generation of nitric oxide caused by balloon injury. Surprisingly, no significant increase in the tissue content of cyclic GMP was obtained in balloon-injured carotid arteries from fish oil-fed rats. This lack of effect is probably due to the small number ($n = 4$) of samples and the substantial fluctuation of the cyclic GMP content between samples. Alternatively, these data may also suggest that nitric oxide relaxes balloon-injured arteries from fish oil-fed rats mostly by a cyclic GMP-independent mechanism(s). This idea is supported by the fact that nitric oxide can cause relaxation of vascular smooth muscle by enhancing the activity of the Na^+-K^+-ATPase (Gupta *et al.*, 1994). In addition, the enhanced hyporeactivity caused by balloon injury in carotid arteries from fish oil-fed rats compared to those receiving a control diet cannot be explained by the ability of fish oil to reduce the synthesis of the contractile prostanoid thromboxane A_2 (Codde *et al.*, 1987; Locher *et al.*, 1988), since all experiments were performed in the presence of indomethacin. Dietary feeding with fish oil may lead to a significant alteration in the platelet arterial wall interaction *in vivo*, with a decrease in both platelet deposition at the site of arterial wall injury and a reduction of the associated vasoconstrictor response (Fingerle *et al.*, 1989; Lam *et al.*, 1992). In control rats, superoxide anions seem to play a major role in the events following balloon injury, since the contractions to phenylephrine are depressed further in the presence of SOD, an effect associated with an increased production of cyclic GMP. The release of superoxide anions in balloon-injured arteries from control rats may be due to the presence of neutrophils and macrophages at the site of injury (McCall *et al.*, 1989). The lack of effect of the scavenger of superoxide anions on contractions to the α_1-adrenoceptor agonist, and on the cyclic GMP content in arteries from fish oil-treated rats could result from a decreased adhesion/activation of blood cells, and a lesser release of superoxide anions (Sperling *et al.*, 1993).

The possibility that the injury with a balloon catheter, or the treatment by fish oil affects the medial smooth muscle cells or modifies their soluble guanylate cyclase is unlikely because in the presence of L-NNA phenylephrine evoked a similar maximal response in control arteries without endothelium and in balloon-injured carotid arteries, irrespective of the diet of the animals. In addition, SIN-1, an exogenous donor of nitric oxide (Gerzer *et al.*, 1988), evokes similar relaxations independently of the treatment and the artery.

In summary, this study suggests that fish oil feeding could play an important role in early events following vascular injury by potentiating the arterial hyporeactivity observed 24 h after balloon injury, which can be attributed to an induction of nitric oxide synthase. This effect could influence favourably the pathways that are believed to be important in the development of atherosclerosis.

This study was supported in part by National Institutes of Health grants HL-31183 (P.M.V.) and HL-46356 (V.B.S.) and by an unrestricted Research Award from the Bristol-Meyers Squibb Research Institute. The authors would like to thank Barnabas Desta and Dewayne O.Coney for technical assistance.

References

BEASLEY, D., SCHWARTZ, J.H. & BRENNER, B.M. (1991). Interleukin 1 induces prolonged L-arginine-dependent cyclic guanosine monophosphate and nitrite production in rat vascular smooth muscle cells. *J. Clin. Invest.*, **87**, 602–608.

BLIGH, E.G. & DYER, W.J. (1959). A rapid method of total lipid extraction and purification. *Can. J. Biochem. Physiol.*, **37**, 911–917.

BULLOCK, G.R., TAYLOR, S.G. & WESTON, A.H. (1986). Influence of the vascular endothelium on agonist-induced contractions and relaxations in the rat aorta. *Br. J. Pharmacol.*, **89**, 819–830.

BUSSE, R., LUCKHOFF, A. & BASSENGE, E. (1987). Endothelium-derived relaxant factor inhibits platelet activation. *Naunyn Schmied. Arch. Pharmacol.*, **336**, 566–571.

CAHILL, P.D., SARRIS, G.E., COOPER, A.D., WOOD, P.D., KOSEK, J.C., MITCHELL, R.C. & MILLER, D.C. (1988). Inhibition of vein graft intimal thickening by eicosapentanoic acid: reduced thromboxane production without change in lipoprotein levels or low-density lipoprotein receptor density. *J. Vasc. Surg.*, **7**, 108–118.

CODDE, J.P., BEILIN, L.J., CROFT, K.D. & VANDONGEN, R. (1987). The effect of dietary fish oil and salt on blood pressure and eicosanoid metabolism of spontaneously hypertensive rats. *J. Pharmacol.*, **5**, 137–142.

FINGERLE, J., JOHNSON, R., CLOWES, A., MAJESKY, M. & REIDY, M.A. (1989). Role of platelet in smooth muscle cell proliferation and migration after vascular injury in rat carotid artery. *Proc. Natl. Acad. Sci. U.S.A.*, **86**, 8412–8416.

FLEMING, I., GRAY, G.A., JULOU-SCHAEFFER, G., PARRAT, J.R. & STOCLET, I.C. (1990). Incubation with endotoxin activates the L-arginine pathway in vascular tissue. *Biochem. Biophys. Res. Commun.*, **171**, 562–568.

FURCHGOTT, R.F. & VANHOUTTE, P.M. (1989). Endothelium-derived relaxing and contracting factors. *FASEB J.*, **3**, 2007–2018.

GERZER, R., KARRENBROCK, B., SIESS, W. & HEIM, J.M. (1988). Direct comparison of the effects of nitroprusside, SIN-1, and various nitrates on platelet aggregation and soluble guanylate cyclase activity. *Thromb. Res.*, **52**, 11–21.

GUPTA, S., MCARTHUR, C., GRADY, C. & RUDERMAN, N.B. (1994). Stimulation of vascular Na^+-K^+-ATPase activity by nitric oxide: a cGMP-independent effect. *Am. J. Physiol.*, **35**, H2146–H2151.

HARKER, L.A., KELLY, A.B., HANSON, S.R., KRUPSKI, W., BASS, A., OSTERUD, B., FITZGERALD, G.A., GOOGNIGHT S.H. & CONNOR, W.E. (1993). Interruption of vascular thrombus formation and vascular lesion formation by dietary n-3 fatty acids in fish oil in nonhuman primates. *Circulation*, **87**, 1017–1029.

IGNARRO, L.J. (1989). Biological actions and properties of endothelium-derived nitric oxide formed and released from artery and vein. *Circ. Res.*, **65**, 1–20.

JOLY, G.A., SCHINI, V.B. & VANHOUTTE, P.M. (1992). Balloon injury and interleukin-1 β induce nitric oxide synthase activity in rat carotid artery. *Circ. Res.*, **71**, 331–338.

KILBOURN, R.G & BELLONI, P. (1990). Endothelial cell production of nitrogen oxides in response to interferon in combination with tumor necrosis factor, interleukin-1, or endotoxin. *J. Natl. Cancer Inst.*, **82**, 772–776.

KNOWLES, R.G., SALTER, M., BROOKS, S.L. & MONCADA, S. (1990). Anti-inflammatory glucocorticoids inhibit the induction by endotoxin of nitric oxide synthase in the lung, liver and aorta of rat. *Biochem. Biophys. Res. Commun.*, **172**, 1042–1048.

LAM, J.Y.T., BADIMON, J.J., ELLEFSON, R.D., FUSTER, V. & CHESEBRO, J.H. (1992). Cod liver oil alters platelet-arterial wall response to injury in pigs. *Circ. Res.*, **71**, 769–775.

LANDYMORE, R.W., KINLEY, C.E., COOPER, J.H., MACAULAY, M., SHERIDAN, B. & CAMERON, C. (1985). Cod-liver oil in the prevention of intimal hyperplasia in autogenous vein grafts used arterial bypass. *J. Thorac. Cardiovasc. Surg.*, **89**, 351–357.

LOCHER, R., VOGT, E., STEINER, A. & VETTER, W. (1988). The phospholipidde turnover of vascular smooth muscle cells is influenced by fish oil. *J. Hypertens.*, **6**, S222–S224.

LOCKETTE, W., WEBB, R.C. & CULP, B.R. (1982). Vascular reactivity and high dietary eicosapentaenoic acid. *Prostaglandins*, **24**, 631–639.

MARTIN, W., VILLANI, G.M., JOTHIANANDAN, D. & FURCHGOTT, R.F. (1985). Selective blockade of endothelium-dependent and glyceryl trinitrate-induced relaxation by hemoglobin and methylene blue in the rabbit aorta. *J. Pharmacol. Exp. Ther.*, **232**, 708–716.

MCCALL, T.B., BOUGHTON-SMITH, N.K., PALMER, R.M.J., WHITTLE, B.J.R. & MONCADA, S. (1989). Synthesis of nitric oxide from L-arginine by neutrophils: Release and interaction with superoxide anion. *Biochem. J.*, **261**, 293–296.

MCCORD, J.M. & FRIDOVICH, I. (1970). The utility of superoxide dismutase in studying free radical reaction. *J. Biol. Chem.*, **245**, 1374–1377.

MULSCH, A. & BUSSE, R. (1990). N^G-nitro arginine (N5-[imino(nitro-amino)-methyl]-L-ornithine) impairs endothelium-dependent dilatations by inhibiting cytosolic nitric oxide synthesis from L-arginine. *Naunyn. Schmied. Arch. Pharmacol.*, **341**, 143–147.

RADOMSKI, M.W., PALMER, R.M.J. & MONCADA, S. (1990). Glucocorticoids inhibit the expression of an inducible, but not the constitutive, nitric oxide synthase in the vascular endothelial cells. *Proc. Natl. Acad. Sci. U.S.A.*, **87**, 10043–10047.

RADOMSKI, M.W., PALMER, R.M. & MONCADA, S. (1991). Modulation of platelet aggregation by an L-arginine-nitric oxide pathway. *Trends Pharmacol. Sci.*, **12**, 87–88.

RUBANY, G.M & VANHOUTTE, P.M. (1986). Superoxide anions and hyperoxia inactivate endothelium-derived relaxing factor. *Am. J. Physiol.*, **250**, H122–H127.

SHIMOKAWA, H., LAM, J.Y.T., CHESEBRO, J.H., BOWIE, E.J.W. & VANHOUTTE, P.M. (1987). Effects of dietary supplementation with cod-liver oil on endothelium-dependent responses in porcine coronary arteries. *J. Clin. Invest.*, **76**, 898–905.

SMINOKAWA, H. & VANHOUTTE, P.M. (1989). Dietary omega 3 fatty acids and endothelium-dependent relaxations in porcine coronary arteries. *Am. J. Physiol.*, **256**, H963–H973.

SCHINI, V.B., DURANTE, W., CATOVSKY, S. & VANHOUTTE, P.M. (1993). Eicosapentaenoic acid potentiates the production of nitric oxide evoked by interleukin-1 β in cultured vascular smooth muscle cells. *J. Vasc. Res.*, **30**, 209–217.

SCHINI, V.B., JUNQUERO, D.C., SCOTT-BURDEN, T. & VANHOUTTE, P.M. (1991). Interleukin-1 b induces the production of an L-arginine-derived relaxing factor from cultured smooth cells from rat aorta. *Biochem. Biophys. Res. Commun.*, **176**, 114–121.

SCOTT-BURDEN, T., SCHINI, V.B., ELIZONDO, E., JUNQUERO, D.C. & VANHOUTTE, P.M. (1992). Platelet-derived growth factor suppresses and fibroblast growth factor enhances cytokine-induced production of nitric oxide by cultured smooth muscle cells. Effects on cell proliferation. *Circ. Res.*, **71**, 1088–1100.

SMITH, D.L., WILLIS, A.L., NGUYEN, N., CONNER, D., ZAHEDI, S. & FULKS, J. (1989). Eskimo plasma constituents, dihomo-gamma-linolenic acid, eicosapentaenoic acid and docosahexaenoic acid inhibit the release of atherogenic mitogens. *Lipids*, **24**, 70–75.

SPERLING, R.I., BENINCASO, A.I., KNOELL, C.T., LARKIN, J.K. AUSTEN, K.F. & ROBINSON, D.R. (1993). Dietary o-3 polyunsaturated fatty acids inhibit phosphoinositide formation and chemotaxis in neutrophils. *J. Clin. Invest.*, **91**, 651–660.

VANHOUTTE, P.M. & DOUSTE-BLAZY, P. (1991). *Fish Oil and Blood Vessel Wall Interactions.* Monrouge: John Libbey Eurotext.

WEINER, B.H., OCKENE, I.S. & LEVINE, P.H. (1986). Inhibition of atherosclerosis by cod liver oil in a hyperlipidemic swine model. *N. Engl. J. Med.*, **315**, 841–846.

WOOD, K.S., BUGS, G.M., BYRNS, R.N. & IGNARRO, L.J. (1990). Vascular smooth muscle-derived relaxing factor (MRRF) and its close similarity to nitric oxide. *Biochem. Biophys. Res. Commun.*, **170**, 80–88.

YIN, K., CHU, Z.M. & BEILIN, L.J. (1991). Blood pressure and vascular reactivity changes in spontaneously hypertensive rats fed fish oil. *Br. J. Pharmacol.*, **102**, 991–997.

YIN, K., CHU, Z.M. & BEILIN, L.J. (1992). Study of mechanisms of glucocorticoid hypertension in rats: endothelial related changes and their amelioration by dietary fish oils. *Br. J. Pharmacol.*, **106**, 435–442.

(Received February 10, 1994
Revised December 12, 1994
Accepted February 2, 1995)

British Journal of Pharmacology (1995) 115, 261-266

Group B *Streptococcus* and *E. coli* LPS-induced NO-dependent hyporesponsiveness to noradrenaline in isolated intrapulmonary arteries of neonatal piglets

*Eduardo Villamor, [1]Francisco Pérez-Vizcaíno, *Teresa Ruiz, Juan C. Leza, *Manuel Moro & Juan Tamargo

Department of Pharmacology, Institute of Pharmacology and Toxicology, School of Medicine, Universidad Complutense, 28040 Madrid and *Division of Neonatology, Department of Pediatrics, Hospital Universitario 'S. Carlos', 28040 Madrid, Spain

1 The effects of endotoxin (*E. coli* lipopolysaccharide, LPS) and heat inactivated group B *Streptococcus* (GBS) were studied on the contractile responses to noradrenaline (NA) in isolated pulmonary arteries and on the activity of the constitutive and inducible nitric oxide synthase (NOS) in lung fragments of neonatal piglets.

2 Short-term ($\leqslant 5$ h) incubation with LPS (1 $\mu g\,ml^{-1}$) or GBS (3×10^7 colonies forming units ml^{-1}) did not modify the vascular responsiveness to NA (10^{-8} M–10^{-4} M) in isolated intrapulmonary arteries. However, long-term incubation (20 h) with LPS or GBS produced a significant reduction in the maximal contractile responses and shifted the concentration-response curve for NA downwards.

3 Endothelium removal or the cyclo-oxygenase inhibitor meclofenamate (10^{-5} M) did not affect the GBS- and LPS-induced hyporesponsiveness to NA.

4 The presence of the nitric oxide (NO) precursor, L-arginine (10^{-5} M), 30 min prior to the contractility challenge increased the LPS- and GBS-induced pulmonary vascular hyporesponsiveness to NA. In contrast, the addition, prior to the challenge with NA, of the NOS inhibitor N^G-nitro-L-arginine methyl ester (L-NAME, 10^{-4} M) or coincubation with dexamethasone (3×10^{-6} M), a potent inhibitor of the induction of NOS, or with the protein synthesis inhibitor cycloheximide (10^{-5} M) completely restored the reactivity to NA in LPS- and GBS-treated pulmonary arteries.

5 The incubation for 20 h of lung fragments with LPS and GBS produced a significant increase in the Ca^{2+}-independent (inducible) NOS activity determined by the conversion of radiolabelled L-arginine to citrulline, but did not modify the constitutive NOS activity. This NOS induction was abolished by coincubation with dexamethasone (3×10^{-6} M).

6 These results demonstrated that prolonged incubation with GBS and LPS causes an induction of NOS activity which results in a reduced vascular responsiveness to NA in pulmonary arteries of neonatal piglets. Thus, induction of NOS seems to be responsible for the delayed pulmonary vascular hyporesponsiveness induced by GBS (a Gram-positive) and *E. coli* (a Gram-negative), the most common causal agents of neonatal sepsis.

Keywords: Group B *Streptococcus*; lipopolysaccharide; nitric oxide synthase; pulmonary artery of piglet

Introduction

E. coli, a Gram-negative bacterium, and group B *Streptococcus* (GBS), a Gram-positive bacterium, are the most common causal agents of neonatal sepsis (Anthony, 1985; Guerina, 1991). In general, sepsis is characterized by systemic arterial hypotension, inadequate tissue perfusion and decreased responses of vascular smooth muscle to exogenous vasoconstrictors (Groeneveld *et al.*, 1988). The pulmonary system also demonstrates important abnormalities that include changes in pulmonary haemodynamics and lung mechanics, increased vascular permeability and hypoxemia, and more subtle changes in responses of both airway and the pulmonary circulation to constrictor stimuli (Brigham & Meyrick, 1986). Lipopolysaccharide (LPS), the major component of the outer membrane of Gram-negative bacteria, is the endotoxin presumed to cause injury to the lungs as well as to other organs (Thiemermann, 1994). Gram-positive bacteria do not contain LPS and a toxin common to all Gram-positive organisms has not been identified. However, intravenous infusions of GBS and other Gram-positive bacteria cause pulmonary haemodynamic and gas exchange abnormalities similar to those observed in LPS-injected animals (Rojas *et al.*, 1983; Schreiber *et al.*, 1992) suggesting a common pathway leading to these abnormalities (Auguet *et al.*, 1992).

There is evidence that enhanced release of NO plays an important role in the loss of systemic (McKenna, 1990; Julou-Schaffer *et al.*, 1990; Moncada *et al.*, 1991; for a review see Thiemermann, 1994) and pulmonary (Szabó *et al.*, 1993; Zelenkov *et al.*, 1993) vascular responsiveness that occurs in sepsis. There are at least two distinct isoforms of NO synthase (NOS) which catalyzes the formation of NO from L-arginine (Moncada *et al.*, 1991; Stuehr & Griffith, 1992). A constitutive, Ca^{2+}-dependent isoform (cNOS), is present in vascular endothelial cells. In addition, LPS and cytokines induce a Ca^{2+}-independent, isoform (iNOS) in the lung (Knowles *et al.*, 1990), macrophages (Marletta *et al.*, 1988), endothelial cells (Radomski *et al.*, 1990) and vascular smooth muscle (Busse & Mülsch, 1990). Induction of iNOS has been found in rat pulmonary arteries incubated with LPS (Zelenkov *et al.*, 1993) and in rat lung after exposure to endotoxin (Salter *et al.*, 1991; Szabó *et al.*, 1993; Thiemermann, 1994). Unfortunately, the effects of GBS on vascular reactivity and on cNOS and iNOS are still unknown. Therefore, the aim of this work was: (1) to study and compare the effects of GBS with those of LPS on the contractile responses to noradrenaline (NA) in intact and endothelium-denuded pul-

[1] Author for correspondence.

monary arteries of neonatal piglets, and (2) to determine whether GBS- and LPS-mediated pulmonary vascular hyporesponsiveness could be related to the activation of cNOS and/or iNOS.

Methods

Tissue preparation and incubation

Male neonatal piglets (10–17 days of age, 4277 ± 343 g) obtained from the local abattoir were used in this study. Piglets were killed by exsanguination and the lungs were rapidly immersed in cold (4°C) Krebs solution containing ampicillin (10 μg ml^{-1}) and gentamicin (10 μg ml^{-1}) and transported immediately to the laboratory. The third branch of the pulmonary arteries (internal diameter 1–2 mm) was carefully dissected free of parenchyma and connective tissue and cut into rings of 2–3 mm of length. Pulmonary rings were then incubated in Krebs solution (composition in mM: NaCl 118, KCl 4.75, $NaHCO_3$ 25, $MgSO_4$ 1.2, $CaCl_2$ 2.0, KH_2PO_4 1.2 and glucose 11) containing ampicillin (10 μg ml^{-1}) and gentamicin (10 μg ml^{-1}). The solution was gassed with 95% O_2 and 5% CO_2 and maintained at 37°C.

The pulmonary artery rings were initially incubated in Krebs soltuion in the presence of vehicle, LPS (1 μg ml^{-1}) or heat inactivated GBS (3×10^7 colony forming units, c.f.u. ml^{-1}) for 1, 5 or 20 h. To confirm that LPS and GBS induced iNOS, in some experiments pulmonary rings were coincubated for 20 h in Krebs solution containing dexamethasone (3×10^{-6} M), an inhibitor of NOS induction, (Radomski *et al.*, 1990) or cycloheximide (10^{-5} M, an inhibitor of protein synthesis). After incubation, two L-shaped stainless-steel wires were inserted into the arterial lumen and the rings were introduced in Allhin organ chambers filled with Krebs solution. One wire was attached to the chamber and the other to an isometric force-displacement transducer (Grass FT07) and connected to a polygraph (Grass, model 7) as previously described (Pérez-Vizcaíno *et al.*, 1993). The rings were stretched to a resting tension of 0.5 g and allowed to equilibrate for 60–90 min. During this period tissues were restretched and washed every 30 min with warm Krebs solution. In some experiments the endothelium was removed by gently rubbing the intimal surface of the rings with a metal rod. The presence of functional endothelium was verified by addition of acetylcholine (ACh, 10^{-6} M) in arteries precontracted with NA. The ability of ACh to induce relaxation of unrubbed rings was taken as an indicator of the presence of functional endothelium.

Experimental protocol

In pulmonary rings previously incubated with vehicle, LPS or GBS for 1, 5 or 20 h, concentration-response curves to NA (10^{-8} M to 10^{-4} M) were constructed by increasing the organ chamber concentration by cumulative increments after a steady state response had been reached with each increment. In three groups of intact pulmonary arteries, following the incubation period of 20 h, cumulative concentration-response curves to NA were performed in the presence of N^G-nitro-L-arginine-methyl ester (L-NAME, 10^{-4} M, an inhibitor of both cNOS and iNOS, Sakuma *et al.*, 1988), L-arginine (10^{-5} M, the precursor of NO, Palmer *et al.*, 1988) or meclofenamate (10^{-5} M, an inhibitor of cyclo-oxygenase) which were added 30 min before the concentration-response curve to NA was obtained.

Assay of NOS

Lung fragments (weight 100–150 mg) were incubated in the same conditions as described for the arterial rings. After incubation, tissues were immediately stored at −80°C until studied. The frozen tissues were homogenized at 0–4°C in 5 vols of a buffer containing 320 mM sucrose, 50 mM Tris, 1 mM EDTA, 1 mM DL-dithiothreitol, 100 μg ml^{-1} phenylmethylsulfonyl fluoride, 10 μg ml^{-1} leupeptin, 100 μg ml^{-1} soybean trypsin inhibitor and 2 μg ml^{-1} aprotinin brought to pH 7.0 at 20°C with HCl. The homogenates were then centrifuged at 4°C at 12000 *g* for 20 min. The pellets were discarded and the supernatants were placed on ice until incubation the same day. NOS activity was determined by measuring in duplicate the conversion of L-[U-^{14}C]-arginine to L-[U-^{14}C]-citrulline by 10 min incubation at 37°C as described in detail by Salter *et al.* (1991). The incubation buffer contained 50 mM L-valine to minimize any interference from arginase. Ca^{2+}-dependent NOS (cNOS) activity was calculated from the difference between the L-[U-^{14}C]-citrulline produced from control samples containing incubation buffer and samples containing buffer plus 1 mM EGTA. The activity of the Ca^{2+}-independent NOS (iNOS) was determined from the difference between samples containing 1 mM EGTA in the incubation buffer and samples containing 1 mM EGTA plus 2 mM N^G-monomethyl-L-arginine (a competitive inhibitor of NOS, Palmer *et al.*, 1988).

Drugs and heat-killed GBS preparation

The following drugs were used: (−)-noradrenaline bitartrate, acetylcholine chloride, lipopolysaccharide from *E. coli* (serotype 055:B5), dexamethasone, cycloheximide, L-NAME, L-arginine (Sigma Chemical Co., London) and meclofenamate (Warner Lambert Co., U.S.A.). Meclofenamate was dissolved in absolute ethanol. The concentrations are expressed as final molar concentration in the tissue chamber. L-[U-^{14}C]-arginine was obtained from Amersham International (U.K.).

GBS type III was isolated from the blood of a neonate who developed early-onset sepsis. Bacteria were grown in Todd-Hewitt broth for 18–36 h at 37°C to late log phase and harvested by centrifugation at 5000 r.p.m. for 15 min. Bacteria were resuspended in sterile isotonic saline to a concentration determined by serial viable counts to be 1×10^9 c.f.u. ml^{-1}. Heat-killed bacteria were obtained by heating bacteria to 60°C for 60 min. GBS killing was confirmed by no growth on blood agar. Endotoxin levels in the heat-killed GBS preparation were undetectable as assayed by a standard Limulus assay kit (Sigma). Aliquots of heat-killed GBS were stored at −80°C until the study day.

Statistical analysis

Results are expressed as means ± s.e.mean of measurements in *n* arteries. Individual cumulative concentration-response curves to NA were fitted to a logistic equation. In most of the experiments the point corresponding to 10^{-4} M NA was below the maximal tension and was therefore excluded from the fitting. The drug concentration exhibiting 50% of the maximal contraction to NA was calculated for each ring and expressed as negative log molar (pD_2). The E_{max} was defined as the maximal tension induced by NA in each ring. Statistically significant differences were calculated by means of an ANOVA analysis followed by a Newman Keuls means comparison testing. $P < 0.05$ was considered statistically significant.

Results

Effects of LPS and GBS in the presence or absence of endothelium

Short-term incubation of intact pulmonary arteries with LPS (1 μg ml^{-1}) or GBS (3×10^7 c.f.u. ml^{-1}) for 1 or 5 h produced no significant effects on the concentration-response curve to NA (Table 1). However, as shown in Figure 1a, when the endothelium-intact arteries were incubated for a

longer period (20 h) with LPS (1 μg ml^{-1}) or GBS (3×10^7 c.f.u. ml^{-1}) and then transferred to the organ bath in the absence of bacterial products, the maximal contractile response to NA was reduced and thus, a downward shift of the concentration-response curve to NA was observed. This was accompanied by a small, but significant, decrease of the pD_2 values (Table 1). These results indicate that pulmonary vascular hyporesponsiveness to NA is a delayed process and suggested the induction of a biological activity. Endothelium-denuded arteries showed significantly greater maximal responses to NA as compared to endothelium-intact arteries ($P<0.01$) incubated with vehicle, LPS or GBS (Table 1). Nevertheless, mechanical removal of endothelial cells did not affect the hyporeactivity to NA observed after long-term incubation (20 h) with LPS or GBS (Figure 1b).

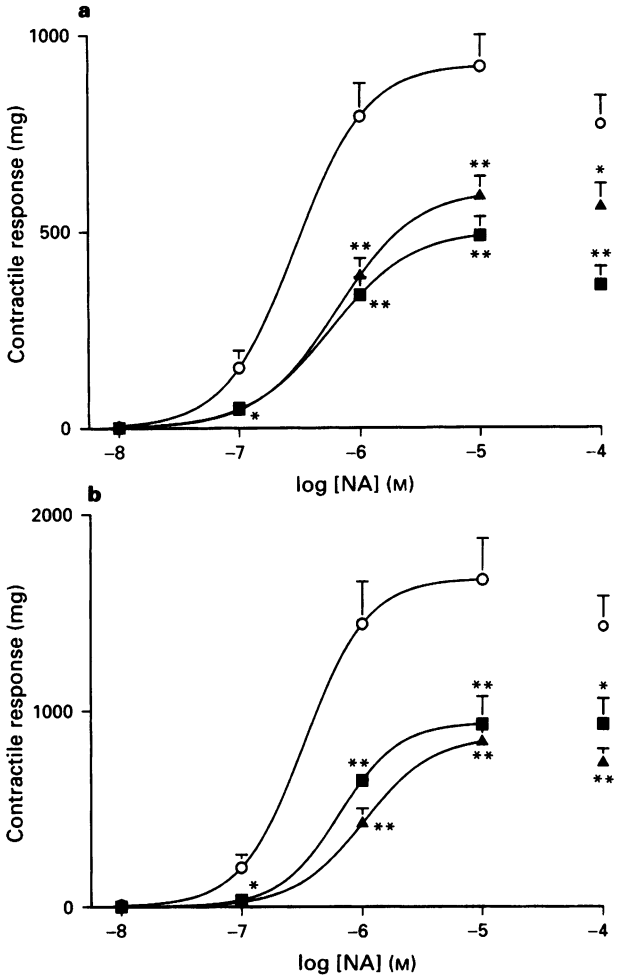

Figure 1 Concentration-response curve to noradrenaline (NA, 10^{-8}–10^{-4} M) in intrapulmonary arterial rings (a) with or (b) without endothelium, preincubated for 20 h in Krebs solution in the presence of vehicle (control, ○), *E. coli* lipopolysaccharide (LPS, 1 μg ml^{-1}, ■) or heat inactivated group B *Streptococcus* (GBS, 3×10^7 c.f.u. ml^{-1}, ▲). The concentration-response curve to NA was carried out in the absence of bacterial products. Data are expressed as means ± s.e.mean of 7–22 observations. *$P<0.05$ and **$P<0.01$ represent significant differences with respect to control group.

Effects of L-arginine, L-NAME and meclofenamate

In order to assess the role of NO production in the hyporesponsiveness to NA, a concentration-response curve to NA was performed in control, LPS- and GBS-treated arteries acutely treated with either the NO-precursor, L-arginine (10^{-5} M), or the NOS inhibitor, L-NAME (10^{-4} M). As shown in Figure 2a and Table 1, in control arteries treated with L-arginine the concentration-response curve to NA was not modified compared to that obtained in arteries in the absence of L-arginine. In contrast, in arteries incubated with LPS or GBS for 20 h, the presence of L-arginine potentiated ($P<0.01$) the hyporesponsiveness to NA. Addition of 10^{-4} M L-NAME to resting arteries produced a small contractile effect averaging 45.7 ± 6.6 mg, 44.3 ± 9.6 mg and 43.1 ± 5.9 mg, in untreated and in arteries treated with LPS and GBS, respectively. Thereafter, L-NAME induced an upward shift of the concentration-response curve to NA in the LPS- and GBS-treated arteries resulting in no differences between control, LPS- or GBS-treated arteries (Figure 2b). Therefore, L-NAME reversed the hyporesponsiveness to NA induced by LPS and GBS.

The possible role of vasodilator prostaglandins in the hyporeactivity to NA was assessed by acute treatment of the arteries with the cyclo-oxygenase inhibitor, meclofenamate. The presence of 10^{-5} M meclofenamate did not affect the hyporesponsiveness to NA in LPS- and GBS-treated arteries (Table 1).

Effect of dexamethasone and cycloheximide

In order to assess the induction of NOS by LPS and GBS, intact pulmonary arteries were simultaneously incubated with LPS and GBS and 3×10^{-6} M dexamethasone or 10^{-6} M cycloheximide for 20 h. As shown in Figure 3, both dexamethasone and cycloheximide completely restored the reactivity to NA in LPS- and GBS-treated arteries. Moreover, dexamethasone (but not cycloheximide)-treated arteries showed greater pD_2 values in control arteries (Table 1).

Table 1 Effects of *E. coli* lipopolysaccharide (LPS, 10 μg ml^{-1}) and group B *Streptococcus* (GBS, 3×10^7 c.f.u. ml^{-1}) on the parameters (E_{max} and pD_2) of the concentration-response curve to noradrenaline (NA) in the absence and presence of various inhibitors

			Control			*LPS*			*GBS*		
Drug		*t(h)*	E_{max} (mg)	pD_2	n	E_{max} (mg)	pD_2	n	E_{max} (mg)	pD_2	n
None	+E	1	1198 ± 141	6.39 ± 0.15	11	1212 ± 153##	6.47 ± 0.43	9	1157 ± 245##	6.31 ± 0.21	8
None	+E	5	1192 ± 212	6.37 ± 0.08	9	1111 ± 127##	6.66 ± 0.15#	8	876 ± 160	6.51 ± 0.19	9
None	+E	20	923 ± 80	6.52 ± 0.07	17	492 ± 47**	6.25 ± 0.10*	13	613 ± 52**	6.17 ± 0.08**	22
None	−E	20	1676 ± 208##	6.46 ± 0.08	7	946 ± 140**##	6.17 ± 0.08*	7	877 ± 68**#	5.98 ± 0.10**	8
Meclofenamate	+E	20	1026 ± 98	6.49 ± 0.08	11	585 ± 55**	6.44 ± 0.06	11	450 ± 77**	6.10 ± 0.04	11
L-Arginine	+E	20	1032 ± 124	6.39 ± 0.09	8	299 ± 50**#	6.07 ± 0.08	11	341 ± 77**##	6.22 ± 0.13	9
L-NAME	+E	20	1047 ± 120	6.72 ± 0.11	10	1023 ± 99##	6.49 ± 0.09	14	1164 ± 55##	6.66 ± 0.08##	12
Dexamethasone	+E	20	876 ± 63	6.89 ± 0.06#	14	923 ± 62##	6.72 ± 0.08#	11	831 ± 64#	6.82 ± 0.06##	11
Cycloheximide	+E	20	879 ± 95	6.64 ± 0.07	7	1107 ± 103##	6.71 ± 0.09#	7	911 ± 82	6.66 ± 0.11	8

t = incubation period. +E = endothelium intact, −E = endothelium denuded. Meclofenamate (10^{-5} M), L-arginine (10^{-5} M) or N^G-nitro-L-arginine methyl ester (L-NAME, 10^{-4} M) were added to the organ bath solution 30 min before the addition of NA. Dexamethasone (3×10^{-6} M) or cycloheximide (10^{-5} M) were included during the 20 h incubation period.
*$P<0.05$ and **$P<0.01$ GBS- or LPS-treated vs control arteries. #$P<0.05$ and ##$P<0.01$ vs arteries +E, 20 h, no drug. The drug concentration exhibiting 50% of the maximal contraction to NA was calculated for each ring and expressed as negative log molar (pD_2). The E_{max} was defined as the maximal tension induced by NA in each ring.

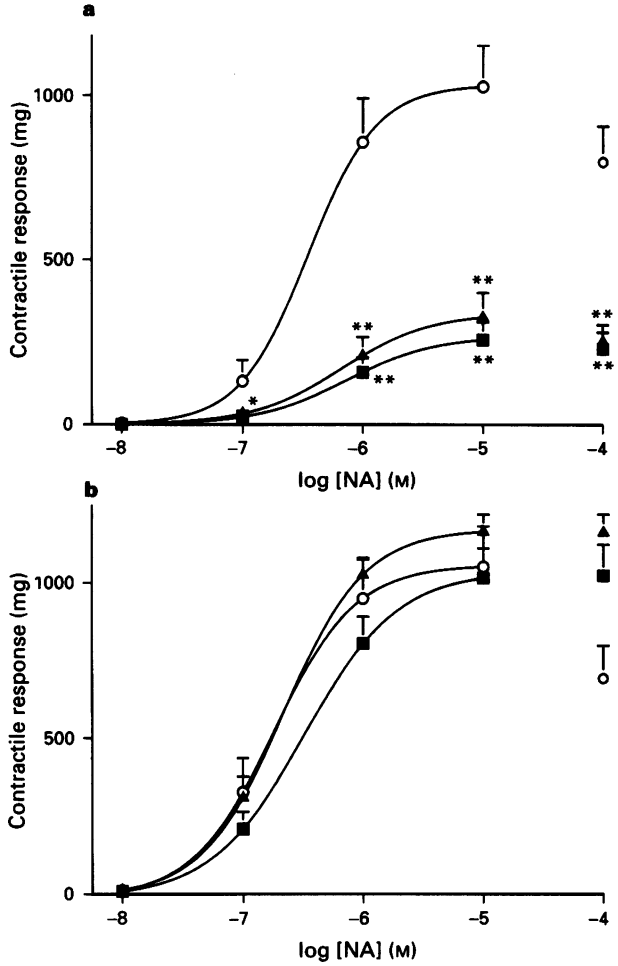

Figure 2 Effects of (a) L-arginine (10^{-5} M) or (b) N^G-nitro-L-arginine methyl ester (L-NAME, 10^{-4} M) on *E. coli* lipopolysaccharide (LPS)- and group B *Streptococcus* (GBS)-induced hyporeactivity to noradrenaline (NA) in intrapulmonary artery rings. Concentration-response curves to noradrenaline (NA, 10^{-8}–10^{-4} M) were performed in intrapulmonary arterial rings previously incubated for 20 h in Krebs solution in the presence of vehicle (control, O), LPS (1 μg ml^{-1}, ■) or heat-inactivated GBS (3×10^7 c.f.u. ml^{-1}, ▲). L-Arginine (10^{-5} M) or L-NAME (10^{-4} M) was added 30 min before addition of NA. The curve was obtained in the absence of bacterial products. Data are expressed as means ± s.e.mean of 8–14 observations. *$P<0.05$ and **$P<0.01$ represent significant differences with respect to control group.

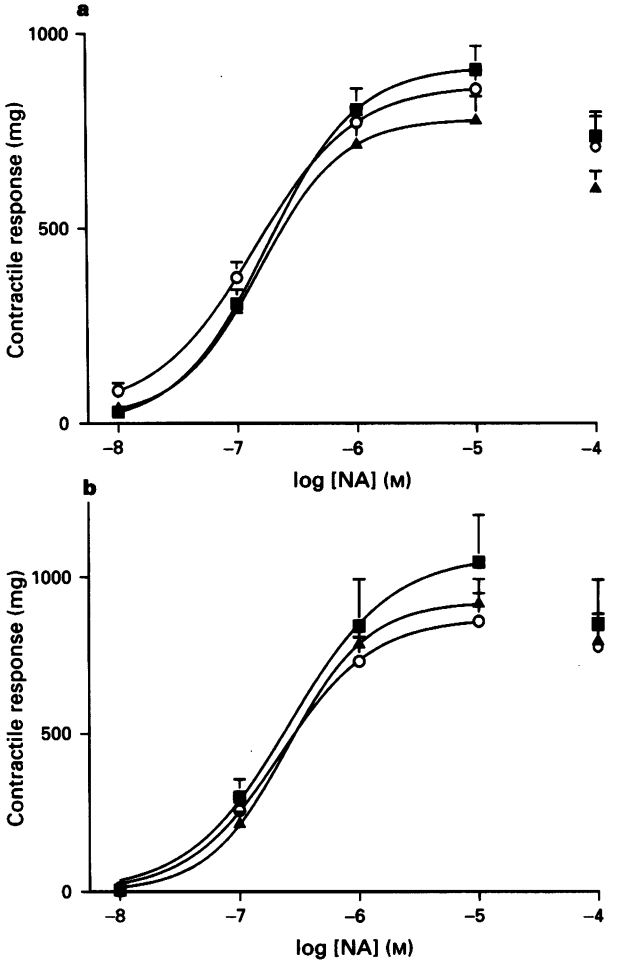

Figure 3 Effects of (a) dexamethasone (3×10^{-6} M) or (b) cycloheximide (10^{-5} M) when coincubated with *E. coli* lipopolysaccharide (LPS) and group B *Streptococcus* (GBS). Concentration-response curves to noradrenaline (NA, 10^{-8}–10^{-4} M) were performed in intrapulmonary arterial rings previously incubated for 20 h in Krebs solution in the presence of vehicle (O), LPS (1 μg ml^{-1}, ■) or heat-inactivated GBS (3×10^7 c.f.u. ml^{-1}, ▲). The curve was obtained in the absence of bacterial products. Data are expressed as means ± s.e.mean of 7–14 observations. *$P<0.05$ and **$P<0.01$ represent significant differences when compared to control group.

Effects of LPS and GBS on NOS activity

NOS activity was measured by the conversion of radiolabelled L-arginine to citrulline (Salter *et al.*, 1991). Using this method, NOS activity was almost undetectable in pulmonary arteries. Therefore, the cNOS (Ca^{2+}-dependent) and iNOS (Ca^{2+}-independent) activities were determined in lung fragments. Control values for cNOS and iNOS activities were 61.5 ± 10.7 and 36.0 ± 6.4 pmol min^{-1} mg^{-1} of tissue, respectively. As shown in Figure 4, no change in cNOS activity was detected after incubation with 1 μg ml^{-1} LPS or 3×10^7 c.f.u. ml^{-1} GBS for 20 h. In contrast, LPS and GBS significantly increased the iNOS activity ($P<0.01$). Dexamethasone (3×10^{-6} M) produced no change in cNOS activity but completely abolished the LPS- and GBS-induced increase in iNOS activity (Figure 4).

Discussion

The present results demonstrated that only after prolonged (>5 h) incubation, did LPS and GBS reduce vascular responsiveness to NA in isolated pulmonary artery rings of neonatal pigs. After incubation, the experiments were performed in the absence of LPS or GBS which indicated that the hyporesponsiveness was a delayed process that was not due to a direct action of bacterial toxins but more likely to the induction of biological activity. The decreased response did not require the presence of an intact endothelium and was not mediated by products of cyclo-oxygenase activity since it was unaffected by endothelium removal or the cyclo-oxygenase inhibitor, meclofenamate, respectively. Our results strongly suggested that induction of iNOS is implicated in the GBS- and LPS-induced pulmonary vascular hyporesponsiveness to NA. To our knowledge this is the first paper showing that GBS produces hyporesponsiveness to NA and induction of iNOS activity.

There is a growing consensus that NO plays a major role in the control of pulmonary vascular smooth muscle tone (Moncada *et al.*, 1991; Dinh-Xuan, 1992; Stamler *et al.*, 1994). Thus, an impaired release of NO has been associated with an increased pulmonary vascular reactivity to constrictor stimuli and may contribute to the pathogenesis of pulmonary hypertension (Moncada *et al.*, 1991; Dinh-Xuan, 1992). In the present experiments, L-arginine potentiated the reduced vascular reactivity to NA in pulmonary arteries of

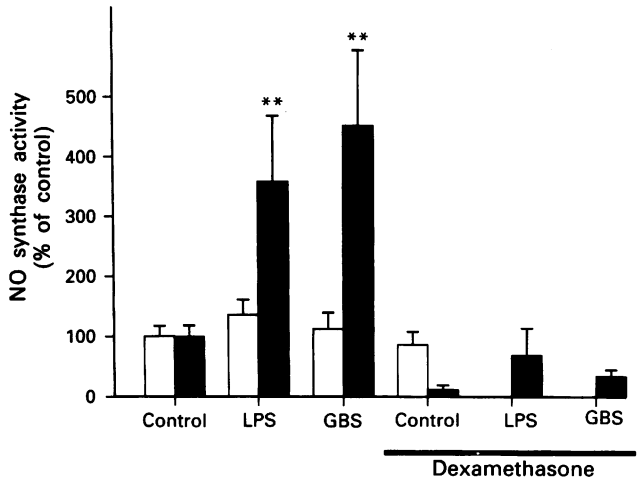

Figure 4 Ca^{2+}-dependent (constitutive, open columns) and Ca^{2+}-independent (inducible, solid columns) nitric oxide synthase (NOS) activities in lung fragments incubated for 20 h in 37°C oxygenated Krebs solution in the presence of vehicle (control), *E. coli* lipopolysaccharide (LPS, 1 $\mu g\ ml^{-1}$) or group B *Streptococcus* (GBS, 3×10^7 c.f.u. ml^{-1}) and in the absence or presence of dexamethasone (3×10^{-6} M). Data are expressed as percentage of the control Ca^{2+}-dependent and Ca^{2+}-independent activities, respectively (means ± s.e.mean of 5–7 observations). Control values for cNOS and iNOS activities were 61.5 ± 10.7 and 36.0 ± 6.4 pmol min^{-1} mg^{-1} of tissue, respectively. $^{**}P < 0.01$ represent significant differences when compared to control group.

newborn piglets incubated with LPS and GBS, while L-NAME completely reversed it. Moreover, dexamethasone, which inhibits the induction of NOS (Radomski *et al.*, 1990) and cycloheximide, an inhibitor of protein synthesis when coincubated with LPS or GBS for 20 h, completely reversed the reduced response to NA. All these results suggest that GBS- and LPS-induced pulmonary vascular hyporesponsiveness to NA is associated with enhanced formation of NO via the iNOS and requires the synthesis *de novo* of the enzyme in the pulmonary vasculature. However, in pulmonary arteries the NOS activity was below the limit of detection. This can be related to the fact that cNOS and iNOS activities in vascular smooth muscle are 5–50 times lower than in lung (Salter *et al.*, 1991; Mitchell *et al.*, 1993). Thus, we assessed the effects of LPS and GBS on both cNOS and iNOS in lung fragments. LPS and GBS had no effect on cNOS but induced a marked increase in iNOS activity which was abolished when lung fragments were incubated with dexamethasone. GBS- and LPS-induction of iNOS in the lung supported the functional evidence of induction of iNOS in pulmonary arteries. As previously reported in rat and rabbit lung (Salter *et al.*, 1991; Mitchell *et al.*, 1993; Szabo *et al.*, 1993), we found that iNOS activity was expressed basally in porcine lung tissue. Since basal iNOS activity was lowered by dexamethasone, it might indicate a certain endotoxin contamination of the incubation media.

GBS is able to produce sepsis only in the neonate and exceptionally in parturients and immunodepressive patients (Anthony, 1985). The mechanism of GBS-induced pulmonary injury in neonates is still a matter of controversy. Gram-positive bacteria do not contain LPS and a common toxin to all Gram-positive organisms has not been identified. It has been shown recently that lipoteichoic acid (LTA), a component of the peptidoglycan layer of the cell wall in most Gram-positive bacteria, decreased the responses to pressor agents and induced iNOS in cultured vascular smooth muscle cells, rat aorta (Auguet *et al.*, 1992) and in anaesthetized rats (De Kimpe *et al.*, 1994). Killed whole *S. aureus* also induced NOS in macrophages (Cunha *et al.*, 1993). Clinical isolates of GSB, including type III, recovered from infants with sepsis, possessed significantly higher levels of LTA in their cell wall than those isolated from asymptomatic carriers (Nealon & Mattingly, 1983). The molecular analysis of GBS LTA demonstrated a close similarity with the Group A *Streptococcus* LTA (Maurer & Mattingly, 1991). Thus, the LTA component of GBS might be responsible for the effects on vascular reactivity and iNOS induction described in the present paper. In addition, two different GBS polysaccharide toxins producing pathophysiological changes mimicking those of GBS infection in neonates have been identified, a non specific mannan polysaccharide (Hellerqvist *et al.*, 1987) and the type III specific capsular polysaccharide (Hemming *et al.*, 1984). However, the type III specific capsular polysaccharide does not seem to be required for the acute phase but it may play a role in the late phase (>2 h) of GBS-induced pulmonary haemodynamic alterations in piglets (Gibson *et al.*, 1989). In the present experiments we used heat-inactivated GSB, i.e. an unfragmented capsule, isolated from the blood of a neonate who developed early-onset sepsis. Heat-inactivated GBS has been previously shown to cause similar haemodynamic effects as the live GBS (Schrieber *et al.*, 1992). Further studies would be necessary to elucidate the specific component of GBS responsible for NOS induction.

The lung is a major target organ in neonatal sepsis (Ablow *et al.*, 1976). In general, the lung plays a determinant role in the sepsis in some animal species that exhibit a pulmonary bacterial clearance (e.g. sheep, pig) but not in species (e.g. dog, rat, rabbit) in which bacteria localize predominantly in the liver and spleen (Winkler, 1988). The uptake of bacteria by pulmonary intravascular macrophages and the subsequent release of inflammatory mediators are central to the pathological changes produced in sepsis-induced adult respiratory distress syndrome in sheep (Warner *et al.*, 1987) and in GBS-induced pulmonary hypertension in newborn piglets (Bowdy *et al.*, 1990). In these models, as in man, sepsis produces a complex pulmonary response in which two different phases have been delimited (Brigham & Meyrick, 1986). Initially there is a marked increase in pulmonary artery pressure and hypoxemia, whereas the second phase is characterized by a returning of pulmonary pressure towards baseline and an increased lung vascular permeability. This latter phase is accompanied by marked increases in guanosine 3':5'-cyclic monophosphate (cyclic GMP, Snapper *et al.*, 1983). NO-mediated vasorelaxation has been correlated with the activation of soluble guanylate cyclase which in turn increases the intracellular concentrations of cyclic GMP (Ignarro *et al.*, 1987; Moncada *et al.*, 1991). Thus, the increased production of NO following the induction of iNOS in pulmonary arteries described here could be responsible for the previously reported increased cyclic GMP production which is a main feature of the latter phase of the pulmonary response to sepsis.

In conclusion, the present results demonstrated that prolonged incubation with GBS, as previously reported with LPS, causes an induction of iNOS which results in a loss of vascular responsiveness to NA in intrapulmonary arteries of neonatal piglets. Thus, the induction of iNOS seems to be a key mediator in the delayed pulmonary vascular hyporesponsiveness characteristic of the pulmonary injury induced by either Gram-positive or Gram-negative sepsis.

This work was supported by a CICYT (92/0157) and Fis (95/0308) Grant. E.V. is a recipient of the Asociación Española de Pediatría/Arbora S.A. Grant for Pediatric Research. We would like to thank Dr Elorza, Dr Romero and Mrs María Gómez for providing the heat-killed Group B *Streptococcus*.

References

ABLOW, R.C., DRISCOLL, S.G., EFFMANN, E.L., GROSS, I., JOLLES, C.J., KAUY, R. & WARSHAW, J.B. (1976). A comparison of early-onset group B streptococcal neonatal infection and the respiratory-distress syndrome of the newborn. *New Engl. J. Med.*, **294**, 65–69.

ANTHONY, B.F. (1985). Epidemiology of GBS in man. *Antibiot. Chemother.*, **35**, 10–16.

AUGUET, M., LONCHAMPT, M.O., DELAFLOTTE, S., GOULIN-SCHULZ, J., CHABRIER, P.E. & BRAQUET, P. (1992). Induction of nitric oxide synthase by lipoteichoic acid from *Staphylococcus aureus* in vascular smooth muscle cells. *FEBS Lett.*, **297**, 183–185.

BOWDY, B.D., MARPLE, S.L., PAULY, T.H., COONROD, J.D. & GILLESPIE, M.N. (1990). Oxygen radical-dependent bacterial killing and pulmonary hypertension in piglets infected with group B Streptococci. *Am. Rev. Respir. Dis.*, **141**, 648–653.

BRIGHAM, K.L. & MEYRICK, B. (1986). Endotoxin and lung injury. *Am. Rev. Respir. Dis.*, **133**, 913–927.

BUSSE, R. & MÜLSCH, A. (1990). Induction of nitric oxide by cytokines in vascular smooth muscle cells. *FEBS Lett.*, **275**, 87–90.

CUNHA, F.Q., MOSS, D.W., LEAL, L.M., MONCADA, S. & LIEW, F.Y. (1993). Induction of macrophage parasiticidal activity by *Staphylococcus aureus* and exotoxins through the nitric oxide synthase pathway. *Immunology*, **78**, 563–567.

DE KIMPE, S.J., THIEMERMANN, C. & VANE, J.R. (1994). Lipoteichoic acid, a cell wall component of Gram-positive bacteria, causes hypotension and induction of nitric oxide synthase in anaesthetized rats. *Br. J. Pharmacol.*, **112**, 442P.

DINH-XUAN, A.T. (1992). Endothelial modulation of pulmonary vascular tone. *Eur. Respir. J.*, **5**, 757–762.

GIBSON, R.L., REDDING, G.J., TRUOG, W.E., HENDERSON, W.R. & RUBENS, C.E. (1989). Isogenic group B streptococci devoid of capsular polysaccharide or β-Hemolysin: pulmonary hemodynamic and gas exchange effects during bacteriemia in piglets. *Pediatr. Res.*, **26**, 241–245.

GROENEVELD, A.B.J., NAUTA, J.J.P. & THIJS, L.G. (1988). Peripheral vascular resistance in septic shock: its relation to outcome. *Intensive Care Med.*, **14**, 141–147.

GUERINA, N.G. (1991). Bacterial and fungal infections. In *Manual of Neonatal Care*. ed. Cloherty, J.P. & Stark, A.R. pp. 146–148. Boston/Toronto/London: Little, Brown and Company.

HELLERQVIST, C.G., SUNDELL, H. & GETTINS, P. (1987). Molecular basis of group B β-haemolytic streptococcal disease. *Proc. Natl. Acad. Sci. U.S.A.*, **84**, 51–55.

HEMMING, V.G., O'BRIEN, W.F., FISCHER, G.W., GOLDEN, S.M. & NOBEL, S.F. (1984). Studies of short-term pulmonary and peripheral vascular responses induced in oophorectomized sheep by infusion of a group B streptococcal extract. *Pediatr. Res.*, **18**, 266–269.

IGNARRO, L.J., BYRNS, R.E., BUGA, G.M. & WOOD, K.S. (1987). Endothelium-derived relaxing factor from pulmonary artery and vein possesses pharmacologic and chemical properties identical to those of nitric oxide radical. *Circ. Res.*, **61**, 866–879.

JULOU-SCHAEFFER, G., GRAY, G.A., FLEMING, I., SCHOTT, C., PARRATT, J.R. & STOCLET, J.-C. (1990). Loss of vascular responsiveness induced by endotoxin involves L-arginine pathway. *Am. J. Physiol.*, **259**, H1038–H1043.

KNOWLES, R.G., MERRETT, M., SALTER, M. & MONCADA, S. (1990). Differential induction of brain, lung and liver nitric oxide synthase by endotoxin in the rat. *Biochem. J.*, **270**, 833–836.

MARLETTA, M.A., YOON, P.A., IYENGAR, R., LEAF, C.D. & WISHNOK, J.S. (1988). Macrophage oxidation of L-arginine to nitrite and nitrate: nitric oxide is an intermediate. *Biochemistry*, **27**, 8706–8711.

MAURER, J.J. & MATTINGLY, S.J. (1991). Molecular analysis of lipoteichoic acid from *Streptococcus agalactie*. *J. Bacteriol.*, **173**, 487–494.

MCKENNA, T.M. (1990). Prolonged exposure of rat aorta to low levels of endotoxin in vitro results in impaired contractility. Association with vascular cytokine release. *J. Clin. Invest.*, **86**, 160–168.

MITCHELL, J.A., KOHLHAAS, K.L., SORRENTINO, R., WARNER, T.D., MURAD, M. & VANE, J. (1993). Induction by endotoxin of nitric oxide synthase in the rat mesentery: lack of effect on action of vasoconstrictors. *Br. J. Pharmacol.*, **109**, 265–270.

MONCADA, S., PALMER, R.M.J. & HIGGS, E.A. (1991). Nitric oxide: physiology, pathophysiology, and pharmacology. *Pharmacol. Rev.*, **43**, 109–142.

NEALON, T.J. & MATTINGLY, S.J. (1983). Association of elevated levels of cellular lipoteichoic acids of group B Streptococci with human neonatal disease. *Infect. Immun.*, **39**, 1243–1251.

PALMER, R.M.J., ASHTON, D.S. & MONCADA, S. (1988). Vascular endothelial cells synthesize nitric oxide from L-arginine. *Nature*, **333**, 664–666.

PEREZ-VIZCAINO, F., CASIS, O., RODRIGUEZ, R., GOMEZ, L.A., GARCIA RAFANELL, J. & TAMARGO, J. (1993). Effects of the novel potassium channel opener, UR-8225, on contractile response in rat isolated smooth muscle. *Br. J. Pharmacol.*, **110**, 1165–1171.

RADOMSKI, M.W., PALMER, R.M.J. & MONCADA, S. (1990). Glucocorticoids inhibit the expression of an inducible, but not the constitutive, nitric oxide synthase in vascular endothelial cells. *Proc. Natl. Acad. Sci. U.S.A.*, **87**, 10043–10047.

ROJAS, J., LARSON, L.E., HELLERQVIST, C.G., BRIGHAM, K.L., GRAY, M.E. & STAHLMAN, M.T. (1983). Pulmonary hemodynamics and ultrastructural changes associated with group B streptococcal toxemia in adult sheep and newborn lambs. *Pediatr. Res.*, **17**, 1002–1008.

SAKUMA, I., STUEHR, D.J., GROSS, S.S., NATHAN, C. & LEVI, R. (1988). Identification of arginine as a precursor of endothelium derived relaxing factor. *Proc. Natl. Acad. Sci. U.S.A.*, **85**, 8664–8667.

SALTER, M., KNOWLES, R.G. & MONCADA, S. (1991). Widespread tissue distribution, species distribution and changes in activity of Ca^{2+}-dependent and Ca^{2+}-independent nitric oxide synthases. *FEBS Lett.*, **291**, 145–149.

SCHREIBER, M.D., COVERT, R.F. & TORGERSN, L. (1992). Hemodynamic effects of heat-killed group B β-hemolytic streptococcus in newborn lambs: role of leukotriene D_4. *Pediatr. Res.*, **31**, 121–126.

SNAPPER, J., BRIGHAM, K.L., HEFLIN, C., BOMBOY, J. & GRABER, S. (1983). Effects of endotoxemia on cyclic nucleotides in the unanesthetized sheep. *J. Lab. Clin. Med.*, **102**, 240–249.

STAMLER, J.S., LOH, E., RODDY, M., CURRIE, K.E. & CREAGER, M.A. (1994). Nitric oxide regulates basal systemic and pulmonary vascular resistance in healthy humans. *Circulation*, **89**, 2035–2040.

STUEHR, D.J. & GRIFFITH, D.W. (1992). Mammalian nitric oxide synthases. *Adv. Enzymol. Mol. Biol.*, **65**, 287–343.

SZABO, C., MITCHELL, J.A., THIEMERMANN, C. & VANE, J.R. (1993). Nitric oxide-mediated hyporeactivity to noradrenaline precedes the induction of nitric oxide synthase in endotoxin shock. *Br. J. Pharmacol.*, **108**, 786–792.

THIEMERMANN, C. (1994). The role of the L-arginine: nitric oxide pathway in circulatory shock. *Adv. Pharmacol.*, **28**, 45–79.

WARNER, A.E., MOLINA, R. & BRAIN, J.D. (1987). Uptake of blood-borne bacteria by pulmonary intravascular macrophages and consequent inflammatory responses in sheep. *Am. Rev. Respir. Dis.*, **136**, 683–693.

WINKLER, G.G. (1988). Pulmonary intravascular macrophages in domestic species: review of structural and functional properties. *Am. J. Anat.*, **181**, 217–234.

ZELENKOV, P., MCLOUGHLIN, T. & JOHNS, R.A. (1993). Endotoxin enhances hypoxic constriction of rat aorta and pulmonary artery through induction of EDRF/NO synthase. *Am. J. Physiol.*, **265**, L346–L354.

(Received September 26, 1994
Revised January 5, 1995
Accepted February 6, 1995)

British Journal of Pharmacology (1995) 115, 267-274

Mechanism of block of a human cardiac potassium channel by terfenadine racemate and enantiomers

Tao Yang, [1]Chandra Prakash, Dan M. Roden & [2]Dirk J. Snyders

Departments of Pharmacology and Medicine, Vanderbilt University School of Medicine, Nashville, Tennessee 37232 6602, U.S.A.

1 The cardiac toxicity of racemic terfenadine (marked QT prolongation and polymorphic ventricular arrhythmias) is probably due to potassium channel blockade. To test whether one of its enantiomers would be a less efficient potassium channel blocker, we compared the mechanism of action of the racemate with that of the individual enantiomers.

2 We synthesized the individual enantiomers of terfenadine and examined under whole cell voltage-clamp conditions the mechanism of action of the racemate, both enantiomers and a major metabolite on a cloned human cardiac potassium channel, hKv1.5. This delayed rectifier is sensitive to quinidine, clofilium and other 'class III' antiarrhythmic drugs at clinically relevant concentrations.

3 Upon depolarization, racemic terfenadine and its enantiomers induced a fast decline of hKv1.5 current towards a reduced steady state current level. During subsequent repolarization the tail currents deactivated more slowly than the control, resulting in a 'crossover' phenomenon.

4 The voltage-dependence of block was biphasic with a steep increase in block over the voltage range of channel opening (−30 to 0 mV), and a more shallow phase positive to 0 mV (where the channel is fully open). The latter was consistent with a binding reaction sensing 21% of the transmembrane electrical field (with reference to the cell interior).

5 The EC_{50} for hKv1.5 block by racemic terfenadine was 0.88 μM, while the values for **R**- and **S**-terfenadine were 1.19 μM and 1.16 μM, respectively. In contrast, the acid metabolite reduced hKv1.5 current by only 5% at a concentration of 50 μM.

6 These findings suggest that terfenadine blocks the hKv1.5 channel after it opens by entering into the internal mouth of the channel. We have previously shown that quinidine blocks hKv1.5 in a similar manner but with an apparent affinity of ~6 μM. Thus, terfenadine and its enantiomers are approximately equipotent open state blockers of this human K^+ channel and about 6 times more potent than quinidine. The similar state-, time-, and voltage-dependence of hKv1.5 block by both enantiomers also indicates that the chiral centre does not significantly constrain the orientation of critical binding determinants of terfenadine with respect to the receptor site.

Keywords: Potassium channels; arrhythmia; torsades de pointes; stereoisomers; histamine H_1 antagonist; pro-arrhythmia; Kv1.5

Introduction

Multiple types of potassium currents have been identified in the heart. These potassium currents maintain the resting potential, control action potential duration and modulate pacemaker activity. Inhibition of the delayed rectifier K^+ currents prolongs action potential duration, an effect which may be antiarrhythmic (Singh & Nademanee, 1985) but also carries a proarrhythmic potential. Indeed, excessive lengthening of repolarization is associated with abnormal electrical activity consisting of early afterdepolarizations triggering a polymorphic ventricular arrhythmia known as torsades de pointes (Roden, 1990). This arrhythmia appears to be a side-effect common to many antiarrhythmic drugs that block cardiac K^+ channels, such as quinidine, procainamide and sotalol.

Some cases of torsades de pointes occur in patients who receive non-antiarrhythmic drugs. An example is the histamine H_1-receptor antagonist, terfenadine which is widely used to alleviate allergic symptoms (McTavish *et al.*, 1990) and which was among the top 10 prescribed drugs in the U.S.A. in 1991 (Simonsen, 1992). Clinical situations in which terfenadine may accumulate have been associated with torsades de pointes (Davies *et al.*, 1989; Monahan *et al.*, 1990; Mathews *et al.*, 1991; Honig *et al.*, 1992). This is consistent with the concept that the drug (or an accumulating metabolite or enantiomer) blocks cardiac K^+ channels (Woosley *et al.*, 1993).

Drug-channel interactions in the heart have been studied largely in native cardiac myocytes of 'representative' mammalian species. However, this approach has some drawbacks such as the problem of the multiple overlapping ionic currents in the native myocytes. Usually a combination of extracellular ion substitution and channel blockers is used to eliminate all currents except the one of interest (Sanguinetti & Jurkiewicz, 1990; Balser *et al.*, 1991). These approaches have the disadvantages that blockers may not be highly specific and that detailed kinetic analysis of drug-channel interactions may not be feasible if drug-induced block of other ionic currents is not strictly time- and voltage-independent. Therefore, to quantify mechanisms of ionic channel block, a model system without contamination by other currents has certain advantages. The expression of cloned cardiac K^+ channels in tissue culture cells provides such a system. Recently, a cloned human cardiac K^+ channel, designated HK2 (Tamkun *et al.*, 1991) or hKv1.5, has been successfully expressed in a mouse L-cell line (Snyders *et al.*, 1993). This hKv1.5 current appears very similar to the fast activating potassium currents observed in rat atrial myocytes (Boyle & Nerbonne, 1991), canine neonatal epicardial ventricular myocytes (Jeck & Boyden, 1992) and human atrial myocytes (Wang *et al.*, 1993). The electrophysiological properties of the hKv1.5 have been characterized in detail

[1] Present address: Department of Drug Metabolism, Central Research, Pfizer Pharmaceutical Inc., Groton, CT 06430, U.S.A.
[2] Author for correspondence.

(Snyders *et al.*, 1993) and this model system has allowed elucidation of the mechanism of block of this channel by quinidine (Snyders *et al.*, 1992).

We used this *in vitro* system to study the mechanism of terfenadine inhibition of this human cardiac K^+ channel. In a recent study it was suggested that terfenadine acts as an open channel blocker of fHK, a cloned channel related to hKv1.5 (Rampe *et al.*, 1993). However, no voltage-dependence of block was demonstrated. We specifically investigated the voltage-dependence of block at depolarized potentials, and the time-dependence of deactivating tail currents at negative potentials to provide evidence for the open channel block mechanism. In the same study the benzhydryl-piperidine part of the molecule displayed low affinity, while hydroxylation of the phenylbutyl part of the molecule reduced the affinity moderately. Because the chiral centre is located in the phenylbutyl end of the molecule it is of interest to explore possible stereoselective channel block. Terfenadine is prescribed as a racemate and its H_1 receptor antagonism does not display stereoselectivity (Zhang *et al.*, 1991). For optically active antiarrhythmic drugs, K^+ channel block may (Mirro *et al.*, 1981) or may not (Carmeliet, 1985) be stereoselective. In the case of terfenadine, identification of stereoselectivity in block might imply that prescription of a non-K^+ channel blocking enantiomer would decrease the risk of torsades de pointes. Therefore, we synthesized the enantiomers of terfenadine and compared their effects to those of racemic terfenadine and of its major acid metabolite in voltage-clamped L-cells.

Methods

Cell culture

The method to establish hKv1.5 expression in clonal L-cell lines has been described previously (Snyders *et al.*, 1992; 1993). Transfected cells were cultured in DMEM supplemented with 10% horse serum and 0.25 mg mg^{-1} G418 (geneticin, Gibco BRL, Grand Island, NY, U.S.A.) in a 5% CO_2 atmosphere. The cultures were passed every 3–5 days using a brief trypsinization. Before electrophysiological experiments, subconfluent cultures were incubated with 2 μM dexamethasone for 24 h, as expression of the channel is under control of a dexamethasone-inducible promoter. The cells were removed from the dish with a cell scraper, and the cell suspension was stored at room temperature (22–23°C) and used within 12 h for all the experiments described here.

Electrical recording

Glass micropipettes were pulled from starbore borosilicate glass (Radnoti, Monrovia, CA, U.S.A.) and heat polished. They were filled with 'intracellular' solution (see below) and connected to the headstage of an Axopatch-1A patch clamp amplifier (Axon Instruments Inc., Foster City, CA, U.S.A.). All currents were recorded at room temperature (22–23°C) and were sampled at 3–10 times the anti-alias filter setting using a 12-bit analog-to-digital converter (Labmaster, Scientific Solutions, Solon, Ohio, U.S.A.). A commercial software package (pClamp, Axon Instruments) was used for data acquisition and command potentials Microelectrode resistance averaged 2.7 ± 0.7 MΩ ($n = 30$, range 1.5–5). The microelectrodes were gently lowered onto the cells and Gigaohm seal formation (16 ± 9 GΩ, range 6–33 GΩ, $n = 26$) was achieved by suction. Following seal formation, cells were lifted from the bottom of the perfusion bath and the membrane patch was ruptured with brief additional suction. The capacitive transients elicited by symmetrical 10 mV steps from −80 mV to −70 mV were recorded at 50 kHz (filtered at 10–20 kHz) for subsequent calculation of capacitive surface area, access resistance and input impedance. Thereafter capacitance and series resistance compensation were optimized; 80% compensation of the effective access resistance (9.1 ± 0.9 MΩ) was usually obtained. With an average current of 1.3 nA at +50 mV the voltage error induced by the residual series resistance was less than 3 mV.

Synthesis of terfenadine enantiomers

The method of chiral synthesis via organoboranes (Brown *et al.*, 1988) was used to synthesize the terfenadine enantiomers as illustrated in Figure 1. Racemic terfenadine was oxidized to its corresponding ketone (4-(1,1-dimethylethyl)phenyl-4-(hydroxy-diphenylmethyl)-1-piperidinebutanone). This ketone was purified, crystallized and its structure was confirmed by n.m.r. This ketone was reduced to **R**(+)-terfenadine using (+)-diisopinocampheyl-chloroborane ((+)-Ipc_2BCl) as a

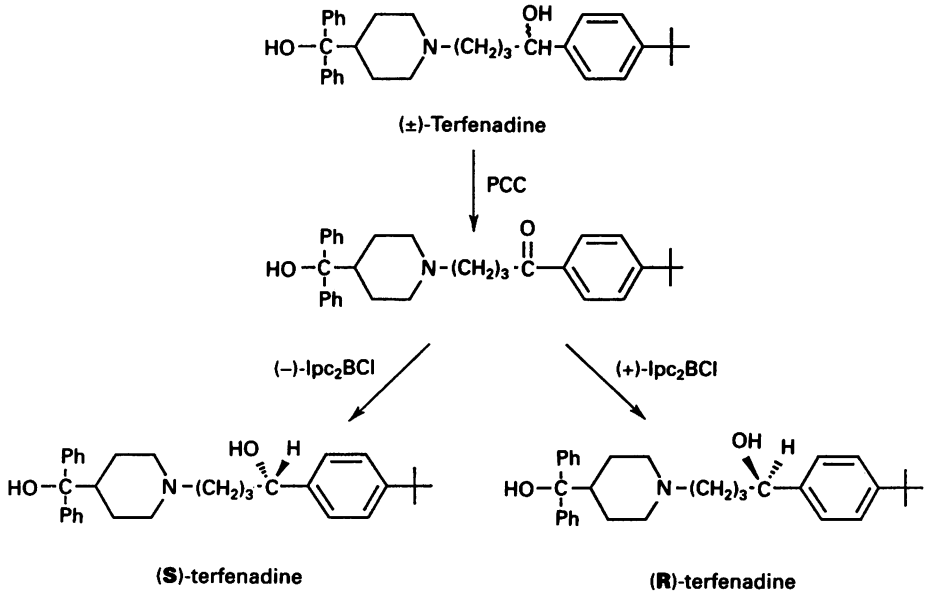

Figure 1 Synthesis of terfenadine enantiomers: racemic terfenadine was oxidized to the corresponding ketone using pyridinum chlorochromate (PCC). The appropriate chiral reducing agents (+)- or (−)-Ipc_2BCl, were used to impose the desired chiral configuration.

chiral reducing agent. Purification on a silica gel column using 1% methanol/methylelne chloride provided the **R**-isomer of terfenadine (reaction yield: 65%). The structure was confirmed by n.m.r. The S(−)-enantiomer was similarly synthesized using (-)-Ipc_2BCl. The purity of each enantiomer was assessed by h.p.l.c. using an Ultron ES-OVM column with methanol/25 mM phosphate buffer (pH 4.6) (25:75) as mobile phase. The **R**-enantiomer was 97.5% pure, and S(-)-terfenadine was 95.2% pure. n.m.r. spectra were recorded in $CDCl_3$ on a Bruker/IBM NR 300.

Other solutions and drugs

The intracellular pipette filling solution contained (in mM): KCl 110, HEPES 10, K_4BAPTA 5, K_2ATP 5, $MgCl_2$ 1, and was adjusted to pH 7.2 with KOH, yielding a final intracellular K^+ concentration of approximately 145 mM. The bath solution contained (mM): NaCl 130, KCl 4, $CaCl_2$ 1.8, $MgCl_2$ 1, HEPES 10, glucose 10, and was adjusted to pH 7.35 with NaOH. Racemic terfenadine (mol.wt. = 472) was purchased from Sigma Chemical CO., St. Louis, MO, U.S.A. Terfenadine carboxylate was provided by Marion Merrell Dow Inc., Cincinnati, OH, U.S.A. All compounds were dissolved in dimethyl sulphoxide (DMSO, Sigma Chemical Co.) to yield stock solutions of 10 mM. This vehicle had no measurable effects on the hKv1.5 current in final working concentrations up to 0.1%. Control solutions contained the same concentrations of DMSO as the test solution.

Pulse protocols and analysis

After obtaining control data, bath perfusion was switched to drug-containing solution. Drug infusion or removal was monitored with test pulses from −80 mV to +50 mV, applied every 30 s until steady-state was obtained (within about 10 min). The holding potential was −80 mV unless indicated otherwise, and the interval between depolarizations for any protocol in control or in drug was 10 s or slower. The protocol to obtain current-voltage (*IV*) relationships and activation curves consisted of 250 ms pulses that were imposed in 10 mV increments between −80 and +60 mV. 'Steady state' *IV* relationships were obtained by measuring currents at the end of the 250 ms depolarizations. Between −80 and −40 mV, only passive linear leak was observed; least squares fit to these data were used for passive leak correction. Deactivating tail currents were recorded upon repolarization to −30 to −50 mV. The activation curve was obtained from the tail current amplitude immediately after the capacitive transient. For steady-state measurements, raw data points were averaged over a small time window (5–10 ms). Activation curves were fitted with a Boltzmann equation of the form $y = 1/(1 + \exp[-(E-E_h)/k])$ where E_h represents the half-activation voltage and k the slope factor. The time course of tail currents and drug-induced 'inactivation' was fitted with a sum of exponentials. The curve-fitting procedure used a non-linear least squares (Gauss-Newton) algorithm. The fit results were displayed in linear and semilogarithmic format together with a plot of the residual deviation of the data from the fitted curve (difference plot). Goodness of the fit was judged by the χ^2_1 criterion (*F*-test) and by inspection for systematic non-random trends in the difference plot.

A first-order blocking scheme was used to describe the drug-channel interaction. The apparent affinity K_D (concentration for 50% block or EC_{50}) and Hill coefficient n were obtained from fitting the fractional block f at various drug concentrations [*D*] to the equation:

$$f = 1/(1 + (K_D/[D])^n) \quad [1]$$

Voltage-dependence of block was determined as follows: leak subtracted current in the presence of drug was normalized to matching control to yield fractional block at each voltage ($f = 1\text{-}I_{terfenadine}/I_{control}$). The voltage-dependence of block was described by a Woodhull (1973) model and was fitted to the equation:

$$f = [D]/([D] + K_D^* \times e^{-\delta zFE/RT}) \quad [2]$$

where z represents the valency, F the Faraday constant, R the gas constant, T the absolute temperature, and δ represents the fractional electrical distance, i.e. the fraction of the transmembrane field sensed by a single charge at the receptor site. K_D^* represents the apparent affinity at a reference voltage (0 mV).

Statistical methods

Results are expressed as mean ± s.e.mean. A paired *t* test was used to compare the effect of each test compound to its control; $P < 0.05$ was considered significant.

Results

Concentration-dependent block of the hKv1.5 current by terfenadine

Figure 2a shows representative recordings of the K^+ current through hKv1.5 channels expressed in mouse L-cells during depolarizations from a holding potential of −80 mV to voltages between −30 and +50 mV in steps of 10 mV. Under control conditions (Figure 2a), the hKv1.5 current rose rapidly with a sigmoidal time course to a peak and then declined slowly (slow and partial inactivation) as reported

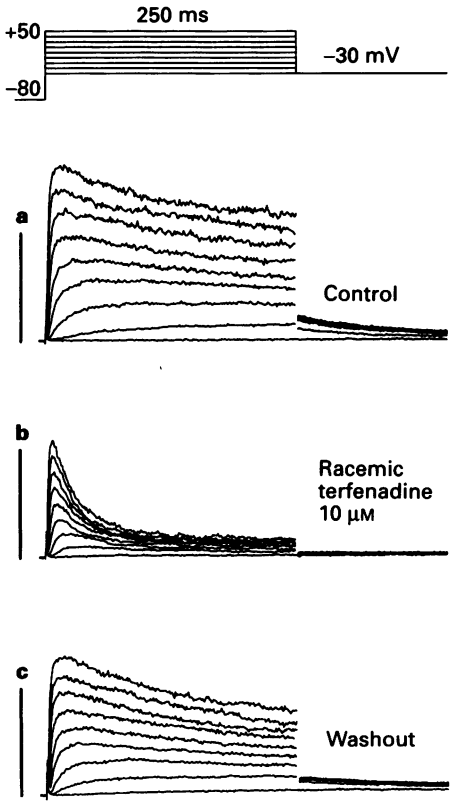

Figure 2 Suppression of hKv1.5 current by terfenadine. Currents are shown for depolarizations from −80 mV to voltages between −30 and +50 mV in steps of 10 mV; tail currents were obtained upon repolarization to −30 mV. Panels (a–c) represent control, 10 μM racemic terfenadine, and washout (20 min), respectively. After addition of terfenadine, the currents at the end of the depolarization were reduced at all levels of voltages. The effect was largely reversed after a 20 min washout. Cell capacitance, 14 pF. Vertical calibration: 0.5 nA. Data filtered at 2 kHz (4 pole Bessel) and digitized at 10 kHz; digital leak subtraction and additional digital filtering at 1 kHz.

previously (Snyders *et al.*, 1992; 1993). The steady-state current amplitude (at the end of 250 ms step) was 1280 ± 120 pA (or 94 ± 9 pA/pF, $n = 30$) at +50 mV. Decaying outward tail currents were observed upon repolarization to −30 mV. Figure 2b shows that this outward K^+ current was markedly suppressed by application of 10 μM racemic terfenadine. The effect was largely reversible after a 20-min wash-out period (Figure 2c). Terfenadine not only reduced the current amplitude, but also altered the time course of the current during depolarization. The current initially activated as in control, but subsequently declined markedly. This decline occurred much faster and to a larger extent than the slow inactivation observed in control. Analysis of this time course of block (see below) indicated that a steady level was achieved within 250 ms, while only a limited degree of slow inactivation occurred over this time. Therefore, the reduction of the hKv1.5 current at end of a-250 ms depolarization ($I_{terfenadine}/I_{control}$) was used as an index of block. In the experiment shown in Figure 2, the K^+ current at +50 mV was reduced to 10% of control in the presence of 10 μM racemic terfenadine. This steady-state reduction of hKv1.5 current was concentration dependent as shown in Figure 3. A non-linear least squares fit of the concentration-response equation [*1*] (see methods) to these data was used to obtain the apparent affinity K_D and Hill coefficient n. In Figure 3, the dotted line represents the fit to the racemic terfenadine data with an apparent K_D of 0.88 μM and n = 0.95. When the data were fit assuming a Hill coefficient of 1, a similar apparent affinity was obtained (K_D of 0.81 μM). Either approach suggested that binding of one terfenadine molecule per channel was sufficient to inhibit potassium permeation.

Voltage-dependent block of the hKv1.5 current by terfenadine

Figure 4 shows that suppression of hKv1.5 current was observed over the whole voltage range over which this current is activated. To determine and quantitate the voltage-dependence of this inhibition, the relative current ($I_{terfenadine}/I_{control}$) was plotted as a function of voltage (Figure 4b). Block increased steeply between −20 mV and 0 mV, coinciding with the voltage range of channel opening (Snyders *et al.*, 1993). This suggests that terfenadine binds primarily to the open channel. Between 0 mV and +60 mV, terfenadine-induced block continued to increase with a more shallow voltage-dependence. It is unlikely that this shallow voltage-dependence was due to channel gating because hKv1.5 activation has reached saturation over this voltage range (Snyders *et al.*, 1993). Terfenadine is a weak base ($pK_a \sim 10$) and is therefore predominantly present in its charged form at the intracellular pH of 7.4. Thus, the voltage-dependence of block could be due to the effect of the transmembrane electrical field on the terfenadine-channel interaction, similar to that reported for the interaction of quinidine with this hKv1.5 channel (Snyders *et al.*, 1992). If terfenadine reaches the receptor from the inside, then channel block is expected to increase in a voltage-dependent manner according to equation [2] (Methods), which incorporates the effect of the transmembrane electrical field (Woodhull, 1973). The parameter δ in this equation represents the fractional electrical distance, i.e., the fraction of the membrane field sensed by the positive charge at the receptor site. The dashed line in Figure 4b represents the fit of this equation to the data points positive to 0 mV (solid symbols). A fractional electrical distance $\delta = 0.24$ was obtained in this experiment with 10 μM racemic terfenadine. The average value ($\delta = 0.21$, see Table 1) was similar to the value $\delta = 0.18$ obtained in previous experiments with quinidine (Snyders *et al.*, 1992).

Change of hKv1.5 current time course by terfenadine

If terfenadine can access its receptor only when the channel is on the open state, then inhibition of the K^+ current would only develop as channels start to open, and block development should be visible if the blocking rate is slower than the opening rate. Figure 5a shows superposition of the currents obtained at +50 mV before and after application of 10 μM racemic terfenadine. Under control conditions, the K^+ current rapidly reached its peak and then inactivated slowly. The time course of this partial inactivation was well fitted by a monoexponential function, yielding a time constant of 188 ± 41 ms ($n = 6$). In the presence of terfenadine, however, the peak current was smaller and reached at an earlier time, and the subsequent current decay displayed a combination of fast and slow phases that were well-fitted with a biexponential function. In these experiments, no significant differences

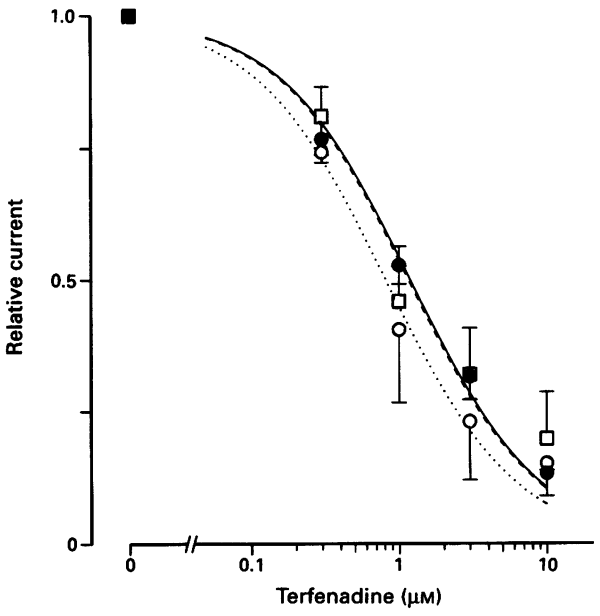

Figure 3 Concentration-dependence of suppression of hKv1.5 current by terfenadine and its enantiomers. Suppression of the steady-state hKv1.5 current (relative to control) at the end of depolarizations to +50 mV was used as index block. Data are shown as mean ± s.e.mean from 3–5 determinations at each concentration. The dotted line represents the fit of the Hill equation [1] to the racemic terfenadine data (○) which yielded an apparent K_D of 0.88 μM and a Hill coefficient of 0.95. The solid and dashed lines represent the fit for the R-(●) and S-enantiomer (□), respectively.

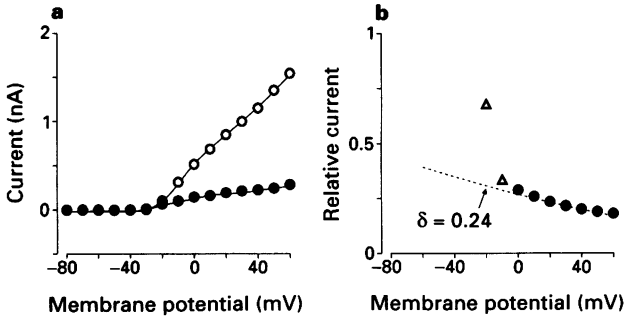

Figure 4 Voltage-dependence of hKv1.5 block by 10 μM terfenadine. (a) Current-voltage relationships (250 ms isochronal) in the absence (open symbols) and presence of drug (●). (b) Normalized block, shown as relative current ($I_{drug}/I_{control}$) from data in (a). Block increased steeply between −20 mV and 0 mV (Δ), corresponding to the voltage range of activation of the hKv1.5 channel. At levels positive to 0 mV, a more shallow voltage-dependence was observed (●). The dotted lines represent the result of the fit of equation [2] to these data, yielding an equivalent electrical distance $\delta = 0.24$ in this case.

were observed for the slow time constants (176 ± 42 vs 188 ± 41, $n = 6$, $P > 0.05$), while the time constant of the fast component was 26 ± 3 ms ($n = 6$). Thus, the fast time constant (τ_{block}) was considered to be a reasonable approximation of the drug-channel interaction kinetics because it is a new component which was sufficiently faster than the slow one to be resolved clearly.

Time course of tail currents

In the absence of drug, the hKv1.5 current deactivated completely at −50 mV, with a time constant of 31 ± 3 ms ($n = 5$). This time constant reflects the closing of the channel, which at this voltage is essentially irreversible (Snyders *et al.*, 1993). If terfenadine interacts only with the open channel, then dissociation of terfenadine from the blocked channel should result in a transient conducting channel, which subsequently could close. Figure 5b shows the superposition of the tail current obtained at −50 mV after a 250 ms depolarization to +50 mV in the absence and presence of racemic terfenadine. In the control experiment shown, the tail current declined with a time constant of 28 ms (Figure 5b). After exposure to 1 μM racemic terfenadine, the initial tail current amplitude was markedly reduced and the time course of the decline of the tail current was slower compared to control ($\tau = 40$ ms). The average values were 23 ± 3 ms and 33 ± 2 ms for control and 1 μM terfenadine, respectively ($n = 3$, $P = 0.04$). Consequently, the superposition of these tails with those in control resulted in a 'crossover' phenomenon (arrow in Figure 5b), compatible with transient unblocking, and providing additional evidence for open channel block.

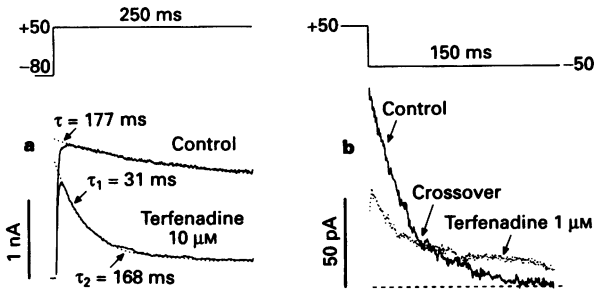

Figure 5 Time-dependent modification by terfenadine of hKv1.5 current during depolarization and repolarization. (a) Superimposed tracings from a holding potential of −80 mV to +50 mV are shown for control and 10 μM terfenadine. In the presence of terfenadine, a fast decline was superimposed on the slow inactivation observed in control. Time constants obtained using a biexponential fit, were $\tau_1 = 31$ ms and $\tau_2 = 168$ ms. The latter was similar to the slow time constant in control (177 ms). (b) Tail currents obtained at −50 mV after a 250 ms depolarization to +50 mV. In the presence of terfenadine (dotted tracing), the initial amplitude was reduced, reflecting block. The subsequent slower decline results in the 'crossover' phenomenon with the control tracing.

Effect of R(+)- and S(−)-enantiomers of terfenadine on hKv1.5 current

To test for potential stereoselectivity in the interaction of terfenadine with the hKv1.5 channel, we used the individual R(+)- and S(−)-enantiomers (Figure 1), synthesized as described above. Figure 6 shows the suppression of hKv1.5 currents by 10 μM of R(+)-terfenadine (Figure 6a, b) and S(−)-terfenadine (Figure 6c, d). As in the case of the racemate, a marked time-dependent reduction of outward current was obtained in the presence of each enantiomer. The steady-state levels of block were similarly high for each enantiomer at this concentration.

The concentration-dependence was assessed from the steady-state suppression (250 ms isochronal values) of hKv1.5 current with concentrations between 0.3 and 10 μM. Averaged data are shown in Figure 3, for comparison with the corresponding results for the racemic mixture. These experiments indicated little difference in the affinity between both enantiomers, with apparent K_D values close to those obtained for the racemic mixture (Figure 3 and Table 1). The time-dependence of block during depolarization was similar for each enantiomer (Figure 6b, d). The time constants for the fast exponential component of current decline at +50 mV were 27 and 29 ms with 10 μM R- and S-terfenadine, respectively (Table 1). Thus, no significant difference was observed for the time constant of block between racemic terfenadine and its enantiomers. The suppression of hKv1.5 current by the individual enantiomers showed the same biphasic voltage-dependence as shown in Figure 4 for the racemate. The average values for the fractional electrical distance δ were 0.19 ± 0.01 for R-terfenadine,

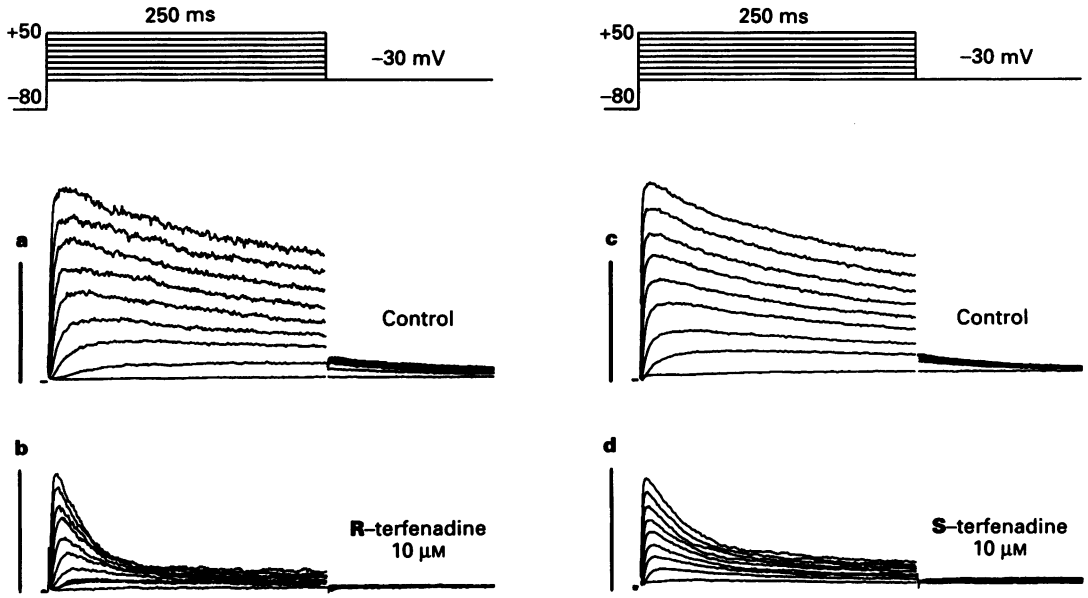

Figure 6 Suppression of hKv1.5 current by R- and S-terfenadine. Tracings for step depolarizations (pulse protocol: top). (a, b) Control and 10 μM R-terfenadine, respectively; (c, d) control and 10 μM S-terfenadine. As for racemic terfenadine, a time-dependent decline of current was observed for both enantiomers. Vertical calibration: 0.5 nA.

Table 1 Fractional electrical distance, affinity and kinetics for terfenadine block

	Racemic	R-*enantiomer*	S-*enantiomer*
δ	0.21 ± 0.02 (5)	0.19 ± 0.01 (5)	0.21 ± 0.02 (6)
τ_B (ms)	26 ± 3 (6)	27 ± 6 (4)	29 ± 5 (4)
K_D (μM)	0.81 ± 1.10	1.19 ± 0.09	1.16 ± 0.20

Mean ± s.e.mean (*n*). δ: Fractional electrical distance (see equation 2, methods), τ_B: time constant of fast decline of current at +50 mV induced by 10 μM terfenadine or its enantiomers. K_D: apparent affinity derived as shown in Figures 3 and 7, with Hill coefficient n = 1.

and 0.21 ± 0.02 for the S-enantiomer (see Table 1 for summary data). Thus neither concentration-, time-, nor voltage-dependence of block indicated stereoselectivity in the binding of the enantiomers to the hKv1.5 channel. The results indicated a similar mechanism consistent with open channel block. This was further confirmed by the observation of a typical tail current 'cross-over' for each enantiomer (data not shown).

Effect of terfenadine carboxylate on hKv1.5 current

Figure 7 shows representative current records for 250 ms depolarizations to +50 mV from a holding potential of −80 mV in the absence and presence of either terfenadine carboxylate or racemic terfenadine in the same cell. Compared to terfenadine (10 μM), a higher concentration of terfenadine carboxylate (50 μM) only slightly reduced the hKv1.5 current. In 6 experiments, 50 μM terfenadine carboxylate reduced the steady state current at +50 mV only by 5 ± 2% (NS), without detectable change of the hKv1.5 channel kinetics. Because this was 50 fold above the apparent K_D for hKv1.5 inhibition by the parent compound and its enantiomers, and at least 100 times above clinically relevant concentrations (Woosley *et al.*, 1993), we did not study the effect of higher concentrations.

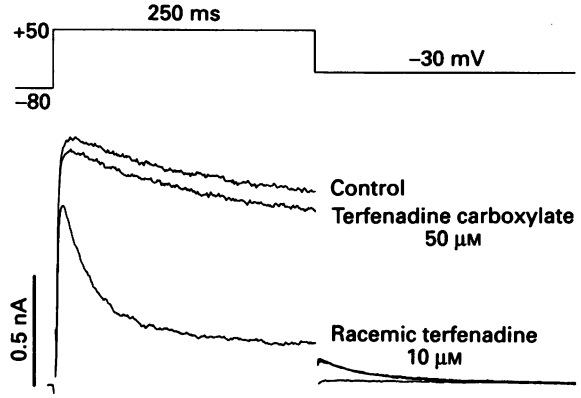

Figure 7 Comparison of the effects of terfenadine and its acid metabolite on hKv1.5 current. Shown are typical current records (voltage clamp protocol on top) in control, and after sequential application of the metabolite, and the parent compound in the same cell. Application of 50 μM terfenadine carboxylate reduced the current by less than 10%, but after washout, subsequent application of terfenadine resulted in the typical response.

Discussion

In this study, we have used our recently developed model system that allows direct study of human cardiac potassium channels (Snyders *et al.*, 1992; 1993) to analyze the mechanism of potassium channel block by terfenadine in detail. The human hKv1.5 channel activates positive to −30 mV, consistent with involvement in the control of cardiac action potential duration (Snyders *et al.*, 1993), as was shown in human atrial myocytes by selective block of this current (Wang *et al.*, 1993). We have previously shown that this channel is sensitive to quinidine in micromolar concentration (Snyders *et al.*, 1992). The results presented in this paper indicate (1) that terfenadine interacts with hKv1.5 in a time-, voltage-, and state-dependent fashion, (2) that both enantiomers are approximately equipotent, and (3) that the carboxylate metabolite is considerably less active, if active at all.

Terfenadine inhibits hKv1.5 current by acting as an open channel blocker

In the presence of terfenadine, the hKv1.5 current was reduced in a time-dependent manner. Upon depolarization, the channel initially opened as in control, but subsequently the current was reduced to a lower steady-state level (Figures 2, 5, 6 and 7). A similar observation was made for the interaction of terfenadine with fHK, a cloned channel similar to hKv1.5 (Rampe *et al.*, 1993). However, in that study, the increase of block with voltage was not significant. Drug-induced time-dependent decline of current can be due to several mechanisms, including block of open channels. Compelling evidence for open channel block includes voltage-dependence of block and the tail current cross-over phenomenon, as was shown for quinidine block of this channel (Snyders *et al.*, 1992). As shown in Figure 4 and Table 1, we observed voltage-dependent open channel block that can be described with the equivalent electrical distance δ. The value for δ was significantly different from 0, and indicates that terfenadine (and its enantiomers) sense about 20% of the applied transmembrane electrical field, referenced from the cytoplasmic side. This analysis assumes that terfenadine approaches the receptor from the inside, consistent with the effect of terfenadine in inside-out patches (Rampe *et al.*, 1993). Another argument for the open channel block model comes from the modification of the kinetics of the tail currents. For the deactivating tail currents at −50 mV, the time course was slowed with respect to control, resulting in the 'cross-over' effect shown in Figure 5.

While the modification of open channel current is consistent with open channel block, the demonstration of voltage-dependent block and tail current cross-over provides further strong evidence for this proposed mechanism of action. Both features indicate that the channel has to open before drug can reach the receptor and inhibit ion flow, and that the drug has to leave the channel before it can fully close. This is very similar to the mechanism of quinidine block of the hKv1.5 channel, but the affinity is about 6 fold higher. This can be understood if we assume that the 29 ms time constant (Table 1) reflects the time course of drug binding to the channel. For a bimolecular reaction (Snyders *et al.*, 1992), the time constant of block corresponds to $1/(k \times [D] + l)$. Together with the apparent affinity of 0.88 μM ($= l/k$), this yields values of $k = 3.5 \times 10^6\ s^{-1}M^{-1}$ and $l = 3\ s^{-1}$. Thus the apparent association rate constant k is only slightly smaller than that of quinidine ($4.5 \times 10^6\ s^{-1}M^{-1}$) obtained with a similar approach (Snyders *et al.*, 1992). The main difference is that the apparent dissociation rate constant l is about 10 fold slower compared to quinidine ($34\ s^{-1}$). Because this dissociation rate constant should reflect the stability of the drug-receptor complex, the slower dissociation may reflect a stronger hydrophobic component of binding, consistent with the high hydrophobicity of this agent. At the molecular level, this mechanism of block indicates that the drug moves some distance into the internal mouth of the channel before reaching the binding site. A hydrophobic component has recently also been observed for binding of tetraethylammonium at the internal quaternary ammonium site in related *Shaker* potassium channels (Choi *et al.*, 1993). In the carbox-

ylate metabolite, the introduction of a formal negative charge reduces the hydrophobicity of part of the molecule, and may also counteract the effect of the positive charge on the tertiary amine. Both effects are potential explanations for the much lower potency of the carboxylate metabolite.

Comparison of in vitro *affinity with* in vivo *pharmacokinetics*

Terfenadine is normally not present in detectable values in human plasma (Woosley *et al.*, 1993), but toxicity has been associated with elevated levels (Coutant *et al.*, 1991). In some cases this was due to (intentional) overdosage (Davies *et al.*, 1989; Kintz & Mangin, 1992), but in most cases the toxicity appeared to result from drug interactions (Cortese & Bjornson, 1992; Peck *et al.*, 1993; Pohjola-Sintonen *et al.*, 1993; Hirschfeld & Jarosinski, 1993; Honig *et al.*, 1993). Terfenadine is metabolized to the active H_1-receptor antagonist, terfenadine carboxylate. This biotransformation is achieved by a specific hepatic enzyme CYP 3A4. When other agents such as erythromycin and ketoconazole compete for this system, the biotransformation is inhibited, resulting in elevated levels of the parent compound (Honig *et al.*, 1992; 1993). Plasma levels of 100 ng ml^{-1} ($\sim$0.2 μM) have been reported in cases of torsades de pointes. Although this level is below the apparent K_D for hKv5.1 block, it should be noted that control of the duration of the cardiac action potential relies on a delicate balance of small currents and that even partial block of one of these currents can result in marked changes in action potential duration. For instance, the human atrial action potential duration was increased by 30% by a concentration of 4-aminopyridine which only blocked 50% of the hKv1.5 current (Wang *et al.*, 1993). Thus partial potassium channel block during the plateau phase may be sufficient to cause substantial changes in action potential duration. In addition, the effective concentration in the myocytes may not be accurately reflected by the plasma concentration, given the lipophilic character of this drug, and our data (obtained at room temperature) may underestimate the potency of terfenadine at physiological temperatures. Moreover, at least one preliminary report suggests that racemic terfenadine may block other potassium channels (Crumb & Brown, 1993).

Relevance of relative potency to clinical toxicity

The biotransformation of racemic terfenadine is not stereoselective (Zamani *et al.*, 1991; Chan *et al.*, 1991), and receptor binding studies have shown a similar affinity of both enantiomers for histamine H_1 receptors (Zhang *et al.*, 1991). In this situation, a less toxic enantiomer might be beneficial without loss of therapeutic efficiency. However, the present *in vitro* data indicate that this possibility is not likely to be realized. Both enantiomers are approximately equipotent, and do not differ significantly in their effects from racemic terfenadine. In contrast, the carboxylate metabolite is not effective as a blocker of hKv1.5 in our study, as in others (Woosley *et al.*, 1993; Rampe *et al.*, 1993). Thus the results of our *in vitro* study do not support the idea of using either enantiomer in an attempt to reduce terfenadine-associated toxicity, but the results do support the approach of using the active metabolite as an H_1-receptor antagonist rather than the parent precursor drug to this end (Woosley *et al.*, 1993).

Multiple ion currents are involved in control of cardiac action potential duration. In human atrium, various components of the delayed rectifier (I_{Ks}, I_{Kr}, hKv1,5-like) have been described recently (Wang *et al.*, 1993). In contrast, information on delayed rectifiers in human ventricle is largely inferential. For example, dofetilide and other methanesulphonanilide antiarrhythmic drugs, which specifically block I_{Kr}, induce QT prolongation, but the I_{Kr} current itself has not yet been identified in human ventricle. Similarly, although the hKv1.5 current has not yet been reported in human ventricle, mRNA for this channel has been demonstrated in human ventricle, and the channel was cloned from a human ventricular cDNA library (Tamkun *et al.*, 1991).

We have used an *in vitro* system that allows the study of an identified human potassium channel. This allowed us to study the blocking mechanism in detail, revealing open channel block as the mechanism of action. Quinidine blocks at least two cardiac delayed rectifiers (hKv1.5 and I_{Ks}) with an open channel block mechanism (Balser *et al.*, 1991; Snyders *et al.*, 1992). It also blocks another delayed rectifier component (I_{Kr}), for which block by other class III agents involves an open channel block mechanism (Furukawa *et al.*, 1989; Follmer & Colatsky, 1990; Sanguinetti & Jurkiewicz, 1990). Therefore it is not unreasonable to expect that the terfenadine open channel block model may generally apply to its interaction with potassium channels other than the hKv1.5 channel. However, because the I_{Kr} and I_{Ks} currents activate on a slower time scale, it may be impossible to resolve the time-dependence of block for these channels. To the extent that the hKv1.5 channel is representative of other human cardiac K^+ channels, the system can serve as a model to analyze mechanisms of cardiac K^+ channel block and associated toxicity.

We appreciate the technical assistance of Craig Short, Jayaveera Kodali and Samir Saleh, and clerical assistance of Melissa Austin. D.M.R. holds the William Stokes chair in Experimental Therapeutics, a gift from the Daiichi Corporation. This study was supported by NIH grants HL47599, HL46681 and GM31304.

References

BALSER, J.R., BENNETT, P.B., HONDEGHEM, L.M. & RODEN, D.M. (1991). Suppression of time-dependent outward current in guinea pig ventricular myocytes. Actions of quinidine and amiodarone. *Circ. Res.*, **69**, 519–529.

BOYLE, W.A. & NERBONNE, J.M. (1991). A novel type of depolarization-activated K^+ current in adult rat atrial myocytes. *Am. J. Physiol.*, **260**, H1236–H1247.

BROWN, H.C., CHANDRASEKHARAN, J. & RAMACHANDRAN, P.V. (1988). Chiral synthesis via organoboranes. 14. Selective reductions. 41. Diisopinocampheylchloroborane, an exceptionally efficient chiral reducing agent. *J. Am. Chem. Soc.*, **110**, 1539–1546.

CARMELIET, E. (1985). Electrophysiologic and voltage clamp analysis of the effects of sotalol on isolated cardiac muscle and Purkinje fibres. *J. Pharmacol. Exp. Ther.*, **232**, 817–825.

CHAN, K.Y., GEORGE, R.C., CHEN, T.M. & OKERHOLM, R.A. (1991). Direct enantiomeric separation of terfenadine and its major acid metabolite by high-performance liquid chromatography, and the lack of stereoselective terfenadine enantiomer biotransformation in man. *J. Chromatogr.*, **571**, 291–297.

CHOI, K.L., MOSSMAN, C., AUBE, J. & YELLEN, G. (1993). The internal quarternary ammonium receptor site of *Shaker* potassium channels. *Neuron*, **10**, 533–541.

CORTESE, L.M. & BJORNSON, D.C. (1992). Potential interaction between terfenadine and macrolide antibiotics [letter]. *Clin. Pharmacy*, **11**, 675.

COUTANT, J.E., WESTMARK, P.A., NARDELLA, P.A., WALTER, S.M. & OKERHOLM, R.A. (1991). Determination of terfenadine and terfenadine acid metabolite in plasma using solid-phase extraction and high-performance liquid chromatography with fluorescence detection. *J. Chromatogr.*, **570**, 139–148.

CRUMB, W.J. & BROWN, A.M. (1993). Terfenadine blockade of a potassium current in human atrial myocytes. *Circulation*, **88**, I-230(Abstract).

DAVIES, A.J., HARINDRA, V., MCEWAN, A. & GHOSE, R.R. (1989). Cardiotoxic effect with convulsions in terfenadine overdose. *Br. Med. J.*, **298**, 325.

FOLLMER, C.H. & COLATSKY, T.J. (1990). Block of delayed rectifier potassium current, I_K, by flecainide and E4031 in cat ventricular myocytes. *Circulation*, **82**, 289–293.

FURUKAWA, T., TSUJIMURA, Y., KITAMURA, K., TANAKA, H. & HABUCHI, Y. (1989). Time- and voltage-dependent block of the delayed K^+ current by quinidine in rabbit sinoatrial and atrioventricular nodes. *J. Pharmacol. Exp. Ther.*, **251**, 756–763.

HIRSCHFELD, S. & JAROSINSKI, P. (1993). Drug interaction of terfenadine and carbamazepine [letter]. *Ann. Intern. Med.*, **118**, 907–908.

HONIG, P.K., WOOSLEY, R.L., ZAMANI, K., CONNER, D.P. & CANTILENA, Jr, L.R. (1992). Changes in the pharmacokinetics and electrocardiographic pharmacodynamics of terfenadine with concomitant administration of erythromycin. *Clin. Pharmacol. Ther.*, **52**, 231–238.

HONIG, P.K., WORTHAM, D.C., ZAMANI, K., CONNER, D.P., MULLIN, J.C. & CANTILENA, L.R. (1993). Terfenadine-ketoconazole interaction. Pharmacokinetic and electrocardiographic consequences. *J. Am. Med. Ass.*, **269**, 1513–1518.

JECK, C.D. & BOYDEN, P.A. (1992). Age-related appearance of outward currents may contribute to developmental differences in ventricular repolarization. *Circ. Res.*, **71**, 1390–1403.

KINTZ, P. & MANGIN, P. (1992). Toxicological findings in a death involving dextromethorphan and terfenadine. *Am. J. Forensic Med. Pathol.*, **13**, 351–352.

MATHEWS, D.R., MCNUTT, B., OKERHOLM, R., FLICKER, M. & MCBRIDE, G. (1991). Torsades de pointes occurring in association with terfenadine use [letter]. *J. Am. Med. Ass.*, **266**, 2375–2376.

MCTAVISH, D., GOA, K.L. & FERRILL, M. (1990). Terfenadine. An updated review of its pharmacological properties and therapeutic efficacy. *Drugs*, **39**, 552–574.

MIRRO, M.J., WATANABE, A.M. & BAILEY, J.C. (1981). Electrophysiological effects of the optical isomers of disopyramide and quinidine in the dog: Dependence on stereochemistry. *Circ. Res.*, **48**, 867–874.

MONAHAN, B.P., FERGUSON, C.L., KILLEAVY, E.S., LLOYD, B.K., TROY, J. & CANTILENA, Jr, L.R. (1990). Torsades de pointes occurring in association with terfenadine use. *J. Am. Med. Ass.*, **264**, 2788–2790.

PECK, C.C., TEMPLE, R. & COLLINS, J.M. (1993). Understanding consequences of concurrent therapies. *J. Am. Med. Ass.*, **269**, 1550–1552.

POHJOLA-SINTONEN, S., VIITASALO, M., TOIVONENE, L. & NEUVONEN, P. (1993). Torsades de pointes after terfenadine-itraconazole interaction. *Br. Med. J.*, **306**, 186.

RAMPE, D., WIBLE, B., BROWN, A.M. & DAGE, R.C. (1993). Effects of terfenadine and its metabolites on a delayed rectifier K^+ channel cloned from human heart. *Mol. Pharmacol.*, **44**, 1240–1245.

RODEN, D.M. (1990). Clinical features of arrhythmia aggravation by antiarrhythmic drugs and their implications for basic mechanisms. *Drug Develop. Res.*, **19**, 153–172.

SANGUINETTI, M.C. & JURKIEWICZ, N.K. (1990). Two components of cardiac delayed rectifier K^+ current. Differential sensitivity to block by class III antiarrhythmic agents. *J. Gen. Physiol.*, **96**, 195–215.

SIMONSEN, L.L. (1992). What are pharmacists dispensing most often? *Pharmacy Times*, April, 47–65.

SINGH, B.N. & NADEMANEE, K. (1985). Control of cardiac arrthymias by selective lengthening of repolarization: theoretical considerations and clinical observations. *Am. Heart. J.*, **109**, 421–430.

SNYDERS, D.J., KNOTH, K.M., ROBERDS, S.L. & TAMKUN, M.M. (1992). Time-, voltage- and state-dependent block by quinidine of a cloned human cardiac potassium channel. *Mol. Pharmacol.*, **41**, 322–330.

SNYDERS, D.J., TAMKUN, M.M. & BENNETT, P.B. (1993). A rapidly activating and slowly inactivating potassium channel cloned from human heart. Functional analysis after stable mammalian cell culture expression. *J. Gen. Physiol.*, **101**, 513–543.

TAMKUN, M.M., KNOTH, K.M., WALBRIDGE, J.A., KROEMER, H., RODEN, D.M. & GLOVER, D.M. (1991). Molecular cloning and characterization of two voltage-gated K^+ channel cDNAs from human ventricle. *FASEB J.*, **5**, 331–337.

WANG, Z., FERMINI, B. & NATTEL, S. (1993). Sustained depolarization-induced outward current in human atrial myocytes. Evidence for a novel delayed rectifier K^+ current similar to Kv1.5 cloned channel currents. *Circ. Res.*, **73**, 1061–1076.

WOODHULL, A.M. (1973). Ionic blockade of sodium channels in nerve. *J. Gen. Physiol.*, **61**, 687–708.

WOOSLEY, R.L., CHEN, Y., FREIMAN, J.P. & GILLIS, R.A. (1993). Mechanism of the cardiotoxic actions of terfenadine. *J. Am. Med. Ass.*, **269**, 1532–1536.

ZAMANI, K., CONNER, D.P., WEEMS, H.B., YANG, S.K. & CANTILENA, Jr, L.R. (1991). Enantiomeric analysis of terfenadine in rat plasma by HPLC. *Chirality*, **3**, 467–470.

ZHANG, M., TER LAAK, A.M. & TIMMERMAN, H. (1991). Optical isomers of the H1 antihistamine terfenadine: synthesis and activity. *Bioorg. Med. Chem. Lett.*, **1**, 387–390.

(Received November 2, 1994
Revised February 2, 1995
Accepted February 7, 1995)

British Journal of Pharmacology (1995) 115, 275-282

Actions of general anaesthetics on a neuronal nicotinic acetylcholine receptor in isolated identified neurones of *Lymnaea stagnalis*

[1]D. McKenzie, [2]N.P. Franks & [2]W.R. Lieb

Biophysics Section, The Blackett Laboratory, Imperial College of Science, Technology and Medicine, South Kensington, London, SW7 2BZ

1 Completely isolated identified neurones from the right parietal ganglion of the pond snail *Lymnaea stagnalis* were studied under two-electrode voltage-clamp. Neuronal nicotinic acetylcholine receptor currents were studied at low acetylcholine (ACh) concentrations ($\leqslant$ 200 nM). At these levels, control currents were non-desensitizing and proportional to the square of the ACh concentration.

2 IC_{50} concentrations were determined for the steady-state inhibition of the ACh-activated current by 31 general anaesthetics plus the non-anaesthetic alcohol *n*-tridecanol. The general anaesthetics included inhalational agents, *n*-alcohols, *n*-alkane-(α,ω)-diols, cycloalcohols and an *n*-alkane.

3 Anaesthetic inhibition was independent of voltage and consistent with two anaesthetic-binding sites on the receptor.

4 IC_{50} concentrations for inhibiting the neuronal nicotinic ACh receptor correlated well ($r = 0.97$) with EC_{50} concentrations for general anaesthesia. The maximum deviation from the line of identity was less than fourfold. The inhalational agents tended to be more potent as inhibitors of the ACh receptor than as general anaesthetics, while the alcohols and diols were less potent.

5 The inhibition of the ACh-induced current by the homologous series of *n*-alcohols exhibited a cutoff at the same position (just after dodecanol) as found for the induction of general anaesthesia in tadpoles.

6 Polarity profile maps of the anaesthetic-binding sites on the neuronal nicotinic ACh receptor were calculated from IC_{50} concentrations for the homologous series of *n*-alcohols and *n*-alkane-(α,ω)-diols. They reveal amphiphilic sites with apolar regions capable of accommodating the hydrocarbon chains of *n*-alcohols as large as decanol. A striking resemblance was found to profiles previously calculated from data for tadpole general anaesthesia.

Keywords: General anaesthesia; neuronal nicotinic acetylcholine receptor; inhalational anaesthetics; alcohols; diols; cycloalcohols; cutoff effect; polarity profiles; identified molluscan neurones

Introduction

Although the nicotinic acetylcholine receptor (AChR) of the neuromuscular junction is the most thoroughly investigated of all neurotransmitter-gated receptor channels, much less is known about its neuronal equivalent. Despite sharing some common properties, such as rapid opening of their channels in response to acetylcholine, muscle and neuronal nicotinic AChRs represent distinct families of receptors with characteristic differences. For example, although both receptors appear to be pentamers, muscle-type receptors are composed of four different types of subunit, whereas neuronal receptors require only one or two different subunit types to be functional (Patrick *et al.*, 1993). Furthermore, neuronal AChRs have a greater tendency to behave as inward rectifiers than do muscle receptor channels (Mathie *et al.*, 1990; Papke, 1993). More pertinent to the present study are possible differences in response to general anaesthetics. Muscle-type nicotinic AChRs in the clonal BC3H1 cell line (Dilger *et al.*, 1993), for example, appear to be much less sensitive to inhibition by isoflurane than neuronal nicotinic AChRs from bovine adrenal chromaffin cells (Pocock & Richards, 1988) and molluscan neurones (Franks & Lieb, 1991a).

The finding (Sargent, 1993) that neuronal nicotinic ACh receptor subunits are much more widely expressed in the mammalian central nervous system than previously realised raises the possibility that anaesthetic inhibition of these receptors may play a role in general anaesthesia. To evaluate this possibility, it is important to study the effect of a wide range of agents on neuronal nicotinic AChRs under controlled conditions. We have chosen a convenient molluscan preparation in which identified central neurones having a single type of nicotinic AChR response can be completely isolated and then exposed under voltage-clamp to known aqueous concentrations of acetylcholine and anaesthetics (Franks & Lieb, 1991a). We have measured the effects on this neuronal nicotinic AChR of 31 anaesthetic agents and find a good correlation between potencies for inhibiting nicotinic AChR activity and for causing general anaesthesia, over about a 20,000 fold range of potencies. Furthermore, we find that the whole animal anaesthetic potency cutoff found in the series of *n*-alcohols is replicated by the neuronal nicotinic AChR. Finally, using our experimentally determined anaesthetic IC_{50} concentrations, we have mapped out the polarity profiles of the anaesthetic binding sites on the receptor protein and find remarkably good agreement with the average profile for the unknown primary target sites underlying general anaesthesia in animals.

Methods

Solutions

The composition of normal saline was (mM): NaCl 50, KCl 2.5, $CaCl_2$ 4, $MgCl_2$ 4, HEPES 10, glucose 5; titrated to pH 7.4 with NaOH. ACh solutions were made up on the day of the experiment. Anaesthetics were dissolved in normal

[1] Present address: Department of Anatomy, Cambridge University, Downing Street, Cambridge CB2 3DY.
[2]Authors for correspondence.

saline, with and without ACh. The volatile anaesthetics and *n*-pentane were made up as fractions of saturated solutions in normal saline at room temperature. The concentrations of the saturated solutions were taken as: chloroform, 66.6 mM (Firestone *et al.*, 1986); diethyl ether, 816 mM (Budavari, 1989); enflurane, 11.9 mM (Seto *et al.*, 1992); fluroxene, 30 mM (Firestone *et al.*, 1986); halothane, 17.5 mM (Raventós, 1956); isoflurane, 15.3 mM (Franks & Lieb, 1991a); methoxyflurane, 9.1 mM (Seto *et al.*, 1992); pentane, 534 μM (Bell, 1973). The *n*-alcohols (carbon numbers ≤C7), the cycloalcohols (carbon numbers ≤C10) and the *n*-alkane-(α,ω)-diols (carbon numbers ≤C9) were added directly or diluted from stock solutions in normal saline. Solutions of higher members of these series were prepared using concentrated ethanolic solutions; the final concentration of ethanol in these anaesthetic-containing solutions was 17 mM or less, and an identical concentration of ethanol was always present in the equivalent control solutions. All chemicals other than anaesthetics were obtained from Sigma Chemical Co. Ltd. (Poole, Dorset).

Anaesthetics

The sources of the anaesthetics were as follows: enflurane, isoflurane, methoxyflurane (Abbott Laboratories Ltd., Queenborough, Kent); *n*-tetradecanol, *n*-pentane-1,5-diol, *n*-hexane-1,6-diol, *n*-octane-1,8-diol, *n*-nonane-1,9-diol, *n*-decane-1,10-diol, *n*-dodecane-1,12-diol (Aldrich Chemical Co. Ltd., Gillingham, Dorset); chloroform, *n*-pentane, ethanol, *n*-propanol, *n*-butanol, *n*-pentanol, *n*-hexanol, *n*-heptanol, *n*-octanol, *n*-nonanol, *n*-decanol, *n*-dodecanol (BDH Chemicals Ltd., Poole, Dorset); diethyl ether (Fisons Scientific Equipment, Loughborough, Leicestershire); cyclodecanol (ICN Biomedicals Ltd., Thame, Oxfordshire); halothane (ICI Ltd., Macclesfield, Cheshire); *n*-heptane-1,7-diol, cyclohexanol, cycloheptanol, cyclooctanol, cyclododecanol (Lancaster Synthesis Ltd., Morecambe, Lancashire); fluroxene (Ohio Medical Products, Madison, Wisconsin, U.S.A.); *n*-undecanol, *n*-tridecanol (Sigma Chemical Co. Ltd., Poole, Dorset).

Electrophysiology

Electrophysiological measurements were made using methods similar to those described previously (Franks & Lieb, 1991a). *Lymnaea stagnalis* snails (1 to 2.5 g) were obtained from Blades Biological (Cowden, Kent). All of the measurements were made on a group of three or four neurones which had a yellow-speckled appearance and lay adjacent to one another and lateral to the neurosecretory region in the ventral portion of the right parietal ganglion. The cells were completely isolated from the right parietal ganglion, which had been dissected away intact from the CNS. Identified neurones were isolated by impaling them with two microelectrodes and then slowly moving the ganglion away until the cell and its axons pulled free. This left the cell suspended in a bath (volume ~50 μl) which was perfused with solution at a rate of 1–2 ml min^{-1}. Under these conditions, solution exchange around the cell was rapid and equilibration was generally complete in a few seconds or less. A two-electrode voltage clamp (Axoclamp 2A, Axon Instruments, Foster City, California, U.S.A.) was used, with the current record filtered (10 Hz, -3 dB) by an 8-pole Bessel filter. Electrodes were fabricated using 1 mm filamented glass capillaries (Clark Electromedical Instruments, Reading, Berkshire) and were filled with either 2.5 M potassium chloride or 2 M potassium acetate. Electrode resistances were usually in the range 10–40 MΩ. All of the electrophysiological measurements were performed at room temperature.

When the recording electrodes were filled with potassium acetate, ACh induced a current which reversed (see Figure 1) at −70 ± 4 mV (mean ± s.e.mean; $n = 5$), close to the expected reversal potentials of potassium and chloride ions. However, this reversal potential did not change measurably ($n = 4$) when the external potassium concentration was doubled, suggesting the current to be carried largely, if not entirely, by chloride ions. This current has characteristics of a nicotinic AChR current (Franks & Lieb, 1991a). A similar ACh-activated inhibitory Cl^- current has been described by others (Kehoe, 1972; Chemeris *et al.*, 1982; Andreev *et al.*, 1984). When the electrodes were filled with potassium chloride, the reversal potential shifted to the right due, presumably, to an elevated concentration of chloride ions inside the cell (see Figure 1). For all of the anaesthetic

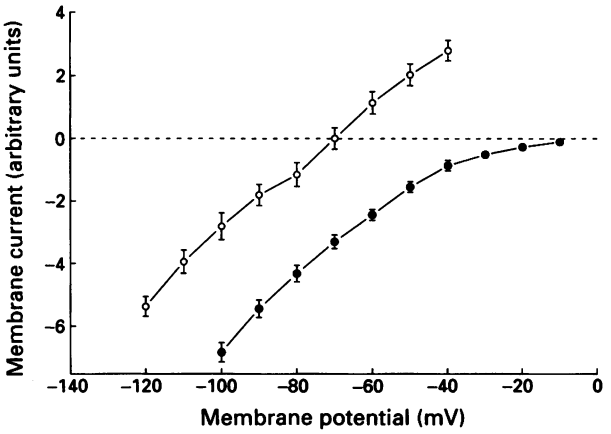

Figure 1 Current-voltage curves for the current activated by 200 nM acetylcholine (ACh). When the recording electrodes were filled with potassium acetate (○, 2 M), the reversal potential was $V_{rev} = -70 \pm 4$ mV (mean ± s.e.mean; $n = 5$ neurones). With potassium chloride (●, 2.5 M) electrodes, the ACh-activated current did not reverse but tended to zero near 0 mV ($n = 3$ neurones). The data for different cells have been combined by setting the slope conductances in the roughly linear region from −90 to −60 mV to be the same. S.e.means are shown except when smaller than the size of the symbol.

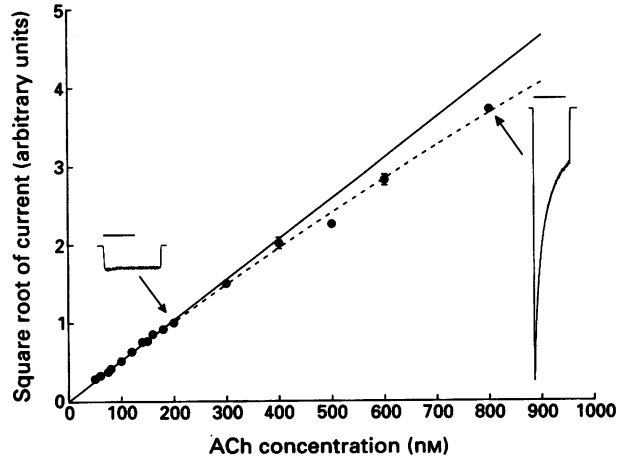

Figure 2 Dose-response curve for the peak acetylcholine (ACh)-activated current. At low concentrations (≤200 nM) of ACh, the induced current increased as the square of the ACh concentration and showed little desensitization (see inset on left). The solid line is a least-squares fit to the data up to 200 nM ACh, the standard concentration used in the anaesthetics experiments. At higher concentrations, the ACh-induced current showed increasingly marked desensitization (see inset on right) and the square root of the peak current began to deviate from linearity (dashed line). The horizontal calibration bars for the insets correspond to 60 s. The data are from four neurones and have been combined by setting the current induced at 200 nM to be the same for all data sets. S.e.means are shown except when smaller than the size of the symbol, apart for the value at 150 nM which was a single point determination.

experiments described here, we used electrodes filled with potassium chloride, since this allowed large Cl^- currents to be measured at around −70 mV, where contributions from anaesthetic-activated potassium currents (Franks & Lieb, 1988; 1991b) could be minimized.

As described in the Results section, all of the anaesthetics tested produced a steady-state level of inhibition, although the time taken to reach this steady-state varied among the anaesthetics. The anaesthetics were either co-applied with the ACh or, more usually, pre-applied before application of ACh. The latter protocol was used particularly when there was evidence that the anaesthetics themselves caused a change in resting current (so that small shifts in the baseline current could be taken into account when calculating IC_{50} values). The percentage inhibition was calculated using control ACh switches before and after anaesthetic administration, with sufficient time being allowed (20-120 s) for steady-state levels to be achieved. The IC_{50} values were calculated by fitting the data to Eqn.1 in the Results section, and these values were combined to give a mean and standard error for each agent. Only in the cases of *n*-tridecanol and *n*-tetradecanol did it prove impossible to achieve experimentally 50% inhibition of the ACh-induced current. For *n*-tridecanol, an IC_{50} concentration was calculated by extrapolation from the inhibition observed at a close to saturating concentration (see Results).

Values are given as means ± s.e.means.

Results

The uninhibited ACh-activated current

The identified, yellow-speckled neurones were usually extremely sensitive to ACh, with a concentration of 200 nM giving currents between 0.5 and 10 nA. At low (≤200 nM) ACh concentrations, currents were non-desensitizing and proportional to the square of the ACh concentration (Figure 2), consistent with two bound ACh molecules being required for opening the receptor channel. At higher ACh concentrations, desensitization began to appear and peak currents deviated from a simple square dependency (Figure 2). For simplicity, therefore, all anaesthetic experiments were performed in the low range of ACh concentrations (≤200 nM), usually at 200 nM ACh.

The anaesthetic-inhibited current

Simultaneous application of ACh and anaesthetic produced an inhibited current that decayed to a constant steady-state level. The magnitude and speed of the decay process varied from agent to agent. For some agents, especially for the volatile anaesthetics, the decay was small and rapid (Figure 3). For other agents, in particular the long-chain anaesthetics, the decay was larger and slower (Figure 4). This decay was roughly exponential and was essentially complete within 90 s. When substantial decay occurred, steady-state inhibition was usually measured by preincubating the neurone with anaesthetic (during general anaesthesia, neurones are exposed to anaesthetics for many minutes) and then repeatedly applying ~20 s pulses of ACh in anaesthetic solution until a constant response was obtained (see Figure 4).

Inhibition of the ACh-induced current by isoflurane was virtually independent of transmembrane potential in the range from −100 mV to −40 mV (Figure 5). In addition, inhibition was square-dependent (Figure 6a) and could be fitted by a straight line of the form

$$\sqrt{\frac{I_o}{I}} = 1 + \frac{A}{K_i} \qquad (1)$$

where I_0/I is the ratio of control to inhibited current at an anaesthetic concentration A, and K_i is the anaesthetic/receptor dissociation constant. This behaviour is consistent with two anaesthetic molecules being able to bind to the receptor channel (each with an identical dissociation constant K_i) but only one molecule being necessary to produce inhibition (Franks & Lieb, 1984; 1991a). Such square-dependent inhibition was found not only for small anaesthetic molecules such as isoflurane but also for very large anaesthetics such as cyclododecanol (Figure 6b).

IC_{50} concentrations for inhibition of the neuronal nicotinic AChR by general anaesthetics

The major result of this work was the determination of IC_{50} concentrations for inhibition of a neuronal nicotinic ACh receptor by a large number (32) of agents (see Table 1).

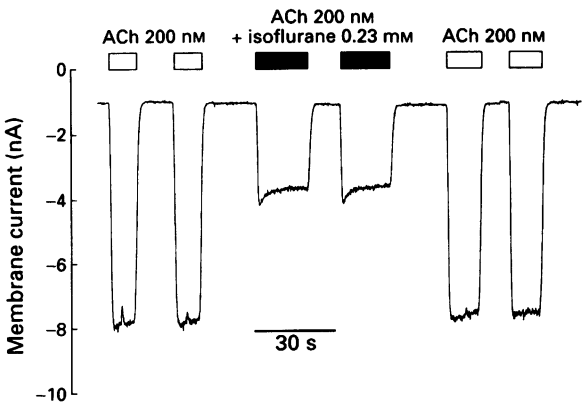

Figure 3 Inhibition of the acetylcholine (ACh)-induced current by the volatile general anaesthetic isoflurane. The inhibited current rapidly (~10 s) reached a steady value. In this example, 0.23 mM isoflurane inhibited the current by ~60%. This isoflurane concentration is ~80% of the EC_{50} for tadpole general anaesthesia (Firestone *et al.*, 1986).

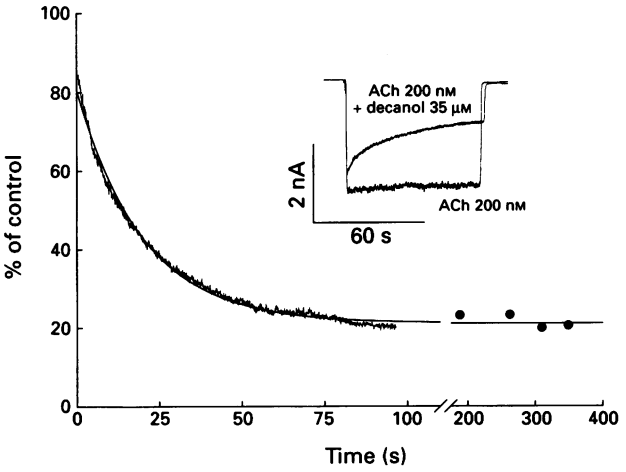

Figure 4 Inhibition of the acetylcholine (ACh)-induced current by the long-chain alcohol *n*-decanol. Many anaesthetics, including decanol, caused an inhibition of the ACh-induced current which took tens of seconds to reach a steady value. The steady state level of inhibition achieved was the same whether the anaesthetic was co-applied with ACh or whether ACh was applied following a prolonged pre-exposure to anaesthetic. The current traces in the inset show the time-course of the inhibition caused by co-application of 35 μM decanol and 200 nM ACh compared to the time-course of the control response. The main graph shows the time-course of the inhibition by 51 μM decanol co-applied with 200 nM ACh, fitted to a single exponential decay process (solid line). The solid symbols show the values of steady-state inhibition achieved after prolonged pre-exposure of the same cell to 51 μM decanol followed by co-application of decanol and 200 nM ACh in 20 s test pulses.

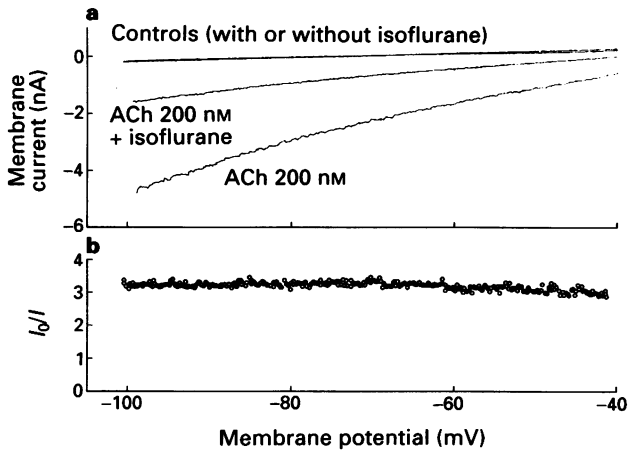

Figure 5 The inhibition of the acetylcholine (ACh)-induced current by isoflurane (0.3 mM) showed no significant voltage-dependence. (a) Quasi-steady-state *I-V* curves generated by slowly (3 mV s^{-1}) ramping the membrane potential from −100 mV to −40 mV. (Notice that in the absence of ACh, isoflurane caused a very small activation of a current which reversed at around −70 mV). (b) The factor (I_0/I) by which the ACh-induced current was inhibited by isoflurane was essentially constant with membrane potential.

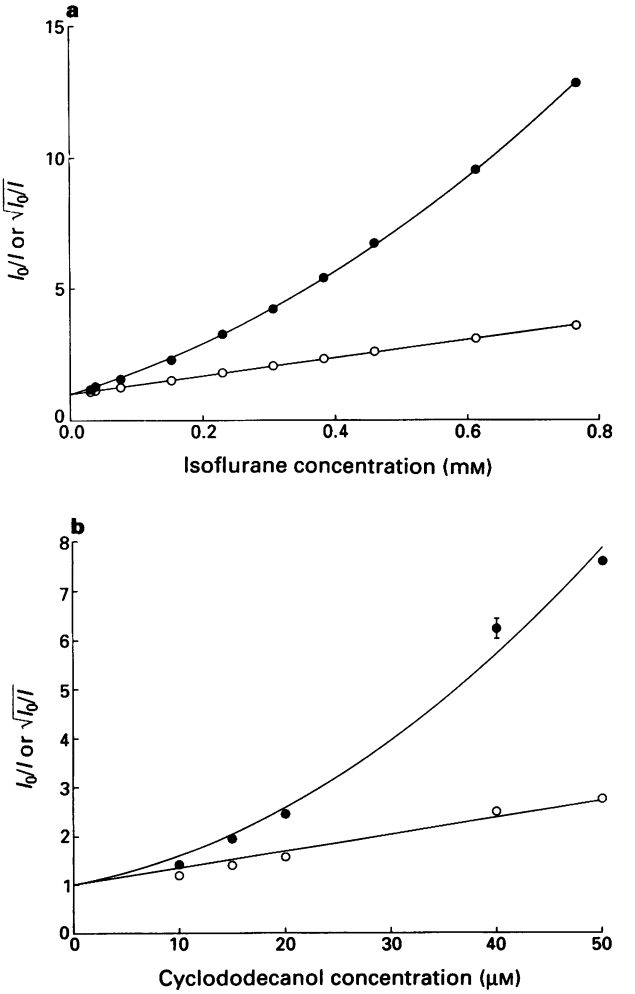

Figure 6 Dose-response relationships for inhibition by (a) isoflurane and (b) cyclododecanol. The ratio of control to inhibited current (I_0/I) (●) and the square root of this ratio (○) are plotted against the aqueous concentration of the anaesthetic. The lines (straight line or quadratic) are least-squares fits constrained to pass through unity on the ordinate axis. S.e.means are shown except when smaller than the size of the symbols. The plot in (a) has been modified from Franks & Lieb (1991a).

These include (in order, from the top of the table) seven inhalational agents, one alkane, twelve *n*-alcohols, seven *n*-alkane-(α,ω)-diols and five cycloalcohols. The IC_{50} concentrations span a 20,000 fold range of values, with *n*-tridecanol (IC_{50} = 15 μM) being the most potent agent and ethanol (IC_{50} = 324 mM) being the least potent agent. The IC_{50} concentration for the non-anaesthetic *n*-tridecanol could not be determined directly (since its IC_{50} is above the saturated concentration) but was extrapolated from an observed inhibition of about 25% with an 89% saturated solution. For *n*-tetradecanol insufficient inhibition (<10%) was obtained with an 82% saturated solution to allow an accurate estimate of the IC_{50}.

IC_{50} concentrations for inhibiting the neuronal nicotinic ACh receptor are highly correlated (correlation coefficient = 0.97 for a log-log relationship) with EC_{50} concentrations for general anaesthesia (Table 1). An unweighted regression of log(IC_{50}) against log(EC_{50}) gives a slope (±s.e.mean) of 0.96 ± 0.04, which is not significantly different from unity. In Figure 7, we have plotted (on a double logarithmic scale) IC_{50} versus EC_{50} values for 31 general anaesthetics; the straight line is the line of identity. It can be seen that the fit is reasonably good, although some agents (e.g. inhalational agents) are in general better inhibitors of the ACh receptor than other agents (e.g. alcohols and diols) when compared to their whole animal EC_{50} values.

Table 1 IC_{50} concentrations for inhibition of the neuronal nicotinic ACh receptor channel and EC_{50} concentrations for general anaesthesia

	ACh receptor-channel		*General anaesthesia*	
Anaesthetic	IC_{50} (μM)	n	EC_{50} (μM)	*Animal*
Halothane	686 ± 24	49	230	Tadpole[a]
Isoflurane	147 ± 6	20	290	Tadpole[b]
Enflurane	318 ± 10	40	600	Mouse[c]
Diethyl ether	37,000 ± 2,800	9	25,000	Tadpole[b]
Methoxyflurane	226 ± 8	21	210	Tadpole[a]
Fluroxene	1,213 ± 21	33	2,300	Tadpole[b]
Chloroform	990 ± 49	44	1,300	Tadpole[d]
n-Pentane	203 ± 4	7	68	Mouse[e]
Ethanol	324,000 ± 26,000	8	190,000	Tadpole[f]
n-Propanol	144,600 ± 6,900	5	73,000	Tadpole[f]
n-Butanol	12,350 ± 580	11	10,800	Tadpole[f]
n-Pentanol	4,750 ± 390	23	2,900	Tadpole[f]
n-Hexanol	1,360 ± 210	6	570	Tadpole[f]
n-Heptanol	439 ± 34	10	230	Tadpole[f]
n-Octanol	190 ± 18	9	57	Tadpole[f]
n-Nonanol	74.8 ± 3.7	4	37	Tadpole[f]
n-Decanol	33.6 ± 6.7	10	12.6	Tadpole[f]
n-Undecanol	28.6 ± 4.7	5	8.1	Tadpole[f]
n-Dodecanol	18.2 ± 5.4	5	4.7	Tadpole[f]
n-Tridecanol	14.9 ± 3.1	4	j	Tadpole[f]
n-Pentane-1,5-diol	42,100 ± 2,900	17	19,000	Tadpole[g]
n-Hexane-1,6-diol	46,900 ± 2,700	8	25,000	Tadpole[g]
n-Heptane-1,7-diol	10,800 ± 1,200	14	3,300	Tadpole[g]
n-Octane-1,8-diol	3,600 ± 260	14	960	Tadpole[g]
n-Nonane-1,9-diol	1,990 ± 70	9	640	Tadpole[g]
n-Decane-1,10-diol	577 ± 21	9	250	Tadpole[g]
n-Dodecane-1,12-diol	59.8 ± 1.5	12	45	Tadpole[g]
Cyclohexanol	5,530 ± 380	19	4,980	Tadpole[h]
Cycloheptanol	1,790 ± 230	7	1,290	Tadpole[h]
Cyclooctanol	1,049 ± 54	8	390	Tadpole[h]
Cyclodecanol	173 ± 36	7	84	Tadpole[h]
Cyclododecanol	17.5 ± 1.6	18	38	Tadpole[i]

IC_{50} concentrations are given as means ± s.e.means for *n* observations on 2 to 10 neurones. General anaesthesia EC_{50} concentrations are given for tadpoles when available in the literature. [a]Kita *et al.* (1981); [b]Firestone *et al.* (1986); [c]Franks & Lieb (1993); [d]Brink & Posternak (1948); [e]Abraham *et al.* (1991); [f]Alifimoff *et al.* (1989); [g]Moss *et al.* (1991a); [h]Curry *et al.* (1991); [i]Curry (1988); [j]Not anaesthetic (Alifimoff *et al.*, 1989).

Discussion and conclusions

Comparison with previous studies and with potencies for general anaesthesia

Overall, the potencies of thirty-one general anaesthetics for inhibiting the *Lymnaea* neuronal nicotinic AChR and for producing general anaesthesia are quite similar, the maximum discrepancy being less than fourfold (see Table 1 and Figure 7). This similarity is consistent with previous reports on rapidly activating acetylcholine receptor chloride channels in other molluscs for enflurane (Arimura & Ikemoto, 1986) and some intravenous general anaesthetics (Cote & Wilson, 1980; Judge & Norman, 1982); similar anaesthetic potencies were reported for molluscan fast acetylcholine receptor cation channels (Cote & Wilson, 1980; Arimura & Ikemoto, 1986), suggesting that anaesthetic sensitivity is independent of the ion specificity of molluscan nicotinic AChR channels. Our results are also consistent with the actions of four volatile and four intravenous general anaesthetics for inhibiting carbachol-induced catecholamine secretion from bovine chromaffin cells, an effect which is thought to be largely due to inhibition of a neuronal nicotinic AChR (Pocock & Richards, 1993).

It thus appears that neuronal nicotinic AChRs may be amongst the most anaesthetic-sensitive of all neuronal ion channels (Franks & Lieb, 1994). Nonetheless, the match we have found (Figure 7) is certainly not perfect, and there are consistent discrepancies between our IC_{50} concentrations determined for the *Lymnaea* neuronal nicotinic AChR and EC_{50} concentrations for general anaesthesia. For example, the volatile general anaesthetic agents, with the exception of halothane, are particularly potent at inhibiting the nicotinic AChR, with the fluorinated ethers isoflurane, enflurane and fluroxene exhibiting exceptional potency. The *n*-alkane pentane and most of the *n*-alcohols and *n*-alkane-α,ω-diols, on the other hand, are rather less potent when compared to their potencies for general anaesthesia, while the cycloalcohols occupy an intermediate position.

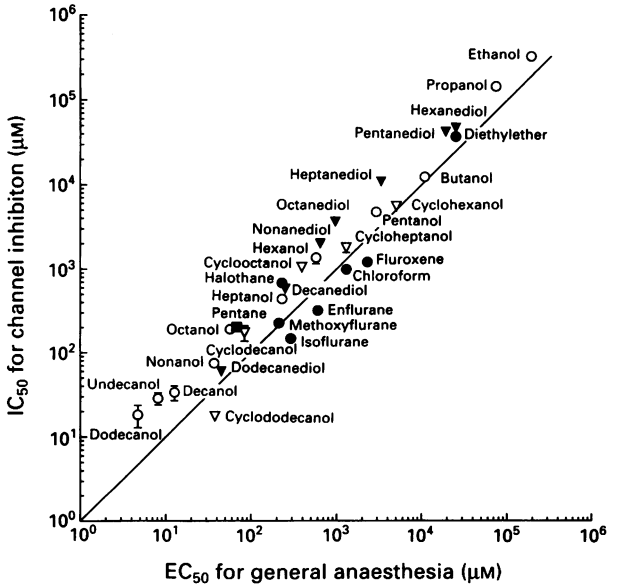

Figure 7 Comparison of the IC_{50} concentrations needed to half-inhibit the acetylcholine (ACh)-induced current with EC_{50} concentrations needed to anaesthetize animals. The line is the line of identity. The errors are s.e.means and where not shown were smaller than the size of the symbols. The symbols are: (●) inhalational anaesthetics; (○) *n*-alcohols; (▽) cycloalcohols; (▼) α,ω-diols; (■) alkanes. IC_{50} values and s.e.means together with values and sources for the animal EC_{50} data are given in Table 1. An unweighted least-squares straight line fit (not shown) through the data gave a slope of 0.96 ± 0.04 with a correlation coefficient of 0.97.

It has been shown previously that the *Lymnaea* neuronal nicotinic AChR is differentially inhibited by the two optical isomers of the widely used inhalational general anaesthetic, isoflurane (Franks & Lieb, 1991a). This stereoselective behaviour is not shared for isoflurane acting on either cholesterol-containing (Dickinson *et al.*, 1994) or cholesterol-free (Franks & Lieb, 1991a; Dickinson *et al.*, 1994) lipid

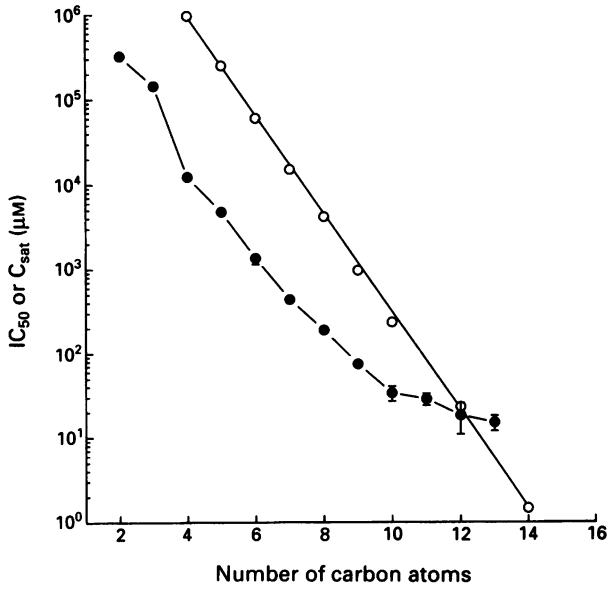

Figure 8 The cutoff effect for the *n*-alcohols. The IC_{50} values (●) for the *n*-alcohols decrease monotonically with the number of carbon atoms in the chain, but the marked reduction in slope after C10 leads to a cutoff at about C12. The next alcohol in the series, tridecanol, has an IC_{50} (estimated by extrapolation) considerably above the maximum aqueous solubility, while tetradecanol barely inhibited the acetylcholine (ACh)-induced current (even at 82% saturation). Values (○) for the maximum aqueous solubilities (C_{sat}), together with the straight line, are from Bell (1973). The errors are s.e.means and where not shown were smaller than the size of the symbols.

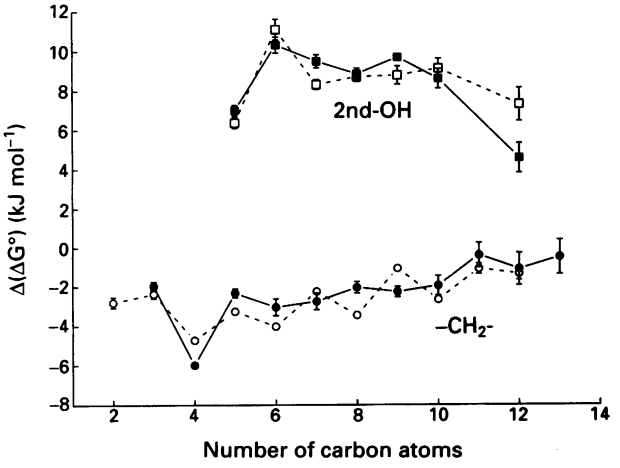

Figure 9 Polarity profiles of anaesthetic-binding sites. Values (± s.e.means) of incremental standard Gibbs free energies $\Delta(\Delta G^\circ)$ were calculated using Eqns. 2–3. (■ and □): $\Delta(\Delta G^\circ_{OH})$, for substituting a hydroxyl group (i.e. a second -OH) for a hydrogen atom on an *n*-alcohol terminal methyl group to obtain the corresponding *n*-alkane-(α,ω)-diol. (● and ○): $\Delta(\Delta G^\circ_{CH_2})$, for adding a methylene ($-CH_2-$) group to an *n*-alcohol. The abscissa scale is the chain-length, expressed as the number of carbon atoms in the final anaesthetic molecule. Solid symbols and continuous lines are neuronal nicotinic acetylcholine receptor data while open symbols and dashed lines are general anaesthesia data. The errors are s.e.means and where not shown were smaller than the size of the symbols.

bilayers and is therefore indicative of the anaesthetic acting directly on the receptor channel protein rather than on surrounding lipids. In addition, the IC_{50} concentration for **R**(−)-isoflurane inhibiting this nicotinic AChR is 50% greater than that for **S**(+)-isoflurane (Franks & Lieb, 1991a), which is the same as the ratio of **R**(−)- to **S**(+)-isoflurane minimum alveolar concentrations (MACs) for general anaesthesia in rats (Lysko *et al.*, 1994) and similar to that found for differences in sleep times in mice (Harris *et al.*, 1992). Although this may well be a coincidence (for example, a preliminary study reported no isoflurane stereoselectivity for tadpole general anaesthesia (Firestone *et al.*, 1992)), it is consistent with the neuronal nicotinic AChR being a potential site of action for general anaesthesia.

The cutoff effect

Further support for this view comes from similarities in the 'cutoff' effects observed for the homologous series of *n*-alcohols acting as inhibitors of the neuronal nicotinic AChR and as general anaesthetics for tadpoles. For general anaesthesia, EC_{50} concentrations monotonically fall (that is, potencies rise) with increasing *n*-alcohol chain-length until a point is reached beyond which even saturated solutions of larger alcohols no longer produce anaesthesia. For tadpoles, the cutoff point comes just after *n*-dodecanol; that is, while dodecanol is the most potent of all *n*-alcohols, even saturated solutions of tridecanol and tetradecanol do not on their own anaesthetize 50% of a population of animals (Alifimoff *et al.*, 1989).

The corresponding behaviour of the neuronal nicotinic AChR is shown in Figure 8. Here we have plotted IC_{50} concentrations against the number of carbon atoms in each *n*-alcohol, together with their corresponding aqueous solubilities, C_{sat}. It can be seen that $\log(IC_{50})$ decreases monotonically with chain length, with a marked reduction in slope after decanol (C10). $\text{Log}(C_{sat})$, however, continues to decrease with no change in slope after C10. These contrasting behaviours of IC_{50} and C_{sat} lead to $IC_{50} > C_{sat}$ for *n*-alcohols with 13 carbon atoms or more (see Figure 8), which means that *n*-tridecanol and larger *n*-alcohols cannot inhibit ACh receptor currents by as much as 50%, even if applied as saturated solutions. We have previously defined the cutoff point for inhibition of an *in vitro* system as the chain-length above which activity cannot be inhibited by 50% even by saturated solutions of higher members of the homologous series (Franks & Lieb, 1985; Curry *et al.*, 1990; Moss *et al.*, 1991b). Using this definition, the *n*-alcohol cutoff point is identical for both neuronal nicotinic AChR inhibition and tadpole general anaesthesia, occurring just after dodecanol.

The alcohol cutoff effect is an exception to the Meyer-Overton rule (of increasing potency for increasing solubility in fat-like solvents) and has been interpreted at the molecular level in terms of both lipid and protein targets. It was once thought to be due to a cutoff in the ability of long-chain alcohols to partition into lipid bilayers (Pringle *et al.*, 1981), but subsequent direct measurements revealed no such cutoff in solubility (Franks & Lieb, 1986). A current lipid hypothesis (Miller *et al.*, 1989; Raines *et al.*, 1993) is that, although long-chain alcohols can indeed partition into lipid bilayers, the disordering effect they cause (postulated to be related to their general anaesthetic potency) disappears near the cutoff point and is replaced by an ordering effect. An untested prediction of this hypothesis is that cutoff alcohols should antagonize the effects of general anaesthetics. A further prediction of this lipid hypothesis for ion channel inhibition is that the cutoff point might be expected to be similar from channel to channel. This does not seem to be the case for a number of ion channels, as has recently been pointed out by Li *et al.* (1994), who found that inhibition by alcohols of a fast ATP-activated current in bullfrog dorsal root ganglion neurones cuts off after *n*-propanol.

An alternative view is that the *n*-alcohols bind to protein pockets of circumscribed dimensions on receptor channels, as has been documented for lipid-free luciferase enzymes (Franks & Lieb, 1984; 1985; Curry *et al.*, 1990; Moss *et al.*, 1991b). For these proteins, the cutoff point varies both between proteins (Franks & Lieb, 1985; Curry *et al.*, 1990) and for different states of the same protein (Moss *et al.*, 1991b). On this view, our results (Figure 8) for the neuronal nicotinic AChR can be interpreted as follows. First, there are two binding sites for anaesthetics on each nicotinic ACh receptor, as indicated by the square-dependent inhibition found for both small and large anaesthetic molecules (see Figure 6). Each site consists of a predominantly apolar pocket on the receptor protein with a polar mouth leading to aqueous solution (see below). As alcohol molecules increase in size, so do the number of their apolar methylene ($-CH_2-$) groups. For molecules smaller than the volume of the apolar pocket, this results in favourable binding energy increases and thus lower IC_{50} concentrations. However, once the pocket is full, after decanol (C10), additional methylene groups are forced into the polar mouth or water and therefore cannot add greatly to the binding energy for transfer from water to the site. The IC_{50} concentrations, consequently, tend to level out after C10, as can be seen from Figure 8. Each added methylene group, however, decreases the aqueous solubility C_{sat} of the alcohol in a roughly log-linear fashion (Figure 8). This combination of a rapidly falling C_{sat} and a levelling IC_{50} means that, inevitably, as the alcohols increase in size a point is reached after which $C_{sat} < IC_{50}$ and larger alcohols are no longer able to function as effective inhibitors.

Mapping the polarity profiles of the anaesthetic-binding sites

The *n*-alcohol and *n*-alkane-(α,ω)-diol data in Table 1 can be used to map out the average polarity profiles of the two anaesthetic-binding sites involved in inhibition of the neuronal nicotinic ACh receptor channel, as has been done previously using data on firefly and bacterial luciferase enzymes (Moss *et al.*, 1991a). The incremental standard Gibbs free energies for adding an apolar methylene ($-CH_2-$) group and for adding a terminal polar hydroxyl group (strictly: for converting an apolar terminal methyl $-CH_3$ group to a polar $-CH_2OH$ group), respectively, to an *n*-alcohol molecule can be calculated from the following formulae (Moss *et al.*, 1991a):

$$\Delta(\Delta G^{\circ}_{CH_2}) = RT \ln\left(\frac{IC^{\text{alcohol}}_{50,m}}{IC^{\text{alcohol}}_{50,m-1}}\right) \quad (2)$$

and

$$\Delta(\Delta G^{\circ}_{OH}) = RT \ln\left(\frac{2\ IC^{\text{diol}}_{50,m}}{IC^{\text{alcohol}}_{50,m}}\right) \quad (3)$$

where R is the gas constant, T is the absolute temperature, and the superscripts (alcohol or diol) and subscripts (*m* or *m*-1) of the IC_{50} terms refer to the type of compound and the number of carbon atoms, respectively. These incremental free energies are for *m* carbon atoms on the final anaesthetic molecule. (Eqns. 2–3 follow from Eqns. 1b and 3, respectively, of Moss *et al.* (1991a) when IC_{50} is proportional to the inhibition constant K_i. This proportionality follows from Eqn.1, from which it is easy to show that $IC_{50} = 0.414\ K_i$) Values of $\Delta(\Delta G^{0}_{CH2})$ and $\Delta(\Delta G^{0}_{OH})$ for inhibition of the ACh receptor channel are plotted as solid symbols in Figure 9, together with corresponding values (open symbols) previously calculated (Moss *et al.*, 1991a) using EC_{50} concentrations for tadpole general anaesthesia.

How can one interpret these polarity profiles? To the extent that adding an apolar methylene group or a terminal

polar hydroxyl group to an *n*-alcohol does not substantially change the position of the anaesthetic molecule in the binding pockets, $\Delta(\Delta G^0_{CH2})$ and $\Delta(\Delta G^0_{OH})$ can be thought of as apolar and polar probes, respectively, of the energetics of binding to the anaesthetic-binding sites. If this assumption is correct, then $\Delta(\Delta G^0_{CH2})$ and $\Delta(\Delta G^0_{OH})$ should give a consistent picture. This seems to be the case. For the neuronal nicotinic AChR, $\Delta(\Delta G^0_{OH})$ is large and positive (between 7 to 11 kJ mol^{-1}) for alcohols with 5 to 10 carbon atoms, indicative of the energetic difficulty of introducing a polar group, while for the same region $\Delta(\Delta G^0_{CH2})$ is substantial and negative (between -2 to -3 kJ mol^{-1}), showing that it is energetically favourable to introduce an apolar group. On the other hand, there is a substantial fall in $\Delta(\Delta G^0_{OH})$ after 10 carbon atoms, while there is a corresponding increase in the algebraic value of $\Delta(\Delta G^0_{CH2})$, both indicative of a more polar region.

These polarity profiles (Figure 9) are consistent with the anaesthetic-binding sites on the neuronal nicotinic AChR being amphiphilic, with an apolar portion capable of accommodating the hydrocarbon chains of alcohols as large as *n*-decanol. For *n*-alcohols larger than decanol, the additional methylene groups are forced into a more polar environment (which for very large alcohols may include external aqueous solution), causing the levelling off of IC_{50} values seen in Figure 8. Interestingly, Figure 9 shows that the polarity profiles for the neuronal nicotinic AChR are surprisingly similar to those for tadpole general anaesthesia, suggesting that the unknown primary target sites underlying general anaesthesia may have similar geometries and polarities. Indeed, solvent correlation studies (Franks & Lieb, 1978; Abraham *et al.*, 1991) have shown that the general anaesthesia sites are on average amphiphilic in nature, but it has not been clear whether or not this reflected a mixed population of polar and apolar sites; the present results with the neuronal nicotinic AChR show that such amphiphilicity can be the property of a single type of site on a receptor channel.

Implications for general anaesthesia

While the muscle type nicotinic ACh receptor has long been used as a model for studying the interactions of anaesthetics and ion channels, it has rarely been argued that nicotinic ACh receptors play an important role in the induction of general anaesthesia. Our results showing the striking similarities between IC_{50} values, the *n*-alcohol cutoff point, the stereoselective effects of the optical isomers of isoflurane (Franks & Lieb, 1991a), and the polarity profiles for anaesthetics acting on a neuronal nicotinic ACh receptor and on animals, at least raises this possibility. This is further strengthened by recent findings (Sargent, 1993) that neuronal nicotinic ACh receptor subunits are more widely distributed in mammalian brain than has previously been thought. Although the sequences of molluscan neuronal nicotinic ACh receptors are still unknown, most nicotinic ACh receptors appear to be members of the superfamily of receptors which includes at least one other member (the $GABA_A$ receptor) which has also been shown to be very sensitive to a wide variety of different anaesthetics. It may well be that, despite the obvious qualitative differences between the effects of anaesthetics on neuronal $GABA_A$ and nicotinic ACh receptors (the former are potentiated while the latter are inhibited), the underlying mechanisms may share common features at the molecular level. One of the most important problems in the future will be to assess which of those receptors that have been found to be sensitive to anaesthetics actually contribute significantly to the clinical state of general anaesthesia.

We thank Ramin Nakisa for providing data acquisition software, Ian Coole for technical assistance, Robert Dickinson for determining the IC_{50} for ethanol, and both Julie Violet and Robert Dickinson for helpful comments on the manuscript. We are grateful to the MRC, the NIH (grant GM 41609), Anaquest Inc., and the BOC Group Inc. for support.

References

ABRAHAM, M.H., LIEB, W.R. & FRANKS, N.P. (1991). Role of hydrogen bonding in general anesthesia. *J. Pharm. Sci.*, **80,** 719–724.

ALIFIMOFF, J.K., FIRESTONE, L.L. & MILLER, K.W. (1989). Anaesthetic potencies of primary alkanols: implications for the molecular dimensions of the anaesthetic site. *Br. J. Pharmacol.*, **96,** 9–16.

ANDREEV, A.A., VEPRINTSEV, B.N. & VULFIUS, C.A. (1984). Two-component desensitization of nicotinic receptors induced by acetylcholine agonists in *Lymnaea stagnalis* neurones. *J. Physiol.*, **353,** 375–391.

ARIMURA, H. & IKEMOTO, Y. (1986). Action of enflurane on cholinergic transmission in identified *Aplysia* neurones. *Br. J. Pharmacol.*, **89,** 573–582.

BELL, G.H. (1973). Solubilities of normal aliphatic acids, alcohols and alkanes in water. *Chem. Phys. Lipids*, **10,** 1–10.

BRINK, F. & POSTERNAK, J.M. (1948). Thermodynamic analysis of the relative effectiveness of narcotics. *J. Cell Comp. Physiol.*, **32,** 211–233.

BUDAVARI, S., Ed. (1989). *The Merck Index*. Rahway, New Jersey: Merck and Co., Inc.

CHEMERIS, N.K., KAZACHENKO, V.N., KISLOV, A.N. & KURCHIKOV, A.L. (1982). Inhibition of acetylcholine responses by intracellular calcium in *Lymnaea stagnalis* neurones. *J. Physiol.*, **323,** 1–19.

COTE, I.L. & WILSON, W.A. (1980). Effects of barbiturates on inhibitory and excitatory reponses to applied neurotransmitters in *Aplysia*. *J. Pharmacol. Exp. Ther.*, **214,** 161–165.

CURRY, S. (1988). The interactions of general anaesthetics with a bacterial luciferase enzyme. *Ph.D. Thesis (University of London)*.

CURRY, S., LIEB, W.R. & FRANKS, N.P. (1990). Effects of general anesthetics on the bacterial luciferase enzyme from *Vibrio harveyi*: an anesthetic target site with differential sensitivity. *Biochemistry*, **29,** 4641–4652.

CURRY, S., MOSS, G.W.J., DICKINSON, R., LIEB, W.R. & FRANKS, N.P. (1991). Probing the molecular dimensions of general anaesthetic target sites in tadpoles (*Xenopus laevis*) and model systems using cycloalcohols. *Br. J. Pharmacol.*, **102,** 167–173.

DICKINSON, R., FRANKS, N.P. & LIEB, W.R. (1994). Can the stereoselective effects of the anesthetic isoflurane be accounted for by lipid solubility? *Biophys. J.*, **66,** 2019–2023.

DILGER, J.P., BRETT, R.S. & MODY, H.I. (1993). The effects of isoflurane on acetylcholine receptor channels. 2. Currents elicited by rapid perfusion of acetylcholine. *Mol. Pharmacol.*, **44,** 1056–1063.

FIRESTONE, L.L., MILLER, J.C. & MILLER, K.W. (1986). Tables of physical and pharmacological properties of anesthetics. In *Molecular and Cellular Mechanisms of Anesthetics*. ed. Roth S.H. & Miller, K.W. pp. 455–470. New York: Plenum.

FIRESTONE, S., FERGUSON, C. & FIRESTONE, L. (1992). Isoflurane's optical isomers are equipotent in *Rana pipiens* tadpoles. *Anesthesiology*, **77,** A758.

FRANKS, N.P. & LIEB, W.R. (1978). Where do general anaesthetics act? *Nature*, **274,** 339–342.

FRANKS, N.P. & LIEB, W.R. (1984). Do general anaesthetics act by competitive binding to specific receptors? *Nature*, **310,** 599–601.

FRANKS, N.P. & LIEB, W.R. (1985). Mapping of general anaesthetic target sites provides a molecular basis for cutoff effects. *Nature*, **316,** 349–351.

FRANKS, N.P. & LIEB, W.R. (1986). Partitioning of long-chain alcohols into lipid bilayers: Implications for mechanisms of general anesthesia. *Proc. Natl. Acad. Sci. U.S.A.*, **83,** 5116–5120.

FRANKS, N.P. & LIEB, W.R. (1988). Volatile general anaesthetics activate a novel neuronal K^+ current. *Nature*, **333,** 662–664.

FRANKS, N.P. & LIEB, W.R. (1991a). Stereospecific effects of inhalational general anesthetic optical isomers on nerve ion channels. *Science*, **254,** 427–430.

FRANKS, N.P. & LIEB, W.R. (1991b). Selective effects of volatile general anesthetics on identified neurons. *Annals N.Y. Acad. Sci.*, **625**, 54–70.

FRANKS, N.P. & LIEB, W.R. (1993). Selective actions of volatile general anaesthetics at molecular and cellular levels. *Br. J. Anaesth.*, **71**, 65–76.

FRANKS, N.P. & LIEB, W.R. (1994). Molecular and cellular mechanisms of general anaesthesia. *Nature*, **367**, 607–614.

HARRIS, B., MOODY, E. & SKOLNICK, P. (1992). Isoflurane anesthesia is stereoselective. *Eur. J. Pharmacol.*, **217**, 215–216.

JUDGE, S.E. & NORMAN, J. (1982). The action of general anaesthetics on acetylcholine-induced inhibition in the central nervous system of *Helix*. *Br. J. Pharmacol.*, **75**, 353–357.

KEHOE, J. (1972). Three acetylcholine receptors in *Aplysia* neurones. *J. Physiol.*, **225**, 115–146.

KITA, Y., BENNETT, L.J. & MILLER, K.W. (1981). The partial molar volumes of anesthetics in lipid bilayers. *Biochim. Biophys. Acta*, **647**, 130–139.

LI, C.Y., PEOPLES, R.W. & WEIGHT, F.F. (1994). Alcohol action on a neuronal membrane receptor: Evidence for a direct interaction with the receptor protein. *Proc. Natl. Acad. Sci. U.S.A.*, **91**, 8200–8204.

LYSKO, G.S., ROBINSON, J.L., CASTO, R. & FERRONE, R.A. (1994). The stereospecific effects of isoflurane isomers *in vivo*. *Eur. J. Pharmacol.*, **263**, 25–29.

MATHIE, A., COLQUHOUN, D. & CULL-CANDY, S.G. (1990). Rectification of currents activated by nicotinic acetylcholine receptors in rat sympathetic ganglion neurones. *J. Physiol.*, **427**, 625–655.

MILLER, K.W., FIRESTONE, L.L., ALIFIMOFF, J.K. & STREICHER, P. (1989). Nonanesthetic alcohols dissolve in synaptic membranes without perturbing their lipids. *Proc. Natl. Acad. Sci. U.S.A.*, **86**, 1084–1087.

MOSS, G.W.J., CURRY, S., FRANKS, N.P. & LIEB, W.R. (1991a). Mapping the polarity profiles of general anesthetic target sites using *n*-alkane-(α,ω)-diols. *Biochemistry*, **30**, 10551–10557.

MOSS, G.W.J., FRANKS, N.P. & LIEB, W.R. (1991b). Modulation of the general anesthetic sensitivity of a protein: A transition between two forms of firefly luciferase. *Proc. Natl. Acad. Sci. U.S.A.*, **88**, 134–138.

PAPKE, R.L. (1993). The kinetic properties of neuronal nicotinic receptors: Genetic basis of functional diversity. *Prog. Neurobiol.*, **41**, 509–531.

PATRICK, J., SÉQUÉLA, P., VERNINO, S., AMADOR, M., LUETJE, C. & DANI, J.A. (1993). Functional diversity of neuronal nicotinic acetylcholine receptors. *Prog. Brain. Res.*, **98**, 113–120.

POCOCK, G. & RICHARDS, C.D. (1988). The action of volatile anaesthetics on stimulus-secretion coupling in bovine adrenal chromaffin cells. *Br. J. Pharmacol.*, **95**, 209–217.

POCOCK, G. & RICHARDS, C.D. (1993). Excitatory and inhibitory synaptic mechanisms in anaesthesia. *Br. J. Anaesth.*, **71**, 134–147.

PRINGLE, M.J., BROWN, K.B. & MILLER, K.W. (1981). Can the lipid theories of anesthesia account for the cutoff in anesthetic potency in homologous series of alcohols? *Mol. Pharmacol.*, **19**, 49–55.

RAINES, D.E., KORTEN, S.E., HILL, W.A.G. & MILLER, K.W. (1993). Anesthetic cutoff in cycloalkanemethanols. A test of current theories. *Anesthesiology*, **78**, 918–927.

RAVENTÓS, J. (1956). The action of Fluothane - a new volatile anaesthetic. *Br. J. Pharmacol. Chemother.*, **11**, 394–410.

SARGENT, P.B. (1993). The diversity of neuronal nicotinic acetylcholine receptors. *Annu. Rev. Neurosci.*, **16**, 403–443.

SETO, T., MASHIMO, T., YOSHIYA, I., KANASHIRO, M. & TANIGUCHI, Y. (1992). The solubility of volatile anaesthetics in water at 25.0°C using ^{19}F NMR spectroscopy. *J. Pharmacol. Biomed. Anal.*, **10**, 1–7.

(Received September 13, 1994
Revised January 31, 1995
Accepted February 8, 1995)

British Journal of Pharmacology (1995) 115, 283-294

Functional evidence equating the pharmacologically-defined α_{1A}- and cloned α_{1C}-adrenoceptor: studies in the isolated perfused kidney of rat

[1]D.R. Blue, Jnr, D.W. Bonhaus, A.P.D.W. Ford, [2]J.R. Pfister, [3]N.A. Sharif, I.A. Shieh, R.L. Vimont, T.J. Williams & D.E. Clarke

Syntex Research, 3401 Hillview Avenue, Palo Alto, CA 94304, U.S.A.

1 The present study characterizes and classifies α_1-adrenoceptor-mediated vasoconstriction in the isolated perfused kidney of rat using quantitative receptor pharmacology and compares the results to radioligand binding studies (made in cloned α_1-adrenoceptor subtypes, native α_{1A}-adrenoceptors in submaxillary gland of rat, and α_{1A}-adrenoceptors in several other tissues of rat).

2 Concentration-effect curves to noradrenaline in the presence of 5-methyl-urapidil were biphasic, indicating α_1-adrenoceptor heterogeneity. The α_1-adrenoceptor subtype mediating the first phase (low affinity for 5-methyl-urapidil) could not be 'isolated' for detailed pharmacological characterization but was defined by a sensitivity to inhibition by chloroethylclonidine and an inability of methoxamine to activate the site. Additionally, vasoconstriction mediated by this α_1-adrenoceptor subtype or subtypes was abolished by nitrendipine (1 μM), thereby allowing characterization of the second, high affinity site for 5-methyl-urapidil.

3 The following antagonists interacted competitively with noradrenaline at the α_1-adrenoceptor for which 5-methyl-urapidil exhibits high affinity (pK_B value): WB 4101 (10.3)$>$prazosin (9.5)$\approx$HV 723 (9.3)$\approx$5-methyl-urapidil (9.2)$>$phentolamine (8.6)$>$spiperone ($pA_2 = 8.1$)$\approx$oxymetazoline (7.9). In contrast, insurmountable antagonism was seen with **S(+)**- and **R(−)**-niguldipine, the **S(+)**-isomer being approximately 30 fold more potent than the **R(−)**-isomer. Receptor protection experiments indicated that **S(+)**-niguldipine interacted directly with α_1-adrenoceptors. Dehydroniguldipine acted as a competitive antagonist ($pK_B = 9.0$). Thus, the results with antagonists define the α_1-adrenoceptor as an α_{1A}-adrenoceptor.

4 An agonist 'fingerprint' was constructed in the presence of nitrendipine to define further the α_{1A}-adrenoceptor. The following order and relativity of agonist potency was obtained: cirazoline (1)$\approx$adrenaline (2)$>$noradrenaline (5)$>$phenylephrine (23)$\approx$amidephrine (31)$>$methoxamine (71)$\gg$isoprenaline (1456)$\approx$dopamine (2210).

5 A high correlative association was shown between the affinity of antagonists obtained functionally in the isolated perfused kidney of rat and pK_i values obtained from binding experiments with the cloned bovine α_{1C}-adrenoceptor ($R^2 = 0.85$), native α_{1A}-adrenoceptors in submaxillary gland of rat ($R^2 = 0.79$), and α_{1A}-adrenoceptors from several other tissues of rat (values taken from the literature, $R^2 = 0.89$).

6 The present study demonstrates that the α_{1A}-adrenoceptor is the predominant α_1-adrenoceptor subtype mediating vasoconstrictor responses to exogenously administered noradrenaline in the isolated perfused kidney of rat. More importantly, α_{1A}-adrenoceptors mediating vasoconstrictor responses to noradrenaline exhibited a pharmacological equivalency to the cloned bovine α_{1C}-adrenoceptor. Thus, definitive functional pharmacological data are provided for equating the two receptors and support results derived recently from molecular and radioligand binding studies.

Keywords: Native α_1-adrenoceptor subtypes; cloned α_1-adrenoceptor subtypes; α_{1A}-adrenoceptors; 5-methyl-urapidil; **S(+)**-niguldipine; chloroethylclonidine; submaxillary gland; kidney

Introduction

Considerable evidence exists for the division of α_1-adrenoceptors into subtypes. In 1986, Flavahan & Vanhoutte proposed the existence of two distinct α_1-adrenoceptor subtypes (α_{1H}- and α_{1L}-adrenoceptors) based on the work of Holck *et al.* (1983) and observations made by Drew (1985). α_{1H}-Adrenoceptors were reported to possess a high affinity for prazosin ($pA_2 > 9$) and yohimbine ($pA_2 > 6.4$) whereas α_{1L}-adrenoceptors were reported to possess a low affinity (pA_2 values <9 and <6.4 respectively). This proposal received little attention due to possible alternative explanations, such as species variation (McGrath *et al.*, 1989), experimental rigour (Docherty *et al.*, 1987; McGrath *et al.*, 1989), and the potential for the involvement of α_2-adrenoceptor subtypes (Bylund, 1985). It should be noted, however, that since the article by Flavahan & Vanhoutte (1986), α_1-adrenoceptors exhibiting both high and low affinity for prazosin have been identified in gerbil (Kimura *et al.*, 1993), rat (Oshita *et al.*, 1991; Ohmura *et al.*, 1992), rabbit (Muramatsu *et al.*, 1990a; Oshita *et al.*, 1993) and dog (Flavahan *et al.*, 1987; Kohno *et al.*, 1994). Thus, a classification scheme proposing α_1-adrenoceptor subtypes based upon divergent affinity estimates for prazosin remains in line with a body of current thinking (Muramatsu *et al.*, 1990b; Oshita *et al.*, 1991). However, the most widely accepted classification scheme for α_1-adrenoceptors operative today considers only those α_1-adrenoceptor subtypes with high affinity for prazosin, and stemmed directly from work by Morrow & Creese (1986).

Morrow & Creese (1986) observed that WB 4101 and phentolamine displaced high affinity [^{3}H]-prazosin ($pK_D \approx$

[1] Author for correspondence.
[2] Present Address: CV Therapeutics, 3172 Porter Dr., Palo Alto, CA 94304, U.S.A.
[3] Present Address: Alcon Labs, 6201 South Freeway, Ft. Worth, TX 76134, U.S.A.

9–10) binding in cortex of rat in a manner consistent with the presence of two distinct binding sites. Binding sites for [^{3}H]-prazosin with high affinity for WB 4101 and phentolamine (Morrow & Creese, 1986), as well as oxymetazoline (Hanft & Gross, 1989a), benoxathian (Han *et al.*, 1987), YM 12617 (Hanft *et al.*, 1989), 5-methyl-urapidil (Gross *et al.*, 1988) and S(+)-niguldipine (Boer *et al.*, 1989) were designated α_{1A}-adrenoceptors, whereas binding sites with low affinity for these ligands were designated α_{1B}-adrenoceptors. Subsequently, the α_{1B}-adrenoceptor subtype has been shown to bind selectively spiperone (Michel *et al.*, 1989) and risperidone (Sleight *et al.*, 1993) and to undergo preferential alkylation by chloroethylclonidine (CEC; Johnson & Minneman, 1987). The identification of α_{1A}- and α_{1B}-adrenoceptor binding sites in human brain (Gross *et al.*, 1989) and the demonstration of functional correlates to these binding sites (Han *et al.*, 1987) served to substantiate the α_{1A}- and α_{1B}-adrenoceptor classification scheme.

In contrast to pharmacological approaches, molecular biological techniques have demonstrated the existence of three α_1-adrenoceptors, all of which exhibit high affinity for prazosin: the cloned α_{1B}-, α_{1C}- and α_{1D}-adrenoceptors (for references, see Ford *et al.*, 1994). Difficulty has arisen, however, in equating cloned and pharmacologically-defined α_1-adrenoceptors. Until recently only the cloned and pharmacologically-defined α_{1B}-adrenoceptors were considered to represent the same molecular entity (Pimoule *et al.*, 1992). Currently, however, the cloned α_{1C}-adrenoceptor, which exhibits high affinity for 5-methyl-urapidil, WB 4101, oxymetazoline and S(+)-niguldipine, is also considered to be the same receptor as the α_{1A}-adrenoceptor described pharmacologically above (Ford *et al.*, 1994; Faure *et al.*, 1994; Clarke *et al.*, 1994; Price *et al.*, 1994; Michel & Insel, 1994). The cloned α_{1D}-adrenoceptor, characterized by its low affinity for 5-methyl-urapidil, oxymetazoline and (+)-niguldipine and its relative resistance to alkylation by CEC, is without a clear-cut functional correlate (Ford *et al.*, 1994), although the α_1-adrenoceptor mediating contraction of the rat aorta *in vitro* is claimed as an α_{1D}-adrenoceptor (Ko *et al.*, 1994; Saussy *et al.*, 1994).

It has been known for more than a decade that α_1-adrenoceptors mediate vasoconstrictor responses to noradrenaline (NA) in the isolated perfused kidney of rat, despite a preponderance of α_2-adrenoceptors in this organ (Schmitz *et al.*, 1981). Radioligand binding and biochemical studies have demonstrated the presence of both α_{1A}- and α_{1B}-adrenoceptor subtypes in rat kidney (Han *et al.*, 1990; Wilson & Minneman, 1990; Michel *et al.*, 1993a). Furthermore, α_{1A}-adrenoceptors have been reported to mediate vasoconstrictor responses to α_1-adrenoceptor agonists both *in vitro* (Eltze *et al.*, 1991; Eltze & Boer, 1992; Blue *et al.*, 1992) and *in vivo* (Elhawary *et al.*, 1992; Sattar & Johns, 1994a,b).

The present study was undertaken to identify and characterize more fully α_1-adrenoceptor-mediated vasoconstriction in the isolated perfused kidney of rat and to compare the results with ligand binding data derived from the cloned hamster α_{1B}-, bovine α_{1C}- and rat α_{1D}-adrenoceptors. Thus, we now present details of functional, pharmacologically-derived data that substantiate the claim for equating the native α_{1A}-adrenoceptor with the cloned, bovine α_{1C}-adrenoceptor (as proposed originally by Ford *et al.*, 1994). Preliminary accounts of some of this work have been presented (Blue & Clarke, 1990; Clarke *et al.*, 1991; Sharif *et al.*, 1991; Blue *et al.*, 1991; Clarke *et al.*, 1994).

Methods

Isolated perfused kidney of rat

Male Sprague-Dawley (Charles River) rats (350–500 g) were anaesthetized with sodium pentobarbitone (55 mg kg^{-1}, i.p.) and the right renal artery and kidney were isolated as described previously (Blue *et al.*, 1992). A cannula was inserted into the mesenteric artery and advanced across the abdominal aorta into the renal artery. The kidney was removed and perfused immediately at a constant rate (6 ml min^{-1}; Masterflex pump, pump head size 7014-21, Cole-Parmer, Chicago, IL, U.S.A.) with Krebs bicarbonate solution (pH 7.4, 37°C) of the following composition (mM): NaCl 118.5, KCl 4.8, $CaCl_2$ 2.5, $MgSO_4$ 1.2, KH_2PO_4 1.2, $NaHCO_3$ 25 and dextrose 5. The Krebs solution was bubbled continuously with 95% O_2 and 5% CO_2. Perfusion pressure was measured by a Spectramed physiological pressure transducer (model number: P23XL) positioned near the kidney and displayed on a Beckman physiograph (model R611). Following removal of the renal capsule, kidneys were allowed to equilibrate for 30 min before exposure to a bolus dose of NA (0.1 μg in 0.1 ml of 0.9% saline). Following this priming dose, kidneys were allowed to equilibrate for an additional 15 min before experiments were begun.

Unless indicated otherwise, experiments were performed in the presence of cocaine (30 μM), corticosterone (30 μM), propranolol (1 μM), indomethacin (10 μM) and EDTA (100 μM) to inhibit neuronal and extraneuronal uptake of catecholamines, vascular β-adrenoceptors, the involvement of prostanoids and auto-oxidation of catecholamines respectively. High concentrations of cocaine and corticosterone are necessary to prevent NA from overcoming uptake blockade when used in high concentrations (e.g. in competition studies with antagonists). Propranolol was omitted from the Krebs solution in experiments where 5-hydroxytryptamine (5-HT) was used as agonist as propranolol is also a 5-HT_2 receptor antagonist (Bond *et al.*, 1989). SCH 23390 (30 nM; a D_1 receptor antagonist) was added to the Krebs solution when dopamine was used as agonist. Nitrendipine (1 μM) was added to the Krebs solution in experiments where blockade of L-type Ca^{2+} channels was desired.

Non-cumulative concentration-effect curves to agonists were obtained by perfusing kidneys until a steady-state response was obtained. Perfusion pressure was allowed to return to baseline levels between each concentration of agonist (studied in 0.5 log increments). In experiments with phentolamine and angiotensin II (see Methods), dose-effect curves were constructed by measuring vasoconstrictor responses to bolus injection of agonist (0.1 ml in 0.9% saline) into the perfusion fluid close to the kidney. Perfusion pressure was allowed to return to baseline before injection of subsequent doses. All results are expressed as a rise in perfusion pressure (mmHg) over baseline, rather than absolute pressure, to normalize for variations in baseline perfusion pressure which averaged 55 mmHg ($n = 200$).

With the exception of CEC, all experiments with antagonists were performed as follows. After construction of a control agonist concentration-effect or dose-effect curve, kidneys were perfused for 60 min with Krebs solution containing antagonist or vehicle. A second curve to the agonist was then constructed in the presence of antagonist or vehicle (time control). For experiments with S(+)-niguldipine, a third concentration-effect curve was constructed after an additional 60 min washout with Krebs solution devoid of antagonist. The entire perfusion apparatus was dismantled and cleaned thoroughly following each experiment with either S(+)- or R(−)-niguldipine due to lasting contamination with these compounds. In time control experiments, both in the absence and presence of nitrendipine (1 μM), concentration-effect curves to infusion of NA were shifted 1.24 fold and 1.5 fold to the right respectively with an insignificant depression of the maximal response ($n = 8$; data not shown). This time-dependent shift in the concentration-effect curve to NA was used to correct dextral shifts produced by antagonists in experiments using NA as agonist. In contrast, time controls for dose-effect curves to bolus injection of NA did not differ in $EC_{100\ mmHg}$ or maximal response ($n = 4$; data not shown).

Experiments with CEC were performed in one of two

ways. First, after construction of a control concentration-effect curve to NA, kidneys were perfused with CEC (10 or 100 μM) for 20 min and then perfused with Krebs solution free of CEC for 40 min before construction of a second concentration-effect curve to NA. Secondly, kidneys were perfused initially with CEC (100 μM) for 20 min and then perfused with Krebs solution free of CEC for 40 min before exposure to the priming dose of NA. Concentration-effect curves to NA, after administration of a priming dose, were then constructed as detailed above.

Preliminary experiments were conducted to rule out a potential role for α_2-adrenoceptors. First, in the presence of prazosin (30 nM), concentration-effect curves to NA were not shifted significantly from corresponding time controls by the selective α_2-adrenoceptor antagonist idazoxan (300 nM; $n = 4$; data not shown). Secondly, Dunn and coworkers (1989) have shown that exogenously administered angiotensin II (50 nM) can unmask α_2-adrenoceptors in the isolated distal saphenous artery of rabbits. Thus, dose-effect curves to NA and the selective α_2-adrenoceptor agonist, UK 14,304, were constructed in the absence and presence of angiotensin II (50 nM). UK 14,304 failed to elicit a vasoconstrictor response (0.01–1000 μg) either in the absence or presence of angiotensin II ($n = 4$, data not shown). Likewise, dose-effect curves to NA were not potentiated by angiotensin II ($n = 4$, data not shown).

Calculation of pK_B and pA_2 values

The pK_B values for competitive antagonists were determined by Schild regression analysis. Regression lines with slopes not significantly different from 1 were constrained to 1 for the estimation of pK_B values. Concentration-ratios were calculated using equiactive responses to agonist and were determined only when control concentration-effect and test curves were parallel. pA_2 estimates for single concentrations of antagonist were calculated as follows:

$$pA_2 \text{ value} = -\log [\text{Antagonist concentration}/(\text{Concentration ratio} - 1)]$$

This method assumes a linear relationship, with a slope of 1, between the $-\log$ molar concentration of the antagonist and the log (concentration-ratio − 1).

Autoradiography

Kidneys were isolated as described above and perfused with CEC (100 μM) or vehicle for 20 min and then perfused with Krebs solution free of CEC for 40 min. Control and CEC-treated kidneys were removed and immediately frozen in dry-ice on microtome chucks. Longitudinal sections (20 μM) were cut from control and CEC-treated kidneys and collected on gelatinised microscope slides. The slides were stored at −20°C for 2 weeks prior to binding assays.

For α_1-adrenoceptor autoradiography, sections were thawed at room temperature and pre-incubated in 170 mM Tris HCl (pH 7.4, 23°C) for 60 min in order to remove possible interfering agents (e.g. neurotransmitters) and residual CEC. Slides were then covered with 0.8 ml of solution containing 0.3 nM [^{3}H]-prazosin (specific activity: 82 Ci mmol^{-1}) in 170 mM Tris HCl plus 50 mM NaCl for 60 min at 23°C to attain equilibrium. Adjacent sections received [^{3}H]-prazosin solution containing 100 μM phentolamine to define non-specific binding. Slides were rinsed in ice-cold buffer for 25 min followed by a rinse in ice-cold water for 15 s. Slides were then dried rapidly in a stream of cold air. Following desiccation overnight, the slides, together with radiation standards, were apposed to ^{3}H-sensitive film in X-ray cassettes for 3 months.

For angiotensin II receptor autoradiography, kidney sections were thawed at 23°C and allowed to dry before being pre-incubated in 500 ml of $NaPO_4$ buffer (20 mM $NaPO_4$, 150 mM NaCl, 10 mM $MgCl_2$ and 10 mM EDTA, pH 7.4) at 23°C for 30 min. Sections were removed from the pre-incubation buffer, air dried and laid flat over glass rods. Sections were then covered with 0.5–0.7 ml of sodium phosphate buffer containing 0.1 nM [^{125}I]-Sar^1-Ile^8-angiotensin II (specific activity: 2200 Ci mmol^{-1}) in the presence or absence of unlabelled competing compound. Nonspecific binding was defined with 10 μM angiotensin II. The assay buffer contained a mixture of the following peptidase inhibitors: captopril (1 μM), bacitracin (60 μg ml^{-1}), phosphoramidon, pepstatin A, bestatin, chymostatin and antipain (each at 1.3 μg ml^{-1}) and amastatin (0.13 μg ml^{-1}). Incubations were terminated after 90 min by rinsing the slides in ice-cold 50 mM Tris HCl (pH 7.4) for 10 min followed by rapid drying in a stream of cold air. The labelled sections were desiccated overnight and then apposed, together with radiation standards, to a radiation-sensitive film in an X-ray cassette. The autoradiograms were generated after 2 weeks exposure.

Autoradiograms for [^{3}H]-prazosin and [^{125}I]-Sar^1-Ile^8-angiotensin II binding were analysed by digital subtraction image analysis.

Radioligand binding

Competition binding assays were performed with [^{3}H]-prazosin (specific activity: 82 Ci mmol^{-1}; 0.1 nM final assay concentration) with approximately 0.3 mg protein in 400 μl of Tris (50 mM)-EDTA (0.5 mM) buffer (pH 7.4). Incubations were at 25°C for 60 min. Reactions were terminated and membranes were harvested by rapid filtration through GF-B filters pretreated with a 0.1% solution of polyethylenimine. Filters were washed three times with 3 ml of ice-cold 0.1 M NaCl solution and dried. The bound radioactivity was determined by liquid scintillation counting. Specific binding was defined as the difference between the binding of [^{3}H]-prazosin in the absence and presence of 10 μM phentolamine. Competition binding assays were performed using 10 different concentrations of displacing antagonist.

Data were first analysed by iterative curve fitting to a four parameter logistic equation to yield Hill coefficients and IC_{50} values. K_i values were calculated according to the Cheng-Prusoff equation.

Statistics

Confidence limits (CL: at 95% probability) were calculated for the slopes of Schild regressions using StatView 512+ (Brain Power Inc., Calabasas, CA, U.S.A.). Differences between mean values were tested for statistical significance ($P < 0.05$) using Student's unpaired t test (two tailed).

For correlations, each pair of concordant tissues was fitted to a linear regression model which included both the slope and intercept. Confirmatory analyses normalizing the intercept to zero were also performed. Tests for correlation and inference on slopes were performed using standard statistical software (SAS PROC REG and PROG CORR, SAS Inc., Cary, NC, U.S.A.). Significance levels were set at the $P < 0.05$ level.

Materials

Drugs were obtained from the following sources: [^{125}I]-Sar^1-Ile^8-angiotensin II and [^{3}H]-prazosin from Dupont-New England Nuclear, Boston, MA, U.S.A.; (−)-noradrenaline HCl, (−)-isoprenaline HCl, (−)-phenylephrine HCl, methoxamine HCl, oxymetazoline HCl, dopamine HCl, 5-hydroxytryptamine HCl, (±)-propranolol HCl, cocaine HCl, corticosterone, indomethacin and EDTA from Sigma Chemical Co., St. Louis, MO, U.S.A.; chloroethylclonidine 2HCl, WB 4101 ((2,6-dimethoxyphenoxyethyl) aminomethyl-1,4-benzodioxane HCl), 5-methyl-urapidil HCl, (−)-adrenaline bitartrate, idazoxan HCl, (+)-SCH 23390 HCl (**R**-(+)-7-chloro-8-hydroxy-3methyl-1-phenyl-2,3,4,5-tetrahydro-1h-3-benzazepine HCl), **S**(+)-niguldipine, **R**(−)-niguldipine from Re-

search Biochemicals Inc., Natick, MA, U.S.A.; nitrendipine, dehydroniguldipine, amidephrine, HV 723 (α-ethyl-3,4,5-trimethoxy-α-(3-((2-(2-methoxyphenoxyethyl)-amino)-propyl) benzene-aceto-nitrile fumarate from the Institute of Organic Chemistry, Syntex Research, Palo Alto, CA, U.S.A.; UK 14,304 (5-bromo-6-[2-imidazolin-2ylamino]-quinoxaline) and prazosin HCl from Pfizer Central Research, U.K. and Pfizer Inc., Groton, CT, U.S.A. respectively; phentolamine mesylate from Ciba Geigy, Summit, NJ, U.S.A.; and cirazoline from Syntelabo, Paris, France. Peptides were obtained from Peninsula Labs (Belmont, CA, U.S.A.).

Stock solutions of drugs were prepared in deionised water with following exceptions: corticosterone (dimethylsulphoxide), indomethacin (0.5% sodium carbonate), 5-methyl-urapidil (predissolved in a drop of 1 M HCl), nitrendipine, S(+)- and R(−)-niguldipine and dehydroniguldipine (ethanol).

The cloned hamster smooth muscle α_{1B}-adrenoceptor (Cotecchia *et al.*, 1988), the cloned rat cerebral cortex α_{1D}-adrenoceptor (Lomasney *et al.*, 1991) and the cloned bovine α_{1C}-adrenoceptor (Schwinn *et al.*, 1990) stably expressed in rat-1 fibroblast cell lines, were purchased from Dr Lee Allen, Duke University, Durham, NC, U.S.A.

Results

Antagonist characterization

Increasing concentrations of noradrenaline (NA; 0.01–3 μM) produced concentration-dependent increases in perfusion pressure spanning approximately two orders of magnitude and attaining maximal vasoconstrictor responses of 200–250 mmHg. Prazosin (1–30 nM), phentolamine (30–300 nM) and WB 4101 (0.3–30 nM) produced parallel dextral shifts of concentration-effect curves to NA and caused a slight but insignificant reduction in the maximal response (Figure 1). Schild regression analysis yielded lines with slopes not significantly different from 1 and pK_B values of 9.5, 8.6 and 10.3, respectively (Table 1).

CEC is a commonly used tool to identify α_{1B}-adrenoceptors. Although CEC binds to all α_1-adrenoceptor subtypes with high affinity for prazosin, as well as α_2-adrenoceptors (Michel *et al.*, 1993b), CEC preferentially alkylates α_{1B}-adrenoceptors. Figure 2 shows concentration-effect curves to NA after pretreatment of kidneys with CEC (10 and 100 μM) for 20 min. Only the highest concentration of CEC (100 μM) produced a statistically significant ($P<0.05$) dextral shift (2.6 ± 0.1) in the concentration-effect curve to NA. Neither concentration of CEC produced a significant depression of the maximal response compared with time controls. The results suggest a limited role for CEC-sensitive α_1-adrenoceptors (α_{1B}- and α_{1D}-adrenoceptors) in NA-mediated vasoconstriction.

Figure 3 shows the effect of perfusion for 20 min with CEC (100 μM) on [^{3}H]-prazosin binding in kidney. CEC reduced [^{3}H]-prazosin binding by approximately 70% without affecting [^{125}I]-Sar^1-Ile^8-angiotensin II binding, suggesting a specific action of CEC.

The most selective ligand available for the α_{1A}-adrenoceptor is the S(+)-isomer of the dihydropyridine Ca^{2+}

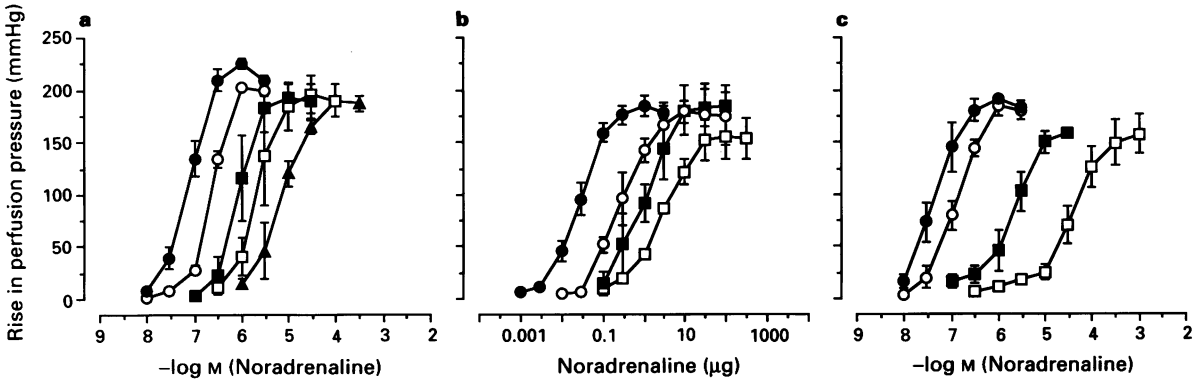

Figure 1 Interaction of noradrenaline (NA) with α_1-adrenoceptor antagonists. (a) Concentration-effect curves to NA in the absence (●, $n=16$) and presence of prazosin: 1 nM (○, $n=4$), 3 nM (■, $n=4$), 10 nM (□, $n=4$) and 30 nM (▲, $n=4$). (b) Dose-effect curves to NA in the absence (●, $n=12$) and presence of phentolamine: 30 nM (○, $n=4$), 100 nM (■, $n=4$) and 300 nM (□, $n=4$). (c) Concentration-effect curves to NA in the absence (●, $n=12$) and presence of WB 4101: 0.3 nM (○, $n=4$), 3 nM (■, $n=4$), 30 nM (□, $n=4$). Kidneys were perfused with Krebs solution containing antagonist for 60 min prior to construction of the second concentration- or dose-effect curve to NA. Each point represents the mean ± s.e.mean where larger than the symbol.

Table 1 Affinity estimates for α_1-antagonists versus noradrenaline in isolated perfused kidney of rat

Antagonist	*Concentrations* (nM)	pK_B	*Slope*	*95% confidence limits*
Prazosin	1, 3, 10, 30	9.5[a]	1.07	0.93–1.21
WB 4101	0.3, 3, 30	10.3[a]	1.01	0.89–1.13
Phentolamine[b]	30, 100, 300	8.6[a]	1.06	0.63–1.49
S(+)-Niguldipine	0.03, 0.1, 0.3	10.5[c]		
R(−)-Niguldipine	3, 30, 300	9.1[c]		
Dehydroniguldipine	10, 30, 100	9.0[a]	1.07	0.80–1.35
5-Methyl-urapidil[d]	3, 10, 30, 100	9.2[a]	1.07	0.94–1.21
	3, 30	9.1[ae]	1.05	0.89–1.25
Oxymetazoline[d]	100, 1000	7.9[a]	1.11	0.83–1.39
HV 723[d]	1, 10	9.3[a]	0.95	0.79–1.11
Spiperone[d]	100	8.1[f]		

[a]Slope constrained to 1. [b]Versus bolus doses of NA. [c]Insurmountable antagonist, affinity estimate based on lowest concentration. [d]Experiment conducted in the presence of nitrendipine (1 μM). [e]Methoxamine as agonist. [f]pA_2 (slope of 1 assumed).

channel antagonist, niguldipine (Boer *et al.*, 1989). The **R**(−)-isomer has lower affinity and is less selective than the **S**(+)-isomer (Boer *et al.*, 1989). Figure 4a and b show composite data for the interaction of NA with **S**(+)- and **R**(−)-niguldipine respectively. **S**(+)-niguldipine (0.03–0.3 nM; Figure 4a) potently, but insurmountably antagonized vasoconstrictor responses to NA. Antagonism by **S**(+)-niguldipine (0.1 nM) was not reversible even after perfusion for 3 h with **S**(+)-niguldipine-free Krebs solution ($n = 4$; data not shown). **R**(−)-niguldipine (3–300 nM; Figure 4b) had approximately 30-times less affinity than **S**(+)-niguldipine and also appeared to deviate from simple competitive antagonism. Antagonism by **S**(+)-niguldipine was not attributable to antagonism of L-type Ca^{2+} channels as other experiments revealed that the dihydropyridine Ca^{2+} channel antagonist, nitrendipine, produced only a limited (5.8 fold) parallel dextral shift of concentration-effect curves to NA (1 μM; $n = 4$; data not shown). Limited dextral shifts (<6 fold) have also been observed using high concentrations of other L-type Ca^{2+} channel antagonists (Blue *et al.*, 1991). Likewise, antagonism by **S**(+)-niguldipine appeared specific for α_1-adrenoceptors as vasoconstrictor responses to 5-hydroxytryptamine (0.01–3 μM) were not affected by **S**(+)-niguldipine (3 nM; $n = 4$; data not shown). In contrast, dehydroniguldipine (10–100 nM; Figure 4c) produced parallel dextral shifts in the concentration-effect curves to NA with no significant reduction in the maximal response, yielding a pK_B estimate of 9.0 (Table 1).

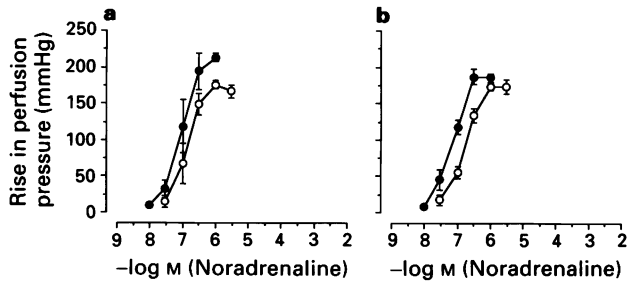

Figure 2 Concentration-effect curves to noradrenaline (NA) before (●) and after (○) treatment with chloroethylclonidine (CEC): (a) 10 μM or (b) 100 μM. Kidneys were perfused with Krebs solution containing CEC for 20 min and then perfused with CEC-free Krebs solution for 40 min before construction of a second concentration-effect curve to NA. Each point represents the mean ± s.e.mean obtained from 4 kidneys.

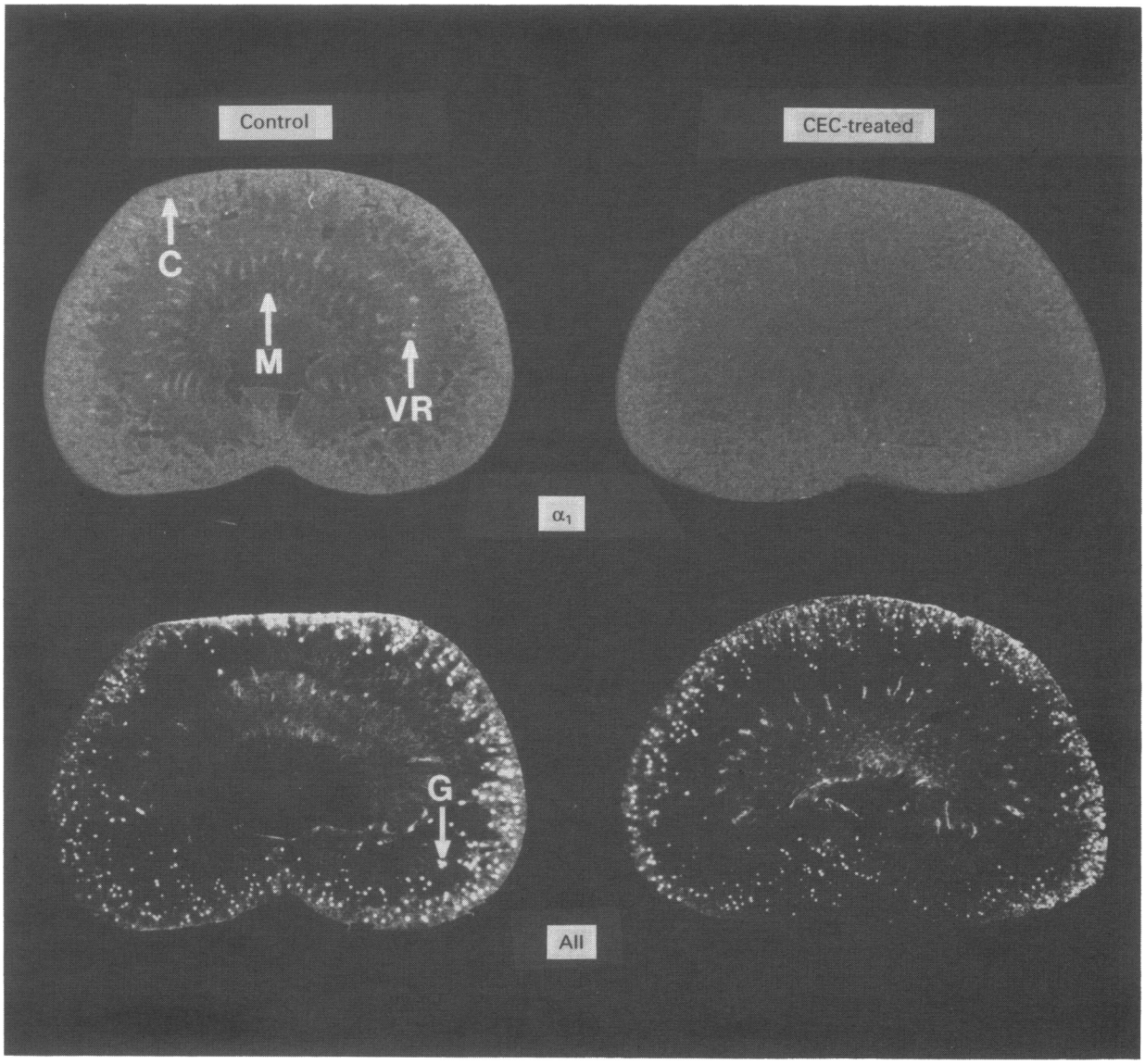

Figure 3 Effect of chloroethylclonidine (CEC; 100 μM) on [^{3}H]-prazosin and [^{125}I]-Sar^1-Ile^8-angiotensin II binding in rat kidney. Kidneys were perfused with Krebs solution containing CEC (100 μM) or vehicle for 20 min and then perfused with CEC-free Krebs solution for 40 min before preparation for autoradiography. C = cortex, M = medulla, VR = vasa recta, G = glomeruli.

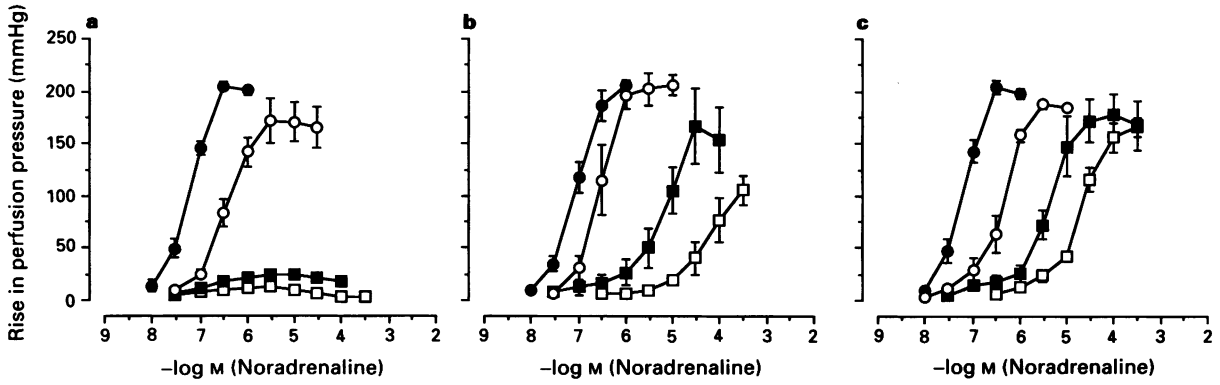

Figure 4 Interaction of noradrenaline (NA) with niguldipine. (a) Concentration-effect curves to NA in the absence (●, $n = 12$) and presence of S(+)-niguldipine: 0.03 nM (○, $n = 4$), 0.1 nM (■, $n = 4$) and 0.3 nM (□, $n = 4$). (b) Concentration-effect curves to NA in the absence (●, $n = 12$) and presence of R(−)-niguldipine: 3 nM (○, $n = 4$), 30 nM (■, $n = 4$) and 300 nM (□, $n = 4$). (c) Concentration-effect curves to NA in the absence (●, $n = 12$) and presence of dehydroniguldipine 10 nM (○, $n = 4$), 30 nM (■, $n = 4$), 100 nM (□, $n = 4$). Kidneys were perfused with Krebs solution containing antagonist for 60 min prior to construction of the second concentration-effect curve to NA. Each point represents the mean ± s.e.mean where larger than the symbol.

The mechanism of insurmountable antagonism was investigated by determining whether prazosin could protect against insurmountable antagonism produced by S(+)-niguldipine. Prazosin (50 nM) competitively antagonized concentration-effect curves to NA (169 fold dextral shift; $pA_2 = 9.5$) and was reversible, in part, after a 60 min washout (Figure 5a). When kidneys were co-perfused with both prazosin (50 nM) and S(+)-niguldipine (0.1 nM), prazosin afforded protection against S(+)-niguldipine (Figure 5b).

5-Methyl-urapidil is another ligand selective for the α_{1A}-adrenoceptor subtype (Gross *et al.*, 1988). In the presence of 5-methyl-urapidil (0.03–3 μM; Figure 6a), concentration-effect curves to NA were biphasic, the first phase being antagonized in an apparently insurmountable fashion by the highest concentration of 5-methyl-urapidil.

The interaction of 5-methyl-urapidil (1 and 10 nM) with methoxamine as agonist was investigated because functional studies in rabbit aorta (mixed population of α_{1L}- and α_{1B}-adrenoceptors) have shown that α_{1B}-adrenoceptors are not activated by methoxamine (Oshita *et al.*, 1993). In contrast to NA, concentration-effect curves to methoxamine were shifted in a parallel, monophasic fashion by 5-methyl-urapidil, yielding a pK_B estimate of 9.1 (Figure 6b). Thus, methoxamine failed to stimulate the low affinity site for 5-methyl-urapidil.

Figure 6c shows concentration-effect curves to NA constructed in the presence of 5-methyl-urapidil (1 μM) both before and after pretreatment of kidneys with CEC (100 μM). The first phase of the concentration-effect curve to NA was significantly reduced, but not abolished, by pretreatment with CEC (Figure 6c; compare closed triangles with open diamonds). This results suggests that the initial phase of the concentration-effect curve to NA in the presence of 5-methyl-urapidil is mediated, in part, by a CEC-sensitive α_1-adrenoceptor.

As nitrendipine produced a small dextral shift similar to that seen with CEC (see above), the ability of nitrendipine (1 μM) to inhibit the first phase of the concentration-effect curve to NA in the presence of 5-methyl-urapidil was investigated. Nitrendipine exerted complete inhibition of the first phase of the concentration-effect curve to NA constructed in the presence of 5-methyl-urapidil (Figure 6c; compare closed triangles with inverted triangles). In light of this result, the interaction of NA and 5-methyl-urapidil (3–100 nM) was re-evaluated with nitrendipine (1 μM) present in the Krebs solution throughout. 5-Methyl-urapidil produced parallel dextral shifts of concentration-effect curves to NA with no significant reduction in the maximal response compared to that seen normally in time controls (Figure 6d). Schild regression analysis yielded a line with a slope not significantly different from 1 and a pK_B value of 9.2 for 5-methyl-urapidil (Table 1).

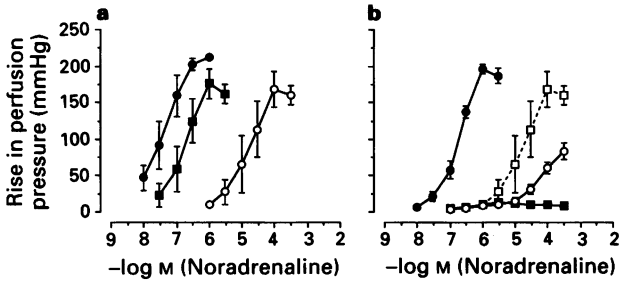

Figure 5 Receptor protection with prazosin against insurmountable antagonism by S(+)-niguldipine. (a) Concentration-effect curves to noradrenaline (NA) in the absence (●) and presence (○) of prazosin (50 nM for 60 min) and following a 60 min washout with prazosin-free Krebs solution (■). (b) Concentration-effect curves to NA before (●) and after coperfusion (○) for 60 min with S(+)-niguldipine (0.1 nM) and prazosin (50 nM) and following removal of prazosin from the Krebs solution (■). The dashed line (□) represents the position of the concentration-effect curve to prazosin (50 nM) alone and is taken from (a). Each point represents the mean ± s.e.mean obtained from 4 kidneys; s.e. are shown where larger than the symbol.

Receptor characterization in the presence of nitrendipine

To characterize further the α_1-adrenoceptor for which 5-methyl-urapidil exhibits high affinity, an agonist profile was obtained with 9 α_1-adrenoceptor agonists in the absence and presence of nitrendipine (1 μM; Figure 7a and b). With the exception of oxymetazoline, all agonists were full agonists relative to NA. The relative order of agonist potency was nearly identical irrespective of whether nitrendipine was present or absent from the Krebs solution (Table 2). Agonist independent pA_2 values for prazosin (obtained in the presence of nitrendipine) suggest that all the agonists produced vasoconstriction via activation of α_1-adrenoceptors with high affinity ($pA_2 > 9$) for prazosin (i.e. α_{1H}-adrenoceptors).

As oxymetazoline behaved as a partial agonist, the ability of oxymetazoline to antagonize vasoconstrictor responses to NA was evaluated. Oxymetazoline (0.1 and 1 μM) produced parallel dextral shifts in the concentration-effect curves to

NA without affecting the maximal response (Figure 7c), yielding a pK_B estimate of 7.9 (Table 1).

Finally, antagonism by HV 723 (an antagonist reported to be selective for α_{1N}- over α_{1L}-adrenoceptors; Muramatsu *et al.*, 1990b) and spiperone (α_{1B}-adrenoceptor-selective: Michel *et al.*, 1989) was evaluated in the presence of nitrendipine (1 μM). Both HV 723 (1 and 10 nM) and spiperone (0.1 μM) produced parallel dextral shifts in the concentration-effect curves to NA with no change in the maximal response. Schild regression analysis yielded a pK_B estimate of 9.3 for HV 723. A pA_2 value of 8.1 was estimated for spiperone (Table 1).

Radioligand binding

The binding of [^{3}H]-prazosin in the rat submaxillary gland and at cloned hamster α_{1B}-, bovine α_{1C}- and rat α_{1D}-adrenoceptors expressed in rat-1 fibroblasts was saturable, of high affinity and consistent with the presence of a single population of binding sites. K_D and B_{max} values respectively were as follows: α_{1B}-clone (49.3 ± 0.70 pM; 2.44 ± 0.17 pmol mg^{-1} protein), α_{1C}-clone (84.7 ± 3.58 pM; 5.2 ± 0.57 pmol mg^{-1} protein), α_{1D}-clone (78.3 ± 0.59 pM; 1.88 ± 0.08 pmol mg^{-1} protein) and submaxillary gland of rat (39 ± 1.7 pM; 193 ± 9.5 fmol mg^{-1} protein). Displacement curves in all

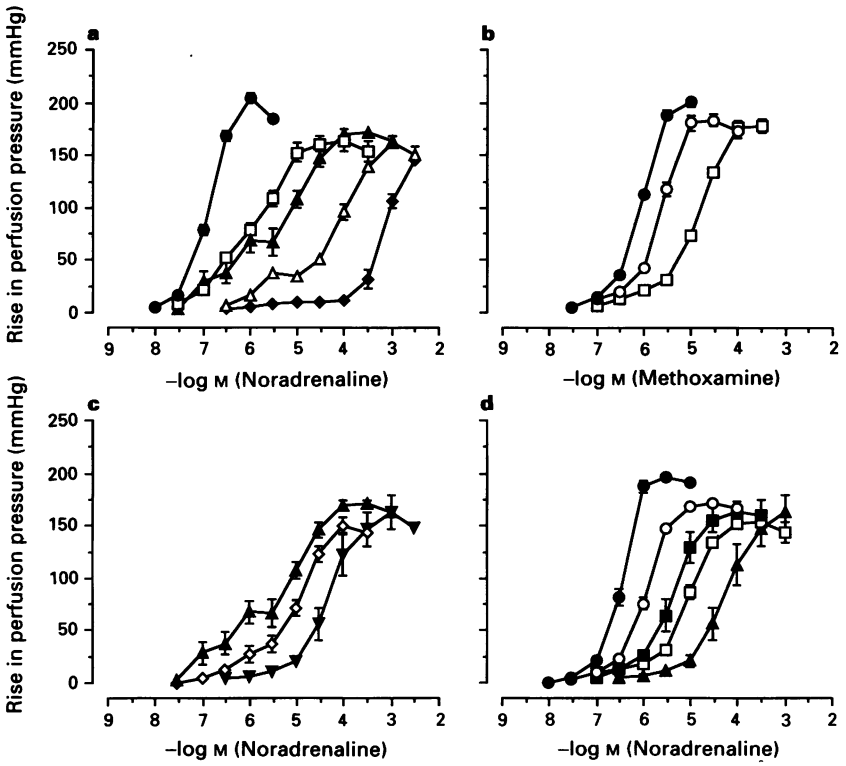

Figure 6 Interaction of 5-methyl-urapidil with α_1-adrenoceptors. (a) Concentration-effect curves to NA in the absence (●, $n = 16$) and presence of 5-methyl-urapidil: 0.03 nM (□, $n = 4$), 0.1 μM (▲, $n = 4$), 1 μM (△, $n = 4$) and 3 μM (◆, $n = 4$). (b) Concentration-effect curves to methoxamine in the absence (●, $n = 8$) and presence of 5-methyl-urapidil: 0.003 μM (○, $n = 4$) and 0.03 μM (□, $n = 4$). (c) Concentration-effect curves to NA obtained in the presence of 0.1 μM 5-methyl-urapidil (▲, $n = 4$) and after pretreatment (100 μM for 20 min) with chloroethylclonidine (◇, $n = 4$) or in the presence of 1 μM nitrendipine (▼, $n = 4$). (d) Concentration-effect curves to NA (constructed in the presence of 1 μM nitrendipine) and measured in the absence (●, $n = 16$) and presence of 5-methyl-urapidil: 0.003 μM (○, $n = 4$), 0.01 μM (■, $n = 4$), 0.03 μM (□, $n = 4$) and 0.1 μM (▲, $n = 4$). Each point represents the mean ± s.e.mean where larger than the symbol.

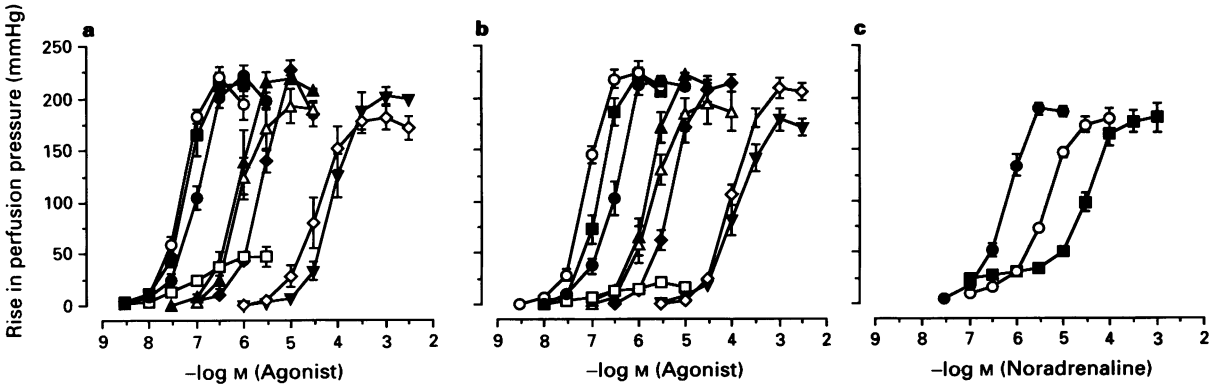

Figure 7 Effect of α_1-adrenoceptor agonists. Agonist profile in (a) the absence and (b) the presence of nitrendipine (1 μM): (○) cirazoline, $n = 4$; (■) adrenaline, $n = 4$; (●) noradrenaline, $n = 4$; (□) oxymetazoline, $n = 4$; (▲) phenylephrine, $n = 4$; (△) amidephrine, $n = 4$; (◆) methoxamine, $n = 4$; (◇) dopamine, $n = 4$; (▼) isoprenaline, $n = 4$. (c) Concentration-effect curves to noradrenaline in the presence of nitrendipine (1 μM) obtained in the absence (●, $n = 8$) and presence of oxymetazoline: 0.1 μM (○), $n = 4$) and 1 μM (●, $n = 4$). Each point represents the mean ± s.e.mean where larger than the symbol.

four preparations were best described by a single site model. Estimated pK_i values are shown in Table 3. Of the cloned α_1-adrenoceptors, only pK_i values from the bovine α_{1C}-adrenoceptor showed a high correlative association with pA_2 values obtained in rat kidney ($R^2 = 0.85$; Figure 8). Likewise, pK_i values from rat submaxillary gland and pK_i values from other α_{1A}-adrenoceptors of rat (abstracted from the literature) correlated well with pA_2 values obtained in rat kidney ($R^2 = 0.79$ and 0.89 respectively; Table 4). As might be expected, strong correlations were observed between pK_i values from rat submaxillary gland, cloned bovine α_{1C}-adrenoceptors, and rat α_{1A}-adrenoceptors, the latter values being drawn from the literature (Table 4).

Discussion

The antagonist affinity profile obtained here demonstrates unequivocally that the α_{1A}-adrenoceptor, as originally defined pharmacologically (see Introduction), is the predominant subtype mediating vasoconstriction in the isolated perfused kidney of rat. Furthermore, we now show that this subtype can be 'isolated' for quantitative evaluation by adding nitrendipine to the perfusion fluid. Thus, the present results extend previous studies on α_1-adrenoceptor classification in kidney of rat (Eltze *et al.*, 1991; Eltze & Boer, 1992; Blue *et al.*, 1992; Elhawary *et al.*, 1992; Sattar & Johns, 1994a,b).

Clear evidence that more than one subtype of α_1-adrenoceptor mediates vasoconstriction to exogenous NA in the kidney was obtained with 5-methyl-urapidil. Concentration-effect curves to NA were found to be biphasic in the presence of 5-methyl-urapidil, the initial phase being antagonized in an apparently insurmountable manner by increasing concentrations of 5-methyl-urapidil. A comprehensive characterization of the α_1-adrenoceptor(s) mediating the initial phase to NA could not be undertaken, however, as the site or sites could not be 'isolated' pharmacologically for study. Partial sensitivity to CEC, and an apparent inability of methoxamine to activate the site(s), provide some descriptive characteristics. Certainly, CEC-sensitive α_1-adrenoceptors were demonstrated independently in functional (Figure 2) and autoradiographic (Figure 3) experiments.

Another characteristic of the α_1-adrenoceptor(s) for which 5-methyl-urapidil exhibited low affinity is that responses mediated by this receptor(s) are sensitive to inhibition by the L-type Ca^{2+} channel antagonist, nitrendipine. Although sen-

Table 2 Relative potency of α_1-adrenoceptor agonists estimated in the absence and presence of nitrendipine in isolated perfused kidney of rat

	No nitrendipine		*Nitrendipine* (1 μM)		
Agonist	$EC_{100\,mmHg}$ (μM)	*Relative potency*	$EC_{100\,mmHg}$ (μM)	*Relative potency*	*Prazosin* pA_2
Cirazoline	0.04	1	0.06	1	9.5[a]
Adrenaline	0.05	1	0.13	2	9.3[a]
Oxymetazoline	0.09[b]	2	NR	–	9.6[cd]
Noradrenaline	0.09	2	0.29	5	9.5[a]
Phenylephrine	0.62	14	1.43	23	9.3[a]
Amidephrine	0.75	17	1.97	31	9.2[a]
Methoxamine	1.90	43	4.55	71	9.3[d]
Dopamine	70.0	1590	138.0	2210	9.6[d]
Isoprenaline	71.0	1610	91.0	1456	9.1[d]

[a]Versus 30 nM prazosin. [b]Calculated at $EC_{50\%}$. [c]pA_2 value obtained in the absence of nitrendipine as oxymetazoline produced no vasoconstriction in the presence of nitrendipine. [d]Versus 3 nM prazosin. NR = no response.

Table 3 Summary of affinity estimates for α_1-adrenoceptor ligands in isolated perfused kidney of rat (pK_B or pA_2 values), submaxillary gland of rat, cloned hamster α_{1B}-, bovine α_{1C}- and rat α_{1D}-adrenoceptors and α_{1A}-adrenoceptors in several different tissues of rat taken from the literature (pK_i values ± s.e.mean)[a]

		Cloned						
Ligand	*Kidney*[b]	α_{1B}	α_{1C}	α_{1D}	*Submaxillary Gland* (α_{1A})	*Literature*[c] (α_{1A})	(n)	*References*[d]
Prazosin	9.5	10.1 (0.02)	9.9 (0.02)	9.9 (0.07)	10.1 (0.01)	10.1 (0.05)	(38)	1–18, 20–27
WB 4101	10.3	8.6 (0.05)	10.0 (0.06)	9.6 (0.04)	10.1 (0.08)	9.9 (0.10)	(18)	1, 2, 5, 7, 9, 12–16, 18, 20–23, 26, 27
Phentolamine	8.6	7.9 (0.07)	8.9 (0.05)	8.1 (0.19)	8.8 (0.10)	8.7 (0.11)	(13)	1–3, 5, 7, 9, 11, 15, 16, 22, 24, 26, 27
S(+)-Niguldipine	10.5	7.0 (0.57)	9.8 (0.30)	7.1 (0.13)	9.7 (0.09)	10.3 (0.18)	(8)	5, 6, 11, 12, 14, 17, 19, 27
R(−)-Niguldipine	9.1	ND	ND	ND	ND	8.9	(2)	5, 11
5-Methyl-urapidil	9.2	7.5 (0.02)	9.4 (0.05)	8.0 (0.03)	9.2 (0.08)	9.0 (0.08)	(22)	4, 5, 7, 10–12, 14, 18–20, 22, 24–27
Oxymetazoline	7.9	6.4 (0.06)	7.8 (0.05)	6.5 (0.13)	8.5 (0.04)	8.3 (0.17)	(6)	7, 9, 14, 24
HV 723	9.3	8.4 (0.11)	9.6 (0.03)	9.4 (0.09)	ND	8.9 (0.11)	(4)	2, 15, 16, 20
Spiperone	8.1	8.9 (0.06)	8.5 (0.04)	8.5 (0.16)	8.1 (0.03)	8.2 (0.08)	(4)	9, 17, 25, 26

[a]All pK_i values were determined with [^{3}H]-prazosin as ligand. [b]pK_B or pA_2 values versus noradrenaline in isolated perfused kidney of rat were taken from Table 1. [c]pK_i values from high affinity binding sites in rat brain, heart, lung, kidney, vas deferens and submaxillary gland. [d]Literature source for α_{1A}-adrenoceptor affinity estimates. ND = not determined. References: (1) Morrow *et al.*, 1985; (2) Morrow & Creese, 1986; (3) Honda *et al.*, 1987; (4) Gross *et al.*, 1988; (5) Boer *et al.*, 1989; (6) Hanft & Gross, 1989a; (7) Hanft & Gross, 1989b; (8) Hanft *et al.*, 1989; (9) Michel *et al.*, 1989; (10) Hanft & Gross, 1990; (11) Michel *et al.*, 1990; (12) Eltze *et al.*, 1991; (13) Feng *et al.*, 1991; (14) Klijn *et al.*, 1991; (15) Oshita *et al.*, 1991; Tsuchihashi *et al.*, 1991; (17) Eltze & Boer, 1992; (18) Hiramatsu *et al.*, 1992; (19) Jackson *et al.*, 1992; (20) Muramatsu, 1992; (21) Ohmura *et al.*, 1992; (22) Yazawa *et al.*, 1992; (23) Ivorra *et al.*, 1993; (24) Michel *et al.*, 1993a; (25) Schwietert *et al.*, 1993; (26) Sleight *et al.*, 1993; (27) Salles & Badia, 1994.

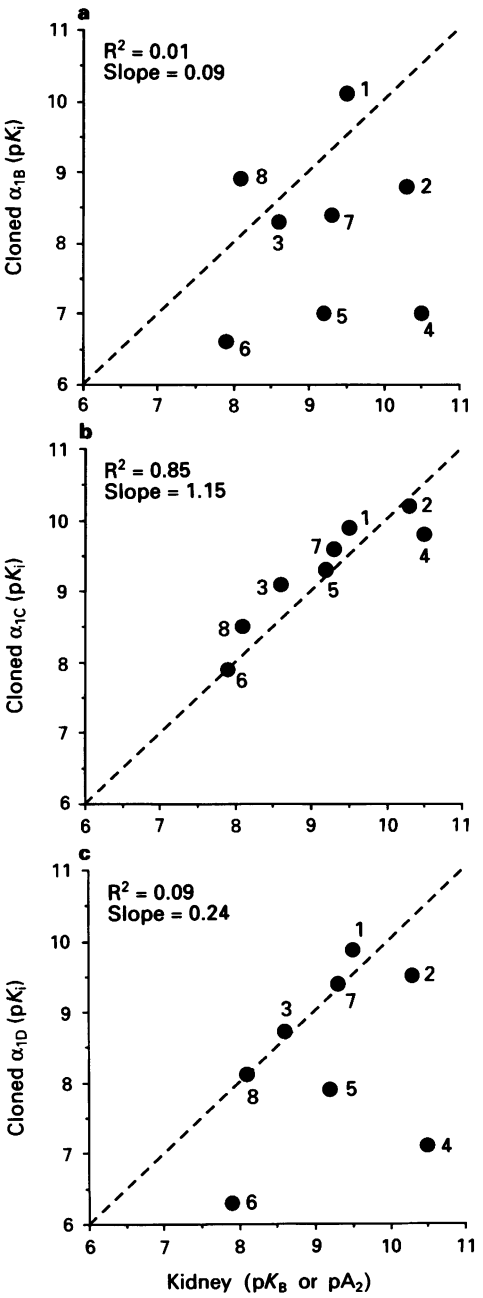

Figure 8 Correlations of antagonist affinity estimates (pA_2 values) at α_1-adrenoceptors in isolated perfused kidney of rat and antagonist affinity estimates (pK_i values) in cloned (a) α_{1B}-adrenoceptors, (b) α_{1C}-adrenoceptors and (c) α_{1D}-adrenoceptors: (1) prazosin; (2) WB 4101; (3) phentolamine; (4) S(+)-niguldipine; (5) 5-methyl-urapidil; (6) oxymetazoline; (7) HV 723; (8) spiperone. Dashed lines indicate the line of identity.

sitivity to nitrendipine does not provide insight into the identity of the receptor, it is nevertheless an important finding as it allows pharmacological 'isolation' of the α_1-adrenoceptor at which 5-methyl-urapidil exerts *high* affinity and, therefore, characterization and classification of the site. For this reason, agonists and antagonists (tested subsequently to using 5-methyl-urapidil) were studied in the presence of nitrendipine (see Table 1).

The α_1-adrenoceptor for which 5-methyl-urapidil exhibited high affinity was characterized using several α_1-adrenoceptor subtype-selective antagonists. Competitive antagonism was observed with prazosin and the α_{1A}-adrenoceptor selective antagonists, WB 4101, phentolamine, 5-methyl-urapidil and oxymetazoline, as well as spiperone (α_{1B}-selective; Michel *et al.*, 1989) and HV 723 (reported to be selective for α_{1N}- over α_{1L}-adrenoceptors; Muramatsu *et al.*, 1990b). The following relative order of antagonist affinity (pK_B value) was obtained: WB 4101 (10.3)> prazosin (9.5)≈HV 723 (9.3)≈5-methyl-urapidil (9.2)> phentolamine (8.6)> spiperone≈oxymetazoline (7.9). This order and relativity of antagonist affinity clearly defines an α_{1A}-adrenoceptor.

The S(+)-isomer of the dihydropyridine Ca^{2+} channel antagonist, niguldipine, is the most selective ligand available for the α_{1A}-adrenoceptor subtype (Boer *et al.*, 1989). In the present study, concentration-effect curves to NA were insurmountably and irreversibly antagonized by subnanomolar concentrations of S(+)-niguldipine. Insurmountable antagonism by S(+)-niguldipine is not attributable to blockade of L-type Ca^{2+} channels as vasoconstrictor responses to NA in rat kidney are largely resistant to nitrendipine (and other L-type Ca^{2+} channel antagonists: see Blue *et al.*, 1991). Indeed, the failure of S(+)-niguldipine to antagonize vasoconstrictor responses to 5-hydroxytryptamine, coupled with the ability of prazosin to protect partially against antagonism by S(+)-niguldipine, suggests strongly that direct binding of S(+)-niguldipine to α_1-adrenoceptors is involved. The insurmountable nature and irreversibility of S(+)-niguldipine may result because of high affinity for the α_{1A}-adrenoceptor (see Rang, 1966) as well as high lipophilicity (Boer *et al.*, 1989). The relative antagonistic potency observed with the S(+)- versus R(−)-isomer of niguldipine (approximately 30 fold) is fully consistent with reported characteristics of α_{1A}-adrenoceptors (Boer *et al.*, 1989; Michel *et al.*, 1990). It is also of interest to note that dehydroniguldipine, a non-chiral analogue of niguldipine, antagonized concentration-effect curves to NA competitively with a potency similar to that of R(−)-niguldipine. This confirms the importance of stereochemistry in the interaction of niguldipine with α_{1A}-adrenoceptors.

In addition to the antagonist affinity profile discussed above, the present study provides a comprehensive agonist potency profile at the α_{1A}-adrenoceptor subtype using 9 ligands. To date, the usefulness of agonists as tools for discrimination and classification of α_1-adrenoceptor subtypes

Table 4 Correlations of affinity estimates for α_1-adrenoceptor ligands in isolated perfused kidney of rat, submaxillary gland of rat, cloned hamster α_{1B}-, bovine α_{1C}- and rat α_{1D}-adrenoceptors and α_{1A}-adrenoceptors in several different tissues of rat taken from the literature

			R-squared (slope)			
	Kidney (α_{1A})	*Submaxillary gland* (α_{1A})	*Literature* (α_{1A})	*Cloned* (α_{1B})	*Cloned* (α_{1C})	*Cloned* (α_{1D})
Kidney (α_{1A})	–	0.79	0.89	0.02*	0.85	0.12*
	–	(1.15)	(1.09)	(0.12)*	(1.14)	(0.28)*
Submaxillary gland (α_{1A})	0.79	–	0.89	0.13*	0.84	0.29*
	(1.15)	–	(0.85)	(0.22)*	(0.95)	(0.35)*
Literature (α_{1A})	0.89	0.89	–	0.08*	0.81	0.16*
	(1.09)	(0.85)	–	(0.20)*	(0.84)	(0.29)*
Cloned α_{1C}	0.85	0.82	0.82	0.22*	–	0.39*
	(1.15)	(0.94)	(0.85)	(0.31)*	–	(0.42)*

*Significantly different from 1 ($P<0.05$). Other R-squared values and slopes of regression lines are not significantly different from 1 and slopes do not differ significantly from the line identity ($P<0.05$).

has been limited. Comparison of agonist potency ratios in rat kidney (Eltze & Boer, 1992; present study) with those obtained in both guinea-pig spleen (α_{1B}-adrenoceptor; Eltze, 1994) and rat thoracic aorta (putative α_{1D}-adrenoceptor; Saussy *et al.*, 1994; Eltze & Boer, 1992), however, suggest that certain agonists (e.g. methoxamine) may exhibit selectivity for the α_{1A}-adrenoceptor subtype (see also Figure 6b).

A most important finding from the present study is the high correlative association between antagonist affinity estimates obtained functionally in the perfused kidney and pK_i values obtained from radioligand binding experiments using the cloned bovine α_{1C}-adrenoceptor. It is this correlation which led us to conclude that the α_{1A}-adrenoceptor mediating vasoconstrictor responses to NA in rat kidney represents a species homologue of the cloned α_{1C}-adrenoceptor (see Ford *et al.*, 1994). This conclusion is now supported by high correlative associations between the affinity of ligands for the cloned bovine α_{1C}-adrenoceptor and their binding affinity for α_{1A}-adrenoceptors in submaxillary gland of rat as well as other rat tissues (values abstracted from the literature). Radioligand binding studies reported recently by others (Faure *et al.*, 1994; Forray *et al.*, 1994; Laz *et al.*, 1994) also support the equivalency of the α_{1A}-adrenoceptor with the α_{1C}-adrenoceptor, and considerable molecular biological evidence now exists for the presence of the α_{1C}-adrenoceptor gene in rat (Alonso-Llamazares *et al.*, 1993; Laz *et al.*, 1994; Rokosh *et al.*, 1994; Faure *et al.*, 1994; Price *et al.*, 1994) despite an initial negative report (Schwinn & Lomasney, 1992).

Apart from radioligand binding data, only one published functional study has attempted to equate the α_{1A}- and α_{1C}-adrenoceptors (Forray *et al.*, 1994). A high correlative association was found between the pA_2 values for 6 α_1-adrenoceptor antagonists measuring human prostatic contraction *in vitro* and their pK_i values at the cloned α_{1C}-adrenoceptor of man. However, only 3 of these antagonists (indoramin, 5-methyl-urapidil, and SNAP 1069) exhibited selectivity for the cloned α_{1C}-adrenoceptor over the cloned human α_{1B}- and α_{1D}-adrenoceptors. Thus, conclusions must be guarded. Indeed, we have reported recently that the α_1-adrenoceptor mediating contraction in prostate of man differs from the α_{1A}-adrenoceptor subtype (Ford *et al.*, 1995) and remains for further definition.

To summarize, the α_{1A}-adrenoceptor is the predominant α_1-adrenoceptor subtype mediating vasoconstrictor responses to exogenously administered NA in the isolated perfused kidney of rat. These α_{1A}-adrenoceptors, characterized functionally, exhibit equivalency to other native α_{1A}-adrenoceptors from rat as well as to the cloned α_{1C}-adrenoceptor, making it unnecessary to postulate the existence of a fourth α_1-adrenoceptor with high affinity for prazosin (Schwinn & Lomasney, 1992). Thus, the following classification of α_1-adrenoceptor with high affinity ($pA_2 > 9$) for prazosin is recommended: α_{1A}-, α_{1B}- and α_{1D}-adrenoceptors (Hieble *et al.*, 1995). Finally, the isolated perfused kidney of rat, studied in the presence of nitrendipine, appears to offer an unequivocal functional preparation for the singular study of the α_{1A}-adrenoceptor. This preparation is important because a candidate functional preparation for the 'classical' α_{1A}-adrenoceptor (vas deferens of rat; Han *et al.*, 1987) has been shown to exhibit clear-cut α_1-adrenoceptor heterogeneity (Ohmura *et al.*, 1992). The presence of α_{1A}-adrenoceptors mediating vasoconstriction in mesenteric (Williams & Clarke, 1994) and renal vascular smooth muscle of rat suggests a role in the maintenance of blood pressure under physiological conditions. Innervation of mesenteric and renal vascular α_{1A}-adrenoceptors by postganglionic sympathetic nerves has been demonstrated (Blue & Clarke, 1992; Williams & Clarke, 1995).

References

ALONSO-LLAMAZARES, A., ZAMANILLO, D., FERNANDEZ, A., CHINCHETRU, M.A. & CALVO, P. (1993). Differential expression of the α_{1C} adrenergic receptor subtype in rat tissues. *NeuroReport*, **4**, 1266–1268.

BLUE, D.R. & CLARKE, D.E. (1990). Characterisation and modulation of vascular α-adrenoceptor responses in rat kidney. *Br. J. Pharmacol.*, **99**, 204P.

BLUE, D.R. Jr., VIMONT, R.L. & CLARKE, D.E. (1992). Evidence for a noradrenergic innervation to α_{1A}-adrenoceptors in rat kidney. *Br. J. Pharmacol.*, **107**, 414–417.

BLUE, D.R., WHITING, R.L. & CLARKE, D.E. (1991). Pharmacological profile of an alpha$_{1A}$-adrenoceptor in the renal vasculature: studies with (+)- and (−)-niguldipine. In *Adrenoceptors: Structure, Mechanisms, Function: Advances in Pharmacological Science*, ed. Abadi, S.Z. pp. 373–374. Basel: Birkhauser verlag.

BOER, R., GRASSEGGER, A., SCHUDT, C. & GLOSSMANN, H. (1989). (+)-Niguldipine binds with very high affinity to Ca^{2+} channels and to a subtype of α_1-adrenoceptors. *Eur. J. Pharmacol.-Mol. Pharmacol. Sec.*, **172**, 131–145.

BOND, R.A., ORNSTEIN, A.G. & CLARKE, D.E. (1989). Unsurmountable antagonism to 5-hydroxytryptamine in rat kidney results from pseudoirreversible inhibition rather than multiple receptors or allosteric receptor modulation. *J. Pharmacol. Exp. Ther.*, **249**, 401–410.

BYLUND, D.B. (1985). Heterogeneity of alpha-2-adrenergic receptors. *Pharmacol. Biochem. Behav.*, **22**, 835–843.

CLARKE, D.E., FORD, A.P.D.W., WILLIAMS, T.J., BONHAUS, D., VIMONT, R. & BLUE, D.R. Jr. (1994). Pharmacological evidence for the equivalency of the α_{1A} adrenoceptor of rat and the cloned bovine α_{1C}-adrenoceptor: a revised α_1-adrenoceptor classification scheme. Abstract from the *Pharmacology of Adrenoceptors Satellite*, King of Prussia, July 22–23.

CLARKE, D.E., WHITING, R.L., PFISTER, J. & BLUE, D.R. (1991). Antagonism of α_1-adrenoceptor subtypes by niguldipine and 5-methyl-urapidil in rat kidney. *Br. J. Pharmacol.*, **102**, 196P.

COTECCHIA, S., SCHWINN, D.A., RANDALL, R.R., LEFKOWITZ, R.J., CARON, M.G. & KOBILKA, B.K. (1988). Molecular cloning and expression of the cDNA for the hamster α_1-adrenergic receptor. *Proc. Natl. Acad. Sci. U.S.A.*, **85**, 7159–7163.

DOCHERTY, J., FLAVAHAN, N.A. & VANHOUTTE, P.M. (1987). α_1-Adrenoceptor subclassification in vascular smooth muscle: a premature proposal? *Trends Pharmacol. Sci.*, **8**, 123–125.

DREW, G.M. (1985). What do antagonists tell us about α-adrenoceptors? *Clin. Sci.*, **68**, 15s–19s.

DUNN, W.R., MCGRATH, J.C. & WILSON, V.G. (1989). Expression of functional postjunctional α_2-adrenoceptors in rabbit isolated distal saphenous artery – a permissive role for angiotensin II? *Br. J. Pharmacol.*, **96**, 259–261.

ELHAWARY, A.M., PETTINGER, W.A. & WOLFF, D.W. (1992). Subtype-selective alpha-1 adrenoceptor alkylation in the rat kidney and its effect on the vascular pressor response. *J. Pharmacol. Exp. Ther.*, **260**, 709–713.

ELTZE, M. (1994). Characterization of the α_1-adrenoceptor subtype mediating contraction of guinea-pig spleen. *Eur. J. Pharmacol.*, **260**, 211–220.

ELTZE, M. & BOER, R. (1992). The adrenoceptor agonist, SDZ NVI 085, discriminates between α_{1A}- and α_{1B}-adrenoceptors subtypes in vas deferens, kidney and aorta of the rat. *Eur. J. Pharmacol.*, **224**, 125–136.

ELTZE, M., BOER, R., SANDERS, K.H. & KOLASSA, N. (1991). Vasodilatation elicited by 5-HT_{1A} receptor agonists in constant-pressure-perfused rat kidney is mediated by blockade of α_{1A}-adrenoceptors. *Eur. J. Pharmacol.*, **202**, 33–44.

FAURE, C., PIMOULE, C., ARBILLA, S., LANGER, S.Z. & GRAHAM, D. (1994). Expression of α_1-adrenoceptor subtypes in rat tissues: implications for α_1-adrenoceptor classification. *Eur. J. Pharmacol. Mol. Pharmacol. Sec.* **268**, 141–149.

FENG, F., PETTINGER, W.A., ABEL, P.W & JEFFRIES, W.B. (1991). Regional distribution of α_1-adrenoceptor subtypes in rat kidney. *J. Pharmacol. Exp. Ther.*, **258**, 263–268.

FLAVAHAN, N.A. & VANHOUTTE, P.M. (1986). α_1-Adrenoceptor subclassification in vascular smooth muscle. *Trends Pharmacol. Sci.*, **7**, 347–349.

FLAVAHAN, N.A., VOS, A.A.A.M. & VANHOUTTE, P.M. (1987). Subclassification of α_1-adrenoceptors mediating contraction of the canine pulmonary artery. *Br. J. Pharmacol.*, **91**, 331P.

FORD, A.P.D.W., ARREDONDO, N.F., BLUE, D.R., BONHAUS, D.W., KAVA, M.S., WILIMANS, T.J., VIMONT, R.L., ZHU, Q.-M., PFISTER, J.R. & CLARKE, D.E. (1995). Do α_{1A}- (α_{1C}-) adrenoceptors (AR) mediate prostatic smooth muscle contraction in man? Studies wtih RS 17053. *Br. J. Pharmacol.*, (in press).

FORD, A.P.D.W., WILLIAMS, T.J., BLUE, D.R. & CLARKE, D.E. (1994). α_1-Adrenoceptor classification: sharpening Occam's razor. *Trends Pharmacol. Sci.*, **15**, 167–170.

FORRAY, C., BARD, J.A., WETZEL, J.M., CHIU, G., SHAPIRO, E., TANG, R., LEPOR, H., HARTIG, P.R., WEINSHANK, R.L., BRANCHEK, T.A. & GLUCHOWSKI, C. (1994). The α_1-adrenergic receptor that mediates smooth muscle contraction in human prostate has the pharmacological properties of the cloned human α_{1C} subtype. *Mol. Pharmacol.*, **45**, 703–708.

GROSS, G., HANFT, G. & MEHDORN, H.M. (1989). Demonstration of α_{1A}- and α_{1B}-adrenoceptor sites in human brain tissue. *Eur. J. Pharmacol.*, **169**, 325–328.

GROSS, G., HANFT, G. & RUGEVICS, C. (1988). 5-Methyl-urapidil discriminates between subtypes of the α_1-adrenoceptor. *Eur. J. Pharmacol.*, **151**, 333–335.

HAN, C., WILSON, K.M. & MINNEMAN, K.P. (1990). α_1-Adrenergic receptor subtypes and formation of inositiol phosphates in dispersed hepatocytes and renal cells. *Mol. Pharmacol.*, **37**, 903–910.

HAN, C., ABEL, P.W. & MINNEMAN, K.P. (1987). α_1-Adrenoceptor subtypes linked to different mechanisms for increasing intracellular Ca^{2+} in smooth muscle. *Nature*, **329**, 333–335.

HANFT, G. & GROSS, G. (1989a). Heterogeneity of α_1-adrenoceptor binding sites in the rat heart – subtype-selective agonists and antagonists. *Br. J. Pharmacol.*, **98**, 652P.

HANFT, G. & GROSS, G. (1989b). Subclassification of α_1-adrenoceptor recognition sites by urapidil derivatives and other selective antagonists. *Br. J. Pharmacol.*, **97**, 691–700.

HANFT, G. & GROSS, G. (1990). The effect of reserpine, desipramine and thyroid hormone on α_{1A}- and α_{1B}-adrenoceptor binding sites: evidence for a subtype-specific regulation. *Br. J. Clin. Pharmacol.*, **30**, 125S–127S.

HANFT, G., GROSS, G., BECKERINGH, J.J. & KORSTANJE, C. (1989). α_1-Adrenoceptors: the ability of various agonists and antagonists to discriminate between two distinct [^{3}H]prazosin binding sites. *J. Pharm. Pharmacol.*, **41**, 714–716.

HIEBLE, J.P., BYLUND, D.B., CLARKE, D.E., EIKENBURG, D.C., LANGER, S.Z., LEFOKOWITZ, R.T., MINNEMAN, K.P. & RUFFOLO, R.R. Jr. (1995). Recommendation for nomenclature of α_1-adrenoceptors: consensus update. *Pharmacol. Rev.*, (in press).

HIRAMATSU, Y., MURAOKA, R., KIGOSHI, S. & MURAMATSU, I. (1992). 5-Methylurapidil may discriminate between α_1-adrenoceptors with a high affinity for WB4101 in rat lung. *Br. J. Pharmacol.*, **105**, 6–7.

HOLCK, M.I., JONES, C.H.M. & HAEUSLER, G. (1983). Differential interactions of clonidine and methoxamine with the postsynaptic α-adrenoceptors of rabbit main pulmonary artery. *J. Cardiovasc. Pharmacol.*, **5**, 240–248.

HONDA, K., NAKAGAWA, C. & TERAI, M. (1987). Further studies on (±)-YM-12617, a potent and selective α_1-adrenoceptor antagonist and its individual optical enantiomers. *Naunyn-Schmied. Arch. Pharmacol.*, **336**, 295–302.

IVORRA, D., GASCON, S., VILA, E. & BADIA, A. (1993). α_1-Adrenoceptor subtypes and inositol phosphates production in heart ventricles of spontaneously hypertensive rats. *J. Cardiovasc. Pharmacol.*, **21**, 931–936.

JACKSON, C.A., MICHEL, M.C. & INSEL, P.A. (1992). Expression of renal α_1-adrenergic subtypes in established hypertension. *J. Cardiovasc. Pharmacol.*, **19**, 857–862.

JOHNSON, R.D. & MINNEMAN, K.P. (1987). Differentiation of α_1-adrenergic receptors linked to phosphatidylinositol turnover and cyclic AMP accumulation in rat brain. *Mol. Pharmacol.*, **31**, 239–246.

KIMURA, T., MURAMATSU, I., KIGOSHI, S. & MURAOKA, R. (1993). Characterization of α_1- and β-adrenoceptor subtypes in the mongolian gerbil cerebral cortex. *Mol. Neuropharmacol.*, **3**, 69–73.

KLIJN, K., SLIVKA, S.R., BELL, K. & INSEL, P.A. (1991). Renal α_1-adrenergic receptor subtypes: MDCK-D1 cells, but not rat cortical membranes possess a single population of receptors. *Mol. Pharmacol.*, **39**, 407–413.

KO, F.-N., GUH, J.-H., YU, S.-M., HOU, Y.-S., WU, Y.-C. & TENG, C.-M. (1994). (−)-Discretamine, a selective α_{1D}-adrenoceptor antagonist, isolated from *Fissistigma glaucescens*. *Br. J. Pharmacol.*, **112**, 1174–1180.

KOHNO, Y., SAITO, H., TAKITA, M., KIGOSHI, S. & MURAMATSU, I. (1994). Heterogeneity of α_1-adrenoceptor subtypes involved in adrenergic contractions of dog blood vessels. *Br. J. Pharmacol.*, **112**, 1167–1173.

LAZ, T.M., FORRAY, C., SMITH, K., BARD, J.A., VAYSSE, P.J.-J., BRANCHEK, T.A. & WEINSHANK, R.L. (1994). The rat homologue of the bovine α_{1C}-adrenergic receptor shows the pharmacological properties of the classical α_{1A}-subtype. *Mol. Pharmacol.*, **46**, 414–422.

LOMASNEY, J.W., COTECCHIA, S., LORENZ, W., LEUNG, W.-Y., SCHWINN, D.A., YANG-FENG, T.L., BROWNSTEIN, M., LEFKOWITZ, R.J. & CARON, M.G. (1991). Molecular cloning and expression of the cDNA for the α_{1A}-adrenergic receptor. *J. Biol. Chem.*, **266**, 6365–6369.

MCGRATH, J.C., BROWN, C.M. & WILSON, V.G. (1989). Alpha-adrenoceptors: a critical review. *Med. Res. Rev.*, **9**, 407–533.

MICHEL, A.D., LOURY, D.N. & WHITING, R.L. (1989). Identification of a single α_1-adrenoceptor corresponding to the α_{1A}-subtype in rat submaxillary gland. *Br. J. Pharmacol.*, **98**, 883–889.

MICHEL, M.C., BUSCHER, R., KERKER, J., KRANEIS, H., ERDBRUGGER, W. & BRODDE, O.E. (1993a). α_1-Adrenoceptor subtype affinities of drugs for the treatment of prostatic hypertrophy: evidence for heterogeneity of chloroethylclonidine-resistant rat renal α_1-adrenoceptor. *Naunyn-Schmied. Arch. Pharmacol.*, **348**, 385–395.

MICHEL, M.C., KERKER, J., BRANCHEK, T.A. & FORRAY, C. (1993b). Selective irreversible binding of chloroethylclonidine at α_1- and α_2-adrenoceptor subtypes. *Mol. Pharmacol.*, **44**, 1165–1170.

MICHEL, M.C., HANFT, G. & GROSS, G. (1990). α_{1B}- but not α_{1A}-adrenoceptors mediate inositol phosphate generation. *Naunyn-Schmied. Arch. Pharmacol.*, **341**, 385–387.

MICHEL, M.C. & INSEL, P.A. (1994). Comparison of cloned and pharmacologically defined rat tissue α_1-adrenoceptor subtypes. *Naunyn-Schmied. Arch. Pharmacol.*, **350**, 136–142.

MORROW, A.L., BATTAGLIA, G., NORMAN, A.B. & CREESE, I. (1985). Identification of subtypes of [^{3}H]-prazosin-labelled α_1 receptor binding sites in rat brain. *Eur. J. Pharmacol.*, **109**, 285–287.

MORROW, A.L. & CREESE, I. (1986). Characterization of α_1-adrenergic receptor subtypes in rat brain: a reevaluation of [^{3}H]WB4104 and [^{3}H]prazosin binding. *Mol. Pharmacol.*, **29**, 321–330.

MURAMATSU, I. (1992). A pharmacological perspective of α_1-adrenoceptors: subclassification and functional aspects. In *α-Adrenoceptors*. pp. 193–202. Tokyo: Excerpta Medica, Ltd.

MURAMATSU, I., KIGOSHI, S. & OSHITA, M. (1990a). Two distinct α_1-adrenoceptor subtypes involved in noradrenaline contraction of the rabbit thoracic aorta. *Br. J. Pharmacol.*, **101**, 662–666.

MURAMATSU, I., OHMURA, T., KIGOSHI, S., HASHIMOTO, S. & OSHITA, M. (1990b). Pharmacological subclassification of α_1-adrenoceptors in vascular smooth muscle. *Br. J. Pharmacol.*, **99**, 197–201.

OHMURA, T., OSHITA, M., KIGOSHI, S. & MURAMATSU, I. (1992). Identification of α_1-adrenoceptor subtypes in the rat vas deferens: binding and functional studies. *Br. J. Pharmacol.*, **107**, 697–704.

OSHITA, M., KIGOSHI, S. & MURAMATSU, I. (1991). Three distinct binding sites for [^{3}H]-prazosin in the rat cerebral cortex. *Br. J. Pharmacol.*, **104**, 961–965.

OSHITA, M., KIGOSHI, S. & MURAMATSU, I. (1993). Pharmacological characterization of two distinct α_1-adrenoceptor subtypes in rabbit thoracic aorta. *Br. J. Pharmacol.*, **108**, 1071–1076.

PIMOULE, C., GRAHAM, D. & LANGER, S.Z. (1992). Characterization of the α_{1B}-adrenoceptor gene product expressed in a stably transfected HeLa cell-line. *Br. J. Pharmacol.*, **105**, 233P.

PRICE, D.T., CHARI, R.S., BERKOWITZ, D.E., MEYERS, W.C. & SCHWINN, D.A. (1994). Expression of α_1-adrenergic receptor subtype mRNA in rat tissues and human SK-N-MC neuronal cells: implications for α_1-adrenergic receptor subtype classification. *Mol. Pharmacol.*, **46**, 221–226.

RANG, H.P. (1966). The kinetics of action of acetylcholine antagonists in smooth muscle. *Proc. R. Soc. B.*, **164**, 488–510.

ROKOSH, D.G., BAILEY, B.A., STEWART, A.F.R., KARNS, L.R., LONG, C.S. & SIMPSON, P.C. (1994). Distribution of α1C-adrenergic receptor mRNA in adult rat tissues by RNase protection assay and comparison with α1B and α1D. *Biochem. Biophys. Res. Commun.*, **200**, 1177–1184.

SALLES, J. & BADIA, A. (1994). Selective enrichment with α_{1A}- and α_{1B}-adrenoceptor subtypes in rat brain cortical membranes. *Eur. J. Pharmacol.*, **266**, 301–308.

SATTAR, M.A. & JOHNS, E.J. (1994a). Evidence for an α_1-adrenoceptor subtype mediating adrenergic vasoconstriction in Wistar Normotensive and stroke-prone spontaneously hypertensive rat kidney. *J. Cardiovasc. Pharmacol.*, **23**, 232–239.

SATTAR, M.A. & JOHNS, E.J. (1994b). α_1-Adrenoceptor subtypes mediating adrenergic vasoconstriction in kidney of two kidney, one-clip Goldblatt and deoxycorticosterone acetate-salt hypertensive rats. *J. Cardiovasc. Pharmacol.*, **24**, 420–428.

SAUSSY, D.L. Jr., GOETZ, A.S., KING, H.K. & TRUE, T.A. (1994). BMY 7378 is a selective antagonist of α_{1D} adrenoceptors (AR): evidence that rat vascular α_1 AR are of the α_{1D} subtype. *Can. J. Physiol. Pharmacol.*, **72** (Suppl.), 323.

SCHMITZ, J.M., GRAHAM, R.M., SAGALOWSKY, A. & PETTINGER, W.A. (1981). Renal alpha-1 and alpha-2 adrenergic receptors: biochemical and pharmacological correlations. *J. Pharmacol. Exp. Ther.*, **219**, 400–406.

SCHWIETERT, H.R., BATINK, H., WILFFERT, B., PFAFFENDORF, M. & VAN ZWIETEN, P.A. (1993). Pharmacological analysis of α_1-adrenoceptor binding sites in rat left ventricular tissue with subtype selective antagonists. *Br. J. Pharmacol.*, **108**, 139P.

SCHWINN, D.A. & LOMASNEY, J.W. (1992). Pharmacological characterization of cloned α_1-adrenoceptor subtypes: selective antagonists suggest the existence of a fourth subtype. *Eur. J. Pharmacol.*, **227**, 433–436.

SCHWINN, D.A., LOMASNEY, J.W., LORENZ, W., SZKLUT, P.J., FREMEAU, R.T. Jr., YANG-FENG, T.L., CARON, M.G., LEFKOWITZ, R.J. & COTECCHIA, S. (1990). Molecular cloning and expression of the cDNA for a novel α_1-adrenergic receptor subtype. *J. Biol. Chem.*, **265**, 8183–8189.

SHARIF, N.A., SHIEH, I.A., BLUE, D.R. & CLARKE, D.E. (1991). Localization and function of alpha$_1$-adrenoceptor (α_1AR) subtypes in rat kidney. *Pharmacologist*, **33**, 214.

SLEIGHT, A.J., KOEK, W. & BIGG, D.C.H. (1993). Binding of antipsychotic drugs at α_{1A}- and α_{1B}-adrenoceptors: risperidone is selective for the α_{1B}-adrenoceptors. *Eur. J. Pharmacol.*, **238**, 407–410.

TSUCHIHASHI, H., MARUYAMA, K., BABA, S., MANO, F., KINAMI, J. & NAGATOMO, T. (1991). Comparison of α_1-adrenoceptors between rat brain and spleen. *Jpn. J. Pharmacol.*, **56**, 523–530.

WILLIAMS, T.J. & CLARKE, D.E. (1995). Pharmacological characterization of α_1-adrenoceptors mediating vasoconstriction to noradrenaline and nerve stimulation in isolated perfused mesentery of rat. *Br. J. Pharmacol.*, **114**, 531–536.

WILSON, K.M. & MINNEMAN, K.P. (1990). Different pathways of [^{3}H]inositol phosphate formation mediated by α_{1a}- and α_{1b}-adrenergic receptors. *J. Biol. Chem.*, **265**, 17601–17606.

YAZAWA, H., TAKANASHI, M., SUDOH, K., INAGAKI, O. & HONDA, K. (1992). Characterization of [^{3}H]YM617, R-(−)-5-[2[[2[ethoxy-ring(n)-^{3}H] (*o*-ethoxyphenoxy)ethyl]amino]-propyl-2- methoxybenzenesulfonamide HCl, a potent and selective alpha-1 adrenoceptor radioligand. *J. Pharmacol. Exp. Ther.*, **263**, 201–206.

(Received November 17, 1994
Revised February 1, 1995
Accepted February 10, 1995)

British Journal of Pharmacology (1995) 115, 295-301

Subcellular localization and molecular pharmacology of distinct populations of [^{3}H]-AMPA binding sites in rat hippocampus

Jeremy M. Henley

*Department of Anatomy, School of Medical Sciences, University of Bristol, University Walk, Bristol, BS8 1TD

1 The subcellular distributions of [^{3}H]-α-amino-3-hydroxy-5-methylisoxazolepropionate ([^{3}H]-AMPA) and [^{3}H]-kainate binding sites in rat hippocampus were investigated by cell fractionation techniques.

2 Two major populations of [^{3}H]-AMPA sites were detected with the majority of binding located intracellularly in the microsomal (P_3) fraction. Most of the remaining sites were in the synaptosomal membrane fraction but some were also present in the nuclear fraction. In contrast, essentially all of the [^{3}H]-kainate binding sites were in the synaptosomal membrane fraction.

3 Saturation binding analysis yielded K_D and B_{max} values for [^{3}H]-AMPA of 147 nM and 2.6 pmol mg^{-1} protein respectively for the synaptosomal membrane-associated sites and 129 nM and 5.3 pmol mg^{-1} protein respectively for the microsomal sites.

4 Both main populations of [^{3}H]-AMPA sites displayed the same rank order of inhibition by competitive ligands, the apparent Mr values of GluR1 subunits were equivalent, suggesting the same degree of post-translational modification and the hydrodynamic properties of the receptor complexes were identical.

5 These data are consistent with the hypothesis that the movement of AMPA receptors between cellular compartments in the postsynaptic neurone could constitute one mechanism underlying long-term potentiation in the hippocampus.

Keywords: Glutamate receptors; excitatory amino acid receptors; AMPA; synaptic plasticity; long-term potentiation; kainate; subcellular fractionation; receptor localization

Introduction

Glutamate receptors (GluRs) are the major class of excitatory receptors in the vertebrate central nervous system. They mediate fast excitatory neurotransmission, they are involved in synaptic formation and stabilization and their prolonged activation is potently neurotoxic (Choi, 1992; Bliss & Collingridge, 1993). Ionotropic GluRs are usually classified into N-methyl-D-aspartate (NMDA) and non-NMDA (kainate and α-amino-3-hydroxy-5-methylisoxazolepropionate, AMPA) subtypes. The cDNAs encoding many of the ionotropic receptor subunits have been cloned and characterized. The sequences which code for the AMPA receptor subunits GluR1-GluR4 show levels of amino acid identity of greater than 70% and they share multiple putative sites for regulation at both the nucleic acid and protein levels (Sommer & Seeburg, 1992; Wenthold *et al.*, 1992; Hollmann & Heinemann, 1994).

The molecular pharmacology and cellular and subcellular distributions of AMPA receptors are of widespread interest because of their underlying roles in normal physiological and pathological processes (Choi, 1992; Bliss & Collingridge, 1993). It is becoming increasingly apparent that AMPA receptors are subject to tight cellular controls and a variety of processes which regulate AMPA receptor expression at the nucleic acid level and which modulate their function at the protein level have been described. To date, these mechanisms include alternative RNA splicing and RNA editing at the nucleic acid level, post-translational modification events such as phosphorylation and glycosylation at the protein level and regulation by phospholipase A_2 and receptor-associated modulatory proteins at the cellular level (for recent reviews see Barnes & Henley, 1992; Swope *et al.*, 1992; Seeburg, 1993).

Another way by which the neurone can control receptor activity is by subcellular compartmentalisation. Indeed, several groups have observed significant levels of GluR1-GluR4 immunoreactivity inside neurones although quantitative analyses of the plasma membrane and intracellular localisations have not been performed (Eshhar *et al.*, 1993; Molnar *et al.*, 1993; Baude *et al.*, 1994). However, recent quantitative autoradiographic experiments carried out on fractionated homogenates from *Xenopus* brain have suggested that in that tissue up to 80% of the [^{3}H]-AMPA and [^{3}H]-6-cyano-7-nitroquinoxaline-2,3,-dione ([^{3}H]-CNQX) (but not [^{3}H]-kainate) binding is missing from synaptosomal membrane preparation compared to whole cell homogenates (Barnes & Henley, 1993).

The aim of this study, therefore, was to determine quantitatively the subcellular compartmentalization of [^{3}H]-AMPA binding in rat hippocampus. The pharmacological and biochemical properties of the sites were compared to gain insight into possible mechanisms by which AMPA receptor processing and compartmentalization may effect the molecular processes underlying synaptic plasticity.

Methods

Wistar rats (250 g) were killed by decapitation and the brains rapidly removed and dissected. Hippocampi were pooled from several rats and either homogenized immediately or frozen rapidly and stored at −80°C.

Subcellular fractionation by differential centrifugation

Fractionation procedures were based on previously described protocols (Maeno *et al.*, 1971; Rodríguez de Lores Arnaiz & Pellegrino de Iraldi, 1984). Rat hippocampi were homogenized with a glass-Teflon homogenizer in 10 volumes of ice-cold 320 mM sucrose and then spun for 10 min at 1000 *g* in a JA 20 rotor. All centrifugation steps were carried out at 4°C and all homogenizations were in ice-cold buffer. The supernatant was saved and the pellet was rehomogenized and recentrifuged twice more. The final pellet (P_1) consists of nuclei and cell debris. The pooled supernatant was centrifuged at 11,500 *g* for 20 min. The supernatant was saved and the pellet was re-

*Part of this work was carried out at: Department of Pharmacology, Medical School, University of Birmingham, Edgbaston, Birmingham, B15 2TT

suspended and respun. The pooled supernatants were spun at 100,000 *g* for 90 min, the resultant pellet from this step comprises microsomes and the supernatant is defined as cell sap. The combined pellets from the 11,500 *g* spins were resuspended in 0.32 M sucrose and layered in 4 ml aliquots onto discontinuous sucrose gradients (4 ml 1.2 M sucrose, 4 ml 0.8 M sucrose) in 12 ml Beckman SW40 centrifuge tubes. The gradients were centrifuged at 58,000 *g* for 110 min. Cell components migrated to the interfaces of the gradient; the 0.32/08 M sucrose interface (P_2A) is myelin; the 0.8/1.2 M sucrose interface (P_2B) comprises synaptosomal membranes and the pellet (P_2C) consists of mitochondria. Each of the fractions was frozen at −80°C, thawed and resuspended to 35 ml in ice-cold Tris-citrate buffer (Tris 50 mM, EDTA 1 mM, EGTA 1 mM, pH 7.4 at 0°C with citric acid) and centrifuged at 48,000 *g* for 20 min to pellet the membranes. This was repeated a total of three times to ensure complete elimination of any remaining endogenous L-glutamate. The final pellet from each fraction was resuspended in Tris-citrate buffer to a final protein concentration of 0.1−0.5 mg ml^{-1} and stored in aliquots at −80°C. A schematic of the subcellular fraction procedure is shown in Figure 1.

Radioligand binding

Hippocampal cell fractions (usually 50 μl) in Tris-citrate buffer were added to test-tubes containing 10 μl of competing compound or vehicle and 10 μl [^{3}H]-AMPA (58 Ci $mmol^{-1}$) at a final concentration of 25 nM. Potassium thiocyanate was included in all [^{3}H]-AMPA binding assays to a final concentration of 100 mM (Honoré & Drejer, 1988). The final assay volume was adjusted to 100 μl with Tris buffer. The reaction mixture was incubated at 0°C for 90 min and then terminated by rapid filtration through GF/B filters pre-soaked in 0.05% polyethylenimine. The filters were washed rapidly with three × 3 ml aliquots of ice-cold Tris buffer and the total wash time 2−3 s. Non-specific binding was defined by inclusion of 1 mM L-glutamate. Radioactivity remaining on the filters was assayed by liquid scintillation spectroscopy at an efficiency of approximately 48%. Binding assays for [^{3}H]-kainate (58 Ci $mmol^{-1}$; 25 nM final concentration) were exactly the same except KSCN was not included and non-specific binding was defined by 100 μM kainate. The binding affinities (K_D) and total number of sites (B_{max}) for [^{3}H]-AMPA were determined by direct fitting to saturation binding curves. The data were

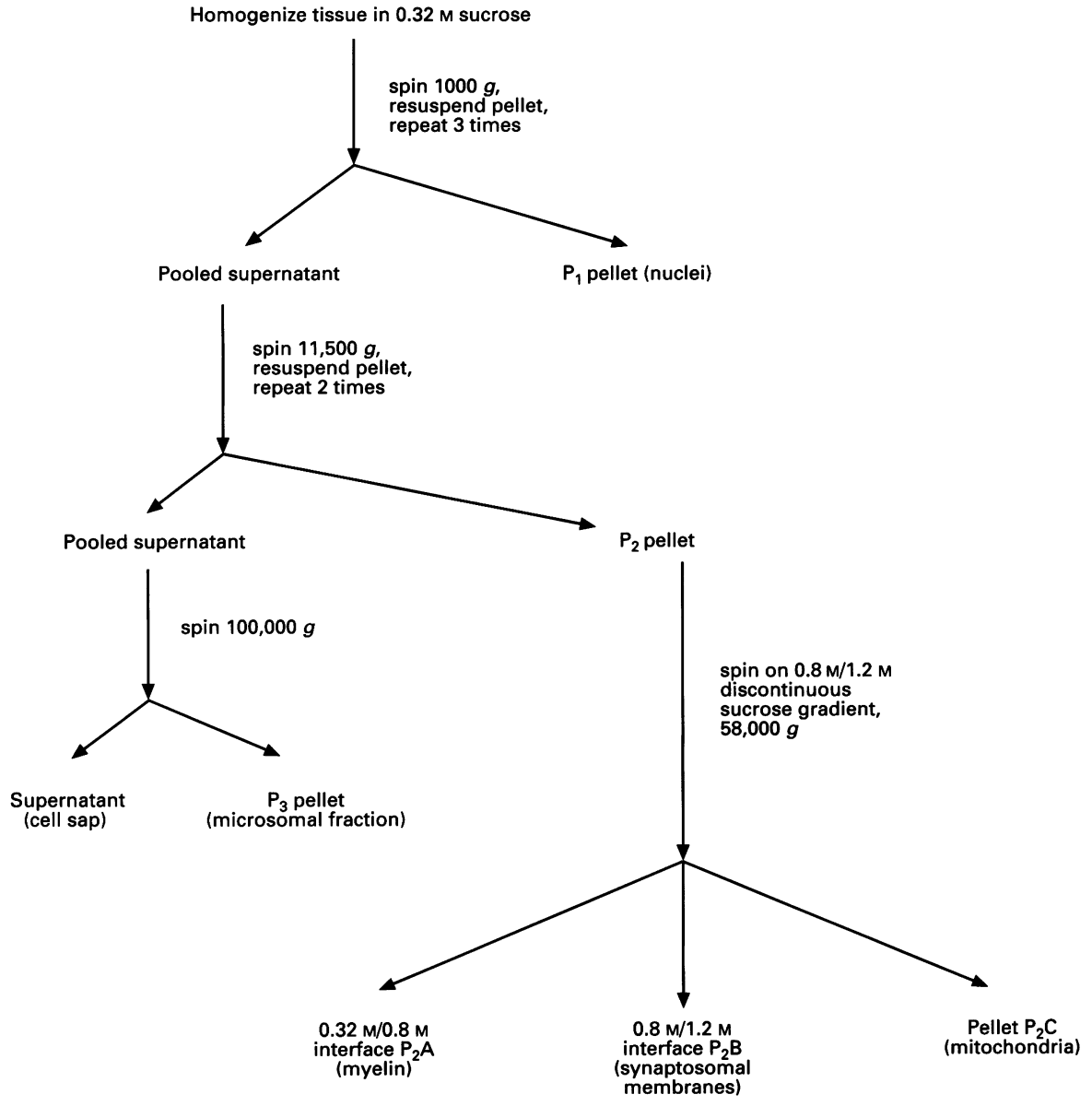

Figure 1 Schematic diagram of the differential centrifugation protocol used to isolate subcellular fractions. Details of the procedure are given in the Methods section.

analysed with the KaleidaGraph programme using the logistic equation:

$$b = B_{max}\cdot[L]^n/[L]^n + K^n$$

where [L] is the free ligand concentration, K is the dissociation constant and ^{n} is the Hill number. A two-site model did not fit the data significantly better than the one-site model used.

SDS-PAGE and Western blotting

The anti-peptide antibody Ab9T was a generous gift from Dr Robert Wenthold, NIH, Bethesda, U.S.A. Hippocampal subcellular fractions were subjected to discontinuous SDS-PAGE on 7.5% acrylamide gels. The electrophoresed protein was blotted on to nitro-cellulose for 30–40 min at ~50 V (~170 mA–100 mA) in CAPS (3-[cyclohexylamino]-1-propanesulphonic acid) transfer buffer (10 mM CAPS pH 11, 10% methanol). Non-specific binding to the blots was blocked by incubation overnight at 4°C in TN buffer (50 mM Tris-HCl (pH 7.4), 0.5 M NaCl) containing 5% (w/v) dry milk powder.

For immunolabelling, blots were incubated for 1 h at 28°C in a Hybaid hybridisation oven with 1.0 μg ml^{-1} Ab9T and 0.15 μg ml^{-1}. The blots were extensively washed (3 x 15 min) in TNT buffer (TN buffer plus 0.1% Triton X-100) and then incubated with the secondary antibody, horse-radish peroxidase (HRP) conjugated swine anti-rabbit IgG for 1 h. Following further extensive washes (3 x 15 min in TNT buffer) the blots were soaked in 3,3-diaminobenzidine-hydrogen peroxide (DAB-H_2O_2) solution to develop the HRP stain. The immunostained blots were washed in distilled water to stop the HRP reaction.

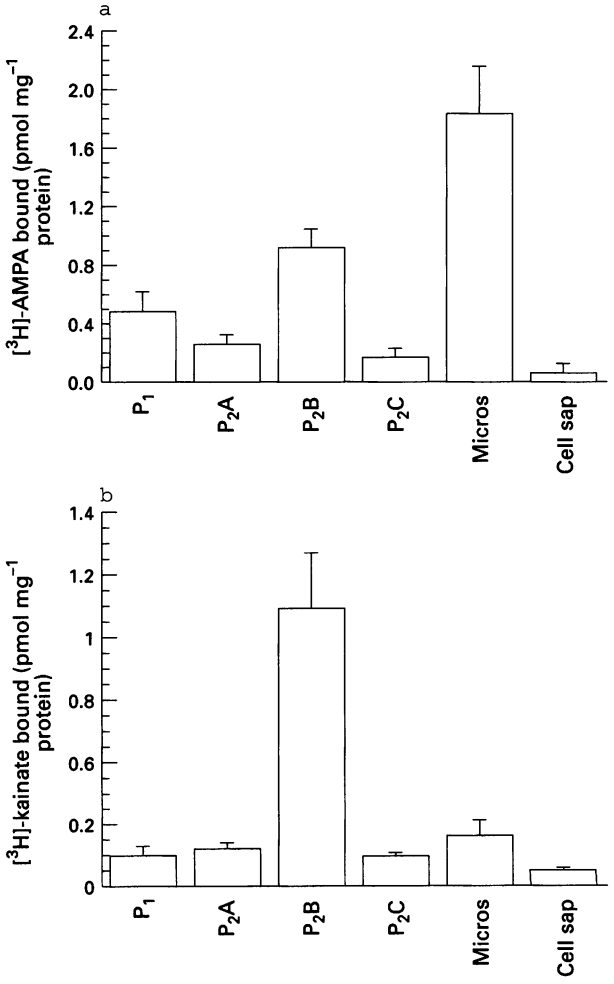

Figure 2 Distributions of (a) [^{3}H]-AMPA and (b) [^{3}H]-kainate binding to rat hippocampal subcellular fractions prepared by differential centrifugation. The data are expressed as pmol of radioligand bound per mg of protein at a single concentration of 25 nM for both radioligands. The results are the means ± s.e.mean of 4 separate experiments for [^{3}H]-AMPA and 3 separate experiments for [^{3}H]-kainate.

Protein solubilisation

[^{3}H]-AMPA sites were solubilized essentially as described elsewhere for *Xenopus* CNS (Henley & Barnard, 1989). Well-washed freeze-thawed synaptosomal membrane or microsomal fractions were resuspended in Tris-citrate buffer containing 1% n-octyl-β-glucopyranoside (octylglucoside). Following incubation with gentle agitation for 1 h at 4°C, the mixture was centrifuged for 1 h at 100,000 g and the supernatant containing solubilized protein was collected and either used immediately or stored at −80°C until required.

Sucrose density gradient centrifugation

Gradients were constructed and sampled as described previously (Henley *et al.*, 1992). Briefly, octylglucoside-solubilized synaptosomal membrane or microsomal extracts (0.5 ml) were layered on to 15 ml 5%–20% sucrose gradients. The gradients were made in Tris-citrate buffer containing 0.8% octylglucoside and were poured using the gradient maker facility on the BioRad Econosystem. Centrifugation was at 4°C for 17 h at g_{max} 260,000 in a Beckman SW-40 rotor. Thirty drop fractions were collected from the bottom of the gradient and assayed for [^{3}H]-AMPA binding as described above.

Electron microscopy

The micrographs show representative examples of freshly prepared subcellular fractionations that were not subjected to any freeze-thaw-wash steps. All of the electron microscopy was performed by use of standard protocols on a commercial contract basis by Birmingham University Electron Microscopy Service.

Protein assays

Protein concentrations were determined by use of the BioRad assay kit with BSA as standard.

Results

The subcellular localizations of [^{3}H]-AMPA and [^{3}H]-kainate binding are shown in Figure 2. Using 25 nM [^{3}H]-AMPA, binding in rat hippocampus was localized predominantly in the microsomal fraction and to a lesser extent in the synaptosomal membrane fraction. In contrast, [^{3}H]-kainate sites were located almost exclusively in the synaptosomal membrane fraction.

Electron micrographs prepared from subcellular fractions which were not subjected to freeze-thaw-wash protocols are shown in Figure 3. Structures and membrane fragments characteristic of each of the sucrose gradient fractions are apparent in each of the pictures. The P_1 nuclear and the P_2A myelin fractions (b, c) comprise mainly filamentous myelin membranes with an assortment of smaller vesicular structures also present. The P_3 microsomal fraction (d) contains mostly small vesicular structures consistent with ribosomes and intact microsomes. In addition some small filamentous membranes are also present in the microsomal fraction. The P_2B synaptosomal membrane fraction (e) shows a very different profile comprising mainly much more electron-dense structures, a characteristic of postsynaptic membranes, and a few mitochondria. The P_2C fraction (f), consists almost entirely of mitochondria with some smaller electron dense structures also present.

Saturation binding curves for [^{3}H]-AMPA binding to both populations of sites are shown in Figure 4. Under the experi-

mental conditions used in this study, a single class of binding sites was detected in each of the subcellular fractions. The K_D and B_{max} values were 147.5 ± 25.6 nM and 2.6 ± 0.3 pmol mg^{-1} protein respectively for synaptosomal membranes and the Hill number (n_H) was 0.97. For microsomal membranes the K_D and B_{max} values were 129.3 ± 22.7 nM and 5.3 ± 0.6 pmol mg^{-1} protein respectively and the n_H was 0.94. The data are the means and s.e.mean values from 4 experiments each using hippocampal tissue pooled from two rats. The K_D values obtained for [^{3}H]-AMPA binding to both subcellular fractions are well within the range of previously reported values fitted to both one and two site models (Honoré & Drejer, 1988; Smith & McIlhinney, 1992). Furthermore, both the K_D and B_{max} values are in good agreement with saturation binding results from different membrane preparation protocols and utilising much higher concentrations of [^{3}H]-AMPA (up to 1 μM) (K.K. Dev, T. Honoré & J.M. Henley, unpublished observation).

Displacement experiments for [^{3}H]-AMPA binding to the two main populations of sites are shown in Figure 5. The inhibition curves were similar for both the microsomal and synaptosomal sites. For microsomal membranes the IC_{50} values were: CNQX, 0.20 ± 0.04 μM; kainate, 6.5 ± 1.5 μM; quisqua-

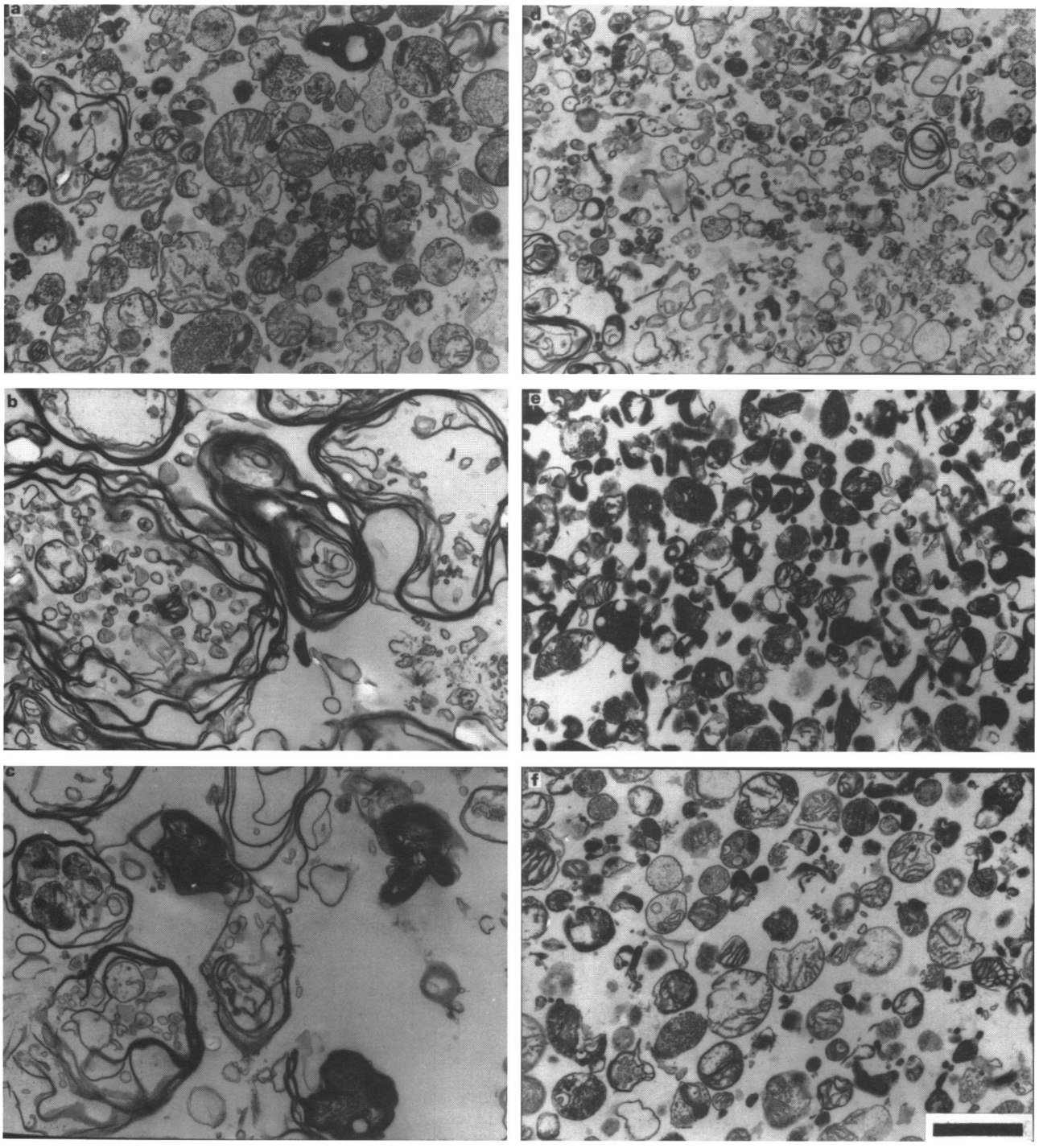

Figure 3 Representative electron micrographs showing the structures present in the subcellular fractions. The panels are: (a) crude homogenate; (b) P_1, nuclear fraction; (c) P_2A, myelin fraction; (d) P_3, microsomal fraction; (e) P_2B, synaptosomal fraction; (f) P_2C, mitochondrial fraction. All of the micrographs are at the same magnification and were prepared by the specialist e.m. facility at Birmingham University. The scale bar in panel (f) corresponds to 1 μm.

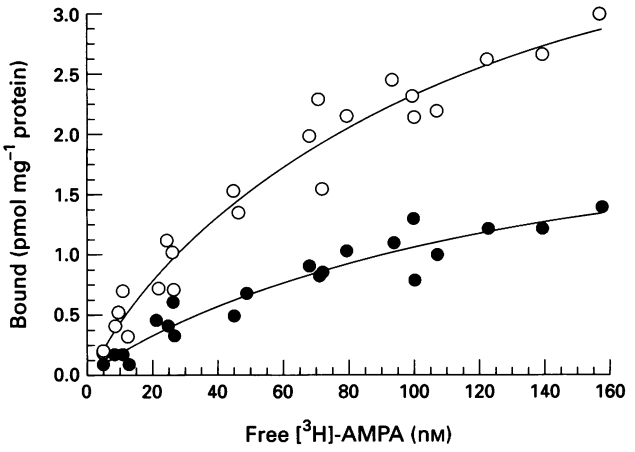

Figure 4 Saturation binding curves for [^{3}H]-AMPA to extensively freeze-thaw-washed synaptosomal membrane fragments (●) and microsomes (○). The data are representative of 4 separate experiments each of which used different synaptosomal and microsomal membrane preparations. Values for the binding affinities and total number of sites are given in the text.

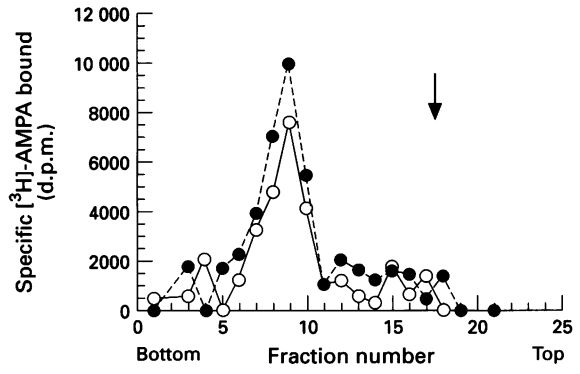

Figure 6 Sedimentation profiles of octylglucoside-solubilized microsomal (○) and synaptosomal (●) [^{3}H]-AMPA binding sites in sucrose density gradients. Approximately 30,000 specific d.p.m., determined with 25 nM [^{3}H]-AMPA, were added to the gradients and the amount of protein was adjusted accordingly. The data show the specific [^{3}H]-AMPA binding activity, expressed in d.p.m., in each of the gradient aliquots. The arrow indicates the position of haemoglobin in fraction 17 in all of the gradients (sedimentation coefficient = 4.5 S).

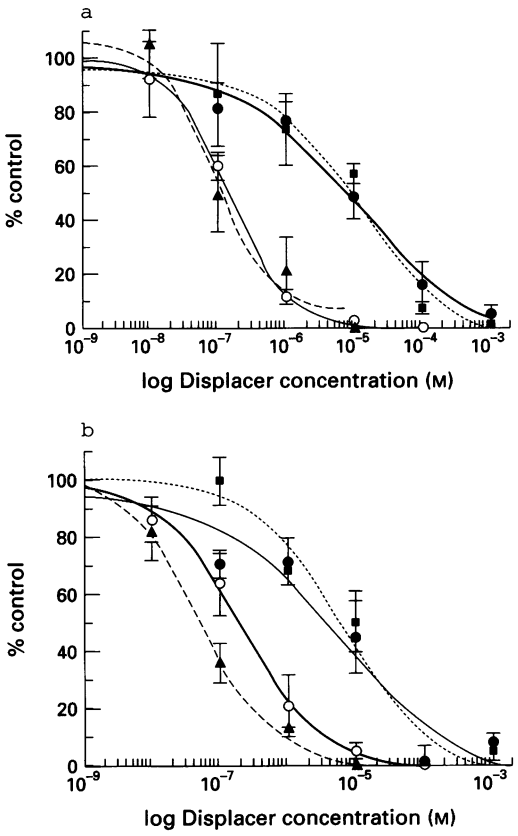

Figure 5 Competition binding curves for [^{3}H]-AMPA to (a) extensively freeze-thaw-washed synaptosomal membrane (P_2B) and (b) microsome fragments by (○) CNQX, (■) L-glutamate, (●) kainate and (△) quisqualate. The data are normalized to 100% in the absence of displacing drug and are the mean ± s.e.mean of at least 4 separate experiments for each displacer. The IC_{50} values are given in the text.

late, 0.05 ± 0.01 μM; L-glutamate, 6.3 ± 2.0 μM. The IC_{50} values for synaptosomal membranes were: CQNX, 0.15 ± 0.01 μM; kainate, 14.4 ± 2.5 μM; quisqualate, 0.09 ± 0.05 μM; L-glutamate, 11.9 ± 3.6 μM. Data for the displacement curves are the means and s.e.mean values of 3–4 experiments each using hippocampal tissue pooled from two rats.

The hydrodynamic properties of the microsomal and synaptosomal [^{3}H]-AMPA binding sites were analysed by sucrose density centrifugation (Figure 6). Within the resolution of the technique, both sets of sites yielded identical sedimentation profiles indicating equivalent sizes, therefore implying that the microsomal sites comprise fully assembled multimeric receptor complexes.

Western blot analysis of the microsomal and synaptosomal fractions was performed using an anti-peptide antibody specific for GluR1 subunit of AMPA receptors. Immunoblots were taken from SDS-PAGE gels run using identical amounts of protein from each fraction. Under exactly the same labelling conditions, darker labelling was observed in the microsomal fraction and qualitatively, the intensity of the HRP-labelled blots were consistent with the [^{3}H]-AMPA binding data in that the microsomal fraction stained more intensely than the synaptosomal fraction. Furthermore, the GluR1 labelled band was the same Mr value in both fractions indicating that the GluR1 polypeptide in the microsomal fraction was glycosylated to the same extent as the synaptosomal membrane subunits. These data suggest that for GluR1 subunits at least, the intracellular and plasma membrane sites have been subjected to the same extent of post-translational processing.

Discussion

The data presented here indicate that a high proportion of [^{3}H]-AMPA binding in the hippocampus is located intracellularly, predominantly in the microsomal fraction. The distribution of [^{3}H]-kainate sites, however, shows a markedly different profile with binding confined mainly to the synaptosomal fraction with little intracellular binding.

Active postsynaptic regions comprise mainly dendritic spines which are approximately 1 μm long protrusions from the body of the dendrite. A possible complicating factor that could influence the interpretation of the results obtained in this study is the contamination of microsomal fraction with postsynaptic synaptosomal membranes originating from these spine structures. During tissue homogenization it is possible that some spines sheared from their parent dendrites could separate from the presynaptic terminal and reseal to form vesicles including the postsynaptic membrane. Vesicles of this size might then migrate to the microsomal rather than the synaptosomal fraction and give an inaccurate distribution of [^{3}H]-AMPA binding.

Two main criteria were used to exclude any artefactual re-

sults of this kind. Firstly, in contrast to the structures observed in the synaptosomal membrane fraction, the micrographs showed no evidence for characteristic postsynaptic densities in the microsomal fraction. Secondly, the subcellular distribution of [^{3}H]-kainate binding was markedly different from that for [^{3}H]-AMPA. High affinity [^{3}H]-kainate binding sites, comprising the KA-1 and KA-2 and/or GluR 5, 6 and 7 subunits, are extremely abundant in areas of the hippocampus, particularly in the CA3 pyramidal cells. However, for [^{3}H]-kainate binding to provide a good control it is crucial that at least a proportion of kainate receptors must be located at the postsynaptic membrane.

Evidence for presynaptic kainate receptors in the hippocampus has come from the observations that high affinity [^{3}H]-kainate binding appears in the CA3 region of the hippocampus between post-natal days 7 and 21, exactly matching the development of the mossy fibres which are axonal projections from the dentate granule cells (Miller *et al.*, 1990). Similarly, a dramatic decrease in high affinity [^{3}H]-kainate binding in the CA3 region occurs if dentate granule cells are lesioned with the resultant degeneration of the mossy fibres, which terminate on the dendritic trees of the CA3 pyramidal cells (Represa *et al.*, 1987). On the other hand, strong evidence for postsynaptic kainate receptors in the hippocampus comes from: (1) high levels of the kainate receptor subunit cDNA KA-1 in CA3 pyramidal cells (Wisden & Seeburg, 1993); (2) the retention of high affinity [^{3}H]-kainate binding in denervated dentate gyrus molecular layer (Ulas *et al.*, 1990); and (3) direct immunocytochemical evidence for exclusively dendritic localizations of GluR 5, 6 and 7 subunits in primate hippocampus with no immunoreactivity in the soma (Good *et al.*, 1992). Thus high affinity [^{3}H]-kainate binding represents a valid marker for synaptic membranes and the lack of [^{3}H]-kainate activity in the microsomal fraction provides good evidence that cross-contamination of the subcellular fractions is not a major factor in the unusual distribution of [^{3}H]-AMPA binding.

The immunohistochemical localizations of the AMPA receptor subunits GluR1–GluR4 have been studied by several different groups. In rat brain sections the regional distribution of antibodies raised against GluR1–GluR4 AMPA receptor subunits were differentially localized within neuronal cell bodies and processes in cerebral cortex, basal ganglia, limbic system, thalamus, cerebellum and brainstem and the precise patterns and cellular localizations appear to be unique for each antibody (Martin *et al.*, 1993). Ultrastructurally, the subunit immunoreactivities were present within cell bodies, dendrites and dendritic spines of specific subsets of neurones and, in the case of GluR1 and GluR4, in some populations of astrocytes (Martin *et al.*, 1993). In rat hippocampal cultures the same group showed that the GluR1 antibody stained all neurones, with the somata and dendrites, but not axons, showing high levels of immunoreactivity. Variable degrees of staining observed in different individual neurones between the dendritic spines and the dendritic shafts with highly punctate hot spots visible, many of which corresponded to synapses. Essentially identical distributions were also observed with a GluR2/3 antipeptide antibody (Craig *et al.*, 1993). Other equally elegant immunohistochemical studies have also shown that the AMPA receptor subunits GluR1–GluR4 are located in postsynaptic densities, the associated dendritoplasm and in the cytoplasm of the soma (Petralia & Wenthold, 1992; Eshhar *et al.*, 1993; Molnar *et al.*, 1993).

Nonetheless, a major constraint on these immunohistochemical investigations is the lack of pharmacological characterization and quantitative data about the actual numbers of receptors present in each of the cellular and subcellular locations. These latter questions have been addressed by the alternative and complementary techniques employed in the present study. My results indicate that in excess of 70% of AMPA receptors are located inside the neurone, predominantly in the microsomal fraction with less than 30% of receptors located in the plasma membrane at any given time. The pharmacological and biochemical characteristics of the synaptosomal membrane and microsomal AMPA receptors appear to be very similar with no marked differences in their [^{3}H]-AMPA binding affinities or displacement profiles.

Although the precise subunit composition of the population of intracellular receptors was not addressed in this study, the abundance of the GluR1 subunit shown in Figure 7 is consistent with the distribution of [^{3}H]-AMPA binding. Furthermore, the similarity of the hydrodynamic profiles of the receptor complexes together with the identical M_r values of the GluR1 subunits from synaptosomal membranes and microsomes suggest that polypeptide glycosylation is complete by the time the protein is inserted into the microsome and that no significant additional glycosylation of GluR1 occurs upon insertion into the synaptosomal membrane.

Long-term potentiation (LTP) in the rat hippocampus is an established model system for the study of the mechanisms of learning and memory (Bliss & Collingridge, 1993). AMPA receptors are integral to LTP since they mediate the synaptic responses that are enhanced. The pivotal role of AMPA receptors in LTP is well documented (Bliss & Collingridge, 1993). While the decrease in the efficacy of synaptic transmission mediated by AMPA receptors could be achieved by a variety of mechanisms at transcriptional, translational and post-translational levels, one attractive mechanism by which rapid onset alterations in the efficacy of synaptic responses could be brought about is the recruitment of additional AMPA receptors from an intracellular pool. These recruited receptors may be identical to those already in the synaptosomal membrane and act solely by increasing the physical number of AMPA receptors available at the postsynaptic membrane. Alternatively, receptors recruited to the synaptosomal membrane could have different subunit compositions and/or different phosphorylation states from those already present. Such differences could lead to a higher affinity for L-glutamate thereby increasing the sensitivity of the postsynaptic membrane. The results from the present study suggest the former of these two possibilities.

The presence of intracellular AMPA receptor subunits in immunohistochemical studies has been explained in terms of normal protein synthesis, transport and degradation. While the results presented in this study are compatible with this hypothesis, the quantitative comparison of the synaptosomal and intracellular AMPA receptor populations, together with the markedly different results obtained for [^{3}H]-kainate binding sites suggests that either AMPA receptor turnover is very rapid or that they are stored in the microsomes, possibly for rapid insertion into the synaptic membrane. With the currently

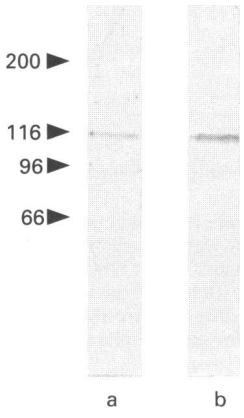

Figure 7 Western blots of (a) synaptosomal and (b) microsomal fractions with the anti-peptide antibody Ab9T directed against GluR1. The same amount of protein (10 μg) was loaded into each lane and the SDS-PAGE gel was run and blotted as described in the Methods. The arrows indicate the positions of BioRad high molecular weight standards.

available data it is not possible to distinguish between these two possibilities and definitive analysis of these dynamic processes will require time course experiments.

I am grateful to the Wellcome Trust and the MRC for financial support.

References

BARNES, J.M. & HENLEY, J.M. (1992). Molecular characteristics of excitatory amino acid receptors. *Prog. Neurobiol.*, **39,** 113–133.

BARNES, J.M. & HENLEY, J.M. (1993). Autoradiographic distribution of glutamatergic ligand binding sites in *Xenopus* brain – evidence for intracellular [^{3}H]-AMPA binding sites. *Brain Res.*, **626,** 259–264.

BAUDE, A., MOLNAR, E., LATAWIEC, D., MCILHINNEY, R.A.J. & SOMOGYI, P. (1994). Synaptic and nonsynaptic localization of the GluR1 subunit of the AMPA-type excitatory amino acid receptor in the rat cerebellum. *J. Neurosci.*, **14,** 2830–2843.

BLISS, T. & COLLINGRIDGE, G. (1993). A synaptic model of memory: long-term potentiation in the hippocampus. *Nature*, **361,** 31–39.

CHOI, D.W. (1992). Excitotoxic cell death. *J. Neurobiol.*, **23,** 1261–1276.

CRAIG, A.M., BLACKSTONE, C.D., HUGANIR, R.L. & BANKER, G. (1993). The distribution of glutamate receptors in cultured rat hippocampal neurons – postsynaptic clustering of AMPA-selective subunits. *Neuron*, **10,** 1055–1068.

ESHHAR, N., PETRALIA, R.S., WINTERS, C.A., NIEDZIELSKI, A.S. & WENTHOLD, R.J. (1993). The segregation and expression of glutamate receptor subunits in cultured hippocampal neurons. *Neuroscience*, **57,** 943–964.

GOOD, P.F., HUNTLEY, G.W., ROGERS, S.W., HEINEMANN, S.F. & MORRISON, J.H. (1993). Organization and quantitative analysis of kainate receptor subunit GluR5–7 immunoreactivity in monkey hippocampus. *Brain Res.*, **624,** 347–353.

HENLEY, J.M. & BARNARD, E.A. (1989). Kainate receptors in *Xenopus* central nervous system: solubilisation with n-octyl-β-*D*-glucopyranoside. *J. Neurochem.*, **52,** 31–37.

HENLEY, J.M., AMBROSINI, A., RODRIGUEZ-ITHURRALDE, D., SUDAN, H., BRACKLEY, P., KERRY, C., MELLOR, I., ABUTIDZE, K., USHERWOOD, P.N.R. & BARNARD, E.A. (1992). Purified unitary kainate/alpha-amino-3-hydroxy-5-methylisooxazole-propionate (AMPA) and kainate/AMPA/N-methyl-D-aspartate receptors with interchangeable subunits. *Proc. Natl. Acad. Sci. U.S.A.*, **89,** 4806–4810.

HOLLMANN, M. & HEINEMANN, S. (1994). Cloned glutamate receptors. *Annu. Rev. Neurosci.*, **17,** 31–108.

HONORÉ, T. & DREJER, J. (1988). Chaotropic ions affect the conformation of quisqualate receptors in rat cortical membranes. *J. Neurochem.*, **51,** 457–461.

HONORÉ, T. & NIELSEN, M. (1985). Complex structure of quisqualate-sensitive glutamate receptors in rat cortex. *Neurosci. Lett.*, **54,** 27–32.

MAENO, H., JOHNSON, E.M. & GREENGARD, P. (1971). Subcellular distribution of adenosine 3′,5′-monophosphate dependent protein kinase in rat brain. *J. Biol. Chem.*, **246,** 134–142.

MARTIN, L.J., BLACKSTONE, C.D., LEVEY, A.I., HUGANIR, R.L. & PRICE, D.L. (1993). AMPA glutanate receptor subunits are differentially distributed in rat brain. *Neuroscience*, **53,** 327–358.

MILLER, L.P., JOHNSON, A.E., GELHARD, R.E. & INSEL, T.R. (1990). The ontogeny of excitatory amino acid receptors in rat forebrain-II. Kaininc acid receptors. *Neuroscience*, **35,** 41–51.

MOLNAR, E., BAUDE, A., RICHMOND, S.A., PATEL, P.B., SOMOGYI, P. & MCILHINNEY, R.A.J. (1993). Biochemical and immunocytochemical characterization of antipeptide antibodies to a cloned GluR1 glutamate receptor subunit – cellular and subcellular distribution in the rat forebrain. *Neuroscience*, **53,** 307–326.

PETRALIA, R.S. & WENTHOLD, R.J. (1992). Light and electron immunocytochemical localization of AMPA-selective glutamate receptors in the rat brain. *J. Com. Neurol.*, **318,** 329–354.

REPRESSA, A., TREMBLAY, E. & BEN-ARI, Y. (1987). Kainate binding sites in the hippocampal mossy fibres: localisation and plasticity. *Neuroscience*, **20,** 739–748.

RODRÍGUEZ DE LORES ARNAIZ, G. & PELLEGRINO DE IRALDI, A. (1985). Subcellular fractionation. In *Neuromethods Series 1: General Neurochemical Techniques*, pp. 19–67. Clifton, New Jersey: Humana Press.

SEEBURG, P.H. (1993). The molecular biology of mammalian glutamate receptor channels. *Trends Neurosci.*, **16,** 359–365.

SOMMER, B. & SEEBURG, P.H. (1992). Glutamate receptor channels – Novel properties and new clones. *Trends Pharmacol. Sci.*, **13,** 291–296.

SMITH, A.L. & MCILHINNEY, R.A.J. (1992). Effects of acromelic acid A on the binding of [3H]-kainic acid and [3H]-AMPA to rat brain synaptic plasma membranes. *Br. J. Pharmacol.*, **105,** 83–86.

SWOPE, S.L., MOSS, S.J., BLACKSTONE, C.D. & HUGANIR, R.L. (1992). Phosphorylation of ligand-gated ion channels – a possible mode of synaptic plasticity. *FASEB J.*, **6,** 2514–2523.

ULAS, J., MONAGHAN, D.T. & COTMAN, C.W. (1990). Kainate receptors in the rat hippocampus – a distribution and time course of changes in response to unilateral lesions of the entorhinal cortex. *J. Neurosci.*, **10,** 2352–2362.

WENTHOLD, R.J., YOKOTANI, N., DOI, K. & WADA, K. (1992). Immunochemical characterisation of the non-NMDA glutamate receptor using subunit specific antibodies. *J. Biol. Chem.*, **267,** 501–507.

WISDEN, W. & SEEBURG, P.H. (1993). A complex mosaic of high-affinity kainate receptors in rat brain. *J. Neurosci.*, **13,** 3582–3598.

(Received November 22, 1994
Revised February 6, 1995
Accepted February 9, 1995)

British Journal of Pharmacology (1995) 115, 302-306

Autoradiography of P_{2x} ATP receptors in the rat brain

[1]Vladimir J. Balcar, Yi Li, Suzanne Killinger & *Maxwell R. Bennett

Department of Anatomy and Histology and *Department of Physiology, The University of Sydney, Australia

1 Binding of a P_{2x} receptor specific radioligand, [^{3}H]-α,β-methylene adenosine triphosphate ([^{3}H]-α,β-MeATP) to sections of rat brain was reversible and association/dissociation parameters indicated that it consisted of two saturable components. Non-specific binding was very low (<7% at 10 nM ligand concentration).

2 The binding was completely inhibited by suramin (IC_{50} ~ 14–26 μM) but none of the ligands specific for P_{2y} receptors such as 2-methylthio-adenosine triphosphate (2-methyl-S-ATP) and 2-chloro-adenosine triphosphate (2-Cl-ATP) nor 2-methylthio-adenosine diphosphate (2-methyl-S-ADP) a ligand for the P_2 receptor on blood platelets ('P_{2T}' type) produced strong inhibitions except for P_1,P_4-di(adenosine-5')tetraphosphate ($A_{p4}A$).

3 Inhibitors of Na^+,K^+-dependent adenosine triphosphatase (ATPase) ouabain, P_1-ligand adenosine and an inhibitor of transport of, respectively, adenosine and cyclic nucleotides, dilazep, had no effect.

4 The highest density of P_{2x} binding sites was found to be in the cerebellar cortex but the binding sites were present in all major brain regions, especially in areas known to receive strong excitatory innervation.

Keywords: Purinoceptors; ATP; suramin; fast neurotransmission; central synapses; cerebellum; excitatory pathways

Introduction

Actions of ATP and other purine derivatives in peripheral and central nervous tissues have been well documented (Burnstock, 1990; Edwards *et al.*, 1992; Evans *et al.*, 1992). The changes in membrane potentials evoked by ATP and related compounds are mediated by receptors ('purinoceptors') classified as P_1, responding preferentially to adenosine, and P_2, sensitive to ATP. P_2 receptors have been further subdivided into P_{2x} and P_{2y} types (Burnstock & Kennedy, 1985). Excitatory purinoceptors of P_{2x}-type have long been known to participate in synaptic responses of smooth muscle cells (Burnstock, 1990) but the presence of P_{2x}-mediated synaptic currents on parasympathetic neurones and in the CNS has been demonstrated only relatively recently (Evans *et al.*, 1992; Edwards *et al.*, 1992).

Furthermore, although Michel & Humphrey (1993) have described the binding of a P_{2x}-specific ligand, [^{3}H]-α,β-methylene adenosine triphosphate ([^{3}H]-α,β-MeATP, Bo & Burnstock, 1990) to membranes prepared from rat cerebral cortex, only a brief report (Bo & Burnstock, 1994) has so far appeared on the binding of [^{3}H]-α,β-MeATP to sections of frozen rat brain. In the present study, we have been using autoradiographic techniques and thaw-mounted sections of frozen rat brain to investigate further the distribution and characteristics of the [^{3}H]-α,β-MeATP binding sites in the rat CNS.

Methods

Rats (Sprague-Dawley, either sex, minimum 12 weeks old) were purchased from the Office of Laboratory Animal Services, The University of Sydney. The animals were anaesthetized with 5% halothane in N_2O/O_2 (65:35) and decapitated. The brains were submerged in Tissue-Tek (Miles Corporation, U.S.A.) and rapidly frozen with a mixture of dry ice and ethanol. The sections (20 μm thick) were prepared on a cryostat, thaw-mounted on gelatine-coated slides and stored at −20°C. The experiments were done usually on the following day but, occasionally, sections stored for longer periods of time (up to five weeks) were used with no observable deleterious effects on the binding.

Binding studies and autoradiography were carried out with previously described techniques (Young & Kuhar, 1979) with some modifications (Greenamyre *et al.*, 1985; Li & Balcar, 1994; Balcar *et al.*, 1995). Sections were preincubated at room temperature (22–25°C) for 30 min with two changes of medium (50 mM Tris-HCl, pH 7.4, used throughout), then incubated in the presence of ^{3}H-labelled [^{3}H]-α,β-MeATP at 2–4°C for 40 min, washed, dried and either extracted with 0.25 M NaOH for liquid scintillation counting (LCS) and protein determination (Lowry *et al.*, 1951) or exposed for 8 days against Amersham Hyperfilm-^{3}H. The film was evaluated by quantitative densitometry and the density of silver grains was converted into fmol of [^{3}H]-α,β-MeATP bound per mg of tissue, using tritium standards (^{3}H-Microscales, Amersham International plc. U.K., RPA 506) which had been exposed simultaneously with the tissue sections (Li & Balcar, 1994; Balcar *et al.*, 1995).

In the experiments studying association, sections were incubated with 10 nM [^{3}H]-α,β-methylene ATP for 0, 0.5, 1, 2, 4, 8, 16, 32 and 64 min. In the dissociation studies, the sections, first labelled with [^{3}H]-α,β-methylene ATP, were transferred into a fresh medium containing 100 μM non-radioactive α,β-methylene ATP and incubated for 0, 0.5, 1, 2, 4, 8, 16, 32 and 64 min. Two sections per time-point were used and the binding was expressed as radioactivity (LSC) per mg protein (Li & Balcar, 1994).

The data were processed by Inplot and Prism software from GraphPad (San Diego, U.S.A.). The values of IC_{50}s (± s.e. mean) were obtained either from the equation $B = B_o/(1 + [I]/IC_{50})$ where B stands for binding, B_o represents the value of control, [I] is the concentration of inhibitor and IC_{50} is [I] which produces 50% inhibition (McGonigle & Molinoff, 1989) or from its more complex form which included the Hill slope coefficient n_H (Levitzki, 1980). Logarithmic forms of the above equations (Triggle & Triggle, 1976) were used to construct the curves describing the relationship between binding and inhibitor concentration (B versus log [I]). The values of IC_{50}s and n_H computed by Prism from the logarith-

[1] Author for correspondence at: Department of Anatomy and Histology, Anderson Stuart Building F13, The University of Sydney NSW 2006, Australia.

mic equations were very similar to those produced by Inplot using the non-transformed equations. However, the data shown are those obtained with Inplot because they included the values of controls in the computations which was not possible when the logarithmic equations were used. If the inclusion of n_H in the equation produced a fit which was significantly better than that resulting from the simpler relationship ($P<0.02$, by F-test, Munson & Rodbard, 1980), n_H was considered significantly different from unity.

The association and dissociations constants were computed by Inplot using previously published equation (Li & Balcar, 1994) or its analogous versions for dissociation and corresponding two-component models. The two-component model was used when the F-test (Munson & Rodbard, 1980) indicated that it fitted the data significantly better ($P<0.02$) than the simpler model.

[^{3}H]-α,β-MeATP, TRQ 6450, 28 Ci mmol^{-1} was purchased from Amersham International, non-radioactive α,β-MeATP, ouabain and adenosine came from Sigma Chemical Co. (St. Louis, U.S.A.) and 2-methylthio-adenosine triphosphate (2-Me-S-ATP), 2-methylthio-adenosine diphosphate (2-Me-S-ADP), 2-chloro-adenosine triphosphate (2-Cl-ATP) and P_1,P_4-di(adenosine-5')tetraphosphate (Ap_4A) were purchased from Research Biochemicals International, Natick, Ma (U.S.A.). Dilazep was a gift from Boehringer Mannheim (Germany).

Results

Binding of 10 nM [^{3}H]-α,β-methylene ATP was reversible with a biphasic time course of association (two-component association exponential fitted the data significantly better, $P<0.01$ by F-test). The smaller component (30% of the binding) reached the half-maximum level at 2.4 ± 0.5 min ($\tau_{1/2}$, mean ± s.e. mean) while the remaining component (70%) had a significantly lower association rate ($\tau_{1/2}$ = 23.8 ± 5.2 min). The opposite was the case for the rates of dissociations ($\tau_{1/2}$ = 0.35 ± 0.09 and 4.6 ± 2.2, respectively, 68 *v.* 32% of the total binding). Preliminary studies using several ligand concentrations (0.5–80 nM) favoured a two-component model ($P<0.005$ by F-test, Munson & Rodbard, 1980) with ^1K_D in the 5–20 nM range and $^2K_D>$ 80 nM. At 10 nM ligand concentration about 95% of [^{3}H]-α,β-MeATP binding was specific (Table 1).

The specific binding of [^{3}H]-α,β-MeATP was not significantly inhibited by the Na^+,K^+-dependent ATPase inhibitor ouabain (100 μM), by P_1 ligand adenosine (10 μM) and by an inhibitor of adenosine (Davies & Chen Chow, 1984) and cyclic AMP (Balcar *et al.*, 1988) uptake, the vasodilator dilazep (10 μM). The binding was, however, completely inhibited by suramin, a broad-spectrum antagonist of P_2 receptors (Dunn & Blakeley, 1988). The half-maximum inhibitions (IC_{50}) were 18.8 ± 1.7 (21.4 ± 1.3) and 20.2 ± 1.5 (21.5 ± 2.7) μM, and the Hill slopes (n_H) were 1.49 ± 0.14 (1.38 ± 0.06) and 1.40 ± 0.14 (1.27 ± 0.11); (mean ± s.e. mean) in coronal and horizontal brain sections, respectively. These were determined at 2, 10, 25, 75, 150 and 300 μM inhibitor concentrations either by quantitative autoradiography or (the values in parentheses) by LSC. Three sections (autoradiography) or one section (LSC) were used at each inhibitor concentration. More extensive studies (Figure 1 and Table 2) indicated that the values of IC_{50}'s varied from 14–17 μM in the cerebellar cortex to 23–26 μM in the thalamus and neostriatum. None of the typical ligands for P_{2y} receptors (2-Me-S-ATP at 50 μM, 2-Cl-ATP at 10 μM) or for the 'P_{2y}' binding site on blood platelets (2-Me-S-ADP, 50 μM) caused significant inhibitions. The only exception was $A_{p4}A$ (Table 1) which is thought to interact preferentially with P_{2y} receptors *in vivo* (Pintor *et al.*, 1993).

The density of binding sites was highest in the cerebellar cortex (Figure 2 and Table 1). In the forebrain all grey-matter regions displayed about equal average density of P_{2x} binding sites (Figure 2 and Table 1). The binding, however, was unevenly distributed within the regions. In sensorimotor areas of the neocortex, the P_{2x} binding sites were found to be particularly abundant in the lamina four while in the hippocampus the most prominently marked area was the molecular layer of CA_4 (Figure 2). In the thalamus, the geniculate nuclei were labelled more strongly than the rest of the grey matter (not shown). The most densely labelled regions in the brainstem were central grey (Figure 2 and Table 1) and the superficial and intermediate zones of the superior colliculus (Figure 2). White matter was not labelled.

Table 1 Densitometric analysis of [^{3}H]-α,β-methylene ATP binding to horizontal and coronal sections of rat brain

A *Horizontal sections*

Brain region	*Density of binding* (fmol mg^{-1} tissue) *Total*	*Nonspecific*
Forebrain	386 ± 5	25 ± 1
Cerebral neocortex	396 ± 5	26 ± 1
Hippocampus	454 ± 5	29 ± 2
Molecular layer of DG	486 ± 8	28 ± 0
Septal nuclei	312 ± 8	26 ± 4
Neostriatum	349 ± 5	26 ± 5
Thalamus	431 ± 7	24 ± 3
Cerebellum	544 ± 11	29 ± 3
Cerebellar cortex	702 ± 13	38 ± 7
Deep cerebellar nuclei	525 ± 9	13 ± 5
Central grey of the midbrain	503 ± 13	28 ± 3
Whole section	415 ± 6	26 ± 0

B *Coronal sections*

Brain region	*Density of binding* (fmol mg^{-1} tissue) *Total*	*Nonpsecific*
Cerebral neocortex	371 ± 13	21 ± 5
Hippocampus	456 ± 16	32 ± 9
Thalamus	397 ± 18	28 ± 4
Whole section	376 ± 13	22 ± 7

The autoradiograms were scanned by Personal Densitometer (Molecular Dynamics) and evaluated as described earlier (Li & Balcar, 1994). The values are means ± s.e.mean obtained from 6 sections (specific binding, 10 nM [^{3}H]-α,β-MeATP) or three sections (nonspecific binding, in the presence of 100 μM nonradioactive α,β-MeATP). DG stands for dentate gyrus.

Discussion

There have been two recent reports of cloning and expression of P_{2x} receptors (Valera *et al.*, 1994; Brake *et al.*, 1994). A putative member of the P_{2x} family of ligand-gated ion channels from vas deferens was activated by 2-Me-S-ATP but not by α,β-MeATP (Brake *et al.*, 1994) while another P_{2x}-like ion channel from the same tissue responded about equally well to both 2-Me-S-ATP and α,β-MeATP (Valera *et al.*, 1994). Northern blotting studies indicated that the former (Brake *et al.*, 1994) but not the latter (Valera *et al.*, 1994) P_{2x} 'receptor' was expressed in the CNS. Results like those serve to emphasize the importance of autoradiographic studies which have a potential to link, and make meaningful, such diverse sets of information as the location in brain regions and ligand/ion-selectivities, respectively, of pharmacologically identifiable receptor-channel complexes. However, as the cloning/expression experiments and binding/autoradiography studies commenced only very recently, it may not yet be feasible to relate one to another. We shall, therefore, keep the discussion within the context of other binding and autoradiographic studies and we shall focus on the methodological aspects.

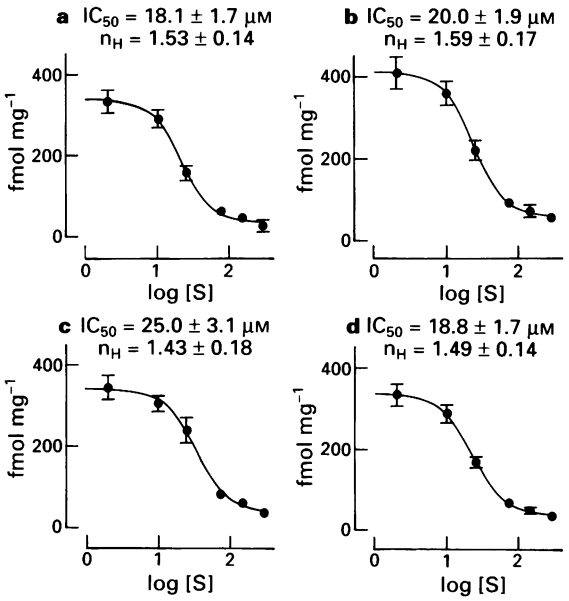

Figure 1 Effect of suramin (S) on the binding of 10 nM [^{3}H]-α,β-MeATP in coronal sections of rat brain. Binding of 10 nM [^{3}H]-α,β-MeATP (total, i.e. not corrected for non-specific binding which was <5%) is expressed as fmol of [^{3}H]-α,β-MeATP bound per mg of tissue wet weight. The values of constants (IC_{50} and n_H) were estimated by analysing inhibition curves over six concentrations of inhibitor: 2, 10, 25, 75, 150 and 300 μM. Individual points are means ± s.d. obtained from three sections incubated in parallel. (a) Cerebral neocortex; (b) hippocampus; (c) thalamus; (d) total section.

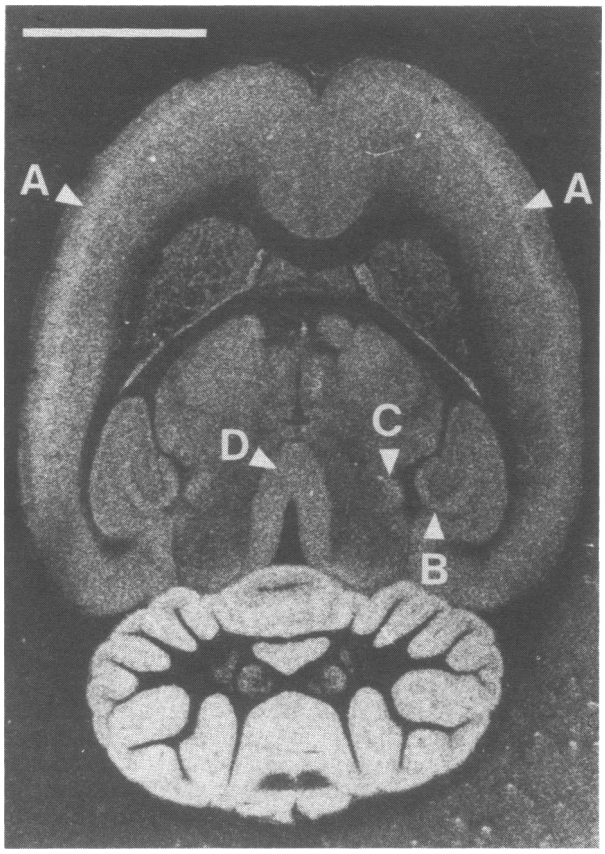

Figure 2 Autoradiography of the binding of 10 nM [^{3}H]-α,β-MeATP in horizontal section of rat brain. Arrows point to the lamina four of the parietal (sensorimotor) neocortex (A), the molecular layer of the dentate gyrus (B), superior colliculus (C) and the central grey of the mesencephalon (D). Nonspecific binding was not detectable under the same conditions of exposure and illumination. Bar = 5 mm.

Table 2 Inhibition of [^{3}H]-α,β-methylene ATP binding to suramin and ATP analogues in horizontal sections in horizontal sections of rat brain

A *Suramin*

Brain region	IC_{50} ± s.e.mean (μM)	n_H ± s.e.mean
Forebrain	21.4 ± 1.3	1.56 ± 0.14
Cerebral neocortex	18.4 ± 2.0	1.64 ± 0.17
Hippocampus	21.5 ± 1.2	1.57 ± 0.14
Molecular layer of DG	19.5 ± 1.5	1.44 ± 0.16
Septal nuclei	19.7 ± 2.0	1.63 ± 0.27
Neostriatum	23.6 ± 1.7	1.68 ± 0.19
Thalamus	26.3 ± 2.4	1.54 ± 0.20
Cerebellum	15.7 ± 1.7	1.28 ± 0.18
Cerebellar cortex	14.8 ± 1.3	1.38 ± 0.18
Deep cerebellar nuclei	15.6 ± 1.0	1.91 ± 0.23
Central grey of the midbrain	20.1 ± 3.0	1.34 ± 0.27
Whole section	20.2 ± 1.5	1.40 ± 0.14

B *Effect of ATP analogues*

	Binding (fmol mg^{-1} tissue)		
Brain region	*Control*	*Ap_4A* (10 μM)	*% Inhibition*
Cerebral neocortex	539 ± 7	309 ± 12	43 ± 2
Hippocampus	539 ± 4	231 ± 20	57 ± 4
Neostriatum	464 ± 14	219 ± 24	53 ± 5
Thalamus	620 ± 17	333 ± 16	44 ± 3
Central grey of the midbrain	573 ± 28	230 ± 18	60 ± 3
Cerebellum	708 ± 13	192 ± 22	73 ± 3
Cerebellar cortex	1015 ± 13	311 ± 42	69 ± 4

No effect: 2-Me-S-ATP (50 μM), 2-Me-S-ADP(50 μM), 2-Cl-ADP (10 μM)

Autoradiograms were scanned by Personal Densitometer (Molecular Dynamics) and evaluated as described earlier (Li & Balcar, 1994). As in Figure 1, the values are (a) means ± s.e.mean obtained by analysing inhibition curves over six concentrations of inhibitor ([S]): 2, 10, 25, 75, 150 and 300 μM or (b) means ± s.e.mean obtained by averaging values from three sections incubated in parallel. The values were not corrected for non-specific binding.

There are strong similarities between the present results and those obtained by Michel & Humphrey (1993) in homogenates of rat cerebral cortex and by Bo & Burnstock (1994) in sections of frozen rat brain. For example, the proportion of non-specific binding is very low and both association/dissociation studies and concentration dependence suggest the presence of two components of binding with high and low affinities, respectively (cf. also $n_H > 1$ in all experiments with suramin). However, in some aspects, the present data differ from the published ones. Thus while we have found strong sensitivity of [^{3}H]-α,β-MeATP binding to suramin, a P_{2y}-preferring ATP analogue 2-Me-S-ATP appeared to be a much weaker inhibitor of [^{3}H]-α,β-MeATP binding in the frozen brain sections than in cortical homogenates (Michel & Humphrey, 1993). In fact, although the P_{2y}-ligand $A_{p4}A$ (Pintor *et al.*, 1993) caused a small inhibition, two other compounds, 2-Cl-ATP and 2-Me-S-ADP produced no measurable effects at concentrations at which they can interact with P_{2y} in the CNS and PNS and 'P_{2T}' sites on blood platelets, respectively (Cusack & Hourani, 1982; 1990; Burnstock, 1990; Barnard *et al.*, 1994).

The most striking difference, however, was between the relative levels of binding in the cerebellar cortex observed by Bo & Burnstock (1994) and in the present experiments, respectively. While the former study did not find that either the cerebellar cortex or any other region of the CNS displayed particularly high density of [^{3}H]-α,β-MeATP binding sites, our experiments indicated that the cerebellar cortex was the most densely labelled structure in the brain. There are important differences between our experimental techniques and those of Bo & Burnstock (1994) and, indeed, we found

much lower binding (~50%) when we used an experimental protocol similar to that of Bo & Burnstock (1994) which includes washing for several minutes at the end of the incubation (by contrast, washing of sections in our experiments is completed in <10 s, Li & Balcar, 1994; Balcar *et al.*, 1995). However, general loss of bound ligand during the washing of sections cannot fully account for the absence of difference between the densities of binding in the cerebellar cortex and forebrain, respectively, and, we favour another interpretation. While evaluating standard curves (optical densities on the Hyperfilm-^{3}H exposed against the radioactive standards containing known amounts of ^{3}H) we noticed that at higher levels of ^{3}H (equivalent to >500 fmol mg^{-1} tissue) the optical density increased much more slowly after three or four weeks than during the first two weeks of exposure. In fact, while the relationship between optical densities and the standards was linear after shorter exposures, more complex standard curves had to be used for exposures longer than three weeks. The longer exposures would, therefore, tend to obscure the presence of more heavily labelled regions which would merely reach the maximum ('saturation') optical density earlier than the rest of the section, final outcome being a relatively uniform distribution of optical densities over the whole autoradiographic image, perhaps with the exception of a few very lightly labelled structures (Bo & Burnstock, 1994). Thus it may be difficult to relate the present data, expressed in fmol mg^{-1} tissue calculated from optical densities obtained after an 8-day exposure to those of Bo & Burnstock (1994) which are given in optical densities after a two-month exposure. Our data, however, may be easier to relate to the distribution of P_{2x} receptors in various brain regions.

Until recently, ATP had been considered a 'modulator' of central synaptic transmission acting predominantly via G-protein linked receptors (Barnard *et al.*, 1994). However, α,β-MeATP does not act on such receptors (Barnard *et al.*, 1994). Rather, P_{2x} receptors function by 'ligand-gating' of ion-specific channels (Barnard *et al.*, 1994). In short, the ATP action on central P_{2x} receptors fits the description of a fast excitatory signalling in the brain.

In fact, some of the regions with high densities of P_{2x} binding sites coincide with target areas of major excitatory fibre tracts: perforant pathway into the hippocampus, specific thalamocortical projections, several excitatory pathways into the central grey of the midbrain, the fibres of the optic tract into the lateral geniculate nucleus and superior colliculus and, especially, mossy, climbing and parallel fibres in the cerebellum.

Consequently, the P_{2x}-mediated synaptic currents demonstrated in medial habenula (Edwards *et al.*, 1992) and the widespread occurrence of [^{3}H]-α,β-MeATP binding shown by the present study imply that no hypothesis relating ATP to the function of excitatory synapses in the central nervous system should disregard contributions from fast-acting ligand-gated receptor-channel complexes of P_{2x} type.

In conclusion, autoradiographic studies revealed the presence of ATP-specific receptor-binding sites of P_{2x} type in many parts of the rat central nervous system. The pattern of distribution of the binding sites is consistent with P_{2x} receptors playing an important part in the process of ATP-mediated fast chemical transmission at central excitatory synapses.

References

BALCAR, V.J., GUNDLACH, A.L. & JOHNSTON, G.A.R. (1988). High affinity uptake of cAMP in rat brain: inhibition by coronary vasodilators dilazep and hexobendine. *Neurochem. Int.*, **12**, 19–24.

BALCAR, V.J., LI, Y. & KILLINGER, S. (1995). Effects of L-*trans*-pyrrolidine-2,4-dicarboxylate and L-*threo*-3-hydroxyaspartate on the binding of [^{3}H]L-aspartate, [^{3}H]α-amino-3-hydroxy-5-methyl-4-isoxazole propionate (AMPA), [^{3}H]DL-*(E)*-2-amino-4-propyl-5-phosphono-3-pentenoate (CGP 39653), [^{3}H]6-cyano-7-nitroquinoxaline-2,3-dione (CNQX) and [^{3}H]kainate studied by autoradiography in rat forebrain. *Neurochem. Int.*, **26**, 155–164.

BARNARD, E.A., BURNSTOCK, G. & WEBB, T.E. (1994). G protein-coupled receptors for ATP and other nucleotides: a new receptor family. *Trends Pharmacol. Sci.*, **15**, 67–70.

BO, X. & BURNSTOCK, G. (1990). High- and low-affinity binding sites for [^{3}H]-α,β-methylene ATP in rat urinary bladder membranes. *Br. J. Pharmacol.*, **101**, 291–296.

BO, X. & BURNSTOCK, G. (1994). Distribution of [^{3}H]α,β-methylene ATP binding sites in rat brain and spinal cord. *Neuroreport*, **5**, 1601–1604.

BRAKE, A.J., WAGENBACH, M.J. & JULIUS, D. (1994). New structural motif for ligand-gated ion channels defined by ionotropic ATP receptor. *Nature*, **371**, 519–523.

BURNSTOCK, G. (1990). Overview. Purinergic mechanisms. In *Biological Actions of Extracellular ATP*. ed. G.R. Dubyak & J.S. Fedan pp. 1–18. New York: The New York Academy of Sciences.

BURNSTOCK, G. & KENNEDY, C. (1985). Review. Is there a basis for distinguishing two types of P_2-purinoceptor? *Gen. Pharmacol.*, **16**, 433–440.

CUSACK, N.J. & HOURANI, S.M. (1982). Competitive inhibition by adenosine 5'-triphosphate of the actions on human platelets of 2-chloro-adenosine 5'-diphosphate, 2-azido-adenosine 5'-diphosphate and 2-methylthio-adenosine 5'-diphosphate. *Br. J. Pharmacol.*, **77**, 329–333.

CUSACK, N.J. & HOURANI, S.M. (1990). Subtypes of P_2-purinoceptors. Studies with analogues of ATP In *Biological Actions of Extracellular ATP*. ed. Dubyak, G.R. & Fedan, J.S. pp. 172–181. New York: The New York Academy of Sciences.

DAVIES, L.P. & CHEN CHOW, S. (1984). Effect of some potent adenosine uptake inhibitors on benzodiazepine binding in the CNS. *Neurochem. Int.*, **6**, 185–189.

DUNN, P.M. & BLAKELEY, A.G.H. (1988). Suramin: a reversible P_2-purinoceptor antagonist in the mouse vas deferences. *Br. J. Pharmacol.*, **93**, 243–245.

EDWARDS, F.A., GIBB, A.J. & COLQUHOUN, D. (1992). ATP receptor-mediated synaptic currents in the central nervous system. *Nature*, **359**, 144–147.

EVANS, R.J., DERKACH, V. & SURPRENANT, A. (1992). ATP mediates fast synaptic transmission in mammalian neurons. *Nature*, **357**, 503–505.

GREENAMYRE, J.T., OLSEN, J.M.M., PENNEY, J.R. & YOUNG, A.B. (1985). Autoradiographic characterization of N-acetyl-D-aspartate-, quisqualate- and kainate-sensitive glutamate binding sites. *J. Pharmacol. Exp. Ther.*, **233**, 254–263.

LEVITZKI, A. (1980). Quantitative aspects of ligand binding to receptors. In *Cellular Receptors for Hormones and Neurotransmitters*. ed. Schulster, D. & Levitzki, A. pp. 10–28. Chichester: John Wiley & Sons.

LI, Y. & BALCAR, V.J. (1994). The Na^+-dependent binding of [^{3}H]L-aspartate in thaw-mounted sections of rat forebrain. *Exp. Brain Res.*, **97**, 415–422.

LOWRY, O.H., ROSEBROUGH, N.J., FARR, A.L. & RANDALL, R.J. (1951). Protein measurements with the Folin phenol reagent. *J. Biol. Chem.*, **193**, 265–275.

MCGONIGLE, P. & MOLINOFF, P.B. (1989). Quantitative aspects of drug-receptor interactions. In *Basic Neurochemistry, 4th edition*, ed. Siegel, G., Agranoff, G.B., Albers, R.W. & Molinoff, P.B. pp. 183–202. New York: Raven Press.

MICHEL, A.D. & HUMPHREY, P.P.A. (1993). Distribution and characterization of [^{3}H]α,β-methylene ATP binding sites in the rat. *Naunyn-Schmied. Arch. Pharmacol.*, **348**, 608–617.

MUNSON, P.J. & RODBARD, D. (1980). LIGAND: a versatile computerized approach for characterization of ligand-binding systems. *Anal. Biochem.*, **107**, 220–239.

PINTOR, J., DIAZ-REY, M.A. & MIRAS-PORTUGAL, M.T. (1993). $A_{p4}A$ and ADP-β-S binding to P_2 purinoceptors present on rat brain synaptic terminals. *Br. J. Pharmacol.*, **108**, 1094–1099.

TRIGGLE, D.J. & TRIGGLE, C.R. (1976). Quantitative aspects of ligand-receptor interactions. In *Chemical Pharmacology of the Synapse*, ed. Triggle, D.J. & Triggle, C.R. pp. 129–232. New York: Academic Press.

VALERA, S., HUSSY, N., EVANS, R.J., ADAMI, N., NORTH, R.A., SURPRENANT, A. & BUELL, G. (1994). A new class of ligand gated ion-channel defined by P_{2x} receptor for extracellular ATP. *Nature*, **371**, 516–519.

YOUNG, W.S. III & KUHAR, M.J. (1979). A new method for receptor autoradiography: [^{3}H]opioid receptors in rat brain. *Brain Res.*, **179**, 255–270.

(Received December 5, 1994
Revised January 24, 1995
Accepted January 25, 1995)

British Journal of Pharmacology (1995) 115, 307-315

Involvement of multiple protein kinase C isozymes in the ACTH secretory pathway of AtT-20 cells

B.W. McFerran, *D.J. MacEwan & [1]†S.B. Guild

Molecular Endocrinology Unit, School of Biological and Medical Sciences, University of St Andrews, St Andrews; *Department of Biochemistry, University of Glasgow, Glasgow G12 8QQ and †Bute Medical Building, School of Biological and Medical Sciences, University of St Andrews, St Andrews KY16 9TS

1 The mouse AtT-20/D16-16 anterior pituitary tumour cell line was used as a model system for the study of protein kinase C (PKC)-mediated enhancement of calcium- and guanine nucleotide-evoked adrenocorticotrophin (ACTH) secretion.

2 A profile of the PKC isozymes present in AtT-20 cells was obtained by Western blotting analysis and it was found that AtT-20 cells express the α, β, ε and ζ isoforms of PKC.

3 PKC isozymes were activated by the use of substances reported to activate particular isoforms of the enzyme. The effects of these substances were investigated in both intact and electrically-permeabilized cells. Phorbol 12-myristate 13-acetate (PMA, $EC_{50} = 1 \pm 0.05$ nM, which activates all isozymes of PKC, except the ζ isozyme), thymeleatoxin (TMX, $EC_{50} = 10 \pm 0.5$ nM, which activates the α, β and γ isozymes) and 12-deoxyphorbol 13-phenylacetate 20-acetate (dPPA, $EC_{50} = 3 \pm 0.5$ nM, a β_1-selective isozyme activator) all stimulated ACTH secretion from intact cells in a concentration-dependent manner. Maximal TMX stimulated ACTH secretion was of a similar degree to that obtained in response to PMA but maximal dPPA-stimulated ACTH secretion was only 60–70% of that obtained in response to PMA or TMX.

4 Calcium stimulated ACTH secretion from electrically-permeabilized cells over the concentration-range of 100 nM to 10 μM. PMA (100 nM), TMX (100 nM) but not dPPA (100 nM) enhanced the amount of ACTH secreted at every concentration of calcium investigated. PMA (100 nM) and TMX (100 nM) significantly enhanced ACTH secretion in the effective absence of calcium (i.e. where the free calcium concentration is 1 nM).

5 GTP-γ-S stimulated ACTH secretion from permeabilized cells in a concentration-dependent manner with a threshold of 1 μM. PMA (100 nM), TMX (100 nM) but not dPPA (100 nM) increased the amount of ACTH secretion evoked by every concentration of GTP-γ-S investigated.

6 The PKC inhibitor, chelerythrine chloride (10 μM), blocked the PMA (100 nM)-evoked enhancement of calcium- and GTP-γ-S-stimulated ACTH secretion but did not significantly alter calcium- or GTP-γ-S-evoked secretion itself.

7 The present paper indicates that AtT-20 cells express multiple isoforms of PKC and that these act at different sites in the secretory pathway for ACTH secretion. The α and ε isozymes of PKC can act distal to calcium entry to modulate the ability of increased cytosolic calcium concentrations to stimulate ACTH secretion. This site of action is either at the level of, or at some stage distal to, a GTP-binding protein which mediates the effects of calcium upon ACTH secretion. The β isozyme of PKC may act at a stage early in the secretory pathway to regulate the cytosolic calcium concentration.

Keywords: Phorbol esters; protein kinase C; calcium; G-protein; anterior pituitary; ACTH

Introduction

Adrenocorticotrophin (ACTH) secretion from anterior pituitary corticotrophs is stimulated by hypothalamic neuropeptides including corticotrophin-releasing factor (CRF) and arginine vasopressin (AVP) (Axelrod & Reisine, 1984; Antoni, 1986). The stimulus-secretion coupling mechanisms mediating the stimulatory effects of these agents on ACTH secretion remain to be completely clarified. CRF acts via the adenosine 3':5'-cyclic monophosphate (cyclic AMP)-dependent protein kinase (PKA) pathway in both anterior pituitary corticotrophs (Aguilera *et al.*, 1983) and in a tumour cell line of the anterior pituitary, AtT-20, which consists of a homogeneous population of ACTH-secreting cells (Luini *et al.*, 1985; Guild & Reisine, 1987). Cyclic AMP has a dual action both enhancing calcium influx into corticotrophs and potentiating the effect of such an increment in cytosolic calcium upon the secretory apparatus (Luini *et al.*, 1985; Guild *et al.*, 1986; Guild & Reisine, 1987; Guild, 1991). The nature of AVP's signal-transduction pathway is less clear than that of CRF but AVP does activate protein kinase C (PKC) in pituitary corticotrophs (Abou-Samra *et al.*, 1986). Although AtT-20 cells do not express functional vasopressin receptors, stimulants of PKC have been shown to alter cytosolic calcium concentrations and stimulate ACTH release from these cells (Reisine & Guild, 1987). Activation of these two protein kinases influences the calcium messenger system and both have a 'pre-' and 'post-' calcium site of action to regulate calcium influx and the effect of particular cytosolic calcium concentrations upon ACTH secretion (Reisine & Guild, 1987; Guild, 1991; McFerran & Guild, 1994).

The mechanisms linking changes in cytosolic calcium concentration to changes in hormone secretion remain largely unknown but it has been suggested that a late stage in stimulus-secretion coupling may involve a direct regulation of exocytosis by guanosine 5'-triphosphate (GTP)-binding proteins, dubbed G_E by Gomperts and his co-workers (Gomperts, 1990). Such a GTP-binding protein has been reported to mediate the effects of calcium upon the secretory apparatus in AtT-20 cells and may be a target for regulation by PKA (Guild, 1991) and PKC (McFerran & Guild, 1994).

[1] Author for correspondence.

Interestingly, PKA and PKC act through distinct mechanisms to influence cytosolic calcium concentrations in AtT-20 cells (Reisine & Guild, 1987; Reisine, 1989) and both have distinct 'post-calcium' sites of action at a late stage in the secretory process, potentiating the effects of calcium and guanine nucleotides upon the secretory apparatus (Guild, 1991; McFerran & Guild, 1994).

Several isoforms of PKC have been identified and characterized (for review, see Hug & Sarre, 1993) and have been specifically implicated as having distinct roles in signal-transduction, stimulus-secretion coupling and growth (Housey *et al.*, 1988; Naor *et al.*, 1989; Akita *et al.*, 1990; Pai *et al.*, 1991; Sharma *et al.*, 1991; Kiley *et al.*, 1992; Leli *et al.*, 1992). In view of the evidence supporting the presence and active role in secretion of pharmacologically distinct forms of PKC in rat anterior pituitary cells (Thomson *et al.*, 1993), the present study profiled the PKC isozymes present in AtT-20 cells and used activators of isozymes of PKC (Ryves *et al.*, 1991) to investigate the contribution of these PKC isoforms to the regulation of ACTH secretion. In particular, the possibility that different PKC isozymes are responsible for the 'pre-' and 'post-' calcium sites of regulation of ACTH secretion was targeted. The distinction between such a 'pre-' and 'post-' calcium site of action required a direct manipulation of the intracellular environment. This was provided by the use of electrically permeabilized cells, a technique which has been used previously to gain access to the cytosol in AtT-20 cells (Guild, 1991). The present paper indicates that AtT-20 cells express multiple isoforms of PKC and that these act at different sites in the secretory pathway for ACTH.

Methods

Culture of AtT-20 cells

Cells of the mouse AtT-20/D16-16 pituitary tumour were grown and subcultured in Dulbecco's Modified Eagle's Medium (DMEM) (glucose 4.5 g l^{-1}) supplemented with 10% (w:v) foetal calf serum as previously described (Reisine, 1984). Cells to be used in ACTH release experiments from intact cells were plated in 24 well (16 mm diameter) multiwell plates (Costar, U.S.A.) at an initial cell density of 10^5 cells/well and were used 5–7 days after subculturing (80–90% confluency). Cells to be used in experiments involving electrically permeabilized cells and the Western blot studies were plated in 75 cm^2 flasks (Nunc, Gibco, U.K.) at an initial density of 2×10^6 cells/flask and were used 7–9 days after subculturing (80–90% confluency).

Preparation of AtT-20 cells for ACTH release experiments

Intact cell preparations The culture medium was removed, cells adhering to the substrate in each well were washed 3 times with 1 ml of DMEM supplemented with 0.1% (w:v) bovine serum albumin (DMEM/BSA) and then incubated for 1 h in 1 ml of fresh DMEM/BSA at 37°C in a humidified atmosphere of 10% CO_2 in air. The DMEM/BSA was then decanted and replaced with 1 ml of fresh DMEM/BSA.

Permeabilized cell preparations The culture medium was removed and the cells liberated from the substrate by trypsin (0.05% w:v)/EDTA (1 mM). The cells were washed twice by centrifugation (200 *g*, 5 min)/resuspension in a balanced salt solution of the following composition (mM): NaCl 145, KCl 5.6, $CaCl_2$ 2, $MgCl_2$ 0.5, glucose 5.6, HEPES 5, sodium ascorbate 0.5, BSA 0.1% (w:v), pH 7.4. After washing, the cells were suspended at a density of 10^6 cells ml^{-1} in this buffer and incubated for a further 30 min at 37°C. The cell suspension was then centrifuged (200 *g*, 5 min) and the cell pellet washed twice by resuspension/centrifugation (200 *g*, 5 min) in the standard permeabilization buffer of the following composition (mM):potassium glutamate 129, PIPES (potassium salt) 20, glucose 5, ATP 5, EGTA 5, $MgCl_2$ 1, BSA 0.1% (w:v), pH 6.6. The cells were finally resuspended in this buffer at a density of 10^7 ml^{-1} and electrically permeabilised by subjection to intense electric fields of brief duration (Knight & Baker, 1982). The optimum permeabilisation parameters of 10 discharges of 2500 V cm^{-1}, previously determined (Guild, 1991), were adopted in these experiments.

Activation of PKC isozymes by drugs

PKC isozymes were activated by the use of substances previously reported to activate particular isoforms of the enzyme (Ryves *et al.*, 1991). The activators of PKC used in these experiments were; phorbol 12-myristate 13-acetate (PMA) (which activates all isozymes of PKC, except the ζ isozyme and is used here as non-selective, general activator of the enzyme); thymeleatoxin (TMX) (which reportedly activates the α, β and γ isozymes) and 12-deoxyphorbol 13-phenylacetate 20-acetate (dPPA) (a reportedly β_1-selective isozyme activator).

Measurement of stimulated ACTH secretion from intact cells

The ability of activators of protein kinase C to stimulate ACTH secretion from intact AtT-20 cells remaining attached to the culture dishes was measured as previously described (Reisine & Guild, 1987; McFerran & Guild, 1994). Briefly, drugs were added to the 1 ml of DMEM/BSA bathing the cells in the wells of the culture dishes. Zero time samples were taken at this point and the remaining cells incubated for 1 h at 37°C in a humidified atmosphere of 10% CO_2 in air. In each experiment, sextuplicate samples were run for each condition. Incubations were terminated by removing the DMEM/BSA bathing the cells, centrifugation (10,000 *g*, 20 s) of this sample and the removal of the supernatant. The ACTH content of the supernatant was measured by radioimmunoassay.

Measurement of calcium- and guanine nucleotide-stimulated ACTH from permeabilized AtT-20 cells

The standard protocol for the determination of ACTH secretion from permeabilized AtT-20 cells was as follows: permeabilized cells were suspended at a cell density of 10^5 cells ml^{-1} in either a series of calcium-EGTA buffers chosen to give a free calcium concentration in the range 1 nM–10 μM for experiments investigating the effects of calcium or in a permeabilization buffer with a free calcium concentration of 1 nM for experiments investigating the effects of guanine nucleotides and prepared as previously described (Guild, 1991). At this point, the zero time samples were centrifuged (200 *g*, 5 min) and an aliquot of the supernatant was stored for subsequent measurement of ACTH content. The cell suspensions were incubated at 37°C for 30 min at which point incubations were terminated by centrifugation (200 *g*, 5 min) and removal of the supernatant. The ACTH content was measured by radioimmunoassay.

In each experiment, sextuplicate samples were run for each condition. The modifications to this standard protocol which were made to permit the measurement of the effect of the protein kinase activators upon calcium- and guanine nucleotide-stimulated ACTH secretion from permeabilized AtT-20 cells are described in the legends to the figures.

Detection of PKC isoforms in AtT-20 cells and rat tissues

Adult male Sprague-Dawley rats were killed by excess CO_2 inhalation and dissections performed. The tissues were

Dounce homogenized in 2 vol ice-cold homogenisation buffer of the following composition: Tris.HCl 20 mM (pH 7.4), ethyleneglycol-*bis*-(β-aminoethyl ether) *N,N,N',N'*-tetraacetic acid (EGTA) 1 mM, dithiothreitol 1 mM, Na F 100 mM, supplemented with a protease inhibitor cocktail of aprotinin, trypsin inhibitor, benzamidine, leupeptin and 4-amidinophenyl-methanesulphonylfluoride at 100, 100, 250, 100 and 100 $\mu g\ ml^{-1}$ respectively (Boehringer Mannheim Corp., Indianapolis, IN, U.S.A.). The homogenates were then boiled for 10 min in sample buffer (5% wt:vol sodium dodecylsulphate, Tris 125 mM, glycerol 10% wt:vol, 2-mercaptoethanol 2% vol:vol, bromophenyl blue 2 $\mu l\ ml^{-1}$ (final concentrations)). AtT-20 cell monolayers were washed once and scraped into ice-cold phosphate buffered saline and treated with sample buffer as described above.

Sodium dodecylsulphate polyacrylamide gel electrophoresis (SDS–PAGE) followed by Western analysis was performed essentially as previously described (Strulovici *et al.*, 1989; 1991) with the following modifications: blocking of non-specific protein binding sites was performed by 5% (wt:vol) non-fat dried milk (in phosphate buffered saline without calcium or magnesium salts supplemented with 0.5% (vol:vol) Tween-20); specific antibody binding was visualised using protein-A horseradish peroxidase followed by enhanced chemiluminescence and autoradiographic exposure. Antisera were used at the following dilutions 1:50 anti-PKC-α, anti-PKC-β and anti-PKC-γ; 1:100 anti-PKC-ε 1:1000 anti-PKC-η and 2 $\mu g\ ml^{-1}$ anti-PKC-δ and anit-PKC-ζ.

The effect of the PKC inhibitor chelerythrine chloride upon the PMA enhancement of calcium- and guanine nucleotide-stimulated ACTH secretion

The PKC inhibitor, chelerythrine chloride (Herbert *et al.*, 1990) was used to investigate whether the observed PMA enhancement of calcium and GTP-γ-S-stimulated ACTH secretion was via a stimulation of PKC. This was tested by measuring calcium- and GTP-γ-S-stimulated ACTH secretion from permeabilized cells in the presence and absence of PMA (100 nM) and the effect of co-incubation with chelerythrine chloride (10 μM).

Radioimmunoassay

The radioimmunoassay for ACTH was performed as previously described (Reisine, 1984). [^{125}I]-ACTH for radioimmunoassay use was produced using the lodogen reagent (1,3,4,6-tetrachloro-3α, 6α-diphenylglycoluril) which was first described as a reagent for iodination by Fraker & Speck (1978). The amount of ACTH released was expressed as the amount present at the end of the specified incubation period less the amount present at zero time.

Statistics

In each experiment sextuplicate determinations for each experimental condition were made and each experiment was repeated three times, on different days. ACTH secretion is expressed as the means ± s.e.mean of the mean values from these 3 separate experiments. Statistical significance was tested by the use of ANOVA tests with Scheffe's *F*-test *post hoc* analysis. A P value <0.05 was considered significant and is the definition of the term used here. Two-way ANOVA was used to test for a statistically significant interaction between two groups (i.e. the concentration-response curves to calcium ions or GTP-γ-S in the presence and absence of PKC activators) and the significance of these interactions is specified.

Materials

The following substances (with their sources) were used: DMEM, foetal calf serum and trypsin/EDTA were purchased from GIBCO, UK.; human ACTH antiserum and human ACTH for standards was the gift of the National Hormone and Pituitary programme, Baltimore, MD, USA. Polyclonal antisera to PKC-α, -β, γ, ε were prepared as previously described (Strulovici *et al.*, 1989; 1991). Other antibodies were purchased from Gibco BRL (Gaithersburg, MD, U.S.A.; PKC-δ and ζ) or was a kind gift from Dr Harald Mishak (NIH, Bethesda, MD, U.S.A.; PKC-η). Immobilon-P polyvinylidene difluoride microporous transfer membranes were obtained from Millipore, Bedford, MA, U.S.A. Protein A conjugated to peroxidase was bought from Calbiochem, San Diego, CA, U.S.A. Enhanced chemiluminescence materials were purchased from Amersham International, Aylesbury, UK.; phorbol 12-myristate 13-acetate was purchased from Sigma UK., thymeleatoxin, 12-deoxyphorbol 13-phenylacetate 20-acetate and chelerythrine chloride were purchased from Calbiochem-NovaBiochem UK. Guanosine 5'-O-(3-thiotriphosphate) (GTP-γ-S) was obtained from Boehringer Mannheim, UK. All other chemicals used were of Analar grade and readily commercially available.

Results

The isoforms of PKC present in AtT-20 cells identified by Western blotting studies

PKC isoform immunoreactivity of whole AtT-20 cells was detected by Western analysis using isoform-specific antisera (Figure 1). Detectable amounts of PKCs α, β, ε and ζ were observed whereas γ, δ and η could not be detected under the

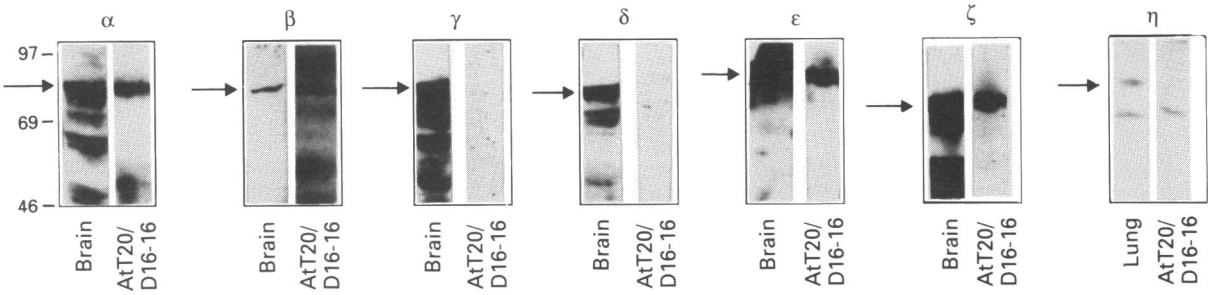

Figure 1 Protein kinase C (PKC) isoform immunoreactivity of whole AtT-20 cells: one dimensional SDS/PAGE followed by Western analysis with PKC isoform-specific anti-sera was performed as described in the Methods section. Each left lane contains whole male rat brain (lung for η) as positive controls for the detectable immunoreactivities. Analysis of whole AtT-20 cells revealed detectable amounts of PKCs α, β, ε and ζ whereas γ, δ and η could not be detected under the present conditions, even after gross autoradiographic overexposure. The arrows indicate the specific bands at the expected molecular masses (approximately 80 kDa (α, β, γ); 76 kDa (δ); 90 kDa (ε); 72 kDa (ζ); 82 kDa (η) which were eradicated by co-incubation of the antisera with the corresponding peptide antigen complexed to bovine serum albumin (100 $\mu g\ ml^{-1}$). The results are representative of at least two separate determinations. For abbreviations in this and subsequent legends, see text.

present conditions, although standards were readily detected in the same experiments.

The effect of PKC activators upon ACTH secretion from intact AtT-20 cells

PMA (1 pM–100 nM) stimulated a concentration-dependent ($EC_{50} = 1 \pm 0.1$ nM, $n = 3$) increase in ACTH secretion (significant ($P<0.05$) at concentrations of PMA of 100 pM and above) (Figure 2). These results are consistent with previous studies showing an activation of PKC by PMA to stimulate ACTH secretion from AtT-20 cells (Reisine & Guild, 1987; Reisine, 1989; McFerran & Guild, 1994). TMX (10 pM–1 μM) and dPPA (10 pM–1 μM) both stimulated ACTH secretion in a concentration-dependent manner ($EC_{50} = 10 \pm 0.5$ nM ($n = 3$) and 3 ± 0.5 nM ($n = 3$) respectively and significant ($P<0.05$) at concentrations of TMX and dPPA of 10 pM and above) (Figure 2). Maximal TMX-stimulated ACTH secretion was of a similar degree to that obtained in response to PMA but maximal dPPA-stimulated ACTH secretion was only 60–70% of that obtained in response to PMA or TMX (Figure 2).

The effect of PKC activators upon calcium-evoked ACTH secretion from permeabilized AtT-20 cells

Calcium-evoked ACTH secretion from permeabilized AtT-20 cells was dependent upon the concentration of free calcium in the permeabilization medium (Figure 3). Calcium stimulated ACTH secretion in a concentration-dependent manner between 100 nM and 10 μM (significant ($P<0.05$) stimulation at concentrations of free calcium ions of 1 μM and above). Co-incubation with PMA (100 nM) resulted in an enhanced ACTH secretion at all concentrations of calcium investigated (Figure 3a). PMA (100 nM) enhanced ACTH secretion in the effective absence of calcium (i.e. where the free calcium concentration is 1 nM). A comparison of the calcium ion concentration-response curves in the presence and absence of PMA (100 nM) by two way ANOVA test revealed that calcium ion-stimulated ACTH secretion was significantly ($P<0.0001$) enhanced by co-incubation with PMA (100 nM) and furthermore there was a significant ($P<0.0017$) interac-

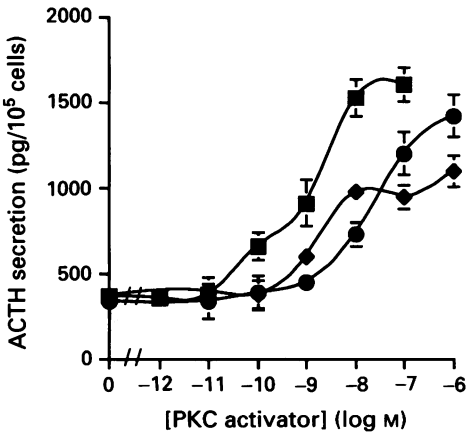

Figure 2 Effect of protein kinase C (PKC) activators on ACTH secretion from intact AtT-20 cells. Intact cells were incubated for 1 h in Dulbecco's Modified Eagles Medium with 0.1% bovine serum albumin (DMEM/BSA) supplemented with the indicated concentration of PMA (■), TMX (●) and dPPA (◆) as described in the Methods. The results are expressed as the mean ± s.e. mean from 3 separate experiments. Absence of error bars indicate that they lie within the symbol used. PMA (1 pM–100 nM, significant ($P<0.05$) at concentrations of PMA of 100 pM and above), TMX (10 pM–1 μM, significant ($P<0.05$) at concentrations of 10 pM and above) and dPPA (10 pM–1 μM, significant ($P<0.05$) at concentrations of 10 pM and above) stimulated ACTH secretion in a concentration-dependent manner.

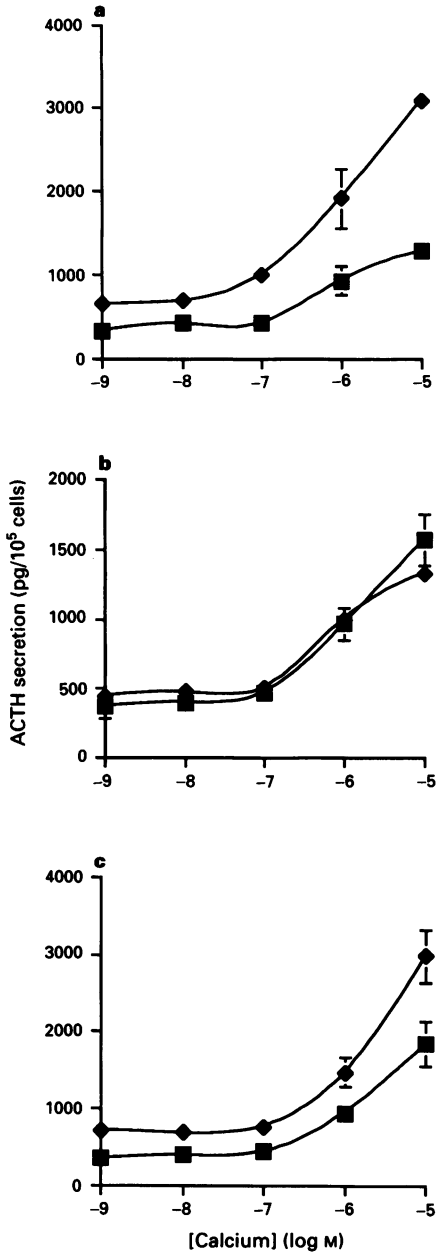

Figure 3 Effect of protein kinase C activators on calcium-dependent ACTH secretion from permeabilized AtT-20 cells. Permeabilized cells were incubated, as described in the Methods, in standard permeabilization medium containing various proportions of calcium and EGTA, such that the indicated concentrations of free calcium resulted, either in the presence (●) or absence (■) of PMA (100 nM, a), dPPA (100 nM, b) or TMX (100 nM, c). The results are expressed as the mean ± s.e. mean from 3 separate experiments. Absence of error bars indicate that they lie within the symbol used. Calcium stimulated ACTH secretion in a concentration-dependent manner between 100 nM and 10 μM (significant ($P<0.05$) stimulation at concentrations of free calcium ions of 1 μM and above). (a) A comparison of the calcium ion concentration-response curves in the presence and absence of PMA (100 nM) by two way ANOVA test revealed that calcium ion-stimulated ACTH secretion was significantly ($P<0.0001$) enhanced by co-incubation with PMA (100 nM) and furthermore there was a significant ($P<0.0017$) interaction between PMA and calcium ions upon ACTH secretion. (b) Co-incubation with dPPA (100 nM) did not significantly alter calcium-evoked ACTH secretion at any concentration of calcium investigated. (c) A comparison of the calcium ion concentration-response curves in the presence and absence of TMX (100 nM) by two way ANOVA test revealed that calcium ion-stimulated ACTH secretion was significantly ($P<0.0001$) enhanced by co-incubation with TMX (100 nM) and furthermore there was a significant ($P<0.0377$) interaction between TMX and calcium ions upon ACTH secretion.

tion between PMA and calcium ions upon ACTH secretion. In contrast to PMA, co-incubation with dPPA (100 nM) did not significantly alter calcium-evoked ACTH secretion at any concentration of calcium investigated (Figure 3b). Co-incubation with TMX (100 nM) resulted in an enhanced ACTH secretion at all concentrations of calcium investigated (Figure 3c). A comparison of the calcium ion concentration-response curves in the presence and absence of TMX (100 nM) by two way ANOVA test revealed that calcium ion-stimulated ACTH secretion was significantly ($P<0.0001$) enhanced by co-incubation with TMX (100 nM) and furthermore there was a significant ($P<0.0377$) interaction between TMX and calcium ions upon ACTH secretion.

The effect of PKC activators upon guanine nucleotide-evoked ACTH secretion from permeabilized AtT-20 cells

GTP-γ-S stimulated ACTH secretion, in the absence of calcium, in a concentration-dependent manner (significant ($P<0.05$) stimulation at concentrations of GTP-γ-S of 10 μM and above) (Figure 4). PMA (100 nM) stimulated ACTH secretion in the absence of GTP-γ-S and enhanced the stimulated ACTH secretion at every concentration of the nucleotide investigated (Figure 4a). A comparison of the GTP-γ-S concentration-response curves in the presence and absence of PMA (100 nM) by two way ANOVA test revealed that GTP-γ-S-stimulated ACTH secretion was significantly ($P<0.0001$) enhanced by co-incubation with PMA (100 nM) but that there was no significant interaction between GTP-γ-S and PMA. In contrast, co-incubation with dPPA (100 nM) did not alter GTP-γ-S-evoked ACTH secretion at any concentration of the nucleotide investigated (Figure 4b). Co-incubation with TMX (100 nM) significantly enhanced ACTH secretion at all concentrations of GTP-γ-S investigated (Figure 4c) in a manner similar to, but to a lesser extent than, that observed with PMA. A comparison of the GTP-γ-S concentration-response curves in the presence and absence of TMX (100 nM) by two way ANOVA test revealed that GTP-γ-S-stimulated ACTH secretion was significantly ($P<0.0001$) enhanced by co-incubation with TMX (100 nM) but that there was no significant interaction between GTP-γ-S and TMX. Thus PMA and TMX but not dPPA enhanced both calcium- and guanine nucleotide-evoked ACTH excretion.

The effect of higher concentrations of dPPA upon calcium- and guanine nucleotide-evoked ACTH secretion from permeabilised AtT-20 cells

The effect of concentrations of dPPA greater than 100 nM (shown to be supra-maximal upon ACTH secretion from intact cells, Figure 1) upon calcium ion (10 μM)- and GTP-γ-S (100 μM)-evoked ACTH secretion was investigated (Table 1). dPPA did not significantly enhance control, calcium ion- or GTP-γ-S-evoked secretion at a concentration of 100 nM (consistent with the results presented in Figures 3 and 4). However, dPPA did significantly ($P<0.05$) enhance calcium ion-evoked secretion and GTP-γ-S-evoked secretion significantly ($P<0.05$) at a concentration of 10 μM (Table 1). These results indicate that high concentrations of dPPA, much greater than those reported for its selective action upon the β1 isoform of PKC, can enhance both calcium ion- and GTP-γ-S-evoked ACTH secretion from permeabilized AtT-20 cells.

The effect of chelerythrine chloride upon calcium- and guanine nucleotide-evoked ACTH secretion from permeabilised AtT-20 cells

Calcium stimulated ACTH secretion in a concentration-dependent manner between 1 nM and 10 μM (significant ($P<0.05$) stimulation at concentrations of free calcium ions of 1 μM and above) (Figure 5a). Co-incubation with PMA (100 nM) resulted in an enhanced ACTH secretion at all concentrations of calcium investigated (Figure 5a). The PKC inhibitor, chelerythrine chloride (10 μM) did not significantly

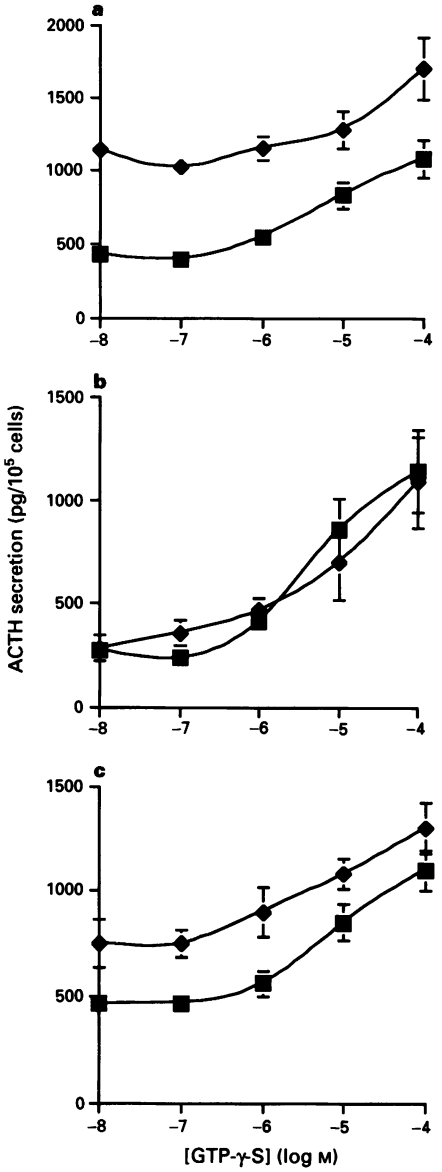

Figure 4 Effect of PMA, TMX and dPPA on GTP-γ-S-stimulated ACTH secretion from permeabilized AtT-20 cells. Permeabilized cells were incubated, as described in the Methods, in standard permeabilization medium supplemented with the indicated concentration of GTP-γ-S either in the presence (●) or absence (■) of PMA (100 nM, a), dPPA (100 nM, b) or TMX (100 nM, c). The results are expressed as the mean ± s.e. mean from 3 separate experiments. Absence of error bars indicate that they lie within the symbol used. GTP-γ-S stimulated ACTH secretion, in the absence of calcium, in a concentration-dependent manner (significant ($P<0.05$) stimulation at concentrations of GTP-γ-S of 10 μM and above). (a) A comparison of the GTP-γ-S concentration-response curves in the presence and absence of PMA (100 nM) by two way ANOVA test revealed that GTP-γ-S-stimulated ACTH secretion was significantly ($P<0.0001$) enhanced by co-incubation with PMA (100 nM) but that there was no significant interaction between GTP-γ-S and PMA (b) Co-incubation with dPPA (100 nM) did not alter GTP-γ-S-evoked ACTH secretion at any concentration of the nucleotide investigated. (c) A comparison of the GTP-γ-S concentration-response curves in the presence and absence of TMX (100 nM) by two way ANOVA test revealed that GTP-γ-S-stimulated ACTH secretion was significantly ($P<0.0001$) enhanced by co-incubation with TMX (100 nM) but that there was no significant interaction between GTP-γ-S and TMX.

alter the ACTH secretion obtained at any concentration of calcium (Figure 5a) but inhibited the PMA-evoked enhancement of ACTH secretion at all of the calcium concentrations (Figure 5a). A comparison of the calcium ion concentration-response curves in the presence and absence of PMA (100 nM), chelerythrine chloride (10 μM) or the combination of PMA and chelerythrine chloride by two way ANOVA test revealed that calcium ion-stimulated ACTH secretion was significantly ($P<0.0001$) enhanced by co-incubation with PMA (100 nM) but not by chelerythrine chloride or the PMA and chelerythrine chloride combination.

GTP-γ-S stimulated ACTH secretion in the absence of calcium in a concentration-dependent manner with a threshold of 1 μM (Figure 5b). PMA (100 nM) stimulated ACTH secretion in the absence of GTP-γ-S and significantly enhanced GTP-γ-S-stimulated ACTH secretion (Figure 5b). Chelerythrine chloride (10 μM) did not significantly alter GTP-γ-S-stimulated ACTH secretion but inhibited the PMA (100 nM)-evoked enhancement of GTP-γ-S-evoked ACTH secretion. (Figure 5b). A comparison of the GTP-γ-S concentration-response curves in the presence and absence of PMA (100 nM), chelerythrine chloride (10 μM) or the combination of PMA and chelerythrine chloride by two way ANOVA test revealed that GTP-γ-S-stimulated ACTH secretion was significantly ($P<0.0001$) enhanced by co-incubation with PMA (100 nM) but not by chelerythrine chloride or the PMA and chelerythrine chloride combination. These results indicate that PMA acts via an activation of PKC to evoke the observed enhancement of calcium- and guanine nucleotide-evoked ACTH secretion in this system.

Discussion

The present study adds to the considerable body of evidence supporting an involvement of PKC in the stimulation of ACTH release from both the normal corticotroph (Abou-Samra *et al.*, 1986) and the model for this secretory cell, the AtT-20 cell line (Reisine & Guild, 1987; Reisine, 1989; McFerran & Guild, 1994). PKC interacts with the ACTH secretory pathway at multiple points as shown by its 'pre-' and 'post-' calcium site of action to regulate calcium influx and the effect of particular cytosolic calcium concentrations upon ACTH secretion (Reisine & Guild, 1987; McFerran & Guild, 1994). Since PKC is now known to consist of several different isoenzymes (for review, see Hug & Sarre, 1993), the question arose as to whether different isozymes of PKC could act at different points in the stimulus-secretion coupling pathway in AtT-20 cells. The family of PKC isozymes can be divided into two main groups, the calcium-dependent or conventional PKC's (cPKC's) and the calcium-independent or novel PKC's (nPKC's) (Ohno *et al.*, 1991). Several isoforms of PKC have been specifically implicated as having

Table 1 Permeabilized cells were incubated in standard permeabilization medium or medium supplemented with GTP-γ-S (100 μM) or calcium ions (10 μM) as indicated: the effect of these treatments in the presence of the indicated concentrations of dPPA upon ACTH secretion was measured as described in the Methods

	ACTH secretion (pg/10^5 cells)		
[dPPA]	*Control*	*GTP* (100 μM)	*Calcium* (10 μM)
0	373 ± 37	840 ± 30	737 ± 68
100 nM	390 ± 40	963 ± 103	860 ± 95
1 μM	460 ± 46	1040 ± 81	1120 ± 113
10 μM	490 ± 16	1250 ± 180	1240 ± 100

ACTH release is expressed as the mean ± s.e.mean from 3 separate experiments. In the absence of dPPA, GTP-γ-S and calcium ions significantly ($P<0.05$) stimulated ACTH secretion above the control value. dPPA did not significantly enhance control, calcium ion- or GTP-γ-S-evoked secretion at a concentration of 100 nM but did significantly ($P<0.05$) enhance calcium ion- and GTP-γ-S-evoked secretion at 10 μM dPPA.

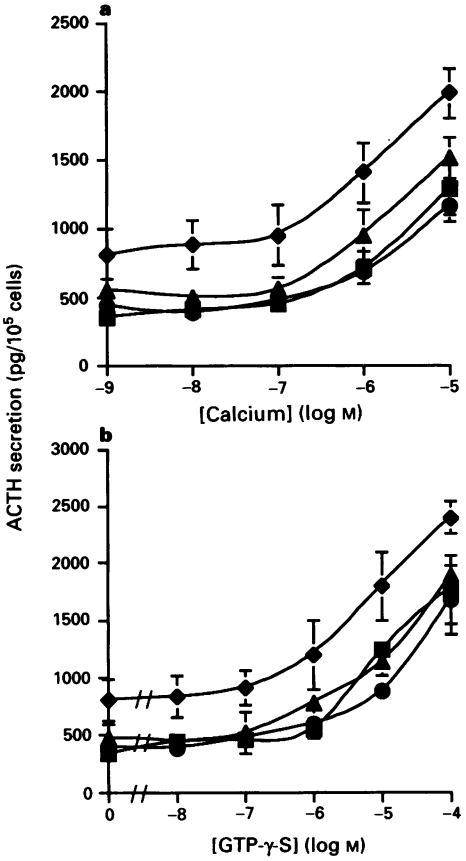

Figure 5 Effect of chelerythrine chloride upon the ability of PMA to potentiate calcium- and GTP-γ-S-evoked ACTH secretion from permeabilized AtT-20 cells. (a) Permeabilized cells were incubated in standard permeabilization medium containing calcium-EGTA buffers designed to give the indicated free calcium concentrations either in the presence (◆) or absence (■) of PMA (100 nM). The effects of chelerythrine chloride (10 μM) upon ACTH secretion evoked by these calcium concentrations (●) and upon the combination of calcium plus PMA (100 nM) (▲) were measured. The results are expressed as the mean ± s.e.mean from 3 separate experiments. Absence of error bars indicate that they lie within the symbol used. Calcium stimulated ACTH secretion in a concentration-dependent manner between 1 nM and 10 μM (significant ($P<0.05$) stimulation at concentrations of free calcium ions of 1 μM and above). A comparison of the calcium ion concentration-response curves in the presence and absence of PMA (100 nM), chelerythrine chloride (10 μM) or the combination of PMA and chelerythrine chloride by two way ANOVA test revealed that calcium ion-stimulated ACTH secretion was significantly ($P<0.0001$) enhanced by co-incubation with PMA (100 nM) but not by chelerythrine chloride or the PMA and chelerythrine chloride combination. (b) Permeabilized cells were incubated in standard permeabilization medium containing calcium-EGTA buffers designed to give 1 nM free calcium supplemented with the indicated concentrations of GTP-γ-S concentrations either in the presence (◆) or absence (■) of PMA (100 nM). The effects of chelerythrine chloride (10 μM) upon ACTH secretion evoked by these GTP-γ-S concentrations (●) and upon the combination of GTP-γ-S plus PMA (100 nM) (▲) were measured. The results are expressed as the mean ± s.e.mean from 3 separate experiments. Absence of error bars indicate that they lie within the symbol used. GTP-γ-S stimulated ACTH secretion in the absence of calcium in a concentration-dependent manner with a threshold of 1 μM. A comparison of the GTP-γ-S concentration-response curves in the presence and absence of PMA (100 nM), chelerythrine chloride (10 μM) or the combination of PMA and chelerythrine chloride by two way ANOVA test revealed that GTP-γ-S-stimulated ACTH secretion was significantly ($P<0.0001$) enhanced by co-incubation with PMA (100 nM) but not by chelerythrine chloride or the PMA and chelerythrine chloride combination.

distinct roles in signal-transduction, stimulus-secretion coupling and growth (Housey *et al.*, 1988; Naor *et al.*, 1989; Akita *et al.*, 1990; Pai *et al.*, 1991; Sharma *et al.*, 1991; Kiley *et al.*, 1992; Leli *et al.*, 1992). In view of all of these findings, it was decided to profile the PKC isozymes present in AtT-20 cells by Western blotting techniques as part of an attempt to establish physiological roles for these isozymes in stimulus-secretion coupling for ACTH secretion. The cPKCs probed for in this study were the α, β and γ isozymes and the nPKCs probed for were the δ, ε, η and ζ isozymes.

The present study indicates that AtT-20 cells contain detectable amounts of PKCs α, β, ε and ζ whereas γ, δ and η could not be detected under the conditions used in this study. Thus AtT-20 cells have the α and β calcium-dependent cPKC isozymes and the ε and ζ calcium-independent nPKCs. This profile of PKC isoforms is identical to another strain of AtT-20 cells, the AtT-20/D16-V line (unpublished observations). PKC isozymes were activated by the use of substances previously reported to activate selectively particular isoforms of the enzyme (Ryves *et al.*, 1991). PMA activates all isozymes of PKC and was used here as a general activator of both cPKCs and nPKCs (although calcium is required for maximal stimulation of cPKCs by PMA, (Ryves *et al.*, 1991) and the ζ isozyme is reported to be insensitive to PMA (see, Hug & Sarre, 1993)). TMX was used in an attempt to activate selectively the α and β isozymes and dPPA was used in an attempt to activate selectively the β_I isozyme. This study used pharmacological agents to investigate if and where the detected isozymes of PKC contributed to the regulation of ACTH secretion from AtT-20 cells. This approach was used recently to support the presence and active role in secretion of pharmacologically distinct forms of PKC in rat anterior pituitary cells (Thomson *et al.*, 1993). However, attributing physiologically relevant roles to PKC isozymes identified by molecular biological and biochemical techniques remains unfulfilled in AtT-20 cells and many other systems.

PMA and TMX stimulated ACTH secretion from intact AtT-20 cells indicating that activation of all PKC isozymes or only the α and β isozymes can elicit the full PKC-evoked ACTH secretion from these cells. The ability of dPPA (and presumably the β isozyme) to evoke a secretory response which was only 60–70% of that obtained to the other two agents may indicate that this isozyme can only evoke a partial stimulation of the secretory pathway. However, intact cells do not permit the differentiation between a 'pre-' and 'post-' calcium site of action by these isozymes and therefore the data from intact cells has to be viewed in concert with that from a cell preparation where the complicating influence of the cell membrane upon calcium metabolism can be circumvented. Such a situation is obtained by the use of electrically permeabilized cells, a technique which has been used previously to gain access to the cytosol in AtT-20 cells (Guild, 1991). The ability of calcium over the physiological range of 100 nM to 10 μM to stimulate ACTH secretion from permeabilized AtT-20 cells is entirely consistent with previous studies using digitonin-(Luini & De Matteis, 1988) and electrically-(Guild, 1991) permeabilized AtT-20 cells. In these studies a free calcium concentration of 10 μM produced maximal stimulation.

PMA and TMX but not dPPA enhanced calcium-dependent ACTH secretion from permeabilized AtT-20 cells. These data confirm the previously suggested 'post'-calcium point of control of the secretory pathway for PKC in AtT-20 cells (Reisine & Guild, 1987; Reisine, 1989; McFerran & Guild, 1994) but indicate that the β isozyme of PKC may not contribute at this site of regulation. Therefore the role of the β_I isozyme of PKC in the stimulus-secretion coupling pathway for ACTH may be at an early stage to stimulate calcium entry into the cell across the plasma membrane (Reisine & Guild, 1987; Reisine, 1989), as reported previously in anterior pituitary tissues (MacEwan & Mitchell, 1991; MacEwan *et al.*, 1991). An action of PMA upon both potassium and calcium channels in the plasma membranes has been shown in AtT-20 cells (Reisine & Guild, 1987; Reisine, 1989) and either of these actions may be due to the action of the β_I isozyme. It may be that the α and ε isozymes (or any, as yet, uncharacterized isozymes) of PKC are responsible for the 'post'-calcium site of enhancement of ACTH secretion from AtT-20 cells (Reisine & Guild, 1987; McFerran & Guild, 1994). This involvement of both calcium-dependent and calcium-independent isozymes of PKC in regulating exocytosis has been reported in both rat basophilic RBL-2H3 cells (Ozawa *et al.*, 1992) and GH_4C_1 rat anterior pituitary tumour cells (Akita *et al.*, 1990).

The ability of TMX to stimulate ACTH secretion from permeabilized AtT-20 cells in the absence of calcium was surprising in the light of the evidence that TMX was selective for the calcium-dependent isozymes of PKC (Ryves *et al.*, 1991). This may indicate that TMX is not as selective an activator of these isozymes of PKC as had been believed (it may even be a partial agonist on the ε isozyme) or that calcium-dependent isozymes of PKC can be partially activated in the absence of calcium. Interestingly, TMX was recently shown to bind to the ε isoform of PKC but was 10–20 fold less potent in its binding to this isoform than its binding to the α and β_I isoforms (Kazanietz *et al.*, 1993). Although binding to the ε isoform does not indicate whether or not TMX can activate this isoform, it does reinforce the caution required in claiming selectivity in the spectrum of activation of PKC isoforms made for these agents. This is also true of the claimed spectrum of activation of dPPA made originally upon data obtained in *in vitro* studies (Ryves *et al.*, 1991). dPPA stimulated PKC-β_I kinase activity at concentrations of 20 nM but did not activate other isoforms of PKC at concentrations up to 2 μM *in vitro* (Ryves *et al.*, 1991). A recent report by some of the same investigators has claimed that dPPA is not a PKC-β_I kinase selective activator when used in intact cells (Kiley *et al.*, 1994). The ability of dPPA to activate other PKC isozymes (assessed by redistribution of PKC isozymes from a digitonin-soluble to a digitonin-insoluble fraction) in that study, however, required concentrations of dPPA in excess of 100 nM (Kiley *et al.*, 1994). This non-selective activation of PKC isozymes in intact cells, therefore, was observed at concentrations of dPPA above that used for selective activation of PKC-β_I in the present study. Consistent with this, in the present study, is that higher concentrations of dPPA (i.e. 10 μM) did produce an enhancement of calcium ion- and GTP-γ-S-evoked ACTH secretion indicating that this agent will activate other isoforms of PKC when present in sufficient quantities. Nonetheless, the present study demonstrates a difference between the actions of PMA and TMX and those of dPPA which would not be the case if these agents were non-selective in their activation of PKC isozymes.

The ability of PMA and TMX but not dPPA to potentiate GTP-γ-S-evoked ACTH secretion suggests that, in AtT-20 cells, the 'post'-calcium site of interaction between calcium and PKC is either at the level of or at some stage distal to G_E. The results indicate that the β isozyme of PKC may not contribute at this site of regulation. The ability of some activators of PKC to stimulate ACTH secretion from permeabilized cells in the absence of calcium and added GTP-γ-S raises the possibility that PKC may mediate the effects of the calcium-G_E system upon secretion. A previous report from this laboratory (McFerran & Guild, 1994) did not support the hypothesis that PKC mediates the effect of calcium-G_E system upon secretion. It would appear that PKC plays a modulatory role in regulating secretion and is not necessary for secretion.

This and previous studies (Guild, 1991; McFerran & Guild, 1994) suggest that not only does a G-protein directly regulate exocytosis but its action is regulated by second messenger systems perhaps by increasing the readily releasable pool of stored, endogenous hormone (Dannies, 1982). It is clear that calcium alone cannot stimulate the maximal possible hormone secretion and that co-operation

with PKC and PKA, which may increase the 'efficacy' of the calcium-G_E system, increased the amount of hormone secreted in response to a particular concentration of calcium (Guild, 1991; McFerran & Guild, 1994). This study also indicates that different isozymes of PKC may act at different points in the stimulus-secretion pathway to regulate ACTH secretion. It is tempting to speculate that different isozymes of PKC contribute to the secretory response depending upon the free cytosolic calcium concentration. At lower calcium concentrations (around the resting calcium concentration of 100 nM) the ε-isoform of PKC may have an important role in stimulating ACTH secretion under circumstances where there is no rise in the cytosolic calcium concentration. As the cytosolic calcium concentration increases above resting values the calcium-dependent cPKCs (here the α and β isoforms detected to be present in AtT-20 cells) may start to exert a greater influence over ACTH secretion. This differential interaction between PKC isozymes and the cytosolic free calcium may go some way to explaining the need for the multiplicity of PKC isozymes present in AtT-20 cells. In addition, the ability of PKC to potentiate calcium-evoked secretion may explain the ability of vasopressin to potentiate corticotrophin-releasing hormone (CRF)-stimulated ACTH secretion from dispersed anterior pituitary cells (Gillies *et al.*, 1982). This suggestion is based upon the observation that vasopressin stimulates PKC activity in pituitary corticotrophs (Abou-Samra *et al.*, 1986) and that CRF stimulates cyclic AMP production and an increase in cytosolic calcium ion concentration in AtT-20 cells (Guild & Reisine, 1987). Hence the potential for an interaction between PKC- and PKA-stimulated mechanisms is provided by these two neuropeptides.

The authors would like to acknowledge gratefully the financial support of the Wellcome Trust, the Royal Society and the Nuffield Foundation. B.W.M. is supported by a Maitland-Ramsay scholarship. Thanks also to Harold Mishak for the gift of PKC antisera.

References

ABOU-SAMRA, A., CATT, K.J. & AGUILERA, G. (1986). Involvement of protein kinase C in the regulation of adrenocorticotrophin release from rat anterior pituitary cells. *Endocrinology*, **118**, 212–217.

AGUILERA, G., HARWOOD, J., WILSON, J., BROWN, J. & CATT, K. (1983). Mechanism of action of corticotrophin-releasing factor and other regulators of corticotrophin release in rat pituitary cells. *J. Biol. Chem.*, **258**, 8039–8045.

AKITA, Y., OHNO, S., YAJIIMA, Y. & SUZUKI, K. (1990). Possible role of Ca^{2+}-independent protein kinase-C isozyme nPKC-ε, in thyrotrophin-releasing hormone-stimulated signal transduction-differential down-regulation of nPKC-ε in GH_4C_1 cells. *Biochem. Biophys. Res. Commun.*, **172**, 184–189.

ANTONI, F.A. (1986). Hypothalamic control of adrenocorticotrophin secretion–Advances since the discovery of 41-residue corticotrophin-releasing factor. *Endocr. Rev.*, **7**, 351–361.

AXELROD, J. & REISINE, T. (1984). Stress hormones: their interaction and regulation. *Science*, **224**, 452–459.

DANNIES, P.S. (1982). Prolactin: multiple intracellular processing routes plus several potential mechanisms for regulation. *Biochem. Pharmacol.*, **31**, 2845–2849.

FRAKER, P. & SPECK, J. (1978). Protein and cell membrane iodination's with a sparingly soluble chloramide, 1,3,4,6-tetrachloro-3α,6α-diaphenylglycoluril. *Biochem. Biophys. Res. Commun.*, **80**, 849–857.

GILLIES, G.E., LINTON, E.A. & LOWRY, P.J. (1982). Corticotrophin releasing activity of the new CRF is potentiated several times by vasopressin. *Nature*, **299**, 355–357.

GOMPERTS, B.D. (1990). G_E: GTP-binding protein mediating exocytosis. *Annu. Rev. Physiol.*, **52**, 591–606.

GUILD, S. (1991). Effects of adenosine 3':5'-cyclic monophosphate and guanine nucleotides on calcium-evoked ACTH release from electrically-permeabilised AtT-20 cells. *Br. J. Pharmacol.*, **104**, 117–122.

GUILD, S., ITOH, Y., KEBABIAN, J.W., LUINI, A. & REISINE, T. (1986). Forskolin enhances basal and potassium-evoked hormone release from normal and malignant pituitary tissue. The role of calcium. *Endocrinology*, **118**, 268–279.

GUILD, S. & REISINE, T. (1987). Molecular mechanisms of corticotrophin-releasing factor stimulation of calcium mobilization and adrenocorticotrophin release from anterior pituitary tumour cells. *J. Pharmacol. Exp. Ther.*, **241**, 125–130.

HERBERT, J.M., AUGEREAU, J.M., GLEYE, J. & MAFFRAND, J.P. (1990). Chelerythrine chloride is a potent and specific inhibitor of protein kinase-C. *Biochem. Biophys. Res. Commun.*, **172**, 993–999.

HOUSEY, G.M., JOHNSON, M.D., HSIAO, W.L.W., O'BRIAN, C.A., MURPHY, J.P., KIRSCHMEIER, P. & WEINSTEIN, I.B. (1988). Overproduction of protein kinase-C causes disordered growth-control in rat fibroblasts. *Cell*, **52**, 343–354.

HUG, H. & SARRE, T.F. (1993). Protein kinase C isozymes: divergence in signal transduction? *Biochem. J.*, **291**, 329–343.

KAZANIETZ, M.G., ARECES, L.B., BAHADOR, A., MISCHAK, H., GOODNIGHT, J., MUSHINISKI, J.F. & BLUMBERG, P.M. (1993). Characterisation of ligand and substrate specificity for the calcium-dependent and calcium-independent protein kinase C isozymes. *Mol. Pharmacol.*, **44**, 298–307.

KILEY, S.C., PARKER, P.J., FABBRO, D. & JAKEN, S. (1992). Hormone-activated and phorbol ester-activated protein kinase C isozymes mediate a reorganisation of the actin cytoskeleton associated with prolactin secretion in GH_4C_1 cells. *Mol. Endocrinol.*, **6**, 120–131.

KILEY, S.C., OLIVIER, A.R., GORDGE, P.C., RYVES, W.J., EVANS, F.J., WAYS, D.K. & PARKER, P.J. (1994). 12-Deoxyphorbol-13-*O*-phenylacetate-10-acetate is not protein kinase C-β isozyme-selective *in vivo*. *Carcinongenisis*, **15**, 319–324.

KNIGHT, D.E. & BAKER, P.F. (1982). Calcium-dependence of catecholamine release from adrenal medulary cells after exposure to intense electric fields. *J. Memb. Biol.*, **68**, 107–140.

LELI, U., PARKER, P.J. & SHEA, T.B. (1992). Intracellular delivery of protein kinase C-α or C-ε isoform specific antibodies promotes acquisition of a morphologically differentiated phenotype in neuroblastoma cells. *FEBS. Letts.*, **297**, 91–94.

LUINI, A. & DE MATTEIS, M.A. (1988). Dual regulation of ACTH secretion by guanine nucleotides in permeabilised AtT-20 cells. *Cell. Mol. Biol.*, **8**, 129–138.

LUINI, A., LEWIS, D., GUILD, S., CORDA, D. & AXELROD, J. (1985). Hormone secretagogues elevate cytosolic calcium by increasing cAMP in corticotrophin-secreting cells. *Proc. Natl. Acad. Sci. U.S.A.*, **82**, 8034–8038.

MACEWAN, D.J. & MITCHELL, R. (1991). Calcium influx through L-type channels into rat anterior pituitary cells can be modulated in 2 ways by protein kinase C-(PKC isoform selectivity of 1,2-Dioctanoyl-sn-glycerol). *FEBS. Letts.*, **291**, 79–83.

MACEWAN, D.J., MITCHELL, R., THOMSON, F.J. & JOHNSON, M.S. (1991). Inhibition of depolarisation-induced calcium influx into GH_3 cells by arachidonic acid – the involvement of protein kinase C. *Biochem. Biophys. Res. Commun.*, **1094**, 346–354.

MCFERRAN, B.W. & GUILD, S.B. (1994). Effects of protein kinase C activators upon the late stages of the ACTH secretory pathway of AtT-20 cells. *Br. J. Pharmacol.*, **113**, 171–178.

NAOR, Z., DAN-COHEN, H., HERMON, J. & LIMOR, R. (1989). Induction of exocytosis in permeabilised pituitary cells by α-type and β-type protein kinase-C. *Proc. Natl. Acad. Sci. U.S.A.*, **86**, 4501–4504.

OHNO, S., AKITA, Y., HATA, A., OSADA, S., KUBO, K., KONNO, Y., AKIMOTO, K., MIZUNO, K., SAIDO, T., KUROKI, T. & SUZUKI, K. (1991). Structural and functional diversities of a family of signal transducing protein-kinases, protein-kinase-C family -2 distinct classes of PKC, conventional cPKC and novel nPKC. *Adv. Enzyme Regul.*, **31**, 287–303.

OZAWA, K., SZALLASI, Z., KAZANIETZ, M.G., BLUMBERG, P.M., MISCHAK, H., MUSHINSKI, J.F. & BEAVEN, M.A. (1992). Ca^{2+}-dependent and Ca^{2+}-independent isozymes of protein kinase C mediate exocytosis in antigen-stimulated rat basophilic RBL-2H3 cells. *FASEB. J.*, **6**, 1749–1756.

PAI, J.K., PACHTER, J.A., WEINSTEIN, I.B. & BISHOP, W.R. (1991). Overexpression of protein kinase C-β enhances phospholipase-D activity and diacylglycerol formation in phorbol ester-stimulated rat fibroblasts. *Proc. Natl. Acad. Sci. U.S.A.*, **88**, 598–602.

REISINE, T. (1984). Somatostatin desensitisation; loss of the ability of somatostatin to inhibit cAMP accumulation and ACTH release. *J. Pharmacol. Exp. Ther.*, **229**, 14–20.

REISINE, T. (1989). Phorbol esters and corticotrophin-releasing factor stimulate calcium influx in the anterior pituitary tumour cell line, AtT-20, through different intracellular sites of action. *Mol. Pharmacol.*, **248**, 984–990.

REISINE, T. & GUILD, S. (1987). Activators of protein kinase C and cyclic AMP-dependent protein kinase regulate intracellular calcium levels through distinct mechanisms in mouse anterior pituitary tumour cells. *Mol. Pharmacol.*, **32**, 488–496.

RYVES, W.J., EVANS, A.T., OLIVIER, A.R., PARKER, P.J. & EVANS, F.J. (1991). Activation of the PKC-isotypes α, β1, γ, δ and ε by phorbol esters of different biological activities. *FEBS Lett.*, **288**, 5–9.

SHARMA, P., EVANS, A.T., PARKER, P.J. & EVANS, F.J. (1991). NADPH-oxidase activation by protein kinase C-isotypes. *Biochem. Biophys. Res. Commun.*, **177**, 1033–1040

STRULOVICI, B., DANIEL-ISSANKANI, S., BAXTER, G., KNOPF, J., SULTZMAN, L., CHERWINSKI, H., NESTOR, J. JR., WEBB, D.R. & RANSOM, J. (1991). Distinct mechanisms of regulation of protein kinase C-ε by hormones and phorbol diesters. *J. Biol. Chem.*, **266**, 168–173.

STRULOVICI, B., DANIEL-ISSANKANI, S., NESTOR, J. JR., CHAN, H. & TSOU, A.P. (1989). Activation of distinct protein kinase C-isozymes by phorbol esters-correlation with induction of interleukin 1-β gene-expression. *Biochem.*, **28**, 3569–3576.

THOMSON, F.J., JOHNSON, M.S., MITCHELL, R., WOLBERS, W-B., ISON, A.J. & MACEWAN, D.J. (1993). The differential effects of protein kinase C activators and inhibitors on rat anterior pituitary hormone release. *Mol. Cell. Endocrinol.*, **94**, 223–234.

(Received June 3, 1994
Revised January 13, 1995
Accepted January 27, 1995)

British Journal of Pharmacology (1995) 115, 316–320

Investigation of the subtype of α_2-adrenoceptor mediating prejunctional inhibition of cardioacceleration in the pithed rat heart

[1]Karen Smith, Katherine Gavin & [2]James R. Docherty

Department of Physiology, Royal College of Surgeons in Ireland, 123 St. Stephen's Green, Dublin 2, Ireland

1 We have investigated the subtype of α_2-adrenoceptor mediating prejunctional inhibition of cardioacceleration in the pithed rat heart in comparison with α_2-adrenoceptor ligand binding sites.

2 In pithed rats, prejunctional α_2-adrenoceptors were investigated in terms of the ability of α_2-adrenoceptor antagonists to shift the inhibitory potency of the α_2-adrenoceptor agonist, xylazine, against the tachycardia to a single electrical stimulus given via the pithing rod.

3 Antagonist potency at prejunctional α_2-adrenoceptors in pithed rat heart was correlated with antagonist affinity at α_2-adrenoceptor ligand binding sites in membranes of rat kidney and submandibular gland labelled with [^{3}H]-yohimbine.

4 The correlation with the prejunctional α_2-adrenoceptor in pithed rat heart was best for the α_{2D}-adrenoceptor ligand binding site of rat submandibular gland ($r = 0.98$, $n = 10$, $P < 0.0001$), as compared to correlations with the α_{2A}-adrenoceptor ligand binding site of human platelet ($r = 0.90$, $n = 9$, $P < 0.001$), the α_{2B}-adrenoceptor ligand binding site of rat kidney ($r = 0.82$, $n = 10$, $P < 0.01$) and with published results for the α_{2C}-adrenoceptor ligand binding site ($r = 0.48$, $n = 6$, NS).

5 It is concluded that the functional prejunctional α_2-adrenoceptor of pithed rat heart closely resembles the α_{2D}-adrenoceptor ligand binding site of rat submandibular gland.

Keywords: Prejunctional α_2-adrenoceptors; α_{2D}-adrenoceptors; pithed rat heart

Introduction

α_2-Adrenoceptors have been subdivided into at least four subtypes, α_{2A}-, α_{2B}-, α_{2C}- and α_{2D}-adrenoceptors, based on ligand binding and molecular cloning studies (Lorenz *et al.*, 1990; Bylund, 1992), although the α_{2D}-adrenoceptor of rat submandibular gland may be a species homologue of the human α_{2A}-adrenoceptor, reducing the number of genes coding for α_2-adrenoceptors to three (Lanier *et al.*, 1991; Harrison *et al.*, 1991; Smith & Docherty, 1992), so that the term $\alpha_{2A/D}$-adrenoceptor could be used to describe these homologues. However, since the functional receptors differ pharmacologically, the term α_{2A}-adrenoceptor is used in this paper to describe the ligand binding site in human platelet and α_{2D}-adrenoceptor to describe the site on rat submandibular gland.

We have previously investigated functional prejunctional α_2-adrenoceptors of adrenergic nerves in a number of tissues and suggested that the prejunctional α_2-adrenoceptors in rat vas deferens and rat submandibular gland resemble the α_{2D}-adrenoceptor ligand binding site of rat submandibular gland (Smith & Docherty, 1992), whereas the functional prejunctional α_2-adrenoceptor of rat atrium differed (Smith *et al.*, 1992).

In this study, we have examined the functional prejunctional α_2-adrenoceptor in pithed rat heart in relation to ligand binding sites in rat kidney (α_{2B}-adrenoceptor: see Michel *et al.*, 1989; Smith & Docherty, 1992), and rat submandibular gland (α_{2D}-adrenoceptor: see Bylund, 1992). For comparison, ligand binding data for human platelet membranes (α_{2A}-adrenoceptor: see Bylund, 1985; 1992) are included.

[1] Present address: Institute of Physiology, University of Glasgow, Glasgow G12 8QQ.
[2] Author for correspondence.

Methods

Male Wistar rats (250–350 g) were obtained from Trinity College Dublin and employed in a number of studies, as outlined below.

Pithed rat preparation

Rats were pithed by the method of Gillespie *et al.* (1970) and ventilated with 100% O_2 at a rate of 60 per min. Heart rate was derived from carotid arterial pressure and drugs were injected into the jugular vein. The pithing rod was used as an electrode positioned at T1 to stimulate the cardio-accelerator nerves with a single stimulus pulse (0.5 ms, supramaximal voltage) every 2 min (see Docherty & Hyland, 1986).

Dose-response curves to the α_2-adrenoceptor agonists, xylazine, clonidine, UK 14,304 and oxymetazoline were constructed from the effects of increasing doses (10 fold increments) administered at 5 min intervals. Prejunctional effects of agonists were assessed as the inhibition of the cardio-acceleration to a single stimulus. Antagonist drugs, or vehicle, were administered intravenously 10 min before starting the agonist dose-response curve. The potency of xylazine was expressed as an ID_{50} (dose causing 50% inhibition of the cardio-acceleration to a single stimulus), and the effects of antagonists were assessed from the difference between agonist potency in the individual antagonist experiment and the mean agonist potency in vehicle experiments. Shifts in agonist potency were expressed as log(DR − 1), where DR is the xylazine dose ratio (difference in potency of xylazine between vehicle experiments and experiments in the presence of antagonist), and mean values (± s.e.mean) were obtained from the effects of the antagonist in n experiments.

Antagonist dose administered was expressed in mol kg^{-1} to allow direct comparison between agents of widely differing molecular weights. Antagonist potency was expressed as an apparent pA_2 ($-\log$ mol kg^{-1}) from the calculation: $-\log$ antagonist dose (mol kg^{-1}) + log(DR − 1). Expression of

antagonist potency in this form allowed direct comparison with ligand binding data.

In some experiments, cardioaccelerator responses to isoprenaline (1–10 ng kg^{-1}) were examined before and following exposure to xylazine (1 mg kg^{-1}) or vehicle, to assess postjunctional actions of xylazine, if any.

Radioligand binding studies

Preparation of human platelet and rat kidney membranes was carried out as described in Connaughton & Docherty (1990), and preparation of submandibular gland membranes was as described for rat kidney. The resultant pellets were used immediately or stored at −20°C for later use. Pellets were reconstituted in 2.5 ml (platelet), 5 volumes (submandibular) or 10 volumes (kidney) of incubation buffer.

In saturation experiments, aliquots of membrane suspension were incubated with various concentrations of [^{3}H]-yohimbine (specific activity: 81 Ci $mmol^{-1}$, Amersham) at 37°C (human platelet: 0.3–20 nM; incubation buffer: Tris-HCl 50 mM, $MgCl_2$ 8 mM, EGTA 5 mM, pH 7.4 at 37°C) or at 25°C (rat kidney: 0.5–30 nM; rat submandibular gland: 2.0–40 nM; incubation buffer: Tris-HCl 50 mM, EDTA 5 mM, pH 7.4 at 25°C). In competition studies, [^{3}H]-yohimbine (5 or 10 nM) was incubated with competing ligands in concentrations from 0.1 nM to 1 mM in 0.5 log unit increments for 30 min. Non-specific binding was determined in the presence of phentolamine (10 μM). Specific binding of [^{3}H]-yohimbine was 70–90% of total binding. Assays were terminated by washing with ice-cold incubation buffer, followed by rapid vacuum filtration through Whatman GF/C filters, using a Brandel Cell Harvester. Radioactivity retained on filters was determined by liquid scintillation spectroscopy.

The inhibition constant (K_i) for inhibition of radiolabelled ligand binding was determined from the formula:

$$K_i = IC_{50}/(1 + [^3H]/k_D)$$

where IC_{50} is the concentration of competing ligand that inhibits radioligand specific binding by 50%, k_D is the dissociation constant for the radioligand (human platelet: 5.50 nM, 95% confidence limits 3.80–7.94 nM, $n = 6$; rat kidney: 8.71 nM, 95% confidence limits 7.41–10.2 nM, $n = 7$; rat submandibular gland: 23.4 nM, 95% confidence limits 18.2–30.2 nM, $n = 4$), and ^{3}H is the concentration of tritiated yohimbine employed (5 nM: platelet and kidney; 10 nM: submandibular gland). B_{max} values obtained in saturation experiments were 115 ± 10 ($n = 6$), 94 ± 13 ($n = 7$) and 146 ± 19 ($n = 4$) fmol mg^{-1} protein in human platelet, rat kidney and rat submandibular gland, respectively.

Statistical evaluation

In functional studies, values are expressed as agonist ID_{50} (dose producing 50% inhibition of the stimulation-evoked tachycardia), antagonist log (DR − 1) (where DR is the xylazine dose-ratio between potency in the presence of antagonist and presence of vehicle), and antagonist pA_2. Antagonist pA_2 was calculated as the sum of antagonist dose (− log mol kg^{-1}) and log(DR − 1). Results are expressed as mean and 95% confidence limits or mean ± s.e. of mean. Effects of antagonist on xylazine ID_{50} were compared with effects of vehicle by Student's t test for unpaired data and Analysis of Variance. Correlation analysis was carried out on an Apple Macintosh using the Statworks and Cricketgraph programmes (Cricket software, Inc.).

Drugs

The following drugs were employed: abanoquil hydrochloride (gift: Pfizer, Sandwich, U.K.); ARC 239 (2-(2,4-(*o*-methoxyphenyl)-piperazin-1-yl)-ethyl-4,4 dimethyl-1,3-(2H,4H)-isoquinolindine chloride; gift: Karl Thomae, Biberach, Germany); BDF 8933 (4-fluoro-2-(imidazolin-2-ylamino)-isiindoline maleate, gift: Beiersdorf, Hamburg, Germany), benozathian hydrochloride (Research Biochemicals, Natick, U.S.A.); chlorpromazine hydrochloride (Sigma, Poole, U.K.), HV 723 (α-ethyl-3,4,5-trimethoxy-α-(3-((2-(2-methoxyphenoxy)ethyl)-amino)-propyl)-benzene acetonitrile fumarate; gift: Hokurika, Seiyaku, Katsuyama, U.K.); idazoxan hydrochloride (Research Biochemicals); isoprenaline hydrochloride (Sigma); oxymetazoline hydrochloride (Sigma); phentolamine hydrochloride (Sigma); prazosin hydrochloride (gift: Pfizer); spiroxatrine hydrochloride (gift: Janssen, Ireland); UK 14,304 (5-bromo-6-(2-imidazolin-2-yl amino)quinoxaline; gift: Pfizer); WB 4101 (2-(2′,6′-dimethoxyphenoxyethyl)aminomethyl-1,4-benzodioxan; Research Biochemicals); xylazine hydrochloride (gift: Bayer, Ireland); yohimbine hydrochloride (Sigma).

Results

Pithed rat preparation

In pithed rat, resting blood pressure was 70.8 ± 1.2/36.0 ± 0.7 mmHg ($n = 81$), and resting heart rate was 256 ± 3 beats min^{-1}. Single pulse stimulation produced a cardioacceleration of 23.4 ± 0.8 beats min^{-1} ($n = 81$). Most antagonist drugs caused a transient inhibition of the stimulation-evoked cardioacceleration but the response had recovered by 10 min (just before beginning the xylazine dose-response curve), except in the case of BDF 8933 (0.1 mg kg^{-1}) which significantly reduced the stimulation-evoked tachycardia to 65.1 ± 8.4% ($n = 5$) (vehicle: 96.6 ± 2.8%, $n = 9$, $P < 0.01$). Chlorpromazine significantly increased the stimulated-evoked tachycardia to 239 ± 26% ($n = 6$) ($P < 0.001$), and the response following chlorpromazine was prolonged in a manner consistent with blockade of noradrenaline re-uptake (see Tuck *et al.*, 1972).

In vehicle experiments, xylazine, clonidine, UK 14,304 and oxymetazoline inhibited the stimulation-evoked tachycardia to a single stimulus with ID_{50} values of 3.80 μg kg^{-1} (95% confidence limits: 3.0–4.8 μg kg^{-1}) ($n = 22$), 0.67 μg kg^{-1} (0.37–0.98) ($n = 6$), 0.57 μg kg^{-1} (0.39–0.81) ($n = 3$) and 0.47 μg kg^{-1} (0.12–1.74) ($n = 5$), respectively. These values are 15.1, 2.51, 1.29 and 1.58 nmol kg^{-1}, respectively. In vehicle experiments, in which saline replaced the test agonist, the response to a single stimulus was not significantly altered (control: 24.4 ± 2.6 beats min^{-1}; response following 5 saline injections over approximately 20 min: 25.9 ± 2.0 beats min^{-1}; $n = 8$).

Responses to xylazine obtained in vehicle experiments were compared with responses to xylazine obtained in experiments in the presence of antagonist, taking as examples ARC 239 (5 mg kg^{-1}), HV 723 (2 mg kg^{-1}), yohimbine (1 mg kg^{-1}) and BDF 8933 (0.1 mg kg^{-1}) (Figure 1). Antagonist doses employed and apparent pA_2 values obtained are shown in Table 1. All antagonists in the doses employed significantly altered the potency of xylazine (Student's t test, $P < 0.05$ or less; Analysis of Variance, $P < 0.0001$) (Table 1).

Xylazine (1 mg kg^{-1}) did not significantly reduce the cardioacceleration produced by isoprenaline. In vehicle experiments, the tachycardia to isoprenaline (3 ng kg^{-1}) was reduced from 36.6 ± 8.1 beats min^{-1} to 31.6 ± 6.8 beats min^{-1} ($n = 5$), whereas xylazine (1 mg kg^{-1}) reduced the tachycardia from 32.0 ± 7.6 beats min^{-1} to 27.8 ± 7.6 beats min^{-1} ($n = 4$) (no significant differences).

Radioligand binding studies

K_i values for the inhibition by ligands of [^{3}H]-yohimbine binding to human platelet, rat kidney and rat submandibular gland membranes were obtained (see Table 2). Hill slopes for all ligands in all 3 tissues were close to unity, so that it was assumed that a single homogeneous population of ligand binding sites was present in all 3 tissues.

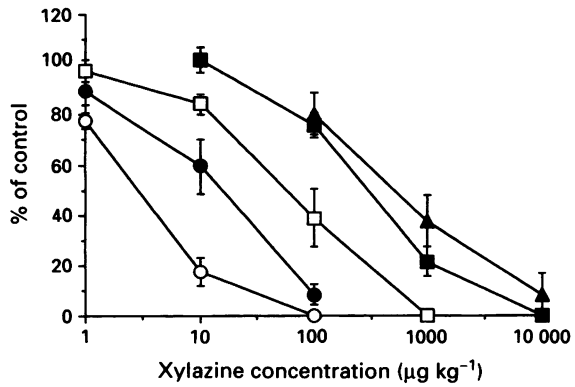

Figure 1 Inhibition by the α_2-adrenoceptor agonists, xylazine, of the tachycardia evoked by a single stimulus in the pithed rat preparation in the presence of antagonist or vehicle. Symbols: vehicle (○), ARC 239 (5 mg kg^{-1}) (●), HV 723 (2 mg kg^{-1}) (□), yohimbine (1 mg kg^{-1}) (■), BDF 8933 (0.1 mg kg^{-1}) (▲). Values (expressed as % of control responses) are mean ± s.e. of mean from at least 4 experiments.

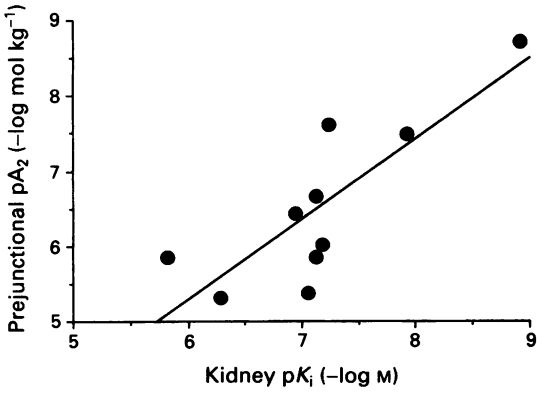

Figure 2 Correlation between antagonist K_i (− log M) obtained at α_{2B}-adrenoceptor ligand binding sites in rat kidney membranes and the antagonist pA_2 obtained against xylazine in the pithed rat heart. $r = 0.82$, $n = 10$, $P < 0.01$.

Correlation between ligand binding sites and the functional prejunctional α_2-adrenoceptor in pithed rat heart

Correlations between α_{2B}- and α_{2D}-adrenoceptor ligand binding sites and the functional site in the pithed rat heart are shown in Figures 2 and 3. The correlation of the functional prejunctional α_2-adrenoceptor of pithed rat heart was better with the α_{2D}-adrenoceptor ligand binding site of rat submandibular gland ($r = 0.98$, $n = 10$, $P < 0.0001$) (Figure 3) than with the α_{2B}-adrenoceptor ligand binding site of rat kidney ($r = 0.82$, $n = 10$, $P < 0.01$) (Figure 2) or with the α_{2A}-adrenoceptor ligand binding site of human platelet ($r = 0.90$, $n = 9$, $P < 0.001$) (Figure 4).

The correlation between published ligand binding data for the α_{2C}-adrenoceptor ligand binding sites and functional site in pithed rat heart was also examined. The correlation between the α_{2C}-site (human α_2-C4 gene expressed in COS-7 cells: Bylund *et al.*, 1992) and the functional receptor of the pithed rat heart was $r = 0.48$ (non-significant; $n = 6$ antagonists, excluding abanoquil, benoxathian, HV 723 and BDF 8933) (Figure 5).

Table 2 Affinities (pK_i, − log M) of test agents at the α_2-adrenoceptor ligand binding sites human platelet (α_{2A}), rat kidney (α_{2B}) and rat submandibular gland (α_{2D})

Test agent	*Platelet*	*Kidney*	*Submand.*
Chlorpromazine	6.48 ± 0.05	6.29 ± 0.03	5.26 ± 0.07
WB 4101	7.08 ± 0.22	6.94 ± 0.03	6.58 ± 0.10
BDF 8933	8.72 ± 0.06	8.91 ± 0.14	8.81 ± 0.20
Prazosin	5.62 ± 0.12	7.12 ± 0.04	6.24 ± 0.12
ARC 239	5.45 ± 0.02	7.06 ± 0.16	5.54 ± 0.13
Yohimbine	8.04 ± 0.10	7.93 ± 0.02	7.34 ± 0.06
Phentolamine	7.61 ± 0.12	7.24 ± 0.12	7.31 ± 0.17
Benoxathian	6.85 ± 0.05	5.82 ± 0.15	5.81 ± 0.05
Abanoquil	/	7.18 ± 0.14	5.98 ± 0.11
HV 723	6.58 ± 0.10	7.13 ± 0.20	6.24 ± 0.06

Values are mean and s.e.mean from at least 3 experiments.

Table 1 Effects of vehicle and antagonists on the prejunctional potency of xylazine in the pithed rat preparation

Test agent	*Xylazine ID_{50}* (μg kg^{-1})	*log(DR − 1)*	*− log antagonist pA_2* (mol kg^{-1})
Vehicle ($n = 22$)	3.80 (3.0–4.8)	/	/
Yohimbine (1 mg kg^{-1}) ($n = 4$)	302 (240–380)	1.89 ± 0.08	7.48
Prazosin (1 mg kg^{-1}) ($n = 4$)	8.91 (6.61–12.0)	0.24 ± 0.11	5.86
BDF 8933 (0.1 mg kg^{-1}) ($n = 5$)	589 (389–891)	2.19 ± 0.18	8.71
Phentolamine (1 mg kg^{-1}) ($n = 5$)	417 (363–479)	2.04 ± 0.06	7.62
HV 723 (2 mg kg^{-1}) ($n = 4$)	60.2 (40.7–89.1)	1.17 ± 0.18	6.66
Chlorpromazine (5 mg kg^{-1}) ($n = 3$)	15.1 (12.6–18.2)	0.47 ± 0.11	5.32
WB 4101 (2 mg kg^{-1}) ($n = 3$)	58.9 (40.7–85.1)	1.16 ± 0.17	6.44
Benoxathian (5 mg kg^{-1}) ($n = 3$)	37.2 (21.4–64.6)	0.94 ± 0.27	5.84
ARC 239 (5 mg kg^{-1}) ($n = 7$)	12.9 (9.55–17.4)	0.43 ± 0.15	5.38
Abanoquil (2 mg kg^{-1}) ($n = 3$)	43.6 (27.5–69.2)	1.02 ± 0.06	6.01

Values are xylazine ID_{50} (dose producing 50% inhibition of the stimulation-evoked tachycardia) and 95% confidence limits, antagonist log (DR − 1) and s.e. of mean, and antagonist pA_2. Antagonist pA_2 was calculated as the sum of − log antagonist dose (mol kg^{-1}) and log(DR − 1), and so has the same s.e. of mean as the log (DR − 1) column.

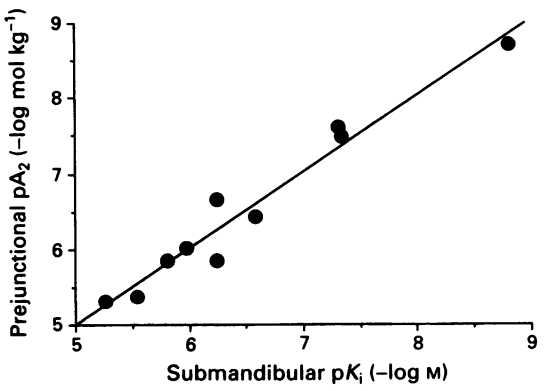

Figure 3 Correlation between antagonist K_i (− log M) obtained at α_{2D}-adrenoceptor ligand binding sites in rat submandibular gland membranes and the antagonist pA_2 obtained against xylazine in the pithed rat heart. $r = 0.98$, $n = 10$, $P < 0.0001$.

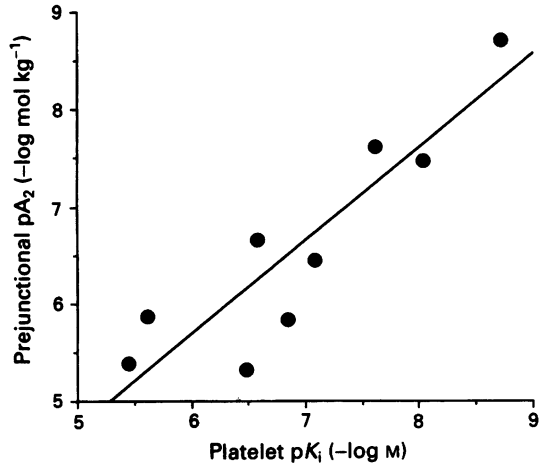

Figure 4 Correlation between antagonist K_i (− log M) obtained at α_{2A}-adrenoceptor ligand binding sites in human platelet membranes and the antagonist pA_2 obtained against xylazine in the pithed rat heart. $r = 0.90$, $n = 9$, $P < 0.001$.

Discussion

The major finding of this study is that the functional prejunctional α_2-adrenoceptor of pithed rat heart closely resembles the α_{2D}-adrenoceptor ligand binding site in rat submandibular gland. This and other points of interest will be discussed.

The main objective of this study was to characterize the subtype of α_2-adrenoceptor found prejunctionally in the pithed rat heart. Using the pithed rat preparation, the inhibition by the α_2-adrenoceptor agonist xylazine of the tachycardia evoked by a single stimulus given via the pithing rod is a useful model of prejunctional α_2-adrenoceptor function, and antagonist potency can be assessed in terms of the shift in agonist potency (see Docherty & McGrath, 1980). Ten antagonist drugs were employed in the present study, of which three (ARC 239, chlorpromazine, prazosin) showed marked selectivity between subtypes (> 10 fold differences in affinity), and doses were chosen which produced a shift in agonist potency. The correlation between the functional prejunctional receptor in the pithed rat heart and the ligand binding site of submandibular gland was so close ($r = 0.98$) and so significant ($P < 0.0001$) that it is virtually certain that these are the same receptor. The correlation between the functional prejunctional receptor in the pithed rat heart and the ligand binding site of rat kidney cortex was relatively poor ($r = 0.82$), ruling out identity with the α_{2B}-adrenoceptor

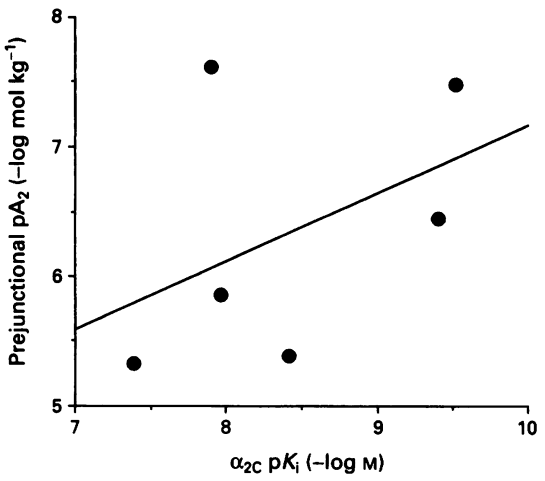

Figure 5 Correlation between antagonist K_i (− log M) obtained at α_{2C}-adrenoceptor ligand binding sites (human α_2-C4 gene expressed in COS-7 cells: Bylund *et al.*,1992) and the antagonist pA_2 obtained against xylazine in the pithed rat heart. $r = 0.48$, $n = 6$, NS.

subtype. The correlation with the published data for the α_{2C}-adrenoceptor ligand binding site (Bylund *et al.*, 1992) was also relatively poor. Hence the functional prejunctional α_2-adrenoceptor of pithed rat heart resembles the functional prejunctional α_2-adrenoceptors of rat vas deferens and submandibular gland in that they all appear to resemble closely the α_{2D}-adrenoceptor ligand binding site of rat submandibular gland (Smith *et al.*, 1992; Smith & Docherty, 1992).

Relative potencies of a series of agonists were also investigated in the pithed rat heart. Clonidine, UK 14,304 and oxymetazoline were approximately equipotent but 10 times more potent then xylazine. This order of potency is similar to that found for these agonists at the functional prejunctional α_2-adrenoceptor of rat vas deferens, which may be of the α_{2D}-adrenoceptor subtype (Smith & Docherty, 1992).

Other authors have examined subtypes of functional prejunctional α_2-adrenoceptors. Functional prejunctional α_2-adrenoceptors in rat submandibular gland (Limberger *et al.*, 1992), rat cerebral cortex (Trendelenberg *et al.*, 1993) and rat kidney (Bohmann *et al.*, 1993) resemble the α_{2D}-adrenoceptor ligand binding site, whereas those in rabbit cerebral cortex (Trendelenberg *et al.*, 1993) and human cerebral cortex (Raiteri *et al.*, 1992) resemble the α_{2A}-adrenoceptor. Since the α_{2A}-adrenoceptor and α_{2D}-adrenoceptor may be species homologues (see Introduction), this would suggest that the $\alpha_{2A/D}$-adrenoceptor may be the predominant prejunctional α_2-adrenoceptor.

However, the functional prejunctional α_2-adrenoceptor in rat isolated atrium does not closely resemble the α_{2D}-adrenoceptor (Smith *et al.*, 1992; Limberger *et al.*, 1992), and this has led to the suggestion that the receptor may resemble the α_{2B}-adrenoceptor ligand binding site of rat kidney cortex (Smith *et al.*, 1992). Indeed, for the 10 antagonists employed in the current study, the correlation between prejunctional potency in rat atrium (authors, unpublished results, see Smith *et al.*, 1992) with the kidney α_{2B}-adrenoceptor ligand binding site ($r = 0.94$) was better than with the rat submandibular α_{2D}-adrenoceptor ligand binding site ($r = 0.89$). This leads to an apparent anomaly that the prejunctional receptor activated by xylazine in the pithed rat heart closely resembles the rat submandibular α_{2D}-adrenoceptor ligand binding site, whereas the prejunctional receptor activated by noradrenaline in rat isolated atrium does not. This may mean that the receptor activated by xylazine to inhibit tachycardia differs from the receptor activated by noradrenaline to inhibit release of transmitter in atria, suggesting two subtypes of prejunctional receptor in atria, although studies *in vitro* may

not examine exclusively nerves involved in control of heart rate. We are currently investigating this problem but have no answer at present.

In conclusion, the prejunctional α_2-adrenoceptor in pithed rat heart mediating the cardioinhibitory actions of xylazine closely resembles the α_{2D}-adrenoceptor ligand binding site of rat submandibular gland.

Supported by the Health Research Board (Ireland) and RCSI. Generous gifts of drugs are gratefully acknowledged.

References

BOHMANN, C., SCHOLLMEYER, P. & RUMP, L.C. (1993). α_2-Autoreceptor subclassification in rat isolated kidney by use of short trains of electrical stimulation. *Br. J. Pharmacol.*, **108**, 262–268.

BYLUND, D.B. (1985). Heterogeneity of alpha-2 adrenergic receptors. *Pharmacol. Biochem. Behav.*, **22**, 835–843.

BYLUND, D.B. (1992). Subtypes of α_1- and α_2-adrenergic receptors. *FASEB J.*, **6**, 832–839.

BYLUND, D.B., BLAXALL, H.S., IVERSEN, L.J., CARON, M.G., LEFKOWITZ, R.J. & LOMASNEY, J.W. (1992). Pharmacological characteristics of α_2-adrenergic receptors: comparison of pharmacologically defined subtypes with subtypes identified by molecular cloning. *Mol. Pharmacol.*, **42**, 1–5.

CONNAUGHTON, S. & DOCHERTY, J.R. (1990). Functional evidence for heterogeneity of peripheral prejunctional α_2-adrenoceptors. *Br. J. Pharmacol.*, **101**, 285–290.

DOCHERTY, J.R. & HYLAND, L. (1985). No evidence for differences between pre- and postjunctional α_2-adrenoceptors. *Br. J. Pharmacol.*, **86**, 335–339.

DOCHERTY, J.R. & MCGRATH, J.C. (1980). A comparison of pre- and postjunctional potencies of several alpha-adrenoceptor agonists in the cardiovascular system and anococcygeus muscle of the rat: evidence for two types of postjunctional alpha-adrenoceptors. *Naunyn-Schmied. Arch. Pharmacol.*, **312**, 107–116.

GILLESPIE, J.S., MACLAREN, A. & POLLOCK, D. (1970). A method of stimulating different segments of the autonomic outflow from the spinal column to various organs in the pithed cat and rat. *Br. J. Pharmacol.*, **40**, 257–267.

HARRISON, J.K., PEARSON, W.R. & LYNCH, K.R. (1991). Molecular characterization of α_1- and α_2-adrenoceptors. *Trends Pharmacol. Sci.*, **12**, 62–67.

LANIER, S.M., DOWNING, S., DUZIE, E. & HOMEY, C.J. (1991). Isolation of rat genomic clones encoding subtypes of the α_2-adrenergic receptor. *J. Biol. Chem.*, **266**, 10470–10478.

LIMBERGER, N., TRENDELENBURG, A.-U. & STARKE, K. (1992). Pharmacological characterisation of presynaptic α_2-autoreceptors in rat submaxillary gland and heart atrium. *Br. J. Pharmacol.*, **107**, 246–255.

LORENZ, W., LOMASNEY, J.W., COLLINS, S., REGAN, J.W., CARON, M.G. & LEFKOWITZ, R.J. (1990). Expression of three α_2-adrenergic receptor subtypes in rat tissues: implications for α_2-receptor classification. *Mol. Pharmacol.*, **38**, 599–603.

MICHEL, A.D., LOURY, D.N. & WHITING, R.L. (1989). Differences between the α_2-adrenoceptor in rat submaxillary gland and the α_{2A}- and α_{2B}-adrenoceptor subtypes. *Br. J. Pharmacol.*, **98**, 890–897.

RAITERI, M., BONANNO, G., MAURA, G., PENDE, M., ANDRIOLI, G.C. & RUELLE, A. (1992). Subclassification of release-regulating α_2-autoreceptors in human brain cortex. *Br. J. Pharmacol.*, **107**, 1146–1151.

SMITH, K. & DOCHERTY, J.R. (1992). Are the prejunctional α_2-adrenoceptors of the rat vas deferens and submandibular gland of the α_{2A}- or α_{2D}-subtype? *Eur. J. Pharmacol.*, **219**, 203–210.

SMITH, K., CONNAUGHTON, S. & DOCHERTY, J.R. (1992). Investigations of prejunctional α_2-adrenoceptors in rat atrium, vas deferens and submandibular gland. *Eur. J. Pharmacol.*, **211**, 251–256.

TRENDELENBERG, A.-U., LIMBERGER, N. & STARKE, K. (1993). Presynaptic α_2-autoreceptors in brain cortex: α_{2D} in the rat and α_{2A} in the rabbit. *Naunyn-Schmied. Arch. Pharmacol.*, **348**, 35–45.

TUCK, D., HAMBERGER, B. & SJOQVIST, F. (1972). Drug interactions: effects of chlorpromazine on the uptake of monoamines into adrenergic neurons in man. *Lancet*, **ii**, 492.

(Received December 5, 1994
Revised January 21, 1995
Accepted January 30, 1995)

British Journal of Pharmacology (1995) 115, 321-329

Activation by ATP of a P_{2U} 'nucleotide' receptor in an exocrine cell

[1]Shaun C. Martin & Trevor J. Shuttleworth

Department of Physiology, University of Rochester School of Medicine and Dentistry, Rochester, NY 14642, U.S.A.

1 We employed the perforated patch whole-cell technique to investigate the effects of ATP and other related nucleotides on membrane conductances in avian exocrine salt gland cells.

2 ATP (10 μM–1 mM) evoked an increase in maxi-K^+ and Cl^- conductances with a reversal potential of −35 mV. At lower concentrations of ATP (≤100 μM) responses were generally oscillatory with a sustained response observed at higher concentrations (≥200 μM).

3 Both oscillatory and sustained responses were abolished by the removal of bath Ca^{2+}. In cells preincubated in extracellular saline containing reduced Ca^{2+}, the application of ATP resulted in a transient increase in current.

4 As increasing concentrations of ATP (and related nucleotides) evoked a graded sequence of events with little run-down we were able to establish a rank order of potency in single cells. The order of potency of ATP analogues and agonists of the various P_2-receptor subtypes was UTP>ATP = 2-methylthio-ATP>ADP. Adenosine (1 μM–1 mM), AMP (1 μM–1 mM), α,β-methylene-ATP (1 μM–1 mM) and β,γ-methylene-ATP (1 μM–1 mM) were without effect.

5 In conclusion, although unable to preclude a role for a P_{2Y}-receptor, our results suggest that ATP binds to a P_{2U}-receptor increasing $[Ca^{2+}]_i$ and subsequently activating Ca^{2+}-sensitive K^+ and Cl^- currents.

Keywords: Extracellular ATP; UTP; P_{2U}-receptor; cytosolic calcium; fluid secretion; potassium current; chloride current; avian salt gland

Introduction

The role of extracellular ATP as a neurotransmitter is widespread (for review see Dubyak & El-Moatassim, 1993). In exocrine cells, such as submandibular glands (Yu & Turner, 1991; Gibb *et al.*, 1994), equine sweat glands (Ko *et al.*, 1994) and lacrimal glands (Sasaki & Gallacher, 1990; 1992), ATP initiates an increase in intracellular $[Ca^{2+}]$ ($[Ca^{2+}]_i$). The rise in $[Ca^{2+}]_i$ subsequently activates Ca^{2+}-sensitive K^+ and Cl^- conductances (Sasaki & Gallacher, 1990; 1992), driving fluid secretion (Dawson & Richards, 1990; Petersen, 1992). Although an ATP-evoked $[Ca^{2+}]_i$ increase is ubiquitous to all exocrine cells tested, clear differences exist in both the resident receptor population and the mechanisms by which receptor activation increases $[Ca^{2+}]_i$.

In accordance with the classification system initially proposed by Burnstock (1978) all purinoceptors currently identified in exocrine glands are of the P_2-class. However, differences occur in the subclass of P_2-receptor found. In equine sweat glands (Ko *et al.*, 1994) and human submandibular duct cells (Yu & Turner, 1991) cellular activation is mediated by the P_{2U} 'nucleotide' receptor. This receptor, as in non-exocrine cells (O'Connor *et al.*, 1991), is linked to phospholipase C (Yu & Turner, 1991) and initiates the production of inositol trisphosphate ($InsP_3$) releasing Ca^{2+} from intracellular stores (Berridge & Irvine, 1989). Depletion of these stores activates a capacitative Ca^{2+}-entry pathway (Putney, 1990) supplementing the intracellular release of Ca^{2+}. In contrast, in lacrimal acinar cells (Sasaki & Gallacher, 1990; 1992), submandibular acinar cells (Hurley *et al.*, 1994) and parotid acini (Soltoff *et al.*, 1992), ATP promotes Ca^{2+}-entry in the absence of inositol phosphate metabolism, opening a Ca^{2+}-permeable non-selective cation channel with properties similar to the ATP-activated cation channel in smooth muscle cells (Benham & Tsien, 1987). The increase in Ca^{2+}-influx then triggers the release of Ca^{2+} from intracellular stores located at the luminal pole (Toescu *et al.*, 1992). In these tissues cellular activation is probably mediated by a P_{2Z}-receptor (McMillian *et al.*, 1993; Hurley *et al.*, 1994), although additional receptor/signalling pathways cannot be discounted (McMillian *et al.*, 1993).

In the present study we examine the effects ATP and other nucleotides on avian salt gland cells, a model exocrine cell. We demonstrate that ATP activates a P_{2U}-receptor which evokes an increase in Ca^{2+}-sensitive K^+ and Cl^- whole-cell currents. This increase in K^+ and Cl^- conductance could provide the basis for fluid secretion (Petersen, 1992).

Methods

Cell isolation and culture

Isolated cells from the nasal salt gland were obtained as previously described (Shuttleworth & Thompson, 1989). Briefly cells were obtained from 4–10 day old ducklings (*Anas platyrhynchos*) which were given 48 h of 1% NaCl drinking water *ad libitum* before being killed. The minced tissue was incubated for 90 min in 0.25% trypsin (Boehringer) then filtered through nylon mesh and centrifuged at 60 *g* for 10 min at room temperature. Cells were resuspended in 0.2 mg ml^{-1} of trypsin inhibitor and 1 mg ml^{-1} collagenase D (Boehringer) and incubated for 10 min. Cells were resuspended, placed on cover slips (25 mm, VWR Scientific No. 2) until firmly attached, and then transferred into sterile L15 containing 23 mM $NaHCO_3$, 100 u ml^{-1} penicillin, 100 μg ml^{-1} streptomycin, 250 ng ml^{-1} amphotericin, 10% dialyzed calf serum (Gibco) and stored in an incubator gassed with 5% CO_2 in air until use.

[1] Author for correspondence at: Dept. of Physiology, Box 642, University of Rochester Medical Center, 601 Elmwood Ave., Rochester, NY 14642, U.S.A.

Electrophysiological recordings

Electrophysiological investigations were carried out on single avian nasal gland cells at room temperature (20–25°C) by the patch-clamp technique (Hamill *et al.*, 1981). The standard extracellular solution contained (in mM): NaCl 132.5, KCl 4.8, $MgCl_2$ 1.2, KH_2PO_4 1.2, $CaCl_2$ 1.3, HEPES (free acid) 5.95, HEPES (Na^+ salt) 9.05 and glucose 6.0, pH 7.4. Bath solution changes were achieved by placing the cell in close proximity (approximately 5 mm) to a row of gravity-fed polythene tubes and constantly removing the bath solution by aspiration. Complete bath solution exchange took less than 10 s. The standard intracellular solution (pipette solution in whole-cell experiments) contained (mM): K glutamate 100, KCl 40, $MgCl_2$ 1.2, HEPES (free acid) 10 and EGTA1, pH 7.2. Where used, the K^+ channel blocker tetraethylammonium chloride (TEA) was obtained from Sigma.

Pipettes of 0.5–2 MΩ (when filled) were pulled from Kimble No. R6 glass (Garner Glass Co., Claremont, California, U.S.A.) and heat polished. Seals of greater than 10 GΩ were produced on the cell membrane. Whole-cell perforated-patch recordings were achieved by the use of the pore-forming antibiotic amphotericin B (Sigma) as previously described (Rea *et al.*, 1991). Briefly, a small volume of amphotericin-free standard intracellular solution was drawn into the pipette and the pipette backfilled with the standard intracellular saline containing amphotericin B. Amphotericin was freshly prepared every 2 h. Access resistance (R_a) rapidly declined after the formation of an on-cell patch as the amphotericin B pores were inserted into the membrane. This could be observed as an increase in the membrane capacitance (C_m). Ionic equilibrium between the cell and the pipette was usually rapid and was judged by the stability of the membrane currents. All cells were left to equilibrate for a minimum of 20 min before any agonists were applied. The access resistance of the patch and the cell capacitance were measured directly by the compensation circuitry of the patch-clamp amplifier (Axopatch-1C, Axon Instruments, Burlingam California, U.S.A.). Any cells with an R_a greater than 12MΩ were rejected. To accommodate for variations in cell size, all currents were normalized as a current density and expressed as picoamperes per picofarad (pA pF^{-1}).

Membrane currents were referenced to the bath using an Ag-Ag_2Cl_2 electrode connected to the bath solution by an agar bridge electrode to minimize the formation of junction potentials when changing solutions. Voltage steps were maintained for 100 ms with a stepping frequency of 1 Hz. At the resolution shown in the figures the current traces appear to be continuous. Currents were filtered at 2 kHz (low pass). Software for pulse generation and data collection was developed for this application by Dr P. Smith (Smith, 1992). Membrane potential measurements were made using a similar protocol to that used to monitor current except the cells were clamped to zero current. Membrane voltage (rather than current) was monitored continuously and every 250 ms the average voltage was calculated and saved.

Results

Changes in conductance evoked by ATP

To evaluate the conductance changes evoked by ATP the whole-cell perforated-patch clamp technique (voltage-clamp

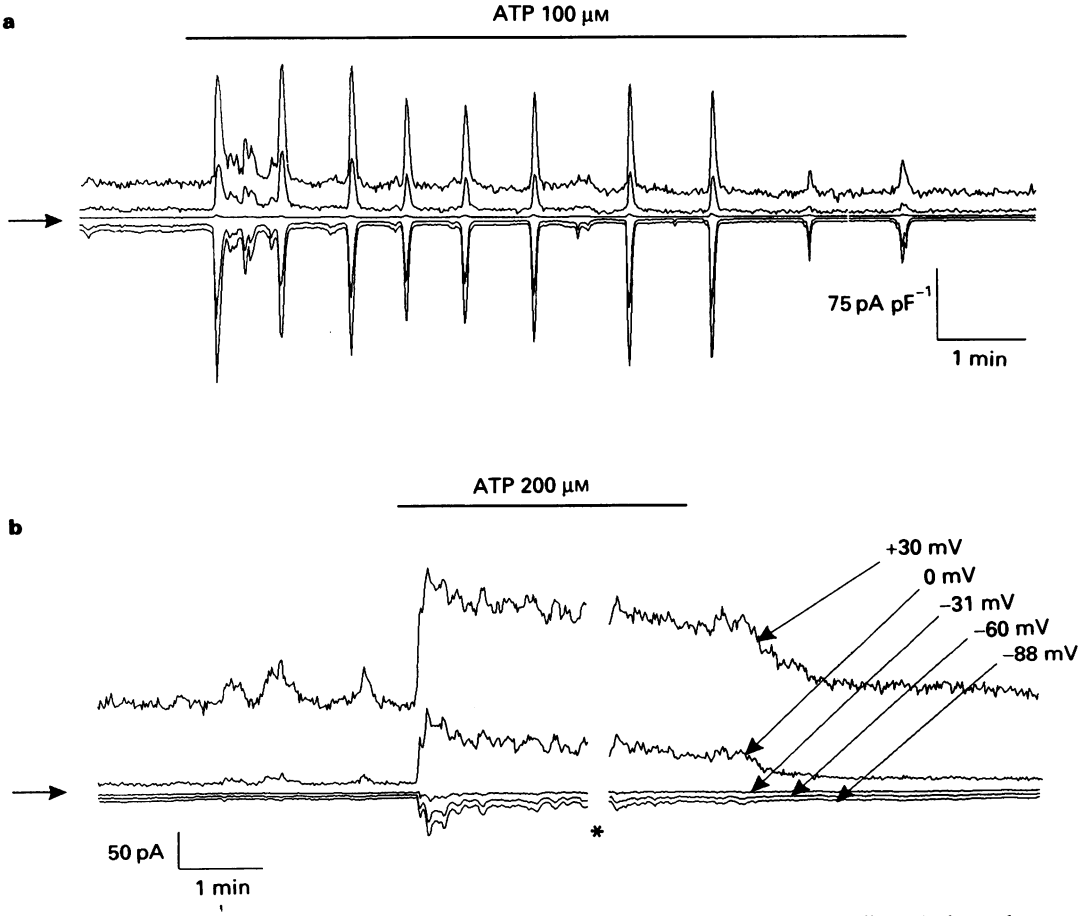

Figure 1 Various membrane conductance changes evoked by ATP. Whole-cell current recordings (voltage-clamp recording configuration) demonstrating oscillatory (a) and sustained (b) responses to ATP. Cells were held at −60 mV and pulsed to the potentials indicated for 100 ms every second. Zero current is indicated by the arrow. Current-voltage recordings were conducted at the asterisk.

recording configuration) was employed. Figure 1 demonstrates that on application of ATP, inward currents were observed at all potentials more negative than E_{Cl^-}, with outward currents observed at 0 mV ($n = 114$). The threshold for ATP-evoked conductance changes showed large variation between cells but was generally in the range 50–100 μM. At lower concentrations (≤100 μM) responses were generally oscillatory (Figure 1a) ($n = 61/80$ applications). These oscillations were of a transient nature with a similar frequency (2–8 spikes min^{-1}) to those observed in the presence of other Ca^{2+}-mobilizing agonists such as carbachol (CCh) (Martin & Shuttleworth, 1994a; Martin *et al.*, 1994). At concentrations ≥200 μM the conductance changes evoked by ATP were generally sustained for the duration of agonist application (Figure 1b) ($n = 10/16$ applications). At these concentrations peak inward currents at −88 mV were 36 ± 10pA pF^{-1}. In contrast, outward currents of 82 ± 16pA pF^{-1} were observed at 0 mV. In the majority of cases little or no current was observed at −31mV. At concentrations where the cell was in a transition stage between oscillatory and sustained phases, a third type of response was observed consisting of small amplitude, high frequency oscillations (more than 10 spikes min^{-1}) on an elevated plateau (Figure 3a). At these concentrations prolonged agonist application often resulted in the oscillations fusing to a plateau similar to that observed at higher concentrations. In all cases removal of the agonist resulted in termination of the response. Furthermore, after an adequate washout period (> 5 min), repetitive applications evoked responses of similar morphology and magnitude.

To evaluate the composition of the ATP response, ionic substitution and pharmacological experiments were conducted. In a previous investigation we demonstrated that agents which evoke an increase in $[Ca^{2+}]_i$, such as CCh and A23187, activate K^+ and Cl^- conductances (Martin & Shuttleworth, 1994a). Figure 2 demonstrates that ATP stimulates similar conductances. If ATP was applied in the presence of TEA (5 mM), a blocker of K_{maxi} in avian salt gland cells (Richards *et al.*, 1989; Martin & Shuttleworth, 1994a), the outward current stimulated by ATP was significantly inhibited with the residual current showing a reversal potential close to E_{Cl^-} (Figure 2a) ($n = 8$). TEA (5 mM) was without effect on the inward currents observed at E_{K^+} and −60 mV ($n = 8$). To demonstrate that the TEA-insensitive current was carried by Cl^- ions a similar experiment was conducted at a high $[Cl^-]_i$ ($[Cl^-]_i$ = 142 mM such that $[Cl^-]_i = [Cl^-]_e$). Under these conditions the reversal potential of the ATP response (in the presence of 5 mM TEA) shifted from −30 mV to approximately 0 mV as predicted by the Nernst equation for Cl^- ions (Figure 2b) ($n = 6$).

Role of Ca^{2+} in the response to ATP

To evaluate the role played by both intracellular and extracellular Ca^{2+} during the ATP response, bath $[Ca^{2+}]$ was reduced from 1.3 mM to approximately 100 μM. Figure 3a shows that reduction of $[Ca^{2+}]_e$ initiated a return to prestimulus levels ($n = 14$). Replacement of extracellular Ca^{2+} rapidly reinstated the ATP-evoked conductance increase. If bath Ca^{2+} was reduced prior to the addition of ATP, the

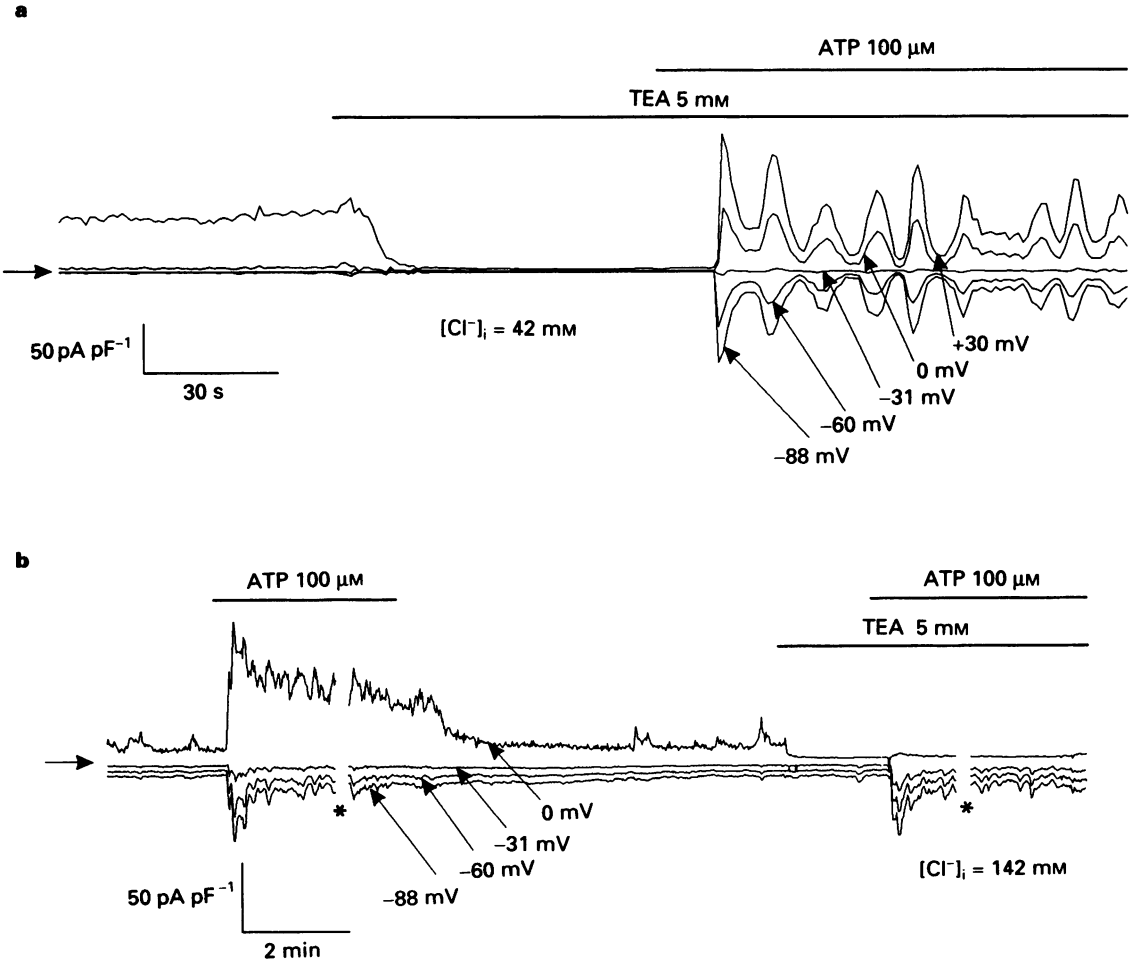

Figure 2 Effects of tetraethylammonium (TEA) and altered $[Cl^-]_i$ on the ATP response. Whole-cell current recordings in which cells were held at −60 mV and pulsed to the potentials indicated. Intracellular $[Cl^-]$ is indicated in the individual figures with Cl^- substituted for glutamate. Zero current is indicated by the arrow. Current-voltage relationships were carried out at the asterisk.

increase in conductance evoked by ATP was only transient, lasting between 1 and 3 min ($n = 12$). If bath Ca^{2+} was replaced at any point during this transient a sustained response was evoked (*cf.* Figure 3b) ($n = 8$). Although physiological Ca^{2+} levels are clearly required to perpetuate the ATP response it is still plausible that the transient increase in Ca^{2+}-dependent currents observed when extracellular Ca^{2+} is reduced could be attributed to a small amount of Ca^{2+}-influx. To address this question we clamped the cell at +60 mV, a potential sufficiently close to E_{Ca} such that Ca^{2+}-influx is completely abolished (Martin & Shuttleworth, 1994b). Figure 3c demonstrates that under these conditions ATP initiates a transient increase in Ca^{2+}-dependent currents substantiating the evidence obtained by reducing extracellular Ca^{2+} ($n = 6$). Furthermore, if the cell is subsequently clamped at −31mV and pulsed to +60 mV for 100 ms every second (thereby reinstating the driving force for Ca^{2+}-influx) the response becomes sustained (results not shown) ($n = 14$).

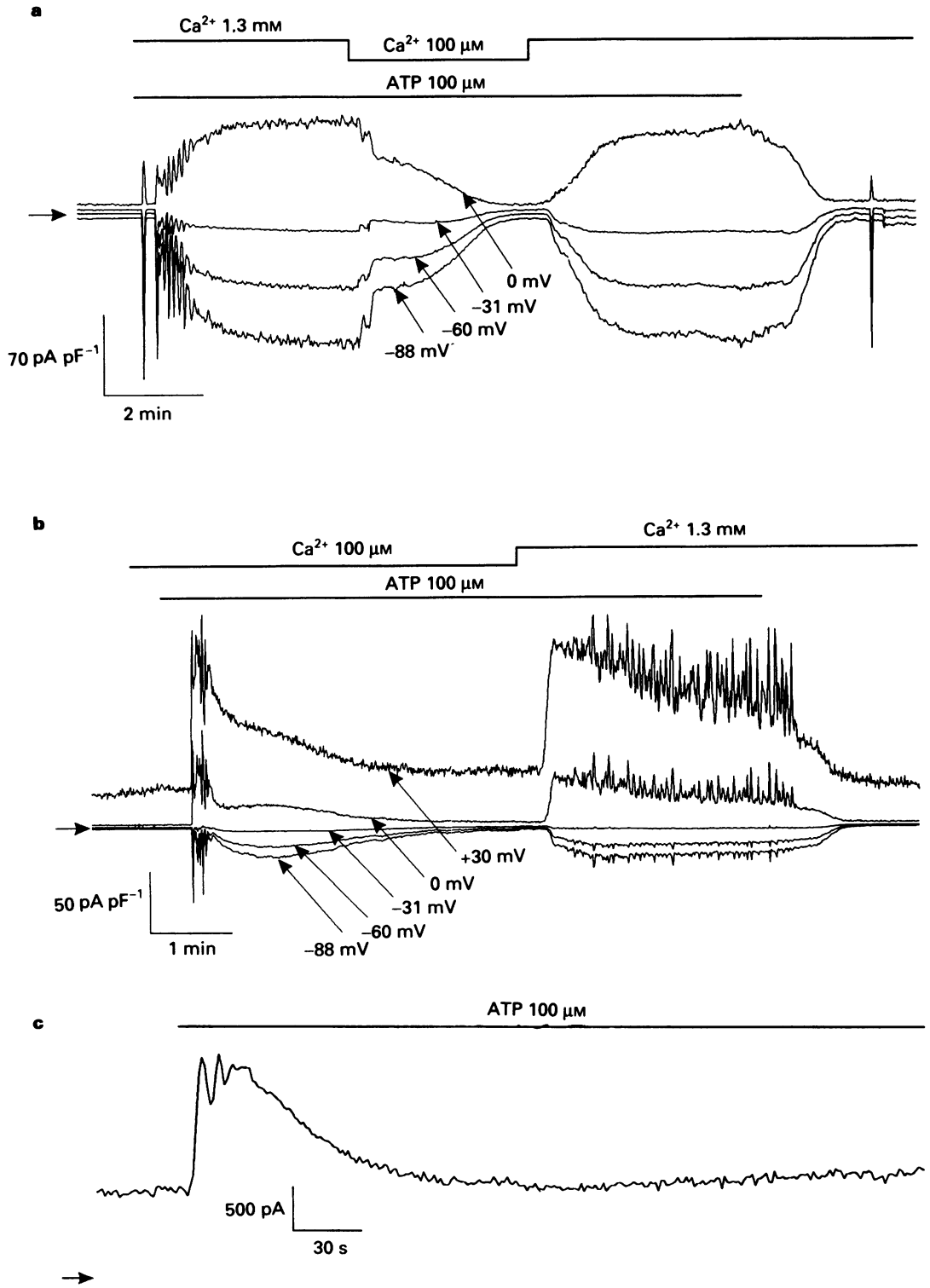

Figure 3 A whole-cell current recording (voltage-clamp recording configuration) demonstrating the effects of Ca^{2+}-removal on the ATP response. In (a) and (b) calcium was reduced by bathing the cell in the standard extracellular solution containing only 100 μM added Ca^{2+}. Cells were held at −60 mV and pulsed to the potentials indicated in the figure. In (c) the cell was maintained in normal extracellular Ca^{2+} (1.3 mM) and voltage-clamped to +60 mV. Zero currents are indicated by the arrows.

Finally, in preliminary experiments using dual-wavelength microfluorimetry on indo-1 loaded cells, ATP (100 μM) evoked a biphasic increase in Ca^{2+} consisting of an initial transient followed by a sustained plateau (results not shown). This provides additional evidence that the effects of ATP are mediated by an increase in $[Ca^{2+}]_i$.

Effects of other nucleotides and ATP analogues

Given the large cell-to-cell variation in threshold ATP concentration, it was necessary to develop a method of quantifying the ATP response to evaluate the effects and relative potencies of other nucleotides and ATP analogues. This was achieved by utilizing the observation that as the concentration of ATP is increased, a graded sequence of events was observed with the following order: low frequency transient oscillations, high frequency spikes on an elevated plateau followed by a sustained plateau. By initially stimulating the cell with ATP then switching to an identical concentration of a distinct agonist it is possible to draw up an order of potency by comparing the individual responses.

To elucidate which receptor subtype was responsible for the ATP effects, the following agonists were incorporated into this protocol: ADP, AMP, adenosine and UTP. Of all

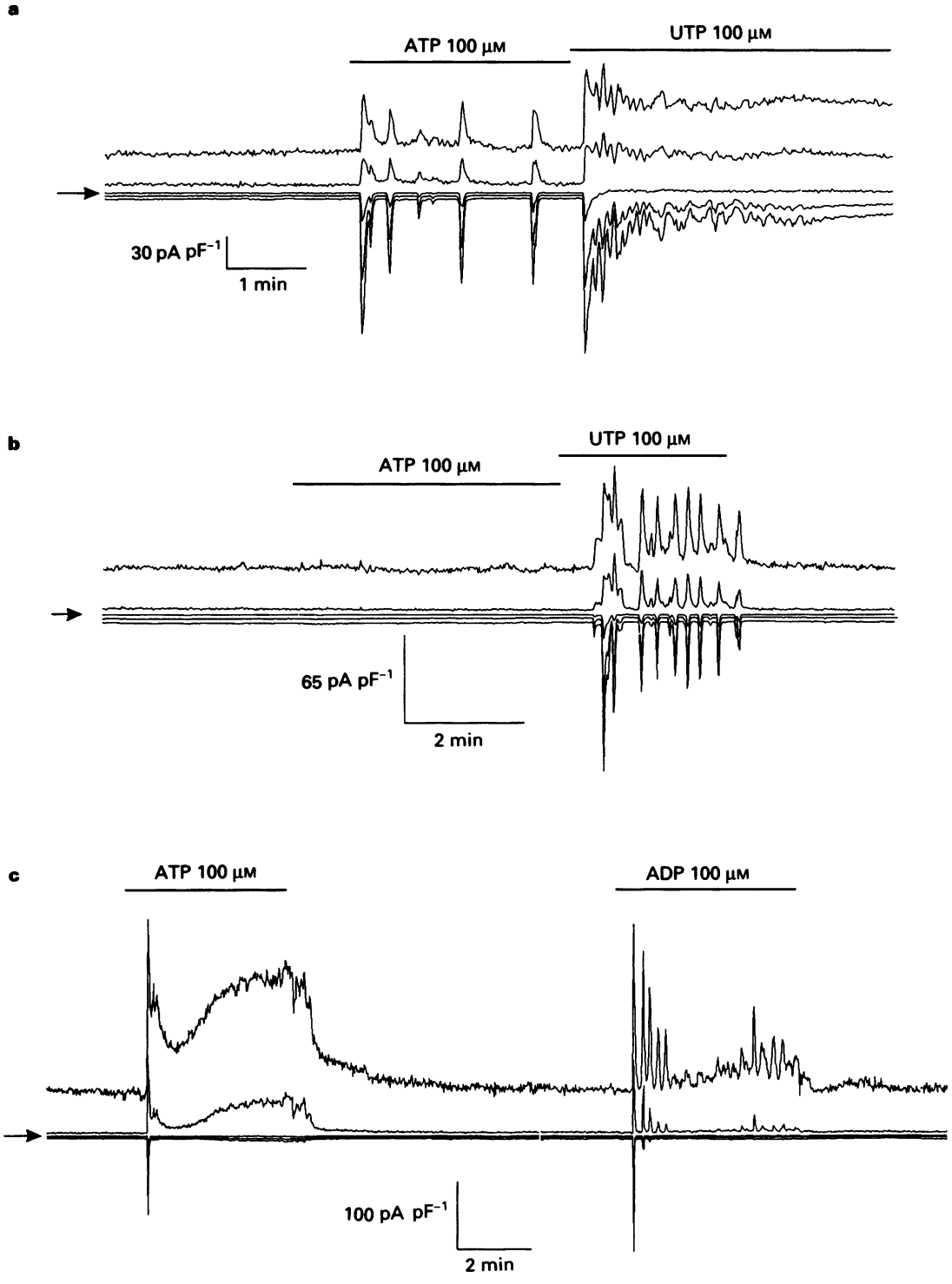

Figure 4 Effects of alternative nucleotides on the avian salt gland cell. The pulse protocol is identical to that employed in Figure 1b. Zero current level is indicated at the arrow.

the agonists tested only UTP proved to be more potent than ATP (18/18 applications). Figure 4a demonstrates that if the cell was triggered by a concentration of ATP which evoked oscillations in current (100 μM), switching to an identical concentration of UTP elicited a sustained increase in conductance. Alternatively if a subthreshold concentration of ATP was administered, the corresponding concentration of UTP initiated oscillations in K^+ and Cl^- current (*cf.* Figure 4b). This protocol demonstrates that UTP is not only more potent than ATP, but also that nucleotides other than ATP can trigger a graded cellular activation. Of all the other nucleotides tested, only ADP mimicked the response to ATP

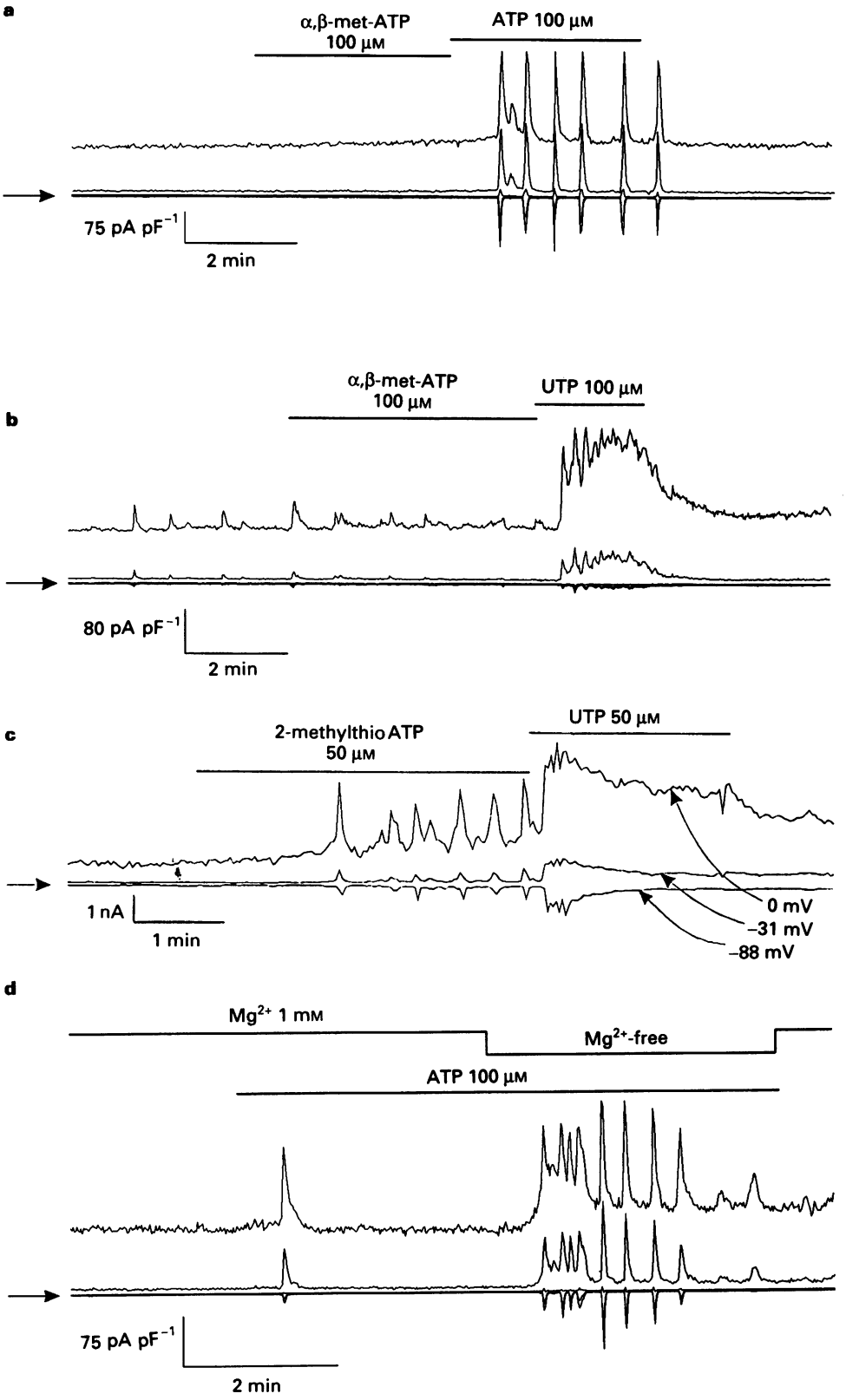

Figure 5 Whole-cell current recording (voltage-clamp recording configuration) demonstrating the effects of agonists for the known receptor subtypes and Mg^{2+}-removal on the ATP response. Extracellular Mg^{2+} was reduced by bathing the cell in the standard solution containing no added Mg^{2+}. The pulse protocols in (a), (b) and (d) are identical to Figure 1b. In (c) the cell is clamped at −31 mV and pulsed to the potentials indicated for 100 ms every 2 s. Zero currents are indicated by the arrows.

(Figure 4c) ($n = 9$). Within the concentration-range tested (50 μM – 1 mM), ADP generally stimulated oscillations in both K^+ and Cl^- currents and, in those cells where comparisons were drawn, ATP was approximately 5 fold more potent than ADP. The relative potency is demonstrated by Figure 4c in which 100 μM ATP activated a sustained increase in membrane conductance whereas 100 μM ADP evoked an oscillatory response. Unlike UTP and ADP, both AMP (10 μM – 1 mM) ($n = 4$) and adenosine (10 μM – 1 mM) ($n = 6$) were without effect on membrane conductance.

To identify further the resident receptor in the avian salt gland, cells were tested with the P_{2X}-receptor agonists α,β-methylene-ATP and β,γ-methylene-ATP, and the P_{2Y}-receptor agonist 2-methylthio-ATP. In all cases the P_{2X}-receptor agonists (1 μM – 1 mM) were without effect on membrane conductance ($n = 12$). To substantiate the absence of a P_{2X}-receptor, cells were preincubated in α,β-methylene-ATP (100 μM). Under these conditions any P_{2X}-receptors should be down-regulated (Burnstock & Kennedy, 1985) yet both ATP (100 μM) (Figure 5a) ($n = 6$) and UTP (100 μM) (Figure 5b) ($n = 3$) still produced characteristic responses. Unlike the P_{2X}-receptor agonists, responses were obtained with 2-methylthio-ATP (100 μM – 1 mM) which showed a similar potency to ATP (10/12 applications). In addition, if oscillations are evoked by the application of 2-methylthio-ATP (50 μM) the response is enhanced by an identical dose of UTP (Figure 5c) ($n = 4$). Finally, the ionic species of ATP binding to the receptor was also investigated. By reducing the extracellular $[Mg^{2+}]$ we were able to increase the ratio of free ATP (i.e. ATP^{3-}, ATP^{4-}) to bound ATP (i.e. MgATP) ($n = 7$). Figure 5d demonstrates that on removal of extracellular Mg^{2+} in the continued presence of a threshold dose of ATP a dramatic potentiation was observed ($n = 8$). Removal of Mg^{2+} in the absence of ATP was without effect on the membrane conductance ($n = 3$).

Discussion

The data presented indicate that, in the exocrine avian salt gland cell, ATP (50 μM – 1 mM) binds to a P_{2U} 'nucleotide' receptor, evoking an increase in $[Ca^{2+}]_i$ which subsequently activates Ca^{2+}-sensitive K^+ and Cl^- conductances. Thus, we found that the conductance increases evoked by ATP were mimicked by UTP, ADP and 2-methylthio-ATP with the following rank order of potency: UTP>>ATP=2-methylthio-ATP>ADP. In contrast, the agonists α,β-methylene-ATP, β,γ-methylene-ATP and the P_1-agonists, adenosine and AMP were without effect.

Burnstock (1978) initially divided purinoceptors into two types, those which increase intracellular cyclic AMP (P_1-receptors) and those which employ Ca^{2+} as an intracellular messenger (P_2-receptors). The P_2-class, the receptor type known to initiate an increase in $[Ca^{2+}]_i$ and fluid secretion in exocrine cells (Sasaki & Gallacher, 1990; 1992; Yu & Turner, 1991; McMillian *et al.*, 1993; Hurley *et al.*, 1994; Gibb *et al.*, 1994; Ko *et al.*, 1994), has been further subdivided into 5 distinct categories, P_{2X}, P_{2Y}, P_{2T} and more recently P_{2U}. The basis for these distinctions is derived from the order of agonist potency of various nucleotides and ATP derivatives. Based on the classification system proposed by Burnstock & Kennedy (1985), and the results presented in the current study we are able to disregard three of the five P_2 subclasses.

The first of these was the P_{2X}-receptor, a receptor commonly associated with smooth muscle cells (Benham & Tsien, 1987). This receptor is characteristically activated by the methylated ATP analogues, α,β-methylene-ATP and β,γ-methylene-ATP, yet in the avian salt gland cell both agents were ineffective. Furthermore, preincubation in α,β-methylene-ATP (100 μM), a procedure known to desensitize the P_{2X}-receptor (Burnstock & Kennedy, 1985), failed to abolish the effects of both ATP and UTP. Combined, these findings exclude the P_{2X} designation. Our observations also preclude the P_{2T}-receptor. To date the P_{2T}-receptor is restricted to platelets and megakaryocytic cells (Murgo *et al.*, 1994). This receptor subtype possesses the distinguishing characteristic that it is stimulated only by ADP with ATP acting as an antagonist. As ATP is approximately 5 times more potent that ADP in our preparation, the P_{2T}-receptor can also be disregarded.

The final type of receptor to be discounted is the P_{2Z}-receptor. P_{2Z}-receptors were originally discovered on mast cells and are involved in receptor-activated cell permeabilization (Tatham *et al.*, 1988). The P_{2Z}-receptor is discounted on the basis of its typical receptor potency order. The P_{2Z}-receptor is highly selective for the ATP^{4-} ion and has strict structural requirements. Generally there is a need for an unmodified adenine ring, subsequently UTP has little or no activity (Gordon, 1986; Erb *et al.*, 1990). Although metal ion-free nucleotides are the more active species in our preparation UTP is the most potent agonist in our system which suggests that the P_{2Z}-receptor type need not be considered.

Given the potency of UTP, the most likely candidate for the receptor subtype in our cells is the P_{2U} 'nucleotide' receptor (O'Connor *et al.*, 1991; O'Connor, 1992). The accepted agonist potency order for the P_{2U}-receptor is UTP = ATP > ADP > 2methylthio-ATP > α,β-methylene-ATP = β,γ-methylene-ATP (O'Connor, 1992). This order of potency is similar to our current findings except that UTP demonstrates a potency approximately 5 fold greater than ATP. Furthermore, as with the P_{2Z}-receptor (Tatham *et al.*, 1988), numerous accounts have demonstrated that metal ion-free nucleotides are the active species at the P_{2U} site (for review see Dubyak & El-Moatassim, 1993). Although consistent with the above features, categorizing our receptor in the P_{2U}-subgroup is only tentative as there are a few discrepancies. The first involves the agonist actions of 2-methylthio-ATP which is conventionally recognised as a P_{2Y}-agonist. In our preparation 2-methylthio-ATP was equipotent with ATP and demonstrated a greater potency than ADP. Although this discrepancy could be due to 2-methylthio-ATP acting as a partial agonist for the P_{2U}-receptor it is more plausible that the avian salt gland cell possesses two distinct P_2-receptor subclasses, as observed in many other cells such as hepatocytes (Dixon *et al.*, 1990) and megakaryocytes (Murgo *et al.*, 1994). However, although a P_{2Y}-receptor cannot be discounted, a P_{2U}-receptor must be present as UTP is unable to activate the P_{2Y}-receptor (O'Connor, 1992), Until specific antagonists for the individual receptor subtypes are developed it is not possible to differentiate between these possibilities.

The presence of a P_{2U}-receptor is not uncommon in exocrine cells. Such receptors have been identified in mouse submandibular cells (Gibb *et al.*, 1994), human submandibular duct cells (Yu & Turner, 1991) and equine sweat gland cells (Ko *et al.*, 1994) and are linked to the activation of phospholipase C (O'Connor *et al.*, 1991; O'Connor, 1992) leading to an increased generation of inositol (1,4,5) trisphosphate which results in the release of Ca^{2+} from intracellular stores. As with the majority of Ca^{2+}-mobilizing agonists, emptying of intracellular stores initiates a Ca^{2+}-influx pathway (Putney, 1990) thereby maintaining the response for the duration of agonist application. Results presented here imply that P_{2U}-receptors initiate a similar chain of events in the avian salt gland. As the response to ATP generally shows little desensitization we were able to investigate the effects of Ca^{2+}-removal in detail.

Given that removal of extracellular Ca^{2+} during a sustained response to ATP terminated the response (*cf.* Figure 3a) the importance of extracellular Ca^{2+} is beyond question. In many cells, including exocrine acinar cells, ATP directly opens a non-selective cation channel permeable to Ca^{2+} (Sasaki & Gallacher, 1990; 1992; Soltoff *et al.*, 1992; Hurley

et al., 1994). However, this channel is unlikely to import Ca^{2+} in the avian salt gland cell. The reasoning behind this is many-fold. If we apply ATP when extracellular Ca^{2+} is reduced, a transient increase in Ca^{2+}-dependent currents is observed (*cf.* Figure 3b and c) which can only result from release from intracellular stores. Furthermore, the oscillatory ATP response cannot be duplicated by the Ca^{2+}-ionophore A23187 (Martin & Shuttleworth, 1994a). This would suggest that the influx of Ca^{2+} in the absence of phosphoinositide metabolism cannot mimic the ATP response. Further evidence against the involvement of a non-selective cation channel is that the whole-cell currents activated by ATP are similar in morphology and reversal potential to the current responses evoked by the Ca^{2+}-mobilizing agonist, CCh (Martin & Shuttleworth, 1994a). This contrasts with the whole-cell currents observed in lacrimal cells where ATP activates a non-selective cation channel (Sasaki & Gallacher, 1990; 1992). In these cells a large transient inward current triggers a response with a reversal potential significantly more negative than that evoked by acetylcholine. The final piece of evidence against the involvement of an ATP-gated channel lies in the receptor employed in the avian salt gland. To date it has yet to be demonstrated that activation of a P_{2U}-receptor can directly open a non-selective cation channel. The only receptors which activate such a channel are the P_{2X}-receptor in preparations such as smooth muscle cells (Benham & Tsien, 1987) and the P_{2Z}-subtype in tissues such as lacrimal and parotid acini (McMillian *et al.*, 1993). As the only possible receptors in the avian salt gland cell are the P_{2U} and possibly, the P_{2Y} variants, both of which employ phospholipase C, the involvement of an ATP-gated cation channel is unlikely.

Although the mechanism by which ATP evokes an increase in $[Ca^{2+}]_i$ varies among exocrine cells the resultant increase in Ca^{2+}-sensitive currents displays remarkable homogeneity. Gallacher (1982) first demonstrated that ATP was a major stimulus in exocrine glands observing an increase in $^{86}Rb^+$ efflux and an increase in amylase output in the mouse parotid on addition of the nucleotide. Further studies revealed that the increase in $[Ca^{2+}]_i$ activates an increase in Ca^{2+}-sensitive K^+ and Cl^- conductances (Sasaki & Gallacher, 1990; 1992). The findings in the present study would support these conclusions with ATP activating Ca^{2+}-sensitive K^+ and Cl^- currents similar to those activated by other Ca^{2+}-mobilizing agonists (Martin & Shuttleworth, 1994a). As the simultaneous activation of both K^+ and Cl^- conductances provides the fundamental basis for fluid secretion (for review see Petersen, 1992) it is not unreasonable to suggest that ATP may play an important physiological role in the mechanism underlying fluid secretion in the avian salt gland. In addition to its effects in isolation, the fact that ATP is stored and co-released with all neurotransmitters cannot exclude its role as a co-transmitter. By fulfilling a role as a co-transmitter it could enhance the Ca^{2+}-responses to low concentrations of Ca^{2+}-mobilizing agonists such as acetylcholine or potentiate cyclic AMP-mediated pathways, a mechanism shown to be of particular importance in the avian salt gland (Martin *et al.*, 1994).

We would like to thank Jill Thompson for excellent technical assistance and help in preparation of the manuscript. We would also like to thank Dr P. Smith for the computer software used for data collection and analysis. This work was supported by National Institutes of Health Grant GM-40457 to T.J.S.

References

BENHAM, C.D. & TSIEN, R.W. (1987). A novel receptor-operated Ca^{2+}-permeable channel activated by ATP in smooth muscle. *Nature*, **328**, 275–278.

BERRIDGE, M.J. & IRVINE, R.F. (1989). Inositol phosphates and cell signalling. *Nature*, **341**, 197–205.

BURNSTOCK, G. (1978). A basis for distinguishing 2 types of purinergic receptor. In *Cell Membrane Receptors for Drugs and Hormones: A Multidisciplinary Approach.* ed. Straub & Bolish pp. 107–118. New York: Raven Press.

BURNSTOCK, G. & KENNEDY, C. (1985). Is there a basis for distinguishing two types of P_2-purinoceptor? *Gen. Pharmacol.*, **16**, 433–440.

DAWSON, D.C. & RICHARDS, N.W. (1990). Basolateral K^+ conductance: role in regulation of NaCl absorption and secretion. *Am. J. Physiol.*, **259**, C181–195.

DIXON, C.J., WOOD, N.M., CUTHBERTSON, K.R.S. & COBBOLD, P.H. (1990). Evidence for two Ca^{2+}-mobilising purinoceptors on rat hepatocytes. *Biochem. J.*, **269**, 499–502.

DUBYAK, G.R. & EL-MOATASSIUM, C. (1993). Signal transduction via P_2-purinergic receptors for extracellular ATP and other nucleotides. *Am. J. Physiol.*, **265**, C577–606.

ERB, L., LUSTIG, K.D., AHMED, A.H., GONZALEZ, F.A. & WEISMAN, G.A. (1990). Covalent incorporation of 3'-O-(4-benzoyl-ATP) into a P_2-purinoceptor in transformed mouse fibroblasts. *J. Biol. Chem.*, **265**, 7424–7431.

GALLACHER, D.V. (1982). Are there purinergic receptors on parotid aciar cells? *Nature*, **296**, 83–86.

GIBB, C.A., SINGH, S., COOK, D.I., PORONNIK, P. & CONIGRAVE, A.D. (1994). A nucleotide receptor that mobilizes calcium in the mouse submandibular salivary gland cell line ST885. *Br. J. Pharmacol.*, **111**, 1135–1139.

GORDON, J.L. (1986). Extracellular ATP: effects, sources and fate. *Biochem J.*, **233**, 309–319.

HAMILL, O.P., MARTY, A., NEHER, E., SAKMANN, B. & SIGWORTH, F.J. (1981). Improved patch-clamp techniques for high resolution current recording from cells and cell-free membrane patches. *Pflügers Arch.*, **391**, 85–100.

HURLEY, T.W., RYAN, M.P. & SHOEMAKER, D.D. (1994). Mobilization of Ca^{2+}-influx, but not of stored Ca^{2+}, by extracellular ATP in rat submandibular gland acini. *Arch. Oral. Biol.*, **39**, 205–212.

KO, W.H., O'DOWD, J.J.M., PEDIANI, J.D., BOVELL, D.L., ELDER, H.Y., JENKINSON, D.M. & WILSON, S.M. (1994). Extracellular ATP can activate autonomic signal transduction pathways in cultured equine sweat gland epithelial cells. *J. Exp. Biol.*, **190**, 239–252.

MARTIN, S.C. & SHUTTLEWORTH, T.J. (1994a). Muscarinic-receptor activation stimulates oscillations in K^+ and Cl^- currents which are acutely dependent on extracellular Ca^{2+} in avian salt gland cells. *Pflügers Arch.*, **426**, 231–238.

MARTIN, S.C. & SHUTTLEWORTH, T.J. (1994b). Ca^{2+} influx drives agonist-activated $[Ca^{2+}]_i$ oscillations in an exocrine cell. *FEBS Lett.*, **352**, 32–36.

MARTIN, S.C., THOMPSON, J. & SHUTTLEWORTH, T.J. (1994). Potentiation of Ca^{2+}-activated secretory activity by a cAMP-mediated mechanism in avian salt gland cells. *Am. J. Physiol.*, **267**, C255–C265.

MCMILLIAN, M.K., SOLTOFF, S.P., CANTLEY, L.C., RUDEL, R. & TALAMO, B.R. (1993). Two distinct cytosolic calcium responses to extracellular ATP in rat parotid acinar cells. *Br. J. Pharmacol.*, **108**, 453–461.

MURGO, A.J., CONTRERA, J.G. & SISTARE, F.D. (1994). Evidence for separate calcium-signalling P_{2T} and P_{2U} purinoceptors in human megakaryocytic Dami cells. *Blood*, **83**, 1258–1267.

O'CONNOR, S.E. (1992). Recent developments in the classification and functional significance of receptors for ATP and UTP, evidence for nucleotide receptors. *Life Sci.*, **50**, 1657–1664.

O'CONNOR, S.E., DAINTY, I.A. & LEFF, P. (1991). Further subclassification of ATP receptors based on agonist studies. *Trends Pharmacol. Sci.*, **12**, 137–141.

PETERSEN, O.H. (1992). Stimulus-secretion coupling: cytoplasmic calcium signals and the control of ion channels in exocrine acinar cells. *J. Physiol.*, **448**, 1–51.

PUTNEY, J.W. (1990). Capacitative calcium entry revisited. *Cell Calcium.*, **11**, 611–624.

REA, J., COOPER, K., GATES, P. & WATSKY, M. (1991). Low access resistance perforated patch recordings using amphotericin B. *J. Neurosci. Methods.*, **37**, 15–26.

RICHARDS, N.W., LOWY, R.J., ERNST, S.A. & DAWSON, D.C. (1989). Two K^+ channel types, muscarinic agonist-activated and inwardly rectifying, in a Cl^- secretory epithelium: the avian salt gland. *J. Gen. Physiol.*, **93**, 1171–1194.

SASAKI, T. & GALLACHER, D.V. (1990). Extracellular ATP activates receptor-operated cation channels in mouse lacrimal acinar cells to promote calcium influx in the absence of phosphoinositide metabolism. *FEBS Lett.*, **264**, 130–134.

SASAKI, T. & GALLACHER, D.V. (1992). The ATP-induced inward current in mouse lacrimal acinar cells is potentiated by isoprenaline and GTP. *J. Physiol.*, **447**, 103–118.

SHUTTLEWORTH, T.J. & THOMPSON, J.L. (1989). Intracellular $[Ca^{2+}]$ and inositol phosphates in avian nasal gland cells. *Am. J. Physiol.*, **257**, C1020–C1029.

SMITH, P.M. (1992). Patch-clamp whole cell pulse protocol measurements using a microcomputer. *J. Physiol.*, **446**, 72P.

SOLTOFF, S.P., MCMILLIAN, M.K. & TALAMO, B.R. (1992). ATP activates a cation-permeable pathway in rat parotid acinar cells. *Am. J. Physiol.*, **262**, C934–C940.

TATHAM, P.E.R., CUSACK, N.J. & GOMPERTS, B.D. (1988). Characterization of the ATP^{4-} receptor that mediates permeabilization of rat mast cells. *Eur. J. Pharmacol.*, **147**, 13–21.

TOESCU, E.C., LAWRIE, A.M., PETERSEN, O.H. & GALLACHER, D.V. (1992). Spatial and temporal distribution of agonist-evoked cytoplasmic Ca^{2+}-signals in exocrine acinar cells analysed by digital image microscopy. *EMBO J.*, **11**, 1623–1629.

YU, H. & TURNER, J.T. (1991). Functional studies in the human submandibular duct cell line, HSG-PA, suggest a second salivary gland receptor subtype for nucleotides. *J. Pharmacol. Exp. Ther.*, **259**, 1344–1350.

(Received September 5, 1994
Revised January 12, 1995
Accepted February 9, 1995)

British Journal of Pharmacology (1995) 115, 330-334

Modulatory effect of bradykinin on the release of noradrenaline from rat isolated atria

Chantal Chulak, Réjean Couture & [1]Sylvain Foucart

Group de Recherche sur le Système Nerveux Autonome, Département de Physiologie, Faculté de Médecine, Université de Montréal, C.P. 6128, Succ. Centre-Ville, Montréal, Québec, Canada H3C 3J7

1 We investigated the modulation by bradykinin (BK) of electrically induced noradrenaline release in rat isolated atria preincubated with [^{3}H]-noradrenaline.

2 BK (1-100 nM) enhanced significantly the stimulation-induced outflow of radioactivity in a concentration-dependent manner with a calculated EC_{50} of 0.58 nM.

3 Des-Arg^9-BK (0.1-100 nM), a selective B_1 receptor agonist, did not modify the stimulation-induced outflow of radioactivity. Hoe 140 (10 nM), a selective B_2 receptor antagonist, but not [Leu^8]-des-Arg^9-BK (100 nM), a selective B_1 receptor antagonist, blocked the facilitatory effect of BK.

4 The effect of BK was not affected by diclofenac (1 μM), a cyclo-oxygenase inhibitor. Bisindolylmaleimide (1 μM), a protein kinase C inhibitor, significantly reduced the facilitatory effect of BK (10 nM), angiotensin II (0.3 μM) and phorbol dibutyrate (0.1 and 1 μM) but not of fenoterol (1 μM).

5 The results suggest that BK enhances noradrenaline release via a prejunctional B_2 kinin receptor in the rat atrium. The effect appears to involve protein kinase C as a second messenger.

Keywords: Noradrenaline release; bradykinin; protein kinase C; kinin receptors; rat atria

Introduction

Two types of bradykinin (BK) receptors have been pharmacologically characterized and cloned: B_1 and B_2 receptors (Hall, 1992; Hess *et al.*, 1992; 1994; Menke *et al.*, 1994). Most of the biological actions of BK are mediated by the B_2 receptor. The function of the B_1 receptor is still unclear but this receptor appears to be inducible during tissue injury or in the presence of interleukins (Marceau *et al.*, 1983; Deblois *et al.*, 1988). However a recent report by Nakhostine *et al.* (1993) suggests that the B_1 receptor is constitutive in the dog vascular system.

Recently, BK was found to potentiate the release of noradrenaline (NA) induced by electrical stimulation in the pithed SHR rat (Dominiak *et al.*, 1992), in rat and mouse vas deferens (Llona *et al.*, 1991) and in rat hypothalamus (Tsuda *et al.*, 1993). This facilitatory action of BK seems to be mediated by a B_2 kinin receptor. In perfused rabbit hearts, BK has been shown to inhibit the overflow of endogenous NA and this inhibitory effect was blocked by indomethacin suggesting the involvement of prostaglandins (Starke *et al.*, 1977). No data are available on the modulatory action of BK in rat atria.

Although the signal transduction mechanism activated by BK in its effect on sympathetic neurotransmission remains to be determined, it has been suggested that BK may interact with dihydropyridine-sensitive Ca^{2+} channels and modulate intracellular Ca^{2+} mobilization in the rat hypothalamus (Tsuda *et al.*, 1993). The intracellular effectors involved in the action of many facilitatory prejunctional receptors of peripheral sympathetic nerve terminals are either adenylate cyclase or protein kinase C (PKC) (Majewski *et al.*, 1990).

Therefore, the first objective of the present study was to examine the effect of BK on [^{3}H]-noradrenaline ([^{3}H]-NA) release induced by electrical stimulation from the rat isolated atrium. The second objective was to determine which receptor mediated the BK effect by use of the selective B_1 agonist (des-Arg^9-BK) and antagonist ([Leu^8]-des-Arg^9-BK) as well as the B_2 selective antagonist D-Arg-(Hyp^3, Thi^5, D-Tic^7, oic^8)bradykinin (Hoe 140). Finally, we used a selective inhibitor of PKC, bisindolylmaleimide (PKCi), to assess the possible involvement of this intracellular pathway in the prejunctional action of BK.

[1] Author for correspondence.

Methods

Experimental protocol

Male Wistar rats (200-250 g, $n = 183$) were decapitated and the hearts quickly removed. The atria were dissected and incubated in a Krebs-Henseleit solution containing [^{3}H]-NA (4 μCi ml^{-1}, 0.2 μM), gassed with 5% CO_2 and 95% O_2 for 20 min at 37°C. Thereafter, the atria were transferred to 0.5 ml perfusion chambers (one pair of atria per chamber) of a Brandel SF6 suprafusion system (Brandel Inc., Gaithersburg, U.S.A.). The rate of superfusion of the tissues was 0.4 ml min^{-1} and the temperature of the system was kept constant at 37°C. The atria were washed with Krebs-Henseleit solution for a period of 75 min during which a priming stimulation (3 Hz frequency for 60 s at an intensity of 50 mA, 1 ms pulses) was given at 40 min. After washing, the effluent was collected for 12 periods of 5 min each (total of 60 min) to estimate the radioactivity. During this collection procedure the atria were stimulated twice (3 Hz frequency for 60 s at an intensity of 50 mA, 1 ms pulses) at 10 min (S_1) and 45 min (S_2). The effect of drugs on the stimulation-induced (S-I) outflow of radioactivity was determined by adding them to the perfusion system 20 min before S_2.

At the end of the experiment, the atria were dissolved in NCS-II (Amersham, Mississauga, Canada). The radioactivity was determined by liquid scintillation counting (Beckman model LS3801, Beckman, Irvine, U.S.A.). Corrections for counting efficiency were made by automatic external standardization. The resting radioactive outflow was taken during the 5 min period before stimulation. The S-I component of the outflow of radioactivity was calculated by subtracting the

resting radioactive outflow from the total radioactivity content of the 5 min period during which the tissue was stimulated. The S-I outflow of radioactivity measured during the second period of stimulation (S_2) was expressed as the percentage of the first period of stimulation (S_1). Drugs were dissolved in Krebs-Henseleit solution and added to the suprafusion system 20 min before S_2 for the remainder of the experiment. Bisindolymaleimide and phorbol dibutyrate were dissolved in dimethylsulphoxide (DMSO).

Drugs and materials

The Krebs-Henseleit solution contained (mM): NaCl 118, KCl 4.7, $CaCl_2$ 2.5, $MgSO_4$ 0.45, glucose 11.1, EDTA 0.067, KH_2PO_4 1.03, $NaHCO_3$ 25 and ascorbic acid 0.14. Following the [^{3}H]-NA incubation period, BSA 0.1% was added to the Krebs-Henseleit solution for the remainder of the experimental protocol. [Ring-2,5,6-^{3}H]-NA was from Du Pont (Mississauga, Canada) and fenoterol hydrobromide from Boehringer Ingelheim (Burlington, Canada). BK, phorbol-12,13-dibutyrate and diclofenac were obtained from Sigma (St-Louis, U.S.A.) and Hoe 140 from Hoechst AG (Frankfurt, Germany). [Leu^8]-des-Arg^9-BK and des-Arg^9-BK were obtained from Hukabel Scientific (Montréal, Canada) and staurosporine, angiotensin II and bisindolylmaleimide from Boehringer Mannheim (Laval, Canada).

Statistics

Values are given as mean ± s.e.mean. Statistical differences were tested using either a one-way or a two-way analysis of variance, which was followed by the appropriate post-operative test (see figure legend). P values <0.05 were taken to indicate a significant difference. The EC_{50} was calculated from the logistic concentration-response curve to BK which was fitted by means of a computer programme.

Results

Effect of BK

In control experiments, the S-I outflow of radioactivity for the two stimulations (S_1 and S_2) was about the same and thus the ratio S_2/S_1 was 104.6 ± 1.9% ($n = 6$), indicating the stability of the system (Figure 1). The total tissue radioactivity (TTR) measured at the end of each experiment was $7.1 \times 10^5 \pm 3.0 \times 10^4$ c.p.m. ($n = 183$). The fractional resting outflow of radioactivity, measured before S_1 and expressed as a percentage of the TTR, was 0.22 ± 0.01% per 5 min. The S-I outflow of radioactivity during S_1 in the absence of treatment, expressed as a percentage of TTR, was 0.38 ± 0.02% ($n = 183$).

BK (1 to 100 nM) significantly enhanced the S-I outflow of radioactivity (Figure 1). The calculated EC_{50} was 0.58 nM. The resting outflow ratio (R_2/R_1 = before S_2/before S_1) was not changed by any dose of BK (data not shown).

Effect of Hoe 140 on the facilitatory action of BK

The selective B_2 receptor antagonist, Hoe 140 (10 nM), did not itself influence significantly the S-I outflow of radioactivity ($S_2/S_1 = 107.3 \pm 2.8\%$, $n = 4$). Hoe 140 (0.1 and 1 nM) attenuated the facilitatory action of BK (1 nM) in the S-I outflow of radioactivity and a higher concentration of Hoe 140 (10 nM) blocked it completely (Figure 2). To assess the selectivity of Hoe 140, the effect of the B_2 antagonist (10 nM) on the facilitatory action of angiotensin (AII) was tested. The S-I outflow of radioactivity was significantly increased by AII (300 nM) ($S_2/S_1 = 173.7 \pm 4.4\%$, $n = 4$) and this increase remained unaffected in the presence of Hoe 140 (10 nM) ($S_2/S_1 = 187.2 \pm 9.5\%$, $n = 6$). The resting outflow ratio (R_2/R_1) was not changed by any treatment (data not shown).

Effect of a B_1 receptor agonist and antagonist

In this series of experiments a selective B_1 receptor agonist, des-Arg^9-BK, and a selective B_1 receptor antagonist, [Leu^8]-des-Arg^9-BK, were used. Des-Arg^9-BK did not affect significantly the S-I outflow of radioactivity at any concentration tested. The control S_2/S_1 value was 100.0 ± 9.9% ($n = 5$), and in the presence of 0.1, 1, 10 and 100 nM of des-Arg^9-BK, the S_2/S_1 values were respectively 102.2 ± 6.3%, 101.3 ± 5.0%, 105.3 ± 12.0% and 106.7 ± 5.9% ($n = 6$ each).

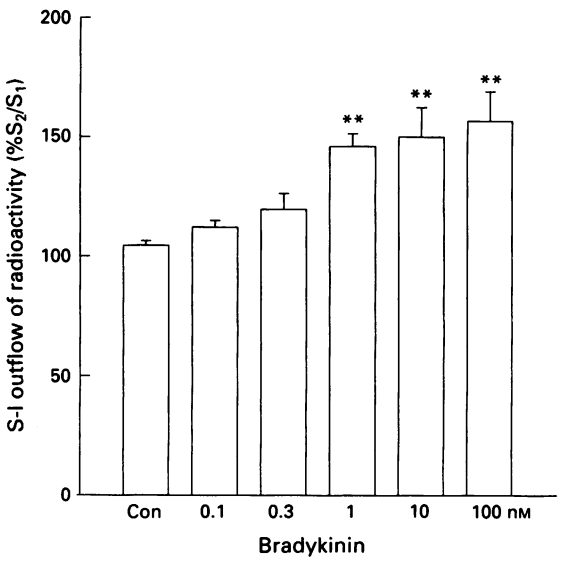

Figure 1 Effect of bradykinin (BK, 0.1 to 100 nM) on the S-I outflow of radioactivity from rat atria incubated with [^{3}H]-noradrenaline. There were two periods of stimulation (S_1 and S_2, 35 min apart, 3 Hz for 60 s each). BK was added 20 min before S_2. The vertical axis represents the S-I outflow of radioactivity in S_2 expressed as a percentage of that in S_1. Values are means ± s.e.mean ($n = 4$ to 7 experiments per group), $^{**}P < 0.01$ represents a significant difference from the control (Con) value as determined by a one-way ANOVA followed by a Bonferroni test.

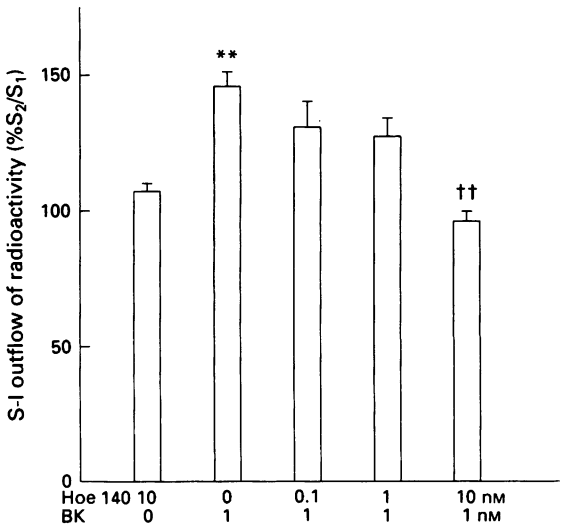

Figure 2 Effect of Hoe 140 (0.1 to 10 nM), on the facilitatory action of bradykinin (BK, 1 nM). There were two periods of stimulation (S_1 and S_2, 35 min apart, 3 Hz for 60 s each). Hoe 140 and BK were added 20 min before S_2. The vertical axis represents the S-I outflow of radioactivity in S_2 expressed as a percentage of that in S_1. Values are means ± s.e.mean ($n = 4$ to 7 experiments per group). $^{**}P < 0.01$ represents a significant difference from Hoe 140 (10 nM) alone, $^{††}P < 0.05$ represents a significant difference form BK (1 nM) alone as determined by a one-way ANOVA followed by a Benferroni test. BK alone value (1 nM) is from Figure 1.

[Leu^8]-des-Arg^9-BK at a concentration of 100 nM did not affect significantly the S-I outflow of [^{3}H]-NA from rat atria (Figure 3). Furthermore, the facilitatory effect of BK (1 nM) was not affected by the addition of the B_1 receptor antagonist (100 nM, Figure 3). The resting outflow ratio (R_2/R_1) was not changed by any treatment (data not shown).

Effect of diclofenac on the facilitatory action of BK

In this series of experiments, we used diclofenac, a cyclo-oxygenase inhibitor, to block prostaglandin production (Figure 3). Diclofenac (1 μM) used alone did not influence the S-I outflow of radioactivity. Furthermore, it did not modify the facilitatory action of BK (1 nM) on the S-I outflow of radioactivity. The resting outflow ratio (R_2/R_1) was not changed by any treatment (data not shown).

Effect of PKC inhibitor on the facilitatory action of BK

To investigate the role of protein kinase C (PKC) in the facilitatory action of BK, we first used staurosporine, a PKC inhibitor (Tamaoki *et al.*, 1986). However, staurosporine appeared to be an inappropriate PKC inhibitor in our experimental conditions since the S-I outflow of radioactivity was affected by this inhibitor: the S_2/S_1 ratio was significantly decreased to 81.8 ± 7.6% ($n = 4$) with staurosporine (300 nM) used alone. Therefore, we used a recently developed PKC inhibitor, bisindolymaleimide (PKCi). PKCi (1 μM) did not influence significantly the S-I outflow or radioactivity (Figure 4). The S_2/S_1 value in the presence of PKCi (1 μM) was 87.5 ± 3.6% ($n = 6$) compared to the DMSO control S_2/S_1 of 100.5 ± 8.3% ($n = 8$). To evaluate the potency of PKCi in inhibiting PKC, we stimulated this pathway with phorbol dibutyrate (PDBu), a well known PKC activator (Wakade *et al.*, 1985; Allgaier & Hertting, 1986). PKCi (1 μM) significantly inhibited the facilitatory action of 0.1 μM and 1 μM PDBu on the S-I outflow of radioactivity (Figure 4). The resting outflow ratio (R_2/R_1) was not changed by any treatment (data not shown).

AII, which enhances NA release through PKC activation (Musgrave *et al.*, 1991; Foucart *et al.*, 1991), was used to demonstrate further the effectiveness of PKCi. As expected, the facilitatory action of AII (0.3 μM) on the S-I outflow of radioactivity was significantly reduced by PKCi (1 μM)

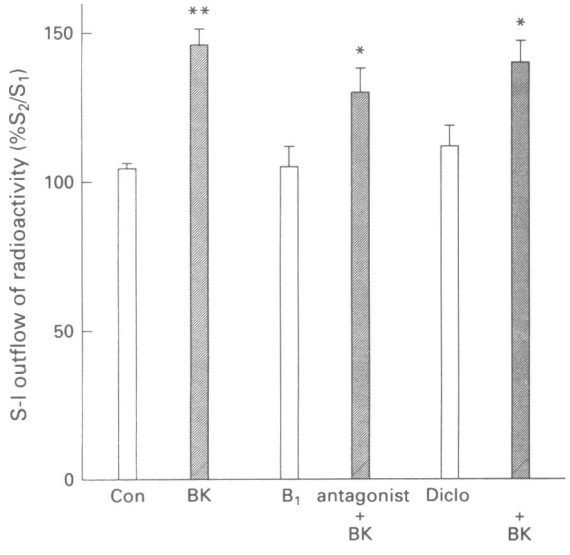

Figure 3 Effect of [Leu^8]-des-Arg^9-BK (B_1 antagonist, 100 nM) and diclofenac (Diclo, 1 μM) on the facilitatory action of bradykinin (BK, 1 nM). There were two periods of stimulation (S_1 and S_2, 35 min apart, 3 Hz for 60 s each). [Leu^8]-des-Arg^9-BK and diclofenac were added 20 min before S_2. The vertical axis represents the S-I outflow of radioactivity in S_2 expressed as a percentage of that in S_1. Values are means ± s.e.mean ($n = 4$ to 7 experiments per group). $^{**}P < 0.01$ or $^{*}P < 0.05$ represents a significant difference from the respective control as determined by a one-way ANOVA followed by a Bonferroni test. BK alone value (1 nM) is from Figure 1.

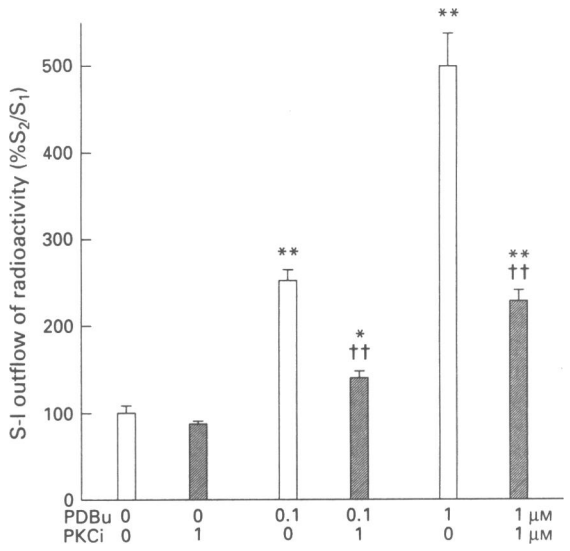

Figure 4 Effect of bisindolylmalemide (PKCi, 1 μM) on the facilitatory action of phorbol dibutyrate (PDBu, 0.1 and 1 μM) on the S-I outflow of radioactivity from rat atria incubated with [^{3}H]-noradrenaline. There were two periods of stimulation (S_1 and S_2 given at 35 min apart, 3 Hz for 60 s each). PKCi and PDBu were added 20 min before S_2. The vertical axis represents the fractional S-I outflow in S_2 expressed as a percentage of that in S_1. Values are means ± s.e.mean ($n = 6$ to 8 experiments per group). $^{*}P < 0.05$ or $^{**}P < 0.01$ represents a significant difference from respective control values, $\dagger\dagger P < 0.01$ represents a significant difference between PDBu alone and in the presence of PKCi (1 μM) as determined by a two-way ANOVA followed by a Bonferroni test.

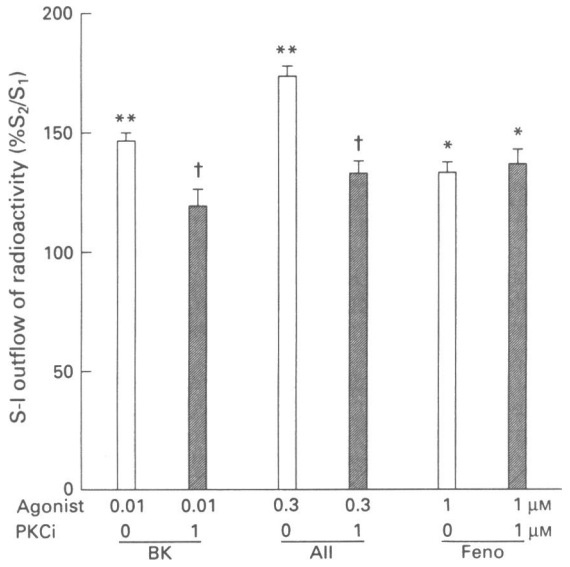

Figure 5 Effect of bisindolylmaleimide (PKCi, 1 μM) on the facilitatory action of bradykinin (BK, 10 nM), angiotensin II (AII, 300 nM) and fenoterol (Feno, 1 μM) on the S-I outflow of radioactivity from rat atria incubated with [^{3}H]-noradrenaline. There were two periods of stimulation (S_1 and S_2 given at 35 min apart, 3 Hz for 60 s each). PCKi, BK, AII and Feno were added 20 min before S_2. The vertical axis represents the fractional S-I outflow in S_2 expressed as a percentage of that in S_1. Values are means ± s.e.mean ($n = 4$ to 8 experiments per group). $^{*}P < 0.05$ or $^{**}P < 0.01$ represents a significant difference from control values (see Figure 1), $\dagger P < 0.05$ represents a significant difference from respective peptide in presence of PKCi (1 μM) as determined by a two-way ANOVA followed by a Bonferroni test.

(Figure 5). The facilitatory action of BK (10 nM) was also significantly reduced by PKCi (1 μM). However, the facilitatory action of a β_2-adrenoceptor agonist, fenoterol (1 μM), was not affected by PKCi (1 μM). The resting outflow ratio (R_2/R_1) was not changed by any treatment (data not shown).

Discussion

The electrical stimulation-induced (S-I) outflow of radioactivity from rat atria pre-incubated with [^{3}H]-NA was used as an index of NA release from sympathetic fibres (Johnston *et al.*, 1987). BK increased dose-dependently this S-I outflow of radioactivity from rat atria as demonstrated in other experimental preparations such as the pithed SHR rat (Dominiak, 1992), the rat and mouse vas deferens (Llona *et al.*, 1991) and rat hypothalamic slices (Tsuda *et al.*, 1993). The calculated EC_{50} was 0.58 nM while it was 42 nM for the positive inotropic action of BK on the rat left atrium (Minshall *et al.*, 1994).

The facilitation by BK of the S-I outflow of radioactivity is likely to be mediated by a B_2 receptor subtype since it was blocked by the selective B_2 receptor antagonist, Hoe 140 (Hock *et al.*, 1991; Lembeck *et al.*, 1991), but not affected by the selective B_1 receptor antagonist, [Leu^8]-des-Arg^9-BK. In addition, the selective B_1 receptor agonist, des-Arg^9-BK, was inactive. The results are in accordance with other studies which have found that the prejunctional action of BK is mediated through a B_2 receptor (Llona *et al.*, 1991; Dominiak *et al.*, 1992).

The use of diclofenac was necessary since BK actions have been related to prostaglandins in many tissues (Hall, 1992). Furthermore, it was shown that prostaglandins can inhibit or enhance the S-I outflow of noradrenaline depending on the prostaglandin type synthesized and the tissue used (Starke, 1977). Indeed, in rabbit isolated heart, BK inhibited NA release through the transjunctional action of prostaglandins (Starke *et al.*, 1977). The present data show that the facilitatory action of BK on the S-I outflow of radioactivity was not affected by diclofenac, suggesting that prostaglandins are not involved and that the effect of BK is directly on nerve terminals in the isolated rat atrium.

PKC is one of the intracellular effectors involved in the action of facilitatory prejunctional receptors of sympathetic nerve endings (Majewski *et al.*, 1990). Indeed, the involvement of this protein kinase in the S-I release of NA has been shown in different experimental preparations, including rabbit hippocampus (Allgaier & Hertting, 1986), cat cerebral arteries (Balfagon *et al.*, 1989), rat salivary gland (Wakade *et al.*, 1985) and rat atria (Ishac & De Luca, 1988). Moreover, postjunctional B_2 receptor activation is linked to the PKC pathway in several tissues such as the rabbit jugular vein and circular muscle of the guinea-pig ileum (Calixto & Madeiros, 1991; 1992). In order to investigate the implication of this intracellular effector in the action of BK, we used the PKC inhibitor, PKCi (Toullec *et al.*, 1991). PKCi clearly inhibited the effects of PDBu and Ang II on the S-I outflow of radioactivity, which are known to increase NA release through the activation of PKC (Wakade *et al.*, 1985; Foucart *et al.*, 1991; Musgrave *et al.*, 1991). Since β_2-adrenoceptor agonists exert their facilitatory action on NA release through PKA activation (Johnston *et al.*, 1987), the results obtained with fenoterol indicate further the selectivity of PKCi. Considering that PKCi reduced with efficiency the action of BK, it is suggested that the prejunctional facilitatory action of BK in rat atria is mediated through activation of the PKC pathway.

In conclusion, BK facilitates the release of [^{3}H]-NA in rat isolated atria. The facilitatory effect is mediated through activation of a B_2 receptor and probably involves activation of PKC as an intracellular second messenger.

The work was supported by a grant from the Medical Research Council of Canada. S.F. is a junior scholar from the Fonds de la Recherche en Santé du Québec. C.C. holds a studentship from the Groupe de Recherche sur le Système Nerveux Autonome of the Université de Montréal. The technical assistance of Ms Louise Grondin is gratefully acknowledged.

References

ALLGAIER, C. & HERTTING, G. (1986). Polymyxin B, a selective inhibitor of protein kinase C, diminishes the release of noradrenaline and the enhancement of release caused by phorbol 12,13-dibutyrate. *Naunyn-Schmied. Arch. Pharmacol.*, **334**, 218–221.

BALFAGON, G., DE SAGARRA, M.R., BARRUS, M.T., ARRIVAS, S., CAPILLA, M.I. & MARIN, J. (1989). Effect of phorbol esters on noradrenaline release from cerebral arteries. *Brain Res.*, **477**, 196–201.

CALIXTO, J.B. & MEDEIROS, Y.S. (1991). Characterization of bradykinin mediating pertussis toxin-insensitive biphasic response in circular muscle of isolated guinea-pig ileum. *J. Pharmacol. Exp. Ther.*, **259**, 659–665.

CALIXTO, J.B. & MEDEIROS, Y.S. (1992). Effect of protein kinase C and calcium on bradykinin-mediated contractions of rabbit vessels. *Hypertension*, **19** (suppl. II), II87–II93.

DEBLOIS, D., BOUTHILLIER, J. & MARCEAU, F. (1988). Effect of glucocorticoids, monokines and growth factors on the spontaneously developing responses of the rabbit isolated aorta to des-Arg^9-bradykinin. *Br. J. Pharmacol.*, **93**, 969–977.

DOMINIAK, P., SIMON, M., BLÖCHL, A. & BRENNER, P. (1992). Changes in peripheral sympathetic outflow of pithed spontaneously hypertensive rats after bradykinin and des-Arg-bradykinin infusions: influence of converting-enzyme inhibition. *J. Cardiovasc. Pharmacol.*, **20** (suppl. 9), S35–S38.

FOUCART, S., MUSGRAVE, I.F. & MAJEWSKI, H. (1991). Long term treatment with phorbol esters suggests a permissive role for protein kinase C in the enhancement of noradrenaline release. *Mol. Neuropharmacol.*, **1**, 95–101.

HALL, J.M. (1992). Bradykinin receptors: pharmacological properties and biological roles. *Pharmacol. Ther.*, **56**, 131–190.

HESS, J.F., BORKOWSKI, J.A., STONESIFER, G.Y., MACNEIL, T., STRADER, C.D. & RANSOM, R.W. (1994). Cloning and pharmacological characterization of bradykinin receptors. *Brazilian J. Med. Biol. Res.*, **27**, 1725–1731.

HESS, J.F., BORKOWSKI, J.A., YOUNG, G.S., STRADER, C.D. & RANSOM, R.W. (1992). Cloning and pharmacological characterization of human bradykinin (BK-2) receptor. *Biochem. Biophys. Res. Commun.*, **45**, 1–8.

HOCK, F.J., WIRTH, K., ALBUS, U., LINZ, W., GERHARDS, H.J., WIEMER, G., HENKE, S.T., BREIPOHL, G., KÖNIG, W., KNOLLE, J. & SCHÖLKENS, B.A. (1991). Hoe 140 a new potent and long acting bradykinin-antagonist: *in vitro* studies. *Br. J. Pharmacol.*, **102**, 769–773.

ISHAC, E.J.N. & DE LUCA, A. (1988). The influence of activation or inhibition of protein kinase C on the release of radioactivity from rat isolated atria labelled with [^{3}H]-noradrenaline. *Br. J. Pharmacol.*, **94**, 713–720.

JOHNSTON, H., MAJEWSKI, H. & MUSGRAVE, I.F. (1987). Involvement of cyclic nucleotides in prejunctional modulation of noradrenaline release in mouse atria. *Br. J. Pharmacol.*, **91**, 773–781.

LEMBECK, F., GRIESBACHER, T., ECKHARDT, M., HENKE, S., BREIPHOL, G. & KNOLLE, J. (1991). New, long-acting, potent bradykinin antagonists. *Br. J. Pharmacol.*, **102**, 297–304.

LLONA, I., GALLEGUILLOS, X., BELMAR, J. & HUIDOBRO-TORO, J.P. (1991). Bradykinin modulates the release of noradrenaline from vas deferens nerve terminals. *Life Sci.*, **48**, 2585–2592.

MAJEWSKI, H., COSTA, M., FOUCART, S., MURPHY, T.V. & MUSGRAVE, I.F. (1990). Second messengers are involved in facilitatory but not inhibitory receptor actions at sympathetic nerve endings. In *Presynaptic Receptors and the Question of Autoregulation of Neurotransmitter Release*. ed. Stanley, K. & Westfall, T.C. *Ann. New York Acad. Sci.*, **604**, 266–275.

MARCEAU, F., LUSSIER, A., REGOLI, D. & GIROUD, J.P. (1983). Pharmacology of kinins: their relevance to tissue injury and inflammation. *Gen. Pharmacol.*, **14**, 209–229.

MENKE, J.G., BORKOWSKI, J.A., BIERILO, K.K., MACNEILL, T., DERRICK, A.W., SHNECK, K.A. RANSOM, R.W. STRADER, C.D., LINEMEYER, D.L. & HESS, J.F. (1994). Expression cloning of a human B_1 bradykinin receptor. *J. Biol. Chem.*, **269**, 21583–21586.

MINSHALL, R.D., YELAMANCHI, V.P., DJOKOVIC, A., MILETICH, D.J., ERDÖS, E.G., RABITO, S.F. & VOGEL, S.M. (1994). Importance of sympathetic innervation in the positive inotropic effects of bradykinin and ramiprilat. *Circ. Res.*, **74**, 441–447.

MUSGRAVE, I.F., FOUCART, S. & MAJEWSKI, H. (1991). Evidence that angiotensin II enhances noradrenaline release from sympathetic nerves in mouse atria by activating protein kinase C. *J. Auton. Pharmacol.*, **11**, 211–220.

NAKHOSTINE, N., RIBUOT, C., LAMONTAGNE, D., NADEAU, R. & COUTURE, R. (1993). Mediation of B_1 and B_2 receptors of vasodepressor responses to intravenously administered kinins in anaesthetized dogs. *Br. J. Pharmacol.*, **110**, 71–76.

STARKE, K. (1977). Regulation of noradrenaline release by presynaptic receptor systems. *Rev. Physiol. Biochem. Pharmacol.*, **77**, 1–124.

STARKE, K., PESCAR, B.A., SCHUMACHER, K.A. & TAUBE, H.D. (1977). Bradykinin and postganglionic sympathetic transmission. *Naunyn-Schmied. Arch. Pharmacol.*, **299**, 23–32.

TAMAOKI, T., NOMOTO, H., TAKAHASHI, I. KATO, Y., MORIMOTO, M. & TOMITA, F. (1986). Staurosporine, a potent inhibitor of phospholipid/Ca^{++} dependent protein kinase. *Biochem. Biophys. Res. Commun.*, **135**, 397–402.

TOULLEC, D., PIANETTI, P., COSTE, H., BELLEVERGUE, P., GRAND-PERRETT, T., AJAKANES, M., BAUDET, V., BOISSIN, P., BOURSIER, E., LORIOLLE, F., DUHAMEL, L., CHARON, D. & KIRILOVSKY, J. (1991). The bisindolylmaleimide GF 109203X is a potent and selective inhibitor of protein kinase C. *J. Biol. Chem.*, **266**, 15771–15781.

TSUDA, K., TSUDA, S., GOLDSTEIN, M., NISHIO, I. & MASUYAMA, Y. (1993). Effects of bradykinin on [^{3}H]-norepinephrine release in rat hypothalamus. *Clin. Exp. Pharmacol. Physiol.*, **20**, 787–791.

WAKADE, A.R., MALHOTRA, R.K. & WAKADE, T.D. (1985). Phorbol ester, an activator of protein kinase C, enhances calcium-dependent release of sympathetic neurotransmitter. *Naunyn-Schmied. Arch. Pharmacol.*, **331**, 122–124.

(Received October 19, 1994
Revised January 24, 1995
Accepted January 30, 1995)

British Journal of Pharmacology (1995) 115, 335-343

Quinidine-induced open channel block of K^+ current in rat ventricle

R.B. Clark, J. Sanchez-Chapula, E. Salinas-Stefanon, H.J. Duff & [1]W.R. Giles

Departments of Medical Physiology and Medicine, University of Calgary, School of Medicine, Calgary, Alberta, Canada

1 The effects of quinidine on calcium-independent outward K^+ currents in rat ventricular myocytes were studied using whole-cell patch clamp techniques.

2 Quinidine sulphate (6 μM) significantly prolonged repolarization of the ventricular action potential. This effect was larger during early repolarization (25% level) than at later times (90% level).

3 Quinidine reduced the amplitude of a transient outward current, and accelerated its rate of decay by approximately 4 fold at membrane potentials between 0 to +50 mV. Quinidine also reduced the amplitude of a slowly inactivating, tetraethylammonium-sensitive 'pedestal' component of the outward current.

4 The quinidine-induced block of the transient outward current was dependent on time and membrane potential. Maximal block occurred with depolarizations of about 100 ms duration, and longer depolarizations (up to 1.5 s) produced little additional block. The membrane potential dependence of quinidine-induced block was very similar to the membrane potential dependence of activation of the transient outward current. The membrane potential dependence of steady-state inactivation of the transient outward current was not significantly affected by quinidine.

5 These results show that quinidine blocks outward K^+ currents in rat ventricular cells. The time and potential dependence of this block suggests that quinidine blocks the transient outward K^+ current by acting primarily on the open state of these channels.

Keywords: Voltage-clamp; K^+ current; antiarrhythmic drugs; repolarization

Introduction

Quinidine is an antiarrhythmic drug which has both class I and class III actions in mammalian atrium and ventricle (Spinelli & Hoffman, 1989; cf. Nattel, 1991; Rosen *et al.*, 1991). Although its ability to block sodium channels (class I antiarrhythmic actions) has been described in some detail as a use-dependent inhibition (Hille, 1977; Hondeghem & Katzung, 1977; 1984; Clarkson & Hondeghem, 1984), the action potential broadening, or class III actions of quinidine are less well understood (Singh & Nadamane, 1985; Hondeghem & Snyders, 1990; Colatsky *et al.*, 1990; Lynch *et al.*, 1992). Part of the reason for this is that in mammalian heart there is a relatively large number of quite diverse potassium (K^+) currents (Colatsky *et al.*, 1990; Baumgarten & Fozzard, 1991; Gintant *et al.*, 1991). Inhibitory actions of quinidine on a number of these K^+ currents have been described, including effects on the inward rectifier, I_{K1}, in Purkinje fibre and ventricle (Roden & Hoffman, 1985; Salata & Wasserstrom, 1988; Balser *et al.*, 1991b), the time- and voltage-dependent delayed rectifier potassium currents in guinea-pig ventricle (Hiraoka *et al.*, 1986; Roden *et al.*, 1988; Balser *et al.*, 1991a; Wettwer *et al.*, 1992) and rabbit sinoatrial and atrioventricular nodes (Furukawa *et al.*, 1989), the calcium-independent transient outward K^+ current in rabbit atrium (Imaizumi & Giles, 1987), canine cardiac Purkinje cells (Nakayama & Fozzard, 1987) and rat ventricle (Slawsky & Castle, 1994) and the ATP-sensitive K^+ current (Undrovinas *et al.*, 1990).

Previously Imaizumi & Giles (1987) have shown that quinidine is a potent, although somewhat nonselective, blocker of a calcium-independent transient outward current in rabbit atrium. Nakayama & Fozzard (1987) obtained somewhat similar data from a canine Purkinje fibre preparation. A consistent and quite striking feature of both of these sets of results was that when this transient outward K^+ current was inhibited by quinidine, the times course of decay was accelerated significantly, suggesting that quinidine may act as an open channel blocker (cf., Armstrong, 1971), as had been described previously for the actions of quinidine in neurones (Hermann & Gorman, 1984; Oyama *et al.*, 1992) and pituitary melanotrophs (Kehl, 1991). Recently, Snyders *et al.* (1992) have shown that quinidine can act as an effective open channel blocker of one of the delayed rectifier K^+ currents (HK2: hKv1.5) cloned from human ventricle when it is expressed in a mouse L cell line.

The main goal of this study was to determine the mechanism by which quinidine can block the outward potassium currents which repolarize mammalian ventricular muscle. Rat ventricular muscle was chosen since recent very detailed data describing the types, relative magnitudes, and kinetics of the potassium currents in this tissue were available (Apkon & Nerbonne, 1991). Our results show that in single myocytes from this mammalian ventricular tissue, quinidine is a potent blocker of both a transient outward potassium current and a slowly inactivating or 'pedestal type' of potassium current which is somewhat similar to hKv1.5 from human ventricle. Evidence is presented describing the mechanism of this open channel block. These results are compared to and contrasted with previously published actions of quinidine on K^+ channels in native membranes of heart cells, and cloned heart K^+ channels expressed in reconstitution systems (Snyders *et al.*, 1992; Yatani *et al.*, 1993).

Methods

Solutions

Standard HEPES-buffered Tyrode solution contained (mM): NaCl 140, KCl 5, $CaCl_2$ 1.8, $MgCl_2$ 1, HEPES 10 and

[1] Author for correspondence.

glucose 5.5. 'Low calcium' solution was prepared by omitting $CaCl_2$ from standard Tyrode solution. The 'enzymatic' solution used in cell dissociation contained (mM): NaCl 130, KCl 5, $MgCl_2$ 1, HEPES 10, glucose 5.5, taurine 10, collagenase (Type I; Sigma Chemical Co., St. Louis, MO, U.S.A.) 0.8 mg ml^{-1} and protease (type XIV; Sigma Chem. Co.) 60 $\mu g\ ml^{-1}$.

The 'washout' solution was a modification of standard Tyrode solution, in which $CaCl_2$ was reduced to 100 μM and 1 mg ml^{-1} bovine serum albumin (type V; Sigma Chem. Co.) was added. All solutions were gassed with 100% O_2 and pH was adjusted to 7.4 by addition of appropriate amounts of 1.0 M NaOH.

The control 'external' solution used in action potential recordings was the same as standard HEPES-buffered Tyrode. For voltage-clamp experiments, 3 mM $CoCl_2$ was added to block the voltage-dependent calcium current. 4-aminopyridine (4-AP) and tetraethylammonium chloride (TEA) were added to the external solution where indicated. In some experiments, tetrodotoxin (TTX; Sigma Chem. Co.) was added at a concentration of 10 μM. Quinidine sulphate (Sigma Chem. Co.) was added to the external solution to give a final concentration of 6 μM.

The pipette solution contained (mM): K-aspartate 70, KCl 70, $MgSO_4$ 1, KH_2PO_4 0.45, HEPES 10, EGTA 10 and Na_2-ATP 5. The pH of the solution was adjusted to 7.2 with appropriate amounts of 1 M KOH.

Cell dissociation procedure

The dissociation method was similar to that described by Clark *et al.* (1993). Rats weighing 250–350 g were killed by cervical dislocation. Their hearts were immediately removed and mounted on a modified Langendorff perfusion system for retrograde perfusion of the coronary circulation. Temperature was maintained at 36 ± 1°C throughout all perfusion steps. An initial 5 min period of perfusion with standard HEPES-buffered Tyrode solution was used to remove as much blood as possible from the heart. Three further steps of perfusion were as follows: 7 min with 'low Ca' solution, 15 min with 'enzymatic' solution and 5 min with 'washout' solution. The heart was then removed from the perfusion system, and the atria and ventricles were separated. Small pieces of the epicardium from the apex, and endocardium from the base of the left ventricle were placed separately in small flasks containing 'washout' solution, where the pieces were gently stirred until the fragments were dissociated into single cells.

Electrophysiological and data-recording procedures

A few drops of cell suspension were placed in a superfusion chamber (vol. 200 μl) mounted on the modified stage of an inverted microscope (IMT; Olympus, Toyko, Japan). The myocytes were left for several minutes to allow them to settle onto the bottom of the chamber. Thereafter, the cells were superfused (about 0.5 ml min^{-1}) with control 'external' solution. A multi-way valve was used to select either control or quinidine-containing solutions. Cells were exposed to quinidine-containing solutions for 5–10 min before recordings were taken. All experiments were carried out at room temperature (21–23°C).

Electrophysiological recordings were made from isolated myocytes using whole-cell patch clamp methods (Hamill *et al.*, 1981). Patch electrodes were made from borosilicate glass (World Precision Inst., Sarasota, FL., U.S.A.), and had tip resistances of 1–2 MΩ-when filled with pipette solution. Voltage and current-clamp experiments were carried out with a conventional patch-clamp amplifier (PC-501; Warner Instruments, Hamden, Conn., U.S.A.). Pipette series resistance in the whole-cell mode was 5–8 MΩ; 60–80% of this resistance was compensated electronically. Cell capacitance was usually not compensated. Data acquisition and generation of current and voltage-clamp command protocols was carried out with a combined A/D and D/A convertor board (Techmar), which was controlled by 'pCLAMP' software (Axon Instruments, Foster City, CA, U.S.A.). Data were stored on hard disk in a microcomputer (IBM) for later analysis. Current records were fit to exponential functions by a least-squares method programme ('Minsq', Micromath). Sets of data points were fitted to exponential and Boltzmann functions using a commercial graph plotting programme ('Sigmaplot', Jandel Scientific, Corta Madera, CA, U.S.A.). Average values are shown as mean ± s.e. Differences between control and quinidine-treated cells were evaluated statistically by Student's paired or unpaired t test, where appropriate; differences were considered to be significant for $P<0.05$.

Results

Effect of quinidine on rat ventricular action potentials

The average resting membrane potential of rat isolated ventricular cells, bathed in HEPES-buffered Tyrode solution containing 5 mM KCl, was −79 ± 2 mV (mean ± s.e., $n=6$). Action potentials in the isolated cells had both a rapid upstroke and initial repolarization followed by a second, slower phase of repolarization (Figure 1a). The average amplitude of the action potentials was 113 ± 3 mV, and the duration, measured at the 25% and 90% repolarization levels, was 7.0 ± 0.5 ms and 49 ± 8 ms, respectively when stimulated at 0.1 Hz. The characteristics of these action potentials from isolated myocytes were similar to those recorded from intact ventricular muscle.

Application of quinidine sulphate (6 μM) did not affect the resting potential of isolated myocytes (−78 ± 2 mV; $n=6$). The average amplitude of the action potentials was slightly but significantly ($P<0.05$) reduced (107 ± 4 mV; $n=6$). Examples of the effects of quinidine on the action potential of two different rat ventricular myocytes are shown in Figure 1a. The action potential in the presence of quinidine had a much slower rate of initial repolarization, which produced a more distinct early plateau region than in the controls. The late phase of repolarization was also prolonged by quinidine, although the effect on this phase of the action potential was less pronounced than on initial repolarization. In the presence of quinidine, action potential duration at the 25% repolarization level was 21 ± 3 ms, 3 fold larger than controls, while the duration at the 90% level was 73 ± 9 ms, an approximately 1.5 fold increase over control values. Both values were significantly ($P<0.05$) increased compared to controls.

Effects of quinidine on outward currents in rat ventricular myocytes

The broadening of the action potential in rat ventricular myocytes by quinidine suggested that part of its action may have resulted from inhibition of one or more of the components of outward current in these cells. It has been demonstrated previously (Apkon & Nerbonne, 1991) that outward currents in rat ventricular myocytes consist of at least two different time and voltage-dependent components with different pharmacological sensitivities to K^+-channel blockers, a rapidly activating and inactivating transient component which is blocked by 4-AP ('transient outward current') and a slowly inactivating 'pedestal' component which is sensitive to TEA. It was therefore of interest to compare the effects of 4-AP and TEA on quinidine-induced changes in action potential repolarization. Results from one experiment are shown in Figure 1b and c. Exposure of the cell to 4-AP (5 mM) produced a marked prolongation of the action potential (Figure 1b); addition of quinidine (6 μM) to the 4-AP-containing solution produced little additional effect. In con-

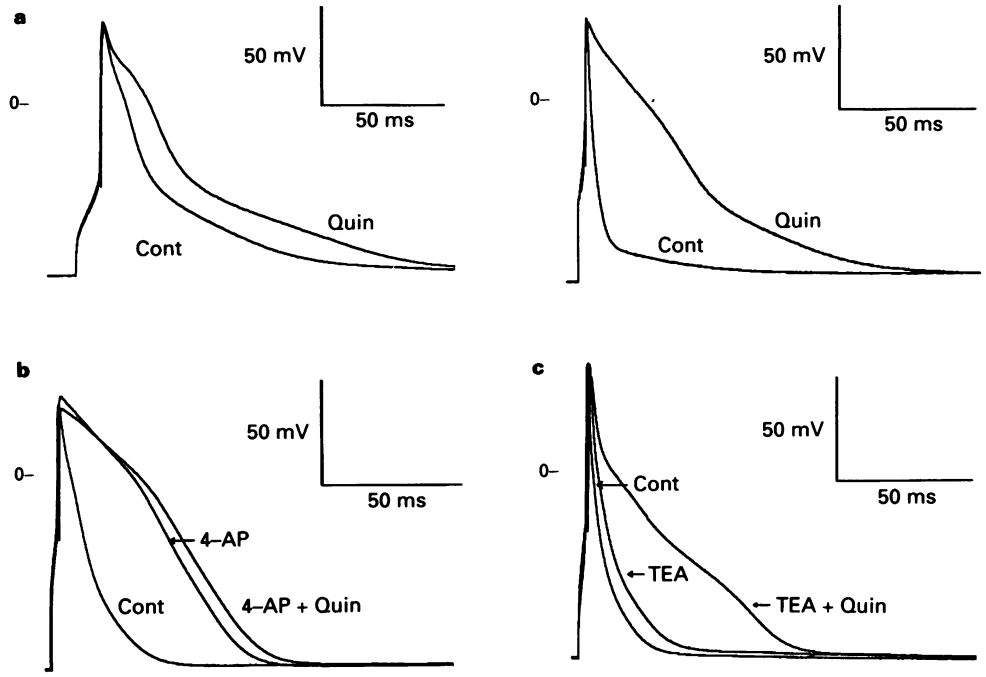

Figure 1 (a) Two examples of the effects of quinidine on the action potentials of different isolated ventricular cells of the rat. Action potentials were produced by 5 ms, 1 nA current pulses applied through the recording electrode at 0.1 Hz. Exposure to solution containing 6 μM quinidine sulphate (Quin) for 8 min resulted in a broadening of the action potential waveform. (b) Effect of 4-aminopyridine (4-AP) on the changes in action potential waveform induced by quinidine. An action potential was first recorded in control 'external' solution (Cont). External solution containing 5 mM 4-AP (4-AP) was then added, followed by a solution containing 4-AP and 6 μM quinidine sulphate (4-AP + Quin). (c) Effect of tetraethylammonium chloride (TEA) on the changes in action potential waveform induced by quinidine. Same cell as in (b). Action potentials were recorded in control solution, then 10 mM TEA, and finally in 10 mM TEA and 6 μM quinidine sulphate. The stimulation rate was 1 Hz in (b) and (c).

trast, exposure of the same cell to TEA (10 mM) alone produced a relatively small broadening of the action potential (Figure 1c), but addition of quinidine to the TEA solution resulted in a large additional prolongation.

Voltage-clamp experiments were carried out to assess the effects of quinidine on each of the outward currents of rat ventricular myocytes. An example of the quinidine-induced inhibition of the transient outward current in a rat ventricular myocyte is shown in Figure 2a. This experiment was done in the presence of 10 mM external TEA which blocked most of the slowly inactivating component of outward current. Quinidine (6 μM) reduced the amplitude of the transient outward current by about 15–20%. Figure 2b shows the effect of quinidine on the current-voltage relation for the peak transient outward current for membrane potentials in the range −30 to +50 mV, averaged from 8 cells taken from the epicardium of the apex of the left ventricle. Previous studies (Clark *et al.*, 1993) have shown that the transient outward current is largest in cells taken from this region of the rat heart. Note that quinidine reduced the amplitude of the transient outward current at all potentials over this range.

Quinidine also reduced the magnitude of the slowly inactivating outward current in rat ventricular myocytes, as shown in Figure 3a. This experiment was done on a myocyte taken from the endocardium of the base of the left ventricle; myocytes from this region of the rat heart have very little transient outward current (Clark *et al.*, 1993). Note that quinidine reduced the magnitude of the slow outward current in this cell by about 50%. Figure 3b shows that quinidine (6 μM) reduced the amplitude of the slowly inactivating outward current by about 50% at membrane potentials positive to −10 mV. These data were averaged from 6 endocardial/base cells in which the transient outward current was negligible.

Imaizumi & Giles (1987) noted that quinidine increased the rate of decay of a calcium-independent transient outward current in rabbit atrium. Quinidine produced a similar increase in the rate of decay of the transient outward current in rat ventricle, as described recently by Slawsky & Castle (1994). This can be seen in Figure 4a, where transient outward currents produced by a voltage-clamp step from −70 to +30 mV have been superimposed to compare the time course of decay of the current in control and in the presence of quinidine. The time course of decay of the current was fitted to an exponential function; the time constant was 41.3 ms in the control and was 18.6 ms after application of quinidine. Figure 4b shows dependence of the decay time constant on membrane potential in control conditions and after addition of 6 μM quinidine, averaged from 4 cells. In controls the time constant was 35–45 ms and was not significantly dependent on membrane potential in the range from −10 to +50 mV. The magnitude of the time constant was significantly reduced in the presence of 6 μM quinidine at membrane potentials positive to −10 mV, and decreased in magnitude by about 4 fold for membrane potentials over the range 0 and +50 mV.

Use-dependent block of the transient outward current by quinidine

The effectiveness of quinidine in blocking voltage-dependent sodium channels is increased if the channels are repetitively activated by trains of brief membrane depolarizations (Hondeghem & Katzung, 1984). It was of interest to see if quinidine produced a similar 'use-dependent' block of the transient outward current in rat ventricular cells. Figure 5a illustrates an example of results from an experiment designed to test this possibility. The voltage-clamp protocol consisted of a train of 100 ms test steps to +50 mV, from a holding potential of −70 mV, applied at a frequency of 2 Hz. In the absence of quinidine, the peak current produced by each pulse remained constant during a train of 10 pulses. Following application of quinidine, the amplitude of current pro-

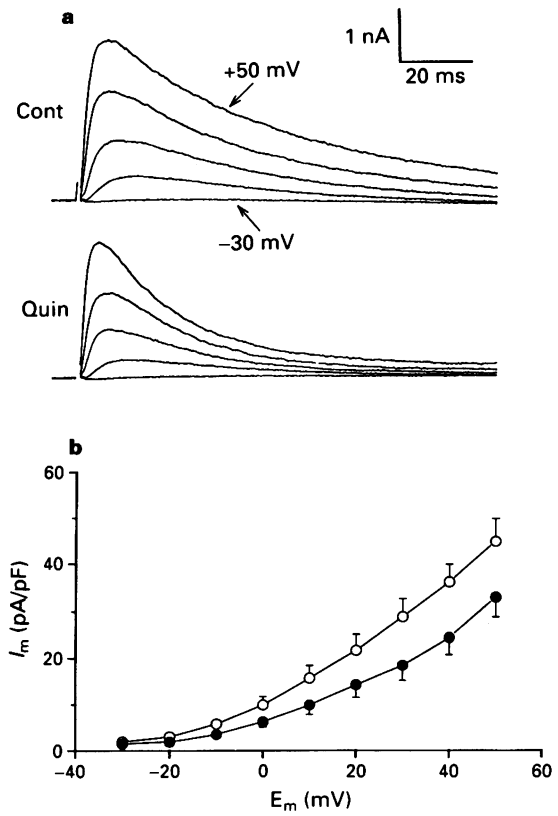

Figure 2 Effect of quinidine on transient outward currents in rat ventricle. (a) Example of transient outward currents, produced by voltage-clamp steps to −30, −10, +30 and +50 mV from a holding potential of −70 mV, in control conditions (Cont), and in the presence of 6 μM quinidine (Quin). The steps were applied at a frequency of 0.03 Hz. Note that quinidine reduced the amplitude of the current at all test potentials, and also increased the rate of decay of the current. The solutions in this experiment contained 10 mM tetraethylammonium chloride. The myocyte was taken from the epicardium of the apex of the left ventricle. (b) Averaged peak current-voltage relation for transient outward current, in control (○) and 6 μM quinidine (●). Peak current was normalized to cell capacitance for each cell. Mean ± s.e., $n = 8$.

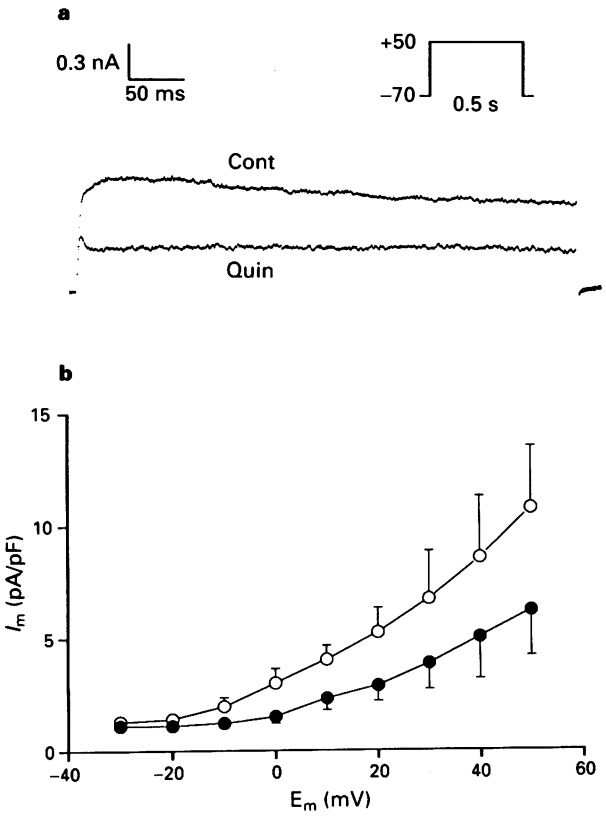

Figure 3 (a) Effect of quinidine on the slowly inactivating outward current in a voltage-clamped myocyte from the endocardium of the base of the rat left ventricle. The transient outward current was negligible in this cell. Quinidine (Quin) (6 μM) produced about 50% reduction in the current magnitude throughout the entire voltage-clamp step. (b) Averaged peak current-voltage relation for slowly inactivating outward current, in control (○) and 6 μM quinidine (●). Mean ± s.e., $n = 6$.

duced by the first pulse of the train was reduced by about 15%, and in contrast to the controls, the current amplitude declined with successive pulses in the train and reached a 'steady state' level of about 60% of the control amplitude after 8–10 pulses. Figure 5b shows averaged data from 8 cells, for pulse trains at frequencies of 0.5 and 2 Hz. The degree of inhibition of outward current amplitude per pulse was larger for the 2 Hz than the 0.5 Hz train, and the degree of 'steady state' block at 2 Hz was about twice that at 0.5 Hz. These use and frequency-dependent effects suggested that block of transient outward current by quinidine is related to states of the channels which are produced by membrane depolarization, i.e., open and inactivated states. The experiments described in the remainder of the paper were designed to elucidate the kinetic basis of the use-dependent quinidine block.

Time and membrane potential dependence of quinidine block of transient outward current

The data in Figure 5 show that in the presence of quinidine, even brief (e.g. 100 ms) depolarizations were sufficient to produce a substantial block of the transient outward current. Figure 6 shows the time-course of development of quinidine-induced block of transient outward current during membrane depolarization. This voltage-clamp protocol consisted of a pair of depolarizing steps to +50 mV from a holding potential of −70 mV. The first was a 'conditioning' step the duration of which was varied between 2 ms and 1.5 s, and the second was a 100 ms 'test' step. The conditioning and test steps were separated by a gap of 0.2 s at the holding potential; this allowed sufficient time for the channels which were not blocked by quinidine to recover from inactivation, but the gap was too short for quinidine-blocked channels to recover (see below). Hence comparison of the test current amplitudes in the presence and absence of the conditioning step gave a measure of the quinidine-induced block. In the absence of quinidine, this protocol produced only a small (<5%) depression of the test current amplitude as the conditioning step duration was varied from 2 ms to 1.5 s. However, in the presence of 6 μM quinidine, conditioning pulses as short as 5 ms produced a measurable decrease in test current amplitude. Conditioning pulses of longer duration resulted in greater depression of the test current, but with a 50 ms conditioning pulse a maximal depression of about 23% was reached and pulses as long as 1.5 s produced no significant additional block.

Figure 7a illustrates results from an experiment which compared the voltage dependence of activation, and quinidine-induced block, of transient outward current. A paired voltage-clamp protocol was used to measure the voltage-dependence of activation of the transient outward current. A 10 ms step to potentials between −30 and +70 mV was used to activate, without significantly inactivating, the transient outward current. The cell was immediately repolarized to −40 mV, and the amplitude of the tail current following repolarization was taken as a measure of transient outward current activation. Figure 7a

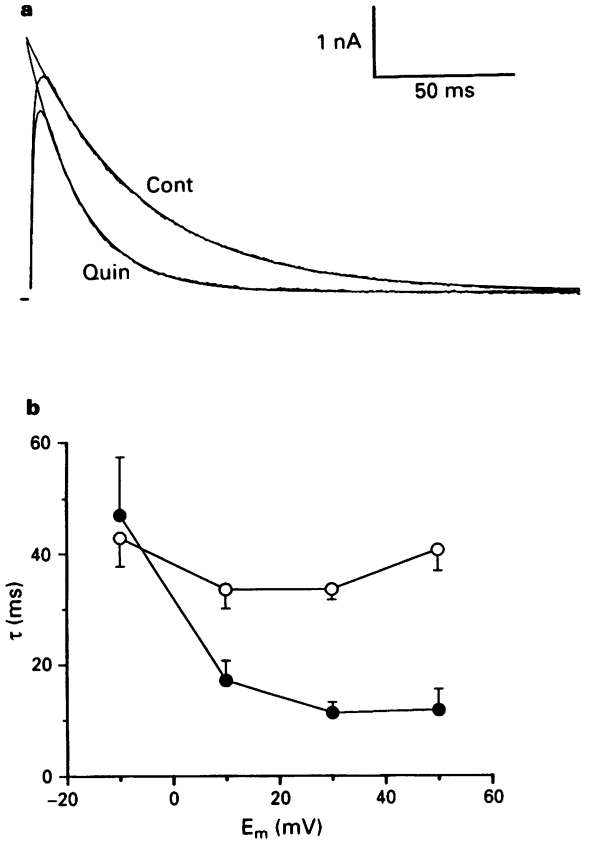

Figure 4 Effect of quinidine on the time course of decay of the transient outward current. (a) Superimposed current records in control and 6 μM quinidine, for voltage-clamp steps to +30 mV, from a holding potential of −70 mV. Single exponentials were fitted to the decay phase of the currents; the time constant for control was 41.3 ms, and in quinidine it was 18.6 ms. (b) Time constant of decay of the transient outward current vs. membrane potential, before (○) and after (●) 6 μM quinidine. Mean (± s.e.) values from 3 different control and 4 different quinidine-treated ventricular cells.

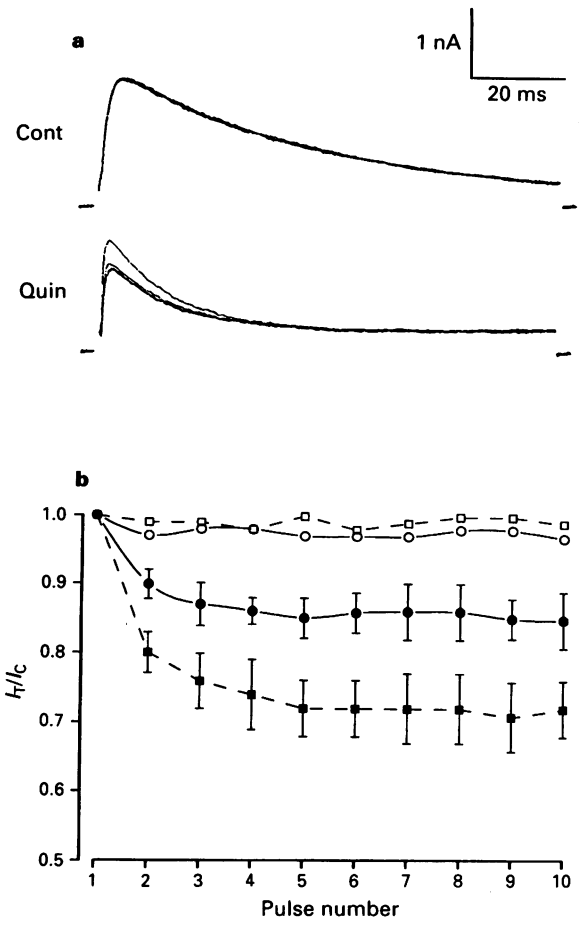

Figure 5 Use- and frequency-dependent effects of quinidine on transient outward current. (a) Effect of quinidine on the amplitude of transient outward current produced by a train of 10 voltage-clamp steps (100 ms; −70 to +50 mV), applied at a rate of 2 Hz. The upper records are 10 superimposed currents recorded in control conditions. Currents produced by the same train of steps after application of 6 μM quinidine are shown below. Transient outward current amplitude decreased with successive steps in the train. (b) Averaged (mean ± s.e.) data from 8 cells, for pulse train frequencies of 0.5 (○, ●) and 2 Hz (□, ■). The current amplitudes for each pulse in the train have been normalized to the first pulse (I_T/I_C). Note that there was no significant change in current amplitude in control (○, □) conditions, but in 6 μM quinidine, (●, ■) the current decreased with successive pulses and reached a 'steady-state' level by the end of the 10 pulse train, and that the block was greater for the 2 Hz train than the 0.5 Hz train.

shows the membrane potential-dependence of the tail current amplitude, normalized to its largest magnitude, at +70 mV (●). The potential dependence of activation was fitted to a Boltzmann function (see Figure 7a), with half-activation at −2 ± 0.5 mV, and a slope at half-activation of 12.7 ± 0.5 mV. The membrane potential-dependence of quinidine-induced block of the transient outward current was measured with the paired voltage-clamp protocol shown schematically in Figure 7a. A 'conditioning' step of 100 ms duration, at potentials between −60 and +80 mV, was followed 300 ms later by a 100 ms 'test' step to +50 mV. In the absence of quinidine, this protocol produced less than 5% depression of transient outward current at the most positive conditioning potentials. In the presence of 6 μM quinidine, conditioning depolarizations positive to about −40 mV produced measurable block of the transient outward current, and the amount of block increased with increased depolarization. Figure 7a shows that although activation of transient outward current and quinidine-induced block had similar membrane potential-dependence, activation was maximal for depolarizations to +40 mV, while the quinidine-induced block continued to increase over the range +40 to +80 mV. This effect may result from voltage-dependence of quinidine block of open transient outward current channels (see Discussion).

The time course of block of transient outward current by quinidine shown in Figure 6 approximately paralleled the inactivation time course of transient outward current (e.g. Figures 2 and 4), suggesting that the block occurred primarily during the time when the transient outward current channels were open; longer depolarizations which completely inactivated transient outward current produced no additional block (Figure 6). Additional data which suggest that quinidine does not significantly block inactivated channels are shown in Figure 7b, where the membrane potential-dependence of 'steady state' inactivation of the transient outward current in the presence and absence of quinidine are compared. 'Conditioning' steps of 1 s duration were applied over the potential range from −100 to −10 mV, followed immediately by a 'test' step to +50 mV. In control conditions, transient outward current was inactivated by conditioning potentials in the range from −60 to −10 mV, and the amplitude of transient outward current evoked by the test step was best-fitted by a Boltzmann function with half-inactivation at −32 ± 1 mV and a slope factor at half-inactivation of 3.9 ± 0.1 mV (see Figure 7b). In the presence of quinidine, there was no significant change in the potential dependence of inactivation; half-inactivation occurred at

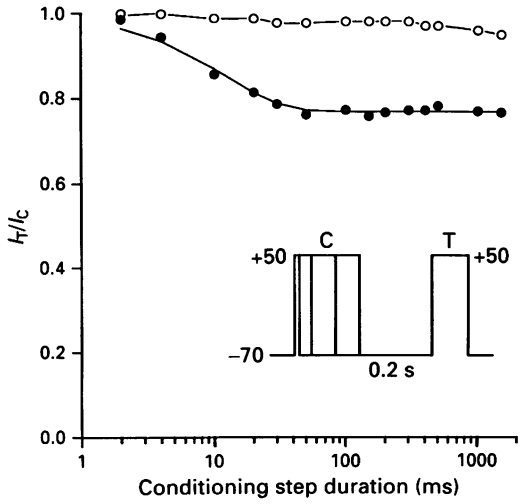

Figure 6 Time course of development of quinidine-induced block of transient outward current during depolarization. The voltage-clamp protocol is shown in the inset. A 'conditioning' step (+50 mV) of variable duration (2 ms to 1.5 s) was followed after a 200 ms interval at −70 mV by a 'test' step (+50 mV). Peak transient outward current in the presence of the conditioning step was normalized to the amplitude of transient outward current in the absence of the conditioning step. The plot shows the normalized amplitude of test current compared to control current (I_T/I_C), as a function of the conditioning pulse duration. Control (○), and 6 μM quinidine (●). Note that conditioning step duration is plotted on a logarithmic scale. The solid line fitted to the quinidine data is a single exponential function with a time constant of 12.1 ms.

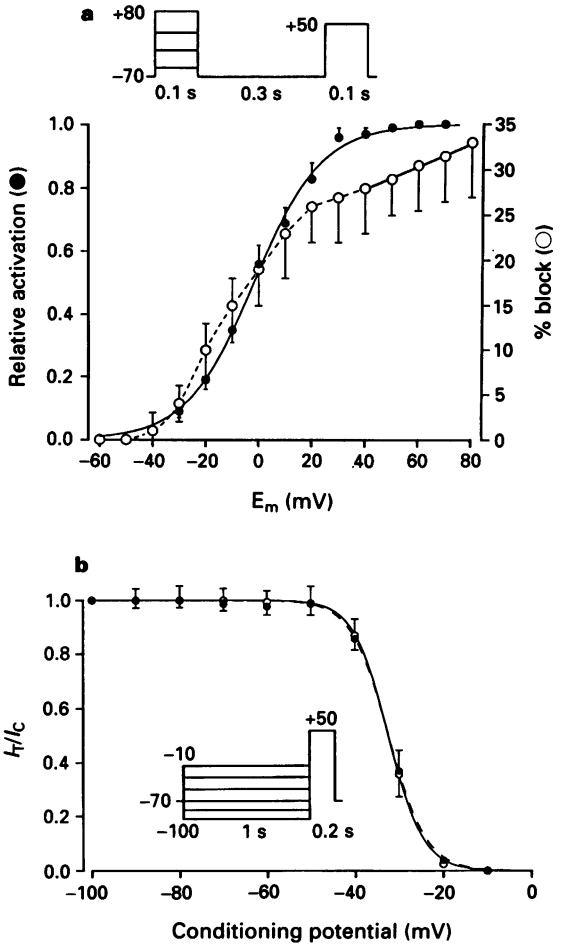

Figure 7 Voltage-dependence of quinidine-induced block of transient outward current. (a) Comparison of the membrane potential-dependence of activation of transient outward current (●), and quinidine-induced block (○). Activation of transient outward current was measured with a two-step voltage-clamp protocol (see text). The solid line is a Boltzmann function of the form

$$1/(1 + \exp[V_{1/2} - V_m)/S_{1/2}])$$

where V_m is membrane potential during the first voltage-clamp step. $V_{1/2}$ is the potential for half-activation, and $S_{1/2}$ is a slope factor at the half-activation potential. Data were pooled from 6 cells. Quinidine-induced block of transient outward current was measured using the voltage-clamp protocol shown; % block (○) was determined by comparing the 'test' (second step) current amplitude in the absence and presence of the 'conditioning' step. The solid line is best fit of equation (*1*) to data from +40 to +80 mV; see text for details. Data from 6 cells. (b) Membrane potential dependence of 'steady state' inactivation of transient outward current. The two-step voltage-clamp protocol used to measure inactivation is shown in inset. Inactivation was measured by the ratio I_T/I_C, where I_T and I_C were current amplitudes in the presence and absence of a conditioning step, respectively. For both controls (○) ($n = 6$) and after quinidine treatment (●) ($n = 6$), the ratio was fitted to a Boltzmann function of the form

$$I_T/I_C = 1/(1 + \exp[(V_m - V_{1/2})/S_{1/2}]$$

See text for values of $V_{1/2}$ and $S_{1/2}$.

−32 ± 1 mV and the slope factor at half-inactivation was 4.2 ± 0.2 mV.

Recovery of transient outward current from quinidine-induced block

The use-dependent behaviour of local anaesthetics during repetitive depolarizations is governed not only by the time course of development of block during depolarization, but also by the amount of recovery from block that occurs in the time intervals between depolarizations. The experiments described below were designed to measure the characteristics of recovery of transient outward current from quinidine-induced block.

Recovery was assessed with a paired pulse voltage-clamp protocol. A 100 ms 'conditioning' step to +50 mV inactivated most of the transient outward current, and the recovery of transient outward current from inactivation at the holding potential (−70 mV) was assessed at different times with a 'test' step (+50 mV, 100 ms). An example of recovery of transient outward current from inactivation is shown in Figure 8a. In control conditions, the transient outward current had almost completely recovered from inactivation when the conditioning-test interval was 140 ms. The time course of recovery from inactivation in controls was fitted to a single exponential function (Figure 8b), with a time constant of 58 ± 4 ms ($n = 9$). In the presence of quinidine, recovery from inactivation was prolonged, with a slow, second phase of recovery following a rapid, initial phase (Figure 8a). The time course of recovery was biexponential (Figure 8b), with 'fast' and 'slow' components with time constants of 59 ± 9 ms and 771 ± 141 ms, respectively ($n = 9$). Figure 8 shows that after a 200 ms interval, the transient outward current had completely recovered from inactivation in control conditions, whereas in the presence of quinidine, substantial block of the transient outward current still remained. This provided the rationale for the 'gapped' voltage-clamp protocols used to measure the time- and voltage-dependence of quinidine block (e.g. Figures 6 and 7).

Discussion

Summary of findings

We have shown that quinidine blocks two components of outward K^+ current in rat isolated ventricular myocytes, a Ca^{2+}-insensitive transient current, and a slowly inactivating delayed rectifier-like component, although only the effects of quinidine on the transient component were examined in

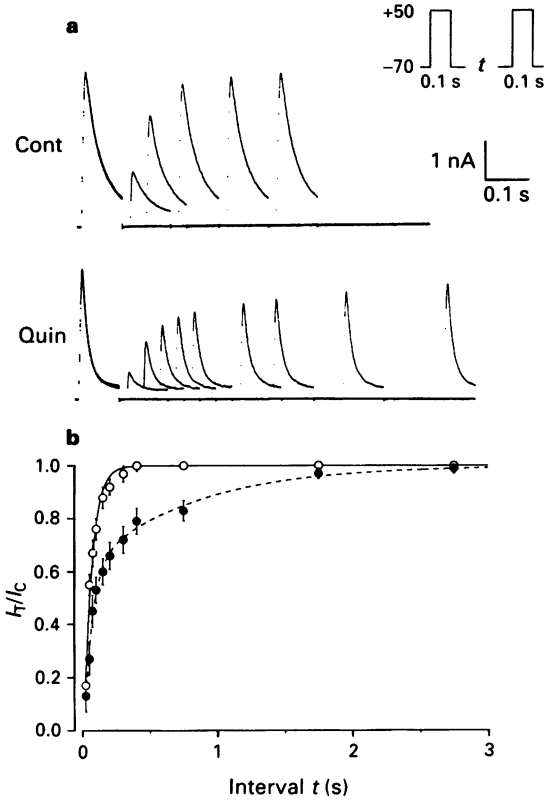

Figure 8 Recovery of transient outward current from quinidine-induced block. (a) A two-pulse protocol was used to measure recovery from inactivation. A 100 ms 'conditioning' step to +50 mV inactivated most of transient outward current; after a variable time t, a 'test' step to +50 mV measured recovery of transient outward current from inactivation. The pulse pairs were applied at 30 s intervals. The currents shown were recorded from the same myocyte in control and in 6 μM quinidine. The solutions contained 10 mM tetraethylammonium chloride. (b) Averaged (mean ± s.e.) recovery data pooled from 9 different cells. 'Test' current amplitude (I_T), normalized to 'conditioning' current amplitude (I_C), is plotted against the time interval between test and conditioning pulses. Control (○; $n = 9$) and after 6 μM quinidine (●). Lines show best-fits of single exponential (Cont) or double exponential (Quin) functions to the data. See text for magnitude of the time constants.

detail. The characteristics of quinidine-induced block of the transient outward current strongly suggested that quinidine blocked open channels, probably from the intracellular side of the membrane. These characteristics included: (*i*) the quinidine-induced increase in the rate of decay of the current, but without significant change in the activation time course (Figures 2 and 4), (*ii*) the use-dependent block (Figure 5), (*iii*) the time course of development of quinidine-induced block paralleled the time course of current (Figure 6), (*iv*) the close correlation between the membrane potential-dependence of current activation and quinidine-induced block (Figure 7), and (*v*) the lack of effect of quinidine on steady-state inactivation of the transient outward current (Figure 7). The implications of these results for models of quinidine-induced block will be discussed in more detail below.

Biophysical analysis of quinidine block of transient outward current

In their simplest form, kinetic models of transient outward current can be written as:

$$[C]_n \rightleftharpoons O \rightleftharpoons I$$

where C, O and I are closed, open and inactivated states of the channel, respectively, and n indicates that there are a series of several closed states leading to an open state (e.g. Zagotta & Aldrich, 1990). At positive membrane potentials, channel 'closure' occurs preferentially by inactivation, hence a prolonged depolarization results in rapid activation of the channel, followed by a slower decay (e.g. Figure 2). This kinetic scheme can be modified to account for block of the open channel by quinidine by adding another pathway:

$$\begin{array}{ccccc} [C]_n & \rightleftharpoons & O & \rightleftharpoons & I \\ & & \downarrow\uparrow & & \\ & & B & & \end{array}$$

where B is a non-conducting, quinidine-blocked channel. This scheme predicts that decay of the current will be accelerated by quinidine, because the open channel can 'close' by two pathways, namely, inactivation ($O \rightleftharpoons I$), and by quinidine block ($O \rightleftharpoons B$). The increase in the rate of decay of the transient outward current in Figures 2 and 4 is consistent with this scheme. In addition, quinidine-induced block cannot occur until the channel opens, which implies that the time course of current activation should be relatively unaffected by quinidine; this result is clearly apparent in the current records in Figure 4.

Quinidine has a positive charge at pH values near 7.2, due to ionization of a tertiary amine group with a pK_a of 8.9. If quinidine blocks transient outward channels by interacting with the open channel, then the block would be expected to be dependent on membrane potential, because the charged ion would interact with the transmembrane electric field in the channel. That this is indeed the case is suggested by the data in Figure 4, which show that the rate of decay of the current in the presence of quinidine is strongly dependent on membrane potential over the range −10 to +50 mV, while it is almost potential-independent in its absence. This suggests that the quinidine blocking step in the kinetic scheme, $O \rightleftharpoons B$, is sensitive to membrane potential. The fact that the rate of decay increased with membrane depolarization is consistent with a positively charged ion moving into the ionic channel from the intracellular side of the membrane. The data in Figure 7a also support this model. These results show that transient outward current activation and block by quinidine increased in parallel with membrane depolarization up to about +30 mV, where this current is fully activated. However, the block produced by quinidine continued to increase at membrane potentials more positive than about +30 mV. This continued increase in block probably reflects the potential dependence of quinidine block of the fully open channel, independent of the effects of membrane potential on channel opening. Assuming this to be the case, the fractional block by quinidine of the transient outward current can be described by the equation (Woodhull, 1973; Snyders *et al.*, 1992)

$$f = [D]/\{[D] + K_d \exp(-\delta F V_m/RT)\} \quad (1)$$

where [D] is the quinidine concentration, K_d is the apparent binding constant (at zero mV membrane potential), and δ is an equivalent electrical distance, i.e., the fraction of the transmembrane potential (V_m) sensed by a single charge at its binding site in the channel. This equation assumes that a single quinidine molecule is required to block a channel (Slawsky & Castle, 1994). Equation (1) was fitted to the data in Figure 7a for membrane potentials from +40 to +80 mV; the best-fit values of δ and K_d were 0.14 and 19.4 μM, respectively. Snyders *et al.* (1992) obtained a similar value of δ (0.19) for quinidine block of a cloned human cardiac delayed rectifier K^+ channel (hKv1.5), expressed in a mouse L cell line.

Comparison with other studies of quinidine-induced block of cardiac K^+ channels

Data from a previous study of the effects of quinidine on Ca^{2+}-independent transient outward current in rabbit atrium (Imaizumi & Giles, 1987) are qualitatively in agreement with

some of the results of the present study. For example, the rate of inactivation of the current was increased by quinidine, the rate of recovery from inactivation was prolonged, and the membrane potential dependence of steady-state inactivation was not affected by quinidine. These similarities suggest that the mechanism of action of quinidine on transient outward current in rabbit atrium and rat ventricle may be identical.

Two studies of the effects of quinidine on rat cardiac transient outward current have appeared recently. Slawsky & Castle (1994) demonstrated many of the features of quinidine-induced block of transient outward current in rat ventricular myocytes shown in the present study, e.g., increased rate of decay of current, use-dependent inhibition, and a slowing of recovery from inactivation in the presence of quinidine, and they interpreted their data in terms of open channel block. Yatani *et al.* (1993) used *Xenopus* oocytes to express a transient outward K^+ channel (RHK1: Kv1.4) cloned from a rat heart cDNA library (Tseng-Crank *et al.*, 1990), and examined the effect of quinidine on macroscopic and single channel currents. Some features of their results were strikingly different from either those in the present study or the findings of Slawsky & Castle (1994); one of the most interesting differences was that quinidine *decreased* the rate of decay of the current, rather than increasing it, as seen in rat myocytes. This effect of quinidine was examined at the single channel level. In control conditions the channels opened in a long, single burst during a membrane depolarization, but after addition of quinidine openings occurred in a series of brief bursts, and the mean open time of the channel during the bursts was reduced by quinidine. Both of these changes in single channel kinetics resulted in the prolongation in time course of inactivation seen in the macroscopic currents. These data were explained by a model in which quinidine blocked the open channel, but the drug was required to dissociate from the channel before it could close during the burst. In addition, Yatani *et al.* (1993) found that the concentration of quinidine required for 50% block of the current was approximately 1 mM, which is more than two orders of magnitude greater than the 50% blocking dose in rat ventricular myocytes (Slawsky & Castle, 1994). There may be several reasons why the effects of quinidine are qualitatively different between these expressed channels and those in the native membrane of rat myocytes. It is not certain that the cloned channel used by Yatani *et al.* (1993) is identical to that found in rat ventricular myocytes, although the rate and potential dependence of inactivation of the cloned channels in control conditions was very similar to that in rat myocytes. It is possible that the native channels are predominantly heteromultimeric, whereas the expressed channels were homomultimeric, since only a single channel clone was injected into the oocytes. It is known that the kinetic and pharmacological properties of heteromultimeric K^+ channels can differ from those of homomultimers (e.g. Isacoff *et al.*, 1990).

Delayed outward K^+ currents are blocked by quinidine in a number of cardiac preparations, including guinea-pig (Hiraoka *et al.*, 1986; Roden *et al.*, 1988; Balser *et al.*, 1991a; Wettwer *et al.*, 1992) and rat (Slawsky & Castle, 1994) ventricle, and rabbit sinoatrial and atrioventricular nodes (Furukawa *et al.*, 1989). In the case of guinea-pig ventricle, quinidine appeared to block multiple components (cf., Sanguinetti & Jurkiewicz, 1990) of delayed rectifier (Balser *et al.*, 1991a; Wettwer *et al.*, 1992). Block by quinidine of the delayed K^+ current in rabbit sinoatrial and atrioventricular nodes (Furukawa *et al.*, 1989), and prolongation of the time constant of tail currents was interpreted in terms of open channel block.

The most comprehensive previous study of the effects of quinidine on a cardiac K^+ channel was carried out by Snyders *et al.* (1992) on a human delayed rectifier channel (hKv1.5) expressed in a stable mouse L cell line. The kinetic and potential-dependent effects of quinidine on this channel were well accounted for by open channel block, in which the quinidine binding site had an equivalent electrical distant of about 20%, referenced to the intracellular side of the membrane. Quinidine produced a rapid phase of 'inactivation' of the current which was qualitatively similar to the effect of quinidine on the time course of the delayed component of outward current in rat ventricular myocytes (cf. Figure 3a).

There are conflicting reports on the effect of quinidine on the inward rectifier K^+ current, I_{K1}. Quinidine was reported to have no significant effect on I_{K1} in rabbit atrium (Imaizumi & Giles, 1987) and Purkinje fibres (Colatsky, 1982), which was in contrast to the results of Salata & Wasserstrom (1988) in canine ventricular myocytes. Balser *et al.* (1991b) reported that quinidine reduced the open probability of single I_{K1} channels recorded from cell-attached patches on guinea-pig ventricular cells, probably by prolonging a closed state of the channels, but these measurements were made at membrane potentials negative to about -100 mV, i.e., far negative to the normal resting potential of the myocytes. The lack of effect of quinidine on the resting membrane potential of rat ventricular myocytes (see Results) is consistent with the study of Slawsky & Castle (1994), which showed that I_{K1} was unaffected even by concentrations of quinidine 100 fold greater than those that blocked transient outward current.

Summary

This study has shown that quinidine is a potent inhibitor of K^+ currents in rat ventricular myocytes, and in the case of Ca^{2+}-independent transient outward current, the mechanism is an open channel block by ionized quinidine. Many other K^+ channels appear to be blocked by quinidine *via* a similar mechanism. This may be expected, given the similarity of the putative ion conducting pore regions, and hence the quinidine binding site, between different K^+ channels (Pongs, 1992).

This study was supported by the Medical Research Council of Canada, the Heart and Stroke Foundation of Canada, and the Alberta Heritage Foundation for Medical Research. H.J.D. and W.R.G. are Alberta Heritage Foundation Medical Scientists.

References

APKON, M. & NERBONNE, J.M. (1991). Characterization of two distinct depolarization-activated K^+ currents in isolated adult rat ventricular myocytes. *J. Gen. Physiol.*, **97**, 973–1011.

ARMSTRONG, C.M. (1971). Interaction of tetraethylammonium ion derivatives with the potassium channels of giant axons. *J. Gen. Physiol.*, **58**, 413–437.

BALSER, J.R., BENNETT, P.B., HONDEGHEM, L.M. & RODEN, D.M. (1991a). Suppression of time-dependent outward current in guinea-pig ventricular myocytes: actions of quinidine and amiodarone. *Circ. Res.*, **69**, 519–529.

BALSER, J.R., RODEN, D.M. & BENNETT, P.B. (1991b). Single inward rectifier potassium channels in guinea-pig ventricular myocytes. Effects of quinidine. *Biophys. J.*, **59**, 150–161.

BAUMGARTEN, C.M. & FOZZARD, H.A. (1991). Cardiac resting and pacemaker potentials. In *The Heart and Cardiovascular System*, 2nd edition, ed. Fozzard, H.A., Haber, E., Jennings, R.B., Katz, A.M. & Morgan, H.E. pp. 963–1001. New York: Raven Press.

CLARK, R.B., BOUCHARD, R.A., SANCHEZ-CHAPULA, E., SALINAS-STEPHANON, E. & GILES, W.R. (1993). Heterogeneity of action potential waveforms and repolarizing potassium currents in rat ventricle. *Cardiovasc. Res.*, **27**, 1795–1799.

CLARKSON, C.W. & HONDEGHEM, L.M. (1985). Evidence for a specific receptor site for lidocaine, quinidine and bupivacaine associated with cardiac sodium channels in guinea-pig ventricular myocardium. *Circ. Res.*, **56**, 496–506.

COLATSKY, T.J. (1982). Mechanism of action of lidocaine and quinidine on action potential duration in rabbit cardiac Purkinje fibers. *Circ. Res.*, **50**, 17–27.

COLATSKY, T.J., FOLLMER, C.H. & STARMER, C.F. (1990). Channel specificity in antiarrhythmic drug action: mechanism of potassium channel block and its role in suppressing and aggravating cardiac arrhythmias. *Circulation*, **82**, 2235–2242.

FURUKAWA, T., TSUJIMURA, Y., KITAMURA, K., TANAKA, H. & HABUCHI, Y. (1989). Time- and voltage-dependent block of the delayed K^+ current by quinidine in rabbit sinoatrial and atrioventricular nodes. *J. Pharmacol. Exp. Ther.*, **251**, 756–763.

GINTANT, G.A., COHEN, I.S., DATYNER, N.B. & KLINE, R.P. (1991). Time-dependent outward currents in the heart. In *The Heart and Cardiovascular System*, 2nd edition. ed. Fozzard, H.A., Haber, E., Jennings, R.B., Katz, A.M. & Morgan, H.E. pp. 1121–1169. New York: Raven Press.

HAMILL, O.P., MARTY, A., NEHER, E., SAKMANN, B. & SIGWORTH, F.J. (1981). Improved patch-clamp techniques for high-resolution current recording from cells and cell-free membrane patches. *Pflügers Arch.*, **391**, 85–100.

HERMANN, A. & GORMAN, A.L.F. (1984). Action of quinidine on ionic currents of molluscan pacemaker neurones. *J. Gen. Physiol.*, **83**, 919–940.

HILLE, B. (1977). Local anaesthetics: hydrophilic and hydrophobic pathways for the drug-receptor reaction. *J. Gen. Physiol.*, **69**, 497–515.

HIRAOKA, M., SAWADA, K. & KAWANO, S. (1986). Effects of quinidine on plateau currents of guinea-pig ventricular myocytes. *J. Mol. Cell. Cardiol.*, **18**, 1097–1106.

HONDEGHEM, L.M. & KATZUNG, B.G. (1977). Time- and voltage-dependent interactions of antiarrhythmic drugs with cardiac sodium channels. *Biochem. Biophys. Acta.*, **472**, 373–398.

HONDEGHEM, L.M. & KATZUNG, B.G. (1984). Antiarrhythmic agents: the modulated receptor mechanism of action of sodium and calcium channel-blocking drugs. *Annu. Rev. Pharmacol. Toxicol.*, **24**, 387–423.

HONDEGHEM, L.M. & SYNDERS, D.J. (1990). Class III antiarrhythmic agents have a lot of potential but a long way to go. *Circulation*, **81**, 686–690.

IMAIZUMI, Y. & GILES, W.R. (1987). Quinidine-induced inhibition of transient outward current in cardiac muscle. *Am. J. Physiol.*, **253**, H704–H708.

ISACOFF, E.Y., JAN, Y.N. & JAN, L.Y. (1990). Evidence for the formation of heteromultimeric potassium channels in *Xenopus* oocytes. *Nature*, **345**, 530–534.

KEHL, S.J. (1991). Quinidine-induced inhibition of the fast transient outward K^+ current in rat melanotrophs. *Br. J. Pharmacol.*, **103**, 1807–1813.

LYNCH, J.J. Jr., SANGUINETTI, M.C., KIMURA, S. & BASSETT, A.L. (1992). Therapeutic potential of modulating potassium currents in the diseased myocardium. *FASEB J.*, **6**, 2952–2960.

NATTEL, S. (1991). Antiarrhythmic drug classifications. *Drugs*, **41**, 672–701.

NAKAYAMA, T. & FOZZARD, H.A. (1987). Quinidine reduces outward current in single canine cardiac Purkinje cells. In *Pharmacological Aspects of Heart Disease*, ed. Beamish, R.E., Panagia, V. & Dhalla, N.S. pp. 33–44. Boston: Martinus Nijhoff.

OYAMA, Y., HARATA, N. & AKAIKE, N. (1992). Accelerating action of quinidine on the decay phase of transient outward current in dissociated hippocampal pyramidal neurons of rats. *Jpn. J. Pharmacol.*, **58**, 185–188.

PONGS, O. (1992). Molecular biology of voltage-dependent potassium channels. *Physiol. Rev.*, **72**, S69–S88.

RODEN, D.M., BENNETT, P.B., SNYDERS, D.J., BALSER, J.R. & HONDEGHEM, L.M. (1988). Quinidine delays I_K activation in guinea-pig ventricular myocytes. *Circ. Res.*, **62**, 1055–1058.

RODEN, D.M. & HOFFMAN, B.F. (1985). Action potential prolongation and induction of abnormal automaticity by low quinidine concentrations in canine Purkinje fibers. *Circ. Res.*, **56**, 857–867.

ROSEN, M.R. *et al.* (1991). The Sicilian Gambit: A new approach to the classification of antiarrhythmic drugs based on their actions on arrhythmogenic mechanisms. *Circulation*, **84**, 1831–1851.

SALATA, J.J. & WASSERSTROM, J.A. (1988). Effects of quinidine on action potentials and ionic currents in isolated canine ventricular myocytes. *Circ. Res.*, **62**, 324–337.

SANGUINETTI, M.C. & JURKIEWICZ, N.K. (1990). Two components of cardiac delayed rectifier K^+ current. Differential sensitivity to block by class III antiarrhythmic agents. *J. Gen. Physiol.*, **96**, 195–215.

SINGH, B.N. & NADAMANE, K. (1985). Control of cardiac arrhythmias by selective lengthening of repolarization: Theoretic considerations and clinical observations. *Am. Heart J.*, **109**, 421–430.

SLAWSKY, M.T. & CASTLE, N.A. (1994). K^+ channel blocking actions of flecainide compared to those of propafenone and quinidine in adult rat ventricular myocytes. *J. Pharmacol. Exp. Ther.*, **269**, 66–74.

SNYDERS, D.J., KNOTH, K.M., ROBERDS, S.L. & TAMKUN, M.M. (1992). Time-, voltage-, and state-dependent block by quinidine of a cloned human cardiac potassium channel. *Mol. Pharmacol.*, **41**, 322–330.

SPINELLI, W. & HOFFMAN, B.R. (1989). Mechanisms of termination of reentrant atrial arrhythmias by class I and III antiarrhythmic agents. *Circ. Res.*, **65**, 1565–1579.

TSENG-CRANK, J.C.L., TSENG, G.N., SCHWARTZ, A. & TANOUYE, M.A. (1990). Molecular cloning and functional expression of a potassium channel cDNA isolated from rat cardiac library. *F.E.B.S. Lett.*, **268**, 63–68.

UNDROVINAS, A.I., BURNASHEV, N., EROSHENKO, D., FLEIDERVISH, I., STARMER, C.F., MAKIELSKI, J.C. & ROSENSHTRAUKH, L.V. (1990). Quinidine blocks adenosine 5′-triphosphate-sensitive potassium channels in heart. *Am. J. Physiol.*, **259**, H1609–H1612.

WETTWER, E., GRUNDKE, M. & RAVENS, U. (1992). Differential effects of the new class III antiarrhythmic agents almokalant, E-4031 and D-sotalol, and of quinidine, on delayed rectifier currents in guinea-pig ventricular myocytes. *Cardiovasc. Res.*, **26**, 1145–1152.

WOODHULL, A.M. (1973). Ion blockage of sodium channels in nerve. *J. Gen. Physiol.*, **61**, 687–708.

YATANI, A., WAKAMORI, M., MIKALA, G. & BAHINSKI, A. (1993). Block of transient outward-type cloned cardiac K^+ channel currents by quinidine. *Circ. Res.*, **73**, 351–359.

ZAGOTTA, W.N. & ALDRICH, R.W. (1990). Voltage-dependent gating of *Shaker* A-type potassium channel in *Drosophila* muscle. *J. Gen. Physiol.*, **95**, 29–60.

(Received September 12, 1994
Revised January 25, 1995
Accepted January 31, 1995)

British Journal of Pharmacology (1995) 115, 344-348

Effect of nitric oxide on integrity, blood flow and cyclic GMP levels in the rat gastric mucosa: modulation by sialoadenectomy

M.A. Tripp & [1]B.L. Tepperman

Department of Physiology, Faculty of Medicine, University of Western Ontario, London, Ontario, Canada N6A 5C1

1 The effects of the nitrosothiol, S-nitroso N-acetylpenicillamine (SNAP) which liberates nitric oxide (NO), on ethanol-mediated gastric damage, blood flow and cyclic GMP levels in siaoloadenectomized (SALX) rats have been investigated.

2 Intraluminal instillation of ethanol (5–50% w/v) dose-dependently induced haemorrhagic damage and decreased NO synthase activity in the gastric mucosa. Both the extent of mucosal damage and inhibition of NO synthase activity were exacerbated in SALX rats.

3 Epidermal growth factor administration (5 and 10 $\mu g\,kg^{-1}$, s.c.) reduced mucosal damage but did not restore NO synthase activity in ethanol-treated SALX rats.

4 SNAP infusion (0.01–1.0 $\mu g\,kg^{-1}\,min^{-1}$, i.v.) attenuated haemorrhagic damage in ethanol-treated rats. The reduction in mucosal damage was significantly greater in SALX rats.

5 SNAP administration also caused an increase in gastric mucosal blood flow and cyclic GMP levels in control rats and both responses were augmented in SALX animals.

6 These data suggest that SALX is associated with increases in mucosal susceptibility to ethanol-mediated damage and reduces mucosal NO synthase activity. Epidermal growth factor does not appear to influence mucosal NO synthase in ethanol-treated rats. Furthermore, SALX augments the responsiveness of the gastric mucosa to NO administration. Therefore, factors from the salivary glands influence gastric NO formation and mucosal responsiveness to a NO donor.

Keywords: Nitric oxide; gastric mucosal integrity; mucosal blood flow; cyclic GMP; sialoadenectomy; epidermal growth factor; S-nitroso N-acetyl penicillamine

Introduction

Removal of the salivary glands (sialoadenectomy; SALX) in rats has been shown to increase the susceptibility of the gastric mucosa to ulcerogens (Skinner & Tepperman, 1981; Olsen *et al.*, 1984; Tepperman & Soper, 1990). The influence of the salivary glands on gastric mucosal integrity has been attributed to a number of peptide or glycopeptide substances which have been extracted from salivary glands or saliva (Skinner *et al.*, 1984) including epidermal growth factor (EGF) (Cohen, 1962). This peptide has been shown to protect the gastric mucosa from the damaging actions of a number of ulcerogens (Pilot *et al.*, 1979; Olsen *et al.*, 1984; Konturek *et al.*, 1988; Itoh *et al.*, 1992). It has been demonstrated that at least a portion of the protective effect of EGF on gastric mucosal integrity may occur via influences on the gastric microcirculation (Tepperman & Soper, 1994).

In addition to salivary factors, nitric oxide (NO) synthesized from L-arginine by the enzyme NO synthase (Moncada *et al.*, 1991) has been shown to play a role in the maintenance of gastric mucosal integrity. Like EGF, the effect of NO on mucosal integrity is mediated by acting on gastric blood flow (Whittle & Tepperman, 1991; Tepperman & Whittle, 1992).

NO has been shown to interact with a number of factors in the regulation of gastric mucosal integrity and blood flow including prostanoids and sensory neuropeptides (Whittle & Tepperman, 1991; Tepperman & Whittle, 1992). Recently we have demonstrated that factors that originate from the rodent salivary glands also interact with NO in the maintenance of mucosal integrity and that this effect may be mediated in part by changes in gastric mucosal blood flow (Tepperman & Soper, 1993). The purpose of the present study was to characterize further this interaction by an examination of the effects of exogenous NO on gastric mucosal integrity and blood flow in the sialoadenectomized rat following administration of S-nitroso N-acetyl-penicillamine (SNAP), an agent which spontaneously releases NO. Furthermore since NO acts on its target cell to stimulate guanylate cyclase and elevate guanosine 3':5'-cyclic monophosphate (cyclic GMP) levels (Moncada *et al.*, 1991) we have also examined the effect of SALX on cyclic GMP levels stimulated by administration of SNAP.

[1] Author for correspondence.

Methods

Animal preparation

Male Sprague Dawley rats (250–350 g) were used in this study. All experiments were performed on sham-operated control rats and sialoadenectomized (SALX) rats. Sialoadenectomy was performed under pentobarbitone anaesthesia (60 $mg\,kg^{-1}$, i.p.) by removal of the submandibular-sublingual gland complexes after the ducts were ligated as previously described (Skinner & Tepperman, 1981; Skinner *et al.*, 1984). SALX and sham-operated animals were administered an antibiotic (Pen-Di-Strep 0.1 ml, i.m.) and then allowed to recover for two weeks before experiments. Effective sialoadenectomy was confirmed by the observation of an increase in prandial drinking by approximately 200% compared to control animals (Epstein *et al.*, 1964). All animals were fasted for 18–20 h before experimentation but were allowed water *ad libitum*. On the day of experimentation animals were anaesthetized with pentobarbitone (60 $mg\,kg^{-1}$), laparotomized and had their stomachs exposed to allow ligation of gastroesophageal and pyloric junctions.

Ethanol was used as an ulcerogen in this study and was administered as a 2 ml bolus through the forestomach.

Animals were given various doses of ethanol (5–50% w/v) as described above or were treated with 50% ethanol after receiving a pretreatment of epidermal growth factor (EGF) or S-nitroso-N-acetyl-penicillamine (SNAP). EGF was given as a bolus 15 min before ethanol in doses of 5 and 10 $\mu g\,kg^{-1}$, s.c. These doses have been shown to reduce effectively mucosal damage in SALX rats (Tepperman *et al.*, 1989). SNAP was administered as a continuous infusion (1.4 $ml\,h^{-1}$), starting 10 min before ethanol administration and maintained throughout the course of the experiment (30 min). SNAP was infused in a concentration range of 0.01–1.0 $\mu g\,kg^{-1}\,min^{-1}$ via a cannula inserted into the tail vein. EGF and SNAP were dissolved in isotonic saline immediately prior to use.

Measurement of haemorrhagic damage

Animals were killed by cervical dislocation 30 min after instillation of ethanol and the gastric mucosa was examined for mucosal damage. The stomachs were excised and opened along the greater curvature. Stomachs were then rinsed with distilled water, pinned flat to a wax plate with mucosa facing upward and fixed in buffered neutral formalin. Each mucosa was then photographed on transparent film (Ektachrome 50 Professional) and the percentage of haemorrhagic mucosal damage was estimated by computerized planimetry on projections of the transparencies. In the group of experiments examining the effects of SNAP on haemorrhagic damage, the difference in the percentage of mucosal area damaged between SNAP-treated and control tissues were compared for SALX and sham-operated rats.

Nitric oxide synthase activity

Mucosal NO synthase activity was assessed by the determination of radiolabelled citrulline formation from the substrate [^{14}C]-arginine as described previously (Tepperman *et al.*, 1993). Briefly, stomachs were excised and opened along the greater curvature and the mucosa was scraped away from underlying muscle. Mucosal tissue was then homogenized in a buffer (3 $\mu l\,mg^{-1}$ tissue) containing 10 mM HEPES, 320 mM sucrose, 1 mM dithiothreitol, soybean trypsin inhibitor (10 $\mu g\,ml^{-1}$), leupeptin (10 $\mu g\,ml^{-1}$) and aprotinin (2 $\mu g\,ml^{-1}$) (pH 7.4). Samples were homogenized for 15 s in a Tekmar Ultra-Turrax homogenizer, centrifuged at 4°C for 25 min at 9000 *g* and 20 μl of each supernatant was added to 50 μl of various incubation solutions. The assay solution contained 50 mM NADPH, 5 mM L-arginine, 40 mM $CaCl_2$, 200 μM $MgCl_2$ 1 mM potassium phosphate, 15 μM [^{14}C]-L-arginine (700,000 d.p.m. ml^{-1}) and 5 mM valine to inhibit any arginase activity. Some assay solutions contained 1 mM EGTA, a calcium chelator, or the NO synthase inhibitor N^G-monomethyl-L-arginine (L-NMMA; 300 μM). Solutions were incubated for 10 min at 37°C and the reaction was terminated by addition of a 1:1 suspension of Dowex 50W (Sigma) in water. The resin was allowed to settle for 10 min and the supernatant was removed for estimation of the radiolabelled product by liquid scintillation counting. Product formation that was inhibited by L-NMMA was used as an index of NO synthase activity. Data are expressed as pmol of [^{14}C]-citrulline formed $min^{-1}\,g^{-1}$ tissue.

Blood flow measurements

Experiments were conducted to examine the effects of the NO donor, SNAP, on gastric mucosal blood flow. A small gastric cannula (o.d. 8.5 mm) was inserted into the gastric lumen via an incision in the non-glandular region of the stomach. A stainless steel laser Doppler flow (LDF) probe (1.9 mm o.d.; Perimed, Piscataway, New Jersey, U.S.A.) was passed through the cannula and rested on the gastric mucosal surface. Mucosal blood flow was recorded continuously by a laser Doppler flow monitor (Periflux 3; Perimed, Piscataway, N.J., U.S.A.). Baseline blood flow was established and all animals received intravenous saline infusion for 3 min before SNAP treatment (0.01–1.0 $\mu g\,kg^{-1}\,min^{-1}$, i.v., for 5 min). Changes in LDF were assessed in response to SNAP and were calculated with a software programme designed for use with the Periflux laser Doppler flowmeter and expressed as percentage change from control in each animal.

Cyclic GMP determination

Experiments were performed to examine the effects of SNAP on guanosine 3′:5′-cyclic monophosphate (cyclic GMP) levels in the gastric mucosa. SNAP was infused intravenously (0.01–1.0 $\mu g\,kg^{-1}\,min^{-1}$) for 2.5 min. Gastric mucosal tissue was then excised and frozen immediately in 7.5% TCA (9 $\mu l\,mg^{-1}$ tissue). All tissues were stored at −80°C and later assayed by the procedure described by the cyclic GMP RIA kit from Amersham using a specific antiserum and [8-^{3}H]-guanosine 3′,5′-cyclic phosphate (1.6 μCi). The assay sensitivity was 2 fmol/well. Cyclic GMP content was expressed as pmol mg^{-1} tissue.

Materials

Epidermal growth factor was purchased from Biomedical Technologies (Stoughton, Mass, U.S.A.) and SNAP was obtained from BIOMOL Research Laboratories Inc. L-NMMA was purchased from Calibiochem (LaJolla, CA, U.S.A.) and radiolabelled arginine was obtained from Amersham (Oakville, Ont, Canada). Dithiothreitol and leupeptin were purchased from Boehringer Mannheim Biochemica (Montreal, Que, Canada). All other reagents in the NOS assay and L-NAME were obtained from Sigma (St. Louis, Missouri, U.S.A.). SNAP was purchased from Biomol Research Laboratories (Plymouth Meeting, PA, U.S.A.). All other reagents used in this study were of analytical grade.

Statistical analysis

All data were compared either by analysis of variance (ANOVA) and Duncan's Multiple Range Test. *P* values less than 0.05 were taken as significant.

Results

The effect of intraluminal ethanol (EtOH; 5–50% w/v) on gastric mucosal haemorrhagic damage is shown in Figure 1. Intraluminal instillation of 5% EtOH did not produce a significant degree of damage in either SALX or sham-operated control rats (Figure 1). Instillation of 25% EtOH resulted in a significant increase in damage in both groups while 50% EtOH resulted in mucosal damage of 40 ± 11% and 65 ± 10% in sham-operated and SALX rats respectively.

NO synthase activity as assessed by [^{14}C]-citulline formation was evident in gastric mucosal scrapings from the stomach of sham-operated and SALX rats (Figure 2). In response to saline in the gastric lumen, NOS activity was observed to be significantly lower in SALX rats when compared to sham-operated control animals. NOS activity was decreased in control and SALX rats in response to increasing concentrations of ethanol instilled into the gastric lumen. At concentrations of 5% and 25% w/v ethanol, NOS activity in the gastric mucosa of SALX rats was significantly lower than the activity observed in control rats. In response to the highest concentration of ethanol examined (50% w/v) NOS activity in both SALX and control rats was significantly reduced when compared to rats receiving saline alone. Furthermore the NOS activities in the gastic mucosa of SALX

and sham-operated rats receiving 50% w/v ethanol were not significantly different from each other (Figure 2).

The effect of administration of EGF to SALX rats receiving 50% w/v ethanol is shown in Figure 3. EGF administration (5 or 10 $\mu g\,kg^{-1}$, sc) significantly reduced mucosal haemorrhagic damage in response to intraluminal ethanol. However EGF had no significant effect on mucosal NOS activity (Figure 3). Similar effects were observed when EGF was administered to animals with intact salivary glands.

SNAP infusion in the concentration range 0.01–1 $\mu g\,kg^{-1}\,min^{-1}$ resulted in a reduction in gastric mucosal haemorrhagic damage in both sham-operated and sialoadenectomized rats (Figure 4). The reduction in mucosal damage in response to SNAP in SALX rats was significantly different from sham-operated controls in response to 0.1 and 1.0 $\mu g\,kg^{-1}\,min^{-1}$ of SNAP. Similarly SNAP infusion resulted in a significant increase in mucosal blood flow as estimated by LDF (Figure 5). In sham-operated control rats only the highest dose of SNAP produced a significant increase in LDF. The increases in LDF in SALX rats receiving 0.1 and 1.0 $\mu g\,kg^{-1}\,min^{-1}$ of SNAP were significantly greater than the mucosal blood flow responses observed in similarly treated sham control rats.

SNAP infusion resulted in a dose-related increase in cyclic GMP levels in the gastric mucosa of sham-operated and SALX rats (Figure 6). The increase in cyclic GMP formation in SALX rats was greater than that observed in control rats with the difference between the groups being significant in rats receiving 0.1 and 1 $\mu g\,kg^{-1}\,min^{-1}$ SNAP (Figure 6).

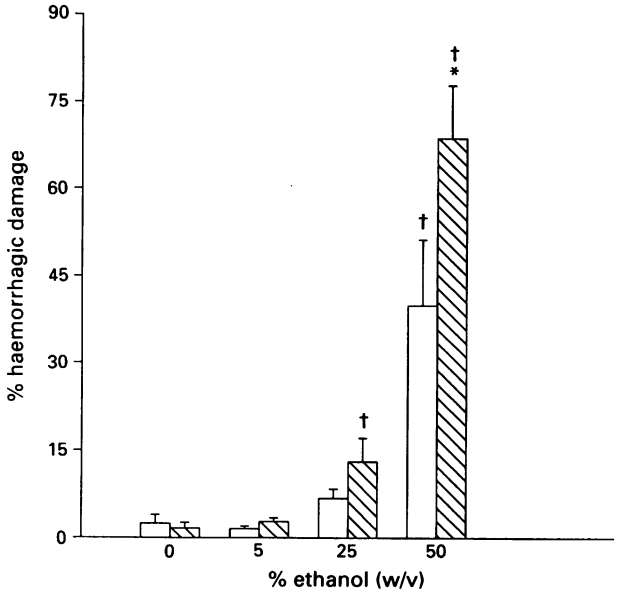

Figure 1 The effect of ethanol (5–50% w/v) on percentage haemorrhagic damage of gastric mucosa of sialoadenectomized (SALX, hatched columns) and sham-operated (Sham, open columns) rats. All values represent means ± s.e.mean of 5–6 animals. Asterisks indicated significant differences between Sham and SALX groups and daggers indicate significant ($P<0.05$) differences from the respective control group in the absence of luminal ethanol as determined by ANOVA and Duncan's multiple range test.

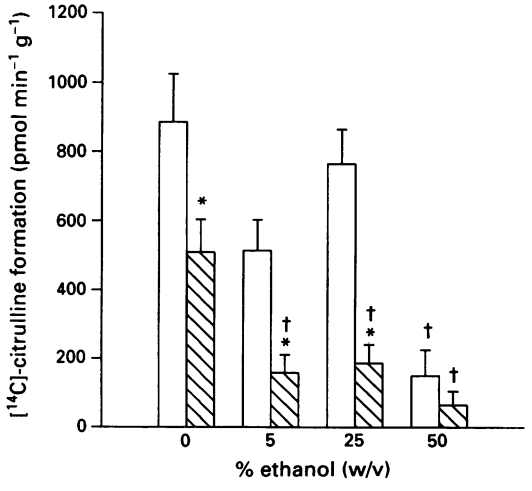

Figure 2 The effect of ethanol (5–50% w/v, i.g.) on gastric mucosal nitric oxide synthase activity as assessed by radiolabelled citrulline formation (pmol $min^{-1}\,g^{-1}$). Experiments were conducted on sialoadenectomized (SALX, hatched columns) and sham-operated (Sham, open columns) rats. All values represent means ± s.e.mean of 5–8 animals. Asterisks indicate significant ($P<0.05$) differences between Sham and SALX groups and daggers represent significant differences from the respective control group in the absence of luminal ethanol as determined by ANOVA and Duncan's multiple range test.

Discussion

The present study demonstrates that sialoadenectomy (SALX) in rats is associated with an increase in the susceptibility of rat gastric mucosa to intraluminal instillation of an ulcerogen. This confirms previous studies in this and other laboratories demonstrating that the degree of mucosal haemorrhagic damage in response to bile salt, cysteamine

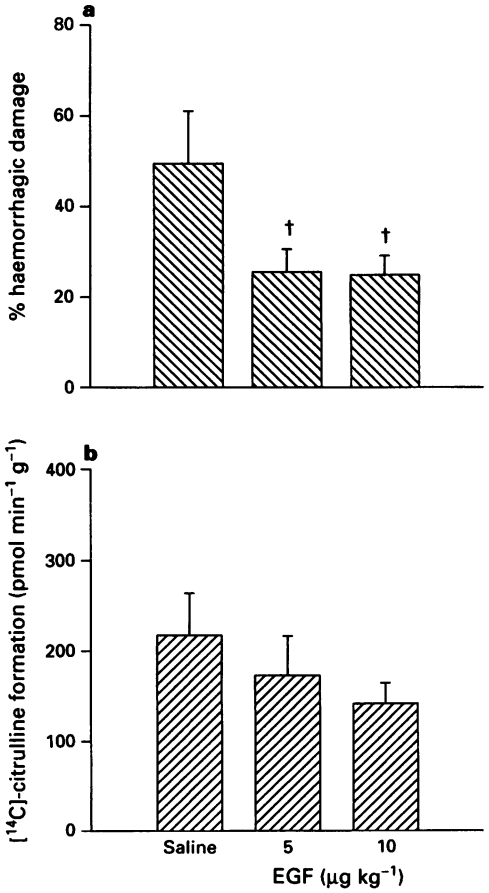

Figure 3 The effect of saline and epidermal growth factor (EGF) (5 and 10 $\mu g\,kg^{-1}$, s.c.) on percentage of haemorrhagic damage (a) and nitric oxide synthase activity (b) of gastric mucosa in response to intraluminal ethanol (50% w/v). Experiments were conducted on sialoadenectomized rats. All values represent means ± s.e.mean of 8–10 animals. Daggers indicate significant ($P<0.05$) changes from control values as determined by ANOVA and Duncan's multiple range test.

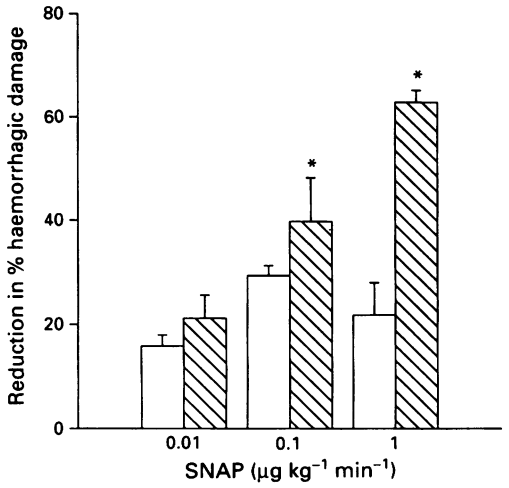

Figure 4 The effect of S-nitroso-N-acetylpenicillamine (SNAP) infusion (0.01–10 μg kg^{-1} min^{-1}, i.v.) reduction in the percentage of haemorrhagic damage of gastric mucosa in response to intraluminal ethanol (50% w/v). Experiments were conducted on sialoadenectomized (SALX, hatched columns) and sham-operated (Sham, open columns) rats. All values are expressed as reduction in % haemorrhagic damage when compared to animals not receiving SNAP and represent means ± s.e.mean of 6–8 animals. Asterisks indicate significant ($P<0.05$) differences between Sham and SALX groups as determined by ANOVA and Duncan's multiple range test.

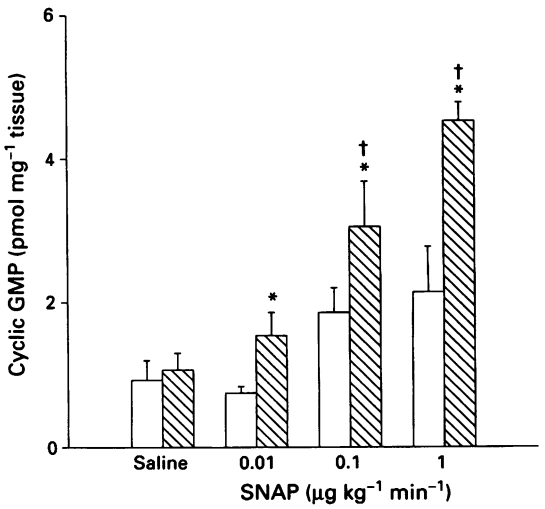

Figure 6 The effect of S-nitroso-N-acetylpenicillamine (SNAP) infusion (0.01–1.0 μg kg^{-1} min^{-1}, i.v.) on gastric mucosal cyclic GMP levels as measured by radioimmunoassay. Experiments were conducted on sialoadenectomized (SALX, hatched columns) and sham-operated (Sham, open columns) rats. All values represent means ± s.e.mean of 4–6 animals. Asterisks indicate significant differences between Sham and SALX rats and daggers represent significant ($P<0.05$) differences from the respective control as determined by ANOVA and Duncan's multiple range test.

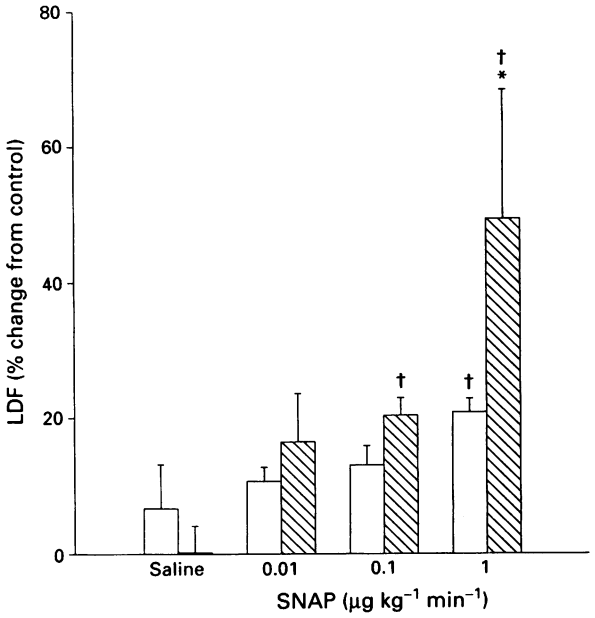

Figure 5 The effect of S-nitroso-N-acetylpenicillamine (SNAP) infusion (0.01–1.0 μg kg^{-1} min^{-1}, i.v.) on gastric mucosal blood flow as assessed by Laser Doppler Flowmetry (LDF). Experiments were conducted on sialoadenectomized (SALX, hatched columns) and sham-operated (Sham, open columns) rats. All values represent means ± s.e.mean of 5–7 animals. Asterisks indicate significant ($P<0.05$) differences between Sham and SALX rats and daggers represent significant differences from the respective control as determined by ANOVA and Duncan's multiple range test.

HCl and ethanol is increased by removal of the salivary glands in experimental animals (Skinner & Tepperman, 1981; Olsen *et al.*, 1984; Konturek *et al.*, 1988). These effects were reversed by administration of extracts of salivary tissue or EGF. EGF has been shown to exert a protective influence on the gastric mucosa (Pilot *et al.*, 1979; Tepperman & Soper, 1990; Itoh *et al.*, 1992) and levels of EGF in saliva have been shown to increase if the mucosa becomes damaged (Gysin *et al.*, 1988). Therefore the absence of EGF may underlie the increase in susceptibility to damage observed previously as well as in the present study.

Using radiolabelled citrulline formation as an index of enzyme activity, NOS activity was found to be reduced in SALX rats when compared to sham-operated controls. This confirms previous findings from this laboratory (Tepperman & Soper, 1993) and suggests that the increase in susceptibility to mucosal damage associated with SALX may be linked to a reduction in NOS activity. A decrease in NO biosynthesis has previously been associated with an increase in the extent of damage (Quintero & Guth, 1992; Ogle & Qiu, 1993; Tepperman *et al.*, 1993) as well as a delay in ulcer healing (Konturek *et al.*, 1993). The mechanism resulting in decreased NOS activity is uncertain. Previous studies from this laboratory have demonstrated that in SALX rats, EGF treatment would reverse the effect of SALX on mucosal NOS activity (Tepperman & Soper, 1993). That study also demonstrated that maximal effects on mucosal integrity were achieved at the doses of EGF used here. However, in the present study EGF treatment did not restore NO synthase activity in rats receiving luminal ethanol. Thus the increase in damage in ethanol-treated SALX rats is not simply due to a reduction in NOS activity. Furthermore it is possible that salivary factors other than EGF influence mucosal NO formation. However, saliva has also been shown to be a source of NO (Bodis & Haregewain, 1993) and the reduction observed here may reflect decreased secretion of saliva in animals with the submandibular glands excised.

In the present study, the NO donor S nitroso-N-acetyl penicillamine (SNAP) reduced mucosal haemorrhagic damage and increased gastric mucosal blood flow. Lopez-Belmonte *et al.* (1993) have similarly observed that low doses of SNAP would reduce haemorrhagic damage in rat stomach in response to endothelin infusion. Furthermore NO donors such as sodium nitroprusside have been shown to increase mucosal blood flow in the gastrointestinal tract (Broughton-Smith *et al.*, 1990; Lopez-Belmonte *et al.*, 1993; Andrews *et al.*, 1994). In the present study both parameters were enhanced in SALX rats suggesting that the responsiveness of

the mucosa to an NO donor is increased by sialoadenectomy. Similarly SNAP infusion resulted in a small increase in cyclic GMP formation in gastric mucosal homogenates. An increase in gastric cyclic GMP in response to NO donors has been previously demonstrated (Brown *et al.*, 1993). In sialoadenectomized rats the increase in cyclic GMP formation was significantly enhanced suggesting an upregulation in gastric mucosal responsiveness to NO. While some have demonstrated tolerance to NO generators (Chung & Fung, 1993) this is the first demonstration of an increase in the responsiveness to NO in the gastric mucosa. The mechanism which mediates the increase in responsiveness is unknown.

In conclusion we have demonstrated that sialoadenectomy which increases the degree of damage in response to a mucosal ulcerogen also reduces mucosal NO formation. Furthermore the NO donor, SNAP reduced the degree of mucosal damage as well as increased mucosal blood flow and cyclic GMP formation. The effect of SNAP was enhanced in SALX rats. Therefore these data suggest that the responsiveness of the gastric mucosa in sialoadenectomized rats to exogenous NO is increased.

This work was supported by a grant from the Medical Research Council of Canada MT6426. M.A.T. was a recipient of a Student Research Fellowship from the American Gastroenterological Association, Foundation, Bethesda, Maryland.

References

ANDREWS, F.J., MALCONTENTI-WILSON, C. & O'BRIEN, P.E. (1994). Protection against gastric ischemia-reperfusion injury by nitric oxide generators. *Dig. Dis. Sci.*, **39**, 366–373.

BODIS, S. & HAREGEWAIN, A. (1993). Evidence for the release and possible neural regulation of nitric oxide in human saliva. *Biochem. Biophys. Res. Commun.*, **194**, 347–350.

BOUGHTON-SMITH, N.K., HUTCHESON, I.R., DEAKIN, A.M., WHITTLE, B.J.R. & MONCADA, S. (1990). Protective effect of S-nitroso-N-acetylpenicillamine in endotoxin-induced acute intestinal damage in the rat. *Eur. J. Pharmacol.*, **191**, 485–488.

BROWN, J.F., KEATES, A.C., HANSON, P.J. & WHITTLE, B.J.R. (1993). Nitric oxide generators and cGMP stimulate mucus secretion by rat gastric mucosal cells. *Am. J. Physiol.*, **265**, (Gastrointest. Liver Physiol., 23), G418–G422.

CHUNG, S.J. & FUNG, H.L. (1993). Relationship between nitroglycerin-induced vascular relaxation and nitric oxide production. *Biochem. Pharmacol.*, **45**, 157–163.

COHEN, S. (1962). Isolation of a mouse submaxillary gland protein accelerating incisor eruption and eyelid opening in the new-born animals. *J. Biol. Chem.*, **237**, 1555–1562.

EPSTEIN, A.N., SPECTOR, D., SAMMAN, A. & GOLDBLUM, C. (1964). Exaggerated prandial drinking in the rat without salivary glands. *Nature*, **201**, 1342–1343.

GYSIN, B., MULLER, R.K.M., OTTEN, U. & FISCHILI, A.E. (1988). Epidermal growth factor content of submandibular glands is increased in rats with experimentally induced gastric lesions. *Scand. J. Gastroenterol.*, **23**, 665–671.

ITOH, M., IMAI, S., JOH, T., KAWAI, T., KATSUMI, K., YOKOCHI, K. & TAKEUCHI, T. (1992). Protection of gastric mucosa against ethanol-induced injury by intragastric bolus administration of epidermal growth factor combined with hydroxypropyl cellulose. *J. Clin. Gastroenterol.*, **14** (Suppl. 1), S127–S130.

KONTUREK, S.J., BRZOZOWSKI, T., MAJKU, J., PYTKO-POLONCZYK, J. & STACHURA, J. (1993). Inhibition of nitric oxide synthase delays heating of chronic gastric ulcers. *Eur. J. Pharmacol.*, **239**, 215–217.

KONTUREK, S.J., DEMBINSKI, A., WARZECHA, Z., BRZOZOWSKI, T. & GREGORY, H. (1988). Role of epidermal growth factor in healing of chronic gastroduodenal ulcers in rats. *Gastroenterology*, **94**, 1300–1307.

LOPEZ-BELMONTE, J., WHITTLE, B.J.R. & MONCADA, S. (1993). The actions of nitric oxide donors in the prevention or induction of injury to the rat gastric mucosa. *Br. J. Pharmacol.*, **108**, 73–78.

MONCADA, S., PALMER, R.M.J. & HIGGS, E.A. (1991). Nitric oxide: physiology, pathophysiology and pharmacology. *Pharmacol. Rev.*, **43**, 109–142.

OGLE, C.W. & QIU, B.S. (1993). Nitric oxide inhibition intensifies cold-restraint induced gastric ulcers in rats. *Experientia*, **49**, 304–307.

OLSEN, P.S., POULSEN, S.S., KIRKEGAARD, P. & NEXO, E. (1984). Role of submandibular saliva and epidermal growth factor in gastric cytoprotection. *Eur. J. Pharmacol.*, **180**, 247–254.

PILOT, M.A., DEREGNANCOURT, J. & CODE, C.F. (1979). Epidermal growth factor increases the resistance of the gastric mucosal barrier to ethanol in rats. *Gastroenterology*, **76**, A1217.

QUINTERO, E. & GUTH, P.H. (1992). Nitric oxide-mediated gastric hyperemia decreases ethanol-induced gastric mucosal injury in uremic rats. *Dig. Dis. Sci.*, **37**, 1324–1328.

SKINNER, K.A., SOPER, B.D. & TEPPERMAN, B.L. (1984). Effect of sialoadenectomy and salivary gland extracts on gastrointestinal mucosal growth and gastrin levels in the rat. *J. Physiol.*, **351**, 1–12.

SKINNER, K.A. & TEPPERMAN, B.L. (1981). Influence of desalivation on acid secretory output and gastic mucosal integrity in the rat. *Gastroenterology*, **81**, 335–339.

TEPPERMAN, B.L., KIERNAN, J.A. & SOPER, B.D. (1989). The effect of sialoadenectomy on gastric mucosal integrity in the rat: roles of epidermal growth factor and prostaglandin E_2. *Can. J. Physiol. Pharmacol.*, **67**, 1512–1519.

TEPPERMAN, B.L. & SOPER, B.D. (1990). Effect of sialoadenectomy on gastric mucosal integrity and growth in the rat: a time course study. *Dig. Dis. Sci.*, **35**, 943–949.

TEPPERMAN, B.L. & SOPER, B.D. (1993). Interaction of nitric oxide and salivary gland epidermal growth factor in the modulation of rat gastric mucosal integrity. *Br. J. Pharmacol.*, **110**, 229–234.

TEPPERMAN, B.L. & SOPER, B.D. (1994). Effect of epidermal growth factor, transforming growth factor α and nerve growth factor on gastric mucosal integrity and microcirculation in the rat. *Regul. Pept.*, **50**, 13–21.

TEPPERMAN, B.L., VOZZOLO, B.L. & SOPER, B.D. (1993). Effect of neutropenia on gastric mucosal integrity and mucosal nitric oxide synthesis in the rat. *Dig. Dis. Sci.*, **38**, 2056–2061.

TEPPERMAN, B.L. & WHITTLE, B.J.R. (1992). Endogenous nitric oxide and sensory neuropeptides interact in the modulation of the rat gastric microcirculation. *Br. J. Pharmacol.*, **105**, 171–175.

WHITTLE, B.J.R. & TEPPERMAN, B.L. (1991). Role of the endogenous vasoactive mediators, nitric oxide, prostanoids and sensory neuropeptides in the regulation of gastric blood flow and mucoscal intergrity. In *Mechanisms of Injury, Protection and Repair of the Upper Gastrointestinal Tract*, ed. Garner, A. & O'Brien, P.E. pp. 127–137. New York: Wiley and Sons.

(Received August 8, 1994
Revised December 6, 1994
Accepted January 31, 1995)

British Journal of Pharmacology (1995) 115, 349-355

Renal vasodilatation by dopexamine and fenoldopam due to α_1-adrenoceptor blockade

S.W. Martin & [1]K.J. Broadley

Department of Pharmacology, Welsh School of Pharmacy, University of Wales Cardiff, Cathays Park, Cardiff CF1 3XF

1 The renal vascular responses of the rat isolated perfused kidney to the dopamine D_1-receptor agonists, dopexamine and fenoldopam, were examined.

2 Both kidneys were perfused *in situ* at constant flow rate (11 ml min^{-1}) with Krebs-bicarbonate solution at 37°C. The perfusion pressure was monitored and to enable vasodilator responses to be measured, the resting perfusion pressure was raised by infusing noradrenaline (6×10^{-9} M).

3 Dose-related vasodilator responses to bolus doses of dopexamine and fenoldopam were obtained. However, these were not antagonized by the D_1-receptor antagonist, SCH 23390, indicating that D_1-receptors were not involved.

4 Bolus doses of the α_1-adrenoceptor antagonist, prazosin, caused similar dose-related vasodilator responses indicating the possibility that α_1-adrenoceptor blocking properties of dopexamine and fenoldopam were responsible for the vasodilatation.

5 α-Adrenoceptor blockade by dopexamine and fenoldopam was confirmed by the parallel displacement of dose-response curves for the vasopressor responses to noradrenaline. pA_2 values were determined by Schild analysis for dopexamine, fenoldopam and prazosin antagonism of noradrenaline in the presence of neuronal (cocaine, 10^{-5} M) and extraneuronal uptake blockade (metanephrine, 10^{-5} M). The values were 6.23, 6.02 and 8.91, respectively. Schild plot slopes of unity were obtained for dopexamine and fenoldopam indicating competitive antagonism. A slope of greater than unity for prazosin may be explained by the lack of equilibrium conditions associated with bolus doses of noradrenaline, the responses of which are affected more by the high affinity antagonist, prazosin, than the two lower affinity antagonists.

6 This study has demonstrated that renal vasodilator responses to the D_1-receptor agonists, dopexamine and fenoldopam, are due to a brief antagonism of the α-adrenoceptor-mediated vasoconstriction induced by noradrenaline. This presumably masks any direct D_1-receptor-mediated vasodilatation.

Keywords: Rat perfused kidneys; vasodilatation; noradrenaline-induced vasoconstrictor tone; dopexamine; fenoldopam; α-adrenoceptor blockade

Introduction

The antihypertensive drug fenoldopam was introduced as a potent, selective renal vasodilator, acting predominantly through stimulation of renal vascular D_1-receptors. Unlike dopamine, it lacks α-adrenoceptor agonist activity (Hahn *et al.*, 1982). Similarly, dopexamine, used in the acute management of low cardiac output conditions, also produces renal vasodilatation by selective stimulation of renal vascular D_1-receptors and lacks α_1-adrenoceptor agonist activity. In addition, the β_2-adrenoceptor agonist activity of this drug promotes reduction of afterload due to vasodilatation and mild positive inotropy (Smith & O'Connor 1988). In the present study, the effects of both drugs were examined in the rat isolated perfused kidney. This preparation has been used as a model for D_1-dopamine receptor-mediated vasodilatation. There are several reports of dopamine and selective D_1-receptor agonists, including fenoldopam, producing falls in perfusion pressure when the basal pressure is raised by vasoconstrictors including prostaglandin $F_{2\alpha}$ (Imbs *et al.*, 1984; Schmidt *et al.*, 1987). However, this paper describes an unexpected observation that although both drugs cause vasodilatation of the rat renal vasculature, constricted with noradrenaline, it is not due to D_1-receptor agonist activity but to α_1-adrenoceptor blockade. This property of the two drugs is then quantified by determination of pA_2 values and compared to prazosin.

[1] Author for correspondence.

Methods

Tissue preparation

Male Wistar rats (300-350 g) were anaesthetized with pentobarbitone sodium (60 mg kg^{-1}, i.p.). The abdomen was opened and a polythene cannula was advanced retrogradely along the abdominal aorta until the tip lay opposite the left renal artery. The mesenteric artery was tied with a cotton ligature and the aorta was ligated immediately below the coeliac artery. Both kidneys were then perfused, at a flow rate of approximately 11 ml min^{-1}, with carboxygenated Krebs-bicarbonate solution at 37°C by means of a Watson-Marlow peristaltic pump (type 502S). The Krebs-bicarbonate solution had the following composition (mM): NaCl 118.4, $NaHCO_3$ 24.9, KCl 4.7, $CaCl_2$ 1.9 (used as the dihydrate), $MgSO_4$ 1.15 (as the heptahydrate), KH_2PO_4 1.15 and glucose 11.7. Ascorbic acid (1 mM) was added to reduce the oxidation of noradrenaline. Although earlier studies have employed a more complex medium for examining renal function in isolated perfused kidneys, this was not essential for the present vascular studies. No deleterious effects were observed upon the responses to noradrenaline over the time period of each experiment.

The vena cava was cut between the left and right renal veins to allow escape of perfusate. Alterations in perfusion pressure, arising from changes in renal vascular resistance, were recorded on a Lectromed polygraph (MT8 P, Welwyn Garden City, Hertfordshire) by means of a pressure transducer (Bell and Howell, type 4-327-L221) situated between the perfusion cannula and the warming coil. A Condon

manometer was also connected in series with the pressure transducer to accommodate some degree of volume change during drug responses.

Construction of dose-response curves

In order to observe substantial vasodilator responses, the renal vasculature was constricted by addition of 6×10^{-9} M noradrenaline to the perfusion medium. When the elevated perfusion pressure (213.2 ± 5.3 mmHg, $n = 6$) had stabilized (about 15 min), non-cumulative dose-response curves to vasodilator drugs were obtained by injection of increasing bolus doses into the perfusion cannula. Vasodilatation was measured as the peak reduction in perfusion pressure at each dose of drug, measured from the stable elevation of pressure induced by noradrenaline. The ED_{50} value was calculated as the dose producing 50% of maximum vasodilatation and the geometric mean with 95% confidence limits was determined.

Calculation of pA_2 values

pA_2 values for the antagonism of vasoconstrictor responses to noradrenaline by dopexamine, fenoldopam and prazosin were calculated (Arunlakshana & Schild, 1959). Following an initial non-cumulative dose-response curve to increasing bolus doses of noradrenaline in the absence of antagonist, a 30 min period of antagonist infusion was allowed before a second dose-response curve was constructed in its presence. Responses were measured as the increase in perfusion pressure. To compensate for time-dependent changes in tissue sensitivity to noradrenaline between the first and second dose-response curves, correction factors derived from time-matched control experiments in the absence of antagonist were applied to the first curve. At each dose of noradrenaline, the response ratio (Curve 2/Curve 1) was calculated for the control experiments. Mean correction ratios ($n \geq 4$) were then multiplied by the corresponding response values of the initial curve of the 'test' experiments. Dose-response curves were then plotted as a percentage of the maximum response and the ED_{50} determined as the dose producing 50% of the maximum response. Dose-ratios were calculated by division of individual ED_{50} values obtained in the presence of antagonist (Curve 2) by the corresponding values in the absence of antagonist (Curve 1). Geometric mean ED_{50} values and their 95% confidence limits were calculated. Values for pA_2 were obtained by plotting log (dose ratio -1) on the ordinate scale against log antagonist concentration on the abscissa scale; the intercept of the regression line on the abscissa scale giving the pA_2 value.

Statistics

Student's t tests were used to test for significant differences between geometric mean ED_{50} values, arithmetic mean maximum responses and pA_2 values and to test the slopes of Schild plots for significant differences from unity. Differences were considered significant with $P < 0.05$. For comparison of more than two means, Tukey's multirange test (95% probability) was used.

Drugs and solutions

Drugs were obtained from the following sources:- cocaine hydrochloride (Hillcross Pharmaceuticals, Burnley, Lancashire, U.K.), dopexamine hydrochloride (Fisons Pharmaceuticals, Loughborough, Leicestershire, U.K.), fenoldopam mesylate (SKB, Philadelphia P.A., U.S.A.), (±)-metanephrine hydrochloride (Sigma, Poole, Dorset, U.K.), (−)-noradrenaline bitartrate (Sigma), pentobarbitone sodium (Sagatal) (Rhone Merieux, Tallaght, Dublin, Ireland), prazosin hydrochloride (Pfizer, Sandwich, Kent, U.K.), (±-propranolol hydrochloride (Inderal) (ICI Pharmaceuticals, Macclesfield, Cheshire, U.K.) and SCH 23390 [(**R**)-(+)-8-chloro-2,3,4,5-tetrahydro-3-methyl-5-phenyl-1*H*-3-benzazepine] as the maleate (Schering Corporation, Bloomfield, NJ, U.S.A.). Stock solutions were prepared as follows:- dopexamine and fenoldopam were made up in 0.9% saline containing 0.05% w/v sodium metabisulphite. Prazosin, cocaine and metanephrine were dissolved in twice distilled water, the latter containing 0.1% w/v sodium metabisulphite. Noradrenaline was dissolved in 0.01 M HCl. SCH 23390 was initially dissolved in a small quantity of 2 M HCl and was then made up to the required concentration by addition of twice distilled water. Stock solutions of dopexamine were stored frozen in small aliquots for a maximum of 5 days. Stock solutions of SCH 23390 were stored in the same way for several weeks. Solutions of prazosin and noradrenaline were prepared immediately prior to the experiment. Working drug concentrations were obtained by serial dilution of stock solutions in Krebs-bicarbonate solution.

Results

Vasodilator responses to dopexamine and fenoldopam

Responses to dopexamine were examined in the presence of β-adrenoceptor blockade by propranolol (10^{-6} M). Both fenoldopam and dopexamine caused dose-related falls in perfusion pressure (Figure 1). The maximum response to dopexamine was consistently greater than that of fenoldopam

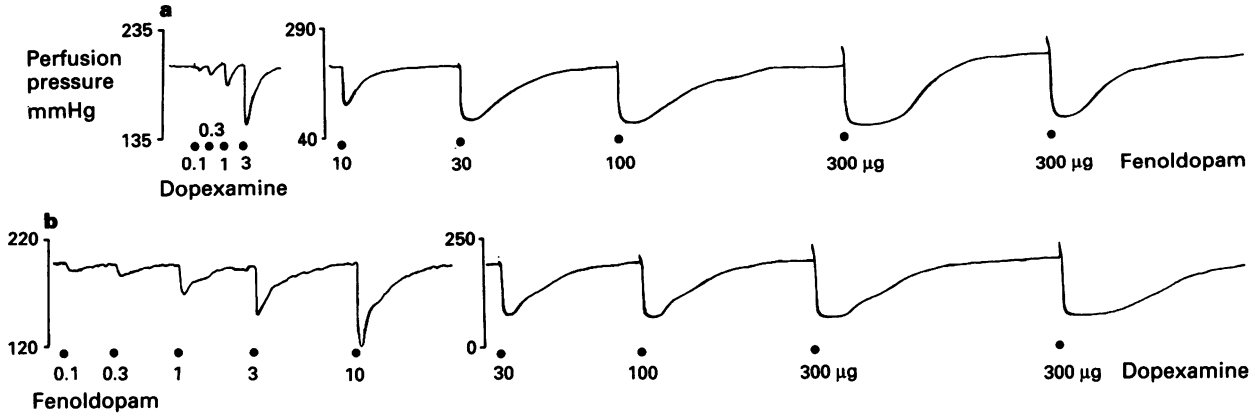

Figure 1 Typical vasodilator responses to dopexamine (a) and fenoldopam (b) in rat isolated perfused kidneys. Traces show the effect of a 300 µg dose of dopexamine following a dose-response curve to dopexamine (a) and *vice versa* (b). Time scale; 10 min between 10 and 30 µg doses of fenoldopam.

(Figure 2). This was shown by administration of a maximum dose of one agonist following completion of the dose-response curve to the other, as illustrated in Figure 1.

Effect of SCH 23390 on responses to dopexamine and fenoldopam

The dose-response curves for vasodilatation in the noradrenaline-constricted kidney preparation in response to bolus doses of dopexamine and fenoldopam were not significantly dextrally displaced in the presence of the competitive D_1-receptor antagonist, SCH 23390 (10^{-6} M) (Figure 3). The basal noradrenaline-induced perfused pressure prior to administration of the dopamine agonist was not affected by the presence of SCH 23390. The mean values prior to dopexamine of 205.5 ± 5.1 and 216.3 ± 4.7 mmHg ($n = 4$) in the absence and presence of SCH 23390, respectively, were not significantly different ($P > 0.05$).

Effect of prazosin

As with dopexamine and fenoldopam, bolus doses of the α_1-adrenoceptor-selective competitive antagonist, prazosin (Cambridge *et al.*, 1977), caused dose-related falls in perfusion pressure (Figure 2). Although the ED_{50} for prazosin (44.8(15.2–132.0)ng) was significantly lower than for dopexamine (3.8(2.6–5.3)μg) and fenoldopam (5.9(4.6–9.7)μg), the maximum decreases in perfusion pressure caused by fenoldopam (122.5 ± 6.3 mmHg) and dopexamine (127.1 ± 5.3 mmHg) were significantly greater than the maximum for prazosin (94.0 ± 2.6 mmHg).

Effects of dopexamine, fenoldopam and prazosin on noradrenaline-induced vasoconstriction

Concentration-response curves for noradrenaline were progressively displaced to the right by dopexamine (Figure 4), fenoldopam (Figure 5) and prazosin. pA_2 values for this antagonism by dopexamine and fenoldopam were determined either in the presence or absence of neuronal and extraneuronal uptake block by cocaine (10^{-5} M) and metanephrine (10^{-5} M), respectively. The pA_2 for prazosin was obtained in the presence of neuronal and extraneuronal uptake block but not in their absence.

In the presence of uptake block, the Schild plots for the antagonism of the vasoconstrictor responses of noradrenaline by dopexamine and fenoldopam (Figure 6a and b) had slopes which were not significantly different from unity (Table 1). The pA_2 value obtained for dopexamine was (6.23 ± 0.11) and a similar value was determined for fenoldopam (6.02 ± 0.21). The antagonism of noradrenaline responses by prazosin yielded a pA_2 of 8.91 ± 0.58, although the slope of the Schild regression (1.28 ± 0.16) was significantly greater than unity ($P < 0.001$) (Figure 6c).

In the absence of uptake block, the slope of the Schild plot for fenoldopam (0.35 ± 0.12, Figure 6e) was significantly less than unity ($P < 0.01$). The pA_2 value (8.36 ± 0.21) was consequently higher than the corresponding value in the presence of uptake blockade. In contrast, the slope of the Schild plot for dopexamine (Figure 6d) remained close to unity (1.08 ± 0.20), resulting in a pA_2 value which was close to that obtained in the presence of uptake block (Table 1).

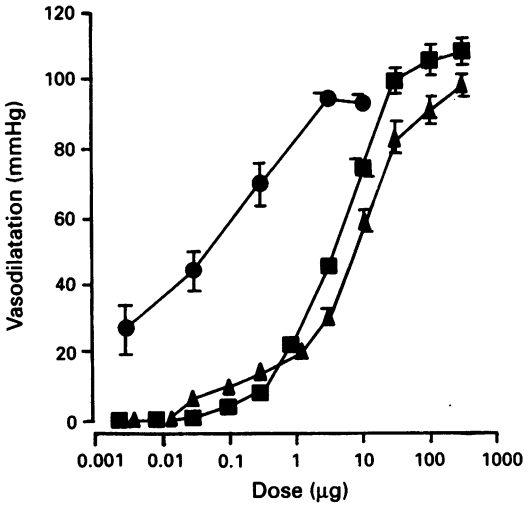

Figure 2 Comparison of the dose-response curves for vasodilatation of the noradrenaline-constricted isolated perfused kidney of the rat by prazosin (●), dopexamine (■) and fenoldopam (▲). Points are mean falls in perfusion pressure (mmHg) (± s.e.mean, $n \geq 4$).

Discussion

In view of the established D_1-receptor agonist activities of fenoldopam (Hahn *et al.*, 1982) and dopexamine (Brown *et al.*, 1985), it was assumed that their vasodilator responses in the noradrenaline-constricted isolated perfused kidney were

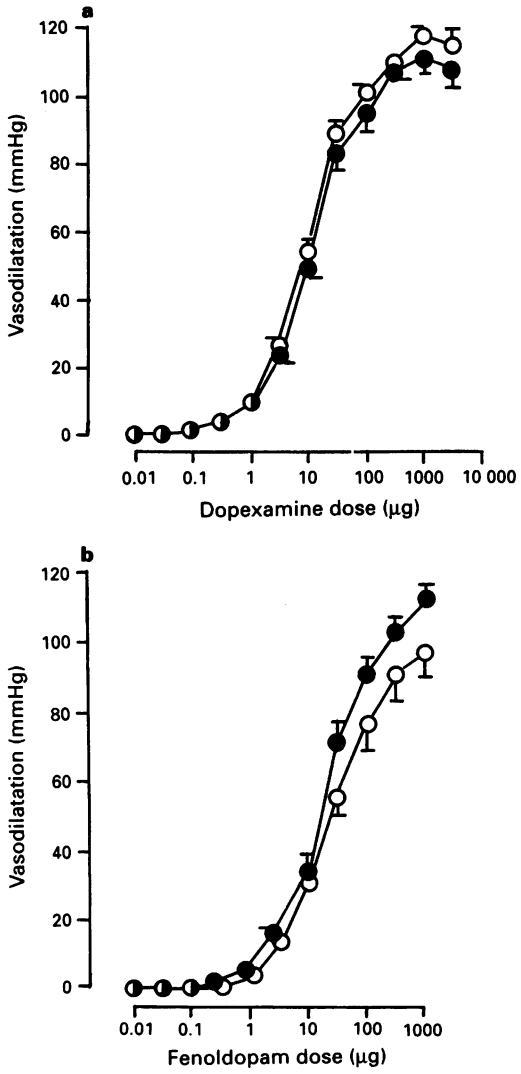

Figure 3 Effect of SCH 23390 (10^{-6} M) on the vasodilator responses of (a) dopexamine and (b) fenoldopam in the rat isolated perfused kidney constricted with noradrenaline. Curves were obtained in the absence (○) or presence (●) of SCH 23390. Curves for dopexamine were constructed in the presence of propranolol (10^{-6} M). Points are mean falls in perfusion pressure (mmHg) (± s.e.mean, $n = 4$).

the result of dopamine D_1- receptor stimulation. Furthermore, this isolated organ is known to exhibit vasodilator responses to dopamine (Imbs *et al.*, 1984; Schmidt *et al.*, 1987). However, the inability of the potent, selective D_1-receptor antagonist, SCH 23390 (Hilditch *et al.*, 1984) to antagonize the vasodilator responses to either fenoldopam or dopexamine at a concentration of 10^{-6} M, suggested that D_1-receptors were not involved. This concentration is known to be sufficient to antagonize D_1-receptor-mediated responses in this tissue (Schmidt *et al.*, 1987) and the splenic artery (Hilditch & Drew, 1985) where pA_2 values of about 10 were obtained. The possibility was considered that the responses were a result of antagonism of the α_1-adrenoceptor-mediated noradrenaline pre-constriction rather than D_1-receptor-mediated relaxation. The similarity of the fenoldopam and dopexamine responses to those produced by the competitive α_1-adrenoceptor antagonist, prazosin (Cambridge *et al.*, 1977) in the same preparation, supported this suggestion. This, together with reports in the literature demonstrating antagonism by fenoldopam of the α_1-adrenoceptor-mediated responses of noradrenaline in the rat (Ohlstein *et al.*, 1985), dog and rabbit (Nakamura *et al.*, 1986) isolated blood vessels, prompted efforts to confirm and quantify the α_1-adrenoceptor antagonist properties of fenoldopam and dopexamine in the noradrenaline-constricted rat isolated perfused kidney.

Both fenoldopam and dopexamine caused concentration-related displacement of the noradrenaline dose-response curves, indicating α_1-adrenoceptor blockade. Since dopexamine has been shown to have uptake blocking activity (Mitchell *et al.*, 1987) which may have influenced the measurement of antagonism, pA_2 values for dopexamine and fenoldopam were determined both in the presence and absence of uptake blockade.

Effect of uptake block on the antagonism of noradrenaline responses by fenoldopam

Since the slope of the Schild plot for fenoldopam was not significantly different from unity in the presence of uptake block, but was significantly less than unity in the absence of uptake block, it seems likely that the low slope obtained under the latter conditions was due to the operation of an agonist uptake mechanism rather than to a lack of competitive antagonism (Blinks, 1967; Furchgott, 1967; Langer & Trendelenburg, 1969). The low slope can be explained in terms of a model proposed by Langer and Trendelenberg (1969) which ascribed three regions to the uptake process. In

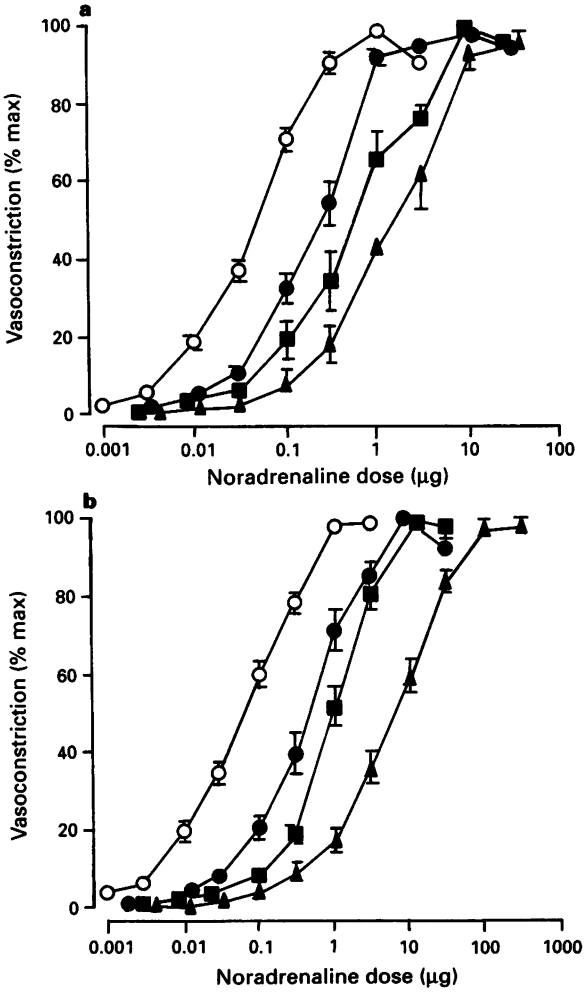

Figure 4 Effect of increasing concentrations of dopexamine on the dose-response curve for vasoconstriction of the rat isolated perfused kidney by noradrenaline in the absence (a) and presence (b) of uptake blockade by cocaine and metanephrine. Curves were obtained in the absence (○) and repeated once in the presence of dopexamine, 3×10^{-6} M (●); 10^{-5} M (■); 3×10^{-5} M (▲). Points are the mean responses expressed as a percentage of the maximum response (± s.e.mean, $n \geq 4$). Pre-antagonist curves are corrected from control experiments.

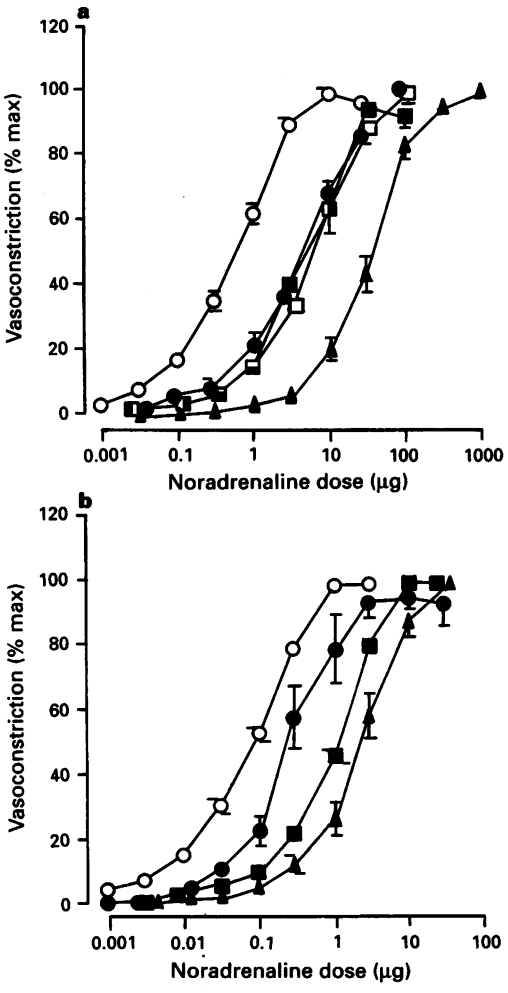

Figure 5 Effects of increasing concentrations of fenoldopam on the dose-response curves for vasoconstriction of the rat isolated perfused kidney by noradrenaline in the absence (a) and presence (b) of uptake blockade by cocaine and metanephrine. Curves were obtained in the absence (○) and repeated once in the presence of fenoldopam, 10^{-6} (□); 3×10^{-6} M (●); 10^{-5} M (■); 3×10^{-5} M (▲). Points are the mean responses expressed as a percentage of the maximum response (± s.e.mean, $n \geq 4$). Pre-antagonist curves are corrected from control experiments.

Region I, a fixed proportion of the agonist is removed from the vicinity of the receptor. As the agonist concentration is increased (for example, to overcome the effect of a competitive antagonist), an increasing proportion of the agonist reaches the receptor due to progressive saturation of the uptake mechanism (Region II) until saturation of uptake is virtually complete and the concentration of agonist at the receptor approaches that in the surrounding medium (Region III). As dose-response curves to the agonist are shifted progressively to the right by increases in antagonist concentration, they pass from Region I, through Region II, in which the increasing proportion of the agonist reaching the receptor has a potentiating effect causing steepening, and sinistral (leftwards) displacement of the EC_{50}. Thus, the dose-ratios are reduced and the slope of the Schild plot is reduced.

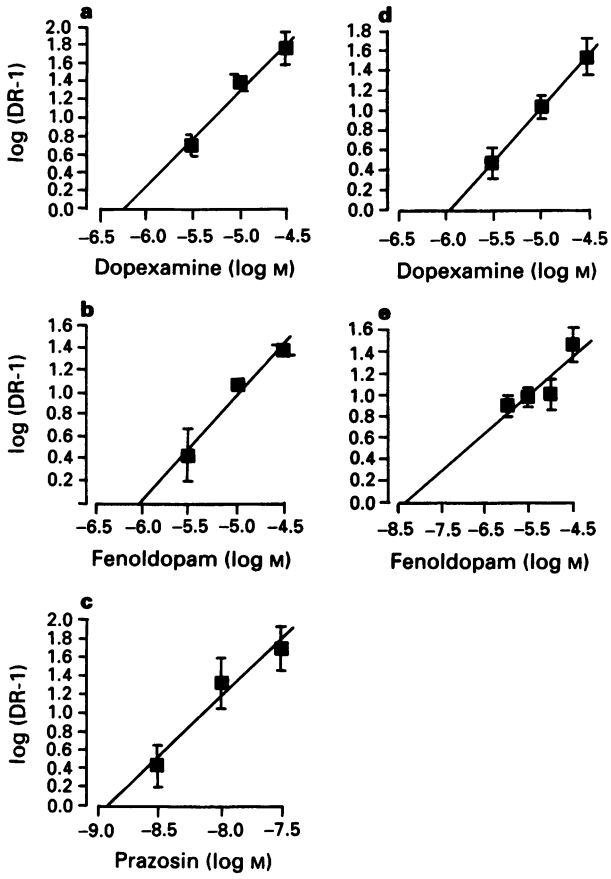

Figure 6 Schild plots for the antagonism of the vasoconstrictor effects of noradrenaline in the rat isolated perfused kidney by dopexamine, fenoldopam and prazosin. Experiments were performed either in the presence of uptake blockade by cocaine (10^{-5} M) and metanephrine (10^{-5} M) (dopexamine a, fenoldopam b, prazosin c) or in the absence of uptake blockade (dopexamine d, fenoldopam e). Points are mean values ± s.e.mean ($n \geq 4$).

Figure 6e shows that in the absence of uptake block, no increase in dose-ratio was observed as the concentration of fenoldopam was increased from 10^{-6} M to 10^{-5} M. Only when the concentration of fenoldopam was raised to 3×10^{-5} M did the dose-ratio appreciate. According to the Langer & Trendelenberg (1969) model, 3×10^{-6} M and 10^{-5} M fenoldopam may have shifted the noradrenaline dose-response curves into Region II, where an increasing proportion of the agonist reaches the receptor due to progressive saturation of neuronal uptake. The resulting potentiation of the noradrenaline responses was sufficient to nullify the effect of increasing the fenoldopam concentration such that the dose-response curves were shifted no further rightwards than in the presence of 10^{-6} M fenoldopam (Figure 5a). This argument assumes that although higher added concentrations of noradrenaline were not in fact used in the presence of 3×10^{-6} and 10^{-5} M fenoldopam, there may be a higher concentration at the receptor. When the antagonist concentration was increased to 3×10^{-5} M, the noradrenaline dose-response curves were shifted into Region III in which saturation of uptake is virtually complete, and with no further opposition to the action of fenoldopam possible, the noradrenaline dose-response curve was driven further rightwards with a consequent increase in ED_{50} and dose-ratio. Due to the magnitude of this final dose-ratio, the slope of the Schild plot was not drastically reduced by the failure of 3×10^{-6} M and 10^{-5} M fenoldopam to increase the dose-ratio appreciably from its value of 10^{-6} M. Rather, the major cause of the reduced slope was the large magnitude of the dose-ratios associated with the 10^{-6}–10^{-5} M concentrations of the antagonist. This, in turn, was the result of an effect associated with the correction (for time-dependent changes in sensitivity) of the pre-antagonist dose-response curve.

Figure 7 shows noradrenaline dose-response curves from time-matched control experiments. The curves were constructed before and after a 'sham' incubation period equivalent to the contact time with fenoldopam. Contrary to expectations, in the absence of uptake block (Figure 7a), Curve 2 was sinistrally displaced; if anything, a dextral displacement was anticipated due to the attenuation of tissue sensitivity with repeated exposure to noradrenaline. In the presence of uptake block, the two curves were virtually superimposed (Figure 7b), suggesting that the operation of the uptake mechanism was, paradoxically, responsible for potentiation of the responses to noradrenaline on repeated exposure.

One possible explanation for this is that supramaximal doses of noradrenaline required to confirm the maximum response may have persisted in the uptake mechanism during washout and resulted in potentiation of responses in the second curve. This is supported by the fact that the ED_{50} for the second curve constructed in the absence of uptake block (63 (37–109)ng) was not significantly different from the ED_{50} for the corresponding curve obtained in the presence of uptake block (56 (40–77)ng). The pre-antagonist curve was therefore displaced to the left by the correction procedure (Figure 8a) and this exaggerated the dose-ratios to a proportionally greater extent at lower concentrations of fenoldopam. This effect caused the marked reduction of the slope of the Schild plot in the absence of uptake block compared

Table 1 Values for pA_2 and Schild plot slope (± s.e.mean) for the antagonism of noradrenaline-induced vasoconstriction of the rat perfused kidney by fenoldopam, dopexamine and prazosin

	No uptake block		*Uptake blocked*		
	Dopexamine	*Fenoldopam*	*Dopexamine*	*Fenoldopam*	*Prazosin*
Slope	1.08 ±0.20	0.35† ±0.12	1.05 ±0.18	0.94 ±0.06	1.28* ±0.16
pA_2	5.95 ±0.21	8.36 ±0.21	6.23^{NS} ±0.11	6.02†† ±0.21	8.91 ±0.58

Uptake mechanisms were blocked with cocaine (10^{-5} M) and metanephrine (10^{-5} M) *Significantly greater than 1.0; †Significantly less than 1.0 by Student's t test ($P<0.05$), ††significantly different ($P<0.05$) or ^{NS}not significantly different from value with no uptake block.

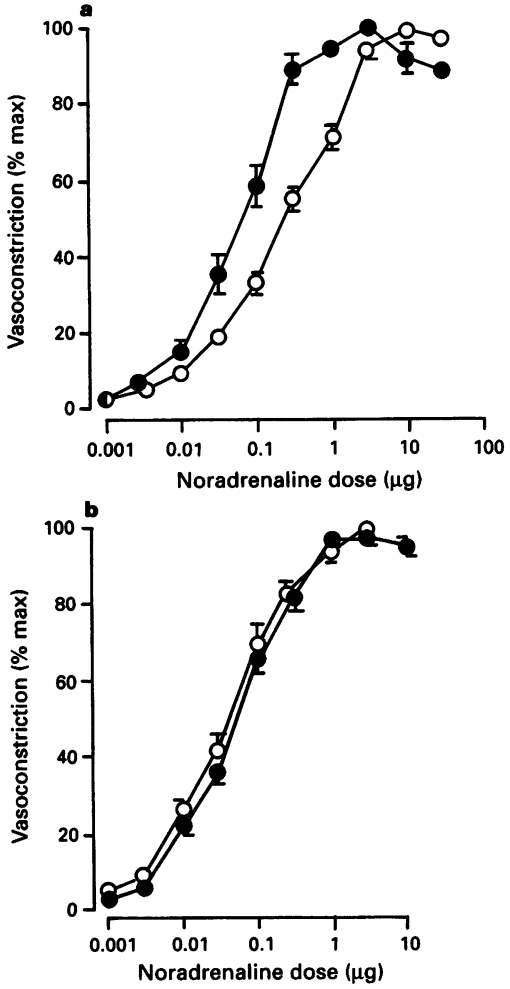

Figure 7 Dose-response curves for vasoconstrictor responses to noradrenaline from time-matched control experiments conducted in the absence of antagonist and obtained in the absence (a) or presence (b) of uptake block. The initial dose-response curve (○) was followed after a sham-incubation without antagonist by a second curve (●). Points are the mean responses expressed as a percentage of the maximum response (± s.e.mean, $n \geqslant 4$).

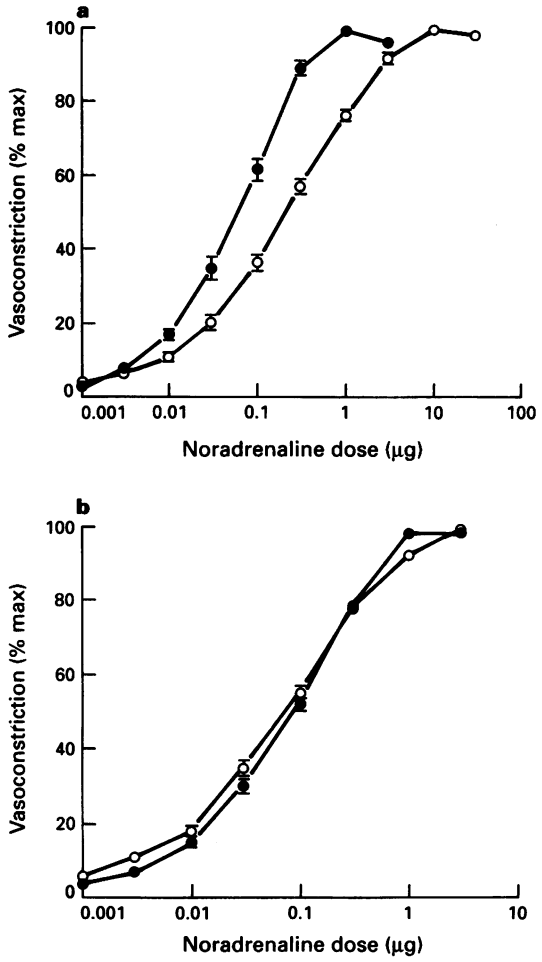

Figure 8 Effects of correction for time-dependent changes in tissue sensitivity upon the pre-antagonist (fenoldopam) noradrenaline dose-response curves. The pre-antagonist curves ($n \geqslant 12$) obtained in the absence (a) or presence (b) of uptake blockade with cocaine (10^{-5} M) and metanephrine (10^{-5} M) are shown. The uncorrected (○) curves and those after correction from control experiments (●) are shown. Points are the mean vasoconstrictor responses expressed as a percentage of maximum response (± s.e.mean).

with that obtained in the presence of uptake block. This indicates the importance of inhibiting the uptake mechanism when using noradrenaline as the agonist.

Effect of uptake block on antagonism of noradrenaline responses by dopexamine

Unlike fenoldopam, dopexamine progressively shifted the noradrenaline dose-response curves rightwards in a concentration-dependent manner in the absence as well as in the presence of uptake block (Figure 4a). This was reflected in the slopes of the Schild plots which were not significantly different from unity in either case. The most obvious reason for dopexamine producing a unity Schild plot slope in the absence of uptake block is that it is a more potent inhibitor of neuronal uptake than cocaine (Mitchell *et al.*, 1987; Nedergaard, 1988; 1989). Inhibition of uptake by dopexamine would potentiate dose-response curves to noradrenaline and thus lessen the degree of antagonism. According to the Langer & Trendelenburg model (1969), there would be no potentiation of the dose-response curve generated in the absence of the antagonist, and dose-ratios would consequently be reduced to a greater extent at low concentrations of dopexamine than at high concentrations. This would result in a steepening of the Schild plot to maintain unity slope in the absence of cocaine.

Effect of prazosin on the responses to noradrenaline

In the presence of uptake blockade, the antagonism of the vasoconstrictor responses of noradrenaline by prazosin resulted in a Schild plot having a slope which was significantly greater than unity. Schild plot slopes exceeding unity can result from lack of equilibrium conditions for the antagonist at the time the response is measured, or from loss of free drug from the external solution (Furchgott, 1972). In addition, a saturable removal mechanism for the antagonist can also give rise to high slopes (Kenakin, 1987). The latter cause can be discounted since prazosin is not a substrate for neuronal or extraneuronal uptake which were, in any case, blocked with cocaine and metanephrine respectively. It is possible that the time allowed for equilibration of prazosin with the receptor (30 min) was not sufficient. Since the rate of onset of antagonist action is concentration-dependent, the effect of low concentrations of prazosin with this length of equilibration may be underestimated, resulting in a steepening of the slope of the Schild plot (Kenakin, 1987). Indeed, in the present case, a disproportionately low dose-ratio value at the lowest concentration of prazosin was the main cause of the high slope obtained. Another possible explanation for the high slope of the Schild plot for prazosin is that bolus injections of noradrenaline, being short-lived in the system, do not allow sufficient time for the drug to reach equilibrium.

As in the present study, Blue & Clarke (1992) found that antagonism by prazosin of the vasoconstrictor responses produced by bolus doses of noradrenaline in the rat perfused kidney apparently deviated from competitive inhibition; the slope of the Schild plot obtained was significantly greater than unity (1.33). On the other hand, when noradrenaline was administered by infusion, the Schild plot for antagonism of the responses by prazosin was not significantly different from unity, indicating competitive kinetics. These authors proposed that lack of equilibrium conditions for the agonist, due to the inherent transience of bolus doses in a perfused system, can lead to a progressive overestimation of the dose-ratio of the antagonist and thus to the slope of the Schild plot exceeding unity when high affinity antagonists such as prazosin are employed. In the present study, the slope of the Schild plot for the antagonism of noradrenaline by prazosin was greater than unity whereas both fenoldopam and dopexamine (in the presence of uptake block) produced slopes which were not significantly different from unity. The hypothesis of Blue & Clarke (1992) can account for this difference in that fenoldopam and dopexamine are weaker antagonists ($pA_2 = 6.2$ and 6.0 respectively, see above) than prazosin, and as such their relatively rapid onset/offset rates would allow both noradrenaline and antagonist (dopexamine or fenoldopam) to attain equilibrium with the α_1-adrenoceptor in spite of the rapid removal of injected noradrenaline from the perfused kidney.

The finding that the two D_1-receptor agonists, dopexamine and fenoldopam, also possess antagonist activity at α_1-adrenoceptors confirmed previous observations for fenoldopam by Ohlstein *et al.* (1985). This property would probably contribute to the antihypertensive activity of fenoldopam (Ventura *et al.*, 1984). α_1-Adrenoceptor blockade by dopexamine would also complement its agonist activity at D_1-dopamine receptors and β_2-adrenoceptors by reducing sympathetic vasoconstrictor tone to the renal vasculature and improving renal blood flow. The reduced vascular tone would also exert favourable effects on cardiac pre- and afterload to improve cardiac performance in low output states. The fact that the vasodilator activities observed in the present study could be attributed to α_1-adrenoceptor blockade was dependent upon the use of noradrenaline to maintain vascular tone. It does not imply that these compounds cannot exert vasodilatation via D_1-receptors when an alternative vasoconstrictor is employed (Schmidt *et al.*, 1987).

This work was supported by Fisons Pharmaceuticals, Loughborough, Leicestershire. We are grateful to Dr J.B. Farmer for helpful discussions and to the companies concerned for gifts of dopexamine, fenoldopam, prazosin and SCH 23390.

References

ARUNLAKSHANA, O. & SCHILD, H.A. (1959). Some quantitative uses of drug antagonists. *Br. J. Pharmacol. Chemother.*, **14**, 48–58.

BLINKS, J.R. (1967). Evaluation of the cardiac effects of several β-adrenergic blocking agents. *Ann. N.Y. Acad. Sci.*, **139**, 673–685.

BLUE, D.R. Jr. & CLARKE, D.E. (1990). Slow off-rate of prazosin accounts for deviations from competitive antagonism in the isolated perfused kidney of rat. *Gen. Pharmacol.*, **23**, 815–821.

BROWN, R.A., DIXON, J., FARMER, J.B., HALL, J.C., HUMPHRIES, R.G., INCE, F., O'CONNOR, S.E., SIMPSON, W.T. & SMITH, G.W. (1985). Dopexamine: a novel agonist at peripheral dopamine and β_2-adrenoceptors. *Br. J. Pharmacol.*, **85**, 599–608.

CAMBRIDGE, D., DAVEY, M.J. & MASSINGHAM, R. (1977). Prazosin, a selective antagonist of post-synaptic alpha-adrenoceptors. *Br. J. Pharmacol.*, **59**, 514–515P.

FURCHGOTT, R.F. (1967). The pharmacological differentiation of adrenergic receptors. *Ann. N.Y. Acad. Sci.*, **139**, 553–570.

FURCHGOTT, R.F. (1972). The classification of adrenoceptors (adrenergic receptors). An evaluation from the standpoint of receptor theory. In *Handbook of Experimental Pharmacology*, Vol. 33, pp. 283–335. Blaschko, H. & Muscholl, E. Berlin: Springer-Verlag.

HAHN, R.A., WARDELL, J.R. Jr., SARAN, H.M. & RIDLEY, P.T. (1982). Characterization of the peripheral and central effects of SKF82526, a novel dopamine receptor agonist. *J. Pharmacol. Exp. Ther.*, **223**, 305–313.

HILDITCH, A. & DREW, G.M. (1985). Characteristics of the dopamine receptors in the rabbit isolated splenic artery. *Eur. J. Pharmacol.*, **72**, 187–196.

HILDITCH, A., DREW, G.M. & NAYLOR, R.J. (1984). SCH23390 is a very potent and selective antagonist at vascular dopamine receptors. *Eur. J. Pharmacol.*, **97**, 333–334.

IMBS, J.L., SCHMIDT, M., EHRHARDT, J.D. & SCHWARTZ, J. (1984). The sympathetic nervous system and renal sodium handling: is dopamine involved? *J. Cardiovasc. Pharmacol.*, **6**, S171–S175.

KENAKIN, T.P. (1987). Drug antagonism. In *Pharmacologic Analysis of Drug-Receptor Interaction*. pp. 205–244. New York: Raven Press.

LANGER, S.Z. & TRENDELENBURG, U. (1969). The effect of a saturable uptake mechanism on the slopes of dose-response curves for sympathomimetic amines and on the shifts of dose-response curves produced by a competitive antagonist. *J. Pharmacol. Exp. Ther.*, **167**, 117–142.

MITCHELL, P.D., SMITH, G.W., WELLS, E. & WEST, P.A. (1987). Inhibition of Uptake$_1$ by dopexamine hydrochloride *in vitro*. *Br. J. Pharmacol.*, **92**, 265–270.

NAKAMURA, S., KOHLI, J.D. & RAJFER, S.I. (1986). α-Adrenoceptor blocking activity of fenoldopam (SK & F 82526), a selective DA_1 agonist. *J. Pharm. Pharmacol.*, **38**, 113–117.

NEDERGAARD, O.A. (1988). Dopexamine hydrochloride is an inhibitor of the Uptake-1 mechanism in rabbit aorta. *Br. J. Pharmacol.*, **96**, 192P.

NEDERGAARD, O.A. (1989). Inhibition of 3H-noradrenaline accumulation by dopexamine hydrochloride in the isolated aorta of the rabbit. *Naunyn-Schmied. Arch. Pharmacol.*, **340**, 270–273.

OHLSTEIN, E.H., ZABKO-POTAPOVICH, B. & BERKOWITZ, B.A. (1985). The DA_1 receptor agonist fenoldopam (SK & F 82526) is also an α_2-adrenoceptor antagonist. *Eur. J. Pharmacol.*, **118**, 321–329.

SCHMIDT, M., KRIEGER, J.P., GIESEN-CROUSE & IMBS, J.L. (1987). Vascular effects of selective dopamine receptor agonists and antagonists in the rat kidney. *Arch. Int. Pharmacodyn.*, **286**, 196–205.

SMITH, G.W. & O'CONNOR, S.E. (1988). An introduction to the pharmacologic properties of Dopacard (Dopexamine hydrochloride). *Am. J. Cardiol.*, **62**, 9C–17C.

VENTURA, H.D., MESSERLI, F.H., FROHLICH, E.D., KOBRIN, I., OIGMAN, W., DUNN, F.G. & CAREY, R.M. (1984). Immediate haemodynamic effects of a dopamine-receptor agonist (fenoldopam) in patients with essential hypertension. *Circulation.*, **69**, 1142–1145.

(Received October 14, 1994
Revised January 18, 1995
Accepted January 27, 1995)

British Journal of Pharmacology (1995) 115, 356-360

Kallikrein rK10-induced kinin-independent, direct activation of NO-formation and relaxation of rat isolated aortic rings

[1]Irene Wassdal, *Robert Hull, *V. Paul Gerskowitch & Torill Berg

Department of Physiology, Medical Faculty, University of Oslo, Oslo, Norway and *James Black Foundation, London

1 rK10, a weak T-kininogenase isolated from the rat submandibular gland, is a protein belonging to the rat kallikrein family. In the present work, we have studied the biological effects of rK10 with respect to its ability to alter vascular resistance, either directly like rK9, *i.e.*, another kallikrein-like protein, trypsin and thrombin, or through the release of kinins like tissue kallikrein (rK1). The direct effect was studied by its vasomotor activity on rat isolated aortic rings since this preparation was insensitive to the action of kinins. Its ability to induce altered vascular resistance through kinin-generation was investigated by blood pressure studies in whole animals. The studies were performed in comparison to rK1.

2 Unlike rK1, which induces hypotension when administered intravenously to rats ($\Delta BP = -56 \pm 5$ mmHg, 5 $\mu g\,kg^{-1}$), rK10 did not have any effect on systemic blood pressure ($\Delta BP = -3 \pm 1$, 5 $\mu g\,kg^{-1}$, i.v.)

3 rK10 was without effect on uncontracted aortic rings, but showed a concentration-dependent (10^{-8}-10^{-6} M) relaxant effect on tissue precontracted with phenylephrine (10^{-6} M). After removal of endothelial cells, no relaxation was observed. The relaxant response to rK10 was transient. rK1 (with and without endothelium), bradykinin and T-kinin (with endothelium) had no effect on contracted or uncontracted aortic rings.

4 The relaxant effect of rK10 was dependent on its enzymatic activity since preincubation with aprotinin (1.02 mM) significantly reduced vasorelaxation from $74 \pm 4\%$ to $24 \pm 3\%$.

5 The relaxant effect was not inhibited by the kinin antagonist Hoe 140 (10^{-7} M; $34 \pm 4\%$ without, versus $30 \pm 2\%$ with Hoe 140), but was totally inhibited by the NO-synthase inhibitor N^{ω}-nitro-L-arginine methyl ester (L-NAME) (2.5×10^{-4} M; $27 \pm 3\%$ without and $2 \pm 1\%$ with L-NAME).

6 These results show that rK10 has the ability to induce vascular relaxation by a specific, direct effect on endothelial cell NO-synthesis, dependent on rK10 proteolytic activity, but independent of its ability to generate kinin. This effect, or its T-kininogenase activity in blood, was not sufficient for rK10 to have an effect on peripheral vascular resistance since intravenous injections of rK10, unlike rK1, did not induce hypotension. Thus, rK10 does not seem to play a role in blood pressure homeostasis but may have a local effect on vascular resistance.

Keywords: Kallikrein rK10; NO; kinin; isolated aortic rings of rat

Introduction

The submandibular gland (SMG) of the rat contains several enzymes belonging to the kallikrein family (Ashley & MacDonald, 1985; Berg *et al.*, 1992). The biological functions of these enzymes are largely unknown. Two have been shown to alter vascular resistance, *i.e.*, vasorelaxation by rK1 (tissue kallikrein) through the release of kinins (Erdøs, 1966; Berg *et al.*, 1987), and vasoconstriction by rK9 through a direct effect on vascular smooth muscles (Yamaguchi *et al.*, 1991; Berg *et al.*, 1992). Also, other proteolytic non-kallikrein enzymes such as trypsin and thrombin have been shown to induce vasorelaxation through a direct effect on endothelium-derived relaxing factor (EDRF) release (Thomas & Ramwell, 1987; Johns *et al.*, 1987). Another enzyme of the kallikrein family, rK10 (Berg *et al.*, 1992), previously named antigen gamma (Berg *et al.*, 1987), endopeptidase K (Gutman *et al.*, 1988), proteinase B (Kato *et al.*, 1987), or T-kininogenase (Xiong *et al.*, 1990), so far found in the rat SMG only, resembles rK1 in its ability to release kinin. However, rK10 differs from rK1 in that it releases T-kinin (Ile-Ser-bradykinin) from T-kininogen (Okamota & Greenbaum, 1983a; Barlas *et al.*, 1987; Gutman *et al.*, 1988; Berg *et al.*, 1991) a substrate present in the rat only (Gutman *et al.*, 1988), whereas rK1, in the rat, releases bradykinin from high and low molecular weight kininogen (Alhenc-Gelas *et al.*, 1981; Kato *et al.*, 1985). T-kinin, like bradykinin, contracts rat uterus and guinea-pig ileum, and induces hypotension (Okamoto & Greenbaum, 1983b). However, kinetic studies have shown that rK10 is not a very efficient kininogenase (Gutman *et al.*, 1988; Berg *et al.*, 1991) compared to human urinary kallikrein (Maier *et al.*, 1983), and its role in vasomotor regulation may be questionable. In the present study, we therefore wanted to characterize further the biological effects of rK10 with respect to its ability to alter vascular resistance, either directly like rK9, trypsin, and thrombin, or through the release of kinins, like rK1. Since it may be assumed that there will be a marked difference in substrate availability between *in vitro* and *in vivo* experiments, and since preliminary studies showed no effect of kinins on isolated aortic rings, the direct effect of rK10 was studied in isolated aortic rings, whereas the vasomotor activity through the presumed release of T-kinin, was studied by its ability to alter arterial blood pressure. The difference between a direct and kinin-mediated response was also tested by the use of a bradykinin-receptor antagonist.

[1] Author for correspondence at: Department of Physiology, Box 1103, Blindern, 0317 Oslo, Norway.

Methods

Effect of rK10 and rK1 on isolated aortic rings

Experimental set up Thoracic aortic rings (3 mm length) were obtained from male Wistar rats (250–350 g), killed by a sharp blow to the head. The rings were set up for isometric recording of force at 37°C in a modified Krebs-Henseleit buffer (composition, mM: Na^+ 143, K^+ 5.9, Ca^{2+} 0.25, Mg^{2+} 1.2, Cl^- 128, $H_2PO_4^-$ 2.2, HCO_3^- 24.9, SO_4^{2-} 1.2, dextrose 10), and gassed with 95% O_2:5% CO_2. The low concentration of Ca^{2+} was chosen due to the observation of less noise in the phenylephrine concentration-response curve than with the 2.5 mM Ca^{2+} which is normally used, although with no loss of sensitivity to phenylephrine. The aortic rings were stretched with an initial preload of 3 g and washed four times with Krebs-Henseleit buffer over the following hour. The α-adrenoceptor agonist, phenylephrine was added, and contraction allowed to develop. The concentration of phenylephrine was established from a cumulative concentration-response curve where phenylephrine (10^{-8}–10^{-3} M) was added until the contraction reached its maximum (100%). A 76 ± 5% ($n = 8$) contraction was obtained with a concentration of 10^{-6} M phenylephrine for aortic rings with intact endothelium. In subsequent studies this concentration of phenylephrine was used to precontract intact rings. Similarly, in denuded aortic rings, phenylephrine (10^{-6} M) gave a 80 ± 2% ($n = 13$) of maximum contraction, which was not significantly different from intact rings. In intact aortic rings treated with L-NAME (2.5×10^{-7}–2.5×10^{-3} M) maximum contractile response to L-NAME was obtained at 2.5×10^{-4} M. From a cumulative concentration-response curve for phenylephrine performed on tissues pretreated with L-NAME (2.5×10^{-4} M), a dose of 3×10^{-7} M phenylephrine was found to produce 73 ± 4% ($n = 8$) of the maximum contraction (NS as compared to intact rings or denuded rings). In experiments where tissue was pretreated with L-NAME, 3×10^{-7} M phenylephrine was used for precontraction. The tension of phenyleprhine-induced precontraction was set at 100% for calculation of relaxant or contractile response in the subsequent experiments. The preparations were then either washed 5 times in Krebs-Henseleit buffer over the next hour (uncontracted preparations) or maintained in a contracted state (contracted preparations). Additions of Krebs-Henseleit buffer amounting to 5% v/v of bath volume elicited no effect. Drugs were therefore added in a volume up to this limit. Removal of the endothelium was carried out before setting up the preparations by gentle rubbing of the intimal surface with a roughened 0.5 mm diameter stainless steel rod. At the end of each experiment, the muscarinic receptor agonist, 5-methylfurmethide (10^{-6} M) was added to test if the endothelium was intact. In rings with intact endothelium, concentration-response experiments showed that this concentration of 5-methylfurmethide produced a relaxation response of 26 ± 3%, whereas in denuded rings, relaxation was not observed (3 ± 2%). Endothelium-independent relaxation was subsequently tested by addition of the β-adrenoceptor agonist, isoprenaline (4×10^{-6} M) which produced a 33 ± 10% relaxation. By choosing these concentrations of 5-methylfurmethide and isoprenaline, the integrity of endothelium and smooth muscle function in the preparation could be tested subsequent to the rK10-induced relaxation. The observed additional relaxation after addition of these two drugs following rK10, agreed with the relaxations obtained with 5-methylfurmethide and isoprenaline alone.

Experimental protocols After preparation of uncontracted and contracted aortic rings with and without endothelium as described above, rK10 or rK1(10^{-8}, 10^{-7}, 3×10^{-7} and 10^{-6} M) was added in a cumulative manner at 5 min intervals, and any contractile or relaxant activity measured isometrically. The 5 min interval was shown in preliminary studies to be sufficient to observe the full relaxant effect of rK10.

After an endothelium-dependent relaxant effect of rK10 had been established, further experiments were carried out on contracted aortic rings with the endothelium intact. To determine if the relaxant effect of rK10 was dependent on its enzymatic activity, rK10 was incubated with aprotinin for 30 min (22°C) before adding it to the organ baths, giving a final concentration of rK10 of 1.5×10^{-6} M and aprotinin of 1.02 mM ($n = 8$) (Berg *et al.*, 1987). Three sets of controls were used: rK10 similarly incubated with Krebs-Henseleit buffer ($n = 8$), Krebs-Henseleit buffer incubated with aprotinin ($n = 8$), and Krebs-Henseleit buffer only. When enzyme activity was tested in samples from the rK10- and the rK10 with aprotinin-incubates using the chromogenic substrate S-2266 as previously described (Berg *et al.*, 1985), rK10 enzyme activity inhibition was confirmed found (96.3 ± 0.1% inhibition).

To determine if bradykinin or T-kinin induced a relaxant effect on contracted aortic rings with intact endothelium, bradykinin (3×10^{-8}–2×10^{-6} M, $n = 8$) or T-kinin (10^{-7}–10^{-6} M, $n = 8$) were added in cumulative manner at 5 min intervals.

In another set of experiments, the tissues were preincubated with the kinin antagonist Hoe 140 (10^{-7} M, $n = 8$) or Krebs-Henseleit buffer ($n = 8$), with the addition of rK10 (1.5×10^{-6} M) to all preparations 5 or 10 min later. The concentration of Hoe 140 was established in separate studies by its ability to inhibit kinin-induced uterine contraction.

The role of endothelium-derived relaxing factor (EDRF), later identified as nitric oxide (NO) (Ignarro *et al.*, 1987; Rees *et al.*, 1990), in the rK10-induced vasorelaxation was tested in similar experiments by addition of NO-synthase inhibitor (L-NAME; 2.5×10^{-4} M, $n = 8$) or Krebs-Henseleit buffer ($n = 8$), followed by the addition of rK10 (1.5×10^{-6} M) to all preparations.

The effect of rK10 on arterial blood pressure (BP) in comparison to rK1 Male Wistar rats (300–350 g) were anaesthetized with Nembutal (70 mg kg^{-1}, *i.p.*), and tracheotomized. BP was recorded continuously through a catheter in the femoral artery connected to a Statham pressure transducer and to a Hewlett Packard polygraph. After a control period of 5 min, a sham injection with PBS followed by rK10 ($n = 5$) or rK1 ($n = 4$) administered as bolus injections (0.15 ml) in increasing doses (0.05, 0.5, 2.5, 5.0 μg kg^{-1} in PBS) at 5 min intervals were given through a catheter in the femoral vein. After each dose, the catheter was flushed with 0.05 ml PBS.

Reagents

Pentobarbitone (Nembutal Sodium) was obtained from Abbott Laboratories, Chicago, IL, U.S.A.; Hoe 140 (D-Arg-[Hyp^3, Thi^5, D-Tic^7, Oic^8]bradykinin) was a kind gift from Hoechst, Frankfurt/Main, Germany. 5-Methylfurmethide was obtained from Wellcome Research Laboratories, Langley Court, Beckenham, Kent, U.K.; phenylephrine hydrochloride and isoprenaline sulphate from Norsk Medisinaldepot, Oslo, Norway; T-kinin and bradykinin from Sigma Chemical Co., St. Louis, MO, U.S.A.; N^{ω}-nitro-L-arginine methylester hydrochloride (L-NAME) from Sigma Chem. Co., St. Louis, U.S.A.; aprotinin from Bayer AG, Leverkusen, Germany, and heparin from Apothekernes Laboratorium A.S., Oslo, Norway. The chromogenic substrate S-2266 (D-valyl-L-leucyl-L-arginine-4-nitroanilide) was from Kabi Diagnostica, Stockholm, Sweden. rK10 and rK1 were purified from the rat SMG as previously described (Berg *et al.*, 1987; Johansen *et al.*, 1987). All other chemicals were of analytical laboratory reagent grade. All drugs and enzymes were dissolved in phosphate-buffered saline (PBS; 0.01 M Na-phosphate, pH 7.4, 0.14 M NaCl).

Statistics

The results are expressed as mean values ± s.e.mean. Dose-dependency was tested by two-way analysis of variance (ANOVA). Differences between dose-response curves were tested by one-way ANOVA. When differences were observed, two-sample Student's t tests were used to test for differences between the groups at a particular dose. A P value less than 0.05 was considered significant.

Results

Effects of rK10, rK1, and kinins on isolated aortic rings

rK10 had no effect on uncontracted aortic rings but showed a concentration-dependent relaxant effect on phenylephrine-contracted tissues ($P<0.0001$). At the highest concentration tested (10^{-6} M), the effect of rK10 induced a 40 ± 6% relaxation. When the endothelium was removed, the vessels failed to relax (Figure 1). The ability of the tissue to relax was confirmed at the end of the experiment, in intact vessels by 5-methylfurmethide (58 ± 7% total relaxation) and in vessels denuded of endothelium by isoprenaline (64 ± 9% total relaxation). Typical recordings are shown in Figure 2. The relaxant effect of rK10 was transient. Tissue kallikrein (rK1) showed no effect on uncontracted tissue with endothelium, or contracted tissue with or without endothelium (Figure 1). Furthermore, no relaxant effect was observed in response to bradykinin or T-kinin with intact endothelium (Figure 1).

The relaxant effect of rK10 on contracted aortic rings was significantly reduced by aprotinin from 74 ± 4% to 24 ± 3% ($P<0.0001$). Aprotinin alone induced a 6 ± 3% relaxation, which was not significantly different from that observed after addition of Krebs-Henseleit buffer.

The relaxant effect of rK10 on contracted aortic rings was not inhibited by the kinin antagonist Hoe 140. The relaxant effect of rK10 was 34 ± 4% without, versus 30 ± 2% with addition of Hoe 140 (5 min preincubation), and 23 ± 6% without, and 26 ± 7% with addition of Hoe 140 (10 min preincubation). Hoe 140 alone had no significant effect on vasomotor tone (3 ± 1% versus 3 ± 1% for Krebs-Henseleit buffer).

The relaxant effect of rK10 was totally inhibited by L-NAME. The relaxation following rK10 alone was 31 ± 6% and after preincubation with L-NAME 2 ± 1% ($P<0.0024$). Validation of the inhibitory effect of L-NAME on NO-dependent relaxation was provided by the observation that L-NAME subsequently inhibited the response to 5-methyl-furmethide (6 ± 2% and 53 ± 9%, with and without L-NAME, respectively, $P<0.0014$), but not the effect of

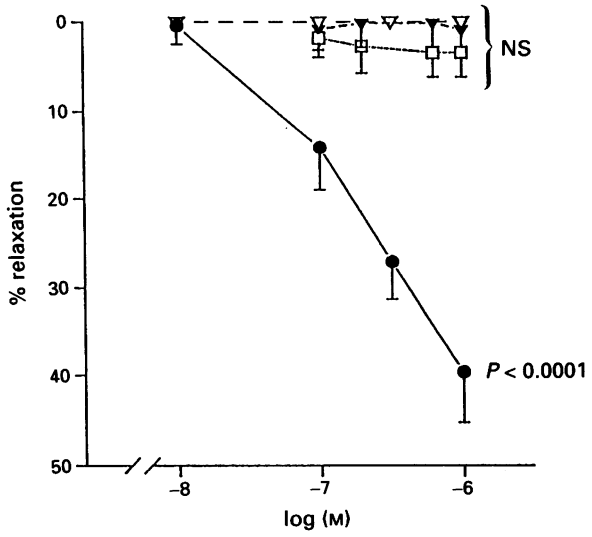

Figure 1 Concentration-response curves for the effect of rK1, rK10, bradykinin (BK) and T-kinin on isolated, contracted aortic rings of the rat. Contraction was developed by adding phenylephrine to the bath (10^{-6} M). In aortic rings with endothelium intact (E+), rK10 induced a significant dose-dependent relaxation ($n=8$) whereas no effect was observed when the endothelium was removed (E−, $n=8$). (●) rK10, E+; (▼) T-kinin, E+; (■) BK, E+; (□) rK1, E+ and E−; (▽) rK10, E−. Relaxation was not observed in response to rK1 with ($n=8$) or without ($n=8$) endothelium, or bradykinin or T-kinin with endothelium ($n=6$).

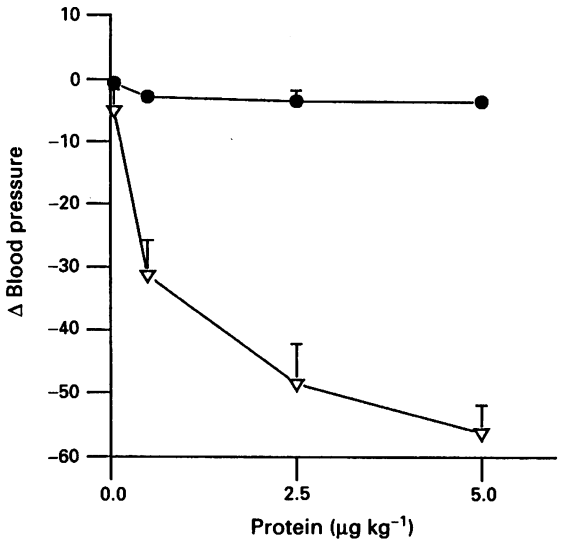

Figure 3 Blood pressure dose-response curves for the effect of rK10 (●) or rK1 (▽) (0.05, 0.5, 2.5, 5.0 μg kg^{-1} in PBS). rK1 induced a dose-dependent drop in BP ($P<0.0001$, $n=4$) significantly different from the nonsignificant response to rK10 ($n=5$).

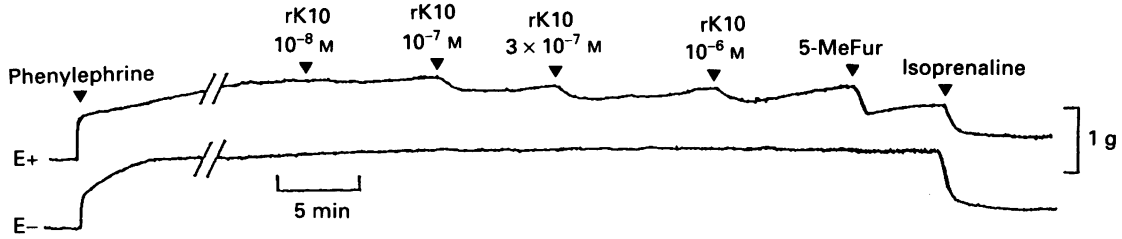

Figure 2 Typical recordings showing the effect of rK10 on contracted aortic rings with (E+) and without (E−) intact endothelium. Contraction was developed by adding phenylephrine to the bath (10^{-6} M). The concentration of rK10 added is indicated above the trace. Addition of 5-methylfurmethide (5-MeFur) (10^{-6} M) and isoprenaline (4×10^{-6} M) demonstrated the ability of the tissue to respond with endothelium-dependent and endothelium-independent relaxation, respectively.

isoprenaline (84 ± 3% and 92 ± 5%, with and without L-NAME, respectively, $P < 0.36$).

The effect of rK10 and rK1 on BP

rK1 induced a dose-dependent hypotensive response with a maximum fall of 56 ± 5 mmHg at maximum dose (5 μg kg^{-1}, *i.v.*) ($P < 0.0001$, $n = 5$). Injections of rK10 (0.05, 0.5, 2.5, 5.0 μg kg^{-1}) did not induce a hypotensive response ($n = 4$) (Figure 3).

Discussion

In the present study, a direct endothelium-dependent vasodilator effect of the kallikrein-like enzyme rK10 on isolated contracted aortic rings was demonstrated. The relaxant effect was found to be dependent on rK10 enzyme activity since preincubation with aprotinin, an inhibitor of rK10 (Berg *et al.*, 1987), significantly reduced relaxation. Some variation in the magnitude of the relaxant response to rK10 was observed throughout the different experiments. These differences were explained by variations in degeneration of the enzyme during storage, since the enzyme activity measurements (S-2266 chromogenic enzyme assay) of the two different rK10-preparations used, showed that variations in the relaxant effect corresponded to variations in specific enzyme activity. The relaxant effect of rK10 on isolated contracted aortic rings was followed by a small contraction. Since rK10 did not have any contractile response on uncontracted vascular rings, this relaxant response was viewed as a transient effect and not as a biphasic response.

Since endothelial denudation and NO-synthase inhibition has been shown to augment phenylephrine-induced contractions (Umans *et al.*, 1993) a comparable phenylephrine-precontractile state (about 75% of maximum contraction) was established for denuded and L-NAME-treated tissue by concentration-response experiments. However, we found no difference in sensitivity to phenylephrine between aortic rings with or without endothelium. On the other hand, after pretreatment with L-NAME, it was necessary to reduce the concentration of phenylephrine by 3.3 times to obtain the desired precontraction tension. This modification ensured that the inhibitory effect of L-NAME was not induced by having reached a supramaximal contraction through the contractile effect of L-NAME, but was indeed due to NO-synthase inhibition.

Two lines of evidence strongly suggest that the relaxant effect of rK10 was not mediated through the formation of kinins. First, the rat aortic rings did not respond to agonists such as bradykinin, T-kinin, or the efficient kininogenase rK1, and second, the relaxant effect was not inhibited by the B_2 kinin receptor antagonist, Hoe 140. Instead, the relaxant effect of rK10 was found to be inhibited by the NO-synthase inhibitor L-NAME, thus indicating that rK10 is mediated through NO-production. The effect of rK10 appeared to be specific for this particular protein, since a similar effect was not observed for the closely related enzyme tissue kallikrein, rK1. The direct enzymatic effect on vascular tension corresponds to that observed for another enzyme from the rat SMG, *i.e.*, rK9, which has been shown to induce a small, but statistically significant concentration-dependent endothelium-independent vasoconstriction of isolated, uncontracted aortic rings. rK9-induced vasoconstriction did not involve the release of angiotensin II (Yamaguchi *et al.*, 1991; Berg *et al.*, 1992) and may indicate another vasomotor reaction due to direct enzymatic activation of smooth muscle receptors. It is possible that enzymes such as rK10 and rK9, through their proteolytic activity may be responsible for a direct conformational change of membrane receptor(s) leading to the activation of NO-synthesis for rK10 or activation of unidentified receptor(s) in smooth muscle cells for rK9.

At the present time we do not know whether the direct vasomotor effect of rK10 is restricted to large arteries, such as the aorta, or whether, resistance vessels show the same reaction. However, the lack of a depressor response after i.v. injections of rK10, may indicate a limited activation, since rK10, unlike rK1, did not have an effect on systemic BP. This is in agreement with previous results where rK10 was found to be a rather inefficient T-kininogenase, (Gutman *et al.*, 1988; Berg *et al.*, 1991) compared to the high/low-molecular kininogenase rK1 (Maier *et al.*, 1983). This may explain the lack of a systemic effect of rK10, in spite of the fact that T-kininogen is the main kininogen in rat plasma (Okamoto & Greenbaum, 1983b). The BP-response for rK1 and rK10 was compared only for similar doses of the two enzymes, since rK10 so far has been detected only in the rat SMG where it is present in approximately the same order of concentration as rK1 (2% and 8% of total gland protein, respectively, Berg *et al.*, 1987). Furthermore, since it may be expected that rK10 will gain access to the vascular compartment in the same way as rK1 (Rabito *et al.*, 1982; Berg *et al.*, 1985), there is no reason to expect that rK10 should enter the blood stream in a higher concentration than rK1. Thus, since the concentration injected induced a large hypotensive response to rK1, we conclude that rK10 does not play a role in BP homeostasis either through a direct effect on vascular resistance or through an ability to generate T-kinin.

In conclusion, the present study demonstrates that in contrast to rK1, rK10 did not have a general effect on blood pressure, but induced a relaxation of isolated aortic rings precontracted with phenylephrine. Furthermore, the relaxation was dependent on endothelial cells and was abolished by NO-synthase inhibition, but was not dependent on the generation of kinin in spite of the fact that rK10 previously has been shown to act as a T-kininogenase. A similar direct effect has also been observed for other proteolytic enzymes on endothelial cells and smooth muscle cells.

This study was supported by The Norwegian Research Council and The Norwegian Council on Cardiovascular Diseases.

References

ALHENC-GELAS, F., MARCHETTI, J, ALLEGRINI, J., CORVOL, P. & MENARD, J. (1981). Measurement of urinary kallikrein activity species differences in kinin production. *Biochim. Biophys. Acta.*, **677**, 477–488.

ASHLEY, P.L. & MACDONALD, R.J. (1985). Kallikrein-related mRNAs of the rat submaxillary gland: nucleotide sequences of four distinct types including tonin. *Biochemistry*, **24**, 4512–4520.

BARLAS, A., GAO, X. & GREENBAUM, L.M. (1987). Isolation of a thiol-activated T-kininogenase from the rat submandibular gland. *FEBS Lett.*, **218**, 66–270.

BERG, T., HOLCK, M. & JOHANSEN, L. (1987). Isolation, characterization, and localization of antigen gamma, a serine protease of the 'Kallikrein-Family' in the rat submandibular gland. *Biol. Chem. Hoppe-Seyler*, **368**, 1455–1467.

BERG, T., JOHANSEN, L. & NUSTAD, K. (1985). Enzymatic activity of rat submandibular gland kallikrein released into blood. *Am. J. Physiol.*, **249**, 1134–1142.

BERG, T., SCHØYEN, H., WASSDAL, I., HULL, R., GERSKOWITCH, P. & TOFT, K. (1992). Characterization of a new kallikrein-like enzyme (KLP-S3) of the rat submandibular gland. *Biochem. J.*, **281**, 819–828.

BERG, T., WASSDAL, I., MINDROIU, T., SLETTEN, K., SCICLI, G., CARRETERO, O.A. & SCICLI, A.G. (1991). T-kininogenase activity of the rat submandibular gland is predominantly due to the kallikrein-like serine protease antigen gamma. *Biochem. J.*, **280**, 19–25.

ERDØS, E.G. (1966). Hypotensive peptides: Bradykinin, kallidin, and eledoisin. *Adv. Pharmacol.*, **4**, 1–90.

GUTMAN, N., MOREAU, T., ALHENC-GELAS, F., BAUSSANT, T., EL MOUJAHED, A., AKPONA, S. & GAUTHIER, F. (1988). T-kinin release from T-kininogen by rat submaxillary gland endopeptidase K. *Eur. J. Biochem.*, **171**, 577–582.

IGNARRO, L.J., BUGA, G.M., WOOD, K.S., BYRNS, R.E. & CHAUDHURI, G. (1987). Endothelium-deriving relaxing factor produced and released from artery and vein is nitric oxide. *Proc. Natl. Acad. Sci. U.S.A.*, **84**, 9265–9269.

JOHANSEN, L., BERGHAUGEN, H. & BERG, T. (1987). Rapid purification of tonin, esterase B, antigen gamma and kallikrein from rat submandibular gland by fast protein liquid chromatography. *J. Chromatog.*, **387**, 347–359.

JOHNS, A., LATEGAN, T.W., LODGE, N.J., RYAN, U.S., VAN BREEMEN, C. & ADAMS, D.J. (1987). Calcium entry through receptor-operated channels in bovine pulmonary artery endothelial cells. *Tissue Cell*, **19**, 733–745.

KATO, H., ENJYOJI, K., MIYATA, T., HAYASHI, I., OH-ISHI, S. & IWANAGA, S. (1985). Demonstration of arginyl-bradykinin moiety on rat HMW Kininogen: Direct evidence for liberation of bradykinin by rat glandular kallikreins. *Biochem. Biophys. Res. Commun.*, **127**, 289–295.

KATO, H., NAKANISHI, E., ENJYOJI, K., HAYASHI, I., OH-ISHI, S. & IWANAGA, S. (1987). Characterization of serine proteinases isolated from rat submaxillary gland: With special reference to the degradation of rat kininogens by these enzymes. *J. Biochem. (Tokyo)*, **102**, 1389–1404.

MAIER, M., AUSTEN, K.F. & SPRAGG, J. (1983). Kinetic analysis of the interaction of human tissue kallikrein with single-chain human high and low molecular weight kininogens. *Proc. Natl. Acad. Sci. U.S.A.*, **80**, 3928–3932.

OKAMOTA, H. & GREENBAUM, L.M. (1983a). Kininogen substrates for trypsin and cathepsin D in human, rabbit and rat plasmas. *Life Sci.*, **32**, 2007–2013.

OKAMOTA, H. & GREENBAUM, L.M. (1983b). Isolation and structure of T-kinin. *Biochem. Biophys. Res. Commun.*, **112**, 701–708.

RABITO, S.F., SCICLI, A.G., KHEER, V. & CARRETERO, O.A. (1982). Immunoreactive glandular kallikrein in rat plasma: a radioimmunoassay for its determination. *Am. J. Physiol.*, **242**, H602–610.

REES, D.D., PALMER, R.M.J., SCHULZ, R., HODSON, H.F. & MONCADA, S. (1990). Characterization of three inhibitors of endothelial nitric oxide synthase *in vitro* and *in vivo*. *Br. J. Pharmacol.*, **101**, 746–752.

THOMAS, G. & RAMWELL, P.W. (1987). Xanthine oxidase and endothelium dependent relaxation. *Biochem. Biophys. Res. Commun.*, **147**, 682–686.

UMANS, J.G., WYLAM, M.E., SAMSEL, R.W., EDWARDS, J. & SCHUMACKER, P.T. (1993). Effects of endotoxin *in vivo* on endothelial and smooth-muscle function in rabbit and rat aorta. *Am. Rev. Respir. Dis.*, **148**, 1638–1645.

XIONG, W., CHEN, L.M. & CHAO, J. (1990). Purification and characterization of a kallikrein-like T-kininogenase. *J. Biol. Chem.*, **265**, 2822–2827.

YAMAGUCHI, T., CARRETERO, O.A. & SCICLI, A.G. (1991). A novel serine protease with vasoconstrictor activity coded by the kallikrein gene S3. *J. Biol. Chem.*, **266**, 5011–5017.

(Received July 20, 1994
Revised February 1, 1995
Accepted February 7, 1995)

British Journal of Pharmacology (1995) 115, 361-367

Stimulation of two vascular smooth muscle-derived cell lines by angiotensin II: differential second messenger responses leading to mitogenesis

Clare Morton, Richard Baines, Imran Masood, *Leong Ng & [1]Michael R. Boarder

Department of Cell Physiology and Pharmacology, *Department of Medicine, University of Leicester, P.O. Box 138, University Road, Leicester, LE1 9HN

1 We show here that angiotensin II (AII) and endothelin-1 (ET-1) stimulate [^{3}H]-thymidine incorporation in a smooth muscle cell line derived from aortae of spontaneously hypertensive rats (SHR), but not in cells derived from normotensive controls (WKY). We have used the differential response of the two cell lines to investigate the relationship between second messenger systems and the mitogenic response.

2 AII produced an increase in accumulation of inositol 1,4,5-triphosphate which was greater in the SHR-derived cell line than in the WKY cells.

3 AII gave an increase in cytosolic Ca^{2+} in each of the cell lines, with both a larger peak (15–30 s) and plateau response (2 min) in the SHR cells. ET-1 gave an enhanced response in the SHR-derived cells with respect to the peak but not the plateau of cytosolic Ca^{2+}.

4 Phospholipase D activity was studied by monitoring the formation of [^{3}P]-phosphatidylbutanol in ^{32}Pi prelabelled cells. AII stimulation gave a larger phospholipase D response in SHR-derived cells, while ET-1 gave a larger response in WKY-derived cells.

5 Stimulation of SHR-derived cells with 100 nM AII for 1 h, followed by 19 h in the absence of agonist, stimulated [^{3}H]-thymidine incorporation over the next 4 h. When the 1 h stimulation with AII was in the presence of increasing concentrations of butanol, which diverts the product of the phospholipase D pathway, there was a loss of stimulated [^{3}H]-thymidine incorporation which was significant at 10 mM butanol and at 30–50 mM reached a maximum loss of 40%.

6 Contrasting with this there was no apparent loss of ET-1-stimulated thymidine incorporation when butanol was present at concentrations up to 40 mM.

7 These results suggest that phospholipase D is one of several pathways in the mitogenic response of SHR-derived vascular smooth muscle cells to AII.

Keywords: Angiotensin II; endothelin-1; vascular smooth muscle; mitogenesis; phospholipase D; phospholipase C

Introduction

Cell surface receptors known to control the cell cycle fall into two principal groups; those with a single transmembrane span and intrinsic tyrosine kinase activity, and those with seven transmembrane domains which are linked to diverse effector mechanisms by heterotrimeric G-proteins (e.g. Pouyssegur & Seuwen, 1992). Recently there has been considerable progress in understanding how the former class, on activation by growth factors such as platelet-derived growth factor, initiates a sequence of events leading to mitogenesis. The mechanisms linking the seven transmembrane receptors to cellular proliferation are more obscure, but often involve a (poly)phosphoinositide specific phospholipase C (PLC) as the primary effector mechanism linked to the receptor by a heterotrimeric G protein. This signalling pathway generates elevated intracellular Ca^{2+} and activation of protein kinase C. While both these have been implicated in mitogenic signalling by seven transmembrane receptors, it is now apparent that there is convergence in the mechanisms underlying cell cycle control between the two principal types of receptors involved. One component which has received some interest recently is the activation of phospholipase D (PLD). This enzyme cleaves specific phospholipids to produce phosphatidic acid as the lipid fragment. It has been shown that in certain cases, activation of tyrosine kinase by growth factors leads to stimulation of PLD (e.g. Zhang *et al.*, 1992; Fukami & Takenawa, 1992; Cook & Wakelam, 1992). There are numerous reports of activation of PLD by receptors which are linked to PLC; in some of these cases tyrosine kinases have also been implicated in the link from receptor to PLD (Uings *et al.*, 1992; Wilkes *et al.*, 1993). Activation of PLD may therefore be considered as an example of convergence of signalling pathways activated by the two classes of receptor.

Evidence for considering the involvement of PLD in certain instances of mitogenic signalling has recently been summarised (Boarder, 1994). The case for a role for PLD is particularly strong for mitogenic responses in vascular smooth muscle cells. In the present study we have utilised two rat aorta-derived cell lines which have different mitogenic responses to both angiotensin II (AII) and endothelin-1 (ET-1) to investigate the relationship between the mitogenic response and the stimulation of PLC and PLD. The two cell lines are derived from one strain of Wistar rat, SHR, which spontaneously develops hypertension and another, WKY, which remains normotensive. It has previously been reported that the SHR-derived cells show an enhanced response to AII and ET-1 with respect to mitogenesis (Paquet *et al.*, 1990; Bunkenberg *et al.*, 1992) and PLC (Resink *et al.*, 1989; Paquet *et al.*, 1990; Osani & Dunn, 1992) but that there were no differences in receptor numbers and affinities between the two cell types (Bolger *et al.*, 1991; Osani & Dunn, 1992). A recent report has shown that SHR-derived cells have an enhanced PLD response to platelet-derived growth factor, which activates an intrinsic tyrosine kinase receptor (Kondo *et al.*, 1994). We have used these differences between these

[1] Author for correspondence.

cell lines to investigate the relationship between the PLC signalling cascade, PLD activation, and the mitogenic response to activation of seven transmembrane receptors. The experiments described provide support for a role for PLD in the mitogenic response to G-protein:PLC linked receptors in cultured vascular smooth muscle cells, but indicate that this relationship is not a simple one.

Methods

Cell preparation and culture

Cells were prepared by the method described by Davies *et al.* (1991). After determining the arterial pressure of 12 week-old SHR and WKY rats (supplied from colonies maintained by the Biomedical Services Unit of Leicester University) by use of a tail cuff, the animals were decapitated and the thoracic aorta removed and stripped of adventitia. The media was cut into 1 mm pieces and enzymatically digested. Following centrifugation the cells were resuspended in growth medium. Clonal cultures were established and after 5 days those colonies with smooth muscle cell morphology were combined. Growth medium comprised Dulbecco's modified Eagle's medium supplemented with 10% foetal calf serum, penicillin (100 i u ml^{-1}), streptomycin (100 $\mu g\ ml^{-1}$) and glutamine (27 mg ml^{-1}). Cells were routinely cultured in 50 ml of the above medium in a 175 cm^2 flask at 37°C in 5% CO_2, 95% air. Cells were used for experiments between passages 6 and 12, seeded into 24 well plates. Cells showed 100% positive smooth muscle actin immunofluorescence.

Incorporation of [^{3}H]-thymidine

Cells at 80% confluence were maintained serum-free for 24 h and then exposed to agonist at the concentration indicated, in a serum-free medium, for 20 h. [^{3}H]-thymidine (0.074 MBq ml^{-1}) was then added followed by a further 4 h incubation. The medium was then aspirated and the cells washed twice with balanced salt solution (BSS, mM: NaCl 125, KCl 5.4, $NaHCO_3$ 16.2, HEPES 30, NaH_2PO_4 1, $MgSO_4$ 0.8, $CaCl_2$ 1.8, glucose 5.5; buffered to pH 7.4 with NaOH and gassed with 95% O_2 5% CO_2). The cell monolayer was then placed on ice and washed sequentially with ice cold 5% trichloroacetic acid and ethanol, taken up into 0.1 M NaOH and scintillation counted. An alternative protocol designed for the butanol experiments employed a 1 h stimulation with the agonist followed by a 19 h incubation with no agonist in serum-free medium before incubation with [^{3}H]-thymidine and extraction as before. When butanol was present it was added 5 min before the agonist and during incubation with agonist, but it was not present during the subsequent periods.

Measurement of Ins(1,4,5)P_3 levels

Cells in 24 well multiwells were washed twice with 1 ml BSS. Agonists were then added in 200 μl of BSS. The incubation was stopped by addition of 100 μl cold 1.5 M trichloroacetic acid. The acid extract was washed with diethylether and assayed for mass of Ins(1,4,5)P_3 by the protein binding procedure of Challiss *et al.* (1988).

Measurement of free intracellular Ca^{2+}

Cells were grown to just reach a confluent monolayer on 9 × 22 mm glass coverslips and then cultured serum-free for 24 h. The cells were loaded for 1 h at 37°C with 4 μM Fura-2 acetoxymethyl ester in Medium 199 buffered to pH 7.4 and supplemented with 10 mM HEPES and 0.1% bovine serum albumin (BSA), followed by 30 min in the absence of the dye. Fluorescence was measured with the coverslip inserted diagonally in a quartz cuvette in 1.8 mM $CaCl_2$, 0.8 mM $MgSO_4$, 15 mM HEPES, 140 mM NaCl, 5 mM KCl and 5 mM glucose, pH 7.4. A Photon Technology International Deltascan dual excitation fluorimeter was used with excitation wavelengths of 340 and 380 nm (5 readings per second) and an emission wavelength of 530 nm, according to the principle described by Grynkiewicz *et al.* (1985). Data are presented as the ratio of the dual wavelength readings.

Assay for phospholipase D activity

PLD activity in intact cells was measured as described in Purkiss & Boarder (1992) and Boarder & Purkiss (1993). Briefly, cells just at confluence in 24 wells were labelled for 24 h at 37°C in a phosphate-free BSS with [^{32}P]-orthophosphoric acid (0.25 MBq ml^{-1}). Preincubations for 10 min included butanol added to the labelling medium at a final concentration of 50 mM, following which the medium was removed and the cells stimulated in BSS with 50 mM butanol and agonists as required until this incubation period was stopped by addition of cold methanol. Drugs were added as indicated to both the preincubation and the incubations. Following extraction with chloroform the ^{32}P-labelled phosphatidylbutanol and phosphatidic acid were separated from other phospholipids by thin layer chromatography on oxalate coated silica plates developed in ethyl acetate:acetic acid:2,2,4-trimethylpentane (9:2:5). The location of phosphatidic acid and phosphatidylbutanol was established by autoradiography and comparison with iodine stained standards, and the spots scraped and scintillation counted. We have previously discussed evidence that this procedure converts essentially all the PLD products to phosphatidylbutanol (Purkiss & Boarder, 1992; Boarder & Purkiss, 1993), in which case the agonist stimulated counts in the phosphatidylbutanol spot are an index of PLD activity.

Materials

[^{3}H]-thymidine, [^{32}P]-P_i and [^{3}H]-Ins(1,4,5)P_3 were purchased from Amersham (Buckinghamshire, UK). Angiotensin II (AII), insulin and fura-2-acetoxymethyl ester were obtained from Sigma (Dorset, UK) and endothelin-1 (ET-1) was obtained from the Peptide Research Institute (Osaka, Japan).

Results

[^{3}H]-thymidine incorporation in response to ET-1 and AII

Initial experiments set out to characterize the stimulation of [^{3}H]-thymidine incorporation into both SHR and WKY cells by various agonists. Figure 1 shows the results of stimulation with ET-1, AII and insulin. The results with WKY cells show that insulin (1 μM), but neither ET-1 nor AII at 100 nM, were capable of stimulating thymidine incorporation (Figure 1a). Insulin combined with either of the other two agonists produced a response which was sometimes, but not reliably, greater than with insulin alone. By contrast the SHR cells gave no response to insulin but a substantial response to both AII and ET-1 (Figure 1b). This dissociation of responses indicated that the two cell types differed in their control of mitogenesis, leading to the subsequent studies. A series of experiments examining the concentration-response relationship for AII and ET-1 stimulation of SHR cells is illustrated in Figure 2, indicating EC_{50} values at low nM levels for both agonists.

Phospholipase C responses to AII and ET-1

The action of AII and ET-1 found on vascular smooth muscle cells are predominantly at AT_1 and ET_A receptors respectively, both of which are G-protein linked to PLC

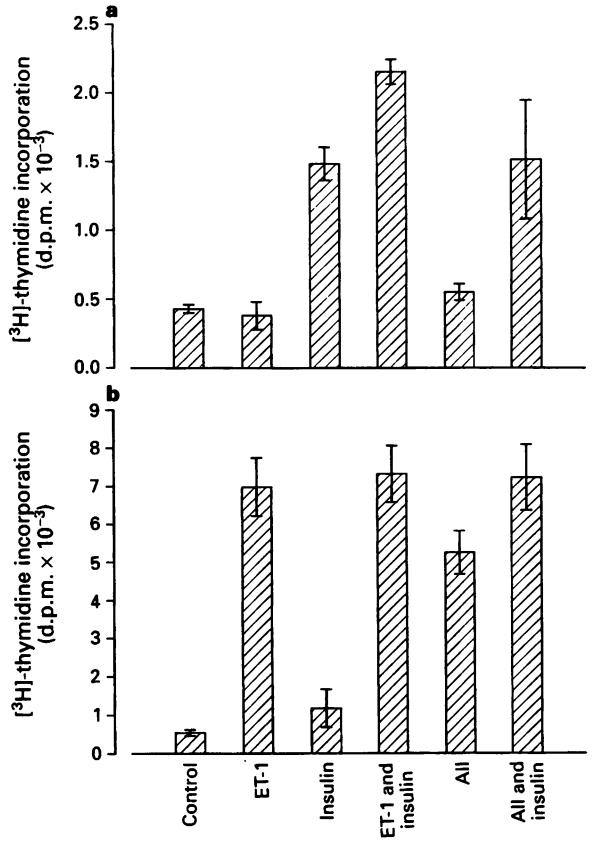

Figure 1 Incorporation of [^{3}H]-thymidine into (a), WKY-derived vascular smooth muscle cells and (b) SHR-derived cells. Agonists were present (angiotensin II AII, and endothelin-1 ET-1 at 100 nM and insulin at 1 μM) as indicated for 24 h, during the last 4 h of which [^{3}H]-thymidine was also present. The results are expressed as counts present in DNA extracted from a well of a 24 well plate, and are mean ± s.e. mean ($n = 3$) from a single experiment representative of 3 separate experiments.

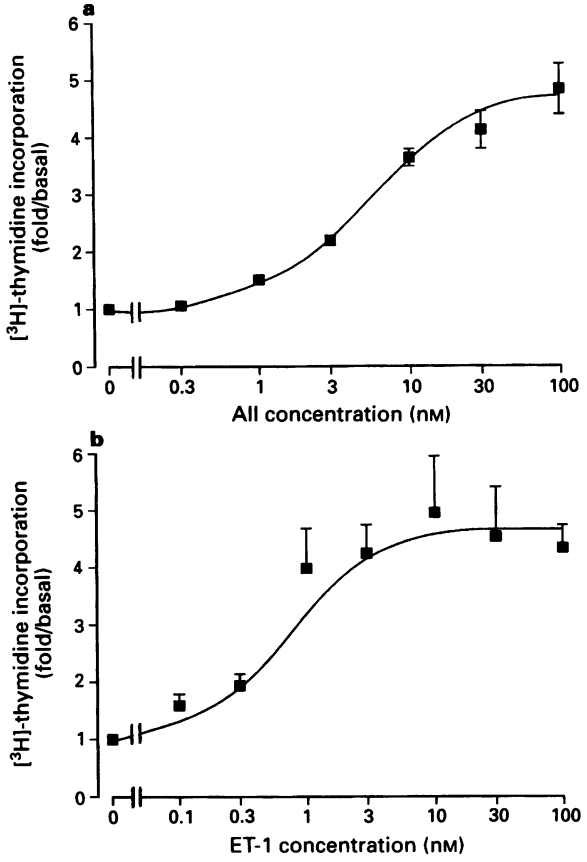

Figure 2 Concentration-response relationship for [^{3}H]-thymidine incorporation into SHR-derived vascular smooth muscle cells with increasing concentrations of (a) angiotensin II (AII) and (b) endothelin-1 (ET-1). Data are normalised to % maximum response and are pooled across 3 separate experiments; error bars are s.e. mean.

(Griendling *et al.*, 1986; Peach & Dostal, 1990; Sakurai *et al.*, 1992) so we investigated the accumulation of Ins(1,4,5)P_3 in response to these two agonists. Figure 3a shows the time course of Ins(1,4,5)P_3 accumulation in SHR and WKY cells to stimulation with 100 nM AII. Starting from the same unstimulated levels (Figure 3a), the peak was at 15 s with both cell types, but higher stimulated levels of Ins(1,4,5)P_3 were seen in SHR than WKY cells. Over 4 separate experiments the peak (15 s) response of the SHR cells was 3.00 ± 0.44 ($P<0.01$) fold that of the WKY cells, while the plateau at 2 min was 2.36 ± 1.38 fold (NS), reflecting variation in the presence of a plateau in WKY cells (data are arithmetic mean ± s.e.mean, $n = 4$, in each case). Using 15 s stimulation the concentration-response relationship for AII was investigated. It was characteristic of these experiments that the higher concentrations of AII gave a reduced response. Figure 3b shows the results of both cell types. Pooled across 4 experiments the apparent EC_{50} values (taken as the concentration of agonist giving 50% of the peak response on the rising phase of the curve) were 50.9 ± 10.0 nM for SHR cells and 46.7 ± 7.6 nM for WKY cells ($n = 4$). Investigation of the time course of raised Ins(1,4,5)P_3 at these concentrations suggested that this reduced response at higher concentrations was not due to a change in the time of the peak response (data not shown).

A similar series of experiments was undertaken with ET-1 (data not shown). The peak response to ET-1 was at 30 s for both cell types, but the height of this peak for SHR cells was 4.56 ± 0.72 fold that of the WKY cells ($P<0.05$) while the plateau at 2 min was 3.33 ± 1.93 fold (NS).

Ca^{2+} responses to AII and ET-1

PLC-linked receptors regulate intracellular Ca^{2+} by Ins(1,4,5)P_3-mediated mobilization of intracellular Ca^{2+} pools and stimulation of Ca^{2+} entry. The change in Ca^{2+} may be related to mitogenic signalling, so we characterized this response in the two cell types. Figure 4 shows typical traces. The responses to ET-1 (100 nM) and to AII (100 nM) were of a similar magnitude. Data not shown established that the plateau phase of these responses, but not the majority of the initial peak, was dependent on extracellular Ca^{2+}. In both cases the magnitude of peak responses was higher in the SHR than the WKY cells. For AII the peak response (expressed as fluorimetric ratios) was 0.865 ± 0.135 in the SHR cells and 0.445 ± 0.067 in the WKY cells ($n = 7$, $P<0.05$), while the plateau was 0.568 ± 0.029 in the SHR cells and 0.169 ± 0.085 in the WKY cells ($n = 7$, $P<0.001$). For ET-1 the peak response was 0.929 ± 0.089 for the SHR cells and 0.526 ± 0.036 for the WKY cells ($n = 3$, $P<0.05$), while the plateau was 0.549 ± 0.061 for the SHR cells and 0.429 ± 0.020 for the WKY cells (NS).

PLD responses to AII and ET-1

To establish the degree of stimulation of PLD in these cells the formation of [^{3}H]-phosphatidylbutanol, a unique product of the PLD pathway, was measured. The time course of [^{32}P]-phosphatidylbutanol accumulation following stimulation of SHR and WKY cells by 100 nM AII is illustrated in Figure 5a, while Figure 5b shows [^{32}P]-phosphatidylbutanol

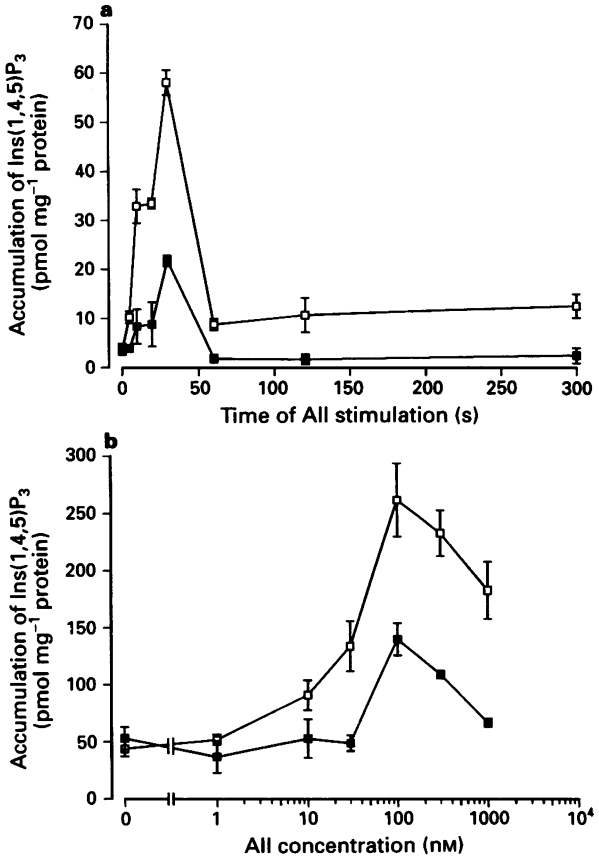

Figure 3 (a) Time course of inositol (1,4,5)trisphosphate ($Ins(1,4,5)P_3$) accumulation in WKY cells (■) and SHR cells (□) in response to 100 nM angiotensin II (AII). (b) Concentration-response curves for accumulation of $Ins(1,4,5)P_3$ with 15 s stimulation by AII in WKY cells (■) and SHR (□). Data are in each case from a single experiment (mean ± s.e. mean, $n = 3$) representative of 4 separate experiments; data pooled across experiments are given in the text.

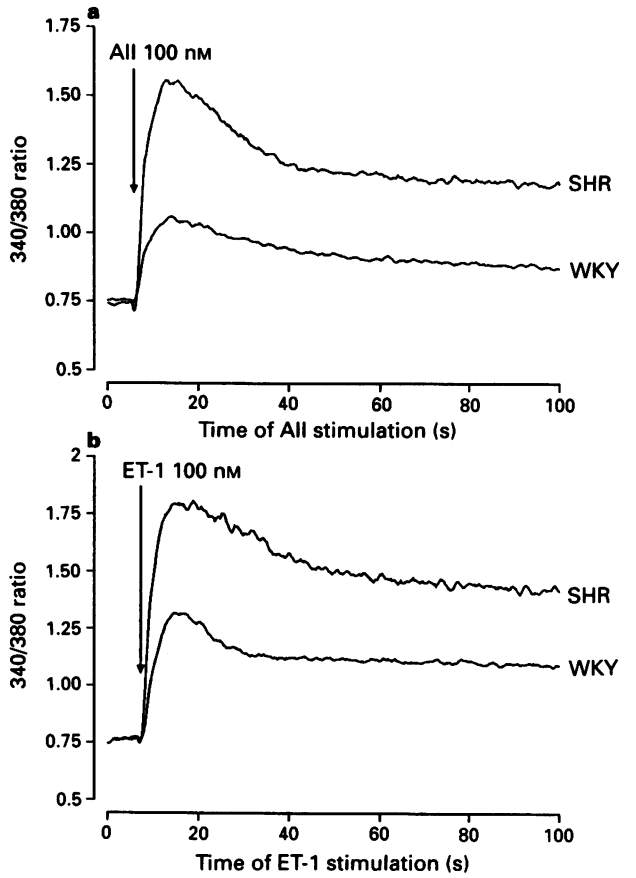

Figure 4 Stimulation of cytosolic Ca^{2+} in WKY- and SHR-derived cells in response to 100 nM angiotensin II (AII) (a) and endothelin-1 (ET-1) (b). Calcium was measured by the Fura 2 procedure and increases indicated by elevations in the ratio flourescence at excitation wavelengths of 340 and 380 nm. The traces shown are representative of 3 for ET-1 and 7 for AII. Data collected across experiments are presented in the text.

accumulation in response to increasing concentrations of AII. In each case the stimulation of PLD by AII showed a similar concentration-response relationship. At the highest concentration of AII used there was a modestly larger response in the SHR cells. Pooled across 3 separate experiments, the response of the WKY cells to AII at 1 μM was 64 ± 8% that of the response of the SHR cells (in each case calculated as c.p.m. [^{32}P]-phosphatidylbutanol mg^{-1} of protein).

Similar experiments were carried out with ET-1. Figure 6 shows the time course of [^{32}P]-phosphatidylbutanol accumulation in the 2 cell types in response to a maximally effective (100 nM) concentration of ET-1. Here the results were very different from those with AII stimulation. When SHR cells were stimulated with ET-1 there was little if any increase in [^{32}P]-phosphatidylbutanol accumulation, while when WKY cells were stimulated there was a large and sustained increase in the levels of this PLD product. This indicates that in response to ET-1 the WKY cells, but not the SHR cells, exhibited a substantial increase in PLD activity.

Effect of butanol on AII-stimulated [^{3}H]-thymidine incorporation

In preliminary experiments we found that we were able to stimulate [^{3}H]-thymidine incorporation in cells just reaching confluence by the following protocol: 24 h serum-free medium prior to and during the experiment, 1 h AII (100 nM), 19 h serum-free medium, 4 h serum-free medium with [^{3}H]-thymidine (0.5 μCi ml^{-1}). This was followed by the standard extraction procedure described. The presence of AII for 1 h gave a stimulation of [^{3}H]-thymidine incorporation 20–24 h later which was several fold over basal. We used this protocol to test for the effect of butanol during the incubation period in the presence of AII. Butanol will inhibit the formation of phosphatidic acid by the PLD pathway in a concentration-dependent manner. The relatively short stimulation with agonist enables the experiment to be carried out without the necessity for prolonged exposure of cells to high concentrations of butanol. A preincubation with butanol for 5 min preceded the stimulation period, so cells were exposed to butanol for 65 min. Results shown in Figure 7a indicate that butanol partially inhibits the AII-stimulated incorporation of [^{3}H]-thymidine. The effect of exposure to butanol was apparent with the lowest concentration used (10 mM). The effect of butanol at concentrations of 30 to 50 mM was similar (Figure 7a). At 50 mM, butanol inhibited 40 ± 6% ($n = 4$ separate experiments, each in triplicate) of the AII-stimulated [^{3}H]-thymidine incorporation. In contrast, there was little effect of butanol at concentrations up to 40 mM on ET-1-stimulated [^{3}H]-thymidine incorporation in SHR cells (Figure 7b).

Effect of chromofuscus PLD

In a previous report on vascular smooth muscle cells it was shown that addition of an exogenous PLD preparation led to enhanced [^{3}H]-thymidine incorporation (Kondo *et al.*, 1992). Here, WKY and SHR cells were incubated with increasing concentrations of *Streptomyces chromofuscus* PLD (0.5–3 u ml^{-1}) for 24 h with the addition of [^{3}H]-thymidine

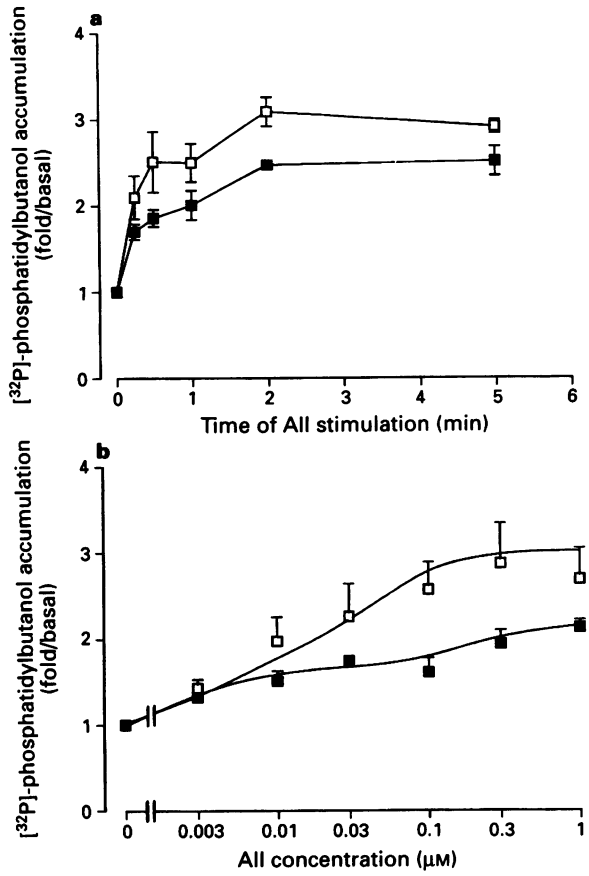

Figure 5 Phospholipase D (PLD) stimulation in WKY- (●) and SHR (○) derived cells in response to (a), incubation for increasing time with 100 nM angiotensin II (AII); (b) incubation with increasing concentrations of AII for 5 min. PLD is expressed as the agonist stimulated accumulation of [^{32}P]-phosphatidylbutanol in the presence of 50 mM butanol. Data are expressed as fold over basal and pooled across 3 experiments; with s.e. mean shown. Two way analysis of variance of data in (b) showed a significant difference between the two cell types ($P<0.001$) in response to the agonist; there was no difference between the cells in the unstimulated levels.

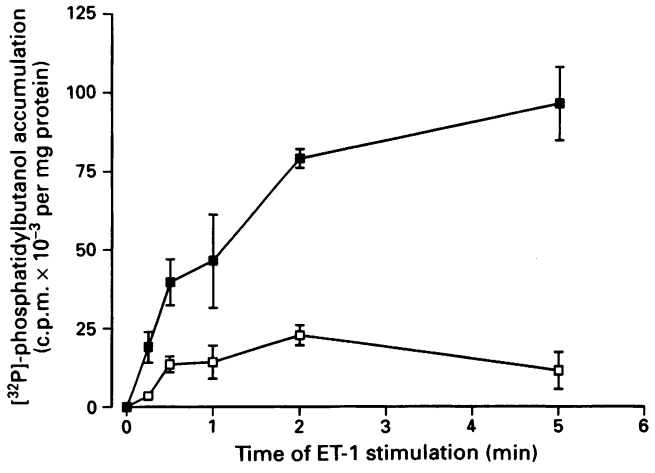

Figure 6 Time course of phospholipase D (PLD) stimulation in WKY- (■) and SHR (□)-derived cells in response to endothelin-1 (ET-1, 100 nM). Data are basal subtracted and pooled across 3 experiments; s.e. mean are shown.

for the final 4 h, as described for the final procedure. A small increase in incorporation was apparent in some instances; however no consistent stimulation was seen (data not shown).

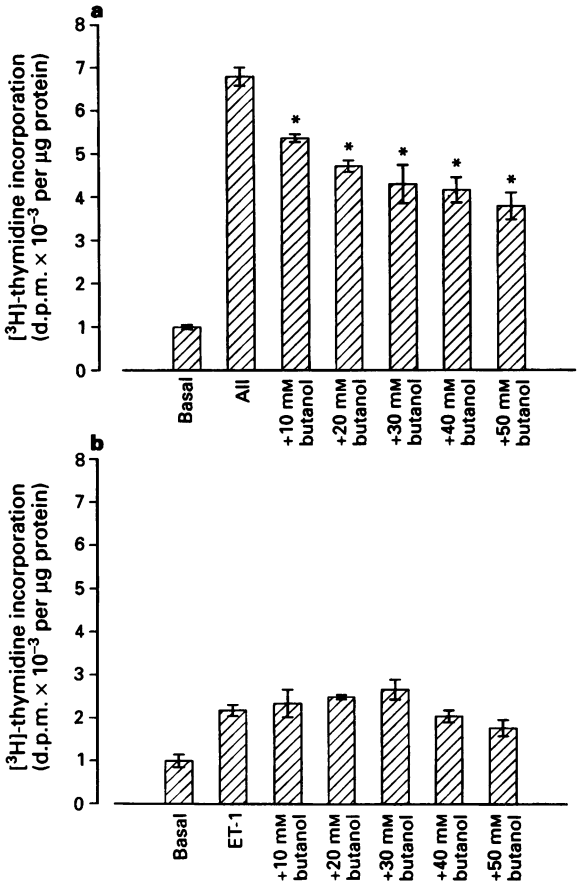

Figure 7 Stimulation of [^{3}H]-thymidine incorporation into SHR-derived vascular smooth muscle cells by (a) 100 nM angiotensin II (AII) and (b) 100 nM endothelin-1 (ET-1) in the presence of increasing concentrations of butanol. The cells were preincubated with butanol where appropriate for 5 min, incubated with butanol and the agonist for 60 min, incubated with neither butanol nor agonist for 19 h, followed by a 4 h incubation in the presence of [^{3}H]-thymidine and extraction of labelled DNA. The experiment is one of three with closely similar results (pooled data in text). *Significantly different ($P<0.005$ or greater) from stimulation in the absence of butanol (Student's unpaired t test).

Discussion

The observation described here that ET-1 and AII stimulate [^{3}H]-thymidine incorporation in SHR, but not WKY, cells is consistent with earlier reports of enhanced mitogenicity of the SHR-derived cells (Paquet *et al.*, 1990; Bunkenberg *et al.*, 1990). The observation in our two cell lines that [^{3}H]-thymidine responses to insulin show the converse relationship (i.e. greater responses in WKY- than SHR-derived cells) was unexpected, and a reflection of the complexity of the signalling pathways that control mitogenesis.

Several papers have documented enhanced PLC responses in SHR-derived smooth muscle cells (Resink *et al.*, 1989; Paquet *et al.*, 1990; Osani & Dunn, 1992). This is the first report characterizing the accumulation of Ins(1,4,5)P_3 in response to stimulation with agonists in SHR- and WKY-derived cells. This is important because this is the inositol phosphate isomer produced by the action of PLC on phosphatidylinositol trisphosphate and because it is the level of this isomer which determines the Ca^{2+} response. The basal levels of both Ins(1,4,5)P_3 and Ca^{2+} were the same for the two cell types. However both Ins(1,4,5)P_3 and Ca^{2+} were the same for the two cell types. However both Ins(1,4,5)P_3 and Ca^{2+} plateau responses to the two agonists were higher for the SHR than the WKY cells, with the exception of the plateau Ca^{2+} response to ET-1. The elevated Ca^{2+} respon-

siveness of SHR-derived cells has been described in a number of studies (e.g. Nabika *et al.*, 1985; Sugiyama *et al.*, 1986), although there are contrary reports of no difference between the cell types (Neusser *et al.*, 1993).

The mechanism by which G-protein-linked receptors activate PLC in vascular smooth muscle cells is unclear. This is because while PLCγ and PLCδ have been reported in these cells, there is an apparent absence of PLCβ (Kato *et al.*, 1992; Homma *et al.*, 1993; Morrero *et al.*, 1994). It is the PLCβ isoforms which are activated by dissociated G-protein subunits, whether they are α_q-GTP or βγ subunits. It has been shown that SHR and WKY cells differ with respect to PLCδ (Kato *et al.*, 1992). This enzyme has no confirmed mode of activation; it is not stimulated by G-protein α-subunits, and stimulation by βγ-subunits is weak compared to that of PLCβ isoforms (Park *et al.*, 1993). More significant is its sensitivity to elevations in cytosolic Ca^{2+}; it is characteristic of the SHR form of the enzyme that it shows an enhanced responsiveness to modest rises in cytosolic Ca^{2+}. Separate studies have shown that in vascular smooth muscle cells, activation by AII or ET-1 of PLC or PLD activity is sensitive to tyrosine kinase inhibition (Wilkes *et al.*, 1993; Morrero *et al.*, 1994); it has also been shown that stimulation by AII and ET-1 leads to tyrosine phosphorylations and activation of mitogen activated protein (MAP) kinases (Ishida *et al.*, 1992; Koide *et al.*, 1992; Molloy *et al.*, 1993) and PLCγ1 (Morrero *et al.*, 1994). With respect to the differential PLC response of the two cell types, it is likely that this is due to the difference in PLCδ response, possibly downstream of a priming activation of PLCγ or undetectable, but functional, amounts of PLCβ.

Various mechanisms have been proposed whereby heterotrimeric G-protein-linked receptors activate PLD, including direct G-protein links and downstream of raised cytosolic Ca^{2+} and activation of protein kinase C (see Boarder, 1994, for summary). PLD is also activated by growth factors acting on intrinsic tyrosine kinase-linked receptors (Zhang *et al.*, 1992), in a manner which may be unrelated to PLC activation (Fukami & Takenawa, 1992; Cook & Wakelam, 1992). Recent elegant studies have shown that PLD may be activated downstream of a small G-protein called ADP-ribosylating factor, (Brown *et al.*, 1993; Cockroft *et al.*, 1993). In vascular smooth muscle cells we have shown that tyrosine kinase activity is required for the stimulation of PLD by ET-1 (Wilkes *et al.*, 1993); this has also been confirmed for AII stimulation of mitogenesis in the cells used in the present study (C. Morton and M.R. Boarder, unpublished observations). The observation that in these cell lines the PLD response to ET-1 was higher in the WKY cells was contrary to our expectations. In this case the mitogenic and PLC responses were not correlated with the PLD response, making any simple causal relationship between them difficult to support. However, in the case of the AII stimulation the three responses, mitogenic, PLC and PLD, were each higher in the SHR than the WKY cells.

The lack of correlation between the PLD responses to ET-1 and the mitogenic response does not exclude an involvement of PLD in the mitogenic response when AII was the agonist. To investigate these possibilities further we stimulated with AII and examined the consequence of co-incubation of the agonist with butanol, to divert the product of PLD activation through the phosphatidylation reaction to phosphatidylbutanol. Previously we have provided evidence that 40 mM butanol can convert essentially all the PLD product away from phosphatidic acid formation while leaving the PLC response intact (Purkiss & Boarder, 1993; Boarder & Purkiss, 1993). In the absence of a suitable PLD inhibitor, butanol provides a method of inhibiting phosphatidic acid formation by PLD. To avoid the necessity of incubating cells with high butanol concentrations for many hours, we used a relatively short incubation with agonist followed by a long lag period before measuring thymidine incorporation. It had previously been shown that brief stimulations with either exogenous PLD or with PLD activating concentrations of platelet-derived growth factor were able to produce a mitogenic response in vascular smooth muscle cells many hours later (Kondo *et al.*, 1992). Here we have shown that 1 h stimulation with AII and measurement of [^{3}H]-thymidine incorporation after a lag of 19 h is as effective as continuous 20 h stimulation with AII. The mitogenic signalling process initiated during this 1 h period is in part dependent on PLD, as indicated by the inhibition of mitogenesis by butanol at the same concentration range as the diversion of the PLD reaction. However, the dependency was only partial, since the effect of butanol formed a plateau between 30 and 40 mM, leaving about 60% of the mitogenic response intact.

These results provide support for a role for PLD in the mitogenic response of SHR-derived vascular smooth muscle cells to stimulation with AII. While other effects of high butanol concentrations cannot be excluded, we have shown that other signalling pathways remain intact (Boarder & Purkiss, 1993). This includes the demonstration that the stimulation of PLC by ET-1 in rat aorta-derived smooth muscle cells was unaffected by 24 h preincubation with 50 mM butanol, and that after 24 h preincubation with 50 mM butanol, stimulation with insulin was still able to elicit a mitogenic response in A10 cells (Wilkes *et al.*, 1993). Here we have used a protocol which reduces the time of exposure to butanol, and have shown that the plateau of butanol inhibition occurs at the concentrations expected for diversion of the PLD pathway; the observation that this leaves a substantial part of the mitogenic response intact may itself be taken as an indication that the butanol effect on thymidine incorporation is not non-specific.

This conclusion is confirmed by the resistance of ET-1-stimulated thymidine incorporation to the inhibitory influence of butanol up to a concentration of 40 mM. Combined with the lower ET-1 stimulated PLD in SHR compared to WKY cells, these results show that PLD stimulation is not significant in the mitogenic response to ET-1 in the SHR-derived cells. The results point to a difference in the mitogenic signalling mechanisms associated with AT_1 and ET_A receptors in this cell line.

The failure of exogenous PLD to produce a reliable mitogenic response is surprising in view of an earlier report (Kondo *et al.*, 1992), and may be taken as an indication that elevated PLD, while necessary for the full response to AII, is not sufficient in itself to elicit enhanced DNA synthesis. However, there are some inherent complications in understanding the consequences of adding phospholipase preparations to the outside of cells, such as the ability to stimulate activity which is effective inside the cells, and non-specific lipid damage. These complications make this experiment difficult to interpret.

The concentration-response data obtained here show that the stimulation of thymidine incorporation lies to the left of the PLC and PLD responses. This is presumably a reflection of multiple steps downstream of the phospholipases, and possibly of involvement of separate pathways controlling mitogenesis by these receptors in these cells.

The results obtained here also suggest that part of the mitogenic response to heterotrimeric G-protein linked receptors is not dependent on PLD. This view is suggested by the results with ET-1 stimulation, and is reinforced by the partial nature of the inhibition of thymidine incorporation by butanol in response to AII. Further studies are underway to investigate a possible role of the Ras:MAP kinase cascade and tyrosine phosphorylations in the mitogenic response to seven transmembrane receptors in vascular smooth muscle cells.

References

BOARDER, M.R. (1994). A role for phospholipase D in mitogenesis. *Trends Pharmacol. Sci.*, **15**, 57–62.

BOARDER, M.R. & PURKISS, J.R. (1993). Assay of phospholipase D as a neuronal receptor effector mechanism. *Neuroprotocols*, **3**, 157–164.

BOLGER, C.T., LIARD, F., JODOIN, A. & JARAMILLO, J. (1990). Vascular reactivity, tissue levels, and binding sites for endothelin; a comparison in the spontaneously hypertensive and Wistar-Kyoto rats. *Can. J. Physiol. Pharmacol.*, **69**, 406–413.

BROWN, H.A., GUTOWSKI, S., MOOMAW, C.R., SLAUGHTER, C. & STERNWEIS, P.C. (1993). ADP-ribosylation factor, a small GTP-dependent regulatory protein, stimulates phospholipase D activity. *Cell*, **75**, 1137–1144.

BUNKENBERG, B., AMELSVOORT, T., ROGG, H. & WOOD, J.M. (1992). Receptor mediated effects of angiotensin II on growth of vascular smooth muscle cells from spontaneously hypertensive rats. *Hypertension*, **20**, 746–754.

CHALLISS, R.A.J., BATTY, I.H., NAHORSKI, S.R. (1988). Mass measurements of inositol (1,4,5)trisphosphate in rat cerebral cortes slices using a radioreceptor assay; effects of neurotransmitters and depolarisation. *Biochem. Biophys. Res. Commun.*, **157**, 684–691.

COCKROFT, S., THOMAS, G.M.H., FENSOME, A., GENY, B., CUNNINGHAM, E., GOUT, I., HILES, I., TOTTY, NF., TRUONG, O. & HSUAN, J.J. (1993). Phospholipase D: a downstream effector of ARF in granulocytes. *Science*, **263**, 523–526.

COOK, S.J. & WAKELAM, M.J.O. (1992). Epidermal growth factor increases sn-1,2,-diacylglycerol levels and activates phospholipase D catalysed phosphatidylcholine breakdown. *Biochem. J.*, **285**, 247–253.

DAVIES, J.E., NG, L.L., AMEEN, M., SYME, P.D. & ARONSON, J.K. (1991). Evidence for altered Na^+/H^+ antiport activity in cultured skeletal muscle cells and vascular smooth muscle cells from spontaneously hypertensive rats. *Clinical Sci.*, **80**, 509–518.

FUKAMI, K. & TAKENAWA, T. (1992). Phosphatidic acid that accumulates in platelet derived growth factor stimulated Balb/c 3T3 cells is a potent mitogenic signal. *J. Biol. Chem.*, **267**, 10988–10993.

GRIENDLING, K.K., RITTENHOUSE, S.E., BROCK, T.A., EKSTEIN, L.S., GIMBRONE, M.A. & ALEXANDER, R.W. (1986). Sustained diacylglycerol formation from inositol phospholipids in angiotensin II stimulated vascular smooth muscle cells. *J. Biol. Chem.*, **261**, 5901–5906.

GRYNKIEWICZ, G., POENIE, M. & TSIEN, R.Y. (1985). A new generation of Ca^{2+} indicators with greatly improved fluorescent properties. *J. Biol. Chem.*, **260**, 3440–3450.

HOMMA, Y., SAKAMOTO, H., TSUNODA, M., AOKI, M., TAKENAWA, T. & OOYAMA, T. (1993). Evidence for early involvement of phospholipase C-γ2 in signal transduction of platelet derived growth factor in vascular smooth muscle cells. *Biochem. J.*, **290**, 649–653.

ISHIDA, Y., KAWAHARA, Y., TSUDA, T., KOIDE, M. & YOKOHAMA, M. (1992). Involvement of MAP kinase activators in angiotensin II-induced activation of MAP kinases in cultured vascular smooth muscle cells. *FEBS Lett.*, **310**, 41–45.

KATO, T., FUKAMI, K., SHIBASAKI, F., HOMMA, Y. & TAKENAWA, T. (1992). Enhancement of phospholipase Cδ1 activity in the aorta of spontaneously hypertensive rats. *J. Biol. Chem.*, **267**, 6483–6487.

KOIDE, M., KAWAHARA, Y., TSUDA, T., ISHIDA, Y., SHII, K. & YOKOYAMA, M. (1992). Endothelin-1 stimulates tyrosine phosphorylation and the activities of two mitogen activated protein kinases in cultured vascular smooth muscle cells. *J. Hypertension*, **10**, 1173–1182.

KONDO, T., INUI, H., KONISHI, F. & INAGAMI, T. (1992). Phospholipase D mimics PDGF as a competence factor in vascular smooth muscle cells. *J. Biol. Chem.*, **267**, 23609–23616.

KONDO, T., INUI, H., KONISHI, F. & INAGAMI, T. (1994). Enhanced phospholipase D activity in vascular smooth muscle cells derived from spontaneously hypertensive rats. *Clin. Exper. Hypertension*, **16**, 17–28.

MOLLOY, C.J., TAYLOR, D.S. & WEBER, H. (1993). Angiotensin II stimulation of rapid protein tyrosine kinase activity in rat aortic vascular smooth muscle cells. *J. Biol. Chem.*, **268**, 7338–7345.

MORRERO, M.B., PAXTON, W.G., DUFF, J.L., BERK, B.C. & BERSTEIN, K.E. (1994). Angiotensin II stimulates tyrosine phosphorylation of phospholipase C-γ1 in vascular smooth muscle cells. *J. Biol. Chem.*, **269**, 10754–10759.

NABIKA, T., VELLETRI, P.A., LOVENBURG, W. & BEAVEN, M.A. (1985). Increase in cytosolic Ca^{2+} and phospholinositide turnover metabolism induced by angiotensin II and [arg]vasopressin in vascular smooth muscle cells. *J. Biol. Chem.*, **260**, 4661–4670.

NEUSSER, M., TEPEL, M. & ZIDEK, W. (1993). Angiotensin II responses after protein kinase C activation in vascular smooth muscle cells of spontaneously hypertensive rats. *J. Cardiovasc. Pharmacol.*, **21**, 749–753.

OSANI, J. & DUNN, M.J. (1992). Phospholipase C responses in cells from spontaneously hypertensive rats. *Hypertension*, **19**, 446–455.

PAQUET, J.L., BANDOMIN-LEGROS, M., BRUNELLE, G. & MEYER, P. (1990). Angiotensin induced proliferation of aortic myocytes in spontaneously hypertensive rats. *J. Hypertension*, **8**, 565–572.

PARK, D., JHON, D.-Y., LEE, C.-W., LEE, K.-H. & RHEE, S.G. (1993). Activation of phospholipase C isozymes by βγ subunits. *J. Biol. Chem.*, **268**, 4573–4576.

PEACH, M.J. & DOSTAL, D.E. (1990). The angiotensin II receptor and the actions of angiotensin II. *J. Cardiovasc. Pharmacol.*, **16** (suppl. 4), S25–S30.

POUYSSEGUR, J. & SEUWEN, K. (1992). Transmembrane receptors and intracellular pathways that control cell proliferation. *Annu. Rev. Physiol.*, **54**, 195–210.

PURKISS, J.R. & BOARDER, M.R. (1993). Stimulation of phosphatidate synthesis in endothelial cells in response to P_2-receptor activation. *Biochem. J.*, **287**, 31–36.

RESINK, T.J., SCOTT-BURDEN, T., BAUR, U., BURGIN, M. & BUHLER, F.R. (1989). Enhanced responsiveness to angiotensin II in vascular smooth muscle cells from spontaneously hypertensive rats is not associated with alterations in protein kinase C. *Hypertension*, **14**, 293–303.

SAKURAI, T., YANAGISAWA, M. & MASAKI, T. (1992). Molecular characterisation of endothelin receptors. *Trends Pharmacol. Sci.*, **13**, 103–108.

SUGIYAMA, T., YOSHIZUMA, M., TAKAKU, F., URABE, H., TSUKAKOSHI, K. & YAZAKI, Y. (1986). The elevation of cytosolic calcium ions in vascular smooth muscle cells in SHR – measurement of the free calcium ions in single living cells by laser microspectrofluorimetry. *Biochem. Biophys. Res. Commun.*, **141**, 340–345.

UINGS, I.J., THOMPSON, N.T., RANDALL, R.W., SPACEY, G.D., BONSER, R.W., HUDSON, A.H. & GARLAND, L.G. (1992). Tyrosine phosphorylation is involved in receptor coupling to phospholipase D but not to phospholipase C in the human neutrophil. *Biochem. J.*, **281**, 597–600.

WILKES, L.C., PATEL, V., PURKISS, J.R. & BOARDER, M.R. (1993). Endothelin-1 stimulated phospholipase D in A10 vascular smooth muscle derived cells is dependent on tyrosine kinase. *FEBS Lett.*, **322**, 147–150.

ZHANG, W., NAKASHIMA, T., SAKAI, N., YAMADA, H., OKANO, Y. & NOZAWA, Y. (1992). Activation of phospholipase D in platelet derived growth factor (PDGF) in rat C6 glioma cells: possible role in mitogenic signal transduction. *Neurol. Res.*, **14**, 397–401.

(Received September 6, 1994
Revised January 12, 1995
Accepted February 8, 1995)

British Journal of Pharmacology (1995) 115, 368-372

Bradykinin receptors in mouse and rat isolated superior cervical ganglia

[1]G.R. Seabrook, B.J. Bowery & R.G. Hill

Merck Sharp & Dohme Research Laboratories, Neuroscience Research Centre, Terlings Park, Eastwick Road, Harlow, Essex, CM20 2QR

1 The ability of bradykinin and its analogues to depolarize rat and mouse superior cervical ganglia was studied by use of *in vitro* grease-gap recording techniques, and the ability of antagonists selective for bradykinin receptor subtypes to block their effects was examined.

2 Bradykinin (3 μM) depolarized ganglia from both species, although the magnitude of the maximal response was less in mouse (15 $\pm$ 5%, $n = 7$) than rat tissue (33 $\pm$ 6%, $n = 7$), relative to muscarine (1 μM).

3 Interleukin 1β (30 u ml^{-1} for 18 h at 37°C) increased the depolarization caused by bradykinin (3 μM) in mouse ganglia from 15% to 54% ($P < 0.001$, $n = 12$). Responses to the B_1 receptor agonist, [des-Arg^{10}]-kallidin (3 μM) were similarly potentiated but this was only detected after inhibition of peptidase activity with 10 μM captopril (4% to 35%, $n = 5$).

4 In ganglia from both species the rank order of agonist potency was bradykinin = [Lys^0]-bradykinin >> [des-Arg^{10}]-kallidin. However, like responses to [des-Arg^{10}]-kallidin in mouse tissue, both the potency of bradykinin and the maximal depolarization achieved ($EC_{50} = 912$ nM; 80%, $n = 11$) was enhanced following inhibition of angiotensin converting enzyme with 10 μM captopril ($EC_{50} = 50$ nM; 135%, $n = 4$).

5 Responses to bradykinin were selectively antagonized by the B_2 receptor antagonist, Hoe 140 but not by the B_1 antagonist, [Leu^8]-bradykinin$_{1-8}$. From Schild analysis the pA_2 value for Hoe 140 in mouse tissue was 9.65, although the slope of the regression line was significantly greater than unity, indicating non-competitive kinetics (slope = 1.88 $\pm$ 0.18, $n = 9$). The depolarization caused by [Lys^0]-bradykinin was also antagonized by Hoe 140 (3 nM).

6 Thus the predominant bradykinin receptor in mouse superior cervical ganglia is compatible with a B_2 subtype. Furthermore the depolarizations caused by B_1 and B_2 agonists in this tissue can be increased following exposure to interleukin 1β, and by blocking peptide degradation with captopril.

Keywords: B_2 bradykinin receptors; superior cervical ganglia; kallidin, Hoe 140; interleukin 1β; electrophysiology

Introduction

Receptors for the nonapeptide bradykinin have been cloned from human, rat and mouse tissues (McEachern *et al.*, 1991; Hess *et al.*, 1992; Eggerikx *et al.*, 1992; McIntyre *et al.*, 1993). These receptors contain seven putative membrane spanning regions and are linked to the activation of phospholipase C, inositol phosphate production, and intracellular calcium mobilization. The existence of at least two types of bradykinin receptors in mammalian tissue, the B_1 and B_2 subtypes, for which antagonists such as Hoe 140 (B_2; Hock *et al.*, 1991; Rhaleb *et al.*, 1992) and the agonist [des-Arg^{10}]-kallidin (B_1) have different selectivities, has recently been confirmed by cloning of cDNA that encodes the human B_1 receptor (Menke *et al.*, 1994).

In mammals, bradykinin is produced by two pathways; through the direct proteolytic action of kallikreins on high-molecular weight kininogen in plasma following tissue damage, and indirectly by aminopeptidase action on [Lys^0]-bradykinin (kallidin) which itself is derived from low-molecular weight kininogens. Several of these bradykinin-related peptides are also biologically active. These include [Lys^0]-bradykinin, and [des-Arg^9]-bradykinin which is generated via carboxypeptidases that cleave the terminal arginine residue from bradykinin. *In vivo* bradykinin is an efficacious inflammatory agent that has also been implicated in nociception and hyperalgesia (reviewed in Dray & Perkins, 1993). Bradykinin is also a potent vasodilator which increases vascular permeability and can thus cause hypotension (Regoli & Barabe 1980). The receptor subtype(s) that are involved in the pathophysiological effects of these kinins are not fully understood. B_2 receptors are known to be constitutively expressed by smooth muscle and neuronal tissues and in many, but not all cases, the B_2 receptor ligand Hoe 140 is an effective antagonist. In particular, this includes some of the cardiovascular effects and inflammation caused by bradykinin (Correa & Callixto, 1993). Although in some animal models of neurogenic inflammation (Mantione & Rodriguez, 1990) and nociception (Correa & Calixto, 1993) responses that are insensitive to B_2 antagonists like Hoe 140, and which are more consistent with the activation of B_1 receptors, have been described.

Bradykinin has been implicated as an important peptide neurotransmitter in the sympathetic nervous system (Levine *et al.*, 1986; Lee *et al.*, 1991). However, there have been few direct pharmacological investigations into the receptor subtype(s) present in such tissue. Consequently, we have examined the ability of bradykinin receptor agonists to depolarize isolated superior cervical ganglia, and have compared the ability of selective antagonists to inhibit these responses. Furthermore, because it has been suggested that cloned murine B_2 bradykinin receptors exhibit a mixed B_1/B_2 receptor pharmacology (McIntyre *et al.*, 1993, however *cf.* Hess *et al.*, 1994) we have compared the pharmacology of bradykinin receptor subtypes in both rat and mouse superior cervical ganglia.

[1] Author for correspondence.

Methods

The methods for dissecting and recording from isolated rodent superior cervical ganglia were the same as described by Seabrook *et al.* (1992). Ganglia were obtained from male Sprague-Dawley rats (150 to 250 g), or from male C57 mice (40 to 60 weeks old), which were then desheathed and placed in a grease-gap recording chamber. The chamber was perfused (1 to 2 ml min^{-1}) with physiological salt solution (PSS) maintained at 25°C and gassed with 95% O_2 and 5% CO_2. The PSS had the following composition (mM): NaCl 125, KCl 5, KH_2PO_4 1, $CaCl_2$ 2.5, $MgSO_4$ 1, $NaHCO_3$ 25, glucose 10 and tetrodotoxin 0.1 μM. The potential difference between the ganglion cell body (earthed) and the postganglionic trunk was monitored via Ag/AgCl electrodes which were connected via a d.c. amplifier to a chart recorder.

The depolarization caused by bradykinin analogues was normalized with respect to the maximum response obtained with a muscarine under control conditions. Muscarine, 1 μM, was supramaximal in both rat and mouse ganglia. Agonist concentration-effect curves were constructed by semi-cumulative applications of increasing agonist concentrations, the test compound being added to the perfusate for 1 min at 5 min intervals. The appropriate antagonist was then added and following a 60 min equilibration period, the concentration-effect curve was repeated in the continuing presence of the antagonist. The subsequent shifts in the concentration-effect curves were used to construct Schild plots according to the methods of Arunlakshana & Schild (1959), or to estimate the pK_A value (the negative logarithm of the antagonist dissociation constant) using the following equation where the estimated $K_A = -\log$ [(antagonist concentration)/(concentration ratio -1)]. Concentration-effect curves were fitted to the data by least squares analysis of variance to the equation $Y = Y_{max}/(1 + (EC_{50}/\text{agonist concentration})^{n_H})$, where the EC_{50} is the half-maximally effective concentration and n_H is the Hill coefficient, using Grafit (Erithacus Software). Data represent the mean ± s.e. mean, and statistical analysis was carried out using ANOVAR (Microsoft Excel ver. 5.0).

Drugs

The following substances were used: bradykinin, [Lys^0]-bradykinin, bradykinin$_{1-8}$, [des-Arg^{10}]-kallidin, Hoe 140 ([D-Arg^0,Hyp^3,β-(2-thienyl)-Ala^5,D-Tic^7,Oic^8]-bradykinin), and [Leu^8]-bradykinin$_{1-8}$ were purchased from Bachem; captopril and tetrodotoxin from Sigma; and human interleukin 1β from Boehringer Mannheim. The structure of the bradykinin analogues used in the present study, as well as their synonyms, are shown in Figure 1. Drugs were dissolved in either distilled water or in dimethylsulphoxide (final bath concentration <0.1%) as appropriate, and aliquots of peptide stock solutions were stored at −70°C.

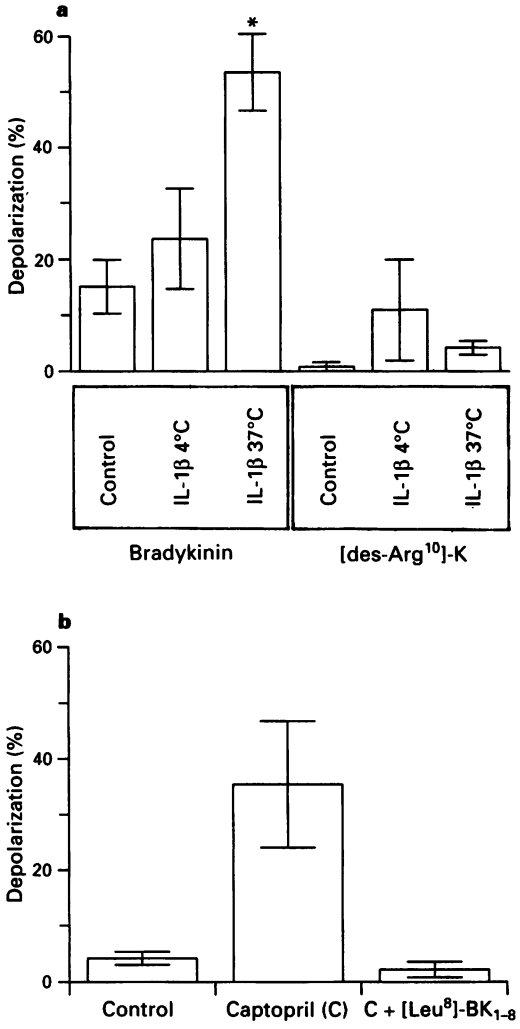

Figure 2 Potentiation of the bradykinin-induced depolarization of mouse superior cervical ganglia by pretreatment with interleukin 1β (IL-1β) and captopril. (a) Depolarization caused by maximal concentration of bradykinin in control ganglia (incubated for 18 h at 34°C) and in those that had been exposed to interleukin 1β (30 u ml^{-1} for 18 h at either 4°C or 37°C). Data are normalized as a percentage depolarization relative to that caused by a supramaximal concentration of muscarine (1 μM). Responses to bradykinin, but not [des-Arg^{10}]-kallidin ([des-Arg^{10}]-K), were significantly potentiated by this treatment (*$P<0.001$ compared with control, ANOVAR). Data from 5 to 12 ganglia for each treatment. (b) Following exposure to IL-1β (18 h at 37°C), treatment of ganglia with captopril (10 μM) potentiated the depolarization caused by [des-Arg^{10}]-kallidin (3 μM, $n = 5$). This effect was blocked by the B_1 receptor antagonist, [Leu^8]-bradykinin$_{1-8}$ ([Leu^8]-BK_{1-8}, 10 μM).

Results

Exogenously applied bradykinin (3 μM) depolarized superior cervical ganglia that had been isolated from both rats and mice. However, relative to the maximum depolarization that was achieved following activation of M_1 muscarine receptors with 1 μM muscarine (e.g. Newberry & Priestley, 1987) the magnitude of the responses was less in mouse (15 ± 5%, $n = 7$) than rat tissue (33 ± 6%, $n = 7$). To examine whether these responses were sensitive to chronic *in vitro* treatment with cytokines, the ability of interleukin 1β (30 u ml^{-1} for 18 h) to potentiate these depolarizations was studied. In mice, the depolarization caused by bradykinin (3 μM) was increased from 15% to 54 ± 7% ($P<0.001$, $n = 12$) with IL-1β (Figure 2). This effect was temperature-dependent in that lowering the incubation temperature from 37°C to 4°C precluded the action of IL-1β. In contrast to responses to bradykinin, responses to the B_1 agonist, [des-Arg^{10}]-kallidin (3 μM) were unaffected by pretreatment with IL-1β (30 u ml^{-1} for 18 h at 37°C). However, potentiation of responses to [des-Arg^{10}]-kallidin (3 μM) was observed after inhibition of peptidase activity with 10 μM captopril (4% to 35 ± 11%,

Lys-**Arg-Pro-Pro-Gly-Phe-Ser-Pro**-Phe-Arg-OH	[Lys^0]-bradykinin = kallidin
-----**Arg-Pro-Pro-Gly-Phe-Ser-Pro**-Phe-Arg-OH	Bradykinin
-----**Arg-Pro-Pro-Gly-Phe-Ser-Pro**-Phe-------OH	Bradykinin$_{1-8}$ = [des-Arg^9]-bradykinin
Lys-**Arg-Pro-Pro-Gly-Phe-Ser-Pro**-Phe-------OH	[des-Arg^{10}] kallidin = [des-Arg^{10}-Lys^0]-bradykinin
-----**Arg-Pro-Pro-Gly-Phe-Ser-Pro**-Leu-------OH	[Leu^8]-bradykinin$_{1-8}$

Figure 1 Comparison between the structure of bradykinin analogues used in the present study. Common amino acids are in bold.

Table 1 Comparison between the potency of bradykinin analogues in rat and mouse isolated superior cervical ganglia, and the affinity of Hoe-140 for receptors activated by bradykinin

	Mouse			*Rat*		
	pEC_{50}/pK_A	nM		pEC_{50}/pK_A	nM	
Agonists						
Bradykinin	6.04 ± 0.22	912	(11)	6.77 ± 0.15	170	(7)
[Lys^0]-bradykinin	5.89 ± 0.37	1,288	(3)	6.51 ± 0.48	309	(3)
[des-Arg^{10}]-kallidin	<5.5	>3,000	(13)	<5.5	>3,000	(3)
[des-Arg^9]-bradykinin	<5.0	>10,000	(4)	NT		
Antagonists						
Hoe 140	10.23 ± 0.22	0.06	(3)	10.61 ± 0.16	0.03	(3)
[Leu^8]-bradykinin$_{1-8}$	<5.0	>10,000	(4)	NT		

Data represent geometric pEC_{50} values or, as in the case of Hoe 140, the estimated antagonist affinity which was calculated from the rightward shift in the bradykinin concentration-effect curve caused by an antagonist concentration of 3 nM. This estimated pK_A value assumes competitive antagonism which was not observed with Hoe 140, but is included simply as a means of comparing the relative effectiveness of Hoe 140 in mouse and rat ganglia at a known antagonist concentration (see text). Numbers in parentheses represent sample sizes. NT = not tested.

$n = 5$). The depolarization caused by bradykinin was selectively blocked by Hoe 140 (see below), whereas those to [des-Arg^{10}]-kallidin and not bradykinin were inhibited by [Leu^8]-bradykinin$_{1-8}$. The depolarization caused by [des-Arg^{10}]-kallidin (3 μM) in the presence of captopril was reduced from 35.4 ± 11.4 ($n = 5$) to 2 ± 1% after treatment with 10 μM [Leu^8]-bradykinin$_{1-8}$ ($n = 5$).

In ganglia from both rats and mice the rank order of agonist potency was bradykinin = [Lys^0]-bradykinin >> [des-Arg^{10}]-kallidin (Table 1, Figure 3). However, like responses to [des-Arg^{10}]-kallidin the potency and efficacy of bradykinin in mouse tissue (EC_{50} = 912 nM; 80 ± 10%, $n = 11$) was significantly increased following inhibition of angiotensin converting enzyme with 10 μM captopril (EC_{50} = 50 nM; 135 ± 32%, $n = 4$). The depolarization caused by bradykinin, or [des-Arg^{10}]-kallidin, in captopril and IL-1β was not enhanced because of a change in sensitivity of treated ganglia to muscarine as the depolarization following activation of m_1 receptors with muscarine (1 μM) was unaffected (458 ± 82 μV, $n = 12$) compared to control (506 ± 65 μV, $n = 8$).

Responses to bradykinin were selectively antagonized by the B_2 receptor antagonist, Hoe 140 but not by the B_1 receptor antagonist, [Leu^8]-bradykinin$_{1-8}$ (Table 1). The shift in the concentration-effect curve to bradykinin with increasing concentrations of Hoe 140 was used to generate a Schild plot (Figure 4). The pA_2 value for Hoe 140 in mouse tissue was determined to be 9.65, although the slope of the regression line was significantly greater than unity (slope = 1.88 ± 0.18, $n = 9$). These data suggest that Hoe 140 was behaving as a non-competitive antagonist in this assay, which precluded the determination of a meaningful antagonist affinity value. Like bradykinin, the depolarization caused by [Lys^0]-bradykinin was also effectively antagonized by Hoe 140 (3 nM, Figure 4b). As in mouse tissue, Hoe 140 was also an effective antagonist of bradykinin responses in rat ganglia. With an identical antagonist concentration (3 nM) the rightward shift in the concentration-effect curve to bradykinin was used to compare the relative effectiveness of Hoe 140 in mouse and rat tissue (Table 1). Using this method the actions of Hoe 140 were indistinguishable in the two species. However, it should be noted that these estimated pK_A values do not reflect the absolute affinity of the antagonist for the receptors because in this assay Schild analysis revealed that Hoe 140 had non-competitive kinetics.

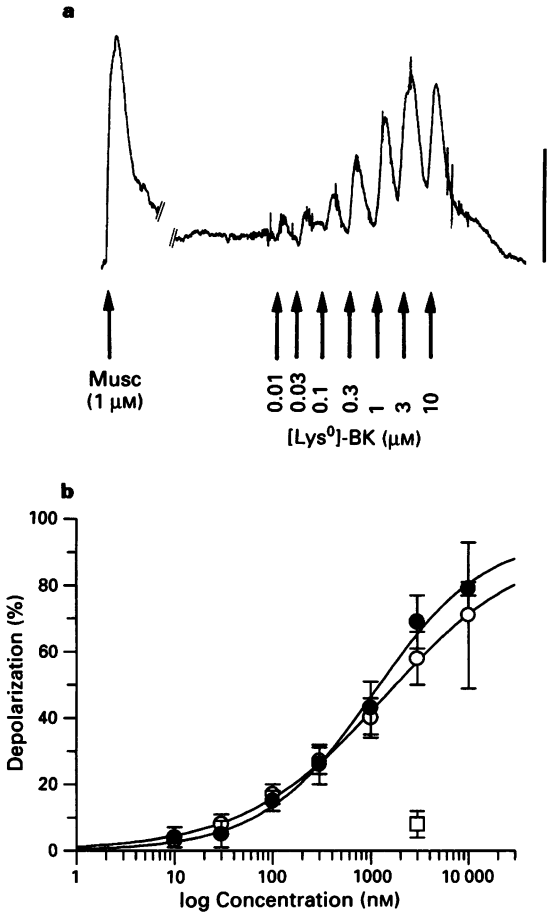

Figure 3 Concentration-dependent depolarization of mouse isolated superior cervical ganglia by bradykinin and its analogues. (a) Voltage trace from an individual recording following exposure of a ganglion to muscarine (1 μM, applied for 1 min at arrow) and by increasing concentrations of [Lys^0]-bradykinin (1 min at 5 min intervals). Vertical calibration bar = 300 μV. (b) Concentration-effect curves for bradykinin (○), [Lys^0]-bradykinin (●) and [des-Arg^{10}]-kallidin (□). Each point represents pooled data from 3 to 6 ganglia. Solid line represents the fit of single site equation to the pooled data. NB the EC_{50} value for each agonist (Table 1) was determined separately using the geometric mean of the individual logarithmic EC_{50} values for each ganglion.

Discussion

One of the most extensively studied neuronal systems in which the physiological effects of bradykinin receptors have been characterized are those of dorsal root ganglia, primarily because these sensory neurones are involved in nociceptive input into the spinal cord. Bradykinin selectively excites a subpopulation of dorsal root ganglia neurones, by mobilizing

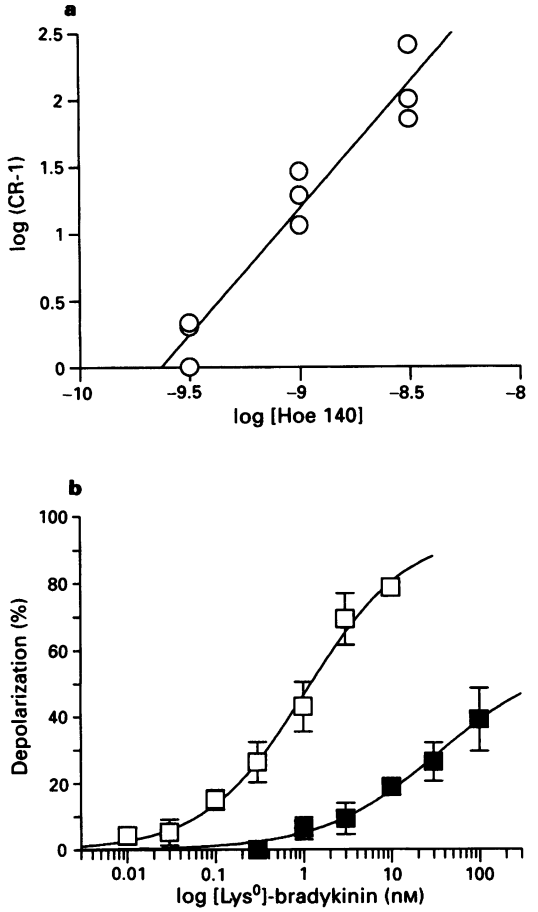

Figure 4 Antagonism of responses in mouse ganglia by the selective B_2 receptor antagonist Hoe 140. (a) Schild plot depicting the antagonism of the depolarization caused by bradykinin with increasing concentrations of Hoe 140 after equilibration for 1 h. The concentration of Hoe 140 that was required to shift the agonist EC_{50} value by two, the pA_2 value, was 9.65 (equivalent to 224 pM). However, the slope of the regression line (solid line) was significantly greater than unity (slope = 1.88 ± 0.18) indicating non-competitive antagonism in this assay. (b) Shift in the concentration-effect curve to [Lys⁰]-bradykinin (□) after incubation in Hoe 140 (3 nM for 1 h; ■). Each point represents the mean and s.e.mean from three preparations. Solid lines represent the fit of a single site equation to the pooled data (see Table 1). Note the flattening of the concentration-effect curve in Hoe 140.

intracellular calcium and activation of an inward cation conductance (Perney & Miller, 1989; McGehee *et al.*, 1992; McGuirk & Dolphin, 1992). Bradykinin receptors have also been implicated in mediating some forms of hyperalgesia and inflammation via regulation of the sympathetic nervous system (Levine *et al.*, 1986; Lee *et al.*, 1991). Consequently to investigate the pharmacology of bradykinin receptors on sympathetic neurones we have compared the ability of bradykinin analogues to depolarize rodent superior cervical ganglia, and have also examined the ability of antagonists selective for bradykinin receptor subtypes to inhibit these responses.

Bradykinin depolarized ganglia that had been isolated from both rats and mice. However, the depolarization obtained with bradykinin (3 μM) was less in mouse versus rat tissue, relative to the maximum depolarization obtained following activation of muscarinic receptors in each species. The weak depolarization observed in mouse tissue was correlated with the 4 fold lower potency of both bradykinin and [Lys⁰]-bradykinin (kallidin) compared to rat tissue under control conditions. Despite this difference, the rank order of agonist potency in both species was consistent with the activation of B_2 receptors in that bradykinin and [Lys⁰]-bradykinin were equipotent agonists, whereas the B_1 receptor selective agonists, [des-Arg¹⁰]-kallidin and [des-Arg⁹]-bradykinin, were relatively inactive. The selectivity of these agonists was identical to that observed in binding studies using cloned murine B_2 receptors (Hess *et al.*, 1994) and was inconsistent with the ligand binding profile of human B_1 receptors (Menke *et al.*, 1994). Although rodent B_1 receptors have yet to be cloned, the relatively weak response to [des-Arg¹⁰]-kallidin suggested that B_1 receptors contributed only a minor component, if any, to the depolarization of these sympathetic ganglia under control conditions.

Hoe 140 is a potent and selective antagonist of B_2 bradykinin receptors (Hock *et al.*, 1991; Rahleb *et al.*, 1992). Like the binding profile of cloned murine B_2 bradykinin receptors (Hess *et al.*, 1994), nanomolar concentrations of Hoe 140 antagonized the depolarization of isolated superior cervical ganglia caused by both bradykinin and [Lys⁰]-bradykinin. The apparent non-competitive nature of the antagonism by Hoe 140 in this assay may be a consequence of the remarkably high affinity of Hoe 140 (230 pM in binding) for the receptor. High affinity receptor ligands typically have very slow off-rates which can effectively preclude a state of equilibrium being reached during the course of an experiment at low antagonist concentrations. There are alternative explanations for Schild plots in which slopes are greater than unity, including positive co-operativity in the binding of an antagonist to the receptor and/or non-specific binding within the tissue (e.g. Kenakin, 1993), although studies in other tissues indicate that Hoe 140 is capable of binding competitively to B_2 receptors (e.g. Rhaleb *et al.*, 1992).

Angiotensin converting enzyme (kininase II) is one of the principle enzymes that degrade kinins into biologically inactive peptides. This enzyme can be selectively inhibited by the competitive blocker, captopril (reviewed in Horovitz, 1981) and was therefore used to determine whether enzymic degradation influenced the potency or efficacy of exogenously applied bradykinin in isolated superior cervical ganglia. Consistent with the presence of kininase II, captopril caused a 70% increase in the maximum depolarization caused by bradykinin in mouse ganglia and this was accompanied by a >10 fold increase in agonist potency.

Responses to kinins in several tissues including smooth muscle, neurones, and endothelium can also be regulated by cytokines. In rabbit aorta the effects of [des-Arg⁹]-bradykinin, an agonist that is *ca.* 10 fold selective for B_1 over B_2 receptors in binding studies (Hess *et al.*, 1994; Menke *et al.*, 1994), are potentiated by pretreatment with interleukin 1β (deBlois *et al.*, 1991). This potentiation was blocked by cycloheximide, an inhibitor of protein synthesis, suggesting that it was probably due to an increase in receptor expression. Recently, Schneck and colleagues have also shown that responses to the more selective B_1 agonist, [des-Arg¹⁰]-kallidin are upregulated by epidermal growth factor in cultures of aortic smooth muscle cells, and that this effect is associated with an increase in number of ligand binding sites (Schneck *et al.*, 1994). To investigate whether interleukins also regulate the expression of bradykinin receptors in sympathetic neurones, ganglia were treated with IL-1β and the responses to bradykinin and [des-Arg¹⁰]-kallidin were examined. In mouse superior cervical ganglia, chronic *in vitro* treatment with IL-1β selectively potentiated the effect of bradykinin in a temperature-dependent manner, in that the increase was precluded by maintaining ganglia at 4°C during the period of incubation with IL-1β. In contrast to bradykinin, responses to the B_1 receptor agonist, [des-Arg¹⁰]-kallidin, were unaffected by this treatment under control conditions. However, after inhibition of angiotensin converting enzyme with captopril, the depolarization caused by [des-Arg¹⁰]-kallidin (3 μM) was also potentiated (from 4% to 35%) by exposure to IL-1β. Furthermore this effect of [des-Arg¹⁰]-kallidin was selectively blocked by the B_1 receptor antagonist, [Leu⁸]-bradykinin$_{1-8}$. Thus angiotensin converting enzyme

modulates the effects of exogenously applied kinins in this tissue, and interleukin treatment can potentiate the effects of both B_1- and B_2-selective agonists on sympathetic neurones.

The induction of bradykinin receptor expression by cytokines has been hypothesized to underlie the persistent state of hyperalgesia that accompanies chronic inflammation (Dray & Perkins, 1993). Furthermore sympathetic neurones are thought to be an important source of prostanoids during inflammation and are involved in a number of pathological hyperalgesic states (Levine *et al.*, 1986; Lee *et al.*, 1991). The ability of interleukin 1β to potentiate responses to both B_1 and B_2 receptor agonists on sympathetic neurones suggests that one or indeed both of these bradykinin receptor subtypes may be involved.

References

ARUNLAKSHANA, O. & SCHILD, H.O. (1959). Some quantitative uses of drug antagonists. *Br. J. Pharmacol. Chemother.*, **14**, 48–58.

CORREA, C.R. & CALIXTO, J.B. (1993). Evidence for participation of B_1 and B_2 kinin receptors in formalin-induced nociceptive response in the mouse. *Br. J. Pharmacol.*, **110**, 193–198.

DEBLOIS, D., BOUTHILLIER, J. & MARCEAU, F. (1991). Pulse exposure to protein synthesis inhibitors enhances vascular responses to des-Arg^9-bradykinin: possible role of interleukin-1. *Br. J. Pharmacol.*, **103**, 1057–1066.

DRAY, A. & PERKINS, M. (1993). Bradykinin and inflammatory pain. *Trends Neurosci.*, **16**, 99–104.

EGGERICKX, D., RASPE, E., BERTRAND, D., VASSART, G. & PARMENTIER, M. (1992). Molecular cloning, functional expression and pharmacological characterisation of a human bradykinin B_2 receptor gene. *Biochem. Biophys. Res. Commun.*, **187**, 1306–1313.

HESS, J.F., BORKOWSKI, J.A., MACNEIL, T., STONESIFER, G.Y., FRAHER, J., STRADER, C.D. & RANSOM, R.W. (1994). Differential pharmacology of cloned human and mouse B_2 bradykinin receptors. *Mol. Pharmacol.*, **45**, 1–8.

HESS, J.F., BORKOWSKI, J.A., YOUNG, G.S., STRADER, C.D. & RANSOM, R.W. (1992). Cloning and pharmacological characterisation of a human bradykinin (BK-2) receptor. *Biochem. Biophys. Res. Commun.*, **184**, 260–268.

HOCK, F.J., WIRTH, K., ALBUS, U., LINZ, W., GERHARDS, H.J., WIEMER, G., HENKE, ST., BREIPHOL, G., KONIG, W., KNOLLE, J. & SCHOLKENS, B.A. (1991). Hoe 140 a new potent and long lasting bradykinin-antagonist: *in vitro* studies. *Br. J. Pharmacol.*, **102**, 769–773.

HOROVITZ, Z.P. (1981). *Angiotensin Converting Enzyme Inhibitors: Mechanism of Action and Clinical Implications.* pp. 1–451. Baltimore-Munich: Urban & Schwarzenberg.

KENAKIN, T. (1993). *Pharmacologic Analysis of Drug-Receptor Interaction.* Chapter 9. pp. 279–321. New York: Raven Press.

LEE, A., CODERRE, T.J., BASBAUM, A.I. & LEVINE, J.D. (1991). Sympathetic neuron factors involved in bradykinin-induced plasma extravasation in rat. *Brain Res.*, **557**, 146–148.

LEVINE, J.D., TAIWO, Y.O., COLLINS, S.D. & TAM, J.K. (1986). Noradrenaline hyperalgesia is mediated through interaction with sympathetic postganglionic neurone terminals rather than activation of primary afferent nociceptors. *Nature*, **323**, 158–160.

MCEACHERN, A.E., SHELTON, E.R., BHAKTA, S., OBERNOLTE, R., BACH, C., ZUPPAN, P., FUJISAKI, J., ALDRICH, R.W. & JARNAGIN, K. (1991). Expression cloning of a rat B_2 bradykinin receptor. *Proc. Natl. Acad. Sci. U.S.A.*, **88**, 7724–7728.

MCGEHEE, D.S., GOY, M.F. & OXFORD, G.S. (1992). Involvement of the nitric oxide-cyclic GMP pathway in the desensitisation of bradykinin responses of cultured rat sensory neurons. *Neuron*, **9**, 315–324.

MCGUIRK, S.M. & DOLPHIN A.C. (1992). G-protein mediation in nociceptive signal transduction: an investigation into the excitatory action of bradykinin in a subpopulation of cultured rat sensory neurones. *Neuroscience*, **49**, 117–128.

MCINTYRE, P., PHILIPS, E., SKIDMORE, E., BROWN, M. & WEBB, M. (1993). Cloned murine bradykinin receptors exhibit a mixed B_1 and B_2 pharmacological selectivity. *Mol. Pharmacol.*, **44**, 346–355.

MENKE, J.G., BORKOWSKI, J.A., BIERILO, K.K., MACNEIL, T., DERRICK, A.W., SCHNECK, K.A., RANSOM, R.W., STRADER, C.D., LINEMEYER, D.L. & HESS, J.F. (1994). Expression cloning of a human B_1 bradykinin receptor. *J. Biol. Chem.*, **269**, 21583–21586.

MANTIONE, C.R. & RODRIGUEZ, R. (1990). A bradykinin $(BK)_1$ receptor antagonist blocks capsaicin-induced ear inflammation in mice. *Br. J. Pharmacol.*, **99**, 516–518.

NEWBERRY, N.R. & PRIESTLEY, T. (1987). Pharmacological differences between two muscarinic responses of the rat superior cervical ganglion. *Br. J. Pharmacol.*, **92**, 817–826.

PERNEY, T.M. & MILLER, R.J. (1989). Two different G-proteins mediate neuropeptide Y and bradykinin-stimulated phospholipid breakdown in cultured sensory neurons. *J. Biol. Chem.*, **264**, 7317–7327.

RHALEB, N-E., ROUISSI, N., JUKIC, D., REGOLI, D., HENKE, S., BREIPOHL, G. & KNOLLE, J. (1992). Pharmacological characterisation of a new highly potent B_2 receptor antagonist (HOE 140: D-Arg-[Hyp^3,Thi^5,D-Tic,Oic^8]bradykinin). *Eur. J. Pharmacol.*, **210**, 115–120.

REGOLI, D. & BARABE, J. (1980). Pharmacology of kinins. *Pharmacol. Rev.*, **32**, 1–46.

SCHNECK, K.A., HESS, J.F., STONESIFER, G.Y. & RANSOM, R.W. (1994). Bradykinin B1 receptors in rabbit aorta smooth muscle cells in culture. *Eur. J. Pharmacol.*, **266**, 277–282.

SEABROOK, G.R., MAIN, M., BOWERY, B., WOOD, N. & HILL, R.G. (1992). Differences in neurokinin receptor pharmacology between rat and guinea-pig superior cervical ganglia. *Br. J. Pharmacol.*, **105**, 925–928.

(Received November 9, 1994
Revised January 18, 1995
Accepted February 13, 1995)

British Journal of Pharmacology (1995) 115, 373-379

Effects of endothelin receptor antagonism with bosentan on peripheral nerve function in experimental diabetes

[1]Elizabeth J. Stevens & David R. Tomlinson

William Harvey Research Institute, Department of Pharmacology, Queen Mary and Westfield College, London E1 4NS

1 The effects of the non-selective endothelin (ET) receptor (ET_A/ET_B) antagonist, bosentan, on sciatic nerve dysfunction in experimental diabetes were investigated.

2 Rats with 5–6 weeks untreated streptozotocin-diabetes exhibited characteristic slowed motor nerve conduction velocity (mean ± s.d., 36.6 ± 3.4 m s^{-1}) and nerve laser Doppler flux (197 ± 64 arbitrary units) compared to age-matched control animals (42.7 ± 2.4 m s^{-1} and 398 ± 77 arbitrary units, respectively). Preventative treatment of diabetic rats with bosentan at 100 mg kg^{-1} day^{-1} p.o. attenuated both these deficits (39.7 ± 3.0 m s^{-1} and 305 ± 56 arbitrary units, respectively) without affecting mean arterial pressure.

3 In control and untreated diabetic rats, ET-1, 1 nmol kg^{-1} i.v., caused an initial hypotension (duration, 30 ± 13 and 26 ± 9 s, respectively; change in mean arterial pressure, −27 ± 13 and −25 ± 7 mmHg, respectively) followed by prolonged hypertension (change in mean arterial pressure, 52 ± 18 and 31 ± 5 mmHg, respectively). Effectiveness of the chronic bosentan treatment was demonstrated by inhibition of the hypotensive response to ET-1 in treated diabetic rats (duration, 5 ± 2 s; change in mean arterial pressure, −4 ± 2 mmHg) although the hypertension was unaltered (change in mean arterial pressure, 32 ± 9 mmHg).

4 Acute i.v. administration of 10 mg kg^{-1} bosentan caused variable and transient rises in nerve laser Doppler flux in control (78 ± 63 arbitrary units) and untreated diabetic rats (93 ± 77 arbitrary units). Acute bosentan blocked the hypotensive response to subsequent ET-1 administration and attenuated the later hypertension (change in mean arterial pressure, 21 ± 9 mmHg in control, 29 ± 10 mmHg in diabetic).

5 Our results indicate that oral treatment of diabetic rats with an ET receptor antagonist can improve sciatic nerve perfusion and conduction, suggesting that the vasoconstrictor action of endogenous ET may contribute to peripheral nerve dysfunction in experimental diabetes.

Keywords: Endothelin-1; bosentan; streptozotocin; diabetes mellitus; nerve conduction; nerve blood flow

Introduction

Reduced peripheral nerve conduction velocity occurs soon after development of both clinical (Gregersen, 1967) and experimental (Eliasson, 1964) diabetes. Although the aetiology of this conduction deficit is unknown, a role for nerve ischaemia is supported by findings of nerve hypoxia in diabetic patients (Newrick *et al.*, 1986) and animals (Tuck *et al.*, 1984), together with poor nerve blood flow in the latter (Tuck *et al.*, 1984; Monafo *et al.*, 1988; Yasuda *et al.*, 1989; Cameron *et al.*, 1991). Furthermore, several compounds which improve nerve conduction in experimental diabetes appear to act by attenuating nerve ischaemia (Yasuda *et al.*, 1989; Stevens *et al.*, 1993b; Maxfield *et al.*, 1993; Cameron *et al.*, 1994a). The mechanism(s) responsible for reduced nerve perfusion remain unclarified, but the disordered endothelial function associated with diabetes (Stout, 1987) may contribute. There is evidence to suggest that the release of the endothelium-derived vasodilator, prostacyclin, is impaired in peripheral nerve from diabetic rats (Ward *et al.*, 1989; Stevens *et al.*, 1993a), while treatment with its stable analogue, iloprost, ameliorates nerve dysfunction (Ohno *et al.*, 1992; Shindo *et al.*, 1992; Cotter *et al.*, 1993). It is possible that either an enhanced production of and/or response to the endothelium-derived, potent vasoconstrictor, endothelin (ET) may also participate in development of reduced nerve perfusion. Clinical studies show variable changes in plasma ET levels of diabetes (Takahashi *et al.*, 1990; Predel *et al.*, 1990), although recent reports indicate similar ET-1 levels to non-diabetic subjects with little dependence on the presence of complications (Bertello *et al.*, 1994; Patino, 1994; Gruden *et al.*, 1994). The likelihood that the conversion of big ET-1 to ET-1 is impaired (Tsunoda *et al.*, 1991) may have masked results from earlier studies with less specific assays. Animal studies also report contradictory change in ET levels (Takahashi *et al.*, 1991; Takeda *et al.*, 1991), although disturbed renal function may be linked with increased ET production (Fukui *et al.*, 1993; Morabito *et al.*, 1994). There is little evidence for a diabetes-induced alteration in vascular responsiveness to ET (Kiff *et al.*, 1991b), but direct effects on nerve function have not been investigated.

Hence, the primary aim of this study was to assess the role of the vasoconstrictor, ET, in peripheral nerve dysfunction in experimental diabetes. We have previously measured sciatic nerve laser Doppler flux, as an index of blood flow, and have demonstrated reductions in streptozotocin-diabetes (Stevens *et al.*, 1993b; 1994). The effects of treatment of diabetic rats with the non-selective ET_A/ET_B receptor antagonist, bosentan (Ro 47-0203), on both sciatic nerve laser Doppler flux and motor conduction velocity were determined. In addition, we also tested the effects of intravenous bosentan administration on nerve laser Doppler flux in untreated control and diabetic rats in an acute protocol, to determine any dynamic influence of ET receptor antagonism on peripheral nerve perfusion. In all animals cardiovascular responses to ET-1 were recorded as a measure of bosentan antagonism. This non-peptide, non-selective antagonist was chosen as the actions of the ET family appear to involve both ET_A and ET_B receptors (Bigaud & Pelton, 1992; Warner *et al.*, 1993) and bosentan has been clearly shown to antagonize both central and regional vascular responses to these peptides (Clozel *et al.*, 1994; Gardiner *et al.*, 1994). In addition, a peptide antagonist

[1] Author for correspondence.

such as BQ-123 may be inadequately selective as its antagonism of the actions of other vasoconstrictor peptides such as angiotensin II, admittedly possibly via antagonism of endothelin receptors (Webb *et al.*, 1992), cannot be excluded.

Methods

Experimental organisation

Male Wistar rats (starting weight 355–400 g and 12–14 weeks of age; Charles River (UK) Ltd., Margate, UK) were assigned at random to three groups. Animals were fasted overnight and the following morning rats of two groups were given a single intraperitoneal injection of 65 mg kg^{-1} streptozotocin. Two days later, blood samples were obtained by tail prick from the streptozotocin-injected rats and blood glucose concentrations were measured by strip-operated reflectance photometry (Reflolux II, Boehringer Mannheim, Mannheim, Germany). All animals had blood glucose concentrations greater than 15 mmol l^{-1} and were thus considered diabetic and included in the experiment.

The aim of the study was to determine the effect of treatment with an ET receptor antagonist on diabetes-induced deficits in sciatic nerve laser Doppler flux and motor conduction velocity. The control group and one diabetic group were left untreated. Immediately after confirmation of diabetes, rats of the second diabetic group received bosentan, a non-peptide, non-selective ET_A/ET_B receptor antagonist, at 100 mg kg^{-1} day^{-1} by gavage for the five to six week protocol. This dose was selected because 100 mg kg^{-1} p.o. bosentan has previously been demonstrated to inhibit pressor responses to big ET-1 for up to 24 h after a single administration in control rats (Clozel *et al.*, 1994); the dose was therefore considered appropriate for use in a once-daily protocol. Animals were studied in mixed batches and, on the day of study, treated rats were dosed 1 h prior to experiment. After death, blood samples from the carotid artery were centrifuged (9000 *g* for 3 min) to provide plasma for later spectrophotometric assay of glucose concentration (GOD-PERID test kit, Boehringer Mannheim, as above).

Nerve laser Doppler flux and cardiovascular variables

In all animals, baseline sciatic nerve laser Doppler flux and systemic arterial pressure were measured in a similar manner to that described previously (Stevens *et al.*, 1993b; 1994). In brief, anaesthesia of rats was induced by halothane and maintained by 1.5 mg ml^{-1} alphaxalone and 0.5 mg ml^{-1} alphadolone (Saffan; Pitman-Moore Ltd, Uxbridge, UK; the manufacturer's solution was diluted 1 in 6 with 0.9% (w/v) saline) infused via the jugular vein at a rate of 8 mg h^{-1}. Systemic arterial pressure and heart rate were monitored via the left carotid artery and laser Doppler flux were measured in the left sciatic nerve using a Moor Instruments (Axminster, UK) fibre optic flow probe (Type P3; tip diameter 1.5 mm) and MBF3D flow monitor. Mean values for systemic arterial pressure, heart rate and nerve laser Doppler flux over 2 min were recorded for each rat. Body temperatures of rats were maintained at 37–38°C via biofeedback by a rectal probe and homeothermic blanket, Near-nerve temperature was monitored via a thermocouple lead connected to a Comark (Rushington, UK) electronic thermometer and was maintained at 35–36°C, with use of infra-red heat when necessary.

Motor nerve conduction velocity

In subgroups of untreated control and diabetic animals and in all bosentan-treated diabetic rats, immediately after nerve laser Doppler flux measurements, left sciatic motor nerve conduction velocity was determined. Stimulation (10 V, 150 μs duration) was via needle electrodes placed at the sciatic notch and ankle. Evoked electromyograms were recorded from the interosseous/plantar muscles and differences in latency were noted. Conduction velocity was calculated by dividing the distance between the stimulating electrodes by the latency difference. For these measurements, near-nerve temperature was maintained at 37°C with infra-red heat.

ET-1 administration

After measurement of conduction velocity, intravenous ET-1 was given to test ET receptor antagonism by bosentan treatment. This was judged in terms of the blockade of pressure responses to the vasoconstrictor in bosentan-treated animals relative to the pressure responses in untreated rats. Specifically, 1 nmol kg^{-1} ET-1, in a volume of 0.5 ml kg^{-1}, was injected via the jugular vein over 24 ± 4 s (mean ± 1 s.d. for all rats). This high dose of ET-1 was selected as one which produces large depressor and pressor changes in arterial pressure but which, in turn, has been shown to be limited by prior administration of bosentan utilised in similar protocols to those performed here (Clozel *et al.*, 1994). Systemic arterial pressure was monitored prior to ET administration and for the following 60 min.

Acute bosentan study

In other subgroups of untreated control and diabetic rats, the acute effects of bosentan administration were examined. After baseline recording of nerve laser Doppler flux and arterial pressure, 10 mg kg^{-1} bosentan, at a volume of 1 ml kg^{-1}, was injected over 35 ± 11 s via the jugular vein. This dose of bosentan was chosen because it has been shown to reduce significantly both depressor and pressor arterial pressure response to ET-1 in a similar protocol (Clozel *et al.*, 1994). Five minutes later, *i.v.* ET-1 was administered to all rats, as described above, to assess antagonism by acute bosentan administration.

Statistical analysis

Data are presented as mean ± 1 s.d. Statistical analyses were carried out by one-way analysis of variance and, where the *F* ratio gave $P < 0.05$ and there was homogeneity of variances (Cochrans C test, $P > 0.05$), group means were compared using Duncan's range tests. For some data (plasma glucose, duration and maximal change in mean systemic arterial pressure during the hypotension, changes in systemic arterial pressures during the hypertension), values were transformed to natural logarithms for statistical analysis to ensure homogeneity of variances.

Materials

Streptozotocin was obtained from ICI Pharmaceuticals (Macclesfield, UK) and was freshly dissolved in 0.9% (w/v) sterile saline to give a solution of 65 mg ml^{-1} prior to injection. Bosentan (Ro 47-0203; free sulphonamide for oral administration, Clozel *et al.*, 1994; 4-tert-butyl-*N*-[6-(2-hydroxy-ethoxy)-5-(2-methoxy-phenoxy)-2,2′-bipyrimidin-4-yl]-benzene-sulphonamide) was prepared as a fresh daily suspension in 5% Arabic gum at 100 mg ml^{-1}. The sodium salt, dissolved in sterile water at 10 mg ml^{-1}, was used for i.v. administration (Clozel *et al.*, 1994). Both forms of bosentan were kindly supplied from F. Hoffman-La Roche Ltd., Basel, Switzerland. ET-1 was obtained from Peptide Institute Inc. (Osaka, Japan) via Scientific Marketing Associates (Barnet, UK) and was dissolved in sterile physiological saline containing 1% bovine serum albumin to give a solution of 2 nmol ml^{-1}.

Results

Animals

Throughout the study, control animals each gained weight, while all diabetic rats lost weight (Table 1). At the end of the protocol, diabetic rats had significantly reduced body weights compared to control animals and were hyperglycaemic. Treatment with bosentan had no effect on these diabetes-induced changes.

Motor nerve conduction velocity

Untreated diabetic animals had significantly reduced sciatic motor nerve conduction velocity (36.6 ± 3.4 m s^{-1}; Figure 1) compared to control animals (42.7 ± 2.4 m s^{-1}; $P<0.01$). This deficit was attenuated in diabetic rats which were treated with bosentan (39.7 ± 3.0 m s^{-1}; not significantly different from control or untreated diabetic values).

Sciatic nerve laser Doppler flux and cardiovascular variables -baseline values

Sciatic nerve laser Doppler flux in untreated diabetic rats (197 ± 64 arbitrary units; Figure 1) was 49% of that for control animals (398 ± 77 arbitrary units) and was significantly ($P<0.01$) different from that for the control group. Values for bosentan-treated diabetic rats (298 ± 55 arbitrary units) were significantly ($P<0.01$) different from those of both the untreated control and diabetic groups. Systolic, diastolic mean arterial pressures, as well as heart rates, were modestly but significantly lower in untreated and bosentan-treated diabetic animals than in control rats (Table 1).

Cardiovascular variables -ET-1 administration

Intravenous administration of ET caused an initial hypotension followed by prolonged hypertension in control and untreated diabetic rats (Figure 2). In parallel to the changes in arterial pressure, there were tachycardiac followed by bradycardic responses to ET-1. Two of the control animals died during the hypertension (systolic pressures greater than 250 mmHg) and are not included in the hypertension data.

The initial hypotension, as judged by duration and maximal change in arterial pressure, was similar and not significantly different between control ($n = 6$) and diabetic ($n = 5$) rats. However, there was little evidence for depressor or tachycardic responses in bosentan-treated diabetic animals (maximal changes in arterial pressure and heart rate, $P<0.01$ *versus* control or diabetic, $n = 9$). The time from ET administration to the peak changes in arterial pressure and heart rate were similar in all rats (17 ± 4 s in control, 23 ± 16 s in untreated diabetic and 21 ± 14 s in bosentan-treated diabetic, no significant differences between groups).

The subsequent hypertension was of variable duration between all rats (note that the y-axis is in min for this section of Figure 2). The maximal changes in systemic arterial pressure were significantly ($P<0.05$) lower for untreated or bosentan-treated diabetic rats compared to those in control animals. The integrated pressure responses to i.v. ET-1 in control animals (areas under the arterial pressure curve during hypertension; 5448 ± 1062 mmHg min) were greater than those in untreated diabetic animals (3569 ± 1351 mmHg min) and responses were lower still in bosentan-treated rats (2695 ± 895 mmHg min). It was noted that blood appeared in the eyes of all the rats of the control group, yet not in those of any other animals.

Acute bosentan administration

Changes in nerve Doppler flux in rats during the acute bosentan part of the study are shown in Figure 3. Intra-

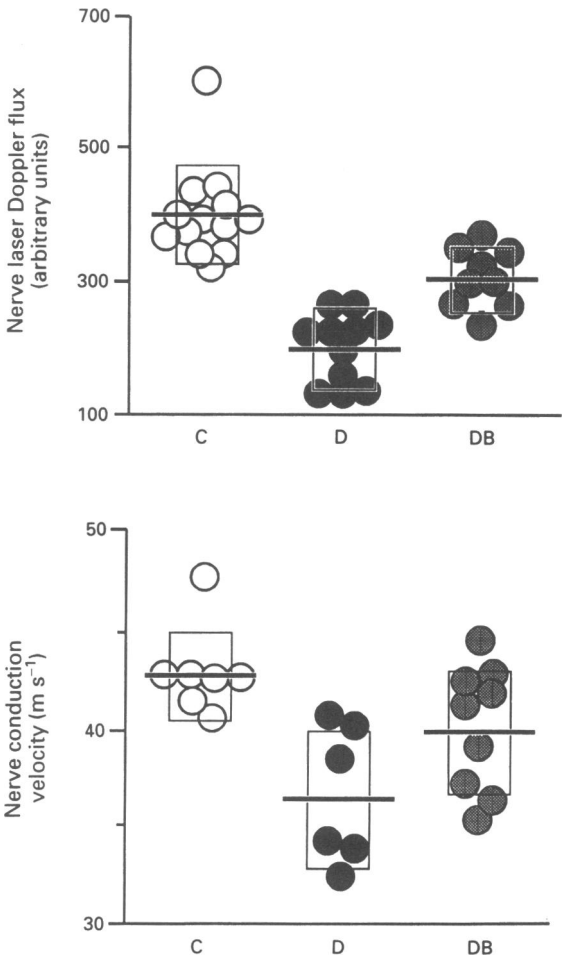

Figure 1 Point-plots showing sciatic nerve motor conduction velocity and laser Doppler flux for control rats (C; open circles), untreated diabetic rats (D; solid circles) and bosentan-treated diabetic rats (DB; cross-hatched). Individual animal data are shown with horizontal bars giving group means and boxes indicating the range of ± 1 s.d.

Table 1 Body weight, final plasma glucose, baseline systemic arterial pressure and heart rate data

	n	*Body weight* (g) *Initial*	*Final*	*Final plasma glucose* (mmol l^{-1})	*Baseline arterial pressures* (mmHg) *Systolic*	*Diastolic*	*Mean*	*Heart rate* (beats min^{-1})
Control	13	379 ± 11	544 ± 30^{x}	10.8 ± 1.9^{x}	140 ± 16^{x}	105 ± 14^{x}	119 ± 15^{x}	394 ± 35^{x}
Untreated diabetic	11	382 ± 14	311 ± 35^{y}	50.7 ± 13.2^{y}	117 ± 9^{y}	91 ± 7^{y}	104 ± 8^{y}	295 ± 39^{y}
Bosentan-treated diabetic	9	378 ± 19	286 ± 41^{y}	48.9 ± 10.3^{y}	115 ± 14^{y}	87 ± 12^{y}	100 ± 11^{y}	283 ± 32^{y}

Data are mean ± 1 s.d. and were analysed by one-way analysis of variance with Duncan's multiple range tests; $P<0.01$ (x versus y). For statistical analysis, plasma glucose data were transformed to natural logarithms to achieve homogeneity of variances

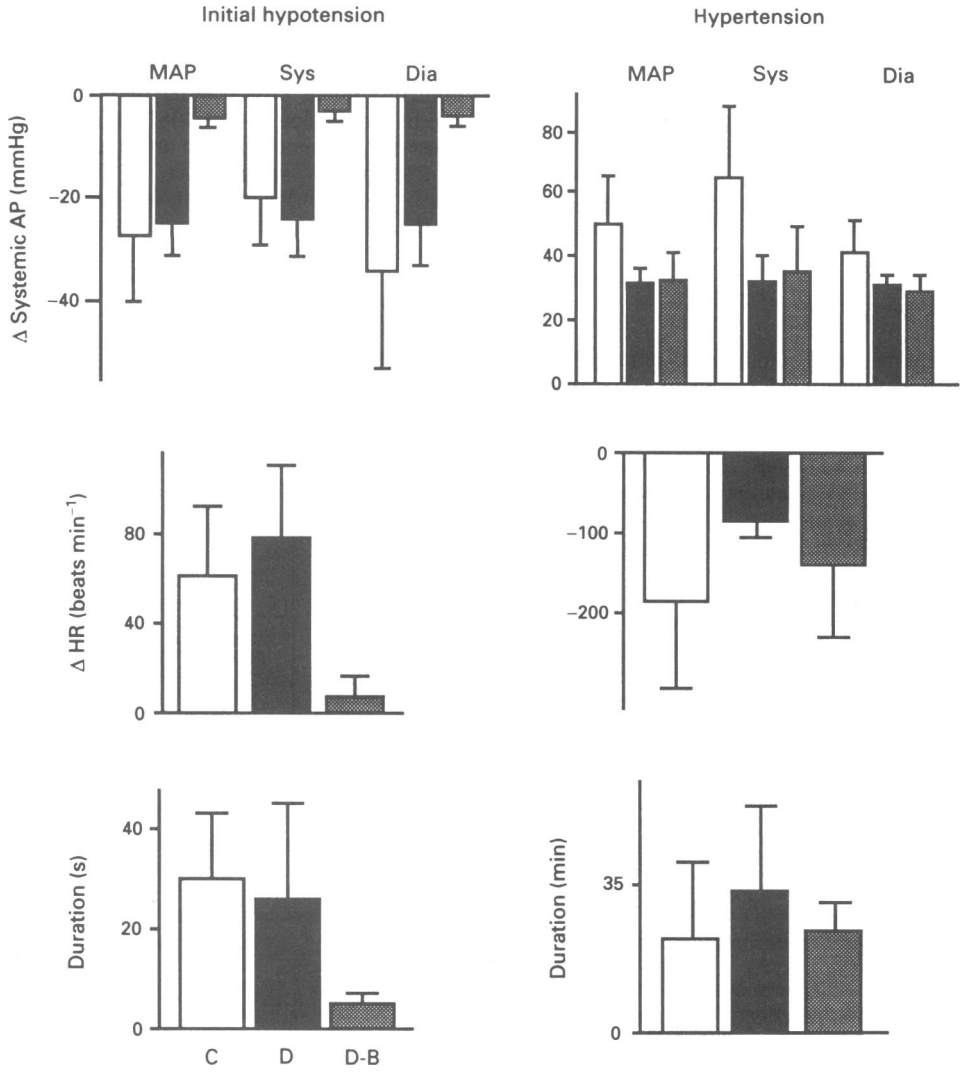

Figure 2 Maximal changes in arterial pressure (MAP = mean, Sys = systolic and Dia = diastolic) and heart rate during the initial hypotension and subsequent hypertension responses to endothelin administration, together with duration of the responses, for control rats (C; open columns), untreated diabetic rats (D; solid columns) and bosentan-treated diabetic rats (D-B; cross-hatched columns). Data are group means ± 1 s.d.

venous bosentan caused slight but brief increases in arterial pressure (maximum change; control 7 ± 5 mmHg, $n = 7$ and diabetic 20 ± 15 mmHg, $n = 6$) which were accompanied by transient decreases in heart rate (maximum change; control -17 ± 12 beats min^{-1} and diabetic -29 ± 20 beats min^{-1}). The maximal changes occurred approximately 1–2 min following the start of bosentan administration (control 90 ± 105 s and diabetic 51 ± 39 s), when there were also transient peaks in nerve Doppler flux (see Figure 3). However, the mean blood pressure or nerve Doppler flux calculated over the 5 min period (from the beginning of the administration) indicated little change from baseline (mean change in arterial pressure 4 ± 11 mmHg and 12 ± 12 mmHg and in nerve Doppler flux 17 ± 25 arbitrary units and 16 ± 34 arbitrary units, in control and diabetic rats, respectively). There was no hypotensive or tachycardic response to the subsequent ET-1 administration, although there was a sustained hypertension (maximum change in mean arterial pressure; controls 21 ± 9 mmHg and diabetics 29 ± 10 mmHg; integrated areas under the arterial pressure curve during hypertension; controls 1987 ± 812 mmHg min and diabetics 2674 ± 1280 mmHg min) and bradycardia (maximum change in heart rate; controls, -116 ± 47 beats min^{-1} and diabetics, -147 ± 52 beats min^{-1}). In response to either bosentan or ET administration, there was little difference between control and diabetic rats.

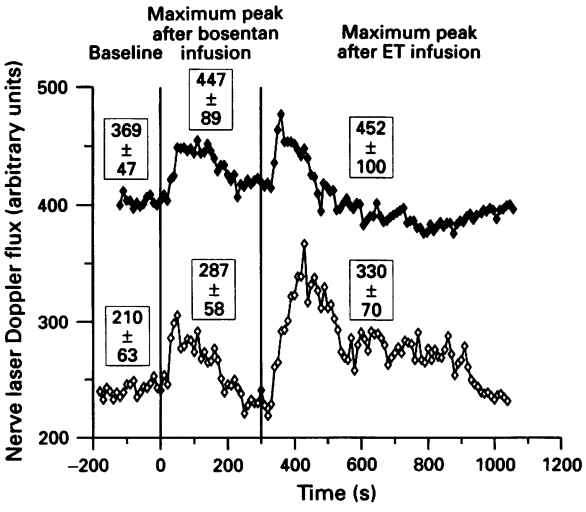

Figure 3 Typical data of nerve laser Doppler flux for one control (◆) and one diabetic (◇) rat in the acute bosentan experiment. Data in boxes are respective group means ± 1 s.d. for baseline values and maximum peaks after bosentan or endothelin (ET) administration. Bosentan administration was at 0 s and ET administration was at 300 s.

Discussion

The main aim of this study was to determine the effect of ET receptor antagonism with bosentan on sciatic nerve motor conduction velocity and laser Doppler flux -early indices of peripheral nerve dysfunction in experimental diabetes.

Untreated diabetic rats failed to gain body weight throughout the experimental protocol, resulting in reduced final weights compared to those of control animals and they were also hyperglycaemic; these are characteristics of streptozotocin-diabetes. Treatment with bosentan had no effect on these changes and thus effects on nerve function could not be attributed to alterations in the severity of diabetes in treated animals.

Untreated diabetic rats exhibited the typical slowed motor nerve conduction velocity reported many times (for example, Eliasson, 1964; Mayer & Tomlinson, 1983) and also demonstrated similar reductions in nerve laser Doppler flux to those which we have previously published (Stevens *et al.*, 1993b; 1994). The deficit of approximately 50% in nerve laser Doppler flux in diabetic rats is consistent with results from other research groups who have either used Doppler flowmetry (Yasuda *et al.*, 1989; Maxfield *et al.*, 1993; Kappelle *et al.*, 1993; Cameron *et al.*, 1994b) or other methods (Tuck *et al.*, 1984; Monafo *et al.*, 1988; Cameron *et al.*, 1991; Hotta *et al.*, 1992) to estimate nerve perfusion in experimental diabetes. The validity of Doppler flowmetry as an index of nerve blood flow requires comment and, in the aforementioned papers (Stevens *et al.*, 1993b; 1994), we discussed the limitations and fidelity of the technique. Nerve Doppler flux values are derived from the number and velocity of erythrocytes passing the probe and thus reflecting the emitted laser signal (Vongsavan & Matthews, 1993). We therefore refer to such data only as an index for whole blood flow through the nerve, but suggest that the decreases in untreated diabetic animals do reflect diminished perfusion. It has been demonstrated that peripheral nerve cannot autoregulate its blood supply (Low & Tuck, 1984) and so adequate perfusion will be dependent on systemic supply. Arterial pressures were slightly reduced in untreated diabetic rats compared to those of the control group and so, in this particular study, this may have contributed to the indicated decrease in nerve blood flow, but the proportional reduction was much greater for Doppler flux than for arterial pressure. Furthermore, daily bosentan treatment had no effect on resting systemic arterial pressure, whilst significantly increasing nerve Doppler flux, implying that the velocity of red blood cells in the sciatic nerve was increased in treated diabetic rats. This suggests an effect of chronic bosentan treatment on the vasomotor tone of the endoneurial circulation of the sciatic nerve.

The mode of action of bosentan on nerve microcirculation is debatable. As mentioned, treatment with this agent was with little effect on baseline arterial pressure and this is in agreement with work by Clozel and co-workers (1994). The apparent increase in nerve perfusion was thus presumably due to antagonism of the constrictor effect of endogenous ET in local microvessels. Such an effect could not have been sufficient to influence overall cardiovascular function, which may have been the consequence of differential antagonism of ET receptors in regional vascular beds. Kiff *et al.* (1991a, b) have shown a vasoconstriction in the hindquarters of conscious diabetic rats (in parallel with renal and mesenteric hyperaemia), which may account for the observed reductions in perfusion of peripheral nerve. Although this was not due to a hyper-responsiveness to ET (Kiff *et al.*, 1991), effective blockade of ET receptors with bosentan in this bed may have occurred with concomitant partial restoration of nerve perfusion. The effectiveness of maintained bosentan administration was demonstrated by abolition of the initial hypotensive response to a high dose of intravenous ET-1; this is in agreement with other reports, indicating blockade of ET_B receptors (Gardiner *et al.*, 1994; Clozel *et al.*, 1994). Also consistent with Gardiner *et al.* (1994) was the difficulty in detecting blockade of the marked and prolonged vasoconstriction associated with ET-1 administration. This may have been the result of several synergistic factors. With hindsight, the dose of ET-1 selected for this protocol was probably too large and, in principle, a dose-response design would have been better, but the extreme duration of the ET-1 pressor response precludes the latter approach. We therefore selected a dose based upon the extensive dose-response (over multiple animals) studies of Clozel and her colleagues (1994). A second possible reason is that the concomitant inhibition of ET-induced hypotension may have also restricted and/or masked an effect of bosentan on ET-induced vasoconstriction. Thirdly, it may be that the oral dose of bosentan was too low to antagonize completely ET_A receptors in this protocol. However, acute intravenous bosentan administration limited the extent of ET-induced hypertension, as was reported by Clozel *et al.* (1994), indicating that bosentan can antagonize ET_A receptors, provided that dose and route are optimal. It is of interest that the cardiovascular responses to ET were unchanged by diabetes, as noted by Kiff *et al.* (1991a, b). This also implies that there were no differences in the ET-provoked nitric oxide release that is thought to be responsible for the observed initial hypotension (Whittle *et al.*, 1989).

The above discussion referring to sustained bosentan treatment is supported by the effects of acute administration of this agent in animals which did not previously receive treatment. Transient increases in nerve laser Doppler flux, independent of changes in systemic arterial pressure, were evident after bosentan administration, indicating a regional effect on blood flow. Antagonism of cardiovascular responses to ET-1 administration were also seen, as discussed above. In addition, the attenuation of the raised nerve Doppler flux in response to prolonged ET-1-mediated vasoconstriction, suggests effective antagonism of ET receptors in the periphery, as noted by Gardiner *et al.* (1994).

The final consideration is the meaning of the associated prevention of reduced nerve laser Doppler flux and of motor nerve conduction velocity in the bosentan-treated diabetic rats. The high selectivity of bosentan towards ET receptors implicates ET as a causative agent in these two peripheral nerve deficits. ET is a potent vasoconstrictor, which reduces blood flow within the peripheral nerve after topical administration (Zochodne *et al.*, 1992), but has not been reported to affect the process of nerve impulse propagation. It is, therefore, likely that the two findings reported here implicate an ET-derived endoneurial vasoconstriction as the cause of the short-term motor nerve conduction deficit in diabetic rats. It is not known whether alterations in ET production, release and/or receptor numbers within the peripheral nerve in experimental diabetes contribute to this. As ET stimulates the growth of endothelial and smooth muscle cells (Kimura *et al.*, 1988), it is also possible that chronic treatment with bosentan exerted its action via effects on microvessel structure and number. To understand more fully the role of ET, our group aims to study the action of this vasoconstrictor on nerve function after direct administration to the endoneurium. The fact that bosentan did not maintain Doppler flux and conduction velocity at completely normal values in the treated diabetic rats in this study may suggest that the role of ET, although major, is not exclusive of other factors. However, there exists the possibility that a higher dose of bosentan may have prevented the deficits and, as discussed above, it may be of value to investigate a dose-response relationship. Should long-term studies indicate that the nerve conduction deficit studied here is symptomatic of the more meaningful components of diabetic neuropathy, then ET receptor blockade may have a role to play in management.

This study was supported by a grant to the William Harvey Research Institute from Ono Pharmaceuticals. We are grateful to Dr Martine Clozel for her kind gift of bosentan, to Professor Terence Bennett for constructive comments on this work and to Mark Dewhurst for guidance with establishment of the electrophysiology on the Maclab.

References

BERTELLO, P., VEGLIO, F., PINNA, G., GURIOLI, L., MOLINO, P., ALBAN, S. & CHIANDUSSI, L. (1994). Plasma endothelin in NIDDM patients with and without complications. *Diabetes Care*, **17**, 574–577.

BIGAUD, M. & PELTON, J.T. (1992). Discrimination between ET_A- and ET_B-receptor-mediated effects of endothelin-1 and [$Ala^{1,3,11,15}$]endothelin-1 by BQ-123 in the anaesthetized rat. *Br. J. Pharmacol.*, **107**, 912–918.

CAMERON, N.E., COTTER, M.A., ARCHIBALD, V. DINES, K.C. & MAXFIELD, E.K. (1994a). Anti-oxidant and pro-oxidant effects on nerve conduction velocity, endoneurial blood flow and oxygen tension in non-diabetic and streptozotocin-diabetic rats. *Diabetologia*, **37**, 449–459.

CAMERON, N.E., COTTER, M.A., DINES, K.C., MAXFIELD, E.K., CAREY, F. & MIRRLEES, D.J. (1994b). Aldose reductase inhibition, nerve perfusion, oxygenation and function in streptozotocin-diabetic rats: Dose-response considerations and independence from a myo-inositol mechanism. *Diabetologia*, **37**, 651–663.

CAMERON, N.E., COTTER, M.A. & LOW, P.A. (1991). Nerve blood flow in early experimental diabetes in rats: relation to conduction deficits. *Am. J. Physiol.*, **261**, E1–E8.

CLOZEL, M., BREU, V., GRAY, G.A., KALINA, B., LÖFFLER, B.-M., BURRI, K., CASSAL, J.M., HIRTH, G., MÜLLER, M., NEIDHART, W. & RAMUZ, H. (1994). Pharmacological characterization of bosentan, a new potent orally active non-peptide endothelin receptor antagonist. *J. Pharmacol. Exp. Ther.*, (in press).

COTTER, M.A., DINES, K.C. & CAMERON, N.E. (1993). Prevention and reversal of motor and sensory peripheral nerve conduction abnormalities in streptozotocin-diabetic rats by the prostacyclin analogue iloprost. *Naunyn Schmied. Arch. Pharmacol.*, **347**, 534–540.

ELIASSON, S.G. (1964). Nerve conduction changes in experimental diabetes. *J. Clin. Invest.*, **43**, 2353–2358.

FUKUI, M., NAKAMURA, T., EBIHARA, I., OSADA, S., TOMINO, Y., MASAKI, T., GOTO, K., FURUICHI, Y. & KOIDE, H. (1993). Gene expression for endothelins and their receptors in glomeruli of diabetic rats. *J. Lab. Clin. Med.*, **122**, 149–156.

GARDINER, S.M., KEMP, P.A., MARCH, J.E. & BENNETT, T. (1994). Effects of bosentan (Ro 47-0203), an ET_A-, ET_B-receptor antagonist, on regional haemodynamic responses to endothelins in conscious rats. *Br. J. Pharmacol.*, **112**, 823–830.

GREGERSEN, G. (1967). Diabetic neuropathy: influence of age, sex, metabolic control and duration of diabetes on motor conduction velocity. *Neurology*, **17**, 972–980.

GRUDEN, G., CAVALLO-PERIN, P., BAZZAN, M., STELLA, S., VUOLO, A. & PAGANO, G. (1994). Pai-1 and Factor VII activity are higher in IDDM patients with microalbuminuria. *Diabetes*, **43**, 426–429.

HOTTA, N., KAKUTA, H., FUKASAWA, H., KOH, N., SAKAKIBARA, F., KOMORI, H. & SAKAMOTO, N. (1992). Effect of niceritrol on streptozocin-induced diabetic neuropathy in rats. *Diabetes*, **41**, 587–591.

KAPPELLE, A.C., BIESSELS, G.J., VAN BUREN, T., ERKELENS, D.W., DE WILDT, D.J. & GISPEN, W.H. (1993). Effects of nimodipine on sciatic nerve blood flow and vasa nervorum responsiveness in the diabetic rat. *Eur. J. Pharmacol.*, **250**, 43–49.

KIFF, R.J., GARDINER, S.M. COMPTON, A.M. & BENNETT, T. (1991a). Selective impairment of hindquarters vasodilator responses to bradykinin in conscious Wistar rats with streptozotocin-induced diabetes mellitus. *Br. J. Pharmacol.*, **103**, 1357–1362.

KIFF, R.J., GARDINER, S.M. COMPTON, A.M. & BENNETT, T. (1991b). The effects of endothelin-1 and N^G-nitro-L-arginine methyl ester on regional haemodynamics in conscious rats with streptozotocin-induced diabetes mellitus. *Br. J. Pharmacol.*, **103**, 1321–1326.

KIMURA, S., KURIHARA, H., SUGIYAMA, T., TAKAKU, F. & YAZAKI, Y. (1988). Endothelin stimulates c-fos and c-mys expression and proliferation of vascular smooth muscle cells. *FEBS Lett.*, **238**, 249–252.

LOW, P.A. & TUCK, R.R. (1984). Effects of changes of blood pressure, respiratory acidosis and hypoxia on blood flow in the sciatic nerve of the rat. *J. Physiol.*, **347**, 513–524.

MAXFIELD, E.K., CAMERON, N.E., COTTER, M.A. & DINES, K.C. (1993). Angiotensin II receptor blockade improves near function, modulates nerve blood flow and stimulates endoneurial angiogenesis in streptozotocin-diabetic rats and nerve function. *Diabetologia*, **36**, 1230–1237.

MAYER, J.H. & TOMLINSON, D.R. (1983). Prevention of defects of axonal transport and nerve conduction velocity by oral administration of myo-inositol or an aldose reductase inhibitor in streptozotocin-diabetic rats. *Diabetologia*, **25**, 433–438.

MONAFO, W.W., ELIASSON, S.G., SHIMAZAKI, S. & SUGIMOTO, H. (1988). Regional blood flow in resting and stimulated sciatic nerve of diabetic rats. *Exp. Neurol.*, **99**, 607–614.

MORABITO, E., CORSICO, N., SERAFINI, S. & MARTELLI, E.A. (1994). Elevated urinary excretion of endothelins in streptozotocin diabetic rats. *Life Sci.*, **54**, PL197–PL200.

NEWRICK, P.G., WILSON, A.J., JAKUBOWSKI, J.A., BOULTON, A.J.M. & WARD, J.D. (1986). Sural nerve oxygen tension in diabetes. *Br. Med. J.*, **293**, 1053–1054.

OHNO, A., KANAZAWA, A., TANAKA, A., MIWA, T. & ITO, H. (1992). Effect of a prostaglandin I_2 derivative (Iloprost) on peripheral neuropathy of diabetic rats. *Diabet. Res. Clin. Prac.*, **19**, 123–130.

PATINO, F. (1994). Increased plasma endothelin in diabetes: an atherosclerosis marker? *Diabetologia*, **37**, 334.

PREDEL, H.G., MEYER-LEHNERT, H., BACKER, A., STELKENS, H. & KRAMER, H.J. (1990). Plasma concentrations of endothelin in patients with abnormal vascular reactivity. *Life Sci.*, **47**, 1837–1843.

SHINDO, H., TAWATA, M., AIDA, K. & ONAYA, T. (1992). The role of cyclic adenosine 3′,5′-monophosphate and polyol metabolism in diabetic neuropathy. *J. Clin. Endocrinol. Metab.*, **74**, 393–398.

STEVENS, E.J., CARRINGTON, A.L. & TOMLINSON, D.R. (1994). Nerve ischaemia in diabetic rats: time-course of development, effect of insulin treatment plus comparison of streptozotocin and BB models. *Diabetologia*, **37**, 43–48.

STEVENS, E.J., CARRINGTON, A.L. & TOMLINSON, D.R. (1993a). Prostacyclin release in experimental diabetes: effects of evening primrose oil. *Prostaglandins Leukot. Essent. Fatty Acids*, **49**, 699–706.

STEVENS, E.J., LOCKETT, M.J., CARRINGTON, A.L. & TOMLINSON, D.R. (1993b). Essential fatty acid treatment prevents nerve ischaemia and associated conduction anomalies in rats with experimental diabetes mellitus. *Diabetologia*, **36**, 397–401.

STOUT, R.W. (1987). The endothelial cell in diabetes. *Front Diabetes*, **8**, 116–124.

TAKAHASHI, K., GHATEI, M.A., LAM, H.-C., O'HALLORAN, D.J. & BLOOM, S.R. (1990). Elevated plasma endothelin in patients with diabetes mellitus. *Diabetologia*, **33**, 306–310.

TAKAHASHI, K., SUDA, K., LAM, H.-C., GHATEI, M.A., & BLOOM, S.R. (1991). Endothelin-like immunoreactivity in rat models of diabetes mellitus. *J. Endocrinol.*, **130**, 123–127.

TAKEDA, Y., MIYAMORI, I., YONEDA, T. & TAKEDA, R. (1991). Production of endothelin-1 from the mesenteric arteries of streptozotocin-induced diabetic rats. *Life Sci.*, **48**, 2553–2556.

TSUNODA, K., ABE, K., SATO, T., YOKOSAWA, S. & YOSHINAGA, K. (1991). Decreased conversion of big endothelin-I to endothelin-I in patients with diabetes mellitus. *Clin. Exp. Pharmacol. Physiol.*, **18**, 731–732.

TUCK, R.R., SCHMELZER, J.D. & LOW, P.A. (1984). Endoneurial blood flow and oxygen tension in the sciatic nerves of rats with experimental diabetic neuropathy. *Brain*, **107**, 935–950.

VONGSAVAN, N. & MATTHEWS, B. (1993). Some aspects of the use of laser Doppler flow meters for recording tissue blood flow. *Exp. Physiol.*, **78**, 1–14.

WARD, K.K., LOW, P.A., SCHMELZER, J.D. & ZOCHODNE, D.W. (1989). Prostacyclin and noradrenaline in peripheral nerve of chronic experimental diabetes in rats. *Brain.*, **112**, 197–208.

WARNER, T.D., ALLCOCK, G.H., CORDER, R. & VANE, J.R. (1993). Use of the endothelin antagonists BQ-123 and PD 142893 to reveal three endothelin receptors mediating smooth muscle contraction and the release of EDRF. *Br. J. Pharmacol.*, **110**, 777–782.

WEBB, M.L., DICKENSON, K.E.J., DELANEY, C.L., LIU, E.C.-K., SERAFINO, R., COHEN, R.B., MOUSHIZADEGAN, H. & MOORELAND, S. (1992). The endothelin receptor antagonist, BQ-123, inhibits angiotensin II-induced contractions in rabbit aorta. *Biochem. Biophys. Res. Commun.*, **185**, 887–892.

WHITTLE, B.H.R., LOPEZ-BELMONTE, J. & REES, D.D. (1989). Modulation of the vasodepressor actions of acetylcholine, bradykinin, substance P and endothelin in the rat by a specific inhibitor of nitric oxide formation. *Br. J. Pharmacol.*, **98**, 646–652.

YASUDA, H., SONOBE, M., YAMASHITA, M., TERADA, M., HATANAKA, I., HUITIAN, Z. & SHIGETA, Y. (1989). Effect of prostaglandin E_1 analogue TFC 612 on diabetic neuropathy in streptozocin-induced diabetic rats: comparison with aldose reductase inhibitor ONO 2235. *Diabetes*, **38**, 832–838.

ZOCHODNE, D.W., HO, L.T. & GROSS, P.M. (1992). Acute endoneurial ischemia induced by epineurial endothelin in the rat sciatic nerve. *Am. J. Physiol.*, **263**, H1806–H1810.

(Received September 5, 1994
Revised January 26, 1995
Accepted February 10, 1995)

British Journal of Pharmacology

VOLUME 115 (2) MAY 1995

STOCKTON

BRITISH JOURNAL OF PHARMACOLOGY

The *British Journal of Pharmacology* welcomes contributions in all fields of experimental pharmacology including neuroscience, biochemical, cellular and molecular pharmacology. The Board of Editors represents a wide range of expertise and ensures that well-presented work is published as promptly as possible, consistent with maintaining the overall quality of the journal.

Edited for the British Pharmacological Society by

A.T. Birmingham
(Chairman)

R.W. Horton **W.A. Large**
(Secretaries)

Submission of manuscripts: Manuscripts (two copies) should be sent to The Editorial Office, British Journal of Pharmacology, St. George's Hospital Medical School, Cranmer Terrace, London SW17 0RE.

Authors should consult the Instructions to Authors and the Nomenclature Guidelines for Authors in Vol. **114,** 245–255. These Instructions and Guidelines also appear with the journal Index for Volumes **111–113,** 1994. A checklist of the essential requirements is summarised in each issue of the journal, or as the last page of the issue.

The *British Journal of Pharmacology* is published by Stockton Press, a division of Macmillan Press Ltd. It is the official publication of the British Pharmacological Society.

Scope The *British Journal of Pharmacology* is published twice a month. It welcomes contribution in all field of experimental pharmacology including neuroscience, biochemical, cellular and molecular pharmacology. The Board of Editors represents a wide range of expertise and ensures that well-presented work is published as promptly as possible, consistent with maintaining the overall quality of the journal

This journal is covered by Current Contents, Excerpta Medica, BIOSIS and Index Medicus.

Editorial Manuscripts (plus two copies) and all editorial correspondence should be sent to: The Editorial Office, British Journal of Pharmacology, St George's Hospital Medical School, Cranmer Terrace, London SW17 0RE, UK. Tel: +44 (0)181 767 6765; Fax: +44 (0)181 767 5645.

Advertisements Enquiries concerning advertisements should be addressed to: Michael Rowley, Hasler House, High Street, Great Dunmow, Essex CM6 1AP, UK. Tel: +44 (0)1371 874613; Fax: +44 (0)1371 872273.

Publisher All business correspondence, supplement enquiries and reprint requests should be addressed to British Journal of Pharmacology, Stockton Press, Houndmills, Basingstoke, Hampshire RG21 2XS, UK. Tel: +44 (0)1256 29242; Fax: +44 (0)1256 810526. Publisher: Marija Vukovojac. Editorial Assistant: Alice Ellingham. Production Controller: Karen Stuart.

Subscriptions – EU/Rest of World Subscription price per annum (3 volumes, 24 issues) £620, rest of world £820 (Airmail), £685 (Surface mail) or equivalent in any other currency. Orders must be accompanied by remittance. Cheques should be made payable to Macmillan Magazines and sent to: The Subscription Department, Macmillan Press Ltd, Houndmills, Basingstoke, Hampshire RG21 2XS, UK. Where appropriate, subscribers may make payments into UK Post Office Giro Account No. 519 2455. Full details must accompany the payment. Subscribers from EU territories should add sales tax at the local rate.

Subscriptions – USA USA subscribers call toll free 1-800-221-2123 or send check/money order/credit card details to: Stockton Press, 49, West 24th Street, New York, NY 10010; Tel: 212 627 5757, Fax: 212 627 9256. USA annual subscription rates: $1230 Airmail; $1030 Surface (Institutional/Corporate); $225 (Individual making personal payment).

British Journal of Pharmacology (ISSN 0007–1188) is published twice a month by Macmillan Press Ltd, c/o Mercury Airfreight International Ltd, 2323 Randolph Avenue, Avenel, NJ 07001, USA. Subscription price for institutions is $1030 per annum (surface). 2nd class postage is paid at Rahway NJ. Postmaster: send address corrections to Macmillan Press Ltd, c/o Mercury Airfreight International Ltd, 2323 Randolph Avenue, Avenel NJ 07001.

Reprints of any article in this journal are available from Stockton Press, Houndmills, Basingstoke, Hampshire RG21 2XS, UK. Tel: +44 (0)1256 29242; Fax: +44 (0)1256 810526.

ISSN 0007–1188

PREPARATION OF MANUSCRIPTS

Authors are strongly recommended to read the full *Instructions to Authors* and *Nomenclature Guidelines for Authors* (*Br. J. Pharmacol.* 1995, **114,** 245–255) before submitting a manuscript for publication in the *British Journal of Pharmacology*. The manuscript and cover letter should be checked against the following list before mailing.

The original and one copy of the manuscript must be supplied. Manuscripts must be typed in double-line spacing on one side of A4 paper, in type not smaller than 12 characters per inch or 10 point. Both copies to include Tables and a set of labelled Figures. One set of Figures without numbers or letters is also to be included. The text to be arranged in the following subsections:

1. **Title**—To have no more than 150 characters on a separate page, which should also include a Short Title (50 characters maximum) and the name and address of the author for correspondence.
2. **Summary**—To be arranged in numbered paragraphs (Full Papers) or a single paragraph (Special Reports).
   —to include aims, principal results and conclusions.
   —to include Key words (10 maximum) at end of summary.
3. **Introduction**—To contain concise statements of the problem and the aims of the investigation.
4. **Methods**—To have brief but adequate account of the procedures; *full names of drugs* (*including those referred to by manufacturer's code*), sources of drugs and statistical tests to be stated.
5. **Results**—To have no repetition of data in Figures, Tables and text.
6. **Discussion**—Findings and conclusions to be placed in context of other relevant work.
   NB Simple repetition of results and unwarranted speculation are not acceptable.
7. **Acknowledgements**—Sources of support. Sources of drugs not widely available commercially.
8. **References**—All references in the text to be included in the Reference List and *vice versa*. References in alphabetical order with complete citations; Journals publishing 'in press' papers identified.
   References to manuscripts submitted to other journals but not yet accepted are not allowed.
9. **Tables**—Each on a separate page and prepared in accordance with current requirements of the Journal.
10. **Figures**—Both labelled and non-labelled Figures to be prepared in accordance with current requirements of the Journal (see *Instructions to Authors*, 1995, **114,** 245–251) and provided with Figure Number and Authors' names on back (*in pencil*).
    —each legend to be typed on a separate page and carrying keys to symbols.
    —keys to symbols and histograms must not appear on the figures themselves, but in the respective legends.
    —'box style' figures are not in keeping with the Journal style; line drawings etc must have only left-hand and bottom axes.
11. **Manuscripts**—To be accompanied by a declaration signed by each author that
    (a) results are original
    (b) approval of all persons concerned has been given to submit manuscripts for consideration (see also 12b)
    (c) the same material is neither 'in press' (i.e. is in proof or has definitely been accepted for publication) nor under consideration elsewhere. Furthermore it will not be submitted or published elsewhere before a decision has been reached by the Editorial Board of the *British Journal of Pharmacology* and will not be submitted elsewhere if accepted by the *British Journal of Pharmacology*.
    (d) Copyright assignment is included.
12. **Cover letter**—To state clearly
    (a) Corresponding author's full postal address, telephone, telex or Fax number
    (b) where appropriate, that *either* ethical approval has been given for investigation *or* Company or Institutional permission to publish work has been received.
13. **Reminder**—Packaging to be sufficiently robust to protect Figures and to withstand mailing.

Failure to comply with *Instructions to Authors* may lead to substantial delays in processing, review and publication and may even jeopardize acceptance of the manuscript.

NOMENCLATURE

Authors are reminded that accepted receptor and associated terminology is laid out in *Nomenclature Guidelines for Authors*, as published in the *British Journal of Pharmacology, Br. J. Pharmacol.*, 1995, **114,** 253–255.

SPECIAL REPORTS

The purpose of *Special Reports* is to provide rapid publication for **new** and **important** results which the Editorial Board considers are likely to be of special pharmacological significance. *Special Reports* will have publication priority over all other material and so authors are asked to consider carefully the status of their work before submission.

In order to speed publication there is normally no revision allowed beyond very minor typographical or grammatical corrections. If significant revision is required, the Board may either invite rapid re-submission or, more probably, propose that it be re-written as a Full Paper and be re-submitted for consideration. In order to reduce delays, proofs of *Special Reports* will be sent to authors but **essential corrections must reach the Production Office within 48 hours of receipt.** Authors should ensure that their submitted material conforms exactly to the following requirements.

Special Reports should normally occupy no more than two printed pages of the Journal; two illustrations (Figures or Tables, with legends) are permitted. As a guideline, with type face of 12 pitch and double-line spacing, a page of A4 paper could contain about 400 words. The absolute maximum length of the *Special Report* is 1700 words. For each Figure or Table, please deduct 200 words. The manuscript should comprise a Title page with key words (maximum of 10), a Summary consisting of a single short paragraph, followed by Introduction, Methods, Results, Discussion and References (maximum of 10). In all other respects, the requirements are the same as for Full Papers (see current 'Instructions to Authors').

BRITISH JOURNAL OF PHARMACOLOGY VOLUME 115 (2) 1995

STOCKTON

Typeset by Elite Typesetting Techniques, Eastleigh, Hants
and printed in Great Britain by Unwin Brothers Ltd., The Gresham Press, Old Woking, Surrey